

# EMERGING INFECTIOUS DISEASES<sup>®</sup>



Vectorborne Infections

April 2019



Untung Yuli Pratiwawan (aka Wawan Geni) (1982-). *The Little Time*, 2017. Burning techniques applied to canvas, 35.4 in. x 27.6 in./90 cm x 70 cm. Wawan Geni Collection. Digital image courtesy of Wawan Geni.

# EMERGING INFECTIOUS DISEASES<sup>®</sup>

EDITOR-IN-CHIEF

D. Peter Drotman

## Associate Editors

Paul Arguin, Atlanta, Georgia, USA  
 Charles Ben Beard, Fort Collins, Colorado, USA  
 Ermias Belay, Atlanta, Georgia, USA  
 David Bell, Atlanta, Georgia, USA  
 Sharon Bloom, Atlanta, Georgia, USA  
 Richard Bradbury, Atlanta, Georgia, USA  
 Mary Brandt, Atlanta, Georgia, USA  
 Corrie Brown, Athens, Georgia, USA  
 Charles Calisher, Fort Collins, Colorado, USA  
 Benjamin J. Cowling, Hong Kong, China  
 Michel Drancourt, Marseille, France  
 Paul V. Effler, Perth, Australia  
 Anthony Fiore, Atlanta, Georgia, USA  
 David Freedman, Birmingham, Alabama, USA  
 Peter Gerner-Smidt, Atlanta, Georgia, USA  
 Stephen Hadler, Atlanta, Georgia, USA  
 Matthew Kuehnert, Edison, New Jersey, USA  
 Nina Marano, Atlanta, Georgia, USA  
 Martin I. Meltzer, Atlanta, Georgia, USA  
 David Morens, Bethesda, Maryland, USA  
 J. Glenn Morris, Gainesville, Florida, USA  
 Patrice Nordmann, Fribourg, Switzerland  
 Johann D.D. Pitout, Calgary, Alberta, Canada  
 Ann Powers, Fort Collins, Colorado, USA  
 Didier Raoult, Marseille, France  
 Pierre Rollin, Atlanta, Georgia, USA  
 Frank Sorvillo, Los Angeles, California, USA  
 David Walker, Galveston, Texas, USA  
 J. Todd Weber, Atlanta, Georgia, USA  
 Jeffrey Scott Weese, Guelph, Ontario, Canada

## Managing Editor

Byron Breedlove, Atlanta, Georgia, USA

**Copy Editors** Kristina Clark, Dana Dolan, Karen Foster,  
 Thomas Gryczan, Amy Guinn, Michelle Moran, Shannon O'Connor,  
 Jude Rutledge, P. Lynne Stockton, Deborah Wenger

**Production** Thomas Ehemann, William Hale, Barbara Segal,  
 Reginald Tucker

**Editorial Assistants** Kristine Phillips, Susan Richardson

**Communications/Social Media** Sarah Logan Gregory,  
 Tony Pearson-Clarke

## Founding Editor

Joseph E. McDade, Rome, Georgia, USA

Emerging Infectious Diseases is published monthly by the Centers for Disease Control and Prevention, 1600 Clifton Rd NE, Mailstop H16-2, Atlanta, GA 30329-4027, USA. Telephone 404-639-1960, fax 404-639-1954, email [eideditor@cdc.gov](mailto:eideditor@cdc.gov).

The conclusions, findings, and opinions expressed by authors contributing to this journal do not necessarily reflect the official position of the U.S. Department of Health and Human Services, the Public Health Service, the Centers for Disease Control and Prevention, or the authors' affiliated institutions. Use of trade names is for identification only and does not imply endorsement by any of the groups named above.

All material published in Emerging Infectious Diseases is in the public domain and may be used and reprinted without special permission; proper citation, however, is required.

## EDITORIAL BOARD

Timothy Barrett, Atlanta, Georgia, USA  
 Barry J. Beaty, Fort Collins, Colorado, USA  
 Martin J. Blaser, New York, New York, USA  
 Christopher Braden, Atlanta, Georgia, USA  
 Arturo Casadevall, New York, New York, USA  
 Kenneth C. Castro, Atlanta, Georgia, USA  
 Vincent Deubel, Shanghai, China  
 Christian Drosten, Charité Berlin, Germany  
 Isaac Chun-Hai Fung, Statesboro, Georgia, USA  
 Kathleen Gensheimer, College Park, Maryland, USA  
 Rachel Gorwitz, Atlanta, Georgia, USA  
 Duane J. Gubler, Singapore  
 Richard L. Guerrant, Charlottesville, Virginia, USA  
 Scott Halstead, Arlington, Virginia, USA  
 Katrina Hedberg, Portland, Oregon, USA  
 David L. Heymann, London, UK  
 Keith Klugman, Seattle, Washington, USA  
 Takeshi Kurata, Tokyo, Japan  
 S.K. Lam, Kuala Lumpur, Malaysia  
 Stuart Levy, Boston, Massachusetts, USA  
 John S. MacKenzie, Perth, Australia  
 John E. McGowan, Jr., Atlanta, Georgia, USA  
 Jennifer H. McQuiston, Atlanta, Georgia, USA  
 Tom Marrie, Halifax, Nova Scotia, Canada  
 Nkuchia M. M'ikanatha, Harrisburg, Pennsylvania, USA  
 Frederick A. Murphy, Bethesda, Maryland, USA  
 Barbara E. Murray, Houston, Texas, USA  
 Stephen M. Ostroff, Silver Spring, Maryland, USA  
 Marguerite Pappaioanou, Seattle, Washington, USA  
 Mario Raviglione, Geneva, Switzerland  
 David Relman, Palo Alto, California, USA  
 Guénaél Rodier, Saône-et-Loire, France  
 Connie Schmaljohn, Frederick, Maryland, USA  
 Tom Schwan, Hamilton, Montana, USA  
 Rosemary Soave, New York, New York, USA  
 P. Frederick Sparling, Chapel Hill, North Carolina, USA  
 Robert Swanepoel, Pretoria, South Africa  
 Phillip Tarr, St. Louis, Missouri, USA  
 Duc Vugia, Richmond, California  
 John Ward, Atlanta, Georgia, USA  
 Mary E. Wilson, Cambridge, Massachusetts, USA

Use of trade names is for identification only and does not imply endorsement by the Public Health Service or by the U.S. Department of Health and Human Services.

EMERGING INFECTIOUS DISEASES is a registered service mark of the U.S. Department of Health & Human Services (HHS).

∞ Emerging Infectious Diseases is printed on acid-free paper that meets the requirements of ANSI/NISO 239.48-1992 (Permanence of Paper)



# EMERGING INFECTIOUS DISEASES®

Vectorborne Infections

April 2019



## On the Cover

Untung Yuli Prastiawan (aka Wawan Geni) (1982–). *The Little Time*, 2017 (detail). Burning techniques applied to canvas, 35.4 in × 27.6 in/90 cm × 70 cm. Wawan Geni Collection. Digital image courtesy of Wawan Geni.

About the Cover p. 845

## Mucosal Leishmaniasis in Travelers with *Leishmania braziliensis* Complex Returning to Israel

M. Solomon et al. 642

## Tick-Borne Relapsing Fever in the White Mountains, Arizona, USA, 2013–2018

N. Mafi et al. 649

## Lobomycosis in Soldiers, Colombia

C.M. Arenas et al. 654

## Research

## Cost-effectiveness of Latent Tuberculosis Infection Screening before Immigration to Low-Incidence Countries

J.R. Campbell et al. 661



Related material available online:  
[http://wwwnc.cdc.gov/eid/article/25/4/17-1630\\_article](http://wwwnc.cdc.gov/eid/article/25/4/17-1630_article)

## Spatial Dynamics of Chikungunya Virus, Venezuela, 2014

E. Lizarazo et al. 672



Related material available online:  
[http://wwwnc.cdc.gov/eid/article/25/4/17-2121\\_article](http://wwwnc.cdc.gov/eid/article/25/4/17-2121_article)

## Sand Fly–Associated Phlebovirus with Evidence of Neutralizing Antibodies in Humans, Kenya

D.P. Tchouassi et al. 681



Related material available online:  
[http://wwwnc.cdc.gov/eid/article/25/4/18-0750\\_article](http://wwwnc.cdc.gov/eid/article/25/4/18-0750_article)

## Human-Origin Influenza A(H3N2) Reassortant Viruses in Swine, Southeast Mexico

M.I. Nelson et al. 691



Related material available online:  
[http://wwwnc.cdc.gov/eid/article/25/4/18-0779\\_article](http://wwwnc.cdc.gov/eid/article/25/4/18-0779_article)

## Perspective

### Resurgence of Vaccine-Preventable Diseases in Venezuela as a Regional Public Health Threat in the Americas

A.E. Paniz-Mondolfi et al. 625



Related material available online:  
[http://wwwnc.cdc.gov/eid/article/25/4/18-1305\\_article](http://wwwnc.cdc.gov/eid/article/25/4/18-1305_article)

## Synopses

**Medscape**  
EDUCATION  
ACTIVITY

### Clinical Manifestations and Molecular Diagnosis of Scrub Typhus and Murine Typhus, Vietnam, 2015–2017

Scrub typhus was the predominant rickettsial disease diagnosed among hospitalized patients with acute undifferentiated fever in northern Vietnam.

N.V. Trung et al. 633



Related material available online:  
[http://wwwnc.cdc.gov/eid/article/25/4/18-0691\\_article](http://wwwnc.cdc.gov/eid/article/25/4/18-0691_article)



**Staphylococcus aureus**  
Bacteremia in Children of Rural Areas of The Gambia, 2008–2015  
A. Oduola et al. 701

**Pneumonia-Specific *Escherichia coli* with Distinct Phylogenetic and Virulence Profiles, France, 2012–2014**  
B. La Combe et al. 710

Related material available online:  
[http://wwwnc.cdc.gov/eid/article/25/4/18-0944\\_article](http://wwwnc.cdc.gov/eid/article/25/4/18-0944_article)

**Symptoms, Sites, and Significance of *Mycoplasma genitalium* in Men Who Have Sex with Men**  
T.R.H. Read et al. 719

**Differences in Neuropathogenesis of Encephalitic California Serogroup Viruses**  
A.B. Evans et al. 728

Related material available online:  
[http://wwwnc.cdc.gov/eid/article/25/4/18-1016\\_article](http://wwwnc.cdc.gov/eid/article/25/4/18-1016_article)

***Klebsiella pneumoniae* ST307 with *bla*<sub>OXA-181</sub> South Africa, 2014–2016**  
M. Lowe et al. 739

Related material available online:  
[http://wwwnc.cdc.gov/eid/article/25/4/18-1482\\_article](http://wwwnc.cdc.gov/eid/article/25/4/18-1482_article)

**Co-infections in Persons with Early Lyme Disease, New York, USA**  
G.P. Wormser et al. 748

**Middle East Respiratory Syndrome Coronavirus Infection Dynamics and Antibody Responses among Clinically Diverse Patients, Saudi Arabia**  
H.M. Al-Abdely et al. 753

Related material available online:  
[http://wwwnc.cdc.gov/eid/article/25/4/18-1595\\_article](http://wwwnc.cdc.gov/eid/article/25/4/18-1595_article)

***Francisella tularensis* Transmission by Solid Organ Transplantation, 2017**  
C.A. Nelson et al. 767

## Dispatches

***Streptococcus agalactiae* Sequence Type 283 in Farmed Fish, Brazil**  
C.A.G. Leal et al. 776

Related material available online:  
[http://wwwnc.cdc.gov/eid/article/25/4/18-0543\\_article](http://wwwnc.cdc.gov/eid/article/25/4/18-0543_article)

**Genomic Survey of *Bordetella pertussis* Diversity, United States, 2000–2013**  
M.R. Weigand et al. 780

Related material available online:  
[http://wwwnc.cdc.gov/eid/article/25/4/18-0812\\_article](http://wwwnc.cdc.gov/eid/article/25/4/18-0812_article)

**Early Genomic Detection of Cosmopolitan Genotype of Dengue Virus Serotype 2, Angola, 2018**  
S.C. Hill et al. 784

Related material available online:  
[http://wwwnc.cdc.gov/eid/article/25/4/18-0958\\_article](http://wwwnc.cdc.gov/eid/article/25/4/18-0958_article)

**Enterovirus A71 Phenotypes Causing Hand, Foot and Mouth Disease, Vietnam**  
H.M.T. Van et al. 788

Related material available online:  
[http://wwwnc.cdc.gov/eid/article/25/4/18-1367\\_article](http://wwwnc.cdc.gov/eid/article/25/4/18-1367_article)

**Distribution, Host-Seeking Phenology, and Host and Habitat Associations of *Haemaphysalis longicornis* Ticks, Staten Island, New York, USA**  
D.M. Tufts et al. 792

**Aerosol Transmission of *Aspergillus fumigatus* in Cystic Fibrosis Patients in the Netherlands**  
T.G.P. Engel et al. 797

**Pneumonic Plague in a Dog and Widespread Human Exposure in a Veterinary Hospital, United States**  
P.A. Schaffer et al. 800

**Seroprevalence of *Borrelia burgdorferi*, *B. miyamotoi*, and Powassan Virus in Residents Bitten by *Ixodes* Ticks, Maine, USA**  
R.P. Smith, Jr., et al. 804





**Prolonged Shedding of Zika Virus RNA in Vaginal Secretions, Nicaragua**

Y. Reyes et al.

808

**Self-Flagellation as Possible Route of Human T-Cell Lymphotropic Virus Type 1 Transmission**

A.R. Tang et al.

811

**Seroprevalence of Zika and Dengue Virus Antibodies among Migrant Workers, Taiwan, 2017**

G.C. Perng et al.

814

Related material available online:  
[http://wwwnc.cdc.gov/eid/article/25/4/18-1449\\_article](http://wwwnc.cdc.gov/eid/article/25/4/18-1449_article)

***Anopheles sundaicus* Mosquitoes as Vector for *Plasmodium knowlesi*, Andaman and Nicobar Islands, India**

P.T. Vidhya et al.

817

**Research Letters**

**Prior Vaccination and Effectiveness of Communication Strategies Used to Describe Infectious Diseases**

T.S. Valley et al.

821

Related material available online:  
[http://wwwnc.cdc.gov/eid/article/25/4/18-1408\\_article](http://wwwnc.cdc.gov/eid/article/25/4/18-1408_article)

**Peripheral Plasma and Semen Cytokine Response to Zika Virus in Humans**

J.-M. Mansuy et al.

823

**Detection of Epizootic Hemorrhagic Disease Virus Serotype 1, Israel**

N. Golender, V.Y. Bumbarov

825

**Ross River Virus Antibody Prevalence, Fiji Islands, 2013–2015**

M. Aubry et al.

827

**Malignant *Aspergillus flavus* Otitis Externa with Jugular Thrombosis**

M. Moniot et al.

830

Related material available online:  
[http://wwwnc.cdc.gov/eid/article/25/4/18-0710\\_article](http://wwwnc.cdc.gov/eid/article/25/4/18-0710_article)

# EMERGING INFECTIOUS DISEASES®

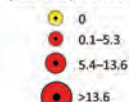
April 2019

No. *H. longicornis* ticks per deer (timed-manual collection)



State and city parks

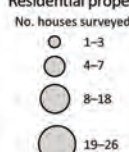
Density of *H. longicornis* ticks in parks (total ticks per 1,000 m<sup>2</sup>)



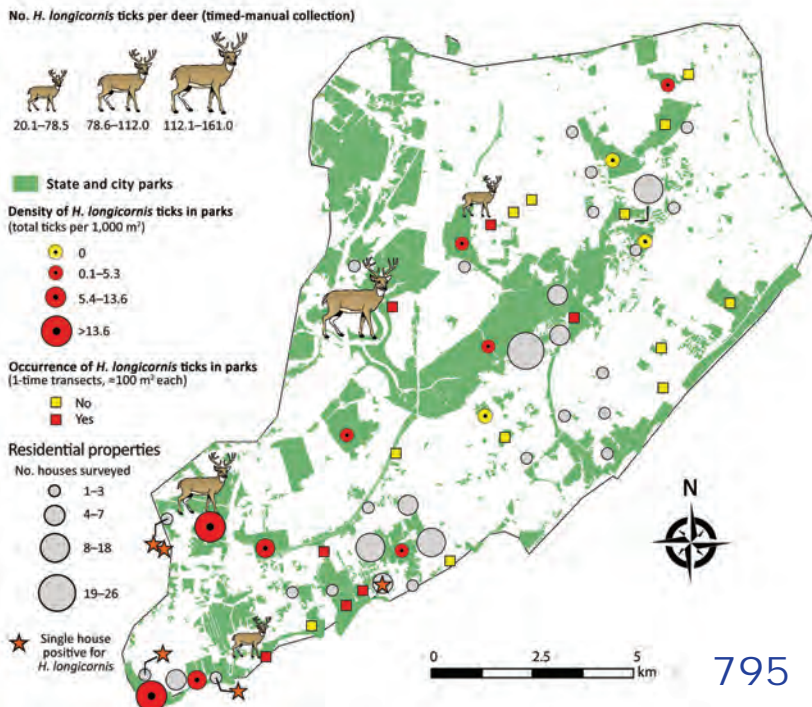
Occurrence of *H. longicornis* ticks in parks (1-time transects, ≈100 m<sup>2</sup> each)



Residential properties



Single house positive for *H. longicornis* (star icon)



795

**Epizootic Hemorrhagic Disease in White-Tailed Deer, Canada**

S.E. Allen et al.

832

**Effects of Political Instability in Venezuela on Malaria Resurgence at Ecuador–Peru Border, 2018**

R. Jaramillo-Ochoa et al.

834

Related material available online:  
[http://wwwnc.cdc.gov/eid/article/25/4/18-1355\\_article](http://wwwnc.cdc.gov/eid/article/25/4/18-1355_article)

***Rickettsia parkeri* and *Candidatus Rickettsia andeanae* in Ticks of the *Amblyomma maculatum* Group, Mexico**

J. Delgado-de la Mora et al.

836

Related material available online:  
[http://wwwnc.cdc.gov/eid/article/25/4/18-1507\\_article](http://wwwnc.cdc.gov/eid/article/25/4/18-1507_article)

**Reduced Susceptibility to Neuraminidase Inhibitors in Influenza B Isolate, Canada**

Y. Abed et al.

838

Related material available online:  
[http://wwwnc.cdc.gov/eid/article/25/4/18-1554\\_article](http://wwwnc.cdc.gov/eid/article/25/4/18-1554_article)

**Combination of Clindamycin and Azithromycin as Alternative Treatment for *Toxoplasma gondii* Encephalitis**

D. Shiojiri et al.

841

**Books and Media**

**The Task Force for Child Survival: Secrets of Successful Coalitions**

J.M. Gould

844

**About the Cover**

**Finesse and Fire, Creativity and Combustion**

B. Breedlove

845

**Etymologia**

***Anaplasma phagocytophilum***

R. Henry

747



## Diagnostic Assistance and Training in Laboratory Identification of Parasites

A free service of CDC available to laboratorians, pathologists, and other health professionals in the United States and abroad



Diagnosis from photographs of worms, histological sections, fecal, blood, and other specimen types



Expert diagnostic review



Formal diagnostic laboratory report



Submission of samples via secure file share

Visit the DPDx website for information on laboratory diagnosis, geographic distribution, clinical features, parasite life cycles, and training via Monthly Case Studies of parasitic diseases.

[www.cdc.gov/dpdx](http://www.cdc.gov/dpdx)  
[dpdx@cdc.gov](mailto:dpdx@cdc.gov)



U.S. Department of  
Health and Human Services  
Centers for Disease  
Control and Prevention



# Resurgence of Vaccine-Preventable Diseases in Venezuela as a Regional Public Health Threat in the Americas

**Alberto E. Paniz-Mondolfi, Adriana Tami, Maria E. Grillet, Marilianna Márquez, Juan Hernández-Villena, María A. Escalona-Rodríguez, Gabriela M. Blohm, Isis Mejías, Huniades Urbina-Medina, Alejandro Rísquez, Julio Castro, Ana Carvajal, Carlos Walter, María G. López, Philipp Schwabl, Luis Hernández-Castro, Michael A. Miles, Peter J. Hotez, John Lednický, J. Glenn Morris Jr., James Crainey, Sergio Luz, Juan D. Ramírez, Emilia Sordillo, Martin Llewellyn, Merari Canache, María Araque, José Oletta**

Venezuela's tumbling economy and authoritarian rule have precipitated an unprecedented humanitarian crisis. Hyperinflation rates now exceed 45,000%, and Venezuela's health system is in free fall. The country is experiencing a massive exodus of biomedical scientists and qualified health-

care professionals. Reemergence of arthropod-borne and vaccine-preventable diseases has sparked serious epidemics that also affect neighboring countries. In this article, we discuss the ongoing epidemics of measles and diphtheria in Venezuela and their disproportionate impact on indigenous populations. We also discuss the potential for reemergence of poliomyelitis and conclude that action to halt the spread of vaccine-preventable diseases within Venezuela is a matter of urgency for the country and the region. We further provide specific recommendations for addressing this crisis.

Author affiliations: Clínica IDB Cabudare, Instituto de Investigaciones Biomédicas IDB, Cabudare, Venezuela (A.E. Paniz-Mondolfi, M. Márquez, M.A. Escalona-Rodríguez, G.M. Blohm); Venezuelan Science Incubator, Barquisimeto, Venezuela (A.E. Paniz-Mondolfi, M. Márquez, M.A. Escalona-Rodríguez, G.M. Blohm, I. Mejías); University of Groningen, University Medical Center Groningen, Groningen, the Netherlands (A. Tami); Facultad de Ciencias de la Salud, Universidad de Carabobo, Valencia, Venezuela (A. Tami); Universidad Central de Venezuela, Caracas (M.E. Grillet, J. Hernández-Villena, A. Rísquez); Universidad Centrooccidental Lisandro Alvarado, Barquisimeto (M. Márquez); University of Florida, Gainesville, Florida, USA (G.M. Blohm, J. Lednický, J.G. Morris Jr.); Rotary International, Houston, Texas, USA (I. Mejías); Sociedad Venezolana de Puericultura y Pediatría, Caracas (H. Urbina-Medina); Sociedad Venezolana de Salud Pública/Red Defendamos la Epidemiología Nacional, Caracas (J. Castro, A. Carvajal, C. Walter, J. Oletta); Sociedad Venezolana de Infectología, Caracas (M.G. López); University of Glasgow, Glasgow, Scotland, UK (P. Schwabl, L. Hernández-Castro, M. Llewellyn); London School of Hygiene and Tropical Medicine, London, UK (M.A. Miles); Baylor College of Medicine National School of Tropical Medicine, Houston (P.J. Hotez); Instituto Leônidas e Maria Deane/FIOCRUZ, Manaus, Brazil (J. Crainey, S. Luz); Universidad del Rosario, Bogotá, Colombia (J.D. Ramírez); Mount Sinai Saint Luke's, New York, New York, USA. (E. Sordillo); Hospital de Niños José Manuel de los Ríos, Caracas (M. Canache); Universidad de Los Andes, Mérida, Venezuela (M. Araque)

DOI: <https://doi.org/10.3201/eid2504.181305>

Residents of Venezuela are struggling to survive in a country with the world's highest annual inflation rate, 46,305% (1), and a minimum monthly wage of just USD \$1.79 (5,196,000 Bolívars). The International Monetary Fund predicted an inflation rate of 1,000,000% by the end of 2018 (1). Sixty-six percent of the population lives in extreme poverty (2), amid escalating violence and a crumbling healthcare infrastructure more typical of conflict zones or war-torn nations. More than 280,000 children are at risk for death from severe malnutrition (3). According to the last official nationwide epidemiologic bulletin, published in 2016, infant and maternal mortality had risen by 30% and 65%, respectively, over the previous year (2); no further national epidemiologic records have been released.

Long-term shortages of essential medicines and medical supplies (only 30% of basic drugs to treat infectious diseases are available in public hospitals) (2), interruption of epidemiologic surveillance systems, weakening of immunization programs, and an unprecedented exodus of trained medical personnel have set the stage for the resurgence of vectorborne and vaccine-preventable infections (4–6). A striking manifestation is the ongoing malaria epidemic in Venezuela (6–9), now approaching half a million cases per

year and continuing to increase at rates exceeding those previously reported anywhere in the world (10).

Recently, the return of measles and other vaccine-preventable childhood infections in Venezuela (Figure 1), as well as the potential for expansion of outbreaks beyond Venezuela's borders, has been recognized by the World Health Organization (WHO) and the Pan American Health Organization (PAHO) (9). In Colombia alone, 25 cases of imported measles in migrants from Venezuela had been recorded as of October 2018 (9,10). The continued mass exodus of  $\approx 2$  million persons from Venezuela since 2014 (9), not only to Colombia (>820,000 migrants) but also to Ecuador (>450,000) and Brazil (>57,000) (11–13), represents an ongoing risk that vaccine-preventable diseases will be carried with them. The United Nations High Commissioner for Refugees (UNHCR) has launched a supplementary appeal for funding for these affected countries (14). Simultaneously, the spread of vaccine-preventable diseases must be tackled urgently within Venezuela, with an emphasis on containing outbreaks locally and at critical border areas.

### Measles

In Venezuela, circulation of wild measles was interrupted in February 2007 after a mass vaccination campaign that

followed outbreaks in 2001 and 2006 (15). However, since 2017, measles has reemerged in Venezuela, particularly within vulnerable indigenous populations, and has subsequently reached neighboring countries (Figure 1, panel A) (16). As of October 23, 2018, Venezuela had contributed 68% (5,525/8,091 cases) of the measles cases reported in the Americas and most of the measles-related deaths (73/85) (16). Genotyping of the measles virus isolated from patients from Venezuela (imported cases) in Brazil, Colombia, Ecuador, and Peru confirmed that the strains were genotype D8, lineage MVi/Hulu Langat.MYS/26.11 (16). The D8 genotype is associated with endemic transmission in Asia and the Pacific (17) and is the main lineage circulating currently in South America (16).

Measles now affects multiple states in Venezuela, and a disproportionate number of cases occur among indigenous populations located in the vast forestlands of the southern region. Measles cases were first reported in epidemiologic week 26 of 2017 in the southern, mineral-rich state of Bolívar; 82% of the cases were detected in the municipality of Caroní (18). From week 26 of 2017 through week 43 of 2018, a total of 7,524 suspected cases were reported, of which 6,252 have been confirmed (727 in 2017 and 5,525 in 2018); 75 deaths were attributed to measles, most of

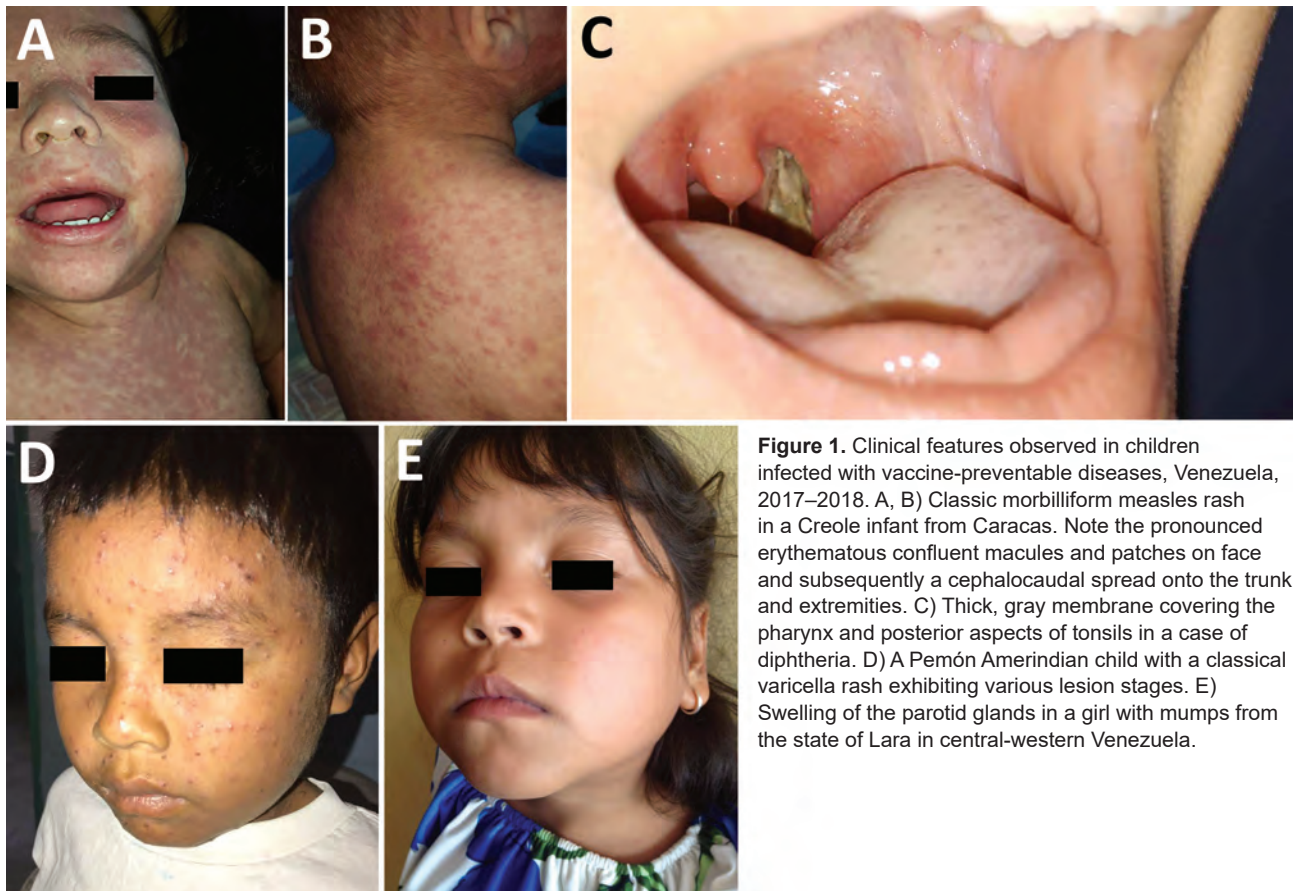


**Figure 1.** Clinical features observed in children infected with vaccine-preventable diseases, Venezuela, 2017–2018. A, B) Classic morbilliform measles rash in a Creole infant from Caracas. Note the pronounced erythematous confluent macules and patches on face and subsequently a cephalocaudal spread onto the trunk and extremities. C) Thick, gray membrane covering the pharynx and posterior aspects of tonsils in a case of diphtheria. D) A Pemón Amerindian child with a classical varicella rash exhibiting various lesion stages. E) Swelling of the parotid glands in a girl with mumps from the state of Lara in central-western Venezuela.



them in the Amazon and Orinoco River Delta regions of the country. The affected regions have widened to include other more populated states such as Apure, Anzoátegui, Delta Amacuro, the Capital District, Miranda, Monagas, Vargas, and Zulia (Figure 2, panel A) (16).

The circulation of measles in Venezuela was preceded by the progressive interruption of the national immunization program since the year 2010, along with the dismantling of the primary healthcare infrastructure. The national coverage rate for the second dose of the measles vaccine was estimated at 52% according to the last reports from the Venezuela Ministry of Health (19,20). This estimate ranks Venezuela toward the bottom of vaccination coverage in the region (20). Current estimates indicate that measles vaccination coverage in the Venezuelan Amazon region has decreased in all municipalities (Alto Orinoco, 40%; Atabapo 18, 6%; Atures 66, 6%; Autana 35, 5%; Manapiare 30, 5%; Maroa 5, 2%; and Rio Negro 41, 7%) (21), notably affecting the Venezuela–Brazil border, where the current measles outbreak threatens to decimate the ancestral aboriginal Yanomami people.

The massive job losses that followed the economic crisis and the dismantling of private industry has meant that most persons in Venezuela have been forced to rely on informal jobs, such as illegal mining. Illegal mining camps, which attract migrant workers from communities throughout Venezuela and from neighboring countries and aboriginal settlements, provide a setting for measles transmission within the camps themselves and for its further spread once the mine workers return to their home communities. Cross-border mobility, migration, and illegal mining activities (21), in which native and indigenous persons are increasingly involved, have been proposed as the probable source of the proliferation of measles in remote areas inhabited by unvaccinated persons (21). Examples of vulnerable aboriginal settlements include those located at the Imataca Forest Reserve; the Paragua, Caura, and Caroní Rivers;

Cerro Guanay Natural Monument; and most important, the Canaima and Cerro Yapakana National Parks (22). Recent reports from the nongovernmental organizations Survival International and Wataniba indicate that  $\approx 100$  cases of measles have occurred among members of the isolated and vulnerable Yanomami populations in the Venezuela–Brazil border region (23). Deaths attributed to measles have already occurred, according to Horonami (a Yanomami nongovernment organization), and high morbidity and mortality rates are expected because these populations are immunologically naive (24,25). Measles is presumed to have entered the Yanomami communities from Brazil after imported cases from Venezuela brought the disease to border populations of Brazil, before spreading back to Yanomami communities in Venezuela (11,25). Further spread of this epidemic wave could devastate the Yanomami people living in the Orinoco highlands of the Amazon, given that humanitarian aid to affected sites is limited or hard to deliver because of the seminomadic characteristics of these indigenous populations and the remoteness of the Yanomami territory.

Other indigenous populations in Venezuela who are particularly vulnerable to the extension of the measles outbreak include the Warao, located in the Orinoco River Delta. During 2018,  $\approx 100$  measles-related deaths occurred among indigenous infants and children in the municipality of Tucupita in the Orinoco River Delta (24). Reports from the municipalities of Pedernales and Antonio Díaz in the same area indicate that the death toll has increased, with 102 additional cases to date (24). Cases have spread rapidly from this region to the neighboring municipality of Barrancas del Orinoco (Venezuela) (25) and to the border state of Roraima (Brazil).

Again, emigration from Venezuela has substantially affected neighboring Brazil and Colombia, as well as other countries in the region, such as Ecuador (26). Measles cases imported from Venezuela have been reported in all 3 nations

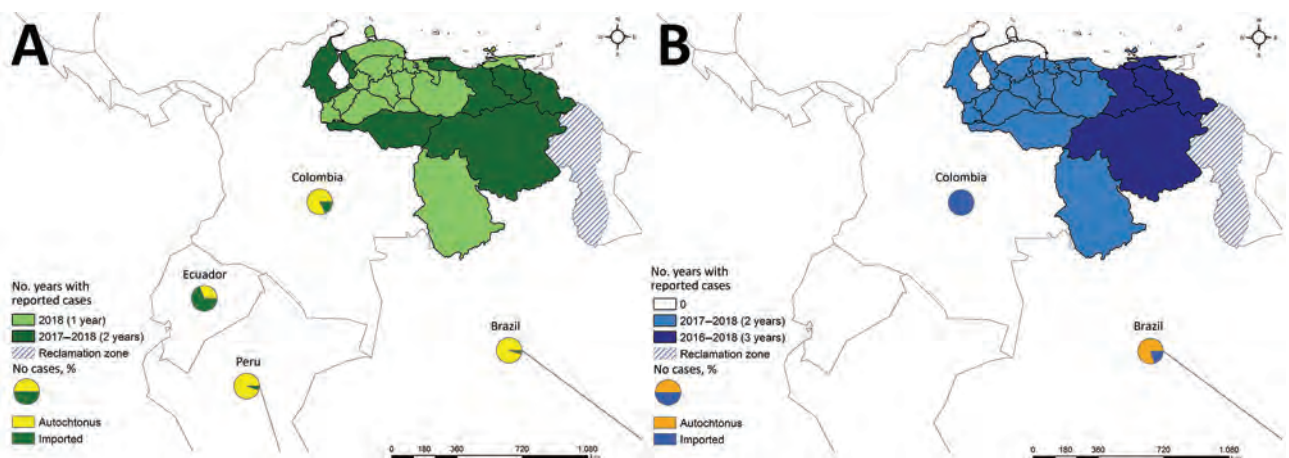


**Figure 2.** States affected by (A) measles and (B) diphtheria, Venezuela, 2017–2018. Circles indicate neighboring countries reporting imported and autochthonous cases of these 2 diseases. Reclamation zone is a territory under dispute between Guyana and Venezuela.

(Figure 1, panels A, B) Thus far, Brazil has reported most of the imported measles cases, mainly from the state of Bolívar in Venezuela), where a major measles outbreak is taking place (27). Not surprisingly, Brazil has the region's second highest measles burden, with 2,801 confirmed cases reported through epidemiologic week 44 of 2018 (Appendix, <https://wwwnc.cdc.gov/EID/article/25/4/18-1305-App1.pdf>) in the neighboring states of Roraima (345 cases) and Amazonas (2,357 confirmed cases and 7,425 suspected cases) (Figure 2, panel A) (10,24). The link to the Venezuela outbreak was established by the isolation and identification of genotype D8 in the first cases of the outbreak in Brazil in February 2018, as confirmed by the Oswaldo Cruz Foundation and unequivocally recognized by PAHO (18,24). In Brazil, the locations principally affected are Boa Vista, Paracaima, Cantá, Rorainópolis, Uramuta, and Manaus (24). These states have received a massive influx of migrants from Venezuela (24). Isolated and import-related cases were also identified in the states of São Paulo (3 cases), Rio Grande do Sul (43 cases), Pará (23 cases), Pernambuco (4 cases), and Rondônia (2 cases), as well as in Rio de Janeiro (19 cases), Sergipe (4 cases), and Distrito Federal (1 case) (24). In addition, the Brazilian Ministry of Health has reported 14 measles deaths through the end of October 2018 in the states of Roraima (4 cases), Amazonas (8 cases), and Pará (2 cases) (24). Of all cases reported by Brazil's Ministry of Health in the state of Roraima through May 2018, a total of 68% corresponded to refugees from Venezuela, and 52.7% were in Warao Amerindians (24). Although Brazil has a free vaccination program with high coverage levels, a recent decrease in polio and measles, mumps, and rubella vaccination rates, linked to local antivaccine movements (28,29) and government underfunding of the healthcare system (30), are worrisome and might worsen the current measles outbreak (28,29).

The Colombia Ministry of Health has also reported 25 measles cases imported from Venezuela (Figure 2, panel A) (16), again confirmed by isolation and molecular identification of genotype D8 in the initial cases (18,31). Most cases were reported from bordering states that received a considerable migratory influx in 2018 and that also had received the most numerous groups comprising the 600,000 immigrants from Venezuela in 2017 (26). Moreover, many residents of Venezuela transit through Colombia to Ecuador, where, by epidemiologic week 44 of 2018, a total of 13 of the 600 suspected cases imported from Venezuela had been confirmed as measles by the Ecuador Ministry of Health (Figure 2, panel A) (8,10). The index case-patient proceeded from Venezuela through the border with Colombia, where  $\approx 286,000$  persons have crossed through the Rumichaca international bridge. As of epidemiologic week 42 of 2018, the Peru Ministry of Health had also reported 2 cases imported from Venezuela (Figure 2, panel A) (16).

The reestablishment of measles transmission because of continuous circulation of either indigenous or imported measles virus for  $\geq 12$  months (32) has threatened the Americas with losing its certification as a measles-free region. On August 24, 2018, PAHO recognized the reestablishment of endemic transmission of measles in Venezuela, thereby suggesting that the Americas was unlikely to remain a certified measles-free region (33,34).

### Diphtheria

Diphtheria, a childhood vaccine-preventable disease, had not been reported in Venezuela during the 24 years before 2016. However, during July–November 2016, a total of 183 suspected diphtheria cases were reported by 16 of the 24 federal entities in Venezuela (Figure 2, panel B) (34), alerting PAHO and WHO to the reappearance of this disease (35). Since 2016, a total of 2,170 cases have been reported to date (324 in 2016, 1,040 in 2017, and 806 cases in 2018 [through October 29]). Of the 2,170 cases, 1,249 were laboratory confirmed; 287 deaths were reported (17 in 2016, 103 in 2017, and 167 in 2018), yielding a case-fatality rate of 22% (34). For 2018, a total of 838 diphtheria cases have been reported in the Americas as of epidemiologic week 41 of 2018 (34). The other 3 countries are Haiti (80 cases), Brazil (6 cases) (36), and Colombia (8 cases). However, 3 of 8 cases in Colombia were imported cases from Venezuela (34).

As in the case of measles, low local vaccination coverage rates have left Venezuela susceptible to the resurgence of diphtheria. By 2016, national coverage with 3 doses of diphtheria-tetanus-pertussis (DTP) vaccine (DTP3) was  $\approx 84\%$ , and reported coverage with 4 doses of DTP barely reached 60% (37). PAHO estimated coverage rates in 2017 of 66% for DTP3 and 38% for 4 doses of DTP (38). Recent unofficial data suggest that for 2018, national DTP3 coverage might not even reach 50% (39), resulting in an important increase in the number of susceptible persons, of whom  $\approx 3$  million are children. Achieving adequate vaccination rates is even more difficult in remote areas, where geographic isolation and ongoing conflicts between armed gangs, guerrilla forces, and military personnel hamper adequate access to rural communities. The southern areas of the Amazon basin, such as Bolívar state, Amazonas state, and the Orinoco River Delta, are particularly at risk because of low pentavalent DTP–*Haemophilus influenzae* type b–hepatitis B vaccination coverage; reported coverage rates are 50% for Bolívar, 37% for Amazonas, and 24% for the Orinoco River Delta, according to data from the Venezuela Ministry of Health (37,40).

Although the first cases of diphtheria in Venezuela were reported in the southern state of Bolívar and were attributed initially to crowding and unhealthy conditions in illegal



mining camps, the disease has spread rapidly throughout the country, reaching epidemic proportions (39). Current data indicate that the number of reported cases likely underestimates the actual magnitude of the outbreak. Reports on the occurrence of diphtheria in isolated Amerindian communities, such as the Pemón and Kariña aboriginal populations, illustrate the geographic reach of the disease.

Diphtheria has now spread to Brazil and Colombia (Figure 2, panel B). In February 2018, PAHO–WHO issued an update on diphtheria in the Americas, highlighting the occurrence of exported cases from Venezuela to Brazil and Colombia (41). In Brazil, a fatal case imported from Venezuela was recorded in the state of Roraima, and in Colombia, another fatal case was reported in the Department of La Guajira (Figure 2, panel B). These cases highlight the vulnerability of the bordering states to the outbreak (41). The lack of infrastructure to receive massive numbers of forced migrants and the associated problems with poor access to essential health and sanitation services are potential facilitators for disease emergence and transmission (41). During epidemiologic week 8 of 2018, PAHO urged health authorities to intensify epidemiologic surveillance, case detection, medical care, and vaccination (39). Since that week, PAHO has confirmed diphtheria cases in Brazil, Colombia, and Venezuela (Figure 2, panel B) (41).

## Polio

In 1971, poliomyelitis became the second vaccine-preventable disease (after smallpox) to be eliminated from the Americas, later followed by measles and rubella (42,43). Venezuela's devastated healthcare infrastructure has halted many of its immunization programs. Estimates indicate that vaccination coverage against polio has dropped below minimum recommended levels (80%); coverage with the third dose of polio vaccine slipped from 87% in 2015 to <79% in 2017 (7), thus establishing the conditions for the potential emergence of vaccine-derived polioviruses (VDPVs). Historically, low vaccination coverage in conflict-affected countries has played an important role in the re-emergence of poliomyelitis because of circulating VDPVs (cVDPVs). Examples include Laos, where an outbreak attributable to cVDPV type 1 cases occurred during 2015–2016; Nigeria and Pakistan, which reported cVDPV type 2 cases throughout 2016; Syria and the Democratic Republic of the Congo, where cVDPV type 2 was present during 2017–2018; and Mogadishu, Somalia (2017) and Kenya (2018), where cVDPV type 2 was isolated from environmental samples (44).

The current reality in Venezuela is a conflux of plummeting vaccination coverages and ongoing outbreaks of other vaccine-preventable diseases. Combined with the weakening of surveillance programs, forced migrations, and a prolonged political, economic, and food crisis without

foreseeable resolution, these factors have set the stage for potential reemergence of poliomyelitis.

## Addressing the Vaccine-Preventable Disease Crisis in Venezuela

During the past decade, crises in Africa and the Middle East have provided numerous examples of the consequences for failure of the control of vaccine-preventable diseases when healthcare delivery is disrupted by political turmoil; these areas have also provided paradigms of successful intervention measures. In Syria, the destruction of healthcare and sanitation infrastructure resulted in the reappearance of polio 15 years after its eradication from that country. At the same time, the number of measles cases expanded to >7,000 confirmed cases nationwide and extended into neighboring countries with higher vaccination coverage (45). Similarly, disruption of immunization programs during the recent political unrest in Yemen led to a measles outbreak with >4,300 cases and a high death rate (46); the number of cases totaled 7,285, according to the most recent data from WHO (47). In both Syria and Yemen, the acknowledgment by WHO of the severity of the crises and assistance marshaling the resources required to mount massive immunization campaigns enabled substantial progress toward containment, although the inability to consistently sustain immunization activities has precluded ideal disease control and the prevention of potential new outbreaks. Subsequently, WHO codified and published an evidence-based approach for vaccination in humanitarian crises that incorporates a framework for decision-making (48). The ongoing diphtheria and measles epidemics in Venezuela and spillover into neighboring countries evoke the reemergence of vaccine-preventable diseases observed in Syria and Yemen and the consequent threat to regional, and potentially global, public health.

The Americas region has been free of wild poliovirus circulation for nearly 3 decades, mainly because of successful immunization programs and vaccination campaigns in high-risk regions. Without doubt, these efforts halted the final chains of transmission and provided strong herd immunity. Similarly, in 2007, Venezuela was able to successfully implement a mass vaccination program that arrested the circulation of measles and ended the 2006 outbreak. Today, however, the crisis in Venezuela has enabled vaccine-preventable diseases such as diphtheria and measles to reemerge (34). The weakening of Venezuela's public health services has led to a breakdown of epidemiologic surveillance systems along with an interruption of the national immunization program, resulting in the decay of infection control practices. In addition, the ongoing massive internal and external exodus of Venezuela residents has become the amplifying factor of these outbreaks beyond Venezuela's borders (8,24,26,29,49).

The Executive Committee of PAHO, at its 162nd session held on June 20, 2018, presented the following document as a point on its agenda: “PAHO Response to Maintain an Effective Agenda for Technical Cooperation in Venezuela and in Neighboring Member States” (49). The document contributes, albeit somewhat late, to addressing the lack of information and to correct misinformation, as well as to refute the government of Venezuela’s official denial of the serious problems afflicting the country. Likewise, the document recognizes the lack of official information but fails to indicate as a priority the resumption of the publication of the Venezuelan Ministry of Health’s Weekly Epidemiologic Bulletins and relevant technical documents from the Venezuela Ministry of Health. We believe that reporting health statistics is an unavoidable obligation of the state to its inhabitants and cannot be substituted by regional and international bulletins or alerts from other countries.

### Recommendations

According to the evaluation approach recommended by WHO, the risk level of the ongoing outbreaks in Venezuela is high. A correspondingly strong response is needed to curtail the expanse of these epidemics. We propose the following measures.

- Global and hemispheric health authorities should urge the Venezuela government to allow the establishment of a humanitarian channel to provide immediate relief efforts addressing extreme food and medicine shortages.
- Epidemiologic surveillance programs, early reporting, and rapid response systems should be restored immediately. Strengthening of infection control practices in healthcare facilities should be implemented with the aid of international agencies while ensuring public health neutrality.
- Emergency relief operations should be put into effect across borders along with authorities in Colombia and Brazil to ameliorate the effects of massive migration by implementation of early nutritional and immunization interventions.
- International agencies should support regional efforts in neighboring countries to promote simultaneous massive vaccination campaigns and vaccination of all refugees from Venezuela arriving in host community populations.
- Adequate supplies for mass vaccination and routine immunization should be ensured, and additional adjunct supplies (e.g., diphtheria antitoxin) should be stockpiled to assist in the establishment of standard treatment protocols and epidemic rapid response measures. These methods are crucial for healthcare delivery and mass vaccination catch-up campaigns to head off the resurgence of vaccine-preventable diseases in Venezuela.

- In areas with low vaccination coverage, improving surveillance for early case detection and increasing vaccination coverage in high-risk age groups should be mandatory. Furthermore, Venezuela is in urgent need to reconstruct its devastated healthcare system, secure sustainable food and medication access, and reinstall proper sanitation policies to reduce the burden of diseases.

On September 27, 2018, the United Nations Human Rights Council adopted a resolution on Venezuela signaling the gravity of the human rights situation and the growing concern by governments worldwide about the country’s humanitarian crisis, including aspects such as malnutrition and the upsurge of preventable diseases (50). PAHO–WHO faces an enormous challenge in attending, without interference, to the complex emergency that affects Venezuela. Emergency funds must be released to acquire medicines, vaccines, laboratory reagents, and other supplies for health programs. As Venezuela rapidly becomes a regional nidus for the emergence of vaccine-preventable diseases, it must take decisive action now alongside regional and national partners to target this emerging regional crisis.

### About the Author

Dr. Paniz-Mondolfi is an infectious diseases pathologist and clinician at the IDB Biomedical Research Institute in Barquisimeto, Venezuela; the Venezuelan Science Incubator; and the Laboratory of Cell Signaling and Parasite Biochemistry (IDEA). His research focuses on emerging pathogens, zoonoses, and epidemic preparedness.

### References

1. Ellsworth B. IMF projects Venezuela inflation will hit 1,000,000 percent in 2018. 2018 Jul 23 [cited 2019 Jan 19]. <https://www.reuters.com/article/us-venezuela-economy/imf-projects-venezuela-inflation-will-hit-1000000-percent-in-2018-idUSKBN1KD2L9>
2. The Lancet. The collapse of the Venezuelan health system. *Lancet*. 2018;391:1331. [http://dx.doi.org/10.1016/S0140-6736\(16\)00277-4](http://dx.doi.org/10.1016/S0140-6736(16)00277-4)
3. ACI Prensa. Children face hunger crisis in Venezuela as malnutrition soars [in Spanish]. 2017 Oct 27 [cited 2018 Aug 31]. <https://www.aciprensa.com/noticias/caritas-venezuela-alerta-que-unos-280-mil-ninos-moririan-a-causa-de-la-desnutricion-51800>
4. Requena J. Economy crisis: Venezuela’s brain drain is accelerating. *Nature*. 2016;536:396. <http://dx.doi.org/10.1038/536396d>
5. Hotez PJ, Basañez MG, Acosta-Serrano A, Grillet ME. Venezuela and its rising vector-borne neglected diseases. *PLoS Negl Trop Dis*. 2017;11:e0005423. <http://dx.doi.org/10.1371/journal.pntd.0005423>
6. Rodríguez-Morales AJ, Paniz-Mondolfi AE. Venezuela’s failure in malaria control. *Lancet*. 2014;384:663–4. [http://dx.doi.org/10.1016/S0140-6736\(14\)61389-1](http://dx.doi.org/10.1016/S0140-6736(14)61389-1)
7. Pan American Health Organization/World Health Organization. Coverage by vaccine: polio3, 2017 [cited 2019 Jan 19]. [http://ais.paho.org/imm/IM\\_JRF\\_COVERAGE.asp](http://ais.paho.org/imm/IM_JRF_COVERAGE.asp)
8. Nebehay S. Malaria on rise in crisis-hit Venezuela, WHO says. 2018 Apr 24 [cited 2018 Aug 15]. <https://www.reuters.com/article/us-health-malaria-venezuela/malaria-on-rise-in-crisis-hit-venezuela-who-says-idUSKBN1HV1ON>



9. Pan American Health Organization/World Health Organization. Measles in the Americas: new epidemiological update. 2018 Jul 20 [cited 2018 Aug 5]. [https://www.paho.org/hq/index.php?option=com\\_content&view=article&id=14515%3Ameasles-in-the-americas-new-epidemiological-update&catid=1443%3Aweb-bulletins&Itemid=135&lang=en](https://www.paho.org/hq/index.php?option=com_content&view=article&id=14515%3Ameasles-in-the-americas-new-epidemiological-update&catid=1443%3Aweb-bulletins&Itemid=135&lang=en)
10. Pan American Health Organization/World Health Organization. Weekly bulletin of measles/rubella. Vol. 24, No. 44 [in Spanish]. 2018 Nov 3 [cited 2018 Nov 13]. [https://www.paho.org/hq/index.php?option=com\\_docman&view=download&category\\_slug=boletin-semanal-s-r-2018-9576&alias=46975-boletin-semanal-de-sarampion-rubeola-44-3-de-noviembre-del-2018&Itemid=270&lang=es](https://www.paho.org/hq/index.php?option=com_docman&view=download&category_slug=boletin-semanal-s-r-2018-9576&alias=46975-boletin-semanal-de-sarampion-rubeola-44-3-de-noviembre-del-2018&Itemid=270&lang=es)
11. United States Agency for International Development. Venezuela regional crisis. 2018 Sep 11 [cited 2018 Nov 9]. [https://www.usaid.gov/sites/default/files/documents/1866/venezuela\\_cr\\_fs05\\_09-11-2018.pdf](https://www.usaid.gov/sites/default/files/documents/1866/venezuela_cr_fs05_09-11-2018.pdf)
12. Colombia M. 442,462 Venezuelans identified in the RAMV registry will receive temporary regularization [in Spanish]. 2018 Jun 13 [cited 2018 Jul 27]. <http://www.migracioncolombia.gov.co/index.php/es/prensa/comunicados/comunicados-2018/junio-2018/7584-442-462-venezolanos-identificados-en-registro-ramv-recibiran-regularizacion-temporal>
13. United Nations High Commissioner for Refugees. Response stepped up in Brazil as Venezuelan arrivals grow. 2018 Apr 6 [cited 2018 Aug 9]. <http://www.unhcr.org/news/briefing/2018/4/5ac72f194/response-stepped-brazil-venezuelan-arrivals-grow.html>
14. United Nations High Commissioner for Refugees. Venezuela situation: responding to the needs of people displaced from Venezuela. Supplementary appeal, January–December 2018. 2018 Mar [cited 2018 Jul 31]. <http://www.unhcr.org/partners/donors/5ab8e1a17/unhcr-2018-venezuela-situation-supplementary-appeal-january-december-2018.html>
15. Sarmiento H, Cobo OB, Morice A, Zapata R, Benitez MV, Castillo-Solórzano C. Measles outbreak in Venezuela: a new challenge to postelimination surveillance and control? *J Infect Dis*. 2011;204(Suppl 2):S675–82. <http://dx.doi.org/10.1093/infdis/jir444>
16. Pan American Health Organization/World Health Organization. Epidemiological update—measles, 24 October 2018. 2018 Oct 24 [cited 2018 Nov 13]. [https://www.paho.org/hq/index.php?option=com\\_docman&view=download&category\\_slug=measles-2204&alias=46783-24-october-2018-measles-epidemiological-update&Itemid=270&lang=en](https://www.paho.org/hq/index.php?option=com_docman&view=download&category_slug=measles-2204&alias=46783-24-october-2018-measles-epidemiological-update&Itemid=270&lang=en)
17. Heywood AE, Gidding HF, Riddell MA, McIntyre PB, MacIntyre CR, Kelly HA. Elimination of endemic measles transmission in Australia. *Bull World Health Organ*. 2009;87:64–71. <http://dx.doi.org/10.2471/BLT.07.046375>
18. Pan American Health Organization/World Health Organization. Epidemiological update—measles, 9 March 2018. 2018 Mar 9 [cited 2018 Aug 15]. [https://www.paho.org/hq/index.php?option=com\\_docman&task=doc\\_view&gid=44007&Itemid=270&lang=en](https://www.paho.org/hq/index.php?option=com_docman&task=doc_view&gid=44007&Itemid=270&lang=en)
19. Pan American Health Organization/World Health Organization. Coverage by vaccine: DTP3. 2017 [cited 2018 Jul 31]. [http://ais.paho.org/imm/IM\\_JRF\\_COVERAGE.asp](http://ais.paho.org/imm/IM_JRF_COVERAGE.asp)
20. Pan American Health Organization/World Health Organization. Vaccination coverage—percentage for countries and territories of the Americas [cited 2018 Oct 31]. <http://www.paho.org/data/index.php/es/temas/inmunizaciones/297-cobertura-vacunacion-por-pais.html>
21. Wataniba Organization. Communiqué from Horonami Yanomami Organization about outbreak of measles in communities of Alto Ocamo (Amazonas) [in Spanish]. 2018 Jul 11 [cited 2018 Aug 9]. [https://www.wataniba.org/wp-content/uploads/2018/07/Comunicado\\_HOY\\_Julio\\_2018.pdf](https://www.wataniba.org/wp-content/uploads/2018/07/Comunicado_HOY_Julio_2018.pdf)
22. Francisco O. Arco Minero y ambiente. *Diario El Universal*. 2016 [cited 2018 Aug 3]. <http://verdadesyrumores.com/index.php/2016/04/03/crisisarco-minero-y-el-ambiente>
23. Servicios de Comunicación Intercultural. Yanomami people threatened by measles outbreak [in Spanish]. 2018 June 29 [cited 2019 Jan 25]. <https://www.servindi.org/29/06/2018/pueblo-yanomami-amenazado-por-brote-de-sarampion>
24. Ministry of Health of Brazil. Ministry of Health updates measles cases [in Portuguese]. 2018 Nov 7 [cited 2018 Nov 18]. <http://portalms.saude.gov.br/noticias/agencia-saude/44613-ministerio-da-saude-actualiza-casos-de-sarampo-14>
25. Venezuelan Alliance for Health. Fourteenth measles alert: the measles epidemic impacts the vulnerable population from the state of Amacuro Delta [in Spanish]. 2018 May 14 [cited 2018 Aug 15]. <http://alianzasalud.org/2-de-abril-de-2018>
26. International Organization for Migration. Migration trends in the Americas: Bolivarian Republic of Venezuela. 2018 Apr [cited 2018 Jul 31]. [http://robuensaires.iom.int/sites/default/files/Informes/National\\_Migration\\_Trends\\_Venezuela\\_in\\_the\\_Americas.pdf](http://robuensaires.iom.int/sites/default/files/Informes/National_Migration_Trends_Venezuela_in_the_Americas.pdf)
27. Pan American Health Organization/World Health Organization. Epidemiological update—measles, 6 April 2018. 2018 Apr 6 [cited 2018 Aug 13]. [https://www.paho.org/hq/index.php?option=com\\_docman&task=doc\\_view&Itemid=270&gid=44328&lang=en](https://www.paho.org/hq/index.php?option=com_docman&task=doc_view&Itemid=270&gid=44328&lang=en)
28. Cambricoli F, Palhares I. Groups against vaccination advance in the country and concern the Ministry of Health [in Portuguese]. 2017 May 21 [cited 2018 Aug 15]. <https://saude.estadao.com.br/noticias/geral,grupos-contrarios-a-vacinacao-avancam-no-pais-e-preocupam-ministerio-da-saude,70001800099>
29. Fraser B. Measles outbreak in the Americas. *Lancet*. 2018;392:373. [http://dx.doi.org/10.1016/S0140-6736\(18\)31727-6](http://dx.doi.org/10.1016/S0140-6736(18)31727-6)
30. Doniec K, Dall'Alba R, King L. Brazil's health catastrophe in the making. *Lancet*. 2018;392:731–2. [http://dx.doi.org/10.1016/S0140-6736\(18\)30853-5](http://dx.doi.org/10.1016/S0140-6736(18)30853-5)
31. Succi RCM. Vaccine refusal—what we need to know. *J Pediatr (Rio J)*. 2018;94:574–81.
32. Katz SL, Hinman AR. Summary and conclusions: measles elimination meeting, 16–17 March 2000. *J Infect Dis*. 2004;189(Suppl 1):S43–7. <http://dx.doi.org/10.1086/377696>
33. Pan American Health Organization/World Health Organization. PAHO urges rapid increase in vaccination coverage to stop spread of measles in the Americas. 2018 Aug 24 [cited 2018 Nov 16]. [https://www.paho.org/hq/index.php?option=com\\_content&view=article&id=14582:paho-urges-rapid-increase-in-vaccination-coverage-to-stop-spread-of-measles-in-the-americas&Itemid=1926&lang=pt](https://www.paho.org/hq/index.php?option=com_content&view=article&id=14582:paho-urges-rapid-increase-in-vaccination-coverage-to-stop-spread-of-measles-in-the-americas&Itemid=1926&lang=pt)
34. Pan American Health Organization/World Health Organization. Epidemiological update—diphtheria, October 29, 2018 [in Spanish]. 2018 Oct 29 [cited 2018 Nov 9]. [https://www.paho.org/hq/index.php?option=com\\_docman&view=download&category\\_slug=difteria-8969&alias=46883-29-de-octubre-de-2018-difteria-actualizacion-epidemiologica&Itemid=270&lang=es](https://www.paho.org/hq/index.php?option=com_docman&view=download&category_slug=difteria-8969&alias=46883-29-de-octubre-de-2018-difteria-actualizacion-epidemiologica&Itemid=270&lang=es)
35. Iris College of General Practitioners. IHR alert: extensive outbreak of diphtheria in Venezuela. 2016 Dec 6 [cited 2018 Aug 13]. [https://www.icgp.ie/go/library/public\\_health\\_alerts/4745104B-0F5C-F480-148C74944F931F3D.html](https://www.icgp.ie/go/library/public_health_alerts/4745104B-0F5C-F480-148C74944F931F3D.html)
36. Pan American Health Organization/World Health Organization. Epidemiological update—diphtheria, April 16, 2018 [in Spanish]. 2018 Apr 16 [cited 2018 Dec 28]. [https://www.paho.org/hq/index.php?option=com\\_docman&view=download&category\\_slug=difteria-8969&alias=44499-16-abril-2018-difteria-actualizacion-epidemiologica-499&Itemid=270&lang=en](https://www.paho.org/hq/index.php?option=com_docman&view=download&category_slug=difteria-8969&alias=44499-16-abril-2018-difteria-actualizacion-epidemiologica-499&Itemid=270&lang=en)
37. Pan American Health Organization/World Health Organization. Immunization: country profiles [cited 2018 July 31]. [https://www.paho.org/hq/index.php?option=com\\_content&view=article&id=2577&Itemid=2065&lang=en](https://www.paho.org/hq/index.php?option=com_content&view=article&id=2577&Itemid=2065&lang=en)
38. Franquis B. 2.9 million children are left out of the Vaccination Plan [in Spanish]. 2018 Apr 30 [cited 2018 Aug 9]. [http://www.el-nacional.com/noticias/salud/millones-ninos-quedan-fuera-del-plan-vacunacion\\_233023](http://www.el-nacional.com/noticias/salud/millones-ninos-quedan-fuera-del-plan-vacunacion_233023)

39. Lodeiro-Colatosti A, Reischl U, Holzmann T, Hernández-Pereira CE, Rísquez A, Paniz-Mondolfi AE. Diphtheria outbreak in Amerindian communities, Wonken, Venezuela, 2016–2017. *Emerg Infect Dis*. 2018;24:1340–4. <http://dx.doi.org/10.3201/eid2407.171712>
40. Venezuelan Society of Public Health. Circular no. 0202 VRSC-DGE 11-10-2016: epidemiologic alert for diphtheria [in Spanish]. 2016 Oct 18 [cited 2018 Dec 28]. <https://www.derechos.org.ve/web/wp-content/uploads/Alerta-N-4-de-la-Red-Defendamos-la-Epidemiologia-Nacional-sobre-Difteria.pdf>
41. Pan American Health Organization/World Health Organization. Epidemiological update—diphtheria, February 28, 2018 [in Spanish]. 2018 Feb 28 [cited 2018 Jul 31]. [https://www.paho.org/ven/index.php?option=com\\_docman&view=document&slug=28-de-febrero-de-2018-difteria-actualizacion-epidemiologica&layout=default&alias=125-28-de-febrero-de-2018-difteria-actualizacion-epidemiologica&category\\_slug=documentos-estrategicos&Itemid=466](https://www.paho.org/ven/index.php?option=com_docman&view=document&slug=28-de-febrero-de-2018-difteria-actualizacion-epidemiologica&layout=default&alias=125-28-de-febrero-de-2018-difteria-actualizacion-epidemiologica&category_slug=documentos-estrategicos&Itemid=466)
42. Pan American Health Organization/World Health Organization. Laboratory tests rule out the presence of wild and vaccine-derived poliovirus in the case of acute flaccid paralysis in Venezuela [cited 2018 Jun 15]. [https://www.paho.org/hq/index.php?option=com\\_content&view=article&id=14445%3ALaboratory-tests-rule-out-the-presence-of-wild-and-vaccine-derived-poliovirus-in-the-case-of-acute-flaccid-paralysis-in-venezuela-&catid=740%3Apress-releases&Itemid=1926&lang=en](https://www.paho.org/hq/index.php?option=com_content&view=article&id=14445%3ALaboratory-tests-rule-out-the-presence-of-wild-and-vaccine-derived-poliovirus-in-the-case-of-acute-flaccid-paralysis-in-venezuela-&catid=740%3Apress-releases&Itemid=1926&lang=en)
43. Pan American Health Organization/World Health Organization. Americas region is declared the world's first to eliminate rubella [in Spanish]. 2015 Apr 29 [cited 2018 Nov 13]. [https://www.paho.org/hq/index.php?option=com\\_content&view=article&id=10798:2015-americas-free-of-rubella&Itemid=1926&lang=es](https://www.paho.org/hq/index.php?option=com_content&view=article&id=10798:2015-americas-free-of-rubella&Itemid=1926&lang=es)
44. Khan F, Datta SD, Quddus A, Vertefeuille JF, Burns CC, Jorba J, et al. Progress toward polio eradication—worldwide, January 2016–March 2018. *MMWR Morb Mortal Wkly Rep*. 2018;67:524–8. <http://dx.doi.org/10.15585/mmwr.mm6718a4>
45. Sharara SL, Kanj SS. War and infectious diseases: challenges of the Syrian civil war. *PLoS Pathog*. 2014;10:e1004438. <http://dx.doi.org/10.1371/journal.ppat.1004438>
46. El Bcheraoui C, Jumaan AO, Collison ML, Daoud F, Mokdad AH. Health in Yemen: losing ground in war time. *Global Health*. 2018;14:42. <http://dx.doi.org/10.1186/s12992-018-0354-9>
47. World Health Organization. Immunization, vaccines and biologicals: measles and rubella surveillance data, 2018. 2018 [cited 2018 Nov 17]. [http://www.who.int/immunization/monitoring\\_surveillance/burden/vpd/surveillance\\_type/Country\\_slides\\_measles.pdf?ua=1](http://www.who.int/immunization/monitoring_surveillance/burden/vpd/surveillance_type/Country_slides_measles.pdf?ua=1)
48. World Health Organization. Vaccination in acute humanitarian emergencies: a framework for decision making. 2017 May [cited 2018 Aug 15]. [http://www.who.int/immunization/documents/who\\_ivb\\_17.03/en](http://www.who.int/immunization/documents/who_ivb_17.03/en)
49. Pan American Health Organization/World Health Organization. PAHO Executive Committee concludes its 162nd session on advancing health in the Americas region. 2018 Jun 22 [cited 2018 Aug 15]. [https://www.paho.org/hq/index.php?option=com\\_content&view=article&id=14472%3Apano-executive-committee-concludes-its-162nd-session-on-advancing-health-in-the-americas-region&catid=740%3Apress-releases&Itemid=1926&lang=en](https://www.paho.org/hq/index.php?option=com_content&view=article&id=14472%3Apano-executive-committee-concludes-its-162nd-session-on-advancing-health-in-the-americas-region&catid=740%3Apress-releases&Itemid=1926&lang=en)
50. Human Rights Watch. Venezuela: landmark UN Rights Council Resolution. 2018 Sep 27 [cited 2018 Sep 29]. <https://www.hrw.org/news/2018/09/27/venezuela-landmark-un-rights-council-resolution>

Address for correspondence: Alberto E. Paniz-Mondolfi, Clínica IDB Cabudare, Instituto de Investigaciones Biomédicas IDB, Department of Tropical Medicine and Infectious Diseases, Av Intercomunal Barquisimeto-Cabudare, Urb Los Rastrojos, Cabudare Estado Lara 3023, Venezuela; email: [albertopaniz@yahoo.com](mailto:albertopaniz@yahoo.com)

## EID Podcast: The Past Is Never Dead— Measles Epidemic, Boston, Massachusetts, 1713

When we consider modern measles prevention, it is worth recalling what epidemics were like before vaccines and organized public health systems. One vivid account of measles describes the disease's deadly spread through a prominent Boston household more than 300 years ago. In 1713, America's first important medical figure, Puritan minister Cotton Mather (1663–1728), called by one authority “the Dr. Spock of the colonial New England,” wrote about a measles epidemic in the American colonies, describing not only its epidemiology and devastation but also the fear it elicited. Mather's account reminds us of the need for such modern medical and public health tools as vaccination, patient isolation, and prevention policies in saving families from the once-unpreventable diseases that compelled us to develop effective medical advances in the first place.



Visit our website to listen:

<http://www2c.cdc.gov/podcasts/player.asp?f=8638047>

# EMERGING INFECTIOUS DISEASES



# Clinical Manifestations and Molecular Diagnosis of Scrub Typhus and Murine Typhus, Vietnam, 2015–2017

Nguyen Vu Trung, Le Thi Hoi, Vu Minh Dien, Dang Thi Huong, Tran Mai Hoa, Vu Ngoc Lien, Phan Van Luan, Sonia Odette Lewycka, Marc Choisy, Juliet E. Bryant, Behzad Nadjm, H. Rogier van Doorn, Allen L. Richards, Nguyen Van Kinh

## Medscape EDUCATION ACTIVITY

In support of improving patient care, this activity has been planned and implemented by Medscape, LLC and Emerging Infectious Diseases. Medscape, LLC is jointly accredited by the Accreditation Council for Continuing Medical Education (ACCME), the Accreditation Council for Pharmacy Education (ACPE), and the American Nurses Credentialing Center (ANCC), to provide continuing education for the healthcare team.

Medscape, LLC designates this Journal-based CME activity for a maximum of 1.00 **AMA PRA Category 1 Credit(s)**<sup>™</sup>. Physicians should claim only the credit commensurate with the extent of their participation in the activity.

Successful completion of this CME activity, which includes participation in the evaluation component, enables the participant to earn up to 1.0 MOC points in the American Board of Internal Medicine's (ABIM) Maintenance of Certification (MOC) program. Participants will earn MOC points equivalent to the amount of CME credits claimed for the activity. It is the CME activity provider's responsibility to submit participant completion information to ACCME for the purpose of granting ABIM MOC credit.

All other clinicians completing this activity will be issued a certificate of participation. To participate in this journal CME activity: (1) review the learning objectives and author disclosures; (2) study the education content; (3) take the post-test with a 75% minimum passing score and complete the evaluation at <http://www.medscape.org/journal/eid>; and (4) view/print certificate. For CME questions, see page 848.

**Release date: March 18, 2019; Expiration date: March 18, 2020**

### Learning Objectives

Upon completion of this activity, participants will be able to:

- Describe the epidemiological features of scrub typhus and murine typhus in northern Vietnam, according to a prospective, hospital-based study at 2 national referral hospitals in Hanoi
- Determine the clinical characteristics of scrub typhus and murine typhus in northern Vietnam, according to a prospective, hospital-based study at 2 national referral hospitals in Hanoi
- Explain laboratory findings of scrub typhus and murine typhus in northern Vietnam, according to a prospective, hospital-based study at 2 national referral hospitals in Hanoi

### CME Editor

**Amy J. Guinn, BA, MA**, Copyeditor, Emerging Infectious Diseases. *Disclosure: Amy J. Guinn, BA, MA, has disclosed no relevant financial relationships.*

### CME Author

**Laurie Barclay, MD**, freelance writer and reviewer, Medscape, LLC. *Disclosure: Laurie Barclay, MD, has disclosed no relevant financial relationships.*

### Authors

*Disclosures: Nguyen Vu Trung, PhD; Le Thi Hoi, PhD; Vu Minh Dien, MD; Dang Thi Huong, MD; Tran Mai Hoa, BS; Vu Ngoc Lien, BS; Phan Van Luan, MSc; Sonia Odette Lewycka, PhD; Marc Choisy, PhD; Juliet E. Bryant, PhD; Behzad Nadjm, MBChB, MD; Allen L. Richards, PhD; and Nguyen Van Kinh, MD, PhD, have disclosed no relevant financial relationships. H. Rogier van Doorn, MD, PhD, has disclosed the following relevant financial relationships: received grants for clinical research from Pfizer Independent Grants for Learning & Change.*

Author affiliations: National Hospital for Tropical Diseases, Hanoi, Vietnam (N.V. Trung, L.T. Hoi, V.M. Dien, D.T. Huong, T.M. Hoa, V.N. Lien, N.V. Kinh); Hanoi Medical University, Hanoi (N.V. Trung, L.T. Hoi, P.V. Luan, N.V. Kinh); Oxford University Clinical Research Unit and Wellcome Trust Major Overseas Programme, Hanoi (S.O. Lewycka, M. Choisy, J.E. Bryant, B. Nadjm, H.R. van Doorn); University of Oxford, UK (S.O. Lewycka,

B. Nadjm, H.R. van Doorn); Institute of Research for Development, Marseille, France (M. Choisy); Merieux Foundation, Lyon, France (J.E. Bryant); Naval Medical Research Center, Silver Spring, Maryland, USA (A.L. Richards); Uniformed Services University of the Health Sciences, Bethesda, Maryland, USA (A.L. Richards)

DOI: <https://doi.org/10.3201/eid2504.180691>

Rickettsioses are endemic to Vietnam; however, only a limited number of clinical studies have been performed on these vectorborne bacteria. We conducted a prospective hospital-based study at 2 national referral hospitals in Hanoi to describe the clinical characteristics of scrub typhus and murine typhus in northern Vietnam and to assess the diagnostic applicability of quantitative real-time PCR assays to diagnose rickettsial diseases. We enrolled 302 patients with acute undifferentiated fever and clinically suspected rickettsiosis during March 2015–March 2017. We used a standardized case report form to collect clinical information and laboratory results at the time of admission and during treatment. We confirmed scrub typhus in 103 (34.1%) patients and murine typhus in 12 (3.3%) patients. These results highlight the need for increased emphasis on training for healthcare providers for earlier recognition, prevention, and treatment of rickettsial diseases in Vietnam.

Rickettsioses are vectorborne infections caused by small, gram-negative, obligatory intracellular bacteria of the genera *Rickettsia* and *Orientia*, belonging to the family *Rickettsiaceae*. The most common vectors for *Rickettsiaceae* are fleas, mites, ticks, and lice. The pathogens are classified into 3 groups on the basis of clinical characteristics of disease and antigenicity: scrub typhus group orientiae (STGO), spotted fever group rickettsiae (SFGR), and typhus group rickettsiae (TGR) (1–3). The presence and distribution of *Rickettsia* and *Orientia* spp. agents in Southeast Asia are poorly defined (4–6). Additional surveillance studies are needed to improve diagnosis and patient treatment.

The extent and severity of disease associated with scrub and murine typhus in Vietnam is unknown because both clinical- and laboratory-based diagnostics are limited and no systematic surveillance programs or reporting systems are in place (7). Frequent cases of scrub typhus and murine typhus were reported among US military personnel stationed in Vietnam during the 1970s (6–8). Cases also have been identified among returning travelers from the region (9,10). One recent study demonstrated that patients with acute undifferentiated fever admitted to a large referral hospital in Hanoi were often infected with scrub typhus (40.9%) and murine typhus (33.3%) (11). A previous study in the same hospital showed that scrub typhus accounted for 3.5% (251/7,226) of all admissions and 33.5% (251/749) of clinical admissions that met the clinical criteria for testing to the infectious diseases department (12). Another clinical study conducted in central Vietnam reported the use of eschar swabbing for molecular diagnosis and genotyping of *O. tsutsugamushi*, which appeared helpful for rapid case detection in the early stage of infection (13). Together, these findings strongly suggest that rickettsioses are common causes of acute fever in Vietnam that are often underdiagnosed and undertreated.

We conducted a prospective hospital-based study of clinically suspected rickettsiosis in the National Hospital for Tropical Diseases (NHTD) and Bach Mai Hospital, 2 large tertiary-care referral hospitals in Hanoi, during 2015–2017. We describe the clinical characteristics of the cases and the assessment of molecular testing results for diagnosing scrub typhus and murine typhus.

## Methods

### Study Design

We conducted a prospective observational study of clinically suspected rickettsioses at NHTD and Bach Mai Hospital. We included patients  $\geq 15$  years of age with fever (temperature  $>37.5^{\circ}\text{C}$ ) of unknown cause or presence of  $\geq 1$  eschar and  $\geq 1$  of the following clinical symptoms: rash, headache, myalgia, lymphadenopathy, hepatomegaly, or splenomegaly. We excluded patients with laboratory-confirmed malaria, dengue, measles, or influenza (via blood smear or rapid tests); patients with clinically and radiologically confirmed pneumonia; and patients with microbiologically confirmed sepsis or urinary tract infection.

We recorded information regarding patient demographics, medical history, clinical and laboratory findings, and treatment in a case record form. We classified outcome at discharge as full recovery, death, or palliative discharge. Palliative discharge is a commonly preferred alternative to dying in the hospital in Vietnam, where a patient for whom ongoing care is considered futile is discharged to permit them to die in their home with their family.

### Ethics Statement

We obtained written informed consent from patients  $\geq 18$  years of age and from patients and their parents or guardians for those 15–17 years of age enrolled at admission. The study protocol was approved by the institutional review boards of NHTD (document no. 01A/HDDD-NDTU) and Bach Mai Hospital (document no. 6/BM-HDDD).

### Specimen Collection and Laboratory Testing

Blood was drawn from all patients at admission for blood culture and basic laboratory tests. These tests included complete blood counts, biochemistry, procalcitonin, and serologic and molecular testing for rickettsioses.

### Serologic Analysis

We screened serum samples at 1:100 dilution and considered net optical density of  $>0.5$  positive, as described (14,15). ELISA antigen preparations were derived from *R. typhi* Wilmington for TGR-specific IgG, *R. conorii* Malish 7 for SFGR-specific IgG, and *O. tsutsugamushi* Karp, Kato, and Gilliam for the detection of STGO-specific IgG.



### Quantitative Real-Time PCR

We collected whole blood in EDTA tubes, then processed it with Ficoll-Paque to obtain leukocyte buffy coats. We extracted DNA from the buffy coats using QIAamp DNA Mini Kits (QIAGEN, <https://www.qiagen.com>) according to the manufacturer's instructions and previously described assays (16–19). Diagnosis of scrub typhus was based on species-specific quantitative real-time PCRs (qPCRs) targeting the corresponding 47-kDa outer membrane protein gene of *O. tsutsugamushi* (Otsu47) and murine typhus was diagnosed based on the outer membrane protein B gene of *Rickettsia typhi* (Rtyph). When both species-specific assays were negative but the genus-specific qPCR assay targeting the 17-kDa antigen gene (Rick17b) was positive, we classified the diagnoses as nonscrub typhus–nonmurine typhus rickettsiosis. We initially tested all buffy coat samples in this study with the Otsu47 qPCR assay to detect *O. tsutsugamushi*. We subsequently assessed Otsu47-negative samples with the genus-specific qPCR assay Rick17b to detect *Rickettsia* spp. We subsequently tested Rick17b-positive samples with the Rtyph qPCR. For each qPCR, we extracted 1  $\mu$ L of nucleic acid from the buffy coats and added it to a final reaction volume of 25  $\mu$ L, using Platinum Quantitative PCR SuperMix-UDG (Invitrogen, <https://www.thermofisher.com>), and performed real-time PCR on an Applied Biosystems 7500 Fast Real-Time PCR System (Applied Biosystems, <https://www.appliedbiosystems.com>).

### Statistical Analysis

We summarized categorical variables as frequencies and percentages and used the Fisher exact test to compare clinical characteristics among different groups. We summarized

non–normally distributed continuous variables as medians with interquartile ranges (IQRs) and compared them using the Mann-Whitney test. We summarized data following normal distribution as means with SDs and compared them using the analysis of variance test for 2-group comparisons. To investigate whether cases from outside the province of Hanoi were biased toward higher severity, we tested the differences in symptoms between Hanoi and the other provinces using the Fisher exact test, with Benjamini and Hochberg correction for multiple comparisons (20). We performed analyses using Stata 12.0 (StataCorp LLC, <https://www.stata.com>).

## Results

### Patient Population and Enrollment

We enrolled 310 persons with suspected rickettsiosis cases during March 2015–March 2017. Eight cases were excluded because diagnostic assays showed positive results for other infections (Figure 1). The median age of the final study population ( $n = 302$ ) was 50 years (IQR 36–60); 158 (52.3%) were men and 144 (47.7%) women. The 302 patients originated from 28 northern provinces. The largest proportion came from the provinces of Hanoi (122, 40.4%), Phu Tho (28, 9.3%), and Hung Yen (17, 5.6%) (Figure 2). Ninety-seven (32.1%) patients were admitted directly from the community to the study hospitals and 205 (67.9%) were referred from other hospitals. Of the 205 transferred patients, 134 (65.4%) were from hospitals outside Hanoi (Table 1). Symptoms did not differ between those admitted in Hanoi and those transferred from other provinces (Table 2).

Of the 302 patients, 171 (56.6%) reported living in rural areas; 127 (42.1%) also reported that they were farmers. During the study, 224 (74.2%) patients were admitted to the hospital in the summer (April–August), with the highest number (61, 20.2%) in the month of May (Figure 3). The median delay in the time from onset of symptoms to treatment was 9 days (range 6–11 days). Eight patients were admitted to the study  $\geq 30$  days after onset of symptoms, 1 of whom was admitted 41 days after symptoms began; all 8 were successfully treated. Furthermore, 83 (27.5%) patients reported use of antimicrobial drugs before initial admission to the hospital, although the identity of these drugs was not given.

We assessed admission serum samples for IgG against STGO, TGR, and SFGR using ELISAs in a subset of 121 of the 302 enrolled patients. Of these, 6 (5.0%) were ELISA positive for STGO IgG, 2 (1.7%) were positive for TGR IgG, and 1 (0.8%) was positive for SFGR IgG. One serum sample was positive for IgG in TGR and SFGR ELISAs. For 6 samples positive by STGO ELISA, 4 also were positive for *O. tsutsugamushi* by Otsu47 qPCR, whereas 20 Otsu47-positive samples were STGO ELISA negative.

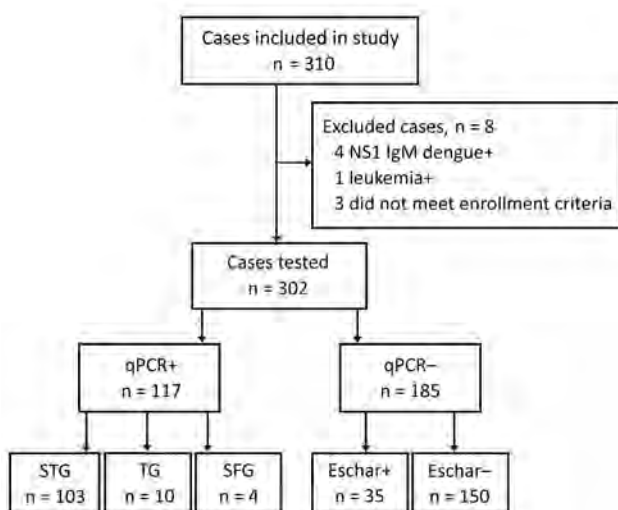


**Figure 1.** Enrollment flow, qPCR results, and presence of eschar among enrollees in study of rickettsial patients, Vietnam, March 2015–March 2017. NS1, nonstructural protein 1; qPCR, quantitative PCR; SFG, scrub typhus group; SFG, spotted fever group; STG, scrub typhus group; +, positive; –, negative.

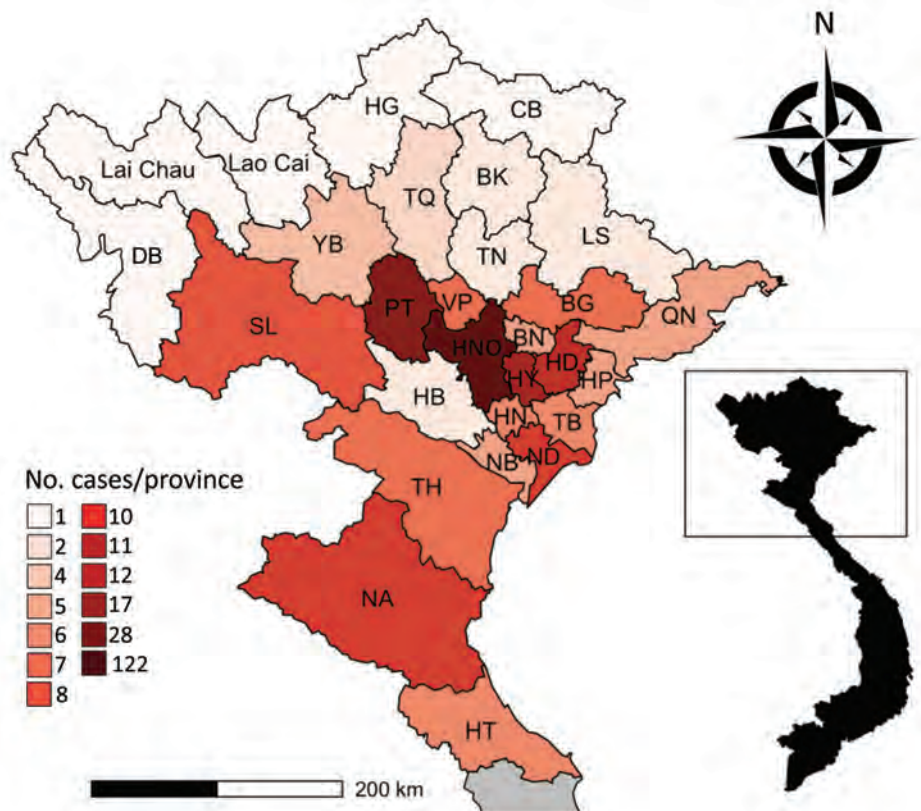


**Figure 2.** Distribution of 302 rickettsial patients, by province, in northern Vietnam, March 2015–March 2017. A) Provinces of northern Vietnam; inset shows location within Vietnam. B) Number of cases by province. BG, Bac Giang; BK, Bac Kan; BN, Bac Ninh; CB, Cao Bang; DB, Dien Bien; HG, Ha Giang; HB, Hoa Binh; HD, Hai Duong; HN, Ha Nam; HP, Hai Phong; HT, Ha Tinh; HY, Hung Yen; LS, Lang Son; NA, Nghe An; NB, Ninh Binh; ND, Nam Dinh; NHO, Hanoi; PT, Phu Tho; QN, Quang Ninh; SL, Son La; TB, Thai Binh; TH, Thanh Hoa; TN, Thai Nguyen; TQ, Tuyen Quang; VP, Vinh Phuc; YB, Yen Bai.

Of 302 enrolled patients, 103 (34.1%) had qPCR-confirmed scrub typhus, 12 (4.0%) had qPCR-confirmed murine typhus, and 2 (0.7%) cases could not be diagnosed beyond genus-specific *Rick17b* qPCR positive (i.e., *Rickettsia* spp.). Thirty-five patients (11.6%) were qPCR-negative but had eschars.

Table 3 gives demographic data, clinical features, and laboratory findings for 115 patients with confirmed scrub typhus (n = 103) and murine typhus (n = 12). There was no major difference in the mean age between these 2 groups, but we did note differences in the geographic distribution of each group. Of the 103 scrub typhus cases, the highest proportion were from Hanoi Province (34, 33.0%), Hai Duong

(10, 9.7%), and Phu Tho (10, 9.7%). Most scrub typhus patients reported rural residence (66, 64.1%). Among 34 scrub typhus patients from Hanoi Province, 19 (55.9%) reported living in rural areas. More men (n = 10) than women (n = 2) had murine typhus; most lived in Hanoi Province (10, 83.3%) and were from urban areas (8, 66.7%). Farming was the most common occupation reported among both groups, 52 (50.5%) for scrub typhus patients and 5 (41.7%) for murine typhus patients.

Patients with confirmed rickettsial disease frequently reported headache, myalgia, and skin hyperaemia (≤78.6% for scrub typhus patients and 91.7% for murine typhus patients). Other symptoms, such as rash, sore throat, cough, nausea, vomiting, abdominal pain, diarrhea, dizziness, lymphadenopathy, hepatomegaly, splenomegaly, and edema, were less frequent in all groups. All cases with lymphadenopathy (n = 19) were confirmed to be scrub typhus.

The most common clinical features among 103 confirmed scrub typhus patients, other than fever, were headache (81, 78.6%), myalgia (73, 70.9%), skin hyperaemia (82, 79.6%), and conjunctivitis (66, 64.1%). Rash was seen in only 34.0% (35) of scrub typhus patients, lymphadenopathy in 18.6% (19), and hepatomegaly in 9.7% (10). Complications in scrub typhus patients were common and included altered mental status (10, 9.7%), jaundice or hyperbilirubinemia (24, 40%), and pulmonary pathology

**Table 1.** Demographic characteristics for 302 patients enrolled in a study of rickettsial diseases, northern Vietnam, March 2015–March 2017\*

Characteristic	Value
Age, y, median (IQR), range	50 (36–60), 16–89
Sex	
M	158 (52.3)
F	144 (47.7)
Admitted from community	97 (32.1)
Transferred from other hospital or clinic	205 (67.9)
Received antimicrobial drugs before admission	83 (27.5)
Residence in rural area	171 (56.6)
Farmer	127 (42.1)

\*Values are no. (%) patients except as indicated. IQR, interquartile range.



(rales) (22, 21.4%). Eschars were found in 53.4% (55) of scrub typhus cases, whereas eschars were not observed in murine typhus cases. Most scrub typhus and murine typhus patients had elevated liver aminotransferases, creatinine, procalcitonin, C-reactive protein, and bilirubin (Table 3). We found no differences in the clinical or laboratory findings between patients with confirmed murine typhus and scrub typhus, though it is noteworthy that no patients with murine typhus had lymphadenopathy.

Patients did not immediately seek treatment, which delayed time from the onset of symptoms to treatment to a median of 9 days (IQR 7–11) for scrub typhus patients and 8.5 days (IQR 5–10) for murine typhus patients. After beginning treatment, 49.2% (31/63) of scrub typhus patients and 60% (6/10) of murine typhus patients were afebrile in <72 h. Average lengths of hospital stays were 7 days (IQR 5–10) for scrub typhus patients and 8 days (IQR 7–8.5) for murine typhus patients. Doxycycline was used to treat 89.2% (91/102) of scrub typhus patients and 91.7% (11/12) of murine typhus patients, and 30 patients (28 with scrub typhus and 2 with murine typhus) were treated with doxycycline plus chloramphenicol. All patients treated with antimicrobial drugs were afebrile within 3–5 days after beginning treatment, ≤3 days for murine typhus and ≤4 days for scrub typhus patients, and all recovered.

Five deaths due to scrub typhus are reported in this study. One patient died in the hospital, and the other 4 patients were discharged from the hospital with a serious medical condition at the request of their family members and died shortly after being discharged. Three (60%) of these patients were ≥60 years of age, and all 5 experienced respiratory failure, hypotension, cardiovascular compromise, elevated aminotransferase levels, coagulation disorder during hospitalization, and markedly elevated serum ferritin levels (>1,500 µg/mL). One also had elevated lactate dehydrogenase (>1,000 U/L). Lung infiltrations and consolidation were the most common imaging findings. All 5 deaths were due to delay in time to appropriate care.

**Table 2.** Comparison of signs and symptoms for patients with scrub typhus from Hanoi Province with patients from other provinces, northern Vietnam, March 2015–March 2017\*

Sign or symptom	p value	
	Noncorrected	Corrected
Headache	0.7041	0.9071
Myalgia	0.8773	0.9071
Eye pain	0.7745	0.9071
Nausea	0.7295	0.9071
Vomiting	0.5109	0.9071
Diarrhea	0.8530	0.9071
Abdominal pain	0.2053	0.6676
Throat pain	0.8128	0.9071
Cough	0.0158	0.2194
Rash	0.8683	0.9071
Eschar	0.0219	0.2194
Skin hyperemia	0.3239	0.8098
Congestive conjunctiva	0.9071	0.9071
Lymphadenopathy	0.0590	0.3479
Edema	0.0696	0.3479
Rales	0.6423	0.9071
Resonance from lungs	0.5542	0.9071
Liver enlargement	0.2089	0.6676
Spleen enlargement	0.5725	0.9071
Convulsions	0.2336	0.6676

\*n = 115; results use Fisher exact test, expressed in p values and corrected using multiple comparisons and the Benjamini and Hochberg method (20).

Of the 185 patients with suspected rickettsial disease who tested negative by molecular methods (qPCR–), 35 had eschar (eschar+) and 150 did not (eschar–). We noted several significant differences when comparing the demographic data, clinical symptoms, and laboratory results between these 2 groups with unknown etiology (Appendix Table 1, <http://wwwnc.cdc.gov/EID/article/25/4/18-0691-Techapp1.pdf>). However, when the eschar+/qPCR– group with unknown etiology (n = 35) was compared to the scrub typhus qPCR+ group (n = 103), they were found to be similar for all but 2 categories (Appendix Table 2). By definition, 1 difference was that the eschar+/qPCR– group was characterized by having an eschar and many individuals in the other group did not. The second difference was that the eschar+/qPCR– group was more likely to have been treated with antimicrobial drugs before enrollment in this study

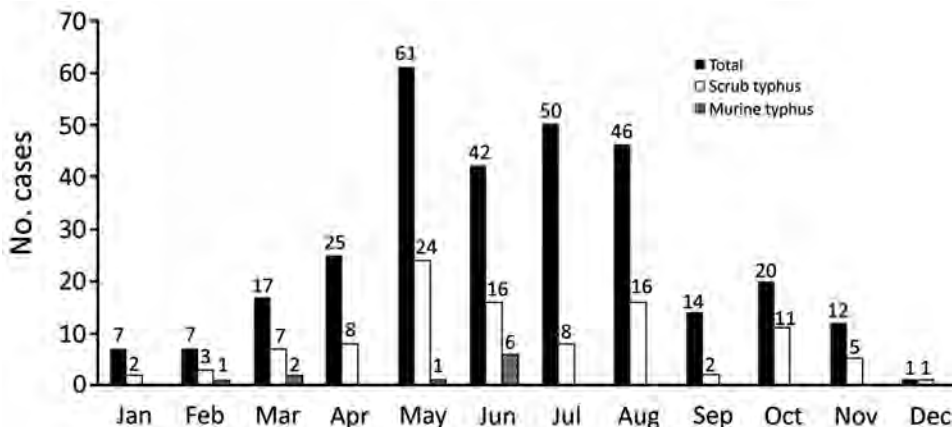


**Figure 3.** Frequency of all enrolled patients and those with confirmed scrub typhus or murine typhus in National Hospital for Tropical Diseases and Bach Mai Hospital, by month, Vietnam, March 2015–March 2017.

SYNOPSIS

**Table 3.** Demographic information, signs and symptoms, and laboratory results for 115 patients with PCR-confirmed scrub typhus or murine typhus, northern Vietnam, March 2015–March 2017\*

Category	qPCR-positive	Scrub typhus, n = 103	Murine typhus, n = 12	p value†
Age, y, mean ± SD	50.0 ± 15.8	50.0 ± 16.5	48.4 ± 8.6	0.709‡
<b>Demographics</b>				
Sex				
M	56 (48.7)	46 (44.7)	10 (83.3)	<b>0.014</b>
F	59 (51.3)	57 (55.3)	2 (16.7)	<b>0.001</b>
Residence				
Hanoi	44 (38.3)	34 (33.0)	10 (83.3)	<b>0.001</b>
Rural area	70 (60.9)	66 (64.1)	4 (33.3)	0.059
Illness during summer, April–August				
Farmer	57 (49.6)	52 (50.5)	5 (41.7)	0.762
Treatment in previous hospitals	82 (71.3)	74 (71.8)	8 (66.7)	0.741
Prior antimicrobial drug treatment, n = 109	33 (30.3)	32 (33.0)	1 (8.3)	0.152
<b>Symptoms at illness onset</b>				
Headache	92 (80.0)	81 (78.6)	11 (91.7)	0.513
Myalgia	81 (69.9)	73 (70.9)	8 (66.7)	0.769
Retro-orbital pain	21 (18.3)	18 (17.5)	3 (25.0)	0.535
Sore throat	13 (11.3)	13 (12.6)	0	0.529
Cough	42 (36.5)	38 (36.9)	4 (33.3)	1.0
Nausea	30 (26.1)	28 (27.2)	2 (16.7)	0.718
Vomiting	21 (18.4)	21 (20.6)	0	0.228
Abdominal pain, n = 114	12 (10.5)	12 (11.8)	0	0.527
Diarrhea	18 (15.7)	15 (14.6)	3 (25.0)	0.664
<b>Physical signs</b>				
Congested skin	90 (78.3)	82 (79.6)	8 (66.7)	0.290
Conjunctivitis	74 (64.4)	66 (64.1)	6 (66.7)	1.0
Eschar	55 (48.8)	55 (53.4)	0	<b>0</b>
Rash	39 (33.9)	35 (34.0)	4 (33.3)	1.0
Lymphadenopathy, n = 114	19 (16.7)	19 (18.6)	0	0.212
Hepatomegaly	11 (9.6)	10 (9.7)	1 (8.3)	1.0
Splenomegaly	7 (6.1)	6 (5.8)	1 (8.3)	0.548
Edema	14 (12.2)	13 (12.6)	1 (8.3)	1.0
Rales	24 (20.9)	22 (21.4)	2 (16.7)	1.0
Decreased breath sounds, n = 114	16 (14.0)	16 (15.7)	0	0.212
Convulsion	10 (8.7)	10 (9.7)	0	0.596
<b>Laboratory test results</b>				
Erythrocytes, T/L, median (IQR)	4.28 (3.9–4.72)	4.25 (3.86–4.69)	4.34 (4.16–4.85)	0.392§
Leukocytes, g/L, median (IQR)	8.73 (6.7–11.1)	9.1 (6.62–11.17)	8.14 (6.9–10.2)	0.631§
Platelets, g/L, median (IQR)	123 (66–194)	128 (65–194)	96 (79.5–196.5)	0.902§
Platelet <100 g/L	49 (42.6)	43 (41.8)	6 (50.0)	0.759
Alanine aminotransferase >40 IU/L, n = 113	102 (90.3)	91 (89.2)	11 (100.0)	0.597
Aspartate aminotransferase ST >37 IU/L, n = 113	106 (93.8)	95 (93.1)	11 (100.0)	1.0
Total bilirubin >17 µmol/L, n = 69	27 (39.1)	24 (40.0)	3 (33.3)	1.0
Albumin <32 g/L, n = 80	39 (48.8)	36 (50.7)	3 (33.3)	1.0
Creatinine >120 µmol/L, n = 113	16 (14.2)	15 (14.9)	1 (8.3)	1.0
Procalcitonin >0.25 ng/mL, n = 101	80 (79.2)	69 (77.5)	11 (91.7)	0.451
C-reactive protein >12 mg/L, n = 93	85 (91.4)	75 (90.4)	10 (100)	0.592
<b>Treatment</b>				
Doxycycline, n = 114	72 (63.2)	63 (61.8)	9 (75.0)	0.839
Chloramphenicol, n = 114	2 (1.8)	2 (2.0)	0 (0.0)	0.839
Doxycycline and chloramphenicol, n = 114	30 (26.3)	28 (27.5)	2 (16.7)	0.839
Albumin transfusion, n = 113	12 (10.6)	12 (11.9)	0 (0.0)	0.357
Respiratory support, n = 111	29 (25.7)	27 (26.7)	2 (16.7)	0.728
<b>Outcomes</b>				
Fever before admission, d, median (IQR)	9 (7–11)	9 (7–11)	8.5 (5–10)	0.130§
Afebrile¶ ≤72 h after treatment began, n = 73	37 (50.7)	31 (49.2)	6 (60.0)	0.736
Median no. days to afebrile, n = 73 (IQR)	3 (3–5)	4 (3–5)	3 (3–5)	0.694§
Median no. days in hospital (IQR)	7 (5–10)	7 (5–10)	8 (7–8.5)	0.822§
Death or palliative discharge	5 (4.4)	5 (4.9)	0 (0.0)	1.0

\*Values are no. (%), except as indicated. Bold text indicates statistical significance. IQR, interquartile range.

†p value calculated using Fisher exact test, except where noted.

‡p value calculated using the analysis of variance test.

§p value calculated using Mann-Whitney test.

¶No temperature recorded >37.5°C over a 24-h period.

than the qPCR+ group. Treatment with antimicrobial drugs is known to rapidly decrease the levels of rickettsial bacteria below detectable levels in blood, which may explain why qPCR results were negative in the eschar+ patients. Moreover, the comparison of the scrub typhus group to the group with unknown etiology that was eschar-/qPCR- showed many significant differences and therefore likely represents diverse etiologies (Appendix Table 3). Collectively, these results indicate that the presence of eschar is an important sign for the diagnosis of scrub typhus in northern Vietnam.

## Discussion

This study contributes to accumulating evidence that rickettsial diseases are a common cause of fever in hospitalized patients in northern Vietnam and suggests a predominance of scrub typhus and a lower prevalence for murine typhus. Of the 302 patients with suspected rickettsial disease we enrolled, we diagnosed scrub typhus in 103 (34.1%) and murine typhus in 12 (4.0%). Rickettsioses peaked during the summer rainy season, when vector populations (e.g., ticks, fleas, and trombiculid mites) are most abundant and active and workers are in the rice fields. Previous studies have similarly reported seasonality that corresponds to summer months and rice harvesting (11,12).

Among a subset of 121 patients with suspected rickettsiosis whose serum samples were tested, 6 (5.0%) showed prevalence of STGO IgG, 2 (1.7%) TGR IgG, and 1 (0.8%) SFGR IgG. This finding differs from what we previously reported for the prevalence of IgG against STGO (1.1%, 10/908), TGR (6.5%, 58/908), and SFGR (1.7%, 15/908) among healthy persons in the rural BaVi District and an urban area of Hanoi using the same ELISAs described here (15). In our previous study, 40% of participants were <20 years of age (15). In contrast, the patients investigated here were older. Scrub typhus incidence has been reported to peak in the fifth decade of life (12), with highest observed prevalence in adults 61–80 years of age (21). Thus, it is not surprising that the average age of qPCR+ scrub typhus cases and eschar+/qPCR- cases in this study was 50.3 years (Appendix Table 3). Note that our seroprevalence is lower than that described for suburban Bangkok, Thailand, and urban and rural Malang, Indonesia (21).

Of note, 4 of 6 qPCR-positive patients had IgG-positive acute-phase serum samples. The positive ELISA results did not appear to be associated with duration of fever before acute-phase blood collection. Two of the samples came from patients with fever of 5 days' duration, suggesting they may have had preexisting *O. tsutsugamushi*-specific IgG. For 2 patients with onset of symptoms at 8 and 10 days, IgG positivity could have been due to the current infection, a previous infection, or both (22,23). We analyzed acute-phase serum samples for 20 Otsu47-positive

samples, and all were negative by STGO ELISA. These examples highlight the importance of collecting paired acute- and convalescent-phase samples at least 14 days apart to serologically confirm the diagnosis of scrub typhus (23).

Our study showed a high proportion of eschars among scrub typhus patients (53.4%), and presence of eschar, a well-known clinical sign for scrub typhus (13), was 1 consideration used for defining suspect cases. The proportion of patients with eschar among our study population was similar to reports from northern (56.2%) and central (62.9%) Vietnam and from Laos and South Korea (11,13,24). The proportion of eschars among scrub typhus patients appears variable and has been reported at  $\leq 7\%$  in children from Thailand (25). We did not recruit young children in this study, which may explain the higher proportion of scrub typhus patients with eschar reported here.

A recent study conducted in Quang Nam Province in central Vietnam demonstrated that the presence of eschar was the chief diagnostic indicator for scrub typhus (13). In that study, the authors used qPCR assays on DNA extracted from swab samples of patients' eschar to identify scrub typhus. They recommended that eschar qPCR should be routinely considered for rickettsial diagnosis in the early phase of infection because it is easy to perform and has a high positive predictive value (13).

We identified 35 patients with an eschar and clinical symptoms consistent with scrub typhus but who tested negative for *O. tsutsugamushi* by qPCR on blood samples. These patients may have had true scrub typhus or spotted fever cases, despite the negative qPCR results. The sensitivity of qPCR for blood may have been inadequate to detect the small number of bacteria present, especially after antimicrobial therapy was commenced (26). Rickettsial DNA is known to disappear quickly from blood after start of appropriate antimicrobial drug therapy. The sensitivity of qPCR on eschar swabs has been reported as higher than for blood samples (18/20 eschar swabs were positive by qPCR vs. 5/20 blood samples from same patients [13]), at 85%–86% with specificity of 100% (13,27). The presence of rickettsiae in eschar and rash samples is not affected by previous antimicrobial drug treatment (23). Thus, for qPCR, the specimen of choice for eschar- or rash-producing rickettsioses is a swab (eschars) or biopsy (eschar or rash) (23).

In our study population, the most common symptoms among qPCR-positive patients included fever, headache, myalgia, conjunctivitis, and rash. Some patients also experienced cough, vomiting, nausea, abdominal pain, lymphadenopathy, hepatomegaly, and splenomegaly. Patients with scrub typhus had a higher frequency of lymphadenopathy, a well-known clinical sign of scrub typhus (28). Headache is frequent with other illnesses, and other studies also have found that clinical characteristics often are not helpful in identifying rickettsial infections. We also saw a high



proportion of scrub typhus patients with conjunctivitis and rash in our study. Rash is a typical finding among patients suspected of having rickettsiosis and was among the inclusion criteria for our study. Rash is reported in  $\approx 45\%$ – $50\%$  of patients with scrub typhus (29,30). However, its frequency varies between areas, as seen in Japan (93%), Thailand (7%), and India (1.7%) (31–33). A few studies conducted in central Vietnam reported that the proportion of scrub typhus patients with rash was low (3 1.2%) or absent, as in a study in central Vietnam (13). Rash may be difficult to diagnose in patients with relatively dark skin, or may be absent at time of examination in the hospital. Most scrub typhus patients had fever for  $>7$  days, time in which rash may have disappeared. We found no major differences in clinical manifestations between patients from Hanoi Province and other provinces of northern Vietnam, suggesting an absence of bias toward higher severity among patients traveling far to the hospital.

Complications of scrub typhus include jaundice, meningoencephalitis, myocarditis, acute respiratory distress, and renal failure (34,35). When treatment is delayed or does not include appropriate antimicrobial drugs, case-fatality rates are up to 6.0% but can be up to 70% (29). Our fatality rate of 4.9% (5/103) is similar to that in previous reports (12).

Murine typhus is a more challenging disease to diagnose clinically than scrub typhus because symptoms are nonspecific. The low number ( $n = 12$ ) of confirmed murine typhus cases in our study makes it difficult to compare murine typhus with scrub typhus and other rickettsial diseases. However, patients with murine typhus experienced myalgia, conjunctivitis, nausea, cough, and vomiting less frequently than patients with scrub typhus, and no lymphadenopathy or eschars were described, which counters previous reports (11). Consistent with other reports, however, murine typhus was associated with elevated liver enzymes, procalcitonin, and C-reactive protein (11,36). These clinical findings may be useful for distinguishing the 2 diseases in areas where both are common (24).

Most scrub typhus and murine typhus patients in our study were treated with doxycycline, the recommended treatment for all ages. Chloramphenicol was used in severe cases as an additional drug. Within 72 hours of starting antimicrobial drug therapy, 49.2% (31/63) of scrub typhus and 60% (6/10) of murine typhus patients were afebrile. These data align with other reports (11). Rapid clinical improvement after using effective antimicrobial drugs is reported to back up clinical diagnoses of rickettsioses (37–39).

This study determined that scrub typhus was the predominant rickettsial disease diagnosed among patients hospitalized with acute undifferentiated fever in northern Vietnam. Public health awareness of scrub typhus and other rickettsial diseases in Vietnam should be enhanced to ensure healthcare providers can diagnose and treat these diseases successfully.

## Acknowledgments

We thank all patients for their participation in this study. We are indebted to all nurses, physicians, and laboratory staff at the National Hospital for Tropical Diseases and Bach Mai Hospital who provided care for the patients, helped collect clinical data, and performed serological and molecular tests. We are grateful to our colleagues from the US Naval Medical Research Center for kindly providing training and technical assistance to establish serological and molecular testing capacity for rickettsial infections at the National Hospital for Tropical Diseases.

This study was supported by the National Foundation for Science and Technology Development of Vietnam [106-YS.042014.10] and was partially supported by the Defense Threat Reduction Agency, work unit #A1266 (A.L.R.) and the Wellcome Trust of Great Britain #106680/Z/14/Z (S.O.L., B.N., M.C., J.E.B., H.R.vD.)

## About the Author

Dr. Trung is an associate professor of the National Hospital for Tropical Diseases and Hanoi Medical University, Hanoi, Vietnam. His primary research interests include bacterial and viral identification by molecular diagnosis.

## References

- Ericson CD, Jensenius M, Fournier PE, Raoult D. Rickettsioses and the international traveler. *Clin Infect Dis*. 2004;39:1493–9. <http://dx.doi.org/10.1086/425365>
- Blanton LS, Dumler JS, Walker DH. *Rickettsia typhi* (murine typhus). In: Dolin R, Blaser MJ, editors. *Mandell, Douglas, and Bennett's principles and practice of infectious diseases*. 8th ed. Philadelphia: Elsevier Inc.; 2014. p. 2221–4.e2.
- Day NPJ, Newton PN. Scrub typhus and other tropical rickettsioses. In: Cohen J, Powderly WG, Opal SM, eds. *Infectious diseases*. 4th ed. Amsterdam: Elsevier Inc.; 2017. p. 1091–1097.e1.
- Duong V, Mai TT, Blasdel K, Lo V, Morvan C, Lay S, et al. Molecular epidemiology of *Orientia tsutsugamushi* in Cambodia and Central Vietnam reveals a broad region-wide genetic diversity. *Infect Genet Evol*. 2013;15:35–42. <http://dx.doi.org/10.1016/j.meegid.2011.01.004>
- Liu D. Rickettsia. In: Tang Y-W, Sussman M, Dongyou L, Poxton I, Schwartzman J, eds. *Molecular medical microbiology*. 2nd ed. Boston: Academic Press; 2015. p. 2043–2056.
- Miller MB, Bratton JL, Hunt J, Blankenship R, Lohr DC, Reynolds RD. Murine typhus in Vietnam. *Mil Med*. 1974;139:184–6. <http://dx.doi.org/10.1093/milmed/139.3.184>
- Lim C, Paris DH, Blacksell SD, Laongnualpanich A, Kantipong P, Chierakul W, et al. How to determine the accuracy of an alternative diagnostic test when it is actually better than the reference tests: A re-evaluation of diagnostic tests for scrub typhus using Bayesian LCMs. *PLoS One*. 2015;10:e0114930. <http://dx.doi.org/10.1371/journal.pone.0114930>
- Berman SJ, Kundin WD. Scrub typhus in South Vietnam. A study of 87 cases. *Ann Intern Med*. 1973;79:26–30. <http://dx.doi.org/10.7326/0003-4819-79-1-26>
- Aung AK, Spelman DW, Murray RJ, Graves S. Rickettsial infections in Southeast Asia: implications for local populace and febrile returned travelers. *Am J Trop Med Hyg*. 2014;91:451–60. <http://dx.doi.org/10.4269/ajtmh.14-0191>

10. Azuma M, Nishioka Y, Ogawa M, Takasaki T, Sone S, Uchiyama T. Murine typhus from Vietnam, imported into Japan. *Emerg Infect Dis*. 2006;12:1466–8. <http://dx.doi.org/10.3201/eid1209.060071>
11. Hamaguchi S, Cuong NC, Tra DT, Doan YH, Shimizu K, Tuan NQ, et al. Clinical and epidemiological characteristics of scrub typhus and murine typhus among hospitalized patients with acute undifferentiated fever in Northern Vietnam. *Am J Trop Med Hyg*. 2015;92:972–8. <http://dx.doi.org/10.4269/ajtmh.14-0806>
12. Nadjm B, Thuy PT, Trang VD, Dang Ha L, Kinh NV, Wertheim HF. Scrub typhus in the northern provinces of Vietnam: an observational study of admissions to a national referral hospital. *Trans R Soc Trop Med Hyg*. 2014;108:739–40. <http://dx.doi.org/10.1093/trstmh/tru145>
13. Le Viet N, Laroche M, Thi Pham HL, Viet NL, Mediannikov O, Raoult D, et al. Use of eschar swabbing for the molecular diagnosis and genotyping of *Orientia tsutsugamushi* causing scrub typhus in Quang Nam province, Vietnam. *PLoS Negl Trop Dis*. 2017;11:e0005397. <http://dx.doi.org/10.1371/journal.pntd.0005397>
14. Graf PC, Chretien JP, Ung L, Gaydos JC, Richards AL. Prevalence of seropositivity to spotted fever group rickettsiae and *Anaplasma phagocytophilum* in a large, demographically diverse US sample. *Clin Infect Dis*. 2008;46:70–7. <http://dx.doi.org/10.1086/524018>
15. Trung NV, Hoi LT, Thuong NTH, Toan TK, Huong TTK, Hoa TM, et al. Seroprevalence of scrub typhus, typhus, and spotted fever among rural and urban populations of northern Vietnam. *Am J Trop Med Hyg*. 2017;96:1084–7. <http://dx.doi.org/10.4269/ajtmh.16-0399>
16. Henry KM, Jiang J, Rozmajz PJ, Azad AF, Macaluso KR, Richards AL. Development of quantitative real-time PCR assays to detect *Rickettsia typhi* and *Rickettsia felis*, the causative agents of murine typhus and flea-borne spotted fever. *Mol Cell Probes*. 2007;21:17–23. <http://dx.doi.org/10.1016/j.mcp.2006.06.002>
17. Jiang J, Chan T-C, Temenak JJ, Dasch GA, Ching W-M, Richards AL. Development of a quantitative real-time polymerase chain reaction assay specific for *Orientia tsutsugamushi*. *Am J Trop Med Hyg*. 2004;70:351–6. <http://dx.doi.org/10.4269/ajtmh.2004.70.351>
18. Jiang J, Stromdahl EY, Richards AL. Detection of *Rickettsia parkeri* and *Candidatus Rickettsia andeanae* in *Amblyomma maculatum* Gulf Coast ticks collected from humans in the United States. *Vector-Borne Zoonotic Dis*. 2012;12:175–82. <http://dx.doi.org/10.1089/vbz.2011.0614>
19. Wright CL, Nadolny RM, Jiang J, Richards AL, Sonenshine DE, Gaff HD, et al. *Rickettsia parkeri* in Gulf Coast ticks, southeastern Virginia, USA. *Emerg Infect Dis*. 2011;17:896–8. <http://dx.doi.org/10.3201/eid1705.101836>
20. Benjamini Y, Hochberg Y. Controlling the false discovery rate: a practical and powerful approach to multiple testing. *J R Stat Soc B*. 1995;57:289–300. <http://dx.doi.org/10.1111/j.2517-6161.1995.tb02031.x>
21. Strickman D, Tanskul P, Eamsila C, Kelly DJ. Prevalence of antibodies to rickettsiae in the human population of suburban Bangkok. *Am J Trop Med Hyg*. 1994;51:149–53. <http://dx.doi.org/10.4269/ajtmh.1994.51.149>
22. Kramme S, Van An L, Khoa ND, Van Trin L, Tannich E, Rybniker J, et al. *Orientia tsutsugamushi* bacteremia and cytokine levels in Vietnamese scrub typhus patients. *J Clin Microbiol*. 2009;47:586–9. <http://dx.doi.org/10.1128/JCM.00997-08>
23. Luce-Fedrow A, Mullins K, Kostik AP, St John HK, Jiang J, Richards AL. Strategies for detecting rickettsiae and diagnosing rickettsial diseases. *Future Microbiol*. 2015;10:537–64. <http://dx.doi.org/10.2217/fmb.14.141>
24. Phongmany S, Rolain JM, Phetsouvanh R, Blacksell SD, Soukkhaseum V, Rasachack B, et al. Rickettsial infections and fever, Vientiane, Laos. *Emerg Infect Dis*. 2006;12:256–62. <http://dx.doi.org/10.3201/eid1202.050900>
25. Silpapojakul K, Varachit B, Silpapojakul K. Paediatric scrub typhus in Thailand: a study of 73 confirmed cases. *Trans R Soc Trop Med Hyg*. 2004;98:354–9. <http://dx.doi.org/10.1016/j.trstmh.2003.10.011>
26. Sonthayanon P, Chierakul W, Wuthiekanun V, Blacksell SD, Pimda K, Suputtamongkol Y, et al. Rapid diagnosis of scrub typhus in rural Thailand using polymerase chain reaction. *Am J Trop Med Hyg*. 2006;75:1099–102. <http://dx.doi.org/10.4269/ajtmh.2006.75.1099>
27. Kim DM, Kim HL, Park CY, Yang TY, Lee JH, Yang JT, et al. Clinical usefulness of eschar polymerase chain reaction for the diagnosis of scrub typhus: a prospective study. *Clin Infect Dis*. 2006;43:1296–300. <http://dx.doi.org/10.1086/508464>
28. Liu Y-X, Feng D, Zhang Q, Jia N, Zhao Z-T, De Vlas SJ, et al. Key differentiating features between scrub typhus and hemorrhagic fever with renal syndrome in northern China. *Am J Trop Med Hyg*. 2007;76:801–5. <http://dx.doi.org/10.4269/ajtmh.2007.76.801>
29. Taylor AJ, Paris DH, Newton PN. A systematic review of mortality from untreated scrub typhus (*Orientia tsutsugamushi*). *PLoS Negl Trop Dis*. 2015;9:e0003971. <http://dx.doi.org/10.1371/journal.pntd.0003971>
30. Weng SC, Lee HC, Chen JJ, Cheng YJ, Chi H, Lin CY. Eschar: a stepping stone to scrub typhus. *J Pediatr* 2017;181:320–320 e1. <http://dx.doi.org/10.1016/j.jpeds.2016.10.084>
31. Jamil M, Lyngrah KG, Lyngdoh M, Hussain M. Clinical manifestations and complications of scrub typhus: a hospital based study from North Eastern India. *J Assoc Physicians India*. 2014;62:19–23.
32. Ogawa M, Hagiwara T, Kishimoto T, Shiga S, Yoshida Y, Furuya Y, et al. Scrub typhus in Japan: epidemiology and clinical features of cases reported in 1998. *Am J Trop Med Hyg*. 2002;67:162–5. <http://dx.doi.org/10.4269/ajtmh.2002.67.162>
33. Silpapojakul K, Chupuppakarn S, Yuthasompob S, Varachit B, Chaipak D, Borkerd T, et al. Scrub and murine typhus in children with obscure fever in the tropics. *Pediatr Infect Dis J*. 1991; 10:200–3. <http://dx.doi.org/10.1097/00006454-199103000-00006>
34. Tsay RW, Chang FY. Serious complications in scrub typhus. *J Microbiol Immunol Infect*. 1998;31:240–4.
35. Tsay RW, Chang FY. Acute respiratory distress syndrome in scrub typhus. *QJM*. 2002;95:126–8. <http://dx.doi.org/10.1093/qjmed/95.2.126>
36. Hu M-L, Liu J-W, Wu K-L, Lu S-N, Chiou S-S, Kuo C-H, et al. Short report: Abnormal liver function in scrub typhus. *Am J Trop Med Hyg*. 2005;73:667–8. <http://dx.doi.org/10.4269/ajtmh.2005.73.667>
37. Tsai CC, Lay CJ, Ho YH, Wang LS, Chen LK. Intravenous minocycline versus oral doxycycline for the treatment of noncomplicated scrub typhus. *J Microbiol Immunol Infect*. 2011;44:33–8. <http://dx.doi.org/10.1016/j.jmii.2011.01.007>
38. Watt G, Chouriyagune C, Ruangweerayud R, Watcharapichat P, Phulsuksombati D, Jongsakul K, et al. Scrub typhus infections poorly responsive to antibiotics in northern Thailand. *Lancet*. 1996;348:86–9. [http://dx.doi.org/10.1016/S0140-6736\(96\)02501-9](http://dx.doi.org/10.1016/S0140-6736(96)02501-9)
39. Le-Viet N, Phan DT, Le-Viet N, Trinh S, To M, Raoult D, et al. Dual genotype *Orientia tsutsugamushi* infection in patient with rash and eschar, Vietnam, 2016. *Emerg Infect Dis*. 2018;24:1520–3. <http://dx.doi.org/10.3201/eid2408.171622>

Address for correspondence: Allen L. Richards, Naval Medical Research Center, 503 Robert Grant Ave, Silver Spring, MD 20910-7500, USA; email: allen.richards@comcast.net

# Mucosal Leishmaniasis in Travelers with *Leishmania braziliensis* Complex Returning to Israel

Michal Solomon, Nadav Sahar, Felix Pavlotzky, Aviv Barzilai,  
Charles L. Jaffe, Abedelmajeed Nasereddin, Eli Schwartz

Mucosal leishmaniasis (ML) is a complication of New World cutaneous leishmaniasis (CL) caused mainly by *Leishmania (Viannia) braziliensis*. This retrospective study investigated all cases of ML caused by *L. (V.) braziliensis* in a tertiary medical center in Israel, evaluating the risk factors, clinical presentations, diagnosis, treatment, and outcome of mucosal involvement in ML caused by *L. (V.) braziliensis* in travelers returning to Israel. During 1993–2015, a total of 145 New World CL cases were seen in travelers returning from Bolivia; among them, 17 (11.7%) developed ML. Nasopharyngeal symptoms developed 0–3 years (median 8 months) after exposure. The only significant risk factor for developing ML was the absence of previous systemic treatment. Among untreated patients, 41% developed ML, compared with only 3% of treated patients ( $p = 0.005$ ). Systemic treatment for CL seems to be a protective factor against developing ML.

In the past 2 decades, travel to South and Central America has increased among young adults from Israel, causing potential exposure to tropical diseases, including leishmaniasis (1). New World cutaneous leishmaniasis (CL), endemic in some parts of the Americas, is caused by *Leishmania viannia* and *Leishmania mexicana* species complexes. Infection with *L. viannia* complex, particularly *Leishmania (Viannia) braziliensis*, results in CL that tends to be persistent and may be further complicated by mucosal leishmaniasis (ML) (2). ML is probably caused by early hematogenous or lymphatic spread from cutaneous lesions through parasites that infect and replicate within macrophages of the nasopharyngeal mucosa, setting up a destructive inflammatory process. The interval from onset (or clinical resolution) of CL to clinical manifestations of ML typically is several years but may range from <30 days to decades (3).

Author affiliations: Sheba Medical Center, Tel Aviv, Israel (M. Solomon, N. Sahar, F. Pavlotzky, A. Barzilai, E. Schwartz); Hebrew University–Hadassah Medical School, Jerusalem, Israel (C.L. Jaffe, A. Nasereddin)

DOI: <https://doi.org/10.3201/eid2504.180239>

Persistent nasal congestion or stuffiness is the most commonly reported ML symptom (4,5); associated manifestations may include coryza, epistaxis, tissue/scab expulsion, pruritus, mass sensation, blockage/obstruction, and hyposmia (4,6–9). Persons with ML may have oral or pharyngeal lesions, bleeding, or pain; dysphagia/odynophagia; or dysphonia. Isolated laryngeal disease, without involvement of other mucosal sites, may occur but is relatively unusual (7,9). Abnormalities of the paranasal sinuses (e.g., those detected by computed tomography) have also been reported (5).

Systemic antileishmanial drugs are often used to treat CL caused by *L. viannia* complex, not only to promote healing of the primary lesion but also to reduce the risk of developing ML (2,10). Risk factors for development of ML are considered to be large or multiple cutaneous lesions, male sex, lesions above the waist, head and neck localization, and longstanding skin lesions for which adequate systemic treatment has not been administered (11).

In this study, we describe a cohort of 145 travelers from Israel returning from the Amazon Basin of Bolivia with New World CL. Within this group, 17 travelers developed ML. We compared these case-patients to patients with CL returning from this region without mucosal involvement, thus highlighting the clinical aspects and identifying potential risk factors for developing ML and noting appropriate treatment management.

## Patients and Methods

We conducted a multicenter survey of patients who received a diagnosis of New World CL during 1993–2005 at 8 medical centers in Israel. We collected additional data for 2006–2015 from cases referred to the Center of Geographic and Tropical Medicine or to the Dermatology Clinic at the Sheba Medical Center in Tel Aviv. All patients with New World CL diagnoses were evaluated retrospectively.

Suspected CL was confirmed when cutaneous lesions (ulcers, nodules, or papules) clinically compatible with



leishmaniasis were noted and  $\geq 1$  of the following tests were positive: a smear or biopsy specimen showing *Leishmania* amastigotes within a dermal or mucosal infiltrate, positive PCR assay for *Leishmania (V.) braziliensis*, or positive promastigote cultures (12). Suspected cases of ML were confirmed when either nasal or oral symptoms of ML were noted together with oral or pharyngeal lesions. All the patients were examined by otorhinolaryngology specialists. Diagnoses were confirmed by biopsy, PCR, or culture for leishmaniasis.

Cure of a cutaneous lesion was defined as closure of the primary skin lesion. Cure of a mucosal lesion was defined as disappearance of the nasopharyngeal lesions.

### PCR Diagnosis

We performed DNA preparation and internal transcribed spacer 1 region (ITS1) PCR as described previously (12). In brief, we analyzed DNA samples at the time of original diagnosis for ITS1 PCR using primers LITSR and L5.8S. We performed the reaction with the PCR-Ready Supreme mix (Syntezza Bioscience, <https://syntezza.com>) in 25  $\mu$ L of total reaction. Amplification conditions were as described previously (12). The PCR products were digested with *Hae*III enzyme for restriction fragment polymorphism analysis. The amplicons of  $\approx 300$ –350 bp were analyzed on 1.5% agarose gels and the restriction fragments on 4% agarose gels by electrophoresis at 100 V in 1X Tris-acetate-EDTA buffer (0.04 M Tris-acetate and 1 mmol/L EDTA, pH 8) and visualized by UV light after being stained with ethidium bromide (0.3  $\mu$ g/mL). We used GeneRuler DNA Ladder Mix (Thermo Scientific, <https://www.thermofisher.com>) as the DNA molecular marker. We also examined archived samples from 79 of the travelers in 2016 by HSP-70 PCR using the primers HSP70-F25 and HSP-70-R1310 (PCR-F) followed by DNA sequencing (13). We compared sequences to those in GenBank by using BLAST (<https://blast.ncbi.nlm.nih.gov/Blast.cgi>).

### Statistical Analysis

We used SPSS version 23.0 software (IBM, <https://www.ibm.com>) for data entry and analysis. Continuous variables were expressed as the median and interquartile range (IQR) and categorical variables as a percentage. We used a 2-tailed Fisher exact test to compute p value in the prevalence assessment. A p value  $< 0.05$  was considered significant.

### Results

During the past 22 years, 145 patients in our cohort received a diagnosis of CL from South America (Figure 1). From this cohort, 77 patients were seen during 1993–2005 in 8 medical centers in Israel (including Sheba Medical Center); the remaining 68 cases were a cohort of patients seen at Sheba Medical Center during 2006–2015. Of the cohort of 145 patients, 17 patients (16 men and 1 woman) received a diagnosis of ML (11.7%). All cases were acquired in known *L. (V.) braziliensis*-endemic areas in the Amazon region of Bolivia.

Of the 145 patients, 4 patients had concomitant cutaneous and mucosal lesions. Among the remaining 141 patients, 59 were treated with intravenous (IV) liposomal amphotericin B (L-AmB; 3 mg/kg/d for 6–10 d); 60 were treated with IV sodium stibogluconate (SSG; 20 mg/kg/d for 20 d); and 22 were not given systemic treatment for their primary skin lesion. Of those who were treated systemically, only 4 patients (3.3%) developed ML (3/60 among the IV SSG group and 1/59 among the IV L-AmB group), whereas in the group of 22 patients who were not given systemic treatment, 9 (41%) developed ML ( $p = 0.005$ ) (Figure 2).

To explore other risk factors for developing ML, we compared patients with New World CL and those with ML (Table 1). The results showed no differences in age, sex, or number or location of skin lesions between the 2 groups.

We compiled epidemiologic characteristics and outcomes of the ML patients (Table 2). The mean age of the ML patients at diagnosis was 27.4 years (median 25 years,

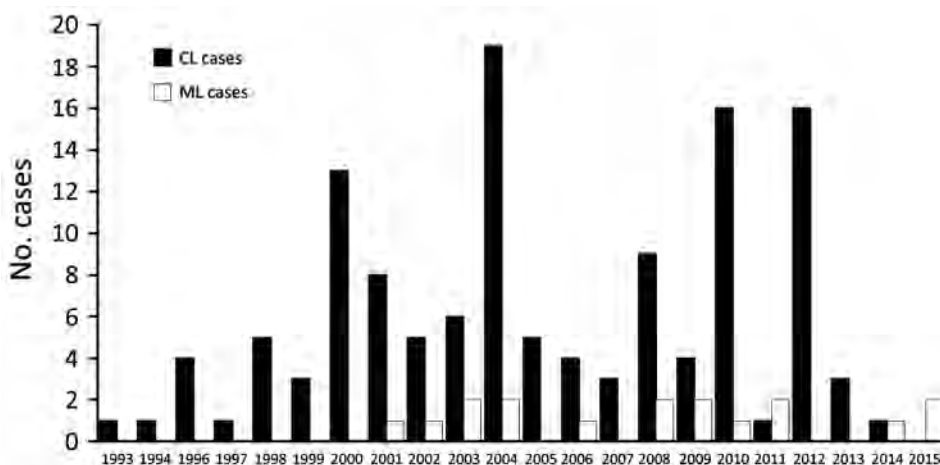


**Figure 1.** Number of CL and ML cases in Israel, 1993–2015. No cases were reported in 1995. CL, cutaneous leishmaniasis; ML, mucosal leishmaniasis.

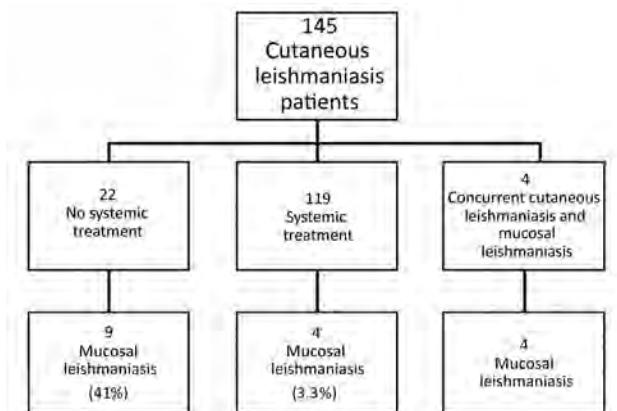


**Figure 2.** Outcomes of cutaneous leishmaniasis cases caused by *Leishmania (Viannia) braziliensis* based on treatment received, Israel, 1993–2015. In comparing the groups of patients,  $p = 0.005$ .

range 22–41 years). ML patients had a total of 42 skin lesions. The number of cutaneous lesions per patient was 2.47 (median 1, range 0–12); 53% had 1 cutaneous lesion, 29% had 2–4 cutaneous lesions, and 12% had >4 lesions. One patient had 12 lesions on his legs, which is rare for *L. (V.) braziliensis* infections, and 1 patient had no primary skin lesions. The distribution of the skin lesions was 29% on the upper limbs, 41% on the lower limbs, 23.5% on the face, and 11.7% on the trunk. Regional lymphadenopathy was found in 41% of the patients. All patients had negative serologic test results for HIV.

Nasopharyngeal symptoms developed 0–3 years after the patients returned from Bolivia (median 8 months), except for 1 case, which developed 20 years after exposure. ML diagnosis was delayed up to 5 years from the onset of symptoms (mean 16.3 months, range 0–60 months). Mucosal symptoms included oral ulceration in 5 patients, nasal obstruction in 12 patients, and lacrimal duct obstruction in 2 patients (in 1 patient, cartilage involvement of the sternoclavicular joint near the primary CL lesion was also noted). Typical nasal involvement is shown in Figure 3.

Regarding diagnosis, in 15 cases, the species diagnosis was based on positive PCR results for *L. braziliensis* taken by scraping of the lesion (mucosal or skin). In the other 2 cases, the species diagnosis could not be verified by PCR and was based on the disease being acquired in the Amazon basin of Bolivia, which is known to be endemic for *L. braziliensis*. Mucosal biopsy was done in 7 patients (41%) and revealed skin granulomas suggesting leishmanial infection, but amastigotes were seen in only 1 case, which demonstrates the limitation of biopsy in these cases.

Among the ML cases, 1 patient did not have a primary skin lesion, 4 patients had concurrent CL at time of diagnosis, and 12 patients developed mucosal symptoms after healing of the primary skin lesion. Among those 12 patients, symptoms developed 1 year (6 patients), 2 years

(4 patients), or more (2 patients) after the initial diagnosis. Eight of those patients were not treated properly (they received paromomycin ointment, itraconazole, and/or intralesional sodium stibogluconate, or no treatment); 3 received IV SSG, and only 1 received IV L-AmB 3 mg/kg for 5 consecutive days and a 6th dose on day 10. The patient who did not have any skin lesions developed mucosal disease 20 years after returning from Bolivia.

### Treatment and Outcome

Treatment of ML was carried out as follows: 10 patients received IV L-AmB at a dose of 3 mg/kg/day for 6–10 days (total 18–30 mg/kg); 6 patients received IV SSG at a dose of 20 mg/kg/day for 20–30 days; and 1 patient was given oral miltefosine at a dose of 150 mg/day for 28 days. With these doses, treatment failure with relapse occurred in 3 patients in the L-AmB group (Figure 4). Of the 3 patients whose ML failed to be cured with L-AmB therapy, 1 patient then received IV SSG and 2 patients were given oral miltefosine. The ML in all 3 of these patients was then cured. The rest of the patients achieved cures of their ML without having relapses, with a mean of follow-up of 9.5 years (median 7 years, range 2.5–16 years, IQR 5–11 years).

Two patients had irreversible nasal cartilage damage upon diagnosis at our center, with a hole in the nasal septum (Figure 3). These complications were a result of misdiagnosis and delayed proper treatment.

### Discussion

Our series describes 145 cases of CL in travelers returning to Israel; among these patients, 17 (11.7%) received diagnoses of ML. The highest-risk areas for ML are south of the Amazon basin in parts of Bolivia, Peru, and Brazil (defined here as the mucosal belt). *Leishmania* species with an increased risk of causing ML include mainly *L. (V.) braziliensis* but also *L. (V.) guyanensis* and *L. (V.) panamensis* (3). Among local populations, observational studies have generally found incidence rates of ML following CL caused by *L. (V.) braziliensis* to be 2%–10% (14) and close to 30% in some reports (15). In Bolivia, ML/CL ratios are highest (16%–37%) in the population living in endemic areas (16,17). Among indigenous persons in rural Bolivia with untreated CL, progression to ML was estimated to occur in 5%–20% of patients (17). Based on retrospective evaluations in an actively surveyed population of >3,000 CL patients in an *L. (V.) braziliensis* focus area in Peru, the lifetime risk of developing ML was 12.8% (18).

Few previous reports exist on ML among travelers returning from Latin America to non-*Leishmania*-endemic countries (10,11,19–21). An estimation of the ML/CL ratio in travelers with *L. (V.) braziliensis* gives a range of 1.2%–8% (14). However, the prolonged follow-up period in our study provides a more firm basis for our finding of a rate of 11%.

**Table 1.** Comparison between patients with New World CL and those with ML, Israel, 1993–2015\*

Characteristic	CL	ML
No. patients	128	17
Sex ratio, M:F	105:23 (82% male)	16:1 (94% male)
Mean age, y	24.2	27.6
Infected in Bolivia	83/100 (83%)	17/17(100%)
No. lesions	1.8	2.3
≥3 lesions	21/128 (16%)	5/17 (29%)
Lesion above waist	61/81 (75%)	9/17 (53%)
PCR positive	68/76 (89%)	15/17 (88%)

\*Differences between categories were not significant. CL, cutaneous leishmaniasis; ML, mucosal leishmaniasis.

Several *Leishmania* species are circulating in the Americas; therefore, the rate of ML might be different from region to region. Our study focused on *L. (V.) braziliensis* infection, notorious for causing ML complications. A report from a *Leishmania*-endemic area of Bolivia indicated that compared with the indigenous population, healthy migrants to this region who developed CL had a 2.3-fold greater risk, of developing ML (22). In this respect, travelers from non-*Leishmania*-endemic countries may similarly be more susceptible to ML. However, based on our data, it seems that the rate among travelers is similar to that of the local population.

The risk for ML following New World CL has been estimated to be highest within 2 years of the onset of the initial skin lesion (9). Indeed, 82% of the patients in our series developed ML symptoms within 2 years after onset of CL lesions.

Mucosal complaints in our study included nasal obstruction, rhinorrhea, nasal discharge, oral ulceration, bone lesion, and lacrimal duct obstruction. Lacrimal duct obstruction is less known; it is described in the literature in 4 patients, 20–75 years of age, who had nasal lesions resulting from ML and sought treatment for chronic dacryocystitis (23). However, based on our case series, invasion of the lacrimal ducts seems to be less uncommon (2/17, 11%).

Delay in diagnosis of ML was common in our study, which found a mean of 16 months from the onset of symptoms until appropriate treatment. A low index of suspicion by clinicians may have contributed to these delays. Increased medical awareness of the risk for CL and ML among travelers to Latin America may reduce delays in diagnosis and optimize chances of cure. Unfortunately, in 2 patients the disease was diagnosed too late, after the patients developed destructive mucosal lesions with a complete hole in the nasal septum that could not be cured (Figure 3, panel C).

**Table 2.** Epidemiologic, clinical, and therapy data of patients with mucosal leishmaniasis, Israel, 1993–2015\*

Patient no.	Age, y/sex	No. primary lesions	Concurrent active CL	Location of primary lesions	Treatment			Response	ML symptoms
					Primary cutaneous lesions	Mucosal lesions	After ML treatment failure		
1	28/M	12	No	Trunk, upper extremities	None	IV SSG	No failure	CR	Oral ulceration, nasal obstruction
2	24/F	1	Yes	Lower extremities	Treated for concurrent CL	IV SSG	No failure	CR	Nasal obstruction
3	28/M	1	No	Lower extremities	None	IV L-AmB	No failure	CR	Nasal obstruction
4	28/M	1	No	Neck	IV SSG	IV L-AmB	No failure	CR	Nasal obstruction
5	26/M	1	No	Lower extremities	IV SSG	IV L-AmB	No failure	CR	Nasal obstruction
6	25/M	1	No	Face	IV SSG	IV L-AmB	No failure	CR	Oral ulceration
7	41/M	1	Yes	Lower extremities	Treated for concurrent CL	IV L-AmB	IV SSG	CL recurrence	Nasal obstruction, lacrimal gland obstruction
8	23/M	4	Yes	Neck, lower extremities	Treated for concurrent CL	IV L-AmB	No failure	None	Nasal obstruction, bone lesion
9	31/M	3	No	Upper and lower extremities	None	IV L-AmB	No failure	CR	Nasal obstruction, rhinorrhea
10	24/M	1	Yes	Upper extremities	Treated for concurrent CL	IV L-AmB	Miltefosine	CR	Nasal obstruction
11	41/M	0	No	No lesions†	None	Miltefosine	No failure	CR	Oral ulceration
12	25/M	1	NA	NA	None	IV SSG	No failure	CR	NA
13	22/M	2	No	NA	None	IV SSG	No failure	CR	Oral ulceration
14	25/M	3	No	Lower extremities	None	IV SSG	No failure	CR	NA
15	24/M	7	No	Face, upper extremities	None	IV SSG	No failure	CR	Oral ulceration, nasal obstruction
16	28/M	1	No	Upper extremities	None	IV L-AmB	No failure	CR	Nasal obstruction
17	23/M	2	No	Trunk	None	IV L-AmB	Miltefosine	CR	Nasal obstruction

\*CL, cutaneous leishmaniasis; CR, complete response; IV L-AmB, intravenous liposomal amphotericin B; IV SSG, intravenous sodium stibogluconate;

ML, mucosal leishmaniasis; NA, not available.

†Patient 11 had no primary cutaneous lesion.



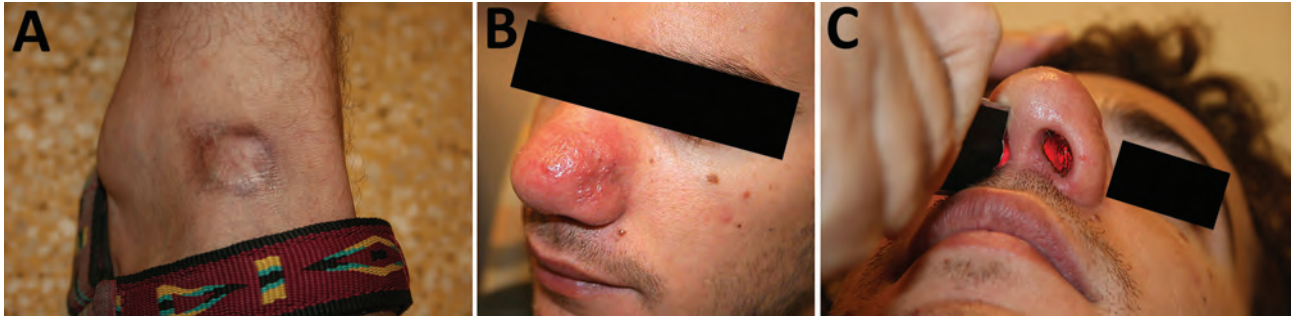


**Figure 3.** Cutaneous leishmaniasis and mucosal leishmaniasis in a traveler returning to Israel from Bolivia. A) Round hyperpigmented patch on the dorsum of right leg, representing old cutaneous leishmaniasis scar. B) Indurated erythematous patch of the nasal skin of the same patient appearing after 1 year. C) Illuminating in the right nostril sheds light into the left side, reflecting a hole within the nasal septum.

In our globalized world, ML should be considered in the differential diagnosis of granulomatous processes in biopsies taken from the nasopharynx, especially in returning travelers. Recent recommendations of the Infectious Diseases Society of America and the American Society of Tropical Medicine and Hygiene state that during all evaluations, persons at risk for ML should be questioned explicitly about the development, evolution, and other characteristics of mucosal symptoms (3). They should also undergo a thorough examination of the naso-oropharyngeal mucosa by an otolaryngologist even if they do not have any mucosal symptoms. These patients should be educated about the importance of seeking medical attention for possible ML if they ever develop persistent, atypical naso-oropharyngeal or laryngeal

manifestations that do not have a clear etiology. The policy at Sheba Medical Center is to check all patients with cutaneous *L. (V.) braziliensis* for ML.

The factors that affect progression to ML are not clear but likely relate to the infecting *Leishmania* species; *L. (V.) braziliensis* is the species most strongly associated with ML (3). Other postulated risk factors for the development of ML include large lesions, multiple CL lesions, presence of lesions for >4 months, micronutrient deficiency, immunosuppression (14,24), location of lesions above the waist (25,26), and concentration of lesions on the head and neck. The explanation for the relationship between ML and CL lesions on the head and neck is that the proximity of the CL lesions to the head increases risk for developing ML because of the shorter

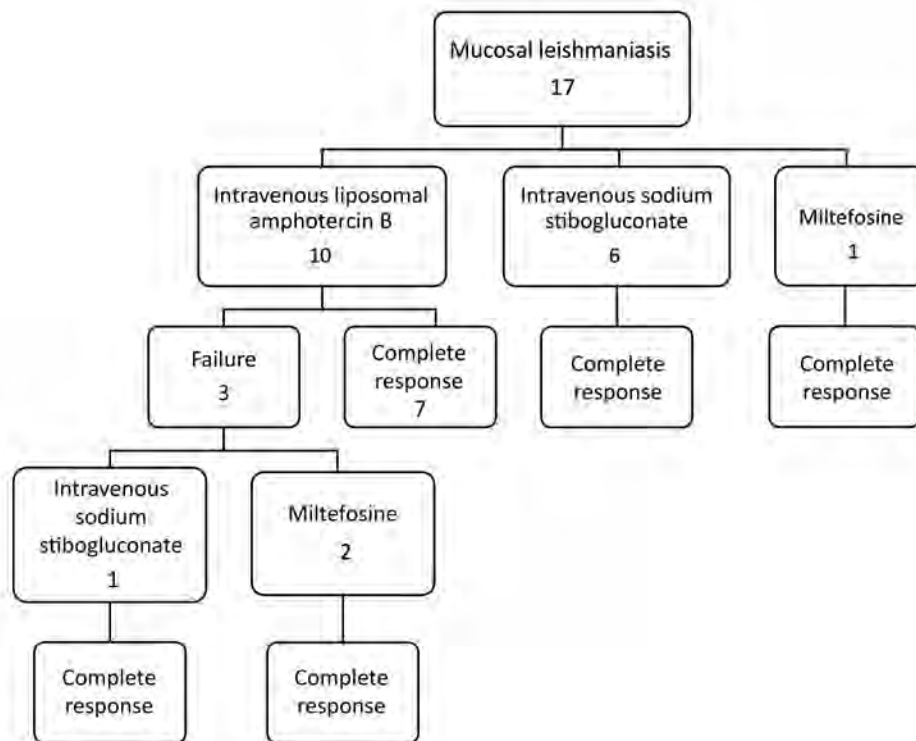


**Figure 4.** Treatment types and results for patients with mucosal leishmaniasis, Israel, 1993–2015.

distance that the parasite-laden macrophages must travel through lymphatic channels to reach the nasopharynx (25,26). However, in our series, none of these risk factors were found to be associated with progression to ML (Table 2). All our patients were young, healthy travelers with no evidence of impaired immunity and were negative for HIV.

One distinct risk factor is that CL patients without prior systemic treatment had a higher risk of developing ML (Figure 2). Of untreated patients, 41% developed ML, compared with 3.3% of treated patients. Thus, effective systemic treatment of New World CL caused by *Leishmania (Viannia)* species can decrease the risk for ML but may not prevent all cases of ML (3). As we mentioned, there was no failure of treatment of ML by IV SSG in our study, whereas 3 patients experienced failure of L-AmB treatment. However, this failure might be the result of a lower dosage; World Health Organization recently recommended 40–60 mg/kg of L-AmB, whereas our patients received the old regimen, which was about half this dose. We otherwise found no difference among the diverse regimens used for systemic treatment (i.e., IV L-AmB, IV SSG, oral miltefosine) in the outcome of the patients. Topical treatment is the most common treatment for Old World cutaneous leishmaniasis. For New World CL caused by *L. braziliensis* complex, topical treatment recently has been discussed as a treatment option. However, our findings recommend using only systemic treatment in this infection because of the risk of development of ML (27).

This study has several limitations. First, the cohort included 2 parts. The first part was a multicenter study from 8 medical centers in Israel, the second patients referred to our tertiary center. As a result, we may have seen more complicated cases of New World CL, including cases of ML. In addition, most of the Israeli patients were returning travelers from Bolivia, which is endemic for *L. (V.) braziliensis*. Therefore, our findings may not represent all New World CL species.

In summary, our findings support that prolonged clinical follow-up of travelers returning from Bolivia with CL is likely warranted. CL in travelers from this region should be managed with systemic therapy according to clinical guidelines (3,14). Furthermore, we noted a high rate of ML in travelers with CL caused by *L. (V.) braziliensis*. Systemic treatment for CL seems to be a protective factor against developing ML. A high index of suspicion is required for prompt diagnosis of ML and optimal management to prevent irreversible damage.

#### Acknowledgments

We thank Ilana Abu for her outstanding nursing support and Sara Lifshitz and Veronika Lagoda for their laboratory support.

C.L.J. holds the Michael and Penny Feiwel Chair of Dermatology, which funded this study in part.

#### About the Author

Dr. Solomon is senior dermatologist at the Chaim Sheba Medical Center, Tel Hashomer, Israel, working with the Center for Travel Medicine and Tropical Diseases. Her research interests include tropical dermatology, especially leishmaniasis.

#### References

1. Scope A, Trau H, Anders G, Barzilai A, Confino Y, Schwartz E. Experience with New World cutaneous leishmaniasis in travelers. *J Am Acad Dermatol*. 2003;49:672–8. [http://dx.doi.org/10.1067/S0190-9622\(03\)01576-7](http://dx.doi.org/10.1067/S0190-9622(03)01576-7)
2. Herwaldt BL. Leishmaniasis. *Lancet*. 1999;354:1191–9. [http://dx.doi.org/10.1016/S0140-6736\(98\)10178-2](http://dx.doi.org/10.1016/S0140-6736(98)10178-2)
3. Aronson N, Herwaldt BL, Libman M, Pearson R, Lopez-Velez R, Weina P, et al. Diagnosis and treatment of leishmaniasis: clinical practice guidelines by the Infectious Diseases Society of America (IDSA) and the American Society of Tropical Medicine and Hygiene (ASTMH). *Clin Infect Dis*. 2016;63:1539–57. <http://dx.doi.org/10.1093/cid/ciw742>
4. Ahluwalia S, Lawn SD, Kanagalingam J, Grant H, Lockwood DN. Mucocutaneous leishmaniasis: an imported infection among travellers to central and South America. *BMJ*. 2004;329:842–4. <http://dx.doi.org/10.1136/bmj.329.7470.842>
5. Camargo RA, Tuon FF, Sumi DV, Gebrim EM, Imamura R, Nicodemo AC, et al. Mucosal leishmaniasis and abnormalities on computed tomographic scans of paranasal sinuses. *Am J Trop Med Hyg*. 2010;83:515–8. <http://dx.doi.org/10.4269/ajtmh.2010.10-0081>
6. Miranda Lessa M, Andrade Lessa H, Castro TW, Oliveira A, Scherifer A, Machado P, et al. Mucosal leishmaniasis: epidemiological and clinical aspects. *Rev Bras Otorrinolaringol (Engl Ed)*. 2007;73:843–7. [http://dx.doi.org/10.1016/S1808-8694\(15\)31181-2](http://dx.doi.org/10.1016/S1808-8694(15)31181-2)
7. Jones TC, Johnson WD Jr, Barretto AC, Lago E, Badaro R, Cerf B, et al. Epidemiology of American cutaneous leishmaniasis due to *Leishmania braziliensis braziliensis*. *J Infect Dis*. 1987;156:73–83. <http://dx.doi.org/10.1093/infdis/156.1.73>
8. Figueroa RA, Lozano LE, Romero IC, Cardona MT, Prager M, Pacheco R, et al. Detection of *Leishmania* in unaffected mucosal tissues of patients with cutaneous leishmaniasis caused by *Leishmania (Viannia)* species. *J Infect Dis*. 2009;200:638–46. <http://dx.doi.org/10.1086/600109>
9. Marsden PD. Mucocutaneous leishmaniasis. *BMJ*. 1990;301:656–7. <http://dx.doi.org/10.1136/bmj.301.6753.656>
10. Lawn SD, Whetham J, Chiodini PL, Kanagalingam J, Watson J, Behrens RH, et al. New world mucosal and cutaneous leishmaniasis: an emerging health problem among British travellers. *QJM*. 2004;97:781–8. <http://dx.doi.org/10.1093/qjmed/hch127>
11. Scope A, Trau H, Bakon M, Yarom N, Nasereddin A, Schwartz E. Imported mucosal leishmaniasis in a traveler. *Clin Infect Dis*. 2003;37:e83–7. <http://dx.doi.org/10.1086/377045>
12. Mousoussan E, Nasereddin A, Jonas F, Schnur LF, Jaffe CL. Comparison of PCR assays for diagnosis of cutaneous leishmaniasis. *J Clin Microbiol*. 2006;44:1435–9. <http://dx.doi.org/10.1128/JCM.44.4.1435-1439.2006>
13. Van der Auwera G, Maes I, De Doncker S, Ravel C, Cnops L, Van Esbroeck M, et al. Heat-shock protein 70 gene sequencing for *Leishmania* species typing in European tropical infectious disease clinics. *Euro Surveill*. 2013;18:20543. <http://dx.doi.org/10.2807/1560-7917.ES2013.18.30.20543>

14. Blum J, Lockwood DN, Visser L, Harms G, Bailey MS, Caumes E, et al. Local or systemic treatment for New World cutaneous leishmaniasis? Re-evaluating the evidence for the risk of mucosal leishmaniasis. *Int Health*. 2012;4:153–63. <http://dx.doi.org/10.1016/j.inhe.2012.06.004>
15. Dimier-David L, David C, Muñoz M, Vargas F, Bustillos R, Valda L, et al. Epidemiological, clinical and biological features of mucocutaneous leishmaniasis in Bolivia after a 221 patient sample [in French]. *Bull Soc Pathol Exot*. 1993;86:106–11.
16. García AL, Parrado R, Rojas E, Delgado R, Dujardin JC, Reithinger R. Leishmaniasis in Bolivia: comprehensive review and current status. *Am J Trop Med Hyg*. 2009;80:704–11. <http://dx.doi.org/10.4269/ajtmh.2009.80.704>
17. David C, Dimier-David L, Vargas F, Torrez M, Dedet JP. Fifteen years of cutaneous and mucocutaneous leishmaniasis in Bolivia: a retrospective study. *Trans R Soc Trop Med Hyg*. 1993;87:7–9. [http://dx.doi.org/10.1016/0035-9203\(93\)90398-A](http://dx.doi.org/10.1016/0035-9203(93)90398-A)
18. Davies CR, Reithinger R, Campbell-Lendrum D, Feliciangeli D, Borges R, Rodriguez N. The epidemiology and control of leishmaniasis in Andean countries. *Cad Saude Publica*. 2000;16:925–50. <http://dx.doi.org/10.1590/S0102-311X2000000400013>
19. Costa JW Jr, Milner DA Jr, Maguire JH. Mucocutaneous leishmaniasis in a US citizen. *Oral Surg Oral Med Oral Pathol Oral Radiol Endod*. 2003;96:573–7. [http://dx.doi.org/10.1016/S1079-2104\(03\)00299-3](http://dx.doi.org/10.1016/S1079-2104(03)00299-3)
20. Lohuis PJ, Lipovsky MM, Hoepelman AI, Hordijk GJ, Huizing EH. *Leishmania braziliensis* presenting as a granulomatous lesion of the nasal septum mucosa. *J Laryngol Otol*. 1997;111:973–5. <http://dx.doi.org/10.1017/S0022215100139106>
21. Rosbotham JL, Corbett EL, Grant HR, Hay RJ, Bryceson AD. Imported mucocutaneous leishmaniasis. *Clin Exp Dermatol*. 1996;21:288–90. <http://dx.doi.org/10.1111/j.1365-2230.1996.tb00097.x>
22. Alcasis A, Abel L, David C, Torrez ME, Flandre P, Dedet JP. Risk factors for onset of cutaneous and mucocutaneous leishmaniasis in Bolivia. *Am J Trop Med Hyg*. 1997;57:79–84. <http://dx.doi.org/10.4269/ajtmh.1997.57.79>
23. Baddini-Caramelli C, Matayoshi S, Moura EM, Araf D, Santo R, Voegels R, et al. Chronic dacryocystitis in American mucocutaneous leishmaniasis. *Ophthal Plast Reconstr Surg*. 2001;17:48–52. <http://dx.doi.org/10.1097/00002341-200101000-00008>
24. Machado-Coelho GL, Caiaffa WT, Genaro O, Magalhães PA, Mayrink W. Risk factors for mucosal manifestation of American cutaneous leishmaniasis. *Trans R Soc Trop Med Hyg*. 2005;99:55–61. <http://dx.doi.org/10.1016/j.trstmh.2003.08.001>
25. Llanos Cuentas EA, Marsden PD, Cuba CC, Barreto AC, Campos M. Possible risk factors in development of mucosal lesions in leishmaniasis. *Lancet*. 1984;324:295. [http://dx.doi.org/10.1016/S0140-6736\(84\)90346-5](http://dx.doi.org/10.1016/S0140-6736(84)90346-5)
26. Osorio LE, Castillo CM, Ochoa MT. Mucosal leishmaniasis due to *Leishmania (Viannia) panamensis* in Colombia: clinical characteristics. *Am J Trop Med Hyg*. 1998;59:49–52. <http://dx.doi.org/10.4269/ajtmh.1998.59.49>
27. Añez N, Rojas A, Scorza-Dagert JV, Morales C. Successful treatment against American cutaneous leishmaniasis by intralesional infiltration of a generic antimonial compound–lidocaine combination. A follow up study. *Acta Trop*. 2018;185:261–6. <http://dx.doi.org/10.1016/j.actatropica.2018.06.001>

Address for correspondence: Eli Schwartz, The Center for Geographic Medicine and Department of Medicine C, The Chaim Sheba Medical Center, Tel Hashomer, 52621 Israel; email: elischwa@post.tau.ac.il

## etymologia revisited

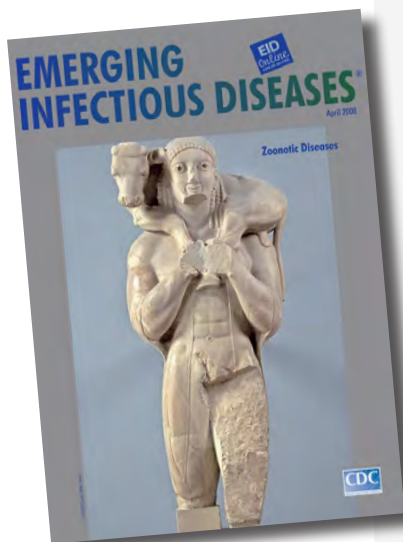
### *Leishmaniasis* [lēsh-ma'-ne-ə-sis]

Disease caused by protozoan parasites of the genus *Leishmania*, named in 1901 for British Army doctor William Leishman, who developed a stain to detect the agent. It is transmitted by the bite of certain species of sand fly, including the genus *Lutzomyia* in the New World and *Phlebotomus* in the Old World.

Leishmaniasis has 2 major forms: cutaneous, characterized by skin sores, and visceral, which affects internal organs and is characterized by high fever, substantial weight loss, swelling of the spleen and liver, and anemia.

If untreated, the disease is universally fatal within 2 years. Visceral leishmaniasis is also called kala-azar, a Hindi term meaning “black fever.” The causal agent, *Leishmania donovani*, was also named for physician Charles Donovan, who discovered the agent in India in 1903. An estimated 500,000 cases occur each year; India has the greatest number, followed by Bangladesh, Brazil, Nepal, and Sudan.

**Source:** Dorland’s illustrated medical dictionary, 31st edition. Philadelphia: Saunders; 2007; <http://www.time.com/time/magazine/article/0,9171,987111-6,00.html>; [zhttp://www.who.int/topics/leishmaniasis/en](http://www.who.int/topics/leishmaniasis/en)



Originally published  
in April 2008

[https://wwwnc.cdc.gov/eid/article/14/4/e1-1404\\_article](https://wwwnc.cdc.gov/eid/article/14/4/e1-1404_article)



---

# Tick-Borne Relapsing Fever in the White Mountains, Arizona, USA, 2013–2018

Neema Mafi, Hayley D. Yaglom, Craig Levy, Anissa Taylor, Catherine O'Grady, Heather Venkat, Kenneth K. Komatsu, Brentin Roller, Maria T. Seville, Shimon Kusne, John Leander Po, Shannon Thorn, Neil M. Ampel

Tick-borne relapsing fever (TBRF) is a bacterial infection transmitted by tick bites that occurs in several different parts of the world, including the western United States. We describe 6 cases of TBRF acquired in the White Mountains of Arizona, USA, and diagnosed during 2013–2018. All but 1 case-patient had recurrent fever, and some had marked laboratory abnormalities, including leukopenia, thrombocytopenia, hyperbilirubinemia, and elevated aminotransaminases. One patient had uveitis. Diagnosis was delayed in 5 of the cases; all case-patients responded to therapy with doxycycline. Two patients had Jarisch-Herxheimer reactions. The White Mountains of Arizona have not been previously considered a region of high incidence for TBRF. These 6 cases likely represent a larger number of cases that might have been undiagnosed. Clinicians should be aware of TBRF in patients who reside, recreate, or travel to this area and especially for those who sleep overnight in cabins there.

The White Mountains comprise a relatively dry, high-elevation region in the eastern part of Arizona that is in close proximity to Phoenix and Tucson, the 2 major metropolitan areas of Arizona, both of which are in lower-elevation deserts. Ranging from 6,000 feet (1,829 m) to >11,000 feet (>3,353 m) in elevation, the White Mountains are a place for recreation and respite for urban dwellers, particularly during the hot summer months, and many cabins and summer homes are located throughout the region. Persons who acquire illnesses in the White Mountains often seek

medical care in the desert metropolitan communities, and physicians there might not be aware of the differences in the diseases or their host habitats in these mountains compared with the lower-elevation deserts.

Tick-borne relapsing fever (TBRF) is a bacterial infection transmitted by tick bites. In the United States, TBRF most often occurs in western states and is usually transmitted by bites of *Ornithodoros* spp. ticks; *Borrelia hermsii* is thought to be the most common cause. We describe 6 cases of TBRF occurring over a 6-year period in persons who visited the White Mountains. Although infection probably was acquired in these mountains, given the timeframe of exposure to illness onset (all had plausible exposure within the ≈7-day incubation period), all cases were diagnosed in either Phoenix or Tucson. We suspect that these cases represent a small proportion of the total number of cases and would alert both clinicians and public health officials to the presence of TBRF in this area.

## The Case-Patients

### Case-Patient 1

A 34-year-old man with no prior medical history had fevers in early July 2013. One week before fever onset, he had spent time with his family in a privately owned cabin in Alpine, Arizona, in the White Mountains. Mice and ticks had been seen in the cabin, but the patient was not aware of any bites. Fevers reaching 39.9°C with chills, headache, arthralgias, and myalgias were reported. These symptoms persisted for ≈3 days, remitted for 3 days, and then recurred for the next 3.5 weeks. Laboratory evaluation of the patient 2 weeks after symptom onset was notable for mild anemia and markedly elevated C-reactive protein but normal leukocyte and platelet counts and aminotransaminases. After ≈25 days, the fevers stopped, but the patient noticed floaters and blurry vision in his right eye. In August, he was seen by a retinal expert in Phoenix, and anterior and posterior uveitis with optic nerve inflammation were noted.

---

Author affiliations: Mayo Clinic, Phoenix, Arizona, USA (N. Mafi, M.T. Seville, S. Kusne, N.M. Ampel); Arizona Department of Health Services, Phoenix (H.D. Yaglom, H. Venkat, K.K. Komatsu); Maricopa County Department of Public Health, Phoenix (C. Levy); Pima County Health Department, Tucson, Arizona, USA (A. Taylor, C. O'Grady); Centers for Disease Control and Prevention, Atlanta, Georgia, USA (H. Venkat); University of Arizona College of Medicine, Tucson (B. Roller, J.L. Po, N.M. Ampel); Northwest Hospital, Tucson (S. Thorn)

DOI: <https://doi.org/10.3201/eid2504.181369>

A Lyme ELISA serologic screening test result was positive, and Western blot revealed IgM bands of 23 and 41 kDa and negative IgG. A Lyme-specific rapid plasma reagin test was negative. An infectious diseases consultant recommended treatment for possible TBRF, and oral doxycycline (100 mg 2×/d) for 14 days was prescribed. The patient had complete resolution of his visual symptoms 2 months after completing antimicrobial therapy. Immunofluorescent serologic tests for *B. hermsii* conducted 9 weeks after symptom onset demonstrated an IgM titer of 1:64 and an IgG titer of 1:512.

### Case-Patient 2

A 64-year-old woman with a medical history of hypothyroidism and hypertension sought care at an emergency department in Tucson in late October 2016 because of a 10-day history of fevers with rigors, fatigue, body aches, and generalized malaise. The symptoms began on October 24, one day after she returned from her cabin in the White Mountains, where she had spent 10 days with her husband doing various recreational activities. The patient denied insect bites or stings. Physical examination revealed a well-appearing female in no acute distress with mild resting tachycardia, normal temperature, and right upper quadrant tenderness to palpation. Laboratory values were remarkable for a total leukocyte count of 2,900 cells/μL with normal differential, platelet count of 32,000/μL, total bilirubin of 2.3 mg/dL, alkaline phosphatase of 483 IU/L, alanine aminotransferase of 78 IU/L, and aspartate aminotransferase of 137 IU/L. The patient was admitted to the hospital, and a subsequent Wright-stain peripheral blood smear demonstrated numerous spirochete-like organisms on light microscopic examination (Figure 1). A Lyme disease screening test was positive. A diagnosis of TBRF was made based on the positive blood smear result with

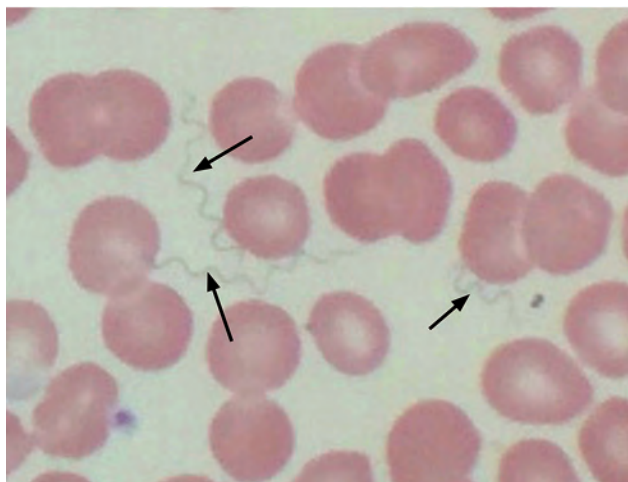


**Figure 1.** Wright stain of peripheral blood demonstrating extracellular spirochetes (arrows) confirming tick-borne relapsing fever in a 64-year-old woman, Tucson, Arizona, USA, October 2016.

matching clinical picture, and the patient was prescribed oral doxycycline (100 mg 2×/d) for 10 days. Within a few hours of receiving the first dose of doxycycline, she became hypotensive and hypoxic and required a 24-hour stay in the medical intensive care unit for supportive care. After her intensive care unit stay, she had a rapid and complete resolution of her symptoms and normalization of her laboratory values. Serum sent to the Centers for Disease Control and Prevention (CDC; Fort Collins, CO, USA) for Western blot assay against *B. hermsii* showed strongly positive results for both IgM and IgG.

### Case-Patient 3

A 72-year-old man with a medical history of hyperlipidemia and complete heart block requiring a permanent pacemaker spent ≈3 weeks at his cabin in the White Mountains near Greer, Arizona, doing outdoor cleaning in early June 2017. On June 22, he had onset of shaking chills and sought evaluation at a local emergency department, where sinusitis was diagnosed and amoxicillin prescribed. A temperature of 38.1°C was recorded. Several hours after taking a single dose of amoxicillin, he experienced severe rigors, prompting him to return to the emergency department. He was admitted to the hospital, where peripheral leukocyte count was 1,800 cells/μL, platelet count was 44,000/μL, total bilirubin was 2.3 mg/dL, and alanine aminotransferase was 78 IU/L. A peripheral blood smear demonstrated toxic granules in the neutrophils but no organisms. The patient improved without further antimicrobial therapy and was discharged home. One week later, he presented to an emergency department in Phoenix with recurrent fevers, fatigue, and rigors. A peripheral blood leukocytosis with lymphopenia was observed over several days. Because of positive coccidioidal serologic results, fluconazole was started; the patient was discharged home after his fevers resolved during hospital observation. He was seen 2 weeks later after a third episode of fever with rigors and was prescribed oral doxycycline (100 mg 2×/d). Within hours of the first doxycycline dose, he developed rigors, dizziness, and tachycardia and discontinued treatment. Subsequently, a PCR test for *B. miyamotoi* on whole blood yielded an indeterminate result. Doxycycline was restarted without further adverse effects, and the patient completed a 2-week course. Immunofluorescent serologic testing for *B. hermsii* demonstrated an IgG titer of 1:128. Serum sent to CDC for tickborne diseases was found to be positive by Western blot assay for *B. hermsii* IgM and IgG. The patient later recalled a possible insect or tick bite on his forearm during his stay at his cabin.

### Case-Patient 4

A previously healthy 4-year-old boy stayed in a cabin near Greer during the last week of May and the first week of

June 2017 and experienced 1 month of recurring fever, chills, sweats, body aches, and headaches beginning on June 5. Blood samples sent to CDC at 28 and 43 days after symptoms started demonstrated *B. hermsii* IgM and IgG by Western blot assay. The patient completed a course of doxycycline and completely recovered. During the investigation, local and state public health authorities learned of  $\geq 6$  other family members who visited the same cabin over a 2-year period, and all reported febrile illnesses. Only 1, case-patient 5, was tested for and diagnosed with TBRF.

#### Case-Patient 5

A 41-year-old man stayed in the same cabin as case-patient 4 from late May through early June 2017. On June 2, the man had onset of fever reaching 39.4°C with sweats, chills, headaches, fatigue, and dizziness. He visited healthcare providers multiple times during the month of June for evaluation of these symptoms. ELISA and Western blot tests for Lyme disease and coccidioidomycosis were positive. Finally, on August 30,  $\approx 12$  weeks after symptoms began, a serum sample sent to CDC was positive by Western blot assay for *B. hermsii* IgM and IgG. The patient was treated with doxycycline (100 mg 2 $\times$ /d), and his symptoms resolved.

#### Case-Patient 6

A 71-year-old woman with a medical history of hypertension, hypothyroidism, and past splenectomy for idiopathic thrombocytopenic purpura had sudden onset of fever, chills, generalized weakness, and myalgias in late July 2018, four days after visiting her family-owned cabin in Alpine. She subsequently sought care at an emergency department in Tucson. She had a temperature of 38.9°C and was found to be tachypneic, hypotensive, and hypoxemic. She was admitted to the intensive care unit, where it was noted that her initial peripheral leukocyte count was 11,400 cells/ $\mu$ L, platelet count was 39,000/ $\mu$ L, and serum creatinine was 2.7 mg/dL. Spirochetes were identified on peripheral blood smear by using light microscopic examination. During her hospital stay, the patient experienced acute respiratory failure and septic shock and required mechanical ventilation. A diagnosis of TBRF was made, and doxycycline (100 mg 2 $\times$ /d) was initiated for a total of 10 days. The patient improved and was discharged home. She recalled substantial rodent activity in the area of the cabin. No other persons staying at the cabin reported illness.

#### Discussion

Vector-associated illnesses are increasing in frequency across the United States (1). Compared with more common vectorborne illnesses such as Lyme borreliosis, Rocky Mountain spotted fever, tularemia, babesiosis, anaplasmosis, and ehrlichiosis, far less is known about TBRF, so much so that it has been described as a neglected disease (2).

TBRF typically manifests after a 7-day incubation period with recurring episodes of fever in association with headache, myalgias, and other nonspecific symptoms lasting for  $\approx 3$  days and separated by afebrile periods of  $\approx 7$  days' duration. In the United States, *B. hermsii* is thought to be the most common cause of TBRF, and transmission is associated with the bite of soft *O. hermsi* ticks. *Ornithodoros* spp. ticks usually feed at night on rodents, such as tree squirrels and chipmunks, but might choose to feed on human hosts, particularly when the rodent population has been cleared from the local habitat. Feeding is rapid, and most persons who are bitten are not aware of a tick bite. Cabins are a typical site to acquire infection. In addition, soft ticks can live up to 10 years; this long lifespan means that once a cabin or building is infested, it can remain a source of human infection for years unless steps are taken to find and remove rodent infestations and eradicate the ticks. The risk for reinfection for any 1 person has not been calculated; however, repeated exposures, especially at the same sites as initial infection, are possible (3).

The 6 cases we describe occurred among persons inhabiting cabins in the White Mountains of Arizona during the late spring to early fall months. All but 1 person sought care with recurrent fever as their primary complaint; some had profound laboratory abnormalities, including leukopenia, thrombocytopenia, hyperbilirubinemia, and elevated aminotransaminases. One patient had organ-specific disease (uveitis). All case-patients responded promptly to doxycycline therapy; 2 had Jarisch-Herxheimer reactions in association with antimicrobial therapy, a phenomenon previously described (4). Two case-patients had positive serologic results for coccidioidomycosis, which were likely coincidental, given the relatively high incidence of this fungal infection in the desert regions of Arizona (5). The positive tests for Lyme borreliosis were likely attributable to cross-reactivity, as has been previously noted (6).

TBRF in Arizona has been described in the past around or near the Grand Canyon (7–9), several hundred miles from the site of these 6 cases (Figure 2). Apache County, the location of the 2013–2018 cases we have described, has been considered to be a comparatively low-incidence area for TBRF (3).

Unfortunately, no epidemiologic or environmental assessments were performed in these 6 cases. Although the benefits of conducting such studies are recognized, these studies were not performed here primarily because the cases were episodic. Limited resources of the local public health jurisdictions and lack of compliance from cabin owners also contributed. If future cases occur, such assessments would be useful to define whether *B. hermsii* is indeed the cause of the syndromes observed and to better define the



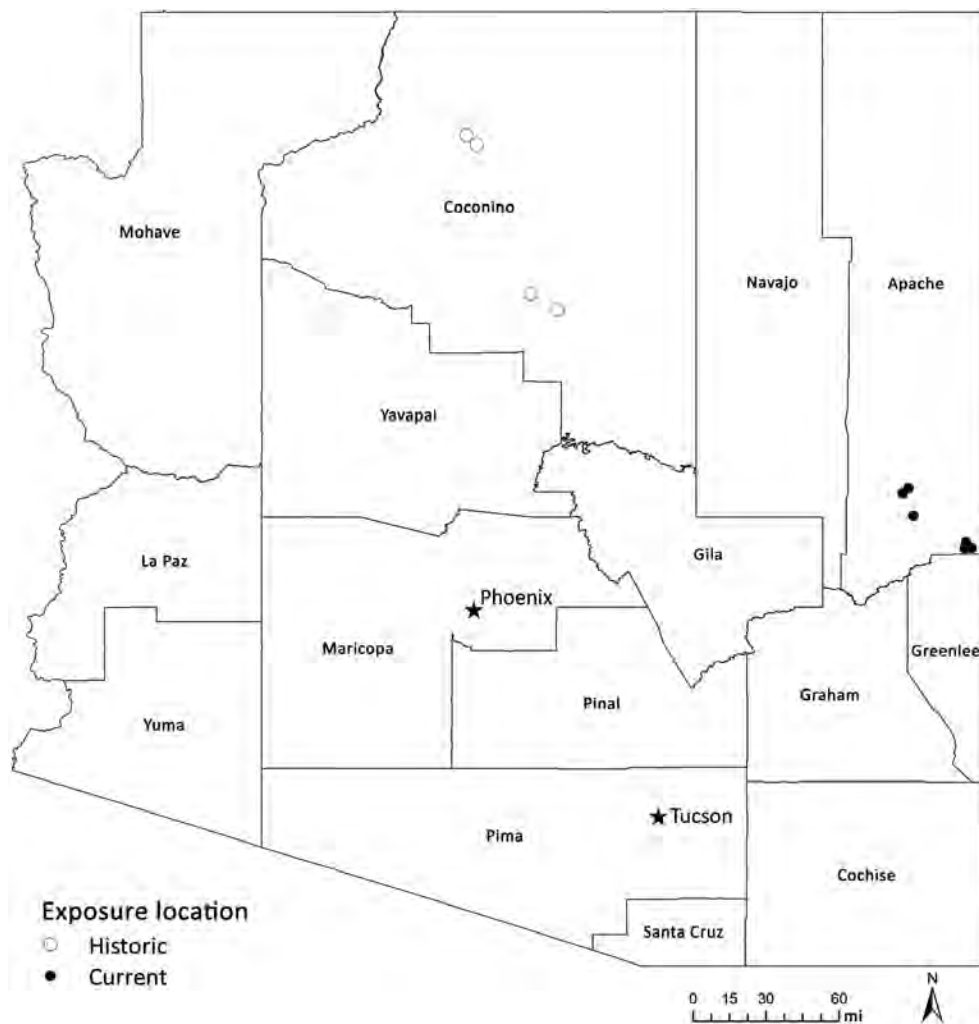


**Figure 2.** Exposure location for historic (1973–2014) tick-borne relapsing fever outbreaks in Coconino County and 6 current (2013–2018) cases in the White Mountains region, Arizona, USA.

ecologic, environmental, and epidemiologic parameters of the disease.

In Arizona, TBRF is a reportable disease by physicians to the local health department according to 2018 Arizona statutes (AR9-6-202). Although TBRF is not a nationally notifiable condition, prompt reporting of TBRF cases was required in  $\geq 12$  states in 2016 (Arizona, California, Colorado, Idaho, Montana, North Dakota, Nevada, New Mexico, Oregon, Texas, Utah, and Washington). Because of frequent travel by US residents, healthcare providers should report cases to the appropriate state or local health department; prompt reporting by clinicians has been critical to the identification and control of several outbreaks. For example, in 2014, a local Arizona hospital notified the Coconino County Public Health Services District (Flagstaff) of a cluster of 5 students with fever, headache, and myalgia who had attended the same camp; the ensuing investigation led to identification of an outbreak of 10 cases of TBRF among a high school football team who had attended an outdoor education camping trip in northern Arizona (9).

The first case of TBRF in Arizona was reported in 1930, involving an exposure near Greer, similar to the 6 cases we have described. In that instance, after staying in the area for 18 days during the summer, a 37-year-old man had repeated bouts of fever with interval periods of well-being lasting several days. During 1 febrile attack, which occurred  $>1$  month after symptoms began, a blood smear demonstrated spirochetes. The patient received an arsenic injection, and his fevers resolved (10).

Far more cases of TBRF probably have occurred recently in the White Mountains than the 6 reported here. Unlike previous recent reports from other parts of Arizona (7–9), the cases we report were not epidemic and therefore could have been easily missed. Therefore, physicians practicing in areas that serve this region should be aware of TBRF and consider the diagnosis when a patient has a nonspecific febrile illness, particularly when that illness is recurrent. In addition, all healthcare providers should assess travel history in patients who have nonspecific febrile illnesses and should consider diseases related to specific

travel exposures. In addition to being able to recognize TBRF, healthcare providers in Arizona should be vigilant for other zoonotic diseases that could result from local exposures, such as hantavirus from deer mice, plague from fleas and prairie dogs, and Rocky Mountain spotted fever transmitted from brown dog ticks.

CDC laboratory testing for TBRF was performed at the Division of Vector-Borne Diseases, National Center for Emerging and Zoonotic Infectious Diseases, Fort Collins, CO, USA. Antibody titers were not provided as part of this testing.

### About the Author

Dr. Mafi is a second-year fellow in infectious diseases at the Mayo Clinic in Phoenix, Arizona. His primary research interests include endemic infectious diseases.

### References

1. Rosenberg R, Lindsey NP, Fischer M, Gregory CJ, Hinckley AF, Mead PS, et al. Vital signs: trends in reported vectorborne disease cases—United States and territories, 2004–2016. *MMWR Morb Mortal Wkly Rep*. 2018;67:496–501. <http://dx.doi.org/10.15585/mmwr.mm6717e1>
2. Talagrand-Reboul E, Boyer PH, Bergström S, Vial L, Boulanger N. Relapsing fevers: neglected tick-borne diseases. *Front Cell Infect Microbiol*. 2018;8:98. <http://dx.doi.org/10.3389/fcimb.2018.00098>
3. Dworkin MS, Schwan TG, Anderson DE Jr, Borchardt SM. Tick-borne relapsing fever. [viii.]. *Infect Dis Clin North Am*. 2008;22:449–68, viii. <http://dx.doi.org/10.1016/j.idc.2008.03.006>
4. Koton Y, Bisharat N. Tick-borne relapsing fever with severe Jarisch-Herxheimer reaction. *Isr Med Assoc J*. 2018;20:62–3.
5. Centers for Disease Control and Prevention. Increase in reported coccidioidomycosis—United States, 1998–2011. *MMWR Morb Mortal Wkly Rep*. 2013;62:217–21.
6. Magnarelli LA, Anderson JF, Johnson RC. Cross-reactivity in serological tests for Lyme disease and other spirochetal infections. *J Infect Dis*. 1987;156:183–8. <http://dx.doi.org/10.1093/infdis/156.1.183>
7. Boyer KM, Munford RS, Maupin GO, Pattison CP, Fox MD, Barnes AM, et al. Tick-borne relapsing fever: an interstate outbreak originating at Grand Canyon National Park. *Am J Epidemiol*. 1977;105:469–79. <http://dx.doi.org/10.1093/oxfordjournals.aje.a112406>
8. Paul WS, Maupin G, Scott-Wright AO, Craven RB, Dennis DT. Outbreak of tick-borne relapsing fever at the North Rim of the Grand Canyon: evidence for effectiveness of preventive measures. *Am J Trop Med Hyg*. 2002;66:71–5. <http://dx.doi.org/10.4269/ajtmh.2002.66.71>
9. Jones JM, Hranac CR, Schumacher M, Horn K, Lee DM, Terriquez J, et al. Tick-borne relapsing fever outbreak among a high school football team at an outdoor education camping trip, Arizona, 2014. *Am J Trop Med Hyg*. 2016;95:546–50. <http://dx.doi.org/10.4269/ajtmh.16-0054>
10. Bannister K. Relapsing fever (febris recurrens, Ruckfallfieber, spirillum fever, tick fever). *Southwest Med*. 1930;14:581–2.

Address for correspondence: Neil M. Ampel, SAVAHCS, Medical Service (1-111), 3601 S Sixth Ave, Tucson, AZ 85723, USA; email: [nampel@email.arizona.edu](mailto:nampel@email.arizona.edu)



Ticks transmit a variety of different pathogens including bacteria, protozoa, and viruses which can produce serious and even fatal disease in humans and animals. Tens of thousands of cases of tickborne disease are reported each year, including Lyme disease. See the EID Lyme Disease Spotlight. Lyme disease is the most well-known tickborne disease. However, other tickborne illnesses such as Rocky Mountain spotted fever, tularemia, babesiosis, and ehrlichiosis also contribute to severe morbidity and more mortality each year.

Symptoms of tickborne disease are highly variable, but most include sudden onset of fever, headache, malaise, and sometimes rash. If left untreated, some of these diseases can be rapidly fatal.



<https://wwwnc.cdc.gov/eid/page/tick-spotlight>

**EMERGING  
INFECTIOUS DISEASES**

# Lobomycosis in Soldiers, Colombia

Claudia M. Arenas,<sup>1</sup> Gerzain Rodriguez-Toro, Andrea Ortiz-Florez, Ingrid Serrato

Lobomycosis is a disease that is endemic to the Amazon rainforest and is caused by the still uncultured fungus *Lacazia loboi*. This disease occurs in loggers, farmers, miners, fishermen, and persons living near coastal rivers of this region. We report 6 soldiers in Colombia in whom lobomycosis developed after military service in the Amazon area. The patients had nodular and keloid-like lesions on the face, neck, trunk, and limbs. The duration of illness ranged from 2 years to 15 years. The initial diagnosis was leishmaniasis on the basis of clinical manifestations and direct smear results, but biopsies confirmed the final diagnosis of lobomycosis. Treatment with surgical excision, itraconazole and clofazimine was satisfactory. However, the follow-up time was short. Healthcare professionals responsible for the diagnosis and treatment of skin diseases need to be able to recognize the clinical signs of lobomycosis and differentiate them from those of cutaneous leishmaniasis.

Lobomycosis (lacaziosis) is a chronic subcutaneous mycosis caused by the still uncultured fungus *Lacazia loboi* (1). Clinical manifestations of this disease are pleomorphic: papules; nodules; and wart-like, ulcerated, and keloid-like lesions located on exposed and cooler areas of the body, particularly the lower limbs and ears (2–7). Lesions might be single or multiple and are classified in localized or disseminated forms according to their distribution (7).

Lobomycosis was first described in 1931 by Jorge Lobo in a 48-year-old man who lived in the Brazilian Amazon and for the previous 19 years had had keloidal nodules in the lumbar region (8). Human lobomycosis has been reported in other countries in South America (Brazil, Colombia, Venezuela, and Peru); ≈500 cases have been reported (2–7). Several names have been used to describe this disease, including lobomycosis, keloidal blastomycosis, Amazonian blastomycosis, Jorge Lobo disease, and lacaziosis. Lacaziosis was named in honor of the Brazil mycologist Carlos da Silva Lacaz, a mycology expert who along with Baruzzi and Rosa published a book that covers all aspects of the disease before 1986 (2). This disease affects men in 88% of cases (7) likely because it is believed to be related

to occupational exposure, especially in forest loggers, rubber tappers, hunters, miners, fishermen, and agricultural workers, as well as residents of the Amazon basin, and indigenous populations in Brazil and Colombia (2–7,9–12). In Manaus, Brazil, lacaziosis was the most common fungal infection in the Brazilian Amazon; it accounted for 50 (42%) of 119 cases (11). Dolphins are the only other animals that have this disease (13–17). The habitats for *L. loboi* are humid forest areas with temperatures 24°C–32°C, large rivers, and coastal waters. Inoculation of *L. loboi* is through the skin is by trauma; for this reason, lacaziosis is considered a mycosis of implantation (14,17).

Diagnosis is difficult and often delayed. In a study of 249 cases diagnosed in the state of Acre, Brazil (7), diagnoses were delayed by an average of 19 years because the organism grows slowly and produces no major symptoms other than mild pruritus or pain if there is trauma in the lesion. Another reason for delayed diagnosis is that patients do not regularly seek medical services or consult healthcare professionals. *L. loboi* has not been cultured, although it is abundant in lesions. Thus, a diagnosis is made by skin biopsy showing a large number of yeasts of uniform size and thick cell walls that form chains linked by thin bridges that are shown by staining with methenamine silver (2,4,9,18). Direct smear and exfoliative cytologic analysis are fast, inexpensive, and accurate diagnostic techniques because they detect abundant numbers of yeast (19,20). We report 6 soldiers in Colombia who acquired lobomycosis when stationed in a jungle area because of military activities.

## Case-Patients

### Case-Patient 1

A 28-year-old soldier reported a 2-year history of confluent erythematous papules with a smooth surface, which formed a plaque resembling a keloid scar, located on the middle third of the right leg (Figure 1, panel A). These lesions appeared while he was patrolling in the rain forest. A direct smear of the lesion resulted in a diagnosis of cutaneous leishmaniasis. He was treated with N-methyl glucamine for 20 days but showed no improvement.

The patient was later referred to the Central Military Hospital in Bogota, Colombia. A skin biopsy specimen

Author affiliations: Hospital Militar Central, Bogota, Colombia (C.M. Arenas, I. Serrato); Universidad del la Sabana, Chia, Colombia (G. Rodriguez-Toro); Fundacion Universitaria Sanitas, Bogota (A. Ortiz-Florez)

DOI: <https://doi.org/10.3201/eid2504.181403>

<sup>1</sup>Current affiliation: Hospital Universitario Centro Dermatologico Federico Lleras Acosta, Bogota, Colombia.



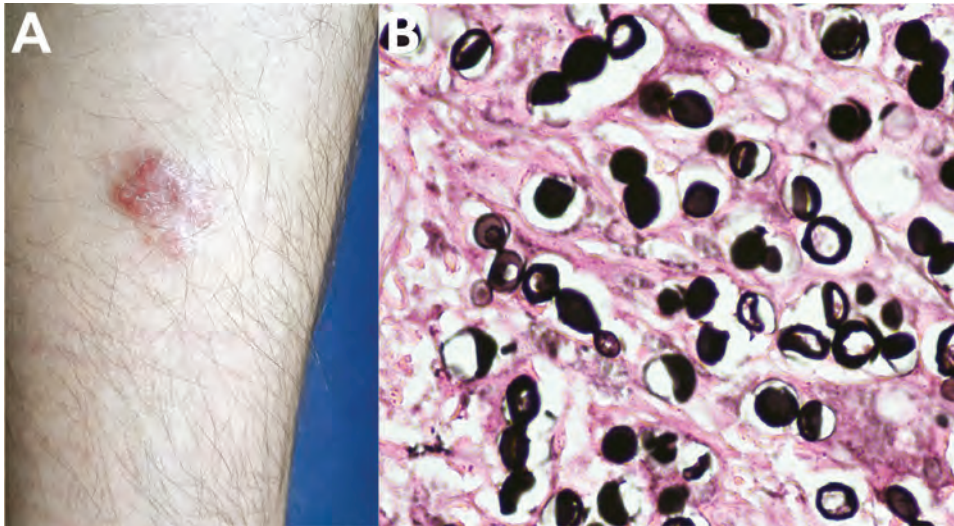


**Figure 1.** Lobomycosis in a 28-year-old soldier (case-patient 1), Colombia. A) Erythematous papules that became confluent and formed an infiltrated plaque with keloidal aspect, smooth surface, located on the middle third of the right leg. B) Grocott-Gomori staining of a biopsy specimen from the lesion shows chains of yeast, some of them in the budding process. Periodic acid–Schiff stain shows yeast of uniform size with a thick cell wall and clear cytoplasm (original magnification  $\times 40$ ).

showed dermal granulomatous inflammation with giant cells and histiocytes and numerous rounded, thick-walled mycotic structures, some with budding and formation of chains of  $\leq 4$  cells. Results of staining with periodic acid–Schiff and Gomori methenamine silver were positive for fungi (Figure 1, panel B). The final diagnosis was lobomycosis. Surgical resection of the lesion was performed, and the infection showed no recurrence at 6 months' follow-up.

#### Case-Patient 2

A 41-year-old soldier from a rural area reported a 15-year history of an ulcerated skin lesion in the sternal notch, which he reported was caused by an insect bite. A direct smear for *Leishmania* spp. was reported as showing a positive result. He was treated with N-methyl glucamine for 20 days, and showed complete healing of the lesion. Eight months later, he relapsed and was treated again with N-methyl glucamine for 20 days and showed complete healing. Two months later, he had a keloid plaque in the sternal notch, which was interpreted as a keloid scar that was treated with intralesional triamcinolone acetonide injections; no improvement was observed.

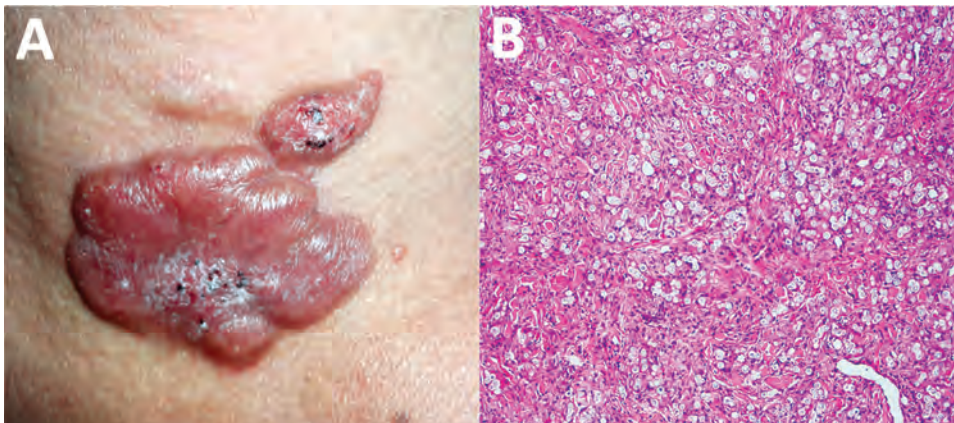


**Figure 2.** Lobomycosis in a 41-year-old soldier (case-patient 2), Colombia. A) Erythematous, lobulated plaque (4 cm  $\times$  2.5 cm) on the sternal notch with hematic crust and black areas on the surface. B) Periodic acid–Schiff staining of a biopsy specimen from the lesion shows the dermis occupied by diffuse, inflammatory granulomata with chains of yeasts (original magnification  $\times 10$ ).

Simultaneously, an acral lentiginous melanoma developed on the second toe of his left foot; an inguinal sentinel node was also positive for melanoma. He was treated by amputation of the first 2 toes and chemotherapy. However, during treatment, the keloid lesion in the sternal notch increased in size. The patient was then referred to the dermatology department of the Central Military Hospital.

Physical examination showed a lobulated, erythematous plaque (4 cm  $\times$  2.5 cm) with a smooth surface with some hematic crust and black areas on the surface (Figure 2, panel A). The suggested diagnoses were metastatic melanoma, lobomycosis, or chromomycosis. A skin biopsy specimen showed typical lobomycosis (Figure 2, panel B). The patient did not receive any treatment for this mycosis; he died as a result of widespread melanoma disease.

#### Case-Patient 3

A 36-year-old soldier reported a 3-year history of a shiny, erythematous, slow-growing, brown nodule with a smooth surface and firm consistency (diameter 1 cm) on the fifth finger of the left hand (Figure 3, panel A). He had no history of trauma and was asymptomatic. A skin biopsy specimen

showed typical features of lobomycosis (Figure 3, panel B). Surgical excision was performed, and he was prescribed oral itraconazole (100 mg /d) for 3 months. There was no recurrence of the lesion after a 1-year follow-up.

#### Case-Patient 4

A 30-year-old soldier reported a 3-year history of an asymptomatic, euchromic, lobed plaque with a smooth and shiny surface on the left cheek (Figure 4, panel A). Slow growth of this lesion became apparent after an insect bite. A direct smear was positive for *Leishmania* spp., and he was given N-methyl glucamine for 20 days. He showed no improvement and was given a second cycle of this drug. A skin biopsy specimen indicated lobomycosis (Figure 4, panel B).

Surgery for the lesion was performed, and the patient was prescribed itraconazole (100 mg/d) for 6 months and clofazimine (50 mg/d) for 6 months. After a 6-month follow-up, he had a recurrence of the lesion. A wide local excision was performed, and he was prescribed oral itraconazole (100 mg/d) for 3 months. He showed no recurrence of the lesion after a 6-month follow-up.

#### Case-Patient 5

A 32-year-old soldier reported a 5-year history of a euchromic nodule (4 cm × 3.5 cm) resembling a keloid scar with a smooth and shiny surface and progressive growth on the right arm (Figure 5, panel A). The patient had no history of trauma and was asymptomatic.

Microscopic findings and staining with periodic acid–Schiff and Gomory methenamine silver showed a diffuse dermal infiltrate of macrophages containing *L. loboi* (Figure 5, panel B). Complete excision was performed. He showed no recurrence of the lesion after a 3-month follow-up.

#### Case-Patient 6

A 24-year-old soldier reported a 2-year history of a keloid-like asymptomatic lesion that slowly increased in size on the right forearm. Physical examination showed an infiltrated, erythematous, violaceous, nonpainful plaque (4 cm × 3 cm)

with a shiny surface (Figure 6, panel A). He had a history of cutaneous leishmaniasis in the right hand and had been treated with N-methyl glucamine for 20 days. After seeing no improvement, a second treatment cycle was prescribed.

The patient showed resolution and formation of a scar 4 years later. Histologic analysis showed macrophages and giant cells, numerous yeast structures of uniform size and thickness, refringence of the cell wall, and chains resembling rosary beads. Staining with periodic acid–Schiff and Grocott was positive for fungi (Figure 6, panel B). Surgical resection was performed, and remission of the lesion was observed at a 6-month follow-up.

#### Discussion

In Colombia, lobomycosis occurs in Amoruas and Motilones aboriginal communities in the Amazon and Orinoco regions and in black persons in the Pacific Coast regions of Cauca and Choco (3,9,21,22). The presence of this disease in soldiers from Colombia who are stationed in jungle or forest regions is a unique situation in which all factors (tropical climate, temperature, humidity, rainfall) related to an optimal habitat for the fungus are present (2–7,17,21,22).

Lobomycosis is found in Central and South America (Mexico, Costa Rica, Panama, Venezuela, Colombia, Guyana, Bolivia, Suriname, Ecuador, and Peru) (2–7). Cases that develop outside the Amazon region need an ecology similar to that of jungle areas (3–7,23). Rare cases have been reported in North America and Europe in persons who have traveled to countries in South America (24–28). However, 2 cases have occurred in persons outside Central and South America who had no history of travel: 1 in a young man who reported swimming in South Africa (29) and 1 in a farmer (woman) who lived in a river basin in Greece (30).

The natural reservoir of *L. loboi* is believed to be aquatic or associated with soil and vegetation. Transmission of this fungus occurs by skin trauma after incubation periods of months to decades. The initial lesion is a papule at the site of local trauma that typically progresses slowly and shows different clinical manifestations. It has also been

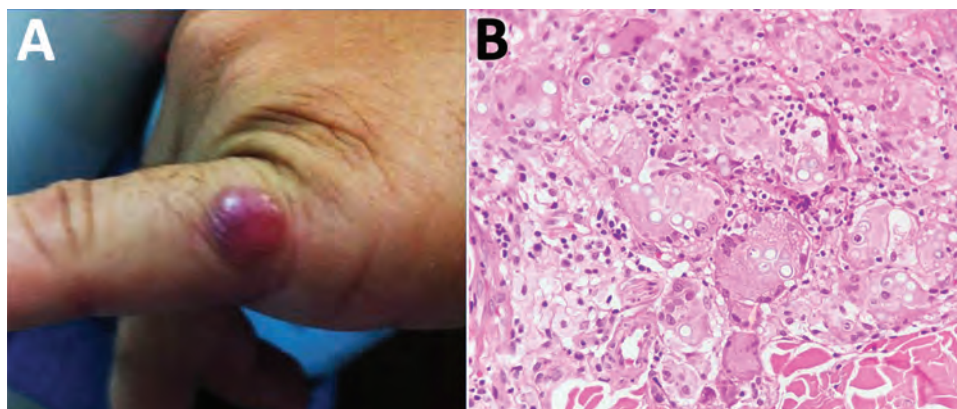


**Figure 3.** Lobomycosis in a 36-year-old soldier (case-patient 3), Colombia. A) Solitary erythematous-violaceous nodule with a shiny surface and firm consistency (diameter 1 cm) located on the fifth finger of the left hand. B) Hematoxylin and eosin staining of a biopsy specimen from the lesion shows giant cells and numerous yeast structures (original magnification ×20).



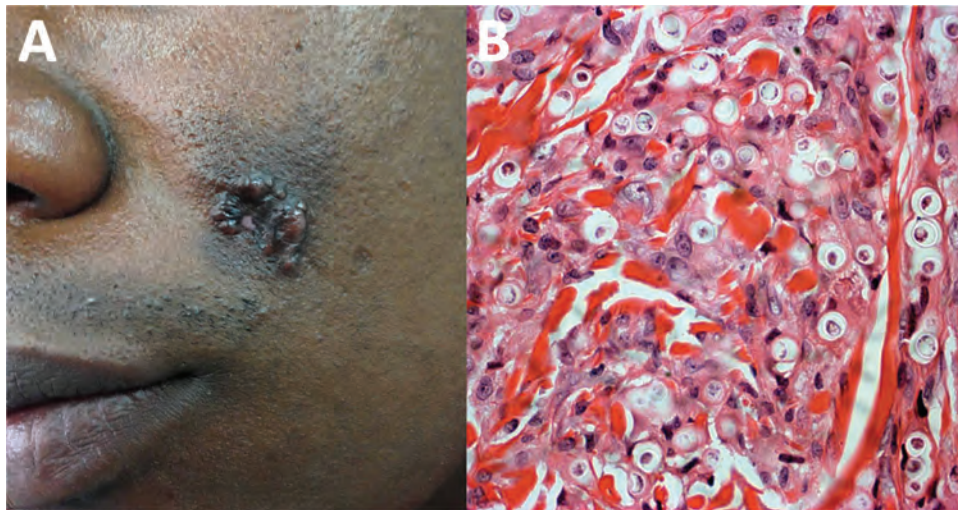


**Figure 4.** Lobomycosis in a 30-year-old soldier (case-patient 4), Colombia. A) Phototype V lesion on the left cheek with papules that became confluent and formed a lobulated plaque with a smooth and shiny surface. B) Periodic acid–Schiff staining of a biopsy specimen from the lesion shows multiple yeasts of uniform size, and thick walls are seen inside phagocytoses (original magnification  $\times 40$ ).

suggested that inoculation of the fungus into tissues can occur through insect bites, as reported by 2 of the soldiers in our study, or by snake bite trauma or helix trauma caused by a fish bone (2,6–9,13,17).

The most common manifestation of lobomycosis is a nodular keloid appearance with slow insidious onset. Case-patients also have macules, plaques, and infiltrative lesions, and as the disease progresses, lesions become verrucous and can ulcerate secondary to trauma (2–13). The lesion might remain localized, single or multiple, confluent in the same region, or can disseminate and become diffuse over several areas of the body (2–13). The 6 soldiers reported localized, circumscribed, nodular, and keloid lesions and chronic evolution, which are the most usual manifestations in 60% of case-patients. Case-patient 4 had a lesion on the face, which is present in only 7% of case-patients, and case-patient 2 had a lesion on the neck, which is present in only 1% of case-patients (7,10,12,31).

The time of evolution for the lesions of the 6 soldiers ranged from 2 to 15 years, which confirms the chronicity of this infection. Other reported case-patients have had evolution times of 35 to 64 years (7,17,31,32). Regional lymph nodes can be affected, but systemic dissemination is

rare. Progression of lobomycosis might lead to deformities affecting quality of life and decreasing work productivity of case-patients (17).

Impaired cellular immune responses cause chronicity of lesions and facilitate the abundance of fungus inside lesions (30%–50% of fungal cells are viable) (33). Macrophages infiltrated by *L. loboi* have increased levels of transforming growth factor- $\beta$  (an interleukin that inhibits expression  $\gamma$ -interferon and nitric oxide), which suppresses the lytic activity of macrophages and promotes fibrosis production, which contributes to the keloid appearance of lesions (34). The inflammatory infiltrate has few lymphocytes and contains neutrophils that are active against the fungus (35). There are no plasmacytoid dendritic cells to promote the Th1 response for antigen presentation and migration to lymph nodes (36). Blood and lymph vessels are decreased in lesions (37). Nodular lesions have cellular components that result in more active immune response cells and less active cells in infiltrative keloids and wart-like and disseminated lesions (38).

Three of the soldiers received diagnoses of leishmaniasis after direct observations of specimens by microscopy. These patients received antileishmanial treatment that

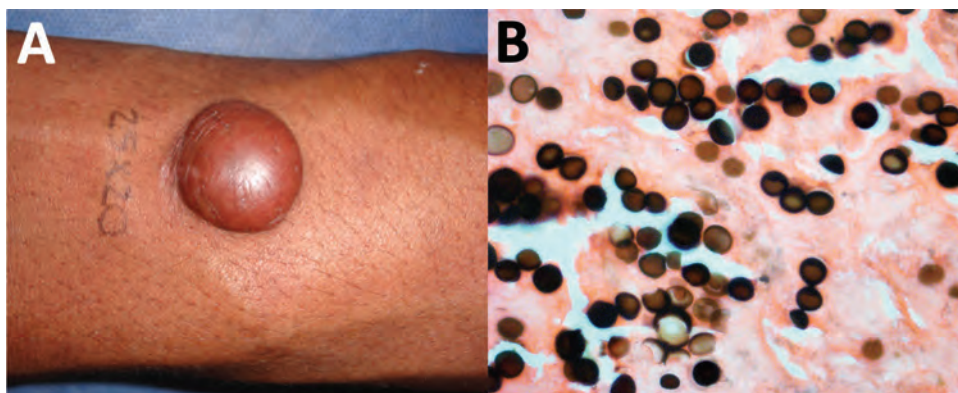


**Figure 5.** Lobomycosis in a 32-year-old soldier (case-patient 5), Colombia. A) Solitary yeast erythematous nodule (4 cm  $\times$  3.5 cm) resembling a keloid scar with a smooth and shiny surface on the right arm. B) Grocott staining of a biopsy specimen from the lesion shows typical chains (original magnification  $\times 40$ ).



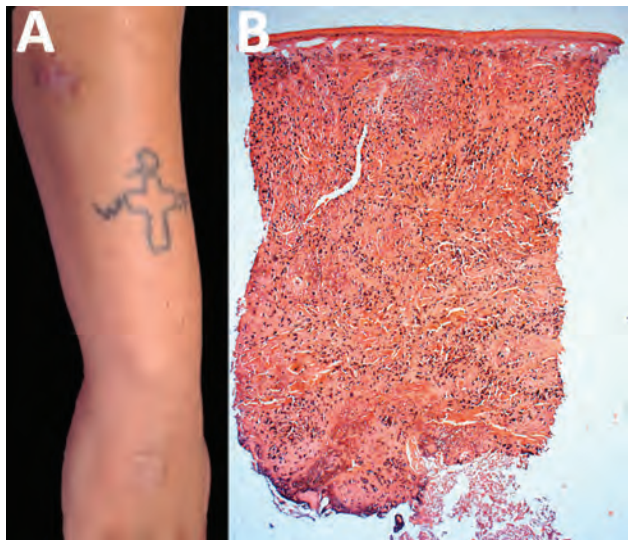


**Figure 6.** Lobomycosis in a 24-year-old soldier (case-patient 6), Colombia. A) Erythematous-violaceous infiltrated plaque (4 cm x 3 cm) with a shiny surface on the right forearm and typical leishmaniasis cicatricial plaque on the same limb. B) Testing of biopsy sample from the lesion. Epidermis shows no hyperplasia or ulceration, but dermis shows diffuse inflammation rich in vacuolated macrophages; Grocott-Gomori staining shows yeast cells (original magnification  $\times 2.5$ ).

resulted in healing for 1 of the patients, suggesting that this patient actually had leishmaniasis. Thus, *L. loboi* could have been implanted on the scar caused by leishmaniasis. A similar condition occurred in a patient in Brazil (31). Lobomycosis has been associated in the same patient with other diseases, such as ringworm, leprosy, paracoccidioidomycosis, chromomycosis, and leishmaniasis (7,13,31), as in case-patient 6 in our study.

Identification of amastigotes in the direct smear for 3 of these soldiers can also be attributed to common geographic areas for leishmaniasis and lobomycosis. During 2004–2012, >50,000 cases of leishmaniasis were reported worldwide (39), many of which were related to combat and destruction of illicit crops. Another reason for detection of lobomycosis and leishmaniasis in the same patient is that health professionals performing cytologic analysis in rural areas do not have enough experience identifying agents other than *Leishmania* spp.

The biopsy specimens of the 6 case-patients confirmed the diagnosis; these specimens showed granulomatous inflammation without abscesses and large numbers of phagocytized yeast of uniform size that formed chains linked by tiny and thin bridges (3,18,40). Once these manifestations are observed, the diagnosis of lobomycosis should not be confused with other diseases. Molecular taxonomy was used to identify an imported case of lobomycosis in a traveler from Europe who visited the Amazon region of Venezuela (41). However, in disease-endemic countries, the

diagnosis should include clinical and microscopic results because molecular diagnosis might not be available (42,43).

Lobomycosis can be confused with other cutaneous diseases. Other diagnoses include cutaneous leishmaniasis, as occurred for 2 of the soldiers, as well as diffuse leishmaniasis, chromomycosis, sporotrichosis, lepromatous or tuberculoid dimorphic leprosy, mycetoma, phaeohyphomycosis, pyoderma, Kaposi sarcoma, sarcoidosis, keloid scars, histiocytosis of Langerhans cells, melanoma, dermatofibrosarcoma, lymphoma, squamous cell carcinoma, and cutaneous metastases (3,17,40,41). Thus, a skin biopsy is necessary to confirm the diagnosis.

Cutaneous leishmaniasis is the most common condition in the differential diagnosis for lobomycosis, especially if the lobomycosis is ulcerated, which is a frequent complication. Four case-patients with lobomycosis, 1 of whom died, were reported to have squamous cell carcinomas (3,44). However, the acrolentiginous melanoma that resulted in the death of case-patient 2 in our report was not related to lobomycosis. Lobomycosis has been reported to occasionally affect the regional lymph nodes (3,45). However, even when disseminated, cutaneous forms do not affect the mucosa or internal organs. Rare spread of lobomycosis to the testes was reported in a case-patient in Costa Rica (3).

Although surgical excision with wide margins is the most recommended treatment for isolated lobomycosis lesions, relapses still occur, as for case-patient 4. Electrocautery and cryosurgery are alternative options. However, there are no effective antimycotic drugs for lobomycosis (17,46).

In Manaus, Brazil, where lobomycosis has been the most common deep mycosis, clofazimine (200 mg/d for 13 months) resulted in improvement in 22 patients (31). This drug might have contributed to healing of leprosy lesions and concomitant lobomycosis for patients in Acre, Brazil, who had completed multidrug therapy for leprosy (7). Rifampin has also shown effective antimycotic activity (17). Itraconazole (100 mg d) and clofazimine (100 mg/d) resulted in healing of an extensive plaque on the face of a woman, who did have recurrent clinical or histological lesions after 3 years of follow-up (47).

We have used itraconazole and surgery treatment for other patients and have observed good results, although the follow-up time should be years. One of the patients we studied showed recurrence of a lesion 10 years after it was removed (30), and a woman who showed remission of a plaque on her face after treatment with itraconazole and clofazimine showed recurrence after 8 years of apparent cure (11). Posaconazole (400 mg 2 $\times$ /d for 27 months) resulted in curing of a patient with lobomycosis in Peru who had a long-lasting lesion (27 years) in the ear (47). In addition, analysis of several genomic DNA sequences and of molecular data showed that cutaneous granulomas in

dolphins were caused by a novel *Paracoccidioides* species (48,49). Those results suggest that a novel, uncultivated strain of *P. brasiliensis* restricted to cutaneous lesions is probably the cause of lacaziosis/lobomycosis in dolphins; however, more research is needed for confirmation.

In conclusion, we report 6 soldiers of the National Army of Colombia who had localized lobomycosis with nodular and keloid-like lesions, acquired while on duty in the Amazonian forests of eastern Colombia in the departments of Caqueta, Meta, and Guaviare, and a jungle area in Montes de Maria in the department of Bolivar. These findings indicate a new and unique epidemiologic situation. Clinical diagnoses and direct smear results were suggestive of cutaneous leishmaniasis for 3 of these case-patients. However, biopsy led to an accurate diagnosis of lobomycosis. Surgery was successful treatment for 3 of the case-patients. Health personnel of the Armed Forces of Colombia, including physicians, bacteriologists, and pathologists, should become better acquainted with this disease to improve its diagnosis and treatment.

### Acknowledgments

We thank Maria Isabel Gonzalez for providing assistance with dermatologic analysis and Angel Jaimes, Carlos Avellaneda, Giovanni Manrique, and Claudia Cruz for providing patient information.

### About the Author

Dr. Arenas is a professor and leader of the Leishmaniasis Program at Hospital Universitario Centro Dermatologico Federico Lleras Acosta, Bogota, Colombia. Her research interests include the epidemiology of tropical infectious diseases.

### References

1. Tabora PR, Tabora VA, McGinnis MR. *Lacazia loboi* gen. nov., comb. nov., the etiologic agent of lobomycosis. *J Clin Microbiol*. 1999;37:2031–3.
2. Lacaz CS, Baruzzi RG, Rosa MC. Jorge Lobo disease [in Portuguese]. Sao Paulo: Editora da USP-IPISIS Grafica e Editora; 1986.
3. Rodriguez-Toro G. Lobomycosis. *Int J Dermatol*. 1993;32:324–32. <http://dx.doi.org/10.1111/j.1365-4362.1993.tb01466.x>
4. De Brito AC, Quaresma JA. Lacaziose (Jorge Lobo's disease): review and update [in Portuguese]. *Anais Brasileiros de Dermatologia*. 2007;82:461–74. <http://dx.doi.org/10.1590/S0365-05962007000500010>
5. Ramos-E-Silva M, Aguiar-Santos-Vilela F, Cardoso-de-Brito A, Coelho-Carneiro S. Lobomycosis. Literature review and future perspectives. *Actas Dermosifiliogr*. 2009;100(Suppl 1):92–100. [http://dx.doi.org/10.1016/S0001-7310\(09\)73173-4](http://dx.doi.org/10.1016/S0001-7310(09)73173-4)
6. Lupi O, Tying SK, McGinnis MR. Tropical dermatology: fungal tropical diseases. *J Am Acad Dermatol*. 2005;53:931–51, quiz 952–4. <http://dx.doi.org/10.1016/j.jaad.2004.10.883>
7. Woods WJ, Belone Ade F, Carneiro LB, Rosas PS. Ten years experience with Jorge Lobo's disease in the state of Acre, Amazon region, Brazil. *Rev Inst Med Trop Sao Paulo*. 2010;52:273–8. <http://dx.doi.org/10.1590/S0036-46652010000500010>
8. Lobo J. A case of blastomycosis produced by a new species found in Recife [in Portuguese]. *Rev Med Pernamb*. 1931;1:763–75.
9. Rodriguez-Toro G, Téllez N. Lobomycosis in Colombian Amer Indian patients. *Mycopathologia*. 1992;120:5–9. <http://dx.doi.org/10.1007/BF00578495>
10. Baruzzi RG, Lacaz CS, Souza PA. Natural history of Jorge Lobo's disease. Occurrence among Indians Caiabi (central Brazil) [in Portuguese]. *Revista do Instituto de Medicina Tropical de Sao Paulo*. 1979;21:302–38.
11. Talhari S, Talhari C. Lobomycosis. *Clin Dermatol*. 2012;30:420–4. <http://dx.doi.org/10.1016/j.clindermatol.2011.09.014>
12. Talhari S, Cunha MG, Schettini AP, Talhari AC. Deep mycoses in Amazon region. *Int J Dermatol*. 1988;27:481–4. <http://dx.doi.org/10.1111/j.1365-4362.1988.tb00925.x>
13. Opromolla DV, Tabora PR, Tabora VB, Viana S, Furtado JF. Lobomycosis: report of 40 new cases [in Portuguese]. *Anais Brasileiros de Dermatologia*. 1999;74:135–41.
14. Bermudez L, Van Bresse M-F, Reyes-Jaimes O, Sayegh AJ, Paniz-Mondolfi AE. Lobomycosis in man and lobomycosis-like disease in bottlenose dolphin, Venezuela. *Emerg Infect Dis*. 2009;15:1301–3. <http://dx.doi.org/10.3201/eid1508.090347>
15. Murdoch ME, Reif JS, Mazzoil M, McCulloch SD, Fair PA, Bossart GD. Lobomycosis in bottlenose dolphins (*Tursiops truncatus*) from the Indian River Lagoon, Florida: estimation of prevalence, temporal trends, and spatial distribution. *EcoHealth*. 2008;5:289–97. <http://dx.doi.org/10.1007/s10393-008-0187-8>
16. Reif JS, Mazzoil MS, McCulloch SD, Varela RA, Goldstein JD, Fair PA, et al. Lobomycosis in Atlantic bottlenose dolphins from the Indian River Lagoon, Florida. *J Am Vet Med Assoc*. 2006;228:104–8. <http://dx.doi.org/10.2460/javma.228.1.104>
17. Paniz-Mondolfi A, Talhari C, Sander Hoffmann L, Connor DL, Talhari S, Bermudez-Villapol L, et al. Lobomycosis: an emerging disease in humans and delphinidae. *Mycoses*. 2012;55:298–309. <http://dx.doi.org/10.1111/j.1439-0507.2012.02184.x>
18. Opromolla D, Belone A, Tabora P, Tabora V. Clinicopathological correlation in 40 new cases of lobomycosis [in Portuguese]. *Anais Brasileiros de Dermatol*. 2000;75:425–34.
19. Talhari C, Chrusciak-Talhari A, de Souza JV, Araújo JR, Talhari S. Exfoliative cytology as a rapid diagnostic tool for lobomycosis. *Mycoses*. 2009;52:187–9. <http://dx.doi.org/10.1111/j.1439-0507.2008.01551.x>
20. Miranda MF, Silva AJ. Vinyl adhesive tape also effective for direct microscopy diagnosis of chromomycosis, lobomycosis, and paracoccidioidomycosis. *Diagn Microbiol Infect Dis*. 2005;52:39–43. <http://dx.doi.org/10.1016/j.diagmicrobio.2005.02.008>
21. Rodriguez-Toro G. New Colombian cases of lobomycosis [in Spanish]. *Biomedica*. 1994;14:239–41. <http://dx.doi.org/10.7705/biomedica.v14i4.2110>
22. Rodriguez Toro G. Jorge Lobo's disease or keloid blastomycosis. New aspects of the entity in Colombia: review [in Spanish]. *Biomedica*. 1989;9:133–46. <http://dx.doi.org/10.7705/biomedica.v9i3-4.1985>
23. Paniz-Mondolfi AE, Reyes Jaimes O, Dávila Jones L. Lobomycosis in Venezuela. *Int J Dermatol*. 2007;46:180–5. <http://dx.doi.org/10.1111/j.1365-4632.2007.02937.x>
24. Symmers WS. A possible case of Lobo's disease acquired in Europe from a bottle-nosed dolphin (*Tursiops truncatus*). *Bull Soc Pathol Exot Filiales*. 1983;76:777–84.
25. Burns RA, Roy JS, Woods C, Padhye AA, Warnock DW. Report of the first human case of lobomycosis in the United States. *J Clin Microbiol*. 2000;38:1283–5.
26. Elsayed S, Kuhn SM, Barber D, Church DL, Adams S, Kasper R. Human case of lobomycosis. *Emerg Infect Dis*. 2004;10:715–8. <http://dx.doi.org/10.3201/eid1004.030416>

27. Arju R, Kothadia JP, Kaminski M, Abraham S, Giashuddin S. Jorge Lobo's disease: a case of keloidal blastomycosis (lobomycosis) in a nonendemic area. *Ther Adv Infect Dis*. 2014;2:91–6. <http://dx.doi.org/10.1177/2049936114559919>
28. Saint-Blancard P, Maccari F, Le Guyadec T, Lanternier G, Le Vagueresse R. Lobomycosis: a mycosis seldom observed in metropolitan France [in French]. *Ann Pathol*. 2000;20:241–4.
29. Al-Daraji WI, Husain E, Robson A. Lobomycosis in African patients. *Br J Dermatol*. 2008;159:234–6. <http://dx.doi.org/10.1111/j.1365-2133.2008.08586.x>
30. Papadavid E, Dalamaga M, Kapniari I, Pantelidaki E, Papageorgiou S, Pappa V, et al. Lobomycosis: a case from southeastern Europe and review of the literature. *J Dermatol Case Rep*. 2012;6:65–9. <http://dx.doi.org/10.3315/jjdr.2012.1104>
31. Talhari S, Cunha MG, Barros ML, Gadelha AD. Jorge Lobo disease. Study of 22 new cases [in Spanish]. *Med Cutan Ibero Lat Am*. 1981;9:87–96.
32. Cáceres S, Rodríguez-Toro G. Lobomycosis; 35 years of evolution [in Spanish]. *Rev Soc Col Dermatol*. 1991;1:43–5.
33. Vilani-Moreno FR, Opromolla DV. Determination of the viability of *Paracoccidioides loboi* in biopsies of patients with Jorge Lobo's disease [in Portuguese]. *Anais Brasileiros de Dermatol*. 1997;72:433–7.
34. Xavier MB, Libonati RM, Unger D, Oliveira C, Corbett CE, de Brito AC, et al. Macrophage and TGF- $\beta$  immunohistochemical expression in Jorge Lobo's disease. *Hum Pathol*. 2008;39:269–74. <http://dx.doi.org/10.1016/j.humpath.2007.06.016>
35. Vilani-Moreno FR, Belone AF, Soares CT, Opromolla DV. Immunohistochemical characterization of the cellular infiltrate in Jorge Lobo's disease. *Rev Iberoam Micol*. 2005;22:44–9. [http://dx.doi.org/10.1016/S1130-1406\(05\)70006-1](http://dx.doi.org/10.1016/S1130-1406(05)70006-1)
36. Pagliari C, Kanashiro-Galo L, Silva AA, Barboza TC, Criado PR, Duarte MI, et al. Plasmacytoid dendritic cells in cutaneous lesions of patients with chromoblastomycosis, lacaziosis, and paracoccidioidomycosis: a comparative analysis. *Med Mycol*. 2014;52:397–402. <http://dx.doi.org/10.1093/mmy/myt026>
37. Quaresma JA, Brito MV, Sousa JR, Silva LM, Hirai KE, Araujo RS, et al. Analysis of microvasculature phenotype and endothelial activation markers in skin lesions of lacaziosis (lobomycosis). *Microb Pathog*. 2015;78:29–36. <http://dx.doi.org/10.1016/j.micpath.2014.11.013>
38. Oliveira Carneiro FR, da Cunha Fischer TR, Brandão CM, Pagliari C, Duarte MI, Quaresma JA. Disseminated infection with *Lacazia loboi* and immunopathology of the lesional spectrum. *Hum Pathol*. 2015;46:334–8. <http://dx.doi.org/10.1016/j.humpath.2014.10.016>
39. Alvar J, Vélez ID, Bern C, Herrero M, Desjeux P, Cano J, et al.; WHO Leishmaniasis Control Team. Leishmaniasis worldwide and global estimates of its incidence. *PLoS One*. 2012;7:e35671. <http://dx.doi.org/10.1371/journal.pone.0035671>
40. Jeunon T, de Jesus Barreto Rodrigues PA, Rocha TC, de Oliveira Bezerra M, Galhardo MC, do Valle AC. Multiple confluent reddish nodules. *Dermatol Pract Concept*. 2013;3:15–20. <http://dx.doi.org/10.5826/dpc.0303a05>
41. Beltrame A, Danesi P, Farina C, Orza P, Perandin F, Zanardello C, et al. Case report: molecular confirmation of lobomycosis in an Italian traveler acquired in the Amazon region of Venezuela. *Am J Trop Med Hyg*. 2017;97:1757–60. <http://dx.doi.org/10.4269/ajtmh.17-0446>
42. Araújo MG, Cirilo NS, Santos SN, Aguilar CR, Guedes AC. Lobomycosis: a therapeutic challenge. *An Bras Dermatol*. 2018;93:279–81. <http://dx.doi.org/10.1590/abd1806-4841.20187044>
43. Vilela R, Mendoza L, Rosa PS, Belone AF, Madeira S, Opromolla DV, et al. Molecular model for studying the uncultivated fungal pathogen *Lacazia loboi*. *J Clin Microbiol*. 2005;43:3657–61. <http://dx.doi.org/10.1128/JCM.43.8.3657-3661.2005>
44. Nogueira L, Mendes L, Rodrigues CA, Santos M, Talhari S, Talhari C. Lobomycosis and squamous cell carcinoma. *An Bras Dermatol*. 2013;88:293–5. <http://dx.doi.org/10.1590/S0365-05962013000200024>
45. Opromolla DV, Belone AF, Taborda PR, Rosa PS. Lymph node involvement in Jorge Lobo's disease: report of two cases. *Int J Dermatol*. 2003;42:938–41. <http://dx.doi.org/10.1111/j.1365-4632.2003.01982.x>
46. Francesconi VA, Klein AP, Santos AP, Ramasawmy R, Francesconi F. Lobomycosis: epidemiology, clinical presentation, and management options. *Ther Clin Risk Manag*. 2014;10:851–60. <http://dx.doi.org/10.2147/TCRM.S46251>
47. Fischer M, Chrusciak Talhari A, Reinell D, Talhari S. Successful treatment with clofazimine and itraconazole in a 46 year old patient after 32 years duration of disease [in German]. *Hautarzt*. 2002;53:677–81. <http://dx.doi.org/10.1007/s00105-002-0351-y>
48. Bustamante B, Seas C, Salomon M, Bravo F. Lobomycosis successfully treated with posaconazole. *Am J Trop Med Hyg*. 2013;88:1207–8. <http://dx.doi.org/10.4269/ajtmh.12-0428>
49. Vilela R, Bossart GD, St Leger JA, Dalton LM, Reif JS, Schaefer AM, et al. Cutaneous granulomas in dolphins caused by novel uncultivated *Paracoccidioides brasiliensis*. *Emerg Infect Dis*. 2016;22:2063–9. <http://dx.doi.org/10.3201/eid2212.160860>

---

Address for correspondence: Andrea Ortiz-Florez, Fundacion Universitaria Sanitas, Calle 169 #16, c-70, Bogota 111161, Colombia; email: andreortiz07@gmail.com



# Cost-effectiveness of Latent Tuberculosis Infection Screening before Immigration to Low-Incidence Countries

Jonathon R. Campbell, James C. Johnston, Victoria J. Cook, Mohsen Sadatsafavi, R. Kevin Elwood, Fawziah Marra

Prospective migrants to countries where the incidence of tuberculosis (TB) is low (low-incidence countries) receive TB screening; however, screening for latent TB infection (LTBI) before immigration is rare. We evaluated the cost-effectiveness of mandated and sponsored preimmigration LTBI screening for migrants to low-incidence countries. We used discrete event simulation to model preimmigration LTBI screening coupled with postarrival follow-up and treatment for those who test positive. Preimmigration interferon-gamma release assay screening and postarrival rifampin treatment was preferred in deterministic analysis. We calculated cost per quality-adjusted life-year gained for migrants from countries with different TB incidences. Our analysis provides evidence of the cost-effectiveness of preimmigration LTBI screening for migrants to low-incidence countries. Coupled with research on sustainability, acceptability, and program implementation, these results can inform policy decisions.

The World Health Organization (WHO) has continued working toward tuberculosis (TB) elimination, aiming to reduce the overall TB burden by  $\approx 90\%$  to  $<1$  case/1 million persons in countries where TB incidence is low (low-incidence countries) (1). Meeting this target will require new and innovative strategies. Typically, the TB burden in low-incidence countries is highest among populations born abroad;  $\approx 70\%$  of TB cases occur in these populations in Canada, the United States, and much of Europe (2). For the most part, TB prevention in these populations has focused on identifying persons with active TB before immigration to reduce transmission after arrival. Stagnant rates of TB suggest additional methods are required to accelerate declines in TB incidence (3).

---

Author affiliations: University of British Columbia, Vancouver, British Columbia, Canada (J.R. Campbell, J.C. Johnston, V.J. Cook, M. Sadatsafavi, R.K. Elwood, F. Marra); British Columbia Centre for Disease Control, Vancouver (J.C. Johnston, V.J. Cook, R.K. Elwood)

DOI: <https://doi.org/10.3201/eid2504.171630>

Universal or targeted postarrival screening for latent TB infection (LTBI) has been suggested as a method to accelerate the decline of TB (4); however, domestic LTBI programs exhibit suboptimal performance (5), are resource intensive (6), and may not be cost-effective (7). One major reason for the reduced effectiveness of postarrival LTBI screening programs is the substantial attrition in the LTBI cascade of care. More than half of patients do not reach the point of initiating treatment, which results in fewer than one fifth completing treatment (5).

Currently, most immigrant-receiving, low-incidence countries employ mandatory preimmigration medical exams (8). As part of these medical exams, a chest radiograph and medical evaluation are performed to detect TB disease before arrival or identify those who may be at increased risk for TB disease in the future; these costs are borne by the patient within their country of origin. Only a select few countries employ some form of mandated LTBI screening (8), and data are scarce on the yield of such programs.

A report sponsored by the US Centers for Disease Control and Prevention (Atlanta, GA, USA) suggested mandatory LTBI screening and treatment as part of routine preimmigration medical exams (9); however, this strategy was viewed as inequitable and unjustly coercive (10) and has never been employed. Alternatively, mandating and fully sponsoring only LTBI screening as a formal part of the immigration process would avoid such ethics quandaries and could substantially reduce postarrival TB incidence. Preimmigration screening coupled with postarrival follow-up could improve the yield of LTBI screening programs  $>2$ -fold (5), because all case-patients reporting postarrival would already have completed LTBI screening.

We evaluated the cost-effectiveness of mandating and fully sponsoring LTBI screening in prospective migrants as part of routine preimmigration medical exams, coupled with passive postarrival follow-up and treatment. We evaluated 6 strategies among migrants from 4 different TB incidence groups to determine the optimal strategy in each group for this intervention.

## Methods

### Model Overview

We chose discrete event simulation for this model because of its flexibility in varying transition times between health states in a single simulation, ability to simulate simultaneous events, and capability to model several different patient covariates. These advantages make it preferable to traditional Markov models and enable the creation of a highly representative cohort in a single simulation (11). We modeled new migrants, which in this evaluation refers specifically to persons who have been granted permanent resident status but have not yet become citizens of the countries they reside in. Of interest were migrants from countries belonging to 4 distinct TB incidence categories: low, <30 cases/100,000 persons/year; moderate,  $\geq 30$  and <100 cases/100,000 persons/year; high,  $\geq 100$  and <200 cases/100,000 persons/year; and very high,  $\geq 200$  cases/100,000 persons/year.

We further defined the 4 populations of interest by 4 covariates: patient age, bacillus Calmette-Guérin (BCG) vaccination status, chest radiograph results, and LTBI prevalence. Patient age was defined based on an age distribution of a reference cohort of permanent residents to Canada in 2014 (12). BCG vaccination was determined through presence of a universal BCG vaccination policy in each country of origin and adjusted by 36-year average BCG vaccine uptake (13–15). For chest radiograph, a reference cohort of permanent residents who came to Ontario during 2002–2011 was used to identify prevalence of abnormal chest radiograph results (15). LTBI prevalence was calibrated in each population using 2-year TB incidence in permanent resident cohorts to Ontario during 2002–2011 (15) and age-adjusted using the results of a meta-analysis of test-positive rates (16).

We estimated LTBI prevalence using several assumptions. First, we assumed that 85% of incident TB resulted from reactivation of LTBI (17); second, that TB reactivation did not change over time post arrival (18); and last, that LTBI prevalence approximately matched reported rates of interferon-gamma release assay (IGRA) positivity in persons from each of the 4 TB incidence categories (16). In sum, an LTBI reactivation rate of 1.1 cases/1,000 person-years approximated literature values and yielded reasonable estimates of LTBI prevalence (17).

The model evaluates implementation of the intervention: preimmigration LTBI screening coupled with postarrival follow-up and treatment. The base case in this model was considered to be preimmigration TB screening without any evaluation for LTBI before or after arrival but with routine postarrival follow-up for those flagged through TB screening. We calibrated baseline TB incidence estimates and rates of postarrival follow-up to TB

incidence data in permanent resident cohorts to Ontario during 2002–2011 (15). We considered 3 preimmigration LTBI screening options and 2 postarrival LTBI treatment options, for a total of 6 unique strategies to compare with the base case (Table 1).

We screened migrants with a tuberculin skin test (TST), IGRA, or sequential screening, in which persons testing positive by TST were given a confirmatory IGRA. We defined a positive TST result as an induration measuring  $\geq 10$  mm and a positive IGRA result using manufacturer's recommendations, with IGRA performance being a composite measure of results from commercially available products (19–21). Although preimmigration testing was mandated, postarrival follow-up and treatment was not mandated and instead assumed to be passive, following published rates of postarrival follow-up in several countries (22). That is, in migrants who tested positive for LTBI, it was recommended that they attend a clinic for treatment postarrival, but no system was in place to enforce this. Those who reported for care postarrival would be treated with 9 months of isoniazid or 4 months of rifampin.

The model took a healthcare system perspective for the fully sponsored and mandated preimmigration LTBI screening: all LTBI screening costs preimmigration, along with typical postarrival costs, were the responsibility of the receiving country's healthcare system. We used a 3% annual discount rate for costs and outcomes (23) and a 25-year time horizon from arrival. The main outcomes of the model were quality-adjusted life-years (QALYs), number of TB cases, and costs per 1,000 permanent residents from each of the 4 populations analyzed. These data were used to calculate the cost-effectiveness ratio, a measure that indicates the cost per additional QALY gained by an intervention strategy compared with the base case (Appendix, <https://wwwnc.cdc.gov/EID/article/25/4/17-1630-App1.pdf>).

A simplified model structure is displayed in Figure 1. In the intervention, migrants were given an LTBI diagnostic test along with the rest of their medical exam; those who tested positive were referred for postarrival follow-up. Those who complied with postarrival follow-up were recommended for LTBI therapy. After initiating treatment, they either completed treatment in full, partially completed treatment, or ceased due to an adverse event that may result in death. After treatment, results for all patients were simulated to the 25-year time horizon, with annual risks of TB reactivation and death.

We made the following assumptions in the model. Those with previous TB or an abnormal chest radiograph result identified during the preimmigration medical exam were also referred for postarrival follow-up. With the intervention, all those who began screening completed it,

**Table 1.** Intervention strategies for screening and treatment of latent TB infection in immigrants\*

Intervention strategy	Preimmigration	Postarrival if test is positive
Base case	TB screening as part of routine preimmigration medical exams, consisting of a chest radiograph, medical history, and symptom screen. If diagnosed with TB, treatment must be completed before immigrating.	Routine follow-up of those with abnormal chest radiograph results or previous TB.
TST/INH	In addition to the base case, a TST is performed at the time of the medical exam. If the result is positive (induration $\geq 10$ mm) referral is made for follow-up postarrival. If the TST result is negative, no further action is taken.	Recommendation for follow-up; if patient reports for follow-up, 9-month course of INH.
TST/RIF	Same as above.	Recommendation for follow-up; at follow-up, 4-month course of RIF.
IGRA/INH	In addition to the base case, an IGRA is placed at the time of the medical exam. If the result is positive (as defined by the manufacturer) referral is made for follow-up postarrival. If the IGRA result is negative, no further action is taken. If the IGRA result is indeterminate, a second is performed; a second consecutive indeterminate is treated as a negative.	Recommendation for follow-up; if patient reports for follow-up, 9-month course of INH.
IGRA/RIF	Same as above.	Recommendation for follow-up; if patient reports for follow-up, 4-month course of RIF.
SEQ/INH	In addition to the base case, a TST is placed at the time of the medical exam. If the result is positive (as defined by an induration $\geq 10$ mm) a second test is performed with an IGRA. If the subsequent IGRA result is positive (as defined by the manufacturer) referral is made for follow-up postarrival. If the initial TST is negative or if the subsequent IGRA is negative, no further action is taken. If the IGRA result is indeterminate, a second is performed; a second consecutive indeterminate is treated as a negative.	Recommendation for follow-up; at follow-up, 9-month course of INH.
SEQ/RIF	Same as above.	Recommendation for follow-up; at follow-up, 4-month course of RIF.

\*No intervention required for migrants with negative results of base case screening. IGRA, interferon-gamma release assay; INH, isoniazid; RIF, rifampin; SEQ, sequential screening; TB, tuberculosis TST, tuberculin skin test.

eliminating dropout during this stage of the LTBI cascade of care. Drug-resistant TB and self-cure of LTBI were not modeled. It was assumed that all those who tested positive were offered LTBI treatment to limit extrapolation of care provider decisions. All reactivation TB cases had a 17.6% chance of causing a secondary case; further transmission was not modeled (Appendix). Modeling was completed in Simio version 8.146.14121 (Simio LLC, <https://www.simio.com>).

### Model Parameters

We derived model estimates from the literature or expert opinion (Table 2). A meta-analysis provided evidence for domestic LTBI program performance (5), therapy efficacy was derived from the literature (24,27,28), and adverse events were imputed from several randomized controlled trials reported in previous analysis (24,25). Diagnostic performance of LTBI screening tests was derived from systematic reviews and modeled to be the same in each country (19–21). Adherence with postarrival follow-up was estimated by reanalysis of reported data (22) (Appendix Figure 1). Death from tuberculosis (3), probability of TB therapy extension (30), and relapse rate (31) were derived from Canada sources. Life tables for Canada estimated background mortality (32).

We derived all costs from Canada sources and assumed that the costs of screening abroad were equal to screening costs in Canada. We derived costs for LTBI treatment and screening, including drugs, screening tests, routine monitoring, and clinician time, from the British Columbia Centre for Disease Control. Adverse event costs, including hospitalization rates and time, and the cost of TB disease were as reported in the literature (30,33,34). We inflated all costs to 2016 Canadian dollars using consumer price indices (35) (Table 3).

We derived health utility data from a study (38) in Canada of migrants who reported for postarrival follow-up. We based adjustments due to adverse events or hospitalization on previous studies (30,33).

### Sensitivity Analysis

We performed a probabilistic sensitivity analysis (PSA) to capture uncertainty of model estimates using an outer sample size of 1,000 and inner sample size of 50,000 (Tables 2, 3). To guide policymakers, we created cost-effectiveness acceptability curves (CEAC) to determine the probability that the most cost-effective intervention strategy in deterministic analysis would fall below various willingness-to-pay (WTP) thresholds. Exploratory sensitivity analysis and additional probabilistic sensitivity analyses are included in the Appendix.



**Results**

**Primary Results**

Among migrants from moderate- to very high-incidence countries, IGRA screening coupled with postarrival rifampin treatment was the optimal intervention strategy in deterministic analysis. Sequential screening coupled with postarrival rifampin treatment was the optimal intervention strategy among migrants from low-incidence countries. Intervention strategies involving TST identified the most migrants for postarrival follow-up, whereas strategies involving sequential screening identified the fewest. Intervention strategies involving rifampin resulted in the fewest TB cases (46% reduction compared with the base case) (Table 4).

**Low-Incidence Countries**

For migrants from low-incidence countries, screening with TST alone resulted in a net loss in population QALYs because of poor specificity of the TST. Sequential screening, the most specific screening method, coupled with postarrival

rifampin treatment yielded the lowest cost per QALY gained at \$191,889. IGRA screening, the most sensitive screening method, coupled with rifampin treatment resulted in the fewest TB cases (46.2% reduction) but had a higher cost per QALY gained (\$373,773) because of its lower specificity compared with that of sequential screening.

**Moderate-Incidence Countries**

For migrants from moderate-incidence countries, the optimal intervention strategy was IGRA screening coupled with postarrival rifampin treatment for those from moderate-incidence countries with a cost per QALY gained of \$43,343. Sequential screening coupled with postarrival rifampin treatment was cheaper overall but had a cost per QALY gained of \$47,561.

**High-Incidence Countries**

Among migrants from high-incidence countries, IGRA screening coupled with postarrival rifampin treatment was the optimal intervention strategy, at a cost per QALY

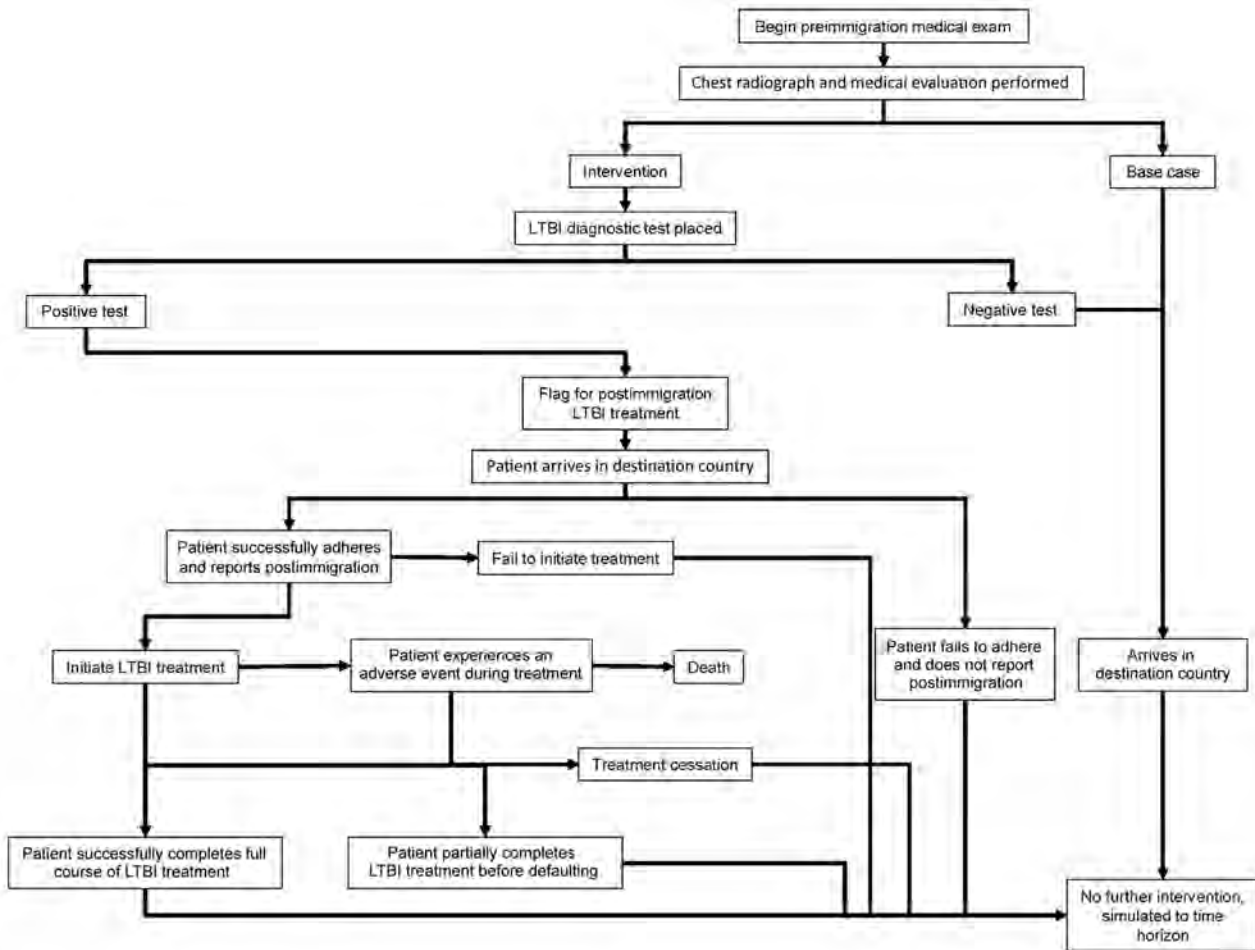


**Figure 1.** Flow structure of model used for cost-effectiveness analysis of screening and interventions of migrants for TB and LTBI. LTBI, latent tuberculosis infection; TB, tuberculosis.

gained of \$26,350. Sequential screening coupled with rifampin treatment was less expensive, but also less efficient, with a cost per QALY gained of \$29,997.

### Very High–Incidence Countries

Among migrants from very high–incidence countries, IGRA screening coupled with postarrival rifampin treatment had a

**Table 2.** Model parameter estimates and values used for sensitivity analyses of intervention strategies for screening and treatment of latent TB infection in immigrants\*

Parameter	Estimate	Range evaluated in PSA	PSA distribution	References
<b>Screening parameters</b>				
TST sensitivity	0.782	0.69–0.87	Beta (43,12)	(19)
TST specificity, no BCG	0.974	0.963–0.982	Beta (770,21)	(20,21)
TST specificity, BCG	0.602	0.561–0.642	Beta (239,158)	(20,21)
IGRA sensitivity	0.889	0.688–0.993	Beta (8,1)	(19)
IGRA specificity	0.957	0.946–0.968	Beta (900,40)	(20,21)
IGRA indeterminate†	0.06	0.05–0.07	Beta (83,1286)	(21)
Complete TST‡	1	Fixed	Fixed	
Complete medical evaluation§	1	Fixed	Fixed	
<b>Population characteristics¶</b>				
LTBI prevalence				
Very high incidence	0.3162	0.2686–0.3880	Varied with reactivation rate	(12,15–17)
High incidence	0.2016	0.1706–0.2464	Varied with reactivation rate	(12,15–17)
Moderate incidence	0.0902	0.0763–0.1102	Varied with reactivation rate	(12,15–17)
Low incidence	0.0159	0.0135–0.0195	Varied with reactivation rate	(12,15–17)
Abnormal chest radiograph results or previous TB				
Very high incidence	0.039	Fixed	Fixed	(15)
High incidence	0.028	Fixed	Fixed	(15)
Moderate incidence	0.029	Fixed	Fixed	(15)
Low incidence	0.008	Fixed	Fixed	(15)
Adherence to postarrival follow-up#	0.684	0.646–0.721	Beta (404.50,186.87)	(22)
<b>Treatment parameters</b>				
Initiate**	0.938	0.907–0.964	Beta (180.83,11.95)	(5)
Complete, INH	0.616	0.561–0.670	Beta (131.66,82.07)	(5)
Complete, RIF	0.814	0.745–0.876	Beta (76.85,17.56)	(5)
Adverse event, INH	0.049	0.044–0.055	Beta (249,4789)	(24,25)
Adverse event, RIF	0.021	0.018–0.025	Beta (109,4877)	(24,25)
Adverse event hospitalization	0.01	0.0005–0.03	Beta (1,99)	(25)
Death, INH	0.00000988	0–0.00002	Beta (2,202495)	(26)
LTBI risk reduction, INH	0.90	0.78–0.95	Normal (–2.3,0.5)††	(27)
LTBI risk reduction, RIF	0.90	0.63–0.97	Normal (–2.3,0.8)††	(28,24)
Partial risk reduction, INH	0.346	0.267–0.490	Combination of normal distributions††, ††	Expert opinion, (25)
Partial risk reduction, RIF	0.30	0.17–0.40	Normal (–0.35,0.1)††	Expert opinion, (24,28)
Adverse event duration	7 d	0–24	Gamma (0.7,10)	Expert opinion, (25)
<b>TB parameters</b>				
Death from TB	0.0476	0.0391–0.0566	Beta (76,1523)	(3)
Reactivation rate	0.0011	0.0009–0.0013	Beta (90.92,82545.55)	(15–17)
Abnormal CXR risk change	3.9	3.0–4.9	Normal (1.36,0.15)††	(29)
Extended therapy	0.124	0.029–0.264	Beta (2.366,16.713)	Expert opinion, (30)
Relapse rate	0.0359	0.0197–0.0654	Normal (–3.327,0.365)††	(30)
Hospitalization duration	17 d	Fixed	Fixed	Expert opinion, (30)
<b>Model parameters</b>				
BCG vaccination, <30 cases	0.605	0.60–0.61	Beta (45137,29502)	(12,13)
BCG vaccination, ≥30 cases	0.998	0.997–0.999	Beta (185381,384)	(12,13)
BCG vaccination uptake	0.837	Fixed	Fixed	(14)
Discount rate	0.03	Fixed	Fixed	(23)
Time horizon	25 y	Fixed	Fixed	NA

\*AE, adverse event; BCG, bacillus Calmette–Guérin; IGRA, interferon-gamma release assay; INH, isoniazid; LTBI, latent tuberculosis infection; NA, not available; PSA, probabilistic sensitivity analysis; RIF, rifampin; TST, tuberculin skin test; TB, tuberculosis.

†Treated as a negative result if it occurred; was equally likely to occur in those with and without LTBI.

‡Without being mandatory, this value is 63.5% (imputed from 43.4% completing screening when 68.4% adhere with a follow-up appointment) (5).

§Without being mandatory, this value is 78% (imputed from 43.7 of 56 individuals completing medical evaluation) (5).

¶Very high incidence, ≥200 cases/100,000; high incidence, ≥100 and <200 cases/100,000; moderate incidence, ≥30 and <100 cases/100,000; low incidence, <30 cases/100,000.

#From a meta-analysis (22); see also Appendix (<https://wwwnc.cdc.gov/EID/article/25/4/17-1630-App1.pdf>).

\*\*This model assumes all who report postarrival due to a positive preimmigration LTBI diagnostic test are offered treatment. Exploratory analysis adjusts this assumption so that only the number who would complete TST screening begin treatment.

††Results from this distribution are exponentiated.

‡‡Formula:  $0.33 \times (\text{Normal}(-1.168,0.228)) + 0.374 \times (\text{Normal}(-0.381,0.169)) + 0.293 \times 1$ .

cost per QALY gained of \$16,291 compared with the base case. Sequential screening with rifampin treatment again was slightly cheaper, resulting in a cost per QALY gained of \$20,165.

### Sensitivity Analysis

Among migrants from low-incidence countries, sequential screening coupled with postarrival rifampin treatment was the most cost-effective option in deterministic analysis. In PSA, this intervention had a probability of cost-effectiveness of 49.1% at a WTP threshold of \$50,000/QALY and 50.7% at a WTP threshold of \$100,000/QALY. This probability did not substantially increase past these thresholds, however, resulting in a probability of cost-effectiveness of 52% at a WTP threshold of \$200,000/QALY (Figure 2, panel A).

Among migrants from moderate-, high-, and very high-incidence countries, IGRA screening coupled with postarrival rifampin treatment was the most cost-effective option in deterministic analysis. This intervention strategy at WTP thresholds of \$50,000/QALY gained had probabilities

of cost-effectiveness of 57.5% among migrants from moderate-incidence countries (Figure 2, panel B), 68.2% among migrants from high-incidence countries (Figure 2, panel C), and of 73.2% among migrants from very high-incidence countries (Figure 2, panel D). At a WTP threshold of \$100,000/QALY gained probabilities of cost-effectiveness were 59.8% among migrants from moderate-incidence countries, 70.6% among migrants from high-incidence countries, and 75.2% among migrants from very high-incidence countries.

### Discussion

The intervention of preimmigration LTBI screening followed by postarrival treatment among new migrants from countries with a TB incidence  $\geq 30$  cases/100,000 persons appears to be an effective method for reducing TB incidence post-arrival. The use of IGRA screening coupled with postarrival rifampin treatment provided the lowest cost-effectiveness ratio in migrants from these countries. This intervention strategy reduced TB incidence by >45% and yielded costs <\$50,000/QALY gained.

**Table 3.** Cost and QALY estimates and values used for sensitivity analysis of intervention strategies for screening and treatment of latent TB infection in immigrants\*

Parameter	Estimate, \$	Range evaluated in PSA	PSA distribution	References
<b>Costs</b>				
Full INH treatment	992	804–1,179	Triangular, 804–1,179	BCCDC, (33,36)
Drug costs	181			
Nurse and clinician costs	741			
Follow-up chest radiograph	42			
Routine tests	28			
Full RIF treatment	575	464–686	Triangular, 464–686	BCCDC, (33,36)
Drug costs	98			
Nurse and clinician costs	421			
Follow-up chest radiograph	42			
Routine tests	14			
Partial INH	462	174–804	Triangular, 174–804	BCCDC, (33,36)
Partial RIF	319	178–464	Triangular, 178–464	BCCDC, (33,36)
Complete TST	31	24–38	Triangular, 24–38	BCCDC, (33,36)
TST cost	11			
Nurse costs (2 visits)	20			
Incomplete TST	21	17–25	Triangular, 17–25	BCCDC, (33,36)
IGRA	54	31–62	Triangular, 31–62	BCCDC, (33,36)
Kit and technician cost	47			
Nurse costs	7			
Chest radiograph	42	32–52	Triangular, 32–52	BCCDC, (33,36)
Cost per radiograph	35			
Nurse costs	7			
TB	20,532	7,141–39,525	Gamma (4,1064,5,000)	Expert opinion, (33,34)
LTBI adverse event	732	549–916	Triangular, 549–916	(33)
Hospitalization	6,641	5,305–9,985	Triangular, 5,305–9,985	(30)
Death	26,933	13,079–40,788	Triangular, 13,079–40,788	(37)
<b>QALYs</b>				
LTBI	0.81		Assumed	(38)
Healthy	0.81	0.58–0.97	Beta (7.85,1.84)	(38)
Adverse event disutility	0.2	0.15–0.25	Triangular, $\pm 25\%$	(30,33)
TB	0.69	0.08–0.24†	Beta (9,51)	(38)
Hospitalization	0.5	0.28–0.51†	Beta (19.5,30.5)	(30)
Death	0	Fixed	Fixed	Standard

\*All costs are in 2016 Can \$. BCCDC, British Columbia Centre for Disease Control; IGRA, interferon-gamma release assay; INH, isoniazid; LTBI, latent tuberculosis infection; PSA, probabilistic sensitivity analysis; RIF, rifampin; TB, tuberculosis; TST, tuberculin skin test.

†Sampled as a percent decrement compared to healthy QALY.



Because prevalence of LTBI was low among migrants from countries with a TB incidence <30 cases/100,000 persons and specificities of LTBI diagnostic tests are imperfect, this intervention may result in a high number of uninfected persons receiving treatment unnecessarily. This finding suggests that with some strategies, the QALYs lost due to treatment side effects among those with false-positive diagnostic results may be greater than the QALYs gained by averted TB in those with true-positive diagnostic results. If screening and treatment must be performed in these low LTBI prevalence populations, more specific screening methods (i.e., sequential screening) are preferred to avoid inappropriate treatment.

Probabilistic sensitivity analysis suggests a certain degree of uncertainty in results. The behavior of CEACs as WTP thresholds increase suggests that the intervention offers small increases in population QALYs or large increases in cost in many replications. It is important to understand how well the model parameters represent the

local setting when using the results of this analysis to inform evidence-based policy. These results suggest that intervention offers domestic benefits to the receiving country, but several factors need to be carefully examined. IGRA use in high-resource settings suffers from variability, in part related to several operational issues (39), and TST variability remains an issue (40). For both types of test, variability may be exacerbated in low-resource settings where LTBI prevalence rates are likely to be higher. In this model, we did not consider the costs of program initiation and maintenance; although they are outside the scope of this analysis, these costs merit careful evaluation when seeking to implement policy.

This model considered only the costs of persons who became permanent residents. The data from Canada indicated that ≈50%–60% of those who begin the process of becoming a permanent resident successfully complete it (3,15). For migrants from very high-incidence countries, assuming only half of migrants receiving preimmigration

**Table 4.** Results in various TB incidence settings of implementing intervention strategies for screening and treatment of latent TB infection in immigrants\*

Intervention	% Identified for postarrival followup	Cost/1,000 persons, \$	No. QALYs/1,000 persons	No. TB cases/1,000 persons	% Reduction in TB incidence	Cost per QALY gained, \$†
<b>Low TB incidence countries</b>						
Base case	0.82	9,681	13,761.03	0.41	NC	NC
SEQ/RIF	4.02	60,996	13,761.30	0.26	36.87	191,889
SEQ/INH	4.02	67,309	13,761.08	0.28	32.00	1,289,335‡
IGRA/RIF	6.43	80,107	13,761.22	0.22	46.16	373,773‡
IGRA/INH	6.43	91,056	13,761.07	0.25	39.07	2,315,425‡
TST/RIF	22.99	120,910	13,760.65	0.24	40.08	Dominated
TST/INH	22.99	162,233	13,760.59	0.27	34.12	Dominated
<b>Moderate TB incidence countries</b>						
Base case	2.88	58,301	13,735.03	2.47	NC	NC
SEQ/RIF	11.99	121,950	13,736.36	1.57	36.52	47,561
IGRA/RIF	14.52	129,036	13,736.66	1.33	46.36	43,343
SEQ/INH	11.99	142,739	13,735.71	1.72	30.55	122,821‡
IGRA/INH	14.52	154,804	13,736.69	1.50	39.47	58,154‡
TST/RIF	38.96	206,145	13,736.84	1.46	40.77	81,548‡
TST/INH	38.96	277,998	13,735.98	1.61	34.88	230,641‡
<b>High TB incidence countries</b>						
Base case	2.79	122,928	13,702.56	5.39	NC	NC
SEQ/RIF	19.13	194,289	13,704.93	3.44	36.06	29,997
IGRA/RIF	23.60	199,878	13,705.48	2.91	45.99	26,350
SEQ/INH	19.13	231,835	13,704.38	3.73	30.73	59,655‡
TST/RIF	44.24	247,488	13,704.35	3.28	39.21	69,421‡
IGRA/INH	23.60	263,572	13,704.93	3.22	40.18	59,154‡
TST/INH	44.24	348,686	13,704.15	3.54	34.36	141,336‡
<b>Very high TB incidence countries</b>						
Base case	3.87	184,357	13,666.32	8.12	NC	NC
SEQ/RIF	27.45	263,628	13,670.25	5.18	36.23	20,165
IGRA/RIF	33.86	268,840	13,671.50	4.41	45.61	16,291
TST/RIF	49.82	318,025	13,670.32	5.62	30.76	33,403‡
SEQ/INH	27.45	318,435	13,671.23	4.86	40.16	27,296‡
IGRA/INH	33.86	337,716	13,671.02	4.97	38.82	32,657‡
TST/INH	49.82	415,877	13,669.91	5.33	34.34	64,494‡

\*Very high incidence, ≥200 cases per 100,000; high incidence: ≥100 and <200 cases/100,000; moderate incidence, ≥30 and <100 cases/100,000; low incidence: <30 cases/100,000. IGRA, interferon-gamma release assay; INH, isoniazid; NC, not calculable; QALY, quality-adjusted life year; RIF, rifampin; SEQ, sequential screening; TB, tuberculosis; TST, tuberculin skin test.

†\*The cost per QALY gained is calculated in comparison to the base case. Dominated indicates that an intervention strategy has higher costs and worse outcomes compared to the base case. Costs are in CAD.

‡This intervention strategy is strictly dominated by another intervention strategy. It is more expensive and has worse outcomes.

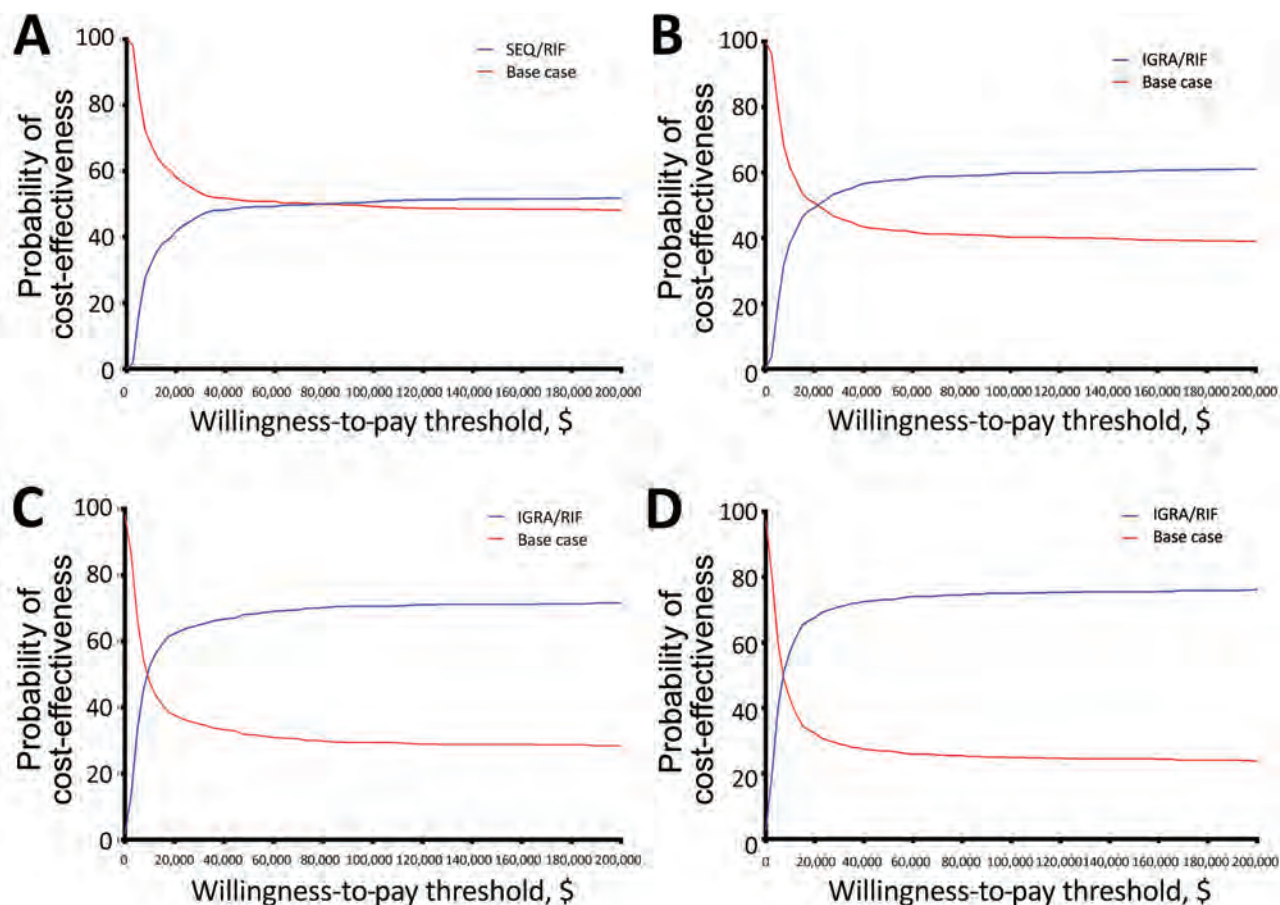


**Figure 2.** Cost-effectiveness acceptability curves of the base case of no intervention compared with intervention strategies in evaluation of screening and treatment of latent tuberculosis infection in immigrants. The graphs demonstrate the probability that an option is more cost-effective at various willingness-to-pay thresholds per quality adjusted life year gained. A) Comparison of the base case with the intervention strategy of preimmigration SEQ screening coupled with postarrival RIF treatment among migrants from low-incidence countries. B) Comparison of the base case with the intervention strategy of preimmigration IGRA screening coupled with postarrival rifampin treatment among migrants from moderate-incidence countries. C) Comparison of the base case with the intervention strategy of preimmigration IGRA screening coupled with postarrival RIF treatment among migrants from high-incidence countries. D) Comparison of the base case with the intervention strategy of preimmigration IGRA screening coupled with postarrival RIF treatment among migrants from very high-incidence countries. IGRA, interferon-gamma release assay; RIF, rifampin; SEQ, sequential.

screening became permanent residents, the cost-effectiveness ratio increased 60% to  $\approx$ \$26,000 when the intervention strategy was IGRA coupled with rifampin. Another consideration is the feasibility of the intervention. In a country like Canada, 2%–3% of new permanent residents are requested to follow up postarrival based on preimmigration medical exams (3,15). If the country implemented preimmigration IGRA screening for migrants from moderate- to very high-incidence countries, 17.6% would be requested to follow up postarrival (3,15). However, coupling IGRA with postarrival rifampin treatment could prevent 3.9% of all TB cases in Canada in the first year (3,12,15). Applied to new permanent residents to Canada in 2014, this process would increase the number requested to follow up postarrival from 6,100 to 45,800 but would result in the prevention of 61 TB cases in the first year (1 case prevented/

651 additional postarrival referrals). If this process were then consistently implemented in successive cohorts in the future, it could annually prevent  $\approx$ 400 TB cases.

Regardless of how preimmigration LTBI screening is implemented, investment in LTBI infrastructure in high TB incidence settings will be essential for global TB elimination. Evidence suggests that introduction of routine preimmigration TB screening in many high-income, low-incidence countries has played a role in improving infrastructure for TB programs in low-resource areas (41). Further introducing LTBI screening as part of these routine medical exams may have similar impact.

The cost-effectiveness of preimmigration LTBI screening and postarrival treatment has not been evaluated since 2003. Previously, Schwartzman and Menzies (42) examined the idea of preimmigration TST screening in addition to

standard preimmigration chest radiograph coupled with post-arrival isoniazid treatment. They found the cost per TB case prevented was approximately Can \$94,500. In our study, using this intervention strategy in very high incidence countries resulted in a cost per TB case prevented of approximately Can \$83,000. Schwartzman et al. (43) later investigated the cost associated with performing a TST in all new legal immigrants from Mexico, a low-incidence country, and coupling it with postarrival isoniazid treatment. This resulted in a cost per TB case prevented of \$1.2 million (2016 Can \$). Using this same intervention strategy in our study resulted in a cost per TB case prevented of \$1.1 million (2016 Can \$). By evaluating new strategies applied to a variety of TB incidence settings, our study represents a much-needed update to the literature.

Our analysis has several strengths. Use of discrete event simulation enabled realistic modeling of time spent in various health states, which is difficult to implement in Markov models. This type of model also allowed age-representative modeling of new migrants for application of age-adjusted LTBI prevalence. The source of most of the cost data was the British Columbia Center for Disease Control, which handles most TB cases in the province of British Columbia. This analysis estimated LTBI prevalence and abnormal chest radiograph prevalence using several years of immigration and TB data from Ontario. The data are likely to be generalizable, because Ontario accepts 40% of new permanent residents (12) and the data fit well with reported LTBI prevalence estimates (16), suggesting these parameters are reflective of long-term TB trends.

In this study, we assumed that all migrants were recommended postarrival LTBI treatment when they had a positive LTBI diagnostic test, which is not necessarily true; for some persons, the risk for serious adverse events may outweigh the benefit of treatment. Social factors and concurrent conditions may increase the risk for reactivation of LTBI. We have shown that the benefits of rifampin treatment for migrants from moderate- to very high-incidence countries who test positive by IGRA preimmigration outweigh the potential risks of adverse events. However, in practice, individual adverse-event risk is considered, and treatment may not be offered to all migrants. Further research designed to identify the specific populations who should be offered treatment would help inform future analyses.

We derived the reactivation rate of LTBI from the literature, but because many of those studies were based on TB incidence in those who were positive by TST, it is possible that the predictive value of the TST caused underestimation of true reactivation rates. Our analysis did not consider 3 months of once-weekly isoniazid and rifampentine as an LTBI treatment modality because it was not universally available. Literature data, however, suggest this modality may yield similar results to rifampin treatment (44).

Our analysis used a healthcare system perspective, which does not consider costs incurred by persons experiencing the intervention (45). It is possible that consideration of costs and benefits from a societal perspective would change the results of this analysis; however, it is also likely that this difference would strengthen the preference for screening with IGRA, which requires only 1 visit, instead of TST, which requires 2, due to reduced absenteeism associated with IGRA testing. Costs per QALY gained may increase for all strategies if the time costs for migrants to follow up for LTBI treatment were considered. Finally, we assumed that TB reactivation was constant, which, while demonstrated previously (18), contradicts the common paradigm of decreasing risk over time (46). Where possible, we performed sensitivity analyses to view the effects our limitations may have on our results to better inform decision makers.

In conclusion, preimmigration IGRA screening coupled with postarrival rifampin treatment among migrants from countries with moderate to very high incidence of TB resulted in the lowest cost-effectiveness ratios. This evidence can be used to support policy decisions surrounding preimmigration LTBI screening in high-income, immigrant-receiving countries, when coupled with evaluations on program implementation, acceptability, and sustainability. Next steps in research should be to identify subgroups at highest risk for progression to TB disease to limit individual risk associated with LTBI treatment and improve the likelihood of feasibility and sustainability.

### Acknowledgments

The authors would like to thank Shannon Kopp and John Darras for their help with costing and Simio LLC (<http://www.simio.com>) for allowing use of their software and replication runner.

J.C.J. and M.S. have received funding from the Michael Smith Foundation for Health Research. M.S. also received salary support from the Canadian Institutes of Health Research.

J.R.C., J.C.J., and F.M. were involved in development of the study objective and design. J.R.C. performed data collection, created the model, performed data analysis and interpretation, and drafted the manuscript. J.C.J. provided expert input on the data informing the model, data interpretation, and performed manuscript editing. M.S. reviewed the model for errors, provided expert input for data analysis, and edited the manuscript. V.J.C. provided expert input on the data informing the model and edited the manuscript. R.K.E. provided expert input on the data interpretation and edited the manuscript. F.M. reviewed the model inputs collected and the data analysis, provided expert input for data interpretation, and edited the manuscript. All authors approved the study objective, design, and final manuscript.



## About the Author

Dr. Campbell received his PhD from the University of British Columbia in Vancouver and is currently a postdoctoral fellow at McGill University in Montreal, Quebec, Canada. His primary research interests include health economics, evidence-based public health policy, and infectious disease.

## References

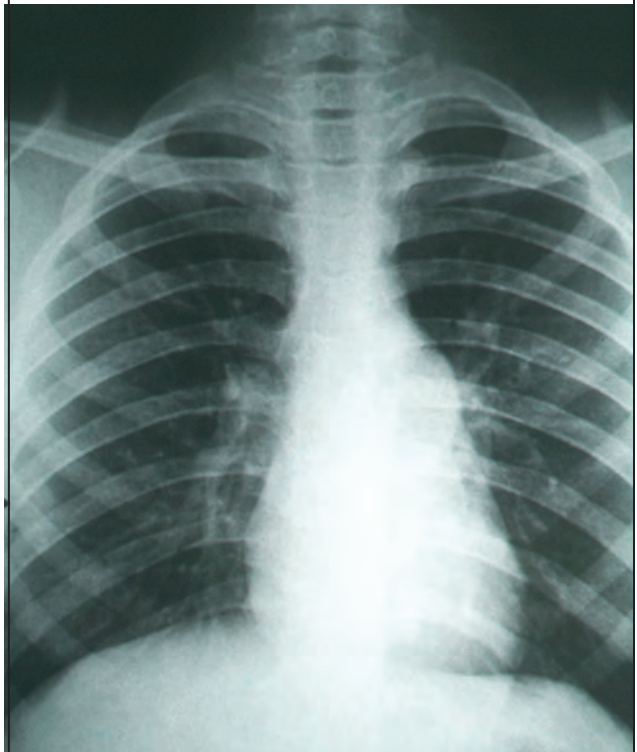
- World Health Organization. Framework towards tuberculosis elimination in low-incidence countries. Geneva: The Organization; 2014 [cited 2018 Mar 7]. [http://www.who.int/tb/publications/elimination\\_framework/en/](http://www.who.int/tb/publications/elimination_framework/en/)
- Pareek M, Greenaway C, Noori T, Munoz J, Zenner D. The impact of migration on tuberculosis epidemiology and control in high-income countries: a review. *BMC Med.* 2016;14:48. <http://dx.doi.org/10.1186/s12916-016-0595-5>
- Public Health Agency of Canada. Canadian tuberculosis standards, 7th ed. Ottawa (ON): Government of Canada; 2014 [cited 2018 Mar 7]. <https://www.canada.ca/en/public-health/services/infectious-diseases/canadian-tuberculosis-standards-7th-edition.html>
- Taylor Z, Nolan CM, Blumberg HM; American Thoracic Society; Centers for Disease Control and Prevention; Infectious Diseases Society of America. Controlling tuberculosis in the United States. Recommendations from the American Thoracic Society, CDC, and the Infectious Diseases Society of America. *MMWR Recomm Rep.* 2005;54(RR-12):1–81.
- Alsdurf H, Hill PC, Matteelli A, Getahun H, Menzies D. The cascade of care in diagnosis and treatment of latent tuberculosis infection: a systematic review and meta-analysis. *Lancet Infect Dis.* 2016;16:1269–78. [http://dx.doi.org/10.1016/S1473-3099\(16\)30216-X](http://dx.doi.org/10.1016/S1473-3099(16)30216-X)
- Campbell J, Marra F, Cook V, Johnston J. Screening immigrants for latent tuberculosis: do we have the resources? *CMAJ.* 2014;186:246–7. <http://dx.doi.org/10.1503/cmaj.131025>
- Campbell JR, Sasitharan T, Marra F. A systematic review of studies evaluating the cost utility of screening high-risk populations for latent tuberculosis infection. *Appl Health Econ Health Policy.* 2015;13:325–40. <http://dx.doi.org/10.1007/s40258-015-0183-4>
- Pareek M, Baussano I, Abubakar I, Dye C, Lalvani A. Evaluation of immigrant tuberculosis screening in industrialized countries. *Emerg Infect Dis.* 2012;18:1422–9. <http://dx.doi.org/10.3201/eid1809.120128>
- Institute of Medicine (US) Committee on the Elimination of Tuberculosis in the United States. Ending neglect: the elimination of tuberculosis in the United States. Geiter L, editor. Washington (DC): National Academies Press; 2000.
- Coker R, van Weezenbeek KL. Mandatory screening and treatment of immigrants for latent tuberculosis in the USA: just restraint? *Lancet Infect Dis.* 2001;1:270–6. [http://dx.doi.org/10.1016/S1473-3099\(01\)00122-0](http://dx.doi.org/10.1016/S1473-3099(01)00122-0)
- Karnon J, Stahl J, Brennan A, Caro JJ, Mar J, Möller J; ISPOR-SMDM Modeling Good Research Practices Task Force. Modeling using discrete event simulation: a report of the ISPOR-SMDM Modeling Good Research Practices Task Force—4. *Value Health.* 2012;15:821–7. <http://dx.doi.org/10.1016/j.jval.2012.04.013>
- Statistics Canada. Report on the demographic situation in Canada: permanent and temporary immigration to Canada from 2012 to 2014. Ottawa (ON): Government of Canada; 2016 [cited 2018 Mar 7]. <http://www.statcan.gc.ca/pub/91-209-x/2016001/article/14615-eng.htm>
- Badar S, Araújo T, Zwerling A, Pai M. BCG world atlas. 2nd edition. 2017 [cited 2018 Mar 7]. <http://www.bcgatlas.org/index.php>
- World Health Organization; UNICEF. WHO-UNICEF estimates of BCG coverage. Geneva: World Health Organization; 2017 [cited 2018 Mar 7]. [http://apps.who.int/immunization\\_monitoring/globalsummary/timeseries/tswucveragebcg.html](http://apps.who.int/immunization_monitoring/globalsummary/timeseries/tswucveragebcg.html)
- Khan K, Hirji MM, Miniota J, Hu W, Wang J, Gardam M, et al. Domestic impact of tuberculosis screening among new immigrants to Ontario, Canada. *CMAJ.* 2015;187:E473–81. <http://dx.doi.org/10.1503/cmaj.150011>
- Campbell JR, Chen W, Johnston J, Cook V, Elwood K, Krot J, et al. Latent tuberculosis infection screening in immigrants to low-incidence countries: a meta-analysis. *Mol Diagn Ther.* 2015;19:107–17. <http://dx.doi.org/10.1007/s40291-015-0135-6>
- Shea KM, Kammerer JS, Winston CA, Navin TR, Horsburgh CR Jr. Estimated rate of reactivation of latent tuberculosis infection in the United States, overall and by population subgroup. *Am J Epidemiol.* 2014;179:216–25. <http://dx.doi.org/10.1093/aje/kwt246>
- Walter ND, Painter J, Parker M, Lowenthal P, Flood J, Fu Y, et al.; Tuberculosis Epidemiologic Studies Consortium. Persistent latent tuberculosis reactivation risk in United States immigrants. *Am J Respir Crit Care Med.* 2014;189:88–95.
- Campbell JR, Krot J, Elwood K, Cook V, Marra F. A systematic review on TST and IGRA tests used for diagnosis of LTBI in immigrants. *Mol Diagn Ther.* 2015;19:9–24. <http://dx.doi.org/10.1007/s40291-014-0125-0>
- Menzies D, Pai M, Comstock G. Meta-analysis: new tests for the diagnosis of latent tuberculosis infection: areas of uncertainty and recommendations for research. *Ann Intern Med.* 2007;146:340–54. <http://dx.doi.org/10.7326/0003-4819-146-5-200703060-00006>
- Pai M, Zwerling A, Menzies D. Systematic review: T-cell-based assays for the diagnosis of latent tuberculosis infection: an update. *Ann Intern Med.* 2008;149:177–84. <http://dx.doi.org/10.7326/0003-4819-149-3-200808050-00241>
- Chan IHY, Kaushik N, Dobler CC. Post-migration follow-up of migrants identified to be at increased risk of developing tuberculosis at pre-migration screening: a systematic review and meta-analysis. *Lancet Infect Dis.* 2017;17:770–9. [http://dx.doi.org/10.1016/S1473-3099\(17\)30194-9](http://dx.doi.org/10.1016/S1473-3099(17)30194-9)
- Sanders GD, Neumann PJ, Basu A, Brock DW, Feeny D, Krahn M, et al. Recommendations for conduct, methodological practices, and reporting of cost-effectiveness analyses. *JAMA.* 2016;316:1093–103. <http://dx.doi.org/10.1001/jama.2016.12195>
- Menzies D, Adjobimey M, Ruslami R, Trajman A, Sow O, Kim H, et al. Four months of rifampin or nine months of isoniazid for latent tuberculosis in adults. *N Engl J Med.* 2018;379:440–53. <http://dx.doi.org/10.1056/NEJMoa1714283>
- Campbell JR, Johnston JC, Sadatsafavi M, Cook VJ, Elwood RK, Marra F. Cost-effectiveness of post-landing latent tuberculosis infection control strategies in new migrants to Canada. *PLoS One.* 2017;12:e0186778. <http://dx.doi.org/10.1371/journal.pone.0186778>
- Salpeter SR. Fatal isoniazid-induced hepatitis. Its risk during chemoprophylaxis. *West J Med.* 1993;159:560–4.
- International Union Against Tuberculosis Committee on Prophylaxis. Efficacy of various durations of isoniazid preventive therapy for tuberculosis: five years of follow-up in the IUAT trial. *Bull World Health Organ.* 1982;60:555–64.
- Reichman LB, Lardizabal A, Hayden CH. Considering the role of four months of rifampin in the treatment of latent tuberculosis infection. *Am J Respir Crit Care Med.* 2004;170:832–5. <http://dx.doi.org/10.1164/rccm.200405-584PP>
- Aldridge RW, Zenner D, White PJ, Williamson EJ, Muzyamba MC, Dhavan P, et al. Tuberculosis in migrants moving from high-incidence to low-incidence countries: a population-based cohort study of 519,955 migrants screened before entry to England, Wales, and Northern Ireland. *Lancet.* 2016;388:2510–8. [http://dx.doi.org/10.1016/S0140-6736\(16\)31008-X](http://dx.doi.org/10.1016/S0140-6736(16)31008-X)
- Holland DP, Sanders GD, Hamilton CD, Stout JE. Costs and cost-effectiveness of four treatment regimens for latent tuberculosis

- infection. *Am J Respir Crit Care Med.* 2009;179:1055–60. <http://dx.doi.org/10.1164/rccm.200901-0153OC>
31. Jasmer RM, Bozeman L, Schwartzman K, Cave MD, Saukkonen JJ, Metchock B, et al.; Tuberculosis Trials Consortium. Recurrent tuberculosis in the United States and Canada. *Am J Respir Crit Care Med.* 2004;170:1360–6. <http://dx.doi.org/10.1164/rccm.200408-1081OC>
  32. Statistics Canada. Life tables, Canada, provinces, and territories. 2016 [cited 2018 Mar 7]. <http://www5.statcan.gc.ca/olc-cel/olc.action?objId=84-537-X&objType=2&lang=en&limit=0>
  33. Marra F, Marra CA, Sadatsafavi M, Morán-Mendoza O, Cook V, Elwood RK, et al. Cost-effectiveness of a new interferon-based blood assay, QuantiFERON-TB Gold, in screening tuberculosis contacts. *Int J Tuberc Lung Dis.* 2008;12:1414–24.
  34. Menzies D, Lewis M, Oxlade O. Costs for tuberculosis care in Canada. *Can J Public Health.* 2008;99:391–6.
  35. Statistics Canada. Consumer price index, annual average, not seasonally adjusted. 2019 [cited 2018 Mar 7]. <https://www150.statcan.gc.ca/t1/tb11/en/tv.action?pid=1810000501>
  36. Tan MC, Marra CA, Sadatsafavi M, Marra F, Morán-Mendoza O, Moadebi S, et al. Cost-effectiveness of LTBI treatment for TB contacts in British Columbia. *Value Health.* 2008;11:842–52. <http://dx.doi.org/10.1111/j.1524-4733.2008.00334.x>
  37. Fassbender K, Fainsinger RL, Carson M, Finegan BA. Cost trajectories at the end of life: the Canadian experience. *J Pain Symptom Manage.* 2009;38:75–80. <http://dx.doi.org/10.1016/j.jpainsymman.2009.04.007>
  38. Bauer M, Ahmed S, Benedetti A, Greenaway C, Lalli M, Leavens A, et al. The impact of tuberculosis on health utility: a longitudinal cohort study. *Qual Life Res.* 2015;24:1337–49. <http://dx.doi.org/10.1007/s11136-014-0858-6>
  39. Tagmouti S, Slater M, Benedetti A, Kik SV, Banaei N, Cattamanichi A, et al. Reproducibility of interferon gamma (IFN- $\gamma$ ) release assays: a systematic review. *Ann Am Thorac Soc.* 2014; 11:1267–76. <http://dx.doi.org/10.1513/AnnalsATS.201405-188OC>
  40. Pouchot J, Grasland A, Collet C, Coste J, Esdaile JM, Vinceneux P. Reliability of tuberculin skin test measurement. *Ann Intern Med.* 1997;126:210–4. <http://dx.doi.org/10.7326/0003-4819-126-3-199702010-00005>
  41. Douglas P, Posey DL, Zenner D, Robson J, Abubakar I, Giovanazzo G. Capacity strengthening through pre-migration tuberculosis screening programmes: IRHWG experiences. *Int J Tuberc Lung Dis.* 2017;21:737–45. <http://dx.doi.org/10.5588/ijtld.17.0019>
  42. Schwartzman K, Menzies D. Tuberculosis screening of immigrants to low-prevalence countries: a cost-effectiveness analysis. *Am J Respir Crit Care Med.* 2000;161:780–9. <http://dx.doi.org/10.1164/ajrccm.161.3.9902005>
  43. Schwartzman K, Oxlade O, Barr RG, Grimard F, Acosta I, Baez J, et al. Domestic returns from investment in the control of tuberculosis in other countries. *N Engl J Med.* 2005;353:1008–20. <http://dx.doi.org/10.1056/NEJMsa043194>
  44. Sterling TR, Villarino ME, Borisov AS, Shang N, Gordin F, Bliven-Sizemore E, et al.; TB Trials Consortium PREVENT TB Study Team. Three months of rifapentine and isoniazid for latent tuberculosis infection. *N Engl J Med.* 2011;365:2155–66. <http://dx.doi.org/10.1056/NEJMoa1104875>
  45. Byford S, Raftery J. Perspectives in economic evaluation. *BMJ.* 1998;316:1529–30. <http://dx.doi.org/10.1136/bmj.316.7143.1529>
  46. Comstock GW. Frost revisited: the modern epidemiology of tuberculosis. *Am J Epidemiol.* 1975;101:363–82. <http://dx.doi.org/10.1093/oxfordjournals.aje.a112105>

Address for correspondence: Fawziah Marra, University of British Columbia, 2405 Wesbrook Mall, Vancouver, BC V6T 1Z3, Canada; email: fawziah@mail.ubc.ca

## EID Podcast: Extensively Drug-Resistant TB

Tuberculosis (TB) remains a major cause of illness and death in the 21st century. There were an estimated 9.6 million incident cases worldwide in 2014. In addition, an estimated 3.3% of new cases and 20% of retreatment cases are multidrug-resistant TB (MDR TB), which is defined as TB resistant to at least rifampin and isoniazid, the 2 most powerful first-line drugs. This resistance threatens global TB control efforts. MDR TB patients need access to treatment, require longer treatment with toxic medications, and have a lower probability of cure.



Visit our website to listen:  
[https://www2c.cdc.gov/podcasts/  
player.asp?f=8644444](https://www2c.cdc.gov/podcasts/player.asp?f=8644444)

**EMERGING  
INFECTIOUS DISEASES**

---

# Spatial Dynamics of Chikungunya Virus, Venezuela, 2014

Erley Lizarazo,<sup>1</sup> Maria Vincenti-Gonzalez,<sup>1</sup> Maria E. Grillet,<sup>2</sup> Sarah Bethencourt, Oscar Diaz, Noheliz Ojeda, Haydee Ochoa, Maria Auxiliadora Rangel, Adriana Tami<sup>2</sup>

Since chikungunya virus emerged in the Caribbean region in late 2013, ≈45 countries have experienced chikungunya outbreaks. We described and quantified the spatial and temporal events after the introduction and propagation of chikungunya into an immunologically naive population from the urban north-central region of Venezuela during 2014. The epidemic curve (n = 810 cases) unraveled within 5 months with a basic reproductive number of 3.7 and a radial spread traveled distance of 9.4 km at a mean velocity of 82.9 m/day. The highest disease diffusion speed occurred during the first 90 days, and space and space–time modeling suggest the epidemic followed a particular geographic pathway with spatiotemporal aggregation. The directionality and heterogeneity of transmission during the first introduction of chikungunya indicated existence of areas of diffusion and elevated risk for disease and highlight the importance of epidemic preparedness. This information will help in managing future threats of new or reemerging arboviruses.

Chikungunya, a reemerging mosquito-borne viral infection, is responsible for one of the most explosive epidemics in the Western Hemisphere in recent years. Since its introduction in the Caribbean region at the end of 2013, chikungunya virus (CHIKV) rapidly expanded within a year to most countries of South, Central, and North America (1,2). CHIKV belongs to the genus *Alpha-virus* (Togaviridae), first isolated in Tanzania during 1952 (3). Its sylvatic (enzootic) cycle in Africa involves nonhuman primates; the virus is transmitted by an ample range of forest-dwelling *Aedes* spp. mosquitoes (4). Within the urban (human) cycle across Asia, the Indian Ocean, and the Americas, CHIKV is transmitted by *Aedes aegypti* and *Ae. albopictus* mosquitoes (5–7). Most (72%–93%)

infected persons develop symptomatic disease characterized by fever, rash, and incapacitating arthralgia, progressing in 42%–60% of patients to chronic, long-lasting relapsing or lingering rheumatic disease (8,9). The lack of population immunity to CHIKV in the Americas alongside the ubiquitous occurrence of competent *Ae. aegypti* mosquitoes and human mobility may explain the rapid expansion of CHIKV across the Americas; cases doubled each month during the epidemic exponential phase (10,11). At the end of 2014, >1 million suspected and confirmed cases, including severe cases and deaths, were reported in 45 countries and territories; this figure reached almost 3 million cases by mid-2016 (12). The real number of cases is most likely higher because of misdiagnosis with dengue virus (DENV) infection and underreporting.

In Venezuela, the first official imported chikungunya case was reported in June 2014, and local transmission followed soon thereafter. Chikungunya quickly spread, causing a large national epidemic affecting the most populated urban areas of northern Venezuela, where DENV transmission is high. Given the paucity of official national data, epidemiologic inference was used to estimate the number of cases. Although nationally the disease attack rate was estimated at 6.9%–13.8% (13), the observed attack rate in populated urban areas was ≈40%–50%, comparable to those reported in the Dominican Republic (14) and Asia and higher than those in La Reunion (15,16).

The rapid expansion and worldwide spread in the last decade make CHIKV one of the most public health–relevant arboviruses (17). With the reemergence of other arboviruses, new large-scale outbreaks in the near future seem likely (18). Clarifying and quantifying the introduction and propagation range in space and time of the initial epidemic wave of chikungunya within the complex urban settings of Latin America will shed light on arboviral transmission dynamics and help in managing future threats of new or emerging arboviruses operating under similar epidemiologic dynamics. We characterized the epidemic wave of chikungunya in a region highly affected by the 2014

---

Author affiliations: University of Groningen, Groningen, the Netherlands (E. Lizarazo, M. Vincenti-Gonzalez, A. Tami); Universidad Central de Venezuela, Caracas, Venezuela (M.E. Grillet); Universidad de Carabobo, Valencia, Venezuela (S. Bethencourt, A. Tami); Fundación Instituto Carabobense para la Salud, Carabobo, Venezuela (O. Diaz, N. Ojeda, H. Ochoa, M.A. Rangel)

DOI: <https://doi.org/10.3201/eid2504.172121>

---

<sup>1</sup>These authors contributed equally to this article.

<sup>2</sup>These authors contributed equally to this article.



outbreak in Venezuela. To this end, we described the spatial progression of the epidemic using geographic information systems (GIS), quantified the global geographic path that CHIKV most likely followed during the first 6 months of the epidemic by fitting a polynomial regression model (trend surface analysis), determined the general direction and speed of the propagation wave of the disease, and identified the local space–time disease clusters through spatial statistics.

**Materials and Methods**

**Study Area**

Carabobo State is situated in the north-central region of Venezuela (Figure 1). It is one of the most densely populated regions (19).

**Study Design and Data Collection**

To determine the spatiotemporal spread of the 2014 chikungunya epidemic at local and global scales, we conducted a retrospective study of patient and epidemiologic data collected through the national Notifiable Diseases Surveillance

System (NDSS). Suspected chikungunya was diagnosed in 810 persons of all ages by their physicians; these patients were reported through the NDSS to the epidemiologic department of the Regional Ministry of Health of Carabobo State. Patients suspected of having chikungunya were those with fever of sudden onset, rash, and joint pain with or without other influenza-like symptoms. Patients who attended public or private healthcare centers across Carabobo State municipalities were included in this study.

Patient data were obtained for June 10–December 3, 2014 (epidemiologic weeks 22–49), coinciding with the Venezuela chikungunya outbreak. Data corresponding to the first visit of the patients to a healthcare center were included and comprised patient address, clinical manifestations, and epidemiologic risk factors. This information was entered in a database, checked for consistency, and analyzed anonymously. We defined the index case as the first chikungunya patient reported by the NDSS within this region.

**Temporal Dynamics of CHIKV Spread**

We described the growth rate of the disease by plotting the cumulative cases per epidemiologic week and fitted a

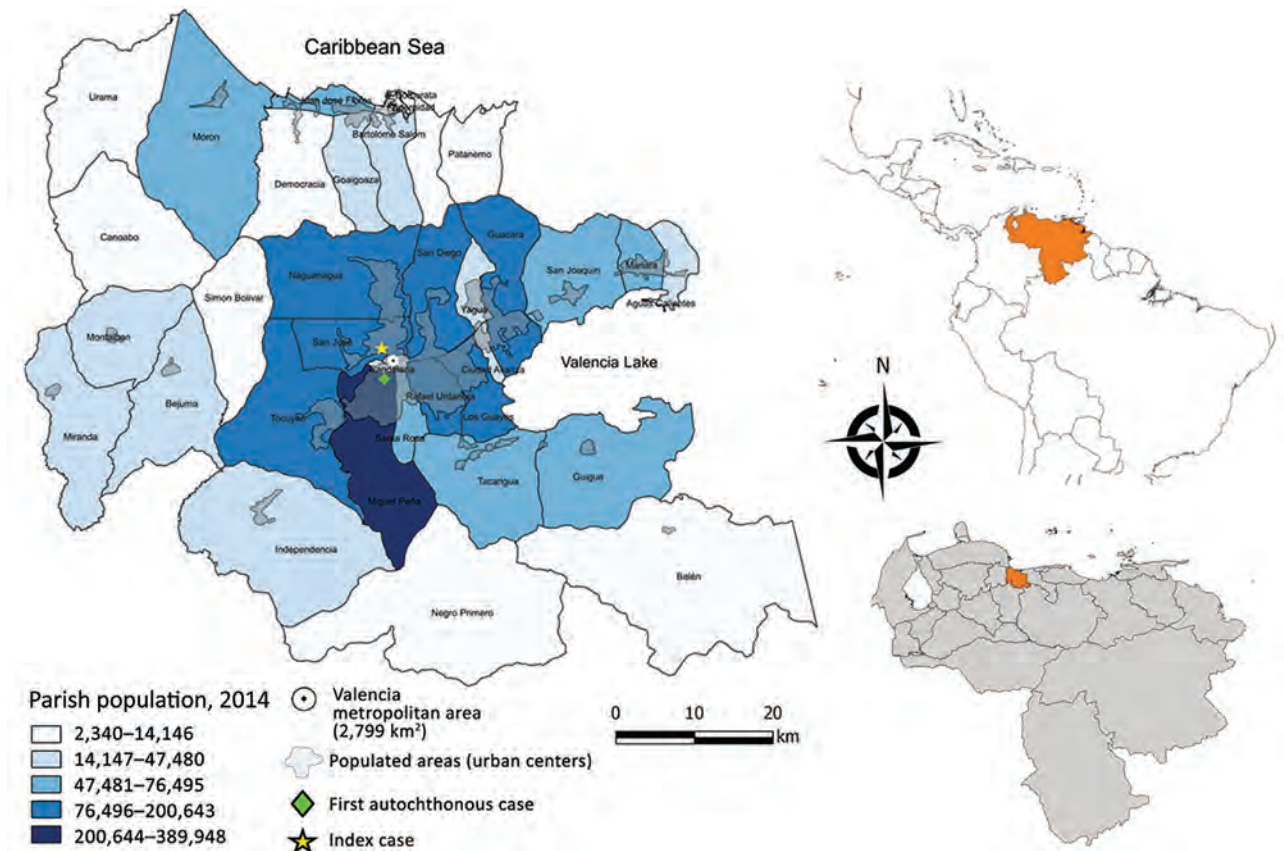


**Figure 1.** Area of study on the spatial dynamics of chikungunya virus, Carabobo state, Venezuela, 2014. Blue shading indicates 2014 population by parish. Most persons live in the capital city of Valencia (892,530 inhabitants); within the metropolitan area, poorer settlements are located mainly in the southern area, and the most organized and urbanized medium- and high-level neighborhoods are situated toward the north-central part. Insets indicate location of Carabobo state in Venezuela and Venezuela in South America.

logistic curve after examining the shape of the epidemic curve (Appendix Figure 1, <https://wwwnc.cdc.gov/EID/article/25/4/17-2121-App1.pdf>). We estimated the average number of secondary cases resulting from a primary case in a completely susceptible population—the epidemic's basic reproductive number ( $R_0$ )—from the initial phase of the epidemic using the exponential growth method (20) and then calculated a real-time estimate of  $R_0$ , called  $R_t$  (21,22), to explore the time-varying transmissibility of chikungunya (Appendix).

### Spatiotemporal Trend of the Epidemic Wave of Chikungunya

We georeferenced the address of every patient into a GIS so that the  $X_i$  (east–west) and  $Y_i$  (north–south) coordinates of each chikungunya case were derived. We drew the weekly spatial progression of the 810 reported cases with respect to the index case in a map. To assess the spreading pattern before the epidemic reached the steady (plateau) state (Figure 2), we selected cases that occurred 0–125 days (up to epidemiologic week 40) after the index case. Within this time range, the case notification rate maintained a sustained growth.

To explore the general spatial trend of chikungunya cases (or the movement of the epidemic wave of infection) across the study area, we developed a map of time of disease spread using trend surface analysis, a global surface fitting method (Appendix). We created the variable *time* (in days) using the symptom onset date from the index case as the baseline date across the 810 case localities; that is, *time* ( $X_i, Y_i$ ). Thus, *time* is considered the number of days elapsed between the appearance of a case in a specific locality  $Z_i$  and the index case. We used results of the trend surface analysis to generate a contour map or smoothed surface; each contour line represented a specific predicted time period in this urban landscape setting since the initial invasion of the virus. The local rate and direction of the spread of infection was estimated as the directional derivative at each case using the trend surface analysis fitted model to obtain local vectors that depicted the direction and speed (inverse of the slope along the direction of the movement) of infection propagation from each locality in  $X$  and  $Y$  directions. In addition, we used kriging, a local geostatistical interpolation method, to generate an estimated continuous surface from the scattered set of points (i.e., *time*) with  $z$  value to better capture the local spatial variation of chikungunya spread across the urban landscape (23). We used ordinary kriging to predict values of the time period since the initial invasion of the virus. We selected the model with the best fit out of 3 theoretical variogram models tested by cross-validation to predict the values at unmeasured locations and their associated errors (Appendix).

We also obtained an empirical basic baseline rate of disease spread to quantify the observed velocity for

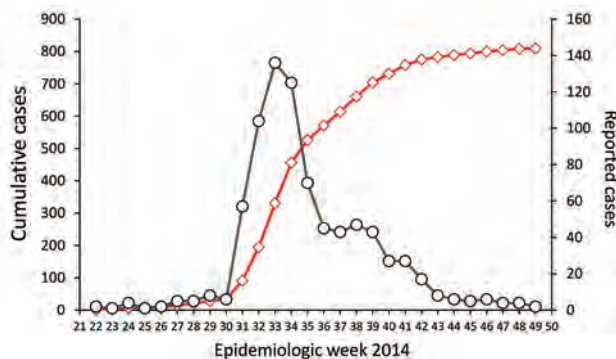


**Figure 2.** Reported chikungunya cases during epidemic, Carabobo state, Venezuela, 2014. Black line with open black dots indicates chikungunya cases; red line with open red diamonds, cumulative cases.

each case  $z_i$  directly from the data by measuring the linear distance (meters) of case  $Z_i$  to the index case and then dividing it by the time in days that elapsed since the index case was reported. We assessed differences between velocities by using the Kruskal-Wallis test, a nonparametric method to test differences between groups when these are nonnormally distributed (24).

Finally, to identify general space–time clusters of chikungunya transmission, we performed a Knox analysis (25), and to identify interactions at specific temporal intervals, we used the incremental Knox test (IKT) (26). For general space–time clusters we selected critical values of 100 m (*distance*) and 3 weeks (*time*) after multiple distance and time windows testing (Appendix Table 2). Our selection was based on the *Aedes* mosquito flight range and the maximum duration of the intrinsic and extrinsic incubation periods of the virus, respectively (27,28). Upon identification of the cluster, we calculated the distance between the first case of a cluster ( $C_1$ ) and the cases within the cluster  $Z_i$ , considering this distance as a measure of virus disease spread. For interactions at specific temporal intervals, we used the IKT in an exploratory mode over the time intervals from 1 day to 31 days and space distances from 25 m to 500 m (Appendix). We conducted spatial analyses using R software (The R-Development Core Team, <http://www.r-project.org>) and ArcGIS version 10.3 (ESRI Corporation, <https://www.esri.com>) using the Spatial Analyst Toolbox and generated maps with Quantum GIS 2.14.3 Essen (QGIS Development Team GNU—General Public License, <https://www.qgis.org>) software). Space-time (Knox) analysis was performed using ClusterSeer 2.0 (Terraseer, <https://www.biomedware.com/software/clusterseer>).

### Ethics Statement

Data were analyzed anonymously, and individuals were coded along with the information of address with a unique numeric identifier. The epidemiologic department of the

Regional Ministry of Health of Carabobo State approved the study.

## Results

### Temporal Dynamics of CHIKV Spread

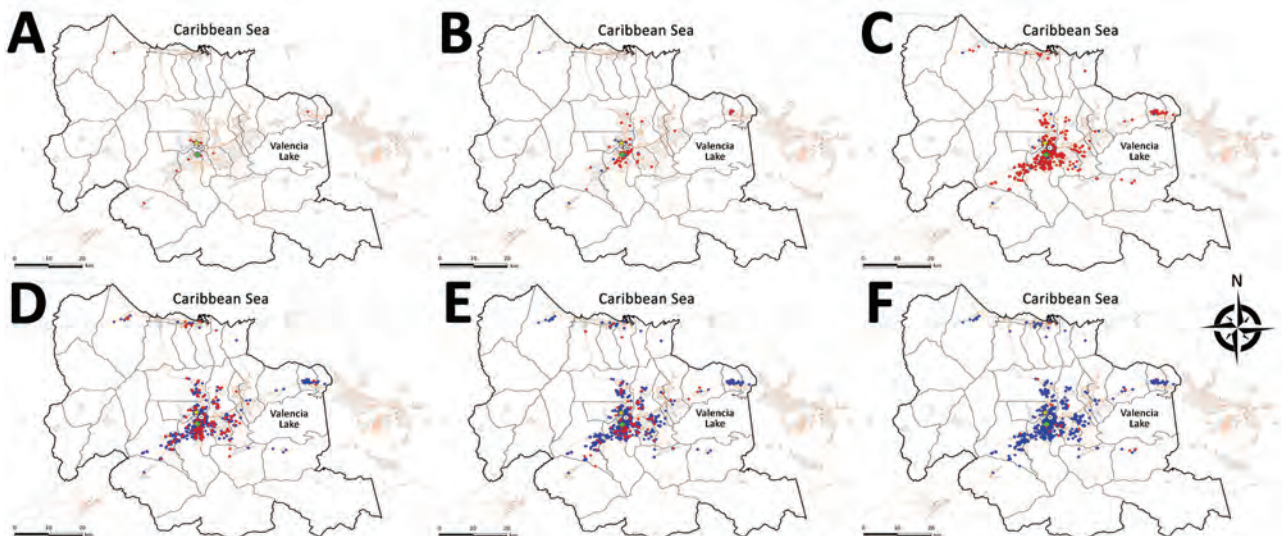
A total of 810 suspected chikungunya cases were reported in Carabobo State in 2014 during epidemiologic weeks 22–49 (28 weeks), representing the first introduction and propagation of the virus in the north-central region of Venezuela. The index case was an imported case (in a returning traveler from the Dominican Republic) in epidemiologic week 22 in the north-central zone of the capital city (Valencia) (Figure 1). The index case was followed by the other imported cases and soon after by locally transmitted cases.

The cumulative cases during epidemiologic weeks 22–49 followed a logistic growth (Appendix Figure 1;  $R = 0.99$ ,  $n = 810$ ;  $p < 0.05$ ). The reported cases displayed a characteristic epidemic curve with a single wave and peaked at epidemiologic week 33, eleven weeks after the index case (Figure 2). The epidemic takeoff occurred at epidemiologic week 31 (i.e., 9 weeks after the index case). The total duration of the outbreak was  $\approx 28$  weeks; however, the main epidemic curve lasted  $\approx 3$  months, from epidemiologic week 30 until epidemiologic weeks 43–44. The initial global growth rate of the epidemic was 0.53 cases per week, and  $R_0 = 3.7$  (95% CI 2.78–4.99) secondary chikungunya cases per primary case (epidemiologic weeks 22–31). We obtained comparable results when we calculated the instantaneous reproductive number ( $R_t = 4.5$ , 95% CI 2.4–7.1) during the epidemic

peak. Beginning with epidemiologic week 34,  $R_t$  values fell below 1, and they gradually decreased from there onward (Appendix Figure 2).

### Spatiotemporal Distribution of the Chikungunya Epidemic

The chikungunya outbreak progressed chronologically and spatially through Carabobo State (Figure 3; Video, <https://wwwnc.cdc.gov/EID/article/25/4/17-2121-V1.htm>). The cases reported in Valencia during the first 6 weeks were located in the central area of the city close to the index case, whereas a few cases were reported in the southwestern part of Valencia and in other small urban towns of Carabobo (Figure 3, panel A). The first autochthonous case occurred during this interval in the south-central area of Valencia, relatively close to the index case (Figure 3, panel A). During epidemiologic weeks 28–31, the number of reported cases increased in parishes around the autochthonous case (Figure 3, panel B). During epidemiologic weeks 32–35, the number of cases exploded exponentially, and the disease spread rapidly throughout the capital city and surrounding smaller urban centers (Figure 3, panel C). New cases were actively reported during 8 continuous weeks (Figure 3, panels C, D) to later decrease from epidemiologic week 40 to epidemiologic week 49 (Figure 3, panels E, F). The epidemic progressed in 2 directions (movement axes) in the region: a north–south direction and a northeastern and southwestern direction. Both shifts consistently overlapped with the populated centers of the region and the main traffic routes (motorways and main roads).



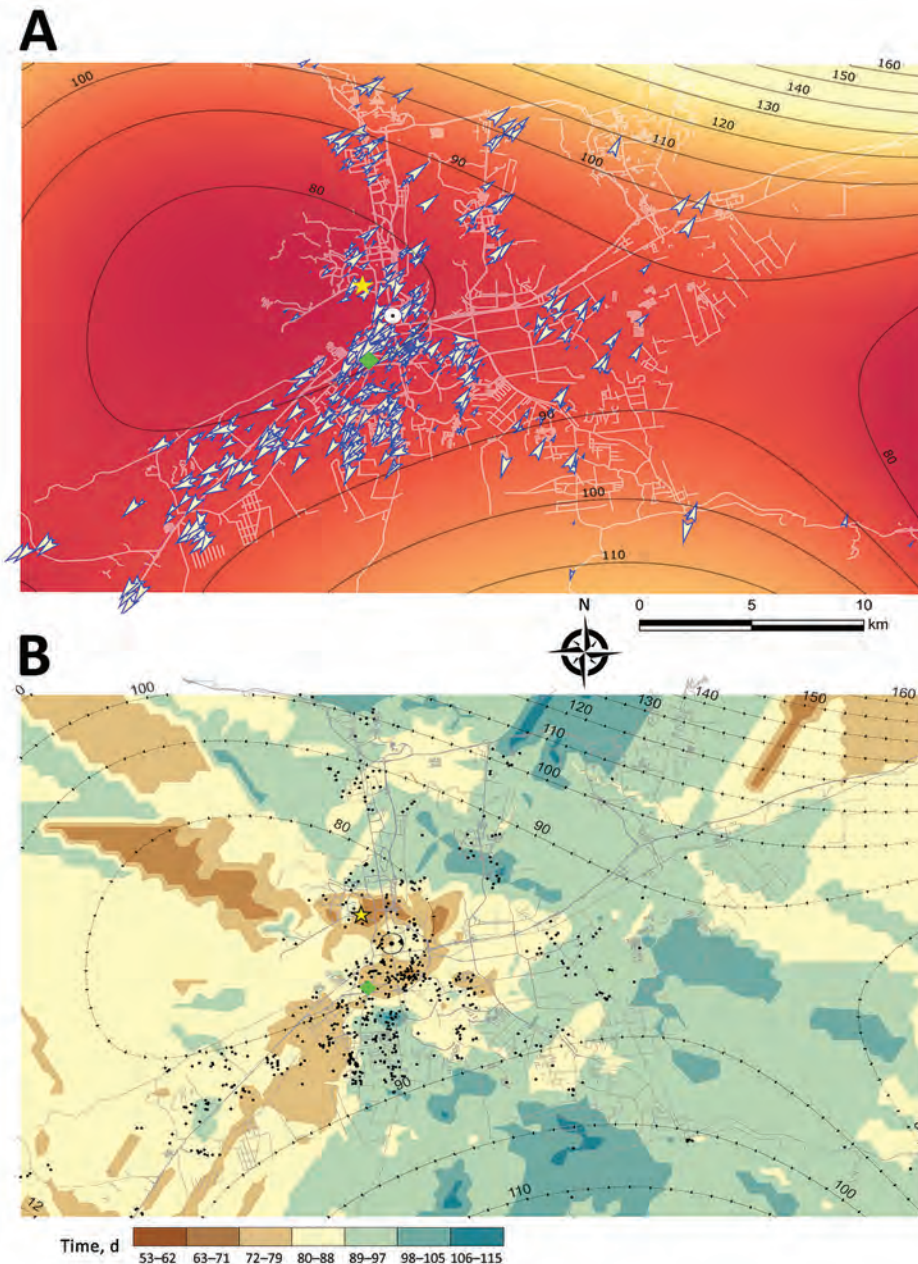
**Figure 3.** Spatial and temporal spread of chikungunya epidemic, Carabobo state, Venezuela, June–December 2014. Time is presented at epidemiologic week intervals as follows: A) weeks 22–27; B) weeks 28–31; C) weeks 32–35; D) weeks 36–39; E) weeks 40–45; F) weeks 46–49. Red circles indicate the appearance of new cases for the given interval; blue indicates the cumulative cases in prior intervals. Light yellow lines depict the road system of the area of study; light gray areas represent the populated areas (urban centers) within the parishes. Yellow star indicates index case; green diamond indicates first autochthonous case.



Figure 4, panel A, depicts the general direction and propagating wave of disease derived from the trend surface analysis. Contour lines that are far apart indicate that the epidemic diffused quickly through the area, whereas lines that are closer together show a slower progression. The direction of diffusion is also given by the edges of the contour lines. The model located the wave of disease dispersal in the central part of the region and included the index case and autochthonous case. The bulk of the outbreak unfolded within 90 days, spreading mainly to the southwestern and northern parts of the capital city. During this time, the maximum radial distance traveled was 9.4 km. A slower diffusion was predicted toward the northeast and southern

part of the region. However, the limitation of the method resulting from edge effects determines that the best area for prediction is the central one.

To visualize the local diffusion of CHIKV at each location, we drew the vector field across the modeled surface (Figure 4, panel A). Overall, the model confirms the previous observation of a general trend or corridor of diffusion of chikungunya cases southwest and northeast of the capital city within the first 80 days. After 90 days, the epidemic wave varied its direction and magnitude by location. Although agreeing with the general pattern shown by the trend surface analysis, the resulting kriging Gaussian (selected) model interpolation surface (Figure 4, panel B;



**Figure 4.** Global and local predicted spreading patterns of chikungunya virus, Carabobo state, Venezuela, 2014. A) Contour map (global scale) of the predicted spreading waves and the velocity vector arrows of each case of chikungunya. The contour map and contour lines in black (traveling waves) were estimated by the best-fit trend surface analysis (third order polynomial model) of time (days) to the first reported case or index case of chikungunya across the landscape. White lines correspond to the road system of the area. The background gradient of color shows the probability of chikungunya virus diffusion according to the prediction of the model: the darker the red, the higher the probability of spread. Each vector (blue outlined arrows) represents the instantaneous velocity derived from the partial, differential equations from the trend surface analysis model (Appendix, <https://wwwnc.cdc.gov/eid/article/25/4/17-2121-App1.pdf>). B) Spatial prediction map for the ordinary kriging (Gaussian model) interpolation of the time (each color represents a different number of days) of chikungunya spread. Contour lines from trend surface analysis depicted in the kriging surface are shown only for comparison purposes. Yellow star indicates index case; green diamond indicates first autochthonous case.

Appendix Table 1) predicts a more heterogeneous spread pattern of chikungunya cases by matching the patchy (uneven population density) distribution of human neighborhoods and the road network. In addition, kriging identified a faster propagation of the epidemiologic wave at the southwestern and eastern areas where the model showed its best fit (Appendix Figure 3, panel A) and a slower movement to the northeastern and south-central areas than estimated by the trend surface analysis.

We calculated the virus diffusion velocities for each parish through the empirical method (Table). The mean velocity of disease spread across the state was 82.9 m ± 53.6 m/day, and overall, the pattern of diffusion of CHIKV was highest in the suburban and rural settlements near the capital city. However, the observed velocities varied significantly by location (n = 735; p<0.05). For instance, the parishes at the center of the capital (San Jose, Catedral, Candelaria, San Blas, Santa Rosa) showed velocities <60 m/day, whereas in the remaining localities, including both rural and suburban towns, the speed was >60 m/day. The maximum velocity of the outbreak was 483 m/day, measured south of the capital.

**Spatiotemporal Clusters of the Epidemic Wave**

Results after multiple space and time parameters testing showed that core clusters remained similar through time (Appendix Figure 4), and the relative risk (RR) within the clusters remained important (RR >1.5) up to 3 weeks (Appendix Figure 5). Using selected critical values, we identified 75 general space–time clusters using Knox analysis (Appendix Table 3; Appendix Figure 6, panel A). These clusters included at least 2 space–time-linked cases and a total of 205 (27.9%) cases that showed a space–time relation. The major accumulation of clusters occurred in the

southern and southwestern parts of the capital. The earliest cluster (cluster 7; Figure 5) was located in the west-central parts of the capital and comprised 3 cases, including the index case. From this cluster, the average distance from each case to the index case was 32 m, and the cases were reported within 25 days after the index case. In addition, the major cluster (cluster 57, 12 cases) was located in the west-central area of the capital 4 km from the index case (Figure 5). The cases belonging to this cluster occurred within 9 days (1.3 cases per day); these cases occurred an average of 70 days (range 69–77 days) after the index case (Appendix Table 3). The median time between the first notified case (symptom onset) and the last case within a cluster was 9 days (range 3–18 days). Furthermore, the average distance between cases within the clusters was 75.2 m ± 25.6 m (range 110.6–39.2 m) (Appendix Table 4). Furthermore, the baseline velocity in Carabobo State was similar to the average velocity within the clusters (69.9 ± 34.4 m/day). These results agree with IKT findings, where the temporal intervals with the strongest spatial clustering and RR occurred at 1–7 days and 25–150 m (Appendix Figures 7, 8).

**Discussion**

We described and quantified the spatial and temporal events that followed the introduction and explosive propagation of CHIKV into an immunologically naive population living in the urban north-central region of Venezuela during 2014. The main epidemic curve developed within 5 months, with a maximum value of the estimate of R<sub>0</sub> = 3.7 by epidemiologic week 12. The speed of disease diffusion was greatest during the first 90 days, and the spatial spread was heterogeneous following mostly a southwest spatial corridor at a variable local rate of diffusion across the

**Table.** Average velocities of chikungunya virus spread across Carabobo state, Venezuela, 2014

Civil parish	No. cases	Velocity, m/day				Location*
		Mean (95% CI)	SD	Minimum	Maximum	
Candelaria	29	39.4 (33.5–45.2)	15.3	17	96	Central
Catedral	11	28.8 (22.4–35.3)	9.5	15	50	Central
Ciudad Alianza	1	146.7	Not applicable	147	147	East-southeast
El Socorro	6	47.2 (13.5–80.9)	32.1	25	98	South-southwest
Guacara†	4	206.2 (–35.1 to 447.6)	151.7	98	430	East-northeast
Guigue‡	5	256.7 (151.7–361.8)	84.6	163	344	Southeast
Independencia†	6	206.7 (138.8–274.5)	64.7	138	310	South-southwest
Los Guayos	42	115.1 (105.3–124.9)	31.4	52	176	East-southeast
Miguel Peña	228	80.6 (75.3–86.0)	40.6	21	483	South
Naguanagua	41	85.9 (77.3–94.6)	27.3	47	174	North
Rafael Urdaneta	84	87.2 (79.5–94.8)	35.3	23	186	Southeast
San Blas	27	43.6 (39.0–48.3)	11.7	21	62	Central
San Diego	35	73.3 (63.5–83.1)	28.5	41	150	North-northeast
San Jose	68	27.6 (21.3–34.0)	26.2	0	202	North-central
Santa Rosa	70	58.4 (55.9–60.9)	10.4	35	97	Central
Tacarigua‡	6	197.0 (147.7–246.3)	47.0	149	259	South-southeast
Tocuyito†	70	149.8 (137.2–162.4)	52.8	61	365	Southwest
Yagua‡	2	111.0 (–3.4 to 225.4)	12.7	102	120	East-northeast
Total	735	82.9 (79.0–86.7)	53.6	0	483	Entire state

\*Location refers to relative locations from the center of the capital city, Valencia.

†Suburban settlements.

‡Rural settlements.



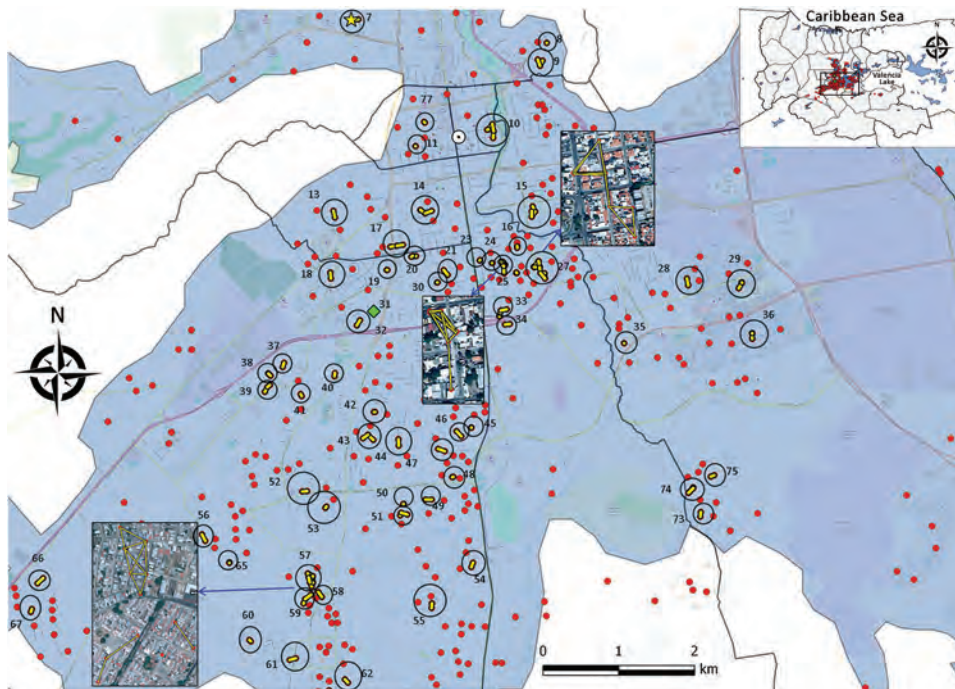


**Figure 5.** Geographic distribution and significant space-time clustering of reported chikungunya cases identified in a section of the capital city, Valencia (metropolitan area), Carabobo state, Venezuela, June–December 2014. Red dots denote case location; black outlined circles identify a significant space-time cluster; yellow lines show the interaction between cases (time–space link). The analysis was performed using 100 m as clustering distance and 3 weeks as time window. Significance level for local clustering detection was  $p < 0.05$ . Inset depicts the geographic location of Carabobo; black rectangle indicates highlighted study area.

landscape. The radial spread traveled distance was 9.4 km at a mean velocity of 82.9 m/day. The chikungunya epidemic showed spatiotemporal aggregation predominantly south of the capital city, where conditions for human–vector contact are favorable.

The temporal dynamics here described,  $R_0$  and its time variable form  $R_t$  suggest high transmissibility of CHIKV in this population. These results agree with previous CHIKV introductions into naive populations (29–31) and with the 2014 predicted values for the mid-latitude countries ( $R_0 = 4–7$ ) of the Americas (31). High values of  $R_0$  are also described during first introduction outbreaks of other *Aedes* mosquito-borne pathogens, such as DENV in Chile ( $R_0 = 27.2$ ) (32) and Zika virus in Brazil ( $R_0 = 1.5–6$ ) (33) and French Polynesia (34). Yet, overall  $R_0$  estimates for dengue are  $\approx 2–6$  (35). The similarity between the  $R_0$  of CHIKV, DENV, and Zika virus infections, all transmitted by the same main vector, the *Ae. aegypti* mosquito, strongly suggests that the major factor driving the exponential increase of the epidemic curve of arboviruses in naive populations is the transmission efficiency of the vector.

Spatially, trend surface and kriging analyses showed a primary wave of disease spread within the first 80 days in the most likely area of transmission (the southwestern center of Valencia), whereas a second wave at 90 days showed the spread of cases toward the southern, western, and northern areas. This sequential pattern is similar to that of dengue, where transmission within neighborhoods most likely is driven by mosquito presence or abundance

and/or short-distance movement of viremic hosts (36–38), whereas long-distance dissemination is probably generated by human mobility patterns through main roads and motorways. Both movements powerfully affected disease transmission (39,40). Moreover, population density modulates the chance of vector–host contact (30,41), a fact reflected in the variation of calculated velocities across different spatial points and the increased diffusion speed of the epidemic toward the southernmost populated area.

Although CHIKV was introduced into a naive population in Venezuela, the distribution of cases was not random but aggregated into 75 significant space-time clusters, indicating an increased likelihood of vector–host contact. The area with most clusters, the southern part of Valencia city, is characterized by densely populated neighborhoods, lower socioeconomic status, and crowded living conditions. Similar factors increased the risk for dengue transmission and clustering (hot spots) in highly endemic urban areas of Venezuela (42). Poverty and human behavior fostering potential mosquito breeding sites (such as storing water at home) were linked with a greater risk for dengue (42,43). In Venezuela, long-lasting deficits in public services, such as frequent and prolonged interruptions in water supply and electricity, have become regular in recent years. These inadequacies have obliged residents to store water, maintaining adequate breeding conditions for *Aedes* vectors during the dry season and throughout the year (44). During the CHIKV epidemic, the proportion of houses infested with *Aedes* larvae/pupae (house index) in Venezuela was  $>20\%$  (45). The World



Health Organization recommends a house index <5% for adequate vector control (46).

In our study, the average distance among cases within chikungunya clusters was 75 m, which coincided with the reported flying range of urban *Ae. aegypti* females during mark-release-recapture studies (37,47). *Ae. aegypti* females have been reported to visit a maximum of 3 houses in a lifetime while not traveling far from their breeding sites (48,49). Thus, the distance traveled by the vector and the number of possible host encounters with an infected vector cannot explain the entire disease epidemic spread. Other factors, such as movement of viremic hosts, a widely distributed vector, and the lack of herd immunity, may play a role, as for DENV, in long-range spread (37).

The lack of entomologic data and estimates of human movement limit our study. We expect that our estimates based on epidemiologic records are accurate because chikungunya is symptomatic in >80% of cases. Likewise, surveillance in Venezuela is based on symptomatic patient reporting by treating doctors.

Our analysis suggests that the epidemic of chikungunya in Venezuela followed a determined geographic course. This propagation was potentiated south and southwest of the study area. Chikungunya is now established in Venezuela, along with other *Aedes* mosquito-borne infections, such as dengue and Zika. However, further epidemics of these and other reemergent arboviruses (i.e., Mayaro virus [18,50]) are likely to arise. The insights gained in our study will help identify and predict future epidemic waves of upcoming vectorborne infections and quickly define intervention areas and improve outbreak preparedness response in Venezuela and countries with similar settings.

### Acknowledgments

We thank Carenne Ludeña for the support and valuable insights regarding the analysis in this research. We thank Jared Aldstadt who kindly shared the R code for the IKT analysis.

This work was supported by the Fondo Nacional de Ciencia y Tecnología e Innovación (FONACIT), grant 201100129, 20130020; and by the Department of Medical Microbiology and Infection Prevention, University Medical Center Groningen (UMCG), University of Groningen, Groningen, the Netherlands. E.L. and M.V.-G. received the Abel Tasman Talent Program grant from the UMCG, University of Groningen, Groningen, the Netherlands. M.E.G. received a travel grant from the Netherlands Organization for Scientific Research (grant no. 040.11.590/2129), the Netherlands, 2017.

### About the Author

Mr. Lizarazo is a PhD candidate at the University Medical Center Groningen. His research interests are vectorborne

diseases and molecular epidemiology. Dr. Vincenti-Gonzalez is a postdoctoral researcher at the University Medical Center Groningen. Her research interests are vectorborne diseases and spatial-temporal dynamics of infectious diseases.

### References

- Weaver SC, Forrester NL. Chikungunya: evolutionary history and recent epidemic spread. *Antiviral Res.* 2015;120:32–9. <http://dx.doi.org/10.1016/j.antiviral.2015.04.016>
- Patterson J, Sammon M, Garg M. Dengue, Zika and chikungunya: emerging arboviruses in the New World. *West J Emerg Med.* 2016;17:671–9. <http://dx.doi.org/10.5811/westjem.2016.9.30904>
- Robinson MC. An epidemic of virus disease in Southern Province, Tanganyika Territory, in 1952–53. I. Clinical features. *Trans R Soc Trop Med Hyg.* 1955;49:28–32. [http://dx.doi.org/10.1016/0035-9203\(55\)90080-8](http://dx.doi.org/10.1016/0035-9203(55)90080-8)
- Powers AM, Logue CH. Changing patterns of chikungunya virus: re-emergence of a zoonotic arbovirus. *J Gen Virol.* 2007;88:2363–77. <http://dx.doi.org/10.1099/vir.0.82858-0>
- Wolfe ND, Kilbourn AM, Karesh WB, Rahman HA, Bosi EJ, Cropp BC, et al. Sylvatic transmission of arboviruses among Bornean orangutans. *Am J Trop Med Hyg.* 2001;64:310–6. <http://dx.doi.org/10.4269/ajtmh.2001.64.310>
- Chevillon C, Briant L, Renaud F, Devaux C. The chikungunya threat: an ecological and evolutionary perspective. *Trends Microbiol.* 2008;16:80–8. <http://dx.doi.org/10.1016/j.tim.2007.12.003>
- Higgs S, Vanlandingham D. Chikungunya virus and its mosquito vectors. *Vector Borne Zoonotic Dis.* 2015;15:231–40. <http://dx.doi.org/10.1089/vbz.2014.1745>
- Marimoutou C, Ferraro J, Javelle E, Deparis X, Simon F. Chikungunya infection: self-reported rheumatic morbidity and impaired quality of life persist 6 years later. *Clin Microbiol Infect.* 2015;21:688–93. <http://dx.doi.org/10.1016/j.cmi.2015.02.024>
- Elsinga J, Gerstenbluth I, van der Ploeg S, Halabi Y, Lourents NT, Burgerhof JG, et al. Long-term chikungunya sequelae in Curaçao: burden, determinants, and a novel classification tool. *J Infect Dis.* 2017;216:573–81. <http://dx.doi.org/10.1093/infdis/jix312>
- Zeller H, Van Bortel W, Sudre B. Chikungunya: its history in Africa and Asia and its spread to new regions in 2013–2014. *J Infect Dis.* 2016;214(suppl 5):S436–40. <http://dx.doi.org/10.1093/infdis/jiw391>
- Pan American Health Organization. Number of reported cases of chikungunya fever in the Americas—cumulative cases (October 23, 2015) [cited 2017 Aug 20]. [http://www.paho.org/hq/index.php?option=com\\_topics&view=readall&cid=5927&Itemid=40931&lang=en](http://www.paho.org/hq/index.php?option=com_topics&view=readall&cid=5927&Itemid=40931&lang=en)
- Pan American Health Organization. Number of reported cases of chikungunya fever in the Americas—cumulative cases (October 23, 2015) [cited 2017 Aug 20]. [http://www.paho.org/hq/index.php?option=com\\_topics&view=readall&cid=5927&Itemid=40931&lang=en](http://www.paho.org/hq/index.php?option=com_topics&view=readall&cid=5927&Itemid=40931&lang=en)
- Oletta JF. Epidemia de fiebre chikungunya en Venezuela, 2014–2015. *Gac Med Caracas.* 2016;124:122–37.
- Pimentel R, Skewes-Ramm R, Moya J. Chikungunya in the Dominican Republic: lessons learned in the first six months [in Spanish]. *Rev Panam Salud Publica.* 2014;36:336–41.
- Gérardin P, Guernier V, Perrau J, Fianu A, Le Roux K, Grivard P, et al. Estimating chikungunya prevalence in La Réunion Island outbreak by serosurveys: two methods for two critical times of the epidemic. *BMC Infect Dis.* 2008;8:99. <http://dx.doi.org/10.1186/1471-2334-8-99>
- Schwartz O, Albert ML. Biology and pathogenesis of chikungunya virus. *Nat Rev Microbiol.* 2010;8:491–500. <http://dx.doi.org/10.1038/nrmicro2368>

17. Weaver SC. Arrival of chikungunya virus in the new world: prospects for spread and impact on public health. *PLoS Negl Trop Dis*. 2014;8:e2921. <http://dx.doi.org/10.1371/journal.pntd.0002921>
18. Hotez PJ, Murray KO. Dengue, West Nile virus, chikungunya, Zika-and now Mayaro? *PLoS Negl Trop Dis*. 2017;11:e0005462. <http://dx.doi.org/10.1371/journal.pntd.0005462>
19. Instituto Nacional de Estadística [cited 2017 Nov 18]. <http://www.ine.gov.ve>
20. Wallinga J, Lipsitch M. How generation intervals shape the relationship between growth rates and reproductive numbers. *Proc Biol Sci*. 2007;274:599–604. <http://dx.doi.org/10.1098/rspb.2006.3754>
21. Nishiura H, Chowell G, Heesterbeek H, Wallinga J. The ideal reporting interval for an epidemic to objectively interpret the epidemiological time course. *J R Soc Interface*. 2010;7:297–307. <http://dx.doi.org/10.1098/rsif.2009.0153>
22. Coelho FC, de Carvalho LM. Estimating the attack ratio of dengue epidemics under time-varying force of infection using aggregated notification data. *Sci Rep*. 2015;5:18455. <http://dx.doi.org/10.1038/srep18455>
23. Dale M, Fortin M. *Spatial analysis: a guide for ecologists*. 2nd ed. Cambridge (UK): Cambridge University Press; 2014.
24. Wallis K. Use of ranks in one-criterion variance analysis. *J Am Stat Assoc*. 1952;47:583–621. <http://dx.doi.org/10.1080/01621459.1952.10483441>
25. Knox EG. The detection of space–time interactions. *Journal of the Royal Statistical Society. Series C, Applied Statistics*. 1964;13 (1):25–29.
26. Aldstadt J. An incremental Knox test for the determination of the serial interval between successive cases of an infectious disease. *Stochastic Environmental Research and Risk Assessment*. 2007;21:487–500. <http://dx.doi.org/10.1007/s00477-007-0132-3>
27. Chan M, Johansson MA. The incubation periods of dengue viruses. *PLoS One*. 2012;7:e50972. <http://dx.doi.org/10.1371/journal.pone.0050972>
28. David MR, Lourenço-de-Oliveira R, Freitas RM. Container productivity, daily survival rates and dispersal of *Aedes aegypti* mosquitoes in a high income dengue epidemic neighbourhood of Rio de Janeiro: presumed influence of differential urban structure on mosquito biology. *Mem Inst Oswaldo Cruz*. 2009;104:927–32. <http://dx.doi.org/10.1590/S0074-02762009000600019>
29. Boëlle P-Y, Thomas G, Vergu E, Renault P, Valleron A-J, Flahault A. Investigating transmission in a two-wave epidemic of chikungunya fever, Réunion Island. *Vector Borne Zoonotic Dis*. 2008;8:207–17. <http://dx.doi.org/10.1089/vbz.2006.0620>
30. Yakob L, Clements ACA. A mathematical model of chikungunya dynamics and control: the major epidemic on Réunion Island. *PLoS One*. 2013;8:e57448. <http://dx.doi.org/10.1371/journal.pone.0057448>
31. Perkins TA, Metcalf CJ, Grenfell BT, Tatem AJ. Estimating drivers of autochthonous transmission of chikungunya virus in its invasion of the Americas. *PLoS Curr*. 2015;7:7.
32. Chowell G, Fuentes R, Olea A, Aguilera X, Nesse H, Hyman JM. The basic reproduction number R0 and effectiveness of reactive interventions during dengue epidemics: the 2002 dengue outbreak in Easter Island, Chile. *Math Biosci Eng*. 2013;10:1455–74. <http://dx.doi.org/10.3934/mbe.2013.10.1455>
33. Ferguson NM, Cucunubá ZM, Dorigatti I, Nedjati-Gilani GL, Donnelly CA, Basáñez M-G, et al. Countering the Zika epidemic in Latin America. *Science*. 2016;353:353–4. <http://dx.doi.org/10.1126/science.aag0219>
34. Nishiura H, Kinoshita R, Mizumoto K, Yasuda Y, Nah K. Transmission potential of Zika virus infection in the South Pacific. *Int J Infect Dis*. 2016;45:95–7. <http://dx.doi.org/10.1016/j.ijid.2016.02.017>
35. Johansson MA, Hombach J, Cummings DAT. Models of the impact of dengue vaccines: a review of current research and potential approaches. *Vaccine*. 2011;29:5860–8. <http://dx.doi.org/10.1016/j.vaccine.2011.06.042>
36. Waterman SH, Novak RJ, Sather GE, Bailey RE, Rios I, Gubler DJ. Dengue transmission in two Puerto Rican communities in 1982. *Am J Trop Med Hyg*. 1985;34:625–32. <http://dx.doi.org/10.4269/ajtmh.1985.34.625>
37. Vazquez-Prokopec GM, Kitron U, Montgomery B, Horne P, Ritchie SA. Quantifying the spatial dimension of dengue virus epidemic spread within a tropical urban environment. *PLoS Negl Trop Dis*. 2010;4:e920. <http://dx.doi.org/10.1371/journal.pntd.0000920>
38. Stoddard ST, Forshey BM, Morrison AC, Paz-Soldan VA, Vazquez-Prokopec GM, Astete H, et al. House-to-house human movement drives dengue virus transmission. *Proc Natl Acad Sci U S A*. 2013;110:994–9. <http://dx.doi.org/10.1073/pnas.1213349110>
39. Mondini A, de Moraes Bronzoni RV, Nunes SHP, Chiaravalloti Neto F, Massad E, Alonso WJ, et al. Spatio-temporal tracking and phylodynamics of an urban dengue 3 outbreak in São Paulo, Brazil. *PLoS Negl Trop Dis*. 2009;3:e448. <http://dx.doi.org/10.1371/journal.pntd.0000448>
40. Tauil PL. Urbanization and dengue ecology [in Portuguese]. *Cad Saude Publica*. 2001;17(Suppl):99–102. <http://dx.doi.org/10.1590/S0102-311X2001000700018>
41. Gubler DJ. Dengue, urbanization and globalization: the unholy trinity of the 21st century. *Trop Med Health*. 2011;39(Suppl):3–11. <http://dx.doi.org/10.2149/tmh.2011-S05>
42. Vincenti-Gonzalez MF, Grillet ME, Velasco-Salas ZI, Lizarazo EF, Amarista MA, Sierra GM, et al. Spatial analysis of dengue seroprevalence and modeling of transmission risk factors in a dengue hyperendemic city of Venezuela. *PLoS Negl Trop Dis*. 2017;11:e0005317. <http://dx.doi.org/10.1371/journal.pntd.0005317>
43. Agha SB, Tchouassi DP, Bastos ADS, Sang R. Assessment of risk of dengue and yellow fever virus transmission in three major Kenyan cities based on *Stegomyia* indices. *PLoS Negl Trop Dis*. 2017;11:e0005858. <http://dx.doi.org/10.1371/journal.pntd.0005858>
44. Barrera R, Avila J, González-Téllez S. Unreliable supply of potable water and elevated *Aedes aegypti* larval indices: a causal relationship? *J Am Mosq Control Assoc*. 1993;9:189–95.
45. Grillet ME, Del Ventura F. Transmisión del virus Zika: Patrones y mecanismos eco-epidemiológicos de una arbovirosis. *Tribuna del Investigador*. 2016;17:42–61.
46. World Health Organization. Guidelines for dengue surveillance and mosquito control. WHO regional publication, Western Pacific Education in Action Series, no. 8. Geneva: The Organization; 1995.
47. Harrington LC, Scott TW, Lerdtusnee K, Coleman RC, Costero A, Clark GG, et al. Dispersal of the dengue vector *Aedes aegypti* within and between rural communities. *Am J Trop Med Hyg*. 2005;72:209–20. <http://dx.doi.org/10.4269/ajtmh.2005.72.209>
48. Rodhain F, Rosen L. Mosquito vectors and dengue virus-vector relationships. In: Gubler D, Kuno G, editors. *Dengue and dengue haemorrhagic fever*. 1st ed. London (UK): CAB International; 1997. p. 45–60.
49. Getis A, Morrison AC, Gray K, Scott TW. Characteristics of the spatial pattern of the dengue vector, *Aedes aegypti*, in Iquitos, Peru. *Am J Trop Med Hyg*. 2003;69:494–505. <http://dx.doi.org/10.4269/ajtmh.2003.69.494>
50. Auguste AJ, Liria J, Forrester NL, Giambalvo D, Moncada M, Long KC, et al. Evolutionary and ecological characterization of Mayaro virus strains isolated during an outbreak, Venezuela, 2010. *Emerg Infect Dis*. 2015;21:1742–50. <http://dx.doi.org/10.3201/eid2110.141660>

---

Address for correspondence: Adriana Tami, Department of Medical Microbiology, University Medical Center Groningen, Hanzeplein 1 (HPC EB80), 9713 GZ Groningen, the Netherlands; email: a.tami@umcg.nl

---

# Sand Fly–Associated Phlebovirus with Evidence of Neutralizing Antibodies in Humans, Kenya

David P. Tchouassi, Marco Marklewitz, Edith Chepkorir, Florian Zirkel,<sup>1</sup>  
Sheila B. Agha, Caroline C. Tigoi, Edith Koskei, Christian Drosten,  
Christian Borgemeister, Baldwin Torto, Sandra Junglen,<sup>2</sup> Rosemary Sang<sup>2</sup>

We describe a novel virus, designated Ntepes virus (NPV), isolated from sand flies in Kenya. NPV has the characteristic phlebovirus trisegmented genome architecture and is related to, but distinct from, Gabek Forest phlebovirus. Diverse cell cultures derived from wildlife, livestock, and humans were susceptible to NPV, with pronounced permissiveness in swine and rodent cells. NPV infection of newborn mice caused rapid and fatal illness. Permissiveness for NPV replication in sand fly cells, but not mosquito cells, suggests a vector-specific adaptation. Specific neutralizing antibodies were found in 13.9% (26/187) of human serum samples taken at the site of isolation of NPV as well as a disparate site in northeastern Kenya, suggesting a wide distribution. We identify a novel human-infecting arbovirus and highlight the importance of rural areas in tropical Africa for arbovirus surveillance as well as extending arbovirus surveillance to include hematophagous arthropods other than mosquitoes.

**D**isease outbreaks caused by Zika, dengue, yellow fever, chikungunya, and Rift Valley fever viruses illustrate the threat posed by arthropodborne viruses (arboviruses), which affect millions of patients worldwide each year (1–3). Major epidemic arboviruses are thought to have originated in tropical Africa, where they are known or thought to have caused local outbreaks before epidemic or pandemic spread. Early recognition of local outbreaks, including precise identification of the disease-causing agent, is key to effective preparedness against epidemics. However, active surveillance is poorly implemented in most seeding countries.

---

Author affiliations: International Centre of Insect Physiology and Ecology, Nairobi, Kenya (D.P. Tchouassi, E. Chepkorir, S.B. Agha, C.C. Tigoi, B. Torto, R. Sang); Charité-Universitätsmedizin Berlin, Berlin, Germany (M. Marklewitz, F. Zirkel, C. Drosten, S. Junglen); German Center for Infection Research, Berlin (M. Marklewitz, F. Zirkel, C. Drosten, S. Junglen); Center for Virus Research, Kenya Medical Research Institute, Nairobi (E. Koskei, R. Sang); University of Bonn, Bonn, Germany (C. Borgemeister)

DOI: <https://doi.org/10.3201/eid2504.180750>

Monitoring programs for vectors of arboviral diseases often prioritize mosquitoes and ticks (4), neglecting other blood-feeding vectors, such as sand flies. Sand flies transmit protozoan parasites that cause leishmaniasis as well as phleboviruses (order *Bunyavirales*, family *Phenuiviridae*, genus *Phlebovirus*) (5,6). Sand fly–borne phlebovirus infections are known to occur in the Mediterranean basin (7,8). Some of these, such as sandfly fever Naples, Sicilian, and Toscana viruses, are of public health importance, especially Toscana virus, which causes meningitis and encephalitis in humans (8–10).

The International Committee for the Taxonomy of Viruses (ICTV) currently recognizes 10 viral species within the genus *Phlebovirus*: Rift Valley fever virus (RVFV), severe fever with thrombocytopenia syndrome (SFTS) virus, Ukuniemi phlebovirus, Bujaru phlebovirus, Candiru phlebovirus, Chilibre phlebovirus, Frijoles phlebovirus, Punta Toro phlebovirus, Salehabad phlebovirus, and sandfly fever Naples phlebovirus (11). The last 7 species are vectored by sand flies. Novel unclassified phleboviruses (e.g., Fermo, Granada, Punique, and Massilia viruses), as well as recently discovered flaviviruses in sand flies, underline the importance of these neglected vectors of arboviral diseases (12–16).

Sand fly–borne phleboviruses have been studied mainly in the Mediterranean region. Prevalence data for sub-Saharan Africa remain scarce. Studies have found serologic evidence of human infections with Karimabad, sandfly fever Naples, and sandfly fever Sicilian viruses in patients from Sudan with febrile illness (7,17,18). Human infections with sandfly fever Naples and Sicilian viruses have been reported in Uganda, Somalia, Djibouti, and Ethiopia (7,19). However, serologic surveys may be compounded by antigenic cross-reactivity between phleboviruses (except in neutralization assays), thereby precluding the unequivocal identification of the circulating sand fly–borne virus (5). Few studies have incorporated viral genetic characterization.

---

<sup>1</sup>Current affiliation: Biotest AG, Dreieich, Germany.

<sup>2</sup>These authors contributed equally to this article.



We describe a previously unknown phlebovirus discovered during vector surveillance in Kenya, which we designate Ntepes virus (NPV), after the place of sampling of virus-infected sand flies. The complete genome of NPV was sequenced, viral species tropism in cell culture assessed, and pathogenicity in vertebrates proven by infection of mice. Human serum samples from Ntepes and other communities yielded evidence of human infection based on specific virus neutralization.

## Methods

### Sandfly Trapping and Virus Isolation

We trapped sandflies using CDC light traps (John W. Hock, <https://johnwhock.com>) in villages of the Marigat district, Baringo County, Kenya, in February 2014 (Figure 1). We homogenized pools of 5–50 female specimens in minimum essential medium (MEM), inoculated an aliquot of the clarified supernatant (50  $\mu$ L) into Vero cells, and incubated it for up to 14 days with daily monitoring for cytopathic effect (CPE). We passaged CPE-positive supernatant onto fresh Vero E6/7 cells; virus stock solution was generated from the first passage and used for all further experiments. We determined the infectious titer by 50% tissue culture infectious dose (TCID<sub>50</sub>) assay using 10-fold serial dilutions from 10<sup>-1</sup> to 10<sup>-12</sup> of the virus stock inoculated in 5 wells each of subconfluent Vero cells seeded in a 96-well plate. We calculated the virus titer

according to Reed and Muench (20). We estimated the minimum infection rate (MIR) in sandflies using the formula [number of positive pools/total specimens tested]  $\times$  1,000.

### Broad Reverse Transcription PCR Screening

We extracted RNA from cytopathic cell culture supernatant (200  $\mu$ L aliquot) using the Viral RNA Mini Kit (QIAGEN, <https://www.qiagen.com>) and eluted it in 50  $\mu$ L of buffer. We performed cDNA synthesis using SuperScript III reverse transcription (Invitrogen, <https://www.thermofisher.com>) and random hexamer primers (TIB Molbiol, <https://www.tib-molbiol.com>), followed by reverse transcription PCR (RT-PCR) for orthobunyaviruses, alphaviruses, and flaviviruses (21–24). We screened for sand fly-borne phleboviruses by targeting the RNA-dependent RNA polymerase (RdRp) gene using degenerate primers (25). We compared the nucleotide sequences to GenBank using blastn (<https://blast.ncbi.nlm.nih.gov/Blast.cgi>) and subjected them to initial phylogenetic analysis in MEGA6 (26). We further extracted RNA from pooled sand flies and tested it by real-time PCR using NPV-specific primers (forward, 5'-GCAAGAAAGCACTGTGGTGG; reverse, 5'-CGTATGATGATCGGCCACCA; probe, 5'-6-FAM-ACAGCCACCTCTGATGATGC-IBFQ).

### Genotyping of Sand Flies and Blood Meal Analysis

We amplified the barcode region of the cytochrome *c* oxidase subunit I (*COI*) gene using published primers (27). We extracted genomic DNA from individual bloodfed sand fly specimens using the QIAGEN DNeasy Blood and Tissue Kit (QIAGEN). We amplified a 500-bp fragment of the 12S mitochondrial rRNA gene as described (28), sequenced the PCR products, and compared them to GenBank database data. We inferred species-level identification on the basis of  $\geq$ 98% identity spanning  $\geq$ 300 bp, as described by Valinsky et al. (29).

### Next-Generation Sequencing, Genome Annotation, and Phylogenetics

We purified and concentrated virions from the supernatant of infected Vero cells by ultracentrifugation through a 36% sucrose cushion. We extracted viral RNA using the QIAGEN RNeasy Kit according to the manufacturer's instructions. We generated cDNA using the Maxima H Minus Double-Stranded cDNA Synthesis Kit and random hexamer primers (Thermo Fisher Scientific, <https://www.thermofisher.com>). We prepared DNA libraries using the Nextera XT DNA Sample Preparation Kit and analyzed them on an Illumina MiSeq instrument with the MiSeq Reagent Kit v3 (Illumina, <https://www.illumina.com>). We identified viral reads by reference mapping to phleboviruses as well as by BLAST comparisons against a local amino acid sequence library containing translations of open reading frames

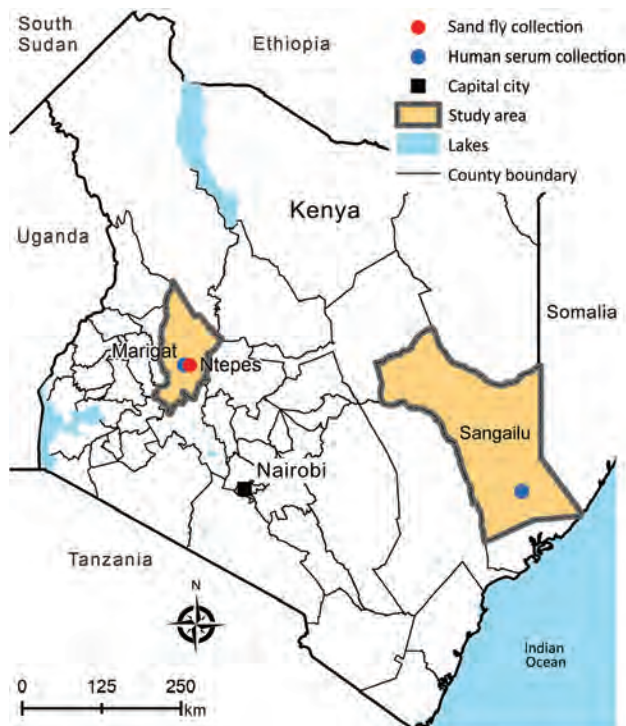


**Figure 1.** Geographic location of sand fly collection site (Ntepes) and district hospitals of Marigat and Sangailu, where human serum samples were collected, Kenya.

(ORFs) of phleboviruses. We closed sequence gaps by conventional RT-PCR followed by Sanger sequencing. We performed genome assembly using Geneious (<http://www.geneious.com>) and confirmed genome terminal sequences by rapid amplification of cDNA ends (RACE-PCR; Life Technologies, <https://www.thermofisher.com>). We identified ORFs using Geneious, compared nucleotide and amino acid sequences with other sequences by blastn and blastx searches against the GenBank database, and identified protein motifs by web-based comparison to the Pfam database (<http://www.pfam.janelia.org>). We identified putative transmembrane regions by prediction of the hydropathy profile using TMHMM (<http://www.cbs.dtu.dk/services/TMHMM-2.0>) and predicted N-linked glycosylation sites using the NetNGlyc 1.0 server (<http://www.cbs.dtu.dk/services/NetNGlyc>).

We aligned nucleotide and amino acid sequences of the ORFs of the respective genome segments with related viral sequences in Geneious using MAFFT (30). Phylogenetic trees were inferred by the maximum-likelihood (ML) method using the best suitable substitution matrix (LG) identified by Modeltest, as implemented in MEGA. We performed confidence testing based on 1,000 bootstrap iterations (31).

#### In Vitro Viral Growth Kinetics

We infected cell lines from insects (LL-5, sand fly; C6/36, mosquito), humans (HEK293-T), small mammals (BHK-21, hamster; VeroE6/7, primate; MEF, mouse; EidNi, bat), and livestock (PK-15, swine; ZN-R, goat; DF-1, chicken; KN-R, cattle) in doublets, at a multiplicity of infection of 0.1. We harvested aliquots of infectious cell culture supernatants every 24 h for periods of 7 d and quantified viral genome copies by real-time RT-PCR with plasmid-based quantification standards.

#### In Vivo Pathogenesis in Suckling Mice

We intracerebrally inoculated 100  $\mu$ L of the viral stock of the first passage, as well as 3 consecutive 2-fold dilutions, into 3–4-day-old Swiss Albino suckling mice. The doses used in the experimental infection were quantified by plaque assays in Vero cells as described previously (32) and corresponded to viral titers of  $4 \times 10^6$ ,  $2 \times 10^6$ ,  $1 \times 10^6$ ,  $5 \times 10^5$ , and  $2.5 \times 10^5$  PFU/mL. We included noninfectious MEM as a negative control. We observed all mice 2 times/day for up to 14 days for signs of disease. We homogenized brains from recently dead mice in 1 mL of cell culture media and plaque-titrated them on Vero cells.

#### Human Serum Samples and Neutralization Tests

Archived serum samples from the Marigat district hospital, taken during 2010–2011, and from Sangailu Health Centre in the Hulugho subcounty in northeastern Kenya,

collected during 2010–2012, were available (Figure 1). We performed a virus neutralization test using 2-fold serial dilutions of serum samples (1:20 to 1:640). We mixed 50  $\mu$ L of the serial serum dilutions with 70 TCID<sub>50</sub> of NPV. Mixtures were incubated at 37°C in the presence of 5% CO<sub>2</sub> for 1 h, then used for infection of a confluent Vero E6/7 cell monolayer seeded in 96-well culture plates with 2 wells/dilution. After 7 days of incubation, we recorded the highest serum dilution at which no CPE was observed in at least 50% of the wells as the neutralization titer.

We tested NPV-reactive human serum samples with RVFV, Gabek Forest virus (GFV), and Karimabad virus (KARV) for serologic cross-reactivity, as described earlier in this article. In addition, we tested GFV- and KARV-positive serum samples with NPV in 2-fold serial dilutions from 1:5 to 1:20 (Table).

#### Ethics Considerations

Approval for the study was granted by the Scientific and Ethical Review Unit and Animal Care and Use Committee of the Kenya Medical Research Institute (SSC Protocol nos. 1560 and KEMRI/SERU/CVR/003/3312). All animal experiments were carried out in accordance with the regulations and guidelines of the Kenya Medical Research Institute.

#### GenBank Accession Numbers

The NPV genome was deposited in GenBank under accession nos. MF695810–MF695812. The *COI* sequence obtained from the virus-positive sand fly pool was deposited in GenBank under accession no. MG913288.

#### Results

##### NPV Isolation and Characterization

In total, 6,434 sand flies were trapped (Figure 1). A subset of 5,481 sandflies was pooled and the resulting 111 pools individually inoculated in VeroE6/7 cells. One pool consisting of 8 females induced CPE 4–5 days postinfection. Sequence analysis of the *COI* gene of the sand flies of this CPE-positive pool suggested that sand flies were of the genus *Sergentomyia*. We identified blood-meal hosts for 62 blood-fed specimens sampled at the same place and time as the pooled specimens. Results revealed that 56 (90.3%) had fed on humans, 2 (3.2%) on snakes, and 1 (1.6%) each on a frog, lizard, cow, and ostrich. The infectious cell culture supernatant tested negative for RVFV, orthobunyaviruses, alphaviruses, and members of genus *Flavivirus*. We amplified a 0.5-kb fragment of the RdRp gene of sand fly–borne phleboviruses using degenerated primers (25). The sequence showed the highest pairwise identity of 79% to GFV and 75% to KARV. We sampled a subset of 953 individual sand fly samples 2 years after the initial study and

tested it in pools of 10 by specific RT-PCR for the cultured virus; results were negative.

Analysis of the complete genome by next-generation sequencing confirmed isolation of a novel phlebovirus. The virus was tentatively termed Ntepes virus, after the location where the sand flies were collected. The virus exhibits the characteristic tripartite-segmented genome organization of phleboviruses, comprising the large (L) segment, which encodes the RdRp protein; the medium (M) segment, encoding a glycoprotein precursor protein (GPC) that is posttranslationally cleaved into 2 viral surface glycoproteins (Gn and Gc) and a nonstructural protein (NSm); and the small (S) segment, encoding the nucleocapsid (N) protein and a nonstructural protein (NS) in an ambisense manner (Figure 2). Highest sequence similarities to GFV were 93% to RdRp, 88% to GPC, 79% to Nsm, 85% to N, and 90% to NS. NPV has the typical conserved genome termini shared among phleboviruses (5'-ACACAAAG and CUUUGUGU-3') (8).

Phylogenetic analyses of NPV RdRp, Gn, Gc, and N proteins and all available sand fly-borne phlebovirus sequences indicate that NPV forms a strongly supported clade with GFV and KARV. NPV branches as a sister taxon to GFV in all genes, suggesting NPV to be a member of the Karimabad species complex (Figure 3). However, the designation of the Karimabad species complex is not yet officially approved by the ICTV. For a provisional genetic classification, we analyzed the intragenetic distances among established phlebovirus species and unclassified isolates based on the RdRp gene. Pairwise nucleotide and amino acid distances between established species ranged from 38% to 62% for nucleotide distances and 39% to 68% for amino acid distances (Appendix Figure, <http://wwwnc.cdc.gov/EID/article/25/4/18-0750-App1.pdf>). For example, amino acid distance between Punta Toro virus and Candiru virus was 39% and between SFTS virus and sandfly fever Naples virus was 68%. Pairwise nucleotide distances ranged from 20% to

**Table.** NT reactivity with NPV, GFV, KARV, and RVFV of serum samples from febrile persons and healthy controls in Kenya\*

Sample ID	Origin	Age, y/sex	Occupation	Acute febrile infection†	Reactivity against			
					NPV	RVFV	GBV	KARV
H01	Marigat	8/F	Student	Fever/chills, head/joint/muscle aches	1:40	None	None	None
H02	Marigat	10/F	Student	Fever/chills, cough, head/joint/muscle aches, eye pain, diarrhea	1:20	None	None	None
H03	Marigat	18/F	Student	Fever/chills, cough, head/joint/muscle aches, jaundice, abdominal pain	1:40	None	None	None
H04	Marigat	19/M	Shop attendant	Acute febrile illness—fever/chills, cough, head/muscle aches	1:20	None	None	None
H05	Marigat	29/M	Driver	Fever/chills, head/joint/muscle aches	1:80	None	None	None
H06	Sangailu	17/F	Housewife	Fever	1:40	None	None	None
H07	Sangailu	25/M	Herdsmen	Fever/chills, headache, diarrhea	1:320	1:1,280	None	None
H08	Sangailu	42/F	Housewife	Fever/chills, headache, abdominal pain	1:40	None	None	None
H09	Sangailu	50/F	Housewife	Fever/chills, cough, head/joint/muscle aches	1:20	None	None	None
H10	Sangailu	24/M	Herder	Fever/chills, head/joint/muscle aches, diarrhea	1:320	None	None	None
H11	Sangailu	53/F	Housewife	Fever, cough, headache, abdominal pain, muscle ache	1:20	None	None	None
H12	Sangailu	26/M	Shepherd	Healthy control	1:20	None	None	None
H13	Sangailu	30/F	Housewife	Healthy control	1:160	None	None	None
H14	Sangailu	65/M	Pastoralist	Healthy control	1:40	1:320	None	None
H15	Sangailu	62/M	Herdsmen	Healthy control	1:80	1:640	None	None
H16	Sangailu	34/F	Housewife	Healthy control	1:80	None	None	None
H17	Sangailu	52/F	Housewife	Healthy control	1:20	None	None	None
H18	Sangailu	50/M	Herdsmen	Healthy control	None	1:1,280	None	None
H19	Sangailu	57/M	Herdsmen	Healthy control	None	1:320	None	None
H20	Sangailu	16/M	Herder	Fever/chills, head/joint/muscle aches, abdominal pain	1:160	1:160	None	None
H21	Sangailu	18/M	Student	Fever, cough, headache, abdominal pains	1:80	None	None	None
H22	Sangailu	9/F	Student	Fever/chills, cough, abdominal pains, joint/muscle aches	1:160	None	None	None
H23	Sangailu	19/F	Housewife	Fever/chills, headache, abdominal pains	1:40	None	None	None
H24	Sangailu	30/F	Housewife	Fever, head/joint/muscle aches, abdominal pain	1:160	1:40	None	None
H25	Sangailu	17/M	Herder	Fever/chills, head/joint/muscle aches, abdominal pain	1:160	None	None	None
H26	Marigat	17/M	Student	Fever/chills, head/joint/muscle aches	1:40	None	None	None

\*GFV, Gabek Forest virus; ID, identification; KARV, Karimabad virus; NPV, Ntepes virus; NT, neutralizing test; RVFV, Rift Valley fever virus.

†Fever defined as body temperature  $\geq 38^{\circ}\text{C}$ .



59% and amino acid distances from 6% to 69% when unclassified tentative species and variants pertaining to established species were included. For example, amino acid distance between Ponticelli virus and Adana virus was 6% and between Naples virus and SFTS virus was 69% (Appendix Figure). NPV showed 7% amino acid distance to GFV and 19% amino acid distance to KARV.

Classical criteria for species demarcation in phleboviruses are based on serology, with established species showing at least 4-fold differences in 2-way neutralization tests (11). We confirmed that NPV did not react with antiserum against its next closest relatives, GFV and KARV, in neutralization tests (Figure 4). NPV Gn protein was 13% different and Gc 4% different from GFV. The Gn protein of phleboviruses is the key component for neutralization and is recognized by specific neutralizing antibodies (33).

Although sequence-based species demarcation criteria have not been determined for phlebovirus species, such criteria exist for the related orthobunyaviruses. Species demarcation criteria are now based on the RdRp gene, which shows  $\geq 6\%$  difference to the closest related virus. Previously unique orthobunyavirus species were defined on  $\geq 10\%$  difference in N protein sequences (11). The N proteins of NPV and GFV differ by 15% (GFV itself is not formally classified as a species, and any of the formally classified phlebovirus species are markedly more distant from NPV in this and other genes; Appendix Figure). We conclude, upon cumulative evidence, that NPV constitutes a putative novel species within the phlebovirus genus.

**Permissiveness in Vertebrates**

To obtain initial data on permissiveness, we performed in vitro growth analyses in a broad range of cell lines derived

from different insect species (sand fly and mosquito), peridomestic wildlife (rodent, nonhuman primate, and bat), and livestock (swine, goat, chicken, and cattle) species, as well as from humans. Results revealed a broad susceptibility to NPV, with peak genome copy numbers in cells derived from swine and rodents (Figure 5, panel A). Cells derived from sand flies but not from mosquitoes were permissive, despite using C6/36 mosquito cells that are normally broadly susceptible to arboviruses because of a defect in their antiviral RNA interference response (34). These findings suggest a host range for NPV similar to those of KARV and GFV, which are transmitted by sand flies and infect rodents (35). It is not known whether rodents are amplificatory or dead-end hosts.

Because GFV is known to induce fatal disease in laboratory mice (36,37), we explored similarities in pathogenicity with NPV. We intracranially inoculated 3–4-day-old Swiss Albino suckling mice, causing tremors, hind-limb paralysis, prostration, and death 5–8 days postinfection (Figure 5, panel B). Time to death was clearly correlated with virus dose. All animals had high infectious virus concentrations in the brain (mean  $2.9 \times 10^6$  PFU/mL). Taken together, the in vitro and in vivo pathogenicity studies of NPV, including the pathogenicity in suckling mice, may suggest that rodents and sand flies may be involved in the maintenance cycle of NPV.

**Evidence for Human Infection with NPV**

To test whether NPV infects humans, we analyzed 187 archived serum samples: 59 samples from the Marigat district hospital in the area where NPV-infected sand flies were trapped, and 128 samples collected in north-eastern Kenya at Sangailu Health Centre (Figure 1). All

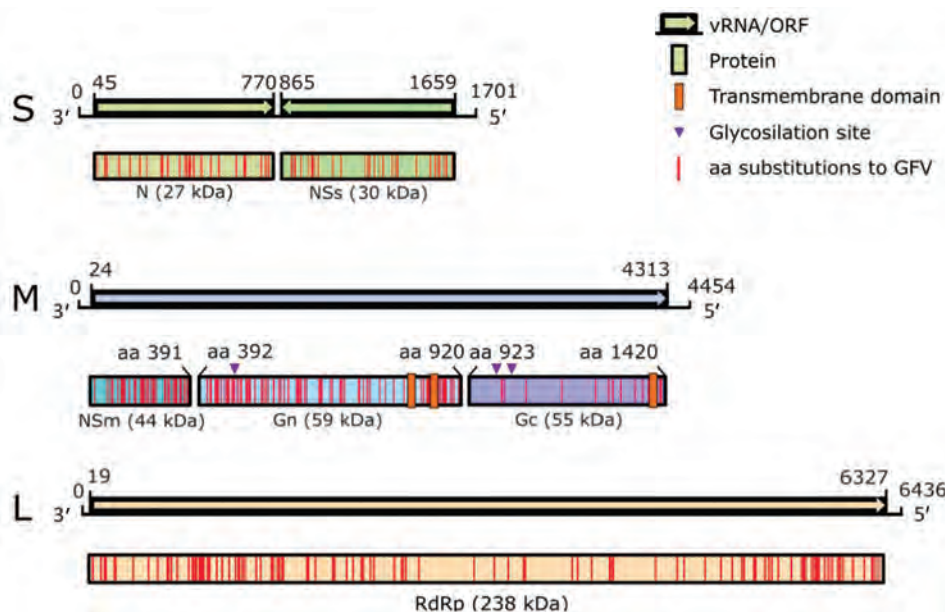


**Figure 2.** Genome organization of novel sand fly-associated phlebovirus Ntepes virus identified in Kenya. Sequence length of the L, M, and S segments (in bp) and encoded predicted proteins RdRp, Gn, Gc, N, and nonstructural proteins NSm and NSs (in kDa) are indicated; ORF positions (length in bp) are also indicated. GFV, Gabek Forest virus; L, large segment (encoding the RdRp protein); M, medium segment (encoding the nonstructural protein NSm and the 2 glycoproteins Gn and Gc); N, nucleocapsid protein; ORF, open reading frame; RdRp, RNA-dependent RNA polymerase; S, small segment (encoding the N protein and nonstructural protein NSs in an ambisense manner); vRNA, virus RNA.

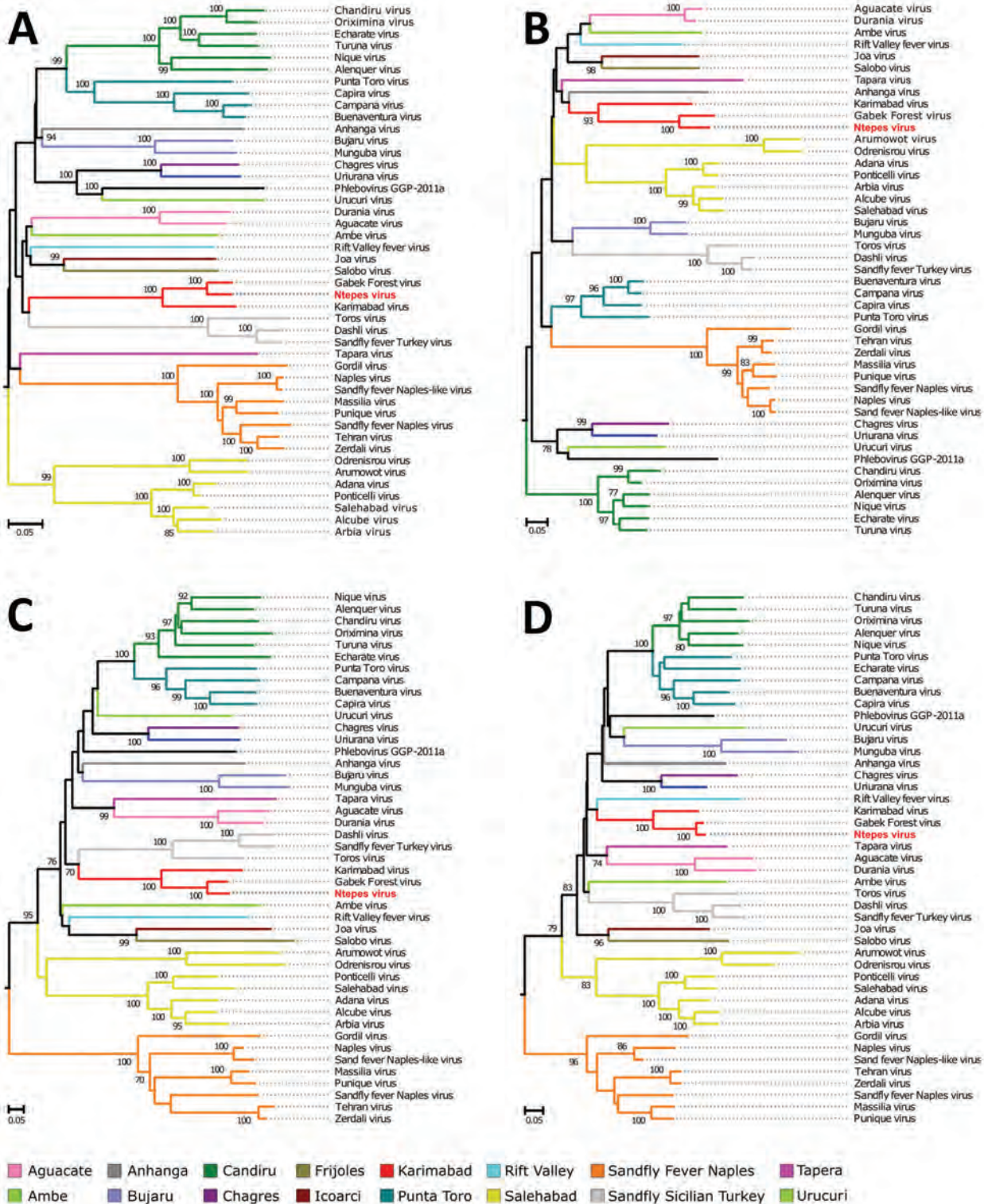


**Figure 3.** Phylogenetic relationship of novel sand fly–associated plebivirus *Ntepes* virus from Kenya (red bold text) in relation to other selected members of the *Phlebovirus* genus. A) RNA-dependent RNA polymerase; B) nucleocapsid protein Gn; C) glycoprotein Gc; D) glycoprotein Gc. The phylogenetic trees were inferred based on complete large, medium, and small protein sequences, applying maximum likelihood analysis in PhyML version 3.0 (<http://www.atgc-montpellier.fr/phyml/versions.php>) using the LG substitution model. Statistical support of the tree topology was evaluated by bootstrap resampling of the sequences 1,000 times. Sequences are identified by virus name and branch colors. Bootstrap values >70 are indicated at the nodes. Scale bar represents numbers of substitutions per site.



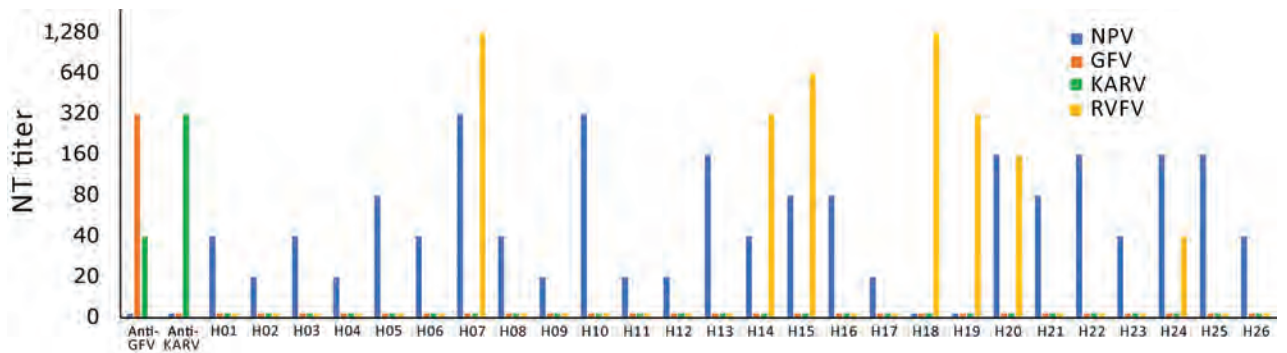


**Figure 4.** Neutralizing activity of novel sand fly–associated phlebovirus Ntepes virus from Kenya in relation to other selected members of the *Phlebovirus* genus. Anti-GFV and anti-KARV samples were tested along with 26 human serum samples. GFV, Gabek Forest virus; H, human; KARV, Karimabad virus; NPV, Ntepes virus; NT, neutralizing test; RVFV, Rift Valley fever virus.

patients from Marigat, as well as 98 patients from Sangailu, had symptoms compatible with acute infectious diseases. The remaining 30 samples from Sangailu came from healthy controls.

Twenty-six (13.9%) serum samples neutralized NPV, with titers ranging from 1:20 to 1:320 (Figure 4). Women and men were infected at equal rates. Positive samples originated from Marigat (10.2%) and Sangailu (15.6%), without statistical differences in rates (Fisher exact test odds ratio [OR] 0.6, 95% CI 0.19–1.70;  $p = 0.37$ ). Detection rates in Sangailu did not differ between healthy and febrile patients (Fisher exact test OR 1.4, 95% CI 0.40–4.3;  $p = 0.58$ ) (Table; Figure 4). No NPV nucleic acids were detected in serum samples by NPV-specific RT-PCR, suggesting no causative link to the present symptoms with NPV. The detection of NPV neutralizing antibodies in geographically unlinked regions of Kenya suggests widespread previous human exposure and infection.

Because NPV is genetically most closely related to GFV and KARV, we tested all NPV-positive serum samples for ability to cross-neutralize GFV or KARV. All tests yielded negative results, providing further support for the classification of NPV as a separate serotype (and species). Because RVFV frequently causes outbreaks in East Africa, we also tested against RVFV, which, according to its phylogenetic relationship with NPV, is not expected to cross-react with NPV. Seven of 26 NPV-neutralizing serum samples were also reactive with RVFV, showing titers that did not correlate in height with titers against NPV (Table; Figure 4). Absence of correlation of titers suggests previous RVFV infection rather than cross-reactivity between RVFV and NPV.

## Discussion

We identified a high percentage of neutralizing antibodies to NPV in humans living in the NPV-endemic area by neutralization assay, confirming that NPV represents a distinct phleboviral species that causes infection in

humans. The fact that the virus was isolated through an exploratory sampling effort is an indicator of the existence of undetected and uncharacterized viruses in this part of Kenya. Although mosquitoes have been the focus of studies on emerging arboviruses, the discovery of a novel sand fly–borne phlebovirus with evidence for human exposure across Kenya indicates the need to broaden vector surveillance activities.

Toscana, sandfly fever Sicilian, and sandfly fever Naples viruses are distributed in the Mediterranean region and northern Africa. GFV has been reported from Sudan, Senegal, Central African Republic, Nigeria, and Benin (38). KARV occurs in eastern and central Asia (7,39,40), as well as Sudan, Egypt, and Nigeria (7). According to this geographic distribution, GFV seems to be the most likely sand fly–borne phlebovirus to co-occur in Kenya. Our results show that NPV-immune serum samples do not react with GFV or KARV, suggesting that the reactivity of the positive human samples was the result of previous infection with NPV.

NPV in Kenya may occupy a niche that is taken by GFV and KARV in northern Africa or eastern and central Asia. Several characteristics of NPV suggest parallels between the host ranges of NPV and GFV. GFV has been detected in rodents (38) but has been detected in arthropods in only a single study in sand flies (35). Further, the virus was shown to be able to infect *Phlebotomus* species under laboratory conditions (Tesh R. Studies of the biology of phleboviruses in sand flies. Paper presented at Yale University School of Medicine, New Haven, CT, USA, 1983), suggesting that GFV is maintained in a transmission cycle that involves rodents and sand flies and that it occasionally infects humans (35). NPV was isolated from sand flies and replicates *in vitro* in sand fly–derived cell lines but not in mosquito cells, similar to sandfly Sicilian and Naples viruses (41). Infection studies with cell lines derived from livestock and peridomestic wildlife species showed that NPV replicates  $\approx 10$ –100 times better in rodent and swine cell



lines than in cells derived from other animals, suggesting the involvement of rodents or swine as potential amplification hosts for NPV.

*COI* gene analyses from the virus-positive sand fly pool suggests that species of the genus *Sergentomyia* have been infected with NPV. Blood-meal analyses revealed that 90% of the analyzed blood-fed sand flies had fed on humans, confirming a likely role as vectors of NPV to humans. Our findings provide new evidence that *Sergentomyia* flies do not strictly feed on reptiles but also feed frequently on humans (42,43).

The NPV antibody prevalence rate in humans (13.9%) is comparable to that of GFV, which is 17%–60% in Sudan, 3%–10% in Egypt, and 3% in Nigeria (7). KARV antibody prevalence is 1%–11% in Sudan, 2% in Egypt, and 1%–62% in regions of Iran and Russia (7). Human serum samples from northern Kenya have been tested and yielded no antibodies against GFV or KARV, which matches our results (7).

NPV appears to have a wide distribution in Kenya; we found equal exposure rates in 2 geographic sets of humans sampled >600 km apart. The serum samples from this study were collected during 2010–2012, suggesting that NPV has been present in humans since at least 2010. Sand fly pools collected in 2014 had low infection rates (MIR 0.18, 1/111 pools, 5–50 sand flies/pool), possibly resulting from collection during a period with low

transmission rates. The estimated MIR is lower compared with previous sand fly infections with phleboviruses such as Punique (MIR 6.7) (14), Massilia (MIR 3.7) (12), and Toscana (MIR 2.2) viruses (44), although comparable to Toros (MIR 0.26) and Zerdali (MIR 0.35) viruses (45). The significance of just 1 isolate of the novel phlebovirus from 111 sand fly pools may seem limited, but it is noteworthy that circulation of RVFV, a phlebovirus with huge epidemic potential, is generally detected at low rates in vectors during interepidemic periods. For instance, multiple surveillance efforts sampling and analyzing thousands of primary and secondary RVFV vectors from outbreak hotspot areas failed to yield any RVFV isolates (46,47), yet RVFV infection rates in mosquitoes during the 2006–2007 outbreak in Kenya were high, ranging between 0.8 and 10.65 per 1,000 for primary vectors (2).

The outcome of infection experiments in mice suggests that NPV could cause diseases such as GFV and RVFV infection (36,37). The neglect of sand fly-borne phleboviruses in Africa is exemplified by outbreaks of acute febrile illness associated with sandfly fever Sicilian virus in Ethiopia, which, for a long time, had remained misdiagnosed as malaria (48), as well as an outbreak of febrile illness probably associated with sandfly fever Naples virus in Sudan (17).

The symptoms reported among most of the tested patients in this study cannot be conclusively linked to NPV

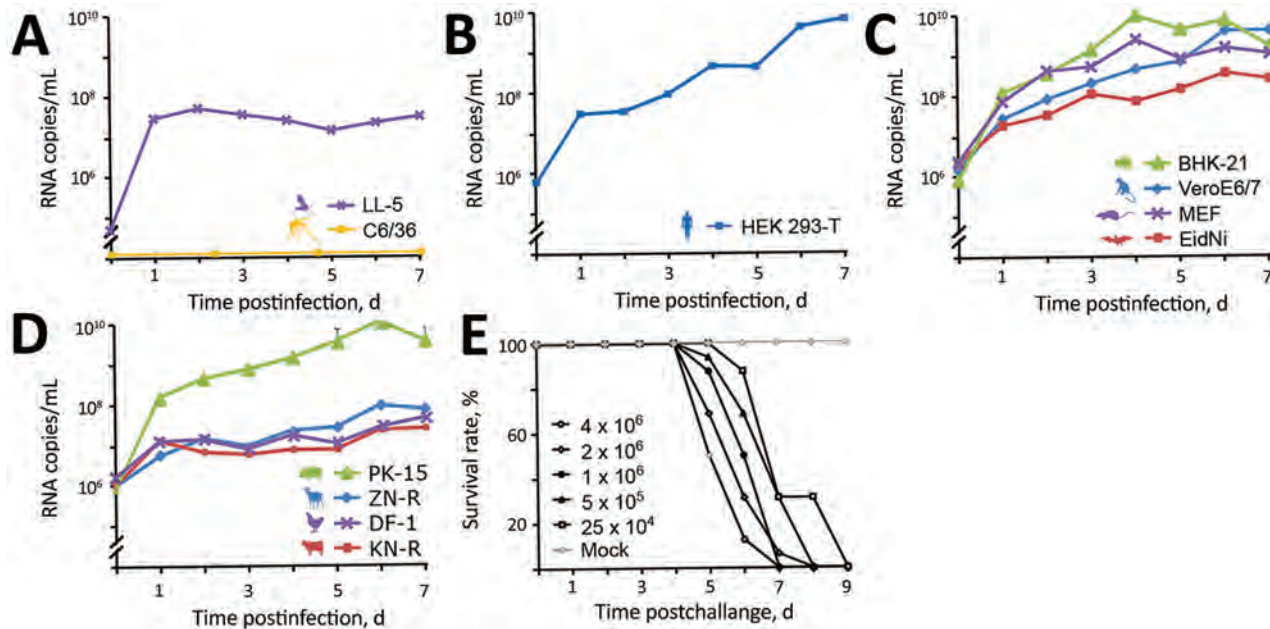


**Figure 5.** In vitro growth kinetics of novel sand fly-associated phlebovirus Ntepes virus from Kenya in different cell lines. A) Insects: LL-5, sand fly; C6/36, mosquito. B) Human: HEK293-T. C) Peridomestic wildlife: hamster, BHK-21; primate, VeroE6/7; mouse, MEF; bat, EidNi. D) Livestock: swine, PK-15; goat, ZN-R; chicken, DF-1; cattle, KN-R. Cells were infected with a multiplicity of infection of 0.1; supernatants were collected every 24 h for 7 d postinfection. Viral genome copies were measured at indicated timepoints by real-time reverse transcription PCR. E) Pathogenicity of Ntepes virus infection in mice. Litters of 2-day-old Swiss Albino suckling mice (8 mice/litter) were intracerebrally inoculated using the indicated virus titers or cell culture media as a control. Animals were monitored daily for signs of disease. Titers are shown in PFU/mL.

infection, as indicated by antibodies in symptomatic patients and healthy controls, demanding further studies of possible disease association. Clinical studies using specific real-time PCR are necessary to detect viral RNA in humans and to measure the clinical impact of NPV.

### Acknowledgments

We thank Mark Rotich for logistical support during field collection of sandflies in Marigat district and Robinson Okiro and Julia Wanjiru for support in the laboratory to sort and pool sand fly samples. Special thanks to John Gachoya for help in mice inoculation, Jackson Kimani for GIS design of the map of the study sites, and the chief and community members at Ntepes for their cooperation and support. We thank Diane E. Griffin and Armanda D.S. Bastos for critical review of the manuscript.

The research is an output from an International Centre of Insect Physiology and Ecology seed grant, awarded to D.P.T. and B.T. D.P.T. also received postdoctoral support through the International Centre of Insect Physiology and Ecology from the UK Department for International Development and the Swedish International Development Cooperation Agency. We also acknowledge financial support from the Swiss Agency for Development and Cooperation and the Kenya government. Work at Charité Berlin was funded by the German Center for Infection Research (grant no. TTU 01.801) as well as by the Deutsche Forschungsgemeinschaft (grant nos. JU 2857/9-1 [to S.J.] and BO 1116/8-1).

### About the Author

Dr. Tchouassi is a disease vector ecologist working as a research scientist at the International Centre of Insect Physiology and Ecology, Nairobi, Kenya. His research interest is in developing and evaluating complementary innovative vector control tools and monitoring of pathogen–vector dynamics for epidemiological assessments.

### References

- Sang RC, Dunster LM. The growing threat of arbovirus transmission and outbreaks in Kenya: a review. *East Afr Med J*. 2001;78:655–61. <http://dx.doi.org/10.4314/eamj.v78i12.8936>
- Sang R, Kioko E, Lutomiah J, Warigia M, Ochieng C, O’Guinn M, et al. Rift Valley fever virus epidemic in Kenya, 2006/2007: the entomologic investigations. *Am J Trop Med Hyg*. 2010;83 (Suppl):28–37. <http://dx.doi.org/10.4269/ajtmh.2010.09-0319>
- Wilder-Smith A, Gubler DJ, Weaver SC, Monath TP, Heymann DL, Scott TW. Epidemic arboviral diseases: priorities for research and public health. *Lancet Infect Dis*. 2017;17:e101–6. [http://dx.doi.org/10.1016/S1473-3099\(16\)30518-7](http://dx.doi.org/10.1016/S1473-3099(16)30518-7)
- Junglen S, Drost C. Virus discovery and recent insights into virus diversity in arthropods. *Curr Opin Microbiol*. 2013;16:507–13. <http://dx.doi.org/10.1016/j.mib.2013.06.005>
- Maroli M, Feliciangeli MD, Bichaud L, Charrel RN, Gradoni L. Phlebotomine sandflies and the spreading of leishmaniases and other diseases of public health concern. *Med Vet Entomol*. 2013; 27:123–47. <http://dx.doi.org/10.1111/j.1365-2915.2012.01034.x>
- Alkan C, Bichaud L, de Lamballerie X, Alten B, Gould EA, Charrel RN. Sandfly-borne phleboviruses of Eurasia and Africa: epidemiology, genetic diversity, geographic range, control measures. *Antiviral Res*. 2013;100:54–74. <http://dx.doi.org/10.1016/j.antiviral.2013.07.005>
- Tesh RB, Saidi S, Gajdamović SJ, Rodhain F, Vesjenjak-Hirjan J. Serological studies on the epidemiology of sandfly fever in the Old World. *Bull World Health Organ*. 1976;54:663–74.
- Elliott RM, Brennan B. Emerging phleboviruses. *Curr Opin Virol*. 2014;5:50–7. <http://dx.doi.org/10.1016/j.coviro.2014.01.011>
- Tesh RB. The genus *Phlebovirus* and its vectors. *Annu Rev Entomol*. 1988;33:169–81. <http://dx.doi.org/10.1146/annurev.en.33.010188.001125>
- Charrel RN, Gallian P, Navarro-Mari J-M, Nicoletti L, Papa A, Sánchez-Seco MP, et al. Emergence of Toscana virus in Europe. *Emerg Infect Dis*. 2005;11:1657–63. <http://dx.doi.org/10.3201/eid1111.050869>
- Maes P, Adkins S, Alkhovsky SV, Avšič-Županc T, Ballinger MJ, Bente DA, et al. Taxonomy of the order Bunyavirales: second update 2018. *Arch Virol*. 2019. <http://dx.doi.org/10.1007/s00705-018-04127-3> [epub ahead of print]
- Charrel RN, Moureau G, Temmam S, Izri A, Marty P, Parola P, et al. Massilia virus, a novel phlebovirus (Bunyaviridae) isolated from sandflies in the Mediterranean. *Vector Borne Zoonotic Dis*. 2009;9:519–30. <http://dx.doi.org/10.1089/vbz.2008.0131>
- Collao X, Palacios G, de Ory F, Sanbonmatsu S, Pérez-Ruiz M, Navarro JM, et al. Granada virus: a natural phlebovirus reassortant of the sandfly fever Naples serocomplex with low seroprevalence in humans. *Am J Trop Med Hyg*. 2010;83:760–5. <http://dx.doi.org/10.4269/ajtmh.2010.09-0697>
- Zhioua E, Moureau G, Chelbi I, Ninove L, Bichaud L, Derbali M, et al. Punique virus, a novel phlebovirus, related to sandfly fever Naples virus, isolated from sandflies collected in Tunisia. *J Gen Virol*. 2010;91:1275–83. <http://dx.doi.org/10.1099/vir.0.019240-0>
- Remoli ME, Fortuna C, Marchi A, Bucci P, Argentini C, Bongiorno G, et al. Viral isolates of a novel putative phlebovirus in the Marche Region of Italy. *Am J Trop Med Hyg*. 2014;90:760–3. <http://dx.doi.org/10.4269/ajtmh.13-0457>
- Ayhan N, Charrel RN. Of phlebotomines (sandflies) and viruses: a comprehensive perspective on a complex situation. *Curr Opin Insect Sci*. 2017;22:117–24. <http://dx.doi.org/10.1016/j.cois.2017.05.019>
- Watts DM, El-Tigani A, Botros BA, Salib AW, Olson JG, McCarthy M, et al. Arthropod-borne viral infections associated with a fever outbreak in the Northern Province of Sudan. *J Trop Med Hyg*. 1994;97:228–30.
- McCarthy MC, Haberberger RL, Salib AW, Soliman BA, El-Tigani A, Khalid IO, et al. Evaluation of arthropod-borne viruses and other infectious disease pathogens as the causes of febrile illnesses in the Khartoum Province of Sudan. *J Med Virol*. 1996;48:141–6. [http://dx.doi.org/10.1002/\(SICI\)1096-9071\(199602\)48:2<141::AID-JMV4>3.0.CO;2-9](http://dx.doi.org/10.1002/(SICI)1096-9071(199602)48:2<141::AID-JMV4>3.0.CO;2-9)
- Rodhain F, Gonzalez J-P, Mercier E, Helync B, Larouze B, Hannoun C. Arbovirus infections and viral haemorrhagic fevers in Uganda: a serological survey in Karamoja district, 1984. *Trans R Soc Trop Med Hyg*. 1989;83:851–4. [http://dx.doi.org/10.1016/0035-9203\(89\)90352-0](http://dx.doi.org/10.1016/0035-9203(89)90352-0)
- Reed LJ, Muench H. A simple method of estimating fifty per cent endpoints. *Am J Epidemiol*. 1938;27:493–7. <http://dx.doi.org/10.1093/oxfordjournals.aje.a118408>
- Kuno G, Mitchell CJ, Chang GJ, Smith GC. Detecting bunyaviruses of the Bunyamwera and California serogroups by a PCR technique. *J Clin Microbiol*. 1996;34:1184–8.
- Kuno G, Chang G-JJ, Tsuchiya KR, Karabatsos N, Cropp CB. Phylogeny of the genus *Flavivirus*. *J Virol*. 1998;72:73–83.

23. Shoemaker T, Boulianne C, Vincent MJ, Pezzanite L, Al-Qahtani MM, Al-Mazrou Y, et al. Genetic analysis of viruses associated with emergence of Rift Valley fever in Saudi Arabia and Yemen, 2000–01. *Emerg Infect Dis.* 2002;8:1415–20. <http://dx.doi.org/10.3201/eid0812.020195>
24. Eshoo MW, Whitehouse CA, Zoll ST, Massire C, Pennella T-TD, Blyn LB, et al. Direct broad-range detection of alphaviruses in mosquito extracts. *Virology.* 2007;368:286–95. <http://dx.doi.org/10.1016/j.virol.2007.06.016>
25. Sánchez-Seco MP, Echevarría JM, Hernández L, Estévez D, Navarro-Mari JM, Tenorio A. Detection and identification of Toscana and other phleboviruses by RT-nested-PCR assays with degenerated primers. *J Med Virol.* 2003;71:140–9. <http://dx.doi.org/10.1002/jmv.10465>
26. Tamura K, Stecher G, Peterson D, Filipski A, Kumar S. MEGA6: molecular evolutionary genetics analysis version 6.0. *Mol Biol Evol.* 2013;30:2725–9. <http://dx.doi.org/10.1093/molbev/mst197>
27. Folmer O, Black M, Hoeh W, Lutz R, Vrijenhoek R. DNA primers for amplification of mitochondrial cytochrome c oxidase subunit I from diverse metazoan invertebrates. *Mol Mar Biol Biotechnol.* 1994;3:294–9.
28. Roca AL, Bar-Gal GK, Eizirik E, Helgen KM, Maria R, Springer MS, et al. Mesozoic origin for West Indian insectivores. *Nature.* 2004;429:649–51. <http://dx.doi.org/10.1038/nature02597>
29. Valinsky L, Ettinger G, Bar-Gal GK, Orshan L. Molecular identification of bloodmeals from sand flies and mosquitoes collected in Israel. *J Med Entomol.* 2014;51:678–85. <http://dx.doi.org/10.1603/MEI13125>
30. Katoh K, Misawa K, Kuma K, Miyata T. MAFFT: a novel method for rapid multiple sequence alignment based on fast Fourier transform. *Nucleic Acids Res.* 2002;30:3059–66. <http://dx.doi.org/10.1093/nar/gkf436>
31. Guindon S, Gascuel O. A simple, fast, and accurate algorithm to estimate large phylogenies by maximum likelihood. *Syst Biol.* 2003;52:696–704. <http://dx.doi.org/10.1080/10635150390235520>
32. Agha SB, Chepkorir E, Mulwa F, Tigo C, Arum S, Guarido MM, et al. Vector competence of populations of *Aedes aegypti* from three distinct cities in Kenya for chikungunya virus. *PLoS Negl Trop Dis.* 2017;11:e0005860. <http://dx.doi.org/10.1371/journal.pntd.0005860>
33. Wu Y, Zhu Y, Gao F, Jiao Y, Oladejo BO, Chai Y, et al. Structures of phlebovirus glycoprotein Gn and identification of a neutralizing antibody epitope. *Proc Natl Acad Sci U S A.* 2017;114:E7564–73. <http://dx.doi.org/10.1073/pnas.1705176114>
34. Brackney DE, Scott JC, Sagawa F, Woodward JE, Miller NA, Schilkey FD, et al. C6/36 *Aedes albopictus* cells have a dysfunctional antiviral RNA interference response. *PLoS Negl Trop Dis.* 2010;4:e856. <http://dx.doi.org/10.1371/journal.pntd.0000856>
35. Traoré-Lamizana M, Fontenille D, Diallo M, Bâ Y, Zeller HG, Mondo M, et al. Arbovirus surveillance from 1990 to 1995 in the Barkedji area (Ferlo) of Senegal, a possible natural focus of Rift Valley fever virus. *J Med Entomol.* 2001;38:480–92. <http://dx.doi.org/10.1603/0022-2585-38.4.480>
36. Tesh RB, Duboise SM. Viremia and immune response with sequential phlebovirus infections. *Am J Trop Med Hyg.* 1987;36:662–8. <http://dx.doi.org/10.4269/ajtmh.1987.36.662>
37. Fisher AF, Tesh RB, Tonry J, Guzman H, Liu D, Xiao S-Y. Induction of severe disease in hamsters by two sandfly fever group viruses, Punta toro and Gabek Forest (Phlebovirus, Bunyaviridae), similar to that caused by Rift Valley fever virus. *Am J Trop Med Hyg.* 2003;69:269–76. <http://dx.doi.org/10.4269/ajtmh.2003.69.269>
38. Kemp GE, Causey OR, Setzer HW, Moore DL. Isolation of viruses from wild mammals in West Africa, 1966–1970. *J Wildl Dis.* 1974;10:279–93. <http://dx.doi.org/10.7589/0090-3558-10.3.279>
39. Tesh R, Saidi S, Javadian E, Nadim A. Studies on the epidemiology of sandfly fever in Iran. I. Virus isolates obtained from Phlebotomus. *Am J Trop Med Hyg.* 1977;26:282–7. <http://dx.doi.org/10.4269/ajtmh.1977.26.282>
40. Gaidamovich SY, Khutoretskaya NV, Asyamov Y, Tsyupa V, Melnikova EE. Sandfly fever in central Asia and Afghanistan. In: Calisher CH, editor. Hemorrhagic fever with renal syndrome, tick- and mosquito-borne viruses. Vienna: Springer; 1991. p. 287–93.
41. Karabatos N. International catalogue of arboviruses including certain other viruses of vertebrates. 3rd ed. San Antonio (TX): American Society of Tropical Medicine and Hygiene; 1985.
42. Jaouadi K, Haouas N, Chaara D, Boudabous R, Gorgii M, Kidar A, et al. Phlebotomine (Diptera, Psychodidae) bloodmeal sources in Tunisian cutaneous leishmaniasis foci: could *Sergentomyia minuta*, which is not an exclusive herpetophilic species, be implicated in the transmission of pathogens? *Ann Entomol Soc Am.* 2013;106:79–85. <http://dx.doi.org/10.1603/AN11186>
43. Maia C, Parreira R, Cristóvão JM, Freitas FB, Afonso MO, Campino L. Molecular detection of *Leishmania* DNA and identification of blood meals in wild caught phlebotomine sand flies (Diptera: Psychodidae) from southern Portugal. *Parasit Vectors.* 2015;8:173. <http://dx.doi.org/10.1186/s13071-015-0787-4>
44. Charrel RN, Izri A, Temmam S, Delaunay P, Toga I, Dumon H, et al. Cocirculation of 2 genotypes of Toscana virus, southeastern France. *Emerg Infect Dis.* 2007;13:465–8. <http://dx.doi.org/10.3201/eid1303.061086>
45. Alkan C, Erisoz Kasap O, Alten B, de Lamballerie X, Charrel RN. Sandfly-borne phlebovirus isolations from Turkey: New insight into the sandfly fever Sicilian and sandfly fever Naples species. *PLoS Negl Trop Dis.* 2016;10:e0004519. <http://dx.doi.org/10.1371/journal.pntd.0004519>
46. Ochieng C, Lutomiah J, Makio A, Koka H, Chepkorir E, Yalwala S, et al. Mosquito-borne arbovirus surveillance at selected sites in diverse ecological zones of Kenya; 2007–2012. *Virol J.* 2013;10:140. <http://dx.doi.org/10.1186/1743-422X-10-140>
47. Sang R, Arum S, Chepkorir E, Mosomtai G, Tigo C, Sigei F, et al. Distribution and abundance of key vectors of Rift Valley fever and other arboviruses in two ecologically distinct counties in Kenya. *PLoS Negl Trop Dis.* 2017;11:e0005341. <http://dx.doi.org/10.1371/journal.pntd.0005341>
48. Woyessa AB, Omballa V, Wang D, Lambert A, Waiboci L, Ayele W, et al. An outbreak of acute febrile illness caused by sandfly fever Sicilian virus in the Afar region of Ethiopia, 2011. *Am J Trop Med Hyg.* 2014;91:1250–3. <http://dx.doi.org/10.4269/ajtmh.14-0299>

---

Address for correspondence: David P. Tchouassi, International Centre of Insect Physiology and Ecology, Nairobi, Kenya; e-mail: dtchouassi@icipe.org; Sandra Junglen, Institute of Virology, Charité-Universitätsmedizin Berlin, Charitéplatz 1, 10117 Berlin, Germany; e-mail: Sandra.junglen@charite.de



---

# Human-Origin Influenza A(H3N2) Reassortant Viruses in Swine, Southeast Mexico

Martha I. Nelson, Carine K. Souza, Nidia S. Trovão, Andres Diaz, Ignacio Mena, Albert Rovira, Amy L. Vincent, Montserrat Torremorell, Douglas Marthaler,<sup>1</sup> Marie R. Culhane

The genetic diversity of influenza A viruses circulating in swine in Mexico complicates control efforts in animals and presents a threat to humans, as shown by influenza A(H1N1)pdm09 virus. To describe evolution of swine influenza A viruses in Mexico and evaluate strains for vaccine development, we sequenced the genomes of 59 viruses and performed antigenic cartography on strains from 5 regions. We found that genetic and antigenic diversity were particularly high in southeast Mexico because of repeated introductions of viruses from humans and swine in other regions in Mexico. We identified novel reassortant H3N2 viruses with genome segments derived from 2 different viruses that were independently introduced from humans into swine: pandemic H1N1 viruses and seasonal H3N2 viruses. The Mexico swine viruses are antigenically distinct from US swine lineages. Protection against these viruses is unlikely to be afforded by US virus vaccines and would require development of new vaccines specifically targeting these diverse strains.

Genetically diverse influenza A viruses (IAV) circulate in swine globally, complicating efforts to control the virus and increasing the threat that a novel virus will emerge in pigs with the capacity to infect humans. This threat was exemplified by the influenza A(H1N1)pdm09 virus, which originated in swine in Mexico, most likely in the west or central–north regions (1). Although IAVs have been endemic in US swine herds since 1919 (2), there is no evidence that IAVs circulated in swine in Mexico before the 1990s. The emergence of Mexico as a hub of swine IAV diversity with pandemic potential is a relatively recent event.

---

Author affiliations: National Institutes of Health, Bethesda, Maryland, USA (M.I. Nelson, N.S. Trovão); National Animal Disease Center, Ames, Iowa, USA (C.K. Souza, A.L. Vincent); Icahn School of Medicine at Mount Sinai, New York, New York, USA (N.S. Trovão, I. Mena); University of Minnesota, Saint Paul, Minnesota, USA (A. Diaz, A. Rovira, M. Torremorell, D. Marthaler, M.R. Culhane)

DOI: <https://doi.org/10.3201/eid2504.180779>

During 1989–2015, >2 million hogs raised in the United States were transported to Mexico, representing >87% of all US swine exports (Figure 1, panel A). During the 1990s, ≈100,000 live hogs were transported annually, on average, from the United States to Mexico (Figure 1, panel B), thus facilitating establishment of 2 major North American swine IAV lineages in Mexico by the end of the decade: triple reassortant swine H3N2 (TRswH3N2) viruses and classical swine H1N1 (CswH1N1) viruses (1) (referred to as lineage 1A according to recently proposed H1 nomenclature [3]). Avian-like Eurasian swine H1N1 (EAswH1N1, lineage 1C [3]) viruses were also introduced into multiple regions of Mexico from Europe. Previously, EAswH1N1 viruses had only been detected in Europe and Asia (4–6), and Mexico is the only country in the Americas where TRswH3N2, CswH1N1, and EAswH1N1 lineages co-circulate and exchange genome segments by reassortment (1).

Increased surveillance of swine IAV in Mexico and other understudied countries has elucidated how international trade of live swine drives the long-distance migration of these viruses. For many decades, countries with less-established swine production have imported breeding stock from North America and Europe, facilitating long-range dissemination of swine IAV lineages to China and Southeast Asia (4,7,8). Swine movements between US regions regularly facilitate long-range swine IAV migration across the country (9), but long-distance movements of pigs between regions in Mexico are less frequent.

The 6 largest swine-producing states in Mexico are located in the west (Jalisco, ≈2.8 million swine), northwest (Sonora, ≈1.7 million swine), east (Puebla, ≈1.6 million swine and Veracruz, ≈1.5 million swine), central–north (Guanajuato, ≈0.9 million swine), and southeast (Yucatan, ≈0.9 million swine) regions (Figure 2). During 1973–2009, Mexico implemented a campaign to eradicate classical swine fever virus (CSFV), including restrictions on animal movements between CSFV-free areas and central regions

---

<sup>1</sup>Current affiliation: Kansas State University, Manhattan, Kansas, USA.

experiencing outbreaks (10) (Figure 2). Lifting of internal movement controls during 2009 provided new opportunities for swine IAV to migrate between regions in Mexico.

To determine the genetic and antigenic diversity of swine IAVs circulating in Mexico, we sequenced genomes of 59 swine IAV samples collected in northwest and southeast Mexico (GenBank accession nos. MG836712–831) (Appendix Table 1, <https://wwwnc.cdc.gov/EID/article/25/4/18-0779-App1.pdf>). We also evaluated the relationship of Mexico swine IAVs to those used in existing vaccines to determine whether new vaccine development is necessary.

## Materials and Methods

### Collection of Swine IAV in Mexico

Respiratory tract samples were collected by veterinarians and farm staff from pigs with clinical signs of respiratory disease on farms in the northwest and southeast regions of Mexico during 2010–2014. These samples were sent ad hoc to the University of Minnesota Veterinary Diagnostic Laboratory (St. Paul, MN, USA) for swine respiratory disease diagnostic investigations. This laboratory conducted matrix gene testing for swine IAV by using a real-time reverse transcription PCR (RT-PCR) (11) and virus isolation in MDCK cells (12) for swine IAV PCR-positive samples, as requested by the submitting party. Hemagglutinin (HA) and neuraminidase (NA) subtyping of RT-PCR-positive samples was completed (13). Sequencing of the HA, but not other segments, was performed previously (14).

We obtained whole-genome sequences from virus isolates or directly from the originally submitted respiratory tract material. RNA was extracted from the original material or virus isolates as described (14). In brief, we extracted virus RNA from 50  $\mu$ L of swab supernatant by using a magnetic bead procedure and obtained segment-specific PCR fragments by using the One-Step RT-PCR (QIAGEN, <https://www.qiagen.com>) and IAV-specific primers for each genome segment as described (15). We obtained 59 complete genomes, 37 from southeast Mexico and 22 from northwest Mexico. All sequences were submitted to GenBank under accessions nos. MG836712–831.

### Phylogenetic Analysis

We generated nucleotide alignments for each of the 8 segments of the virus genome (HA, matrix protein [MP], NA, nucleoprotein [NP], nonstructural [NS], polymerase acidic [PA], polymerase basic 1 [PB1], and polymerase basic 2 [PB2]) by using MUSCLE version 3.8.31 (16). We inferred initial trees for each segment by using neighbor-joining methods to identify major lineages, including pandemic (p), TRswH3N2 (t), CswH1N1 (c), and EAswH1N1 (e): PB2t, PB1p, PB1t, PAp, PAt, H1c, H1p, H3t + H3h, NPp, NPt,

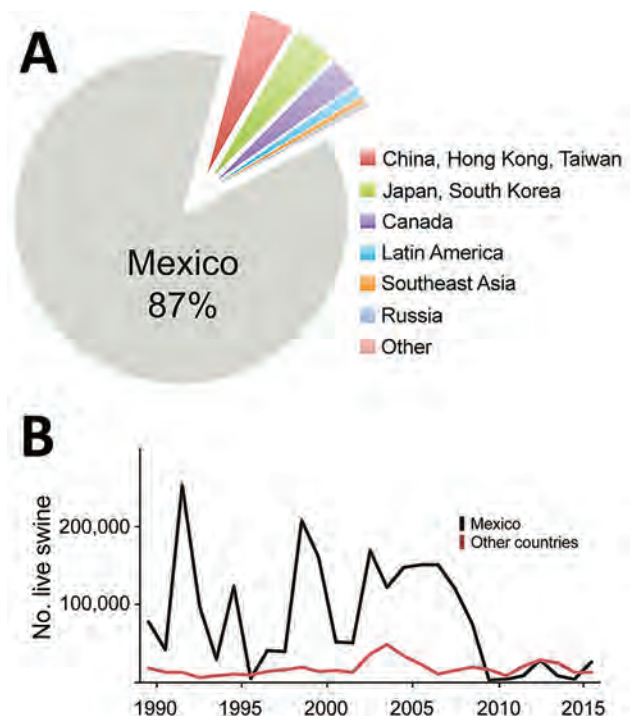


**Figure 1.** Swine exportation to Mexico from the United States and eradication of CSFV in Mexico. A) Hogs exported from the United States to other countries globally during 1989–2015. Of  $\approx 3.7$  million exported,  $\approx 3.1$  million ( $\approx 87\%$ ) were exported to Mexico. B) Since 1989, the number of hogs exported from the United States to Mexico has experienced year-to-year variation. Data are available from the US International Trade Commission (<https://dataweb.usitc.gov>).

N1c, N1e, N1p, N2t + N2h, MPe, MPp, MPt, NSp, and NSt. For simplicity, we visualized human H3N2 (huH3N2) and TRswH3N2 together on the H3 and N2 phylogenies. As additional background data, we downloaded related human and swine sequences from the Influenza Virus Resource (17) that were studied previously, including swine viruses from Mexico, which are indicated with the abbreviation AVX (e.g., A/swine/Mexico/AVX-24/2012[H1N1]) (1).

For each pandemic H1N1 virus alignment, we inferred the phylogenetic relationships by using the maximum-likelihood method in RAXML version 7.2.6 (18) and incorporated a general time-reversible model of nucleotide substitution with a gamma-distributed rate variation among sites. To assess the robustness of each node, we performed a bootstrap resampling process (500 replicates). We used the high-performance computational capabilities of the Biowulf Linux cluster at the National Institutes of Health (Bethesda, MD, USA) (<http://biowulf.nih.gov>). For TRswH3N2, EAswH1N1, CswH1N1, and huH3N2, we inferred time-scaled phylogenies by using Markov chain Monte Carlo (MCMC) methods available in the BEAST package version 1.8.4 (19) and used a relaxed uncorrelated lognormal molecular clock, a constant population



**Figure 2.** Swine exportation to Mexico from the United States and eradication of CSFV in Mexico. The 32 states of Mexico shaded according to the year when CSFV was declared to be eradicated by the Secretariat of Agriculture, Livestock, Rural Development, Fishery and Food of the government of Mexico. International borders are shaded between Mexico and the United States (red), Belize (blue), and Guatemala (violet). The 8 regions of Mexico are indicated, and their borders are shaded orange. CSFV, classical swine fever virus.

demographic model, and a general time reversible-model of nucleotide substitution with a gamma-distributed rate variation among sites. We ran the MCMC chain separately 3 times for each of the datasets for  $\geq 100$  million iterations, with subsampling every 10,000 iterations.

We used the BEAGLE library (20) to improve computational performance. All parameters reached convergence, as assessed visually by using Tracer version 1.6 in BEAST; statistical uncertainty was reflected by values of the 95% highest posterior density. The initial 10% of the chain was removed as burn-in, runs were combined by using Log-Combiner version 1.8.4 in BEAST, and maximum clade credibility trees were summarized by using TreeAnnotator version 1.8.4 in BEAST. We classified H1 viruses by using the H1 swine clade classification tool available at the Influenza Research Database (<http://www.fludb.org>) (3) (Appendix Table 1).

We inferred the timing of the introduction of human seasonal H3N2 viruses into swine in southeast Mexico on the basis of the time to the most recent common ancestor of the clade of viruses identified in swine and the most closely related human viruses, sampled in the mid-1990s. Inferring the precise timing of human-to-swine transmission events that occurred many decades ago is complicated by the lack of sequence data available from swine in previous decades, and the most parsimonious interpretation is that long branch lengths indicate gaps in sampling in swine, rather than humans, an approach that has been described in detail (13).

### Spatial Analysis

The 31 states of Mexico (plus the Federal District) are located within 8 defined regions (Figure 2). We conducted phylogeographic analysis at a regional level to ensure deidentification for swine producers. Swine IAV sequences

were available for 5 regions in Mexico (northwest, west, central–north, east, and southeast). To reduce complexity for maximum clade credibility, we categorized viruses categorized as northwest region (NW), southeast region (SE), or central–north (CN), east (E), or west (W) regions.

We categorized global background sequences as USA/Canada, Asia, Europe, South America, and humans (globally). The location state was specified for each virus sequence, which enabled the expected number of location state transitions in the ancestral history conditional on the data observed at the 3 tips to be estimated by using Markov jump counts (21), providing a quantitative measure of asymmetry in gene flow between regions. The location of viruses in the pandemic H1N1 clade (pH1N1) was left uninformed, which enabled the reconstruction of the location state of the common ancestor of pH1N1 to be unbiased by human data. For computational efficiency we conducted the phylogeographic analysis by using an empirical distribution of 1,000 trees (22), running the MCMC chain for 25 million iterations, and sampling every 1,000 steps. We used a nonreversible diffusion model and Bayesian stochastic search variable selection to improve statistical efficiency for all datasets containing  $>4$  location states. Heat maps were constructed by using the R package to summarize Markov jump counts inferred over phylogenies for all segments and swine IAV lineages (23).

### Movements of Live Swine

We obtained the number of US live swine exports during 1989–2015 from the US International Trade Commission (<https://dataweb.usitc.gov/scripts/REPORT.asp>) by using HS Code 0103. Data were cross-referenced against the United Nations Commodity Trade Statistics Database (<http://comtrade.un.org>), which provides the trade value (in US dollars) for live swine trade between countries for



the years 1996–2012. We obtained the estimated live swine population size of Mexico from the Mexico Secretariat of Agriculture, Livestock, Rural Development, Fisheries and Food (<https://www.siap.gob.mx>). Information on movements of live swine between Mexican states is available only for the relatively small number of pigs that go through plants that pass official government inspections, known as Tipo Inspección Federal plants.

Information on the year of CSFV eradication and opening of border restrictions in each state of Mexico was based on reports of the Secretariat of Agriculture, Livestock, Rural Development, Fisheries and Food. We corroborated these data with reports from the Animal and Plant Health Inspection Service of the US Department of Agriculture (US National Archives) (<https://www.federalregister.gov>; document nos. 02-11897, 02-24753, and E7-10641).

### Antigenic Characterization

Representative H3N2 strains from the United States and Mexico and a human seasonal strain (Appendix Table 2) genetically related to the unique H3N2 swine virus introduced into Mexico were selected from sequence and motif analyses and used for hemagglutination inhibition (HI) assays. The analysis included 5 swine influenza viruses from Mexico reported by Mena et al. (1). Monovalent antiserum against swine IAV H3N2 strains was prepared in swine as described (24) and used for HI assays (25) with 5 H3N2 swine viruses from Mexico as antigens. HI data were used to determine the antigenic relationships between swine H3 from Mexico and the United States by using antigenic cartography 3-dimensional maps (24). Antigenic distances between viruses were calculated in antigenic units (AUs), in which 1 AU is equivalent to a 2-fold loss in HI cross-reactivity (Appendix Table 3). Antigenic distances generated in the 3-dimensional map between the H3N2 antigens were plotted by using GraphPad Prism Version 7.03 (<https://www.graphpad.com>).

## Results

### Genetic Diversity of Swine IAV in Mexico

Phylogenetic analysis of the 59 swine IAV whole-genome sequences generated for this study showed that extensive genetic diversity is circulating in the northwest and southeast regions of Mexico. This viral diversity was produced by 3 evolutionary processes: human-to-swine transmission, long-distance movements of swine, and genomic reassortment. We identified 15 genotypes, including 13 reassortant genotypes with segments from multiple IAV lineages (Figure 3). Three IAV lineages were observed in swine in northwest Mexico: human-origin pH1N1 (1A.3.3.2), TRswH3, and CswH1. These 3 lineages also were identified in southeast Mexico, along with 2 additional lineages: EAswH1N1,

likely introduced from pigs in Europe, and huH3N2, which appears to have been introduced from humans into swine in the 1990s. Eight reassortant genotypes were identified that were not identified in swine in Mexico in previous studies (1), including 1 triple reassortant (TRswH3N2/pH1N1/EAswH1N1, genotype 6) (Figure 3).

Seven of the 8 reassortant genotypes identified in northwest Mexico were generated by reassortment between TRswH3N2 and pH1N1 viruses. Genotype 8 is similar to the pH1N1 precursor viruses identified previously in the west and central-north regions of Mexico (1) and represents the first detection of the genotype outside of the west and central-north regions (Figure 3). Approximately 35% (13/37) of the viruses identified in southeast Mexico were pH1N1/huH3N2 reassortants (Figure 3), in which internal genes were replaced with internal genes of a pH1N1 virus. Seven viruses had possible evidence of co-infection, but only in the MP segment. However, this finding requires further confirmation.

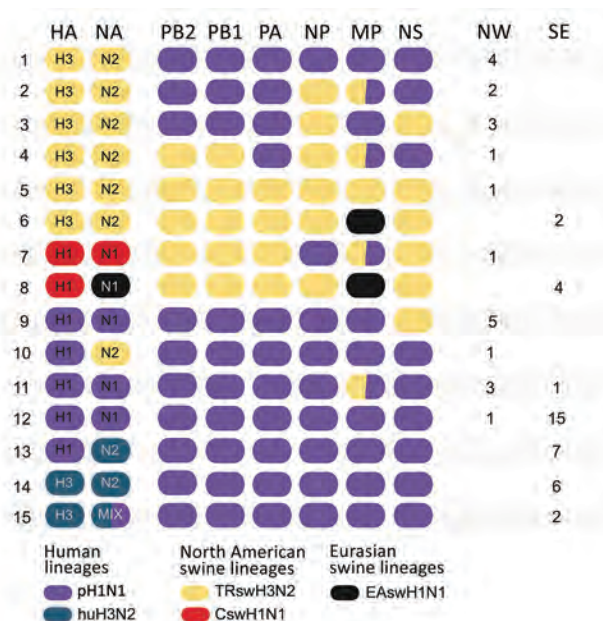


**Figure 3.** Genetic diversity of influenza A viruses (IAVs) circulating in swine in southeast and northwest Mexico. Fifteen genotypes were identified by surveillance in swine herds in Mexico during 2010–2014. Each oval represents 1 of the 8 segments of the virus genome. The surface antigens HA and NA are listed first, followed by the 6 internal gene segments. Shading of each oval corresponds to 1 of 5 major genetic lineages of swine IAV circulating in humans and swine globally. The rightmost columns indicate the number of viruses from each genotype collected from the northwest and southeast regions in Mexico. Ovals shaded with 2 colors represent mixed infections. CswH1, classical swine H1N1; EAswH1, avian-like Eurasian swine H1N1; HA, hemagglutinin; huH3N2, human H3N2; MP, matrix protein; NA, neuraminidase; NP, nucleoprotein; NS, nonstructural; pH1N1, pandemic H1N1 clone; SE, southeast; SW, southwest. TRswH3N2, triple reassortant swine H3N2.

**Genetic Diversity of HA and NA Segments**

Overall, greater genetic diversity was observed in the HA and NA antigens than in the 6 internal gene segments, a pattern that has been observed in other countries (26). CswH1N1-H1β (1A.2), pH1N1 (1A.3.3.2), and TRswH3N2 (cluster IV) viruses were identified in northwest Mexico. Five HAs (CswH1N1-H1γ [1A.3.3.3], pH1N1 [1A.3.3.2], TRswH3N2 [cluster IV], and huH3N2) (Figures 3, 4; Appendix Table 1) were identified in southeast Mexico. Five NA lineages (EAswH1N1, pH1N1, huH3N2, TRswH3N2/N2–1998, and TRswH3N2/N2–2002) (Figure 5) were identified in southeast Mexico. Given the high genetic diversity of H3 viruses, including huH3N2 viruses that were not phylogenetically related to any known US swine lineages (Figure 4), we selected 10 representative H3 viruses from Mexico on the basis of phylogenetic position (Figure 4) and antigenic motif patterns (27) for antigenic characterization.

**Antigenic Analysis of H3 Viruses**

We generated an antigenic map from HI data to visualize antigenic relationships among contemporary H3N2 swine

IAV from multiple regions in Mexico and the United States (Figure 6, panel A). Antigenic distances were extracted from the map to measure distance between H3N2 viruses from Mexico and swine strains from the United States that represent putative antigenic clusters contained in US commercial vaccines (Figure 6, panel B). Of the 10 viruses from Mexico selected for antigenic characterization, 8 were antigenically clustered with H3N2 cluster IV strains from the United States. Two viruses from the southeast region (A/sw/Mex/985778/2013 and A/sw/Mex/84706352130/2015) were more antigenically similar to the human seasonal vaccine strain WU/95 (<3 AUs). The most similar swine strain is the cluster I TX/98.

**Spatial Structure of Swine IAV in Mexico**

We observed no evidence of viral migration between the northwest and southeast regions of Mexico. Although certain clades of pH1N1 viruses from northwest and southeast Mexico share a common ancestor, the low posterior probabilities supporting these nodes indicate that multiple independent human-to-swine transmission events of closely

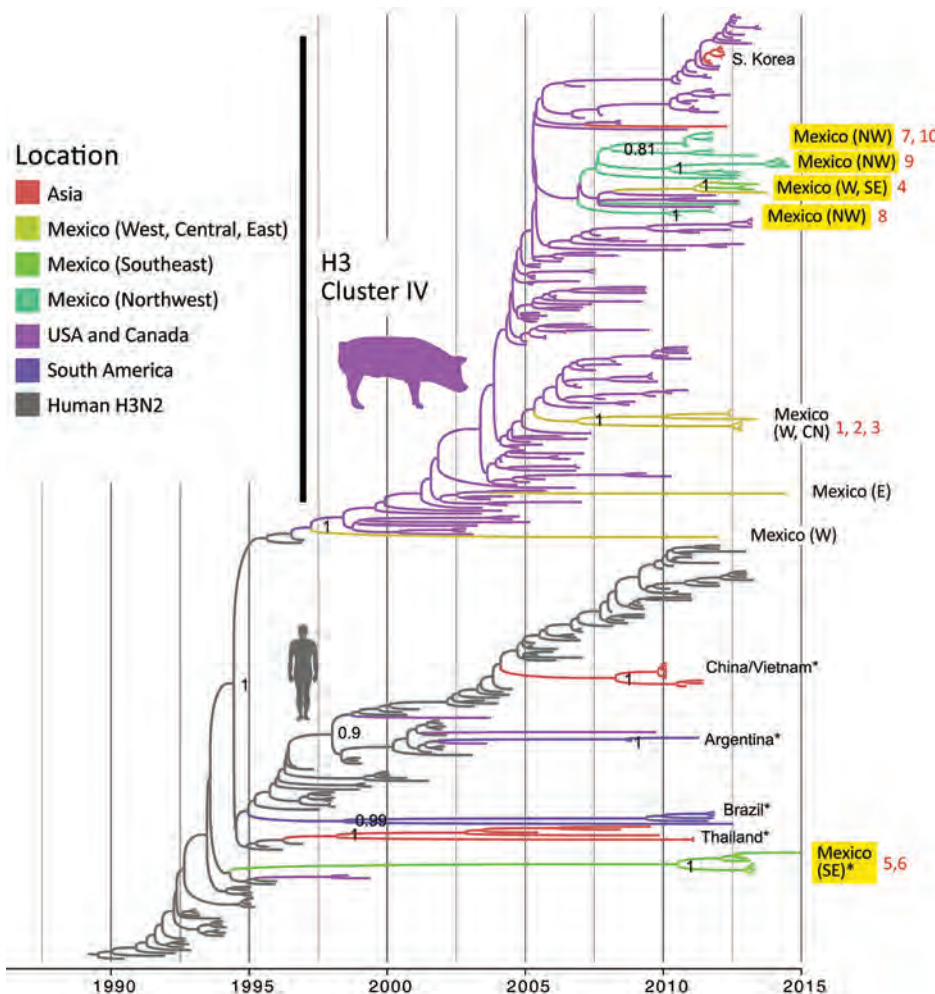


**Figure 4.** Evolutionary relationships between H3 segments of avian influenza viruses collected in humans and swine globally. Time-scaled Bayesian maximum clade credibility tree is inferred for the H3 segment. The tree includes newly generated sequences from northwest and southeast Mexico, along with background sequences from swine in Mexico, Asia, the United States, and Canada, as well as seasonal H3N2 viruses from humans. The color of each branch indicates the most probable location state. Posterior probabilities for key nodes are provided. Clades with viruses from swine in Mexico obtained for this study are highlighted in yellow. \*Major virus introductions into a location, indicating direct introductions from humans. CN, central; NW, northwest; S, south; SE, southeast; W, west. The 10 H3N2 viruses selected for antigenic characterization (Figure 6) are indicated by numbers 1–10 in red. A more detailed phylogeny, including tip labels and all posterior probabilities, is provided in the Appendix Figure (<https://wwwnc.cdc.gov/EID/article/25/4/18-0779-App1.pdf>).

related human pH1N1 viruses are more likely. There might have been 4 independent introductions of pH1N1 virus from humans into swine in southeast Mexico and 5 introductions into the northwest region (Appendix Figure). Similarly, there is no evidence of dispersal of huH3N2 viruses from southeast Mexico to any other regions of Mexico. TRswH3N2 and CswH1N1 viruses from swine in the United States were imported into the northwest region of Mexico, which is located near the US border (Figure 7, panel A), reflecting the large number of live swine transported from the southern United States into Mexico each year (Figure 1). In contrast, TRswH3N2 and CswH1N1 viruses were imported into the southeast region of Mexico primarily from the west region (Figure 7, panel B), an inference that was observed with high support across all phylogenies (Figures 4, 5; Appendix Figure).

The trees indicate that 3 independent introductions of reassortant viruses, including EAswH1N1 segments (genotypes 6 and 8) (Figure 3), occurred during  $\approx 2011$ –2013 on the basis of estimated times to the most recent common ancestor (Figure 8; Appendix Table 4). No additional reassortment events have been observed between genotype 6 or 8 viruses and huH3N2 and pH1N1 viruses also circulating in southeast Mexico.

## Discussion

The recent characterization of the origins of the influenza A(H1N1)pdm09 virus in swine in Mexico underscored the need for efforts to control the unexpectedly diverse swine IAV populations circulating in large swine herds in this country (1). Long-range animal movements between Europe, Mexico, and the United States established an exceptionally diverse population of swine IAV in the west and central-north regions of Mexico, including EAswH1N1 reassortants, which have now disseminated onward into southeast Mexico. Recognition of the genetic diversity of swine IAV in Mexico, including lineages not found in US herds, has stimulated interest from producers in Mexico in developing new vaccines customized to protect against the virus strains in this country, including huH3N2 viruses in southeast Mexico that were introduced from humans in the 1990s and are highly divergent from all known US swine virus strains. The huH3N2 viruses have recently reassorted with pH1N1 viruses, generating novel reassortant genotypes that were identified frequently in southeast Mexico. Eighty percent of H3N2 viruses in swine in southeast Mexico had the HA from the huH3N2 lineage. Our analysis indicates that the huH3N2 viruses have been circulating in swine for many decades, consistent with being fit, well-adapted viruses in pigs. However, the breadth of our sampling is insufficient to draw strong conclusions about whether these viruses are widespread in southeast Mexico, and further surveillance is critical.

Producers invest considerable time and resources into efforts to control swine IAV through vaccination, particularly of sows (28). Influenza vaccines are licensed for swine in Europe and North America, including multivalent formulations targeting the genetically diverse virus populations found in these regions (29,30). Mexico uses some vaccines made in North America, but relies heavily on customized (autogenous) vaccines designed from strains isolated in the field. US producers also frequently use autogenous vaccines because commercial vaccine formulations cannot keep up with the rapid emergence of antigenically novel swine IAV lineages. The H3N2 antigenic maps demonstrate that swine IAV strains detected in most parts of Mexico were antigenically more similar to older US

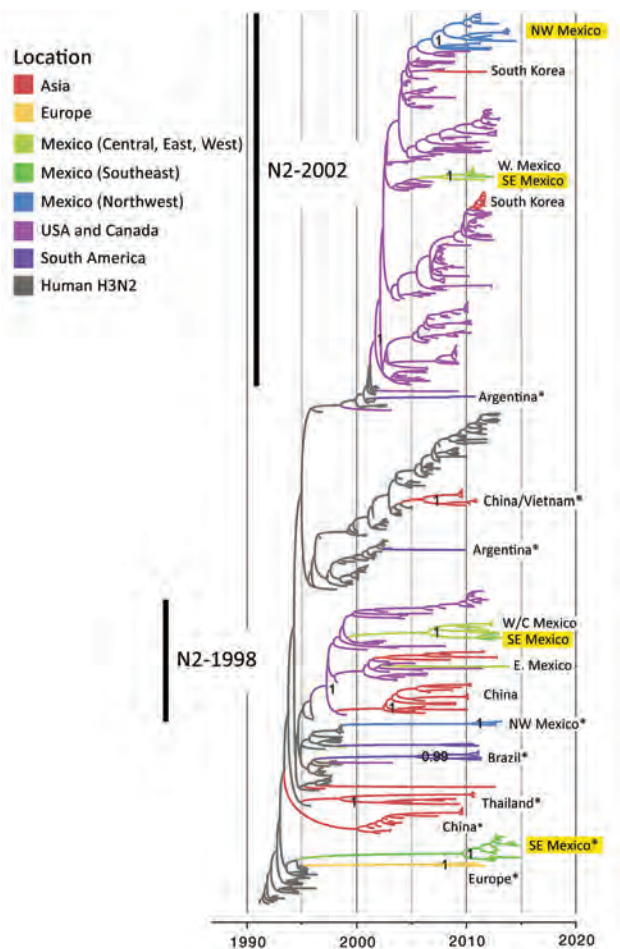


**Figure 5.** Evolutionary relationships between N2 segments of avian influenza viruses collected in humans and swine globally. Time-scaled Bayesian maximum clade credibility tree is inferred for N2 segment. Labeling and shading is similar to that in Figure 4, with the additional labeling of the N2–1998 and N2–2002 lineages. NW, northwest; SE, southeast; W, west; W/C, west/central. \*Direct introduction from humans. A more detailed phylogeny, including tip labels and all posterior probabilities, is provided in the Appendix Figure (<https://wwwnc.cdc.gov/EID/article/25/4/18-0779-App1.pdf>).



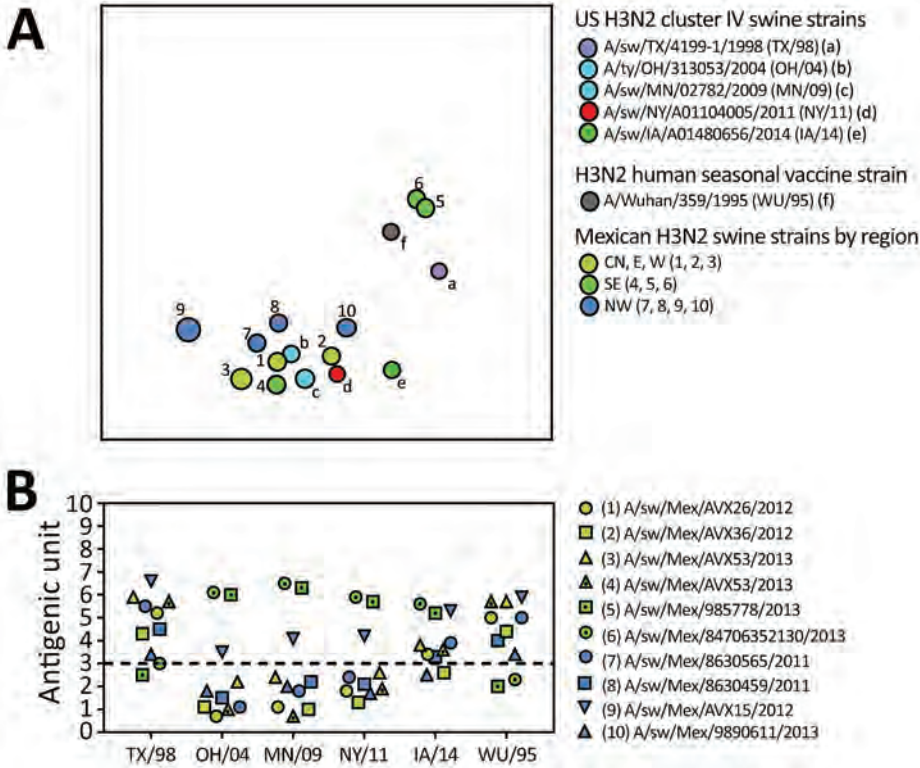


**Figure 6.** Antigenic relationships between contemporary influenza A (H3N2) viruses from Mexico and representative strains from the United States. A) Antigenic map of contemporary swine H3N2 viruses from Mexico and the United States. Antigenic clusters are indicated by color as in Figures 4 and 5. CN, central; E, east; NW, northwest; SE, southeast; W, west. B) Antigenic distance between H3N2 virus from Mexico and representative swine strains from the United States and a putative ancestral human seasonal vaccine virus strain (WU/95). The US swine strains represent antigenic clusters previously defined as TX/98 (cornflower), OH/04 and MN/09 (cyan), NY/11 (red), and IA/14 (green) (27,31).

cluster IV strains that circulated during 2004–2011 (31). Two swine IAV strains from the southeast region of Mexico retained more cross-reactivity with the Wuhan/95 human seasonal H3N2 vaccine strain, compared with other human virus strains and US cluster IV swine viruses, supporting the phylogenetic inference of a separate human-to-swine introduction in the 1990s in Mexico. Although these 2 strains also demonstrated antigenic relatedness to US cluster I swine virus TX/98, phylogenetic analysis

indicates that the introduction into Mexico was separate from that into the United States, albeit from an antigenically similar human seasonal H3N2 ancestor. With such long branch lengths on the phylogenetic tree, we cannot exclude the possibility that human-to-swine transmission occurred in a different country where surveillance of swine is low and where movements of pigs into Mexico could have introduced the virus (e.g., Guatemala), but at this time there is no evidence for such a scenario.

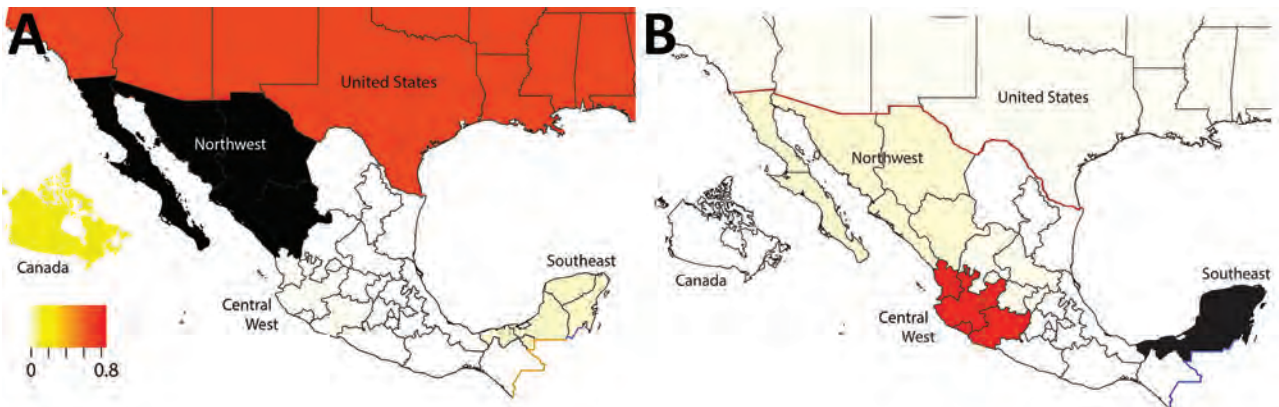


**Figure 7.** Sources of influenza A viruses circulating in swine in northwestern and southeastern Mexico. Each region is shaded according to the proportion of total Markov jump counts from that particular region (source) into A) northwest or B) southeast regions of Mexico (destination). Red indicates high proportion of jumps (major source of viruses); light yellow indicates low proportion of jumps (not a major source of viruses); black indicates destination; white indicates no jumps/no data available. Seven locations were considered in the analysis: Canada, United States, Mexico (northwest), Mexico (central-west), Mexico (central-north), Mexico (east), and Mexico (southeast). Scale bar indicates proportion of total Markov jump counts from a particular region.

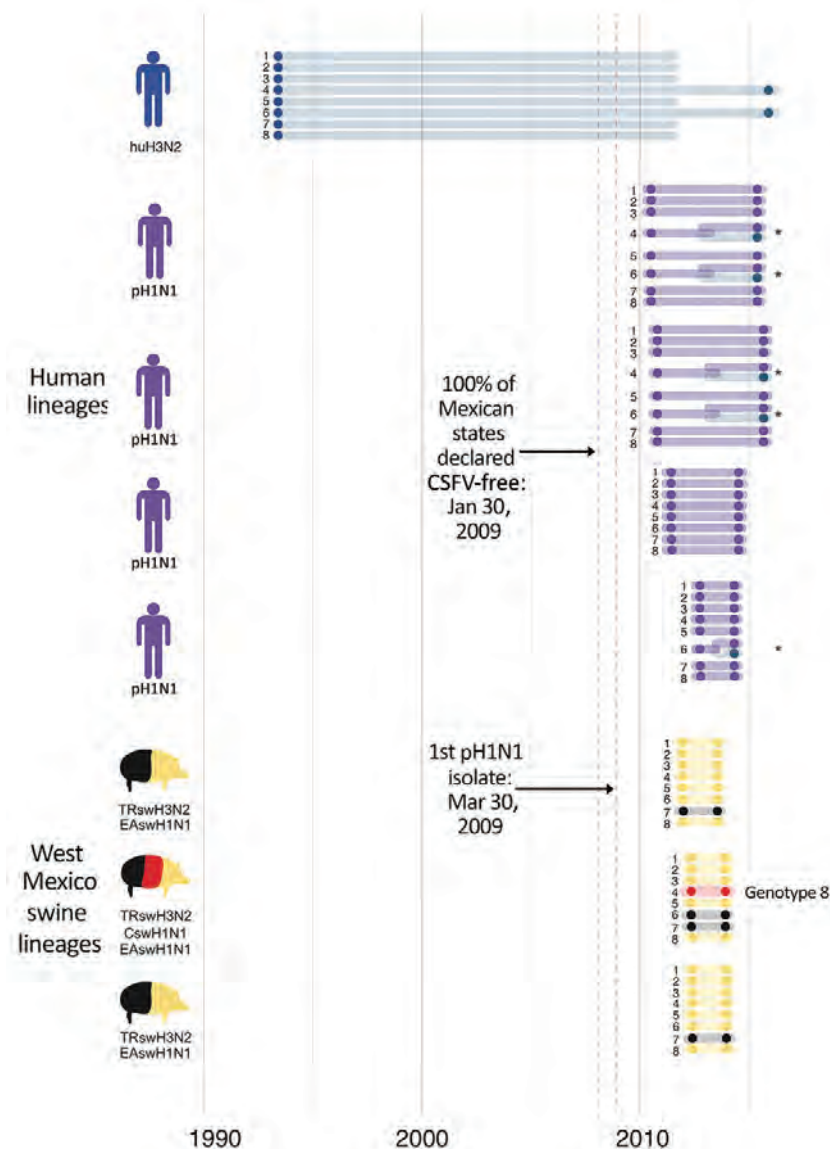


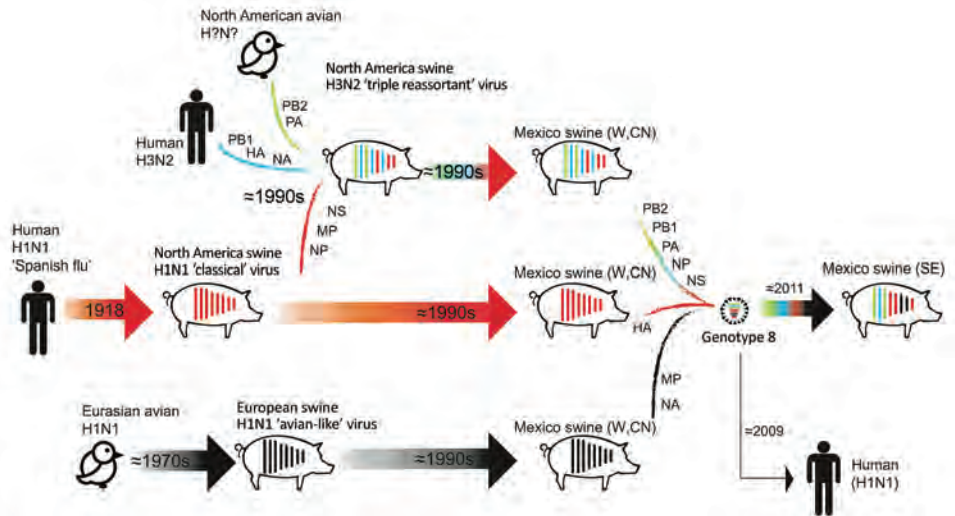
**Figure 8.** Introductions of influenza A viruses into swine in southeast Mexico. Introductions of these viruses from humans and swine into southeast Mexico are indicated as groups of 8 horizontal lines, and each line represents 1 of 8 segments of the virus genome. Segments are numbered 1–8, longest to shortest, according to convention: 1, polymerase basic 2; 2, polymerase basic 1; 3, polymerase acidic; 4, hemagglutinin; 5, nucleoprotein; 6, neuraminidase; 7, matrix protein; 8, nonstructural. The position of each shaded circle along the x-axis represents the estimated timing of virus introduction, estimated directly from the maximum clade credibility trees. Lines and circles are shaded according to the virus lineage, similar to that in Figure 2. \*Reassortment events. Introduction of genotype 8 viruses is indicated. The blue dotted vertical line represents the date of the declaration of Secretariat of Agriculture, Livestock, Rural Development, Fisheries and Food in Mexico that classical swine fever virus had been eradicated from all states in Mexico during January 2009. The red dotted vertical line represents the date of first isolation of pH1N1 virus in humans. CSFV, classical swine fever virus; CswH1, classical swine H1N1; EAswH1, avian-like Eurasian swine H1N1; huH3N2, human H3N2; pH1N1, pandemic H1N1 clade; TRswH3N2, triple reassortant swine H3N2.

Increased surveillance in swine in the years after the 2009 H1N1 pandemic (32) has enhanced our understanding of swine IAV evolution. Whereas movements of humans and wild birds tend to follow symmetric routes of workflows (33), flight patterns (22), and flyways (34), the movements of pigs are often asymmetric, inconsistent with standard gravity models, and driven by fluctuating economic considerations. We demonstrated how genetic diversity that evolved in regions of central Mexico has spread >1,000 miles to southeast Mexico and introduced new lineages, including those of Eurasian origin. Introduction of genotype 8 viruses into southeast Mexico is notable, given their role in the genesis of the 2009 H1N1 pandemic in humans and their complex evolutionary history involving multiple intercontinental migration events and interspecies transmission events (Figure 9). Time-scaled phylogenies consistently

indicate that the west region of Mexico is the original source of the relatively recent ( $\approx$ 2011–2013) incursions of reassortant viruses into the southeast region. Removal of movement restrictions in 2009 might have facilitated virus flow between these regions because the final 3 states to eradicate CSFV in 2009 (Chiapas, Oaxaca, and Tabasco) are geographically situated between the southeast and west/central-north regions of Mexico (Figure 2). However, as is the case in most countries, there are no reliable data on pig movements within Mexico, and our phylogeographic methods cannot exclude the possibility of virus movement through unsampled intermediary locations.

Trade volumes of live swine from the United States into Mexico can fluctuate by orders of magnitude (Figure 1, panel B), driven by economic factors and disease-control efforts, such as during the outbreak of porcine reproductive

**Figure 9.** Evolutionary history of genotype 8 influenza viruses in southeast Mexico, showing interspecies transmission events, reassortment events, and virus migration events leading to the emergence of genotype 8 viruses in swine in Mexico in the W and CN regions and continued spread into SE Mexico in  $\approx 2011$ . Within each pig, vertical lines represent the 8 segments of the influenza A virus genome, ordered longest to shortest, which are shaded according to virus lineage. Arrows represent direct transmission events between hosts. Reassortment events are indicated by multiple lines shaded in different colors. Segments donated from each lineage are indicated. Birds are depicted to reflect uncertainty about the specific avian species that transmitted influenza A viruses to swine in Europe and North America. CN, central; E, east; HA, hemagglutinin; MP, matrix protein; NA, neuraminidase; NP, nucleoprotein; NS, nonstructural; PA, polymerase acidic; PB, polymerase basic; SE, southeast; W, west.



and respiratory syndrome virus in the United States (35). However, it is difficult to explore temporal links with international virus movements given that no swine IAV sequence data for Mexico are available before 2009 (36). The increase in swine IAV surveillance in Mexico since 2009 has been critical for evaluating potential vaccine effectiveness and catalyzing development of new vaccine formulations. Earlier detection of newly emergent strains and better predictions about whether new strains will increase in prevalence will require deeper, population-based surveillance of IAV in swine. Given limited public funding available for surveillance, advances in vaccine effectiveness will require a culture of greater transparency among producers, and guarantees that data shared will not be used to target individual producers or countries.

### Acknowledgment

We thank all swine producers who contributed viruses for this study.

Whole-genome sequencing for this study was generously sponsored by Zoetis Latin America through an agreement with the University of Minnesota (SOW 140-N-3545181). Evolutionary and antigenic analyses were supported by the Center for Research on Influenza Pathogenesis, a National Institute of Allergy and Infectious Diseases–funded Center of Excellence in Influenza Research and Pathogenesis (contract #HHSN272201400008C). This study was supported in part by an in-house collaborative research network for the study of influenza virus epidemiology and evolution (MISMS) led by the Fogarty International Center, National Institutes of Health.

### About the Author

Dr. Nelson is a staff scientist in the Division of International Epidemiology and Population Studies, Fogarty International Center, National Institutes of Health, Bethesda, MD. Her primary research interest is the evolutionary dynamics of rapidly evolving RNA viruses at the human–animal interface.

### References

- Mena I, Nelson MI, Quezada-Monroy F, Dutta J, Cortes-Fernández R, Lara-Puente JH, et al. Origins of the 2009 H1N1 influenza pandemic in swine in Mexico. *eLife*. 2016; 5:e16777. <http://dx.doi.org/10.7554/eLife.16777>
- Koen J. A practical method for field diagnosis of swine diseases. *Am J Vet Med*. 1919;14:468–70.
- Anderson TK, Macken CA, Lewis NS, Scheuermann RH, Van Reeth K, Brown IH, et al. A phylogeny-based global nomenclature system and automated annotation tool for H1 hemagglutinin genes from swine influenza viruses. *mSphere*. 2016;1:pii: e00275–16.
- Vijaykrishna D, Smith GJD, Pybus OG, Zhu H, Bhatt S, Poon LLM, et al. Long-term evolution and transmission dynamics of swine influenza A virus. *Nature*. 2011;473:519–22. <http://dx.doi.org/10.1038/nature10004>
- Watson SJ, Langat P, Reid SM, Lam TT, Cotten M, Kelly M, et al.; ESNIP3 Consortium. Molecular epidemiology and evolution of influenza viruses circulating within European swine between 2009 and 2013. *J Virol*. 2015;89:9920–31. <http://dx.doi.org/10.1128/JVI.00840-15>
- Lam TT, Zhu H, Wang J, Smith DK, Holmes EC, Webster RG, et al. Reassortment events among swine influenza A viruses in China: implications for the origin of the 2009 influenza pandemic. *J Virol*. 2011;85:10279–85. <http://dx.doi.org/10.1128/JVI.05262-11>
- Nelson MI, Viboud C, Vincent AL, Culhane MR, Detmer SE, Wentworth DE, et al. Global migration of influenza A viruses in swine. *Nat Commun*. 2015;6:6696. <http://dx.doi.org/10.1038/ncomms7696>



8. Takemae N, Parchariyanon S, Damrongwatanapokin S, Uchida Y, Ruttanapumma R, Watanabe C, et al. Genetic diversity of swine influenza viruses isolated from pigs during 2000 to 2005 in Thailand. *Influenza Other Respi Viruses*. 2008;2:181–9. <http://dx.doi.org/10.1111/j.1750-2659.2008.00062.x>
9. Nelson MI, Lemey P, Tan Y, Vincent A, Lam TT, Detmer S, et al. Spatial dynamics of human-origin H1 influenza A virus in North American swine. *PLoS Pathog*. 2011;7:e1002077. <http://dx.doi.org/10.1371/journal.ppat.1002077>
10. Vargas Terán M, Calcagno Ferrat N, Lubroth J; TERÁN MV. Situation of classical swine fever and the epidemiologic and ecologic aspects affecting its distribution in the American continent. *Ann N Y Acad Sci*. 2004;1026:54–64. <http://dx.doi.org/10.1196/annals.1307.007>
11. Slomka MJ, Densham ALE, Coward VJ, Essen S, Brookes SM, Irvine RM, et al. Real time reverse transcription (RRT)–polymerase chain reaction (PCR) methods for detection of pandemic (H1N1) 2009 influenza virus and European swine influenza A virus infections in pigs. *Influenza Other Respi Viruses*. 2010;4:277–93. <http://dx.doi.org/10.1111/j.1750-2659.2010.00149.x>
12. Zhang J, Gauger PC. Isolation of swine influenza virus in cell cultures and embryonated chicken eggs. *Methods Mol Biol*. 2014;1161:265–76. [http://dx.doi.org/10.1007/978-1-4939-0758-8\\_22](http://dx.doi.org/10.1007/978-1-4939-0758-8_22)
13. Zhang J, Harmon KM. RNA extraction from swine samples and detection of influenza A virus in swine by real-time RT-PCR. *Methods Mol Biol*. 2014;1161:277–93. [http://dx.doi.org/10.1007/978-1-4939-0758-8\\_23](http://dx.doi.org/10.1007/978-1-4939-0758-8_23)
14. Nelson M, Culhane MR, Rovira A, Torremorell M, Guerrero P, Norambuena J. Novel human-like influenza A viruses circulate in swine in Mexico and Chile. *PLoS Curr*. 2015;7:7.
15. Hoffmann E, Stech J, Guan Y, Webster RG, Perez DR. Universal primer set for the full-length amplification of all influenza A viruses. *Arch Virol*. 2001;146:2275–89. <http://dx.doi.org/10.1007/s007050170002>
16. Edgar RC. MUSCLE: multiple sequence alignment with high accuracy and high throughput. *Nucleic Acids Res*. 2004;32:1792–7. <http://dx.doi.org/10.1093/nar/gkh340>
17. Bao Y, Bolotov P, Dermovoy D, Kiryutin B, Zaslavsky L, Tatusova T, et al. The influenza virus resource at the National Center for Biotechnology Information. *J Virol*. 2008;82:596–601. <http://dx.doi.org/10.1128/JVI.02005-07>
18. Stamatakis A. RAxML-VI-HPC: maximum likelihood-based phylogenetic analyses with thousands of taxa and mixed models. *Bioinformatics*. 2006;22:2688–90. <http://dx.doi.org/10.1093/bioinformatics/btl446>
19. Drummond AJ, Suchard MA, Xie D, Rambaut A. Bayesian phylogenetics with BEAUti and the BEAST 1.7. *Mol Biol Evol*. 2012;29:1969–73. <http://dx.doi.org/10.1093/molbev/mss075>
20. Suchard MA, Rambaut A. Many-core algorithms for statistical phylogenetics. *Bioinformatics*. 2009;25:1370–6. <http://dx.doi.org/10.1093/bioinformatics/btp244>
21. Minin VN, Suchard MA. Counting labeled transitions in continuous-time Markov models of evolution. *J Math Biol*. 2008;56:391–412. <http://dx.doi.org/10.1007/s00285-007-0120-8>
22. Lemey P, Rambaut A, Bedford T, Faria N, Bielejec F, Baele G, et al. Unifying viral genetics and human transportation data to predict the global transmission dynamics of human influenza H3N2. *PLoS Pathog*. 2014;10:e1003932. <http://dx.doi.org/10.1371/journal.ppat.1003932>
23. R Core Team. R: a language and environment for statistical computing. Vienna: R Foundation for Statistical Computing; 2012 [cited 2018 Dec 19]. <http://www.r-project.org/>.
24. Lewis NS, Anderson TK, Kitikoon P, Skepner E, Burke DF, Vincent AL. Substitutions near the hemagglutinin receptor-binding site determine the antigenic evolution of influenza A H3N2 viruses in U.S. swine. *J Virol*. 2014;88:4752–63. <http://dx.doi.org/10.1128/JVI.03805-13>
25. Kitikoon P, Gauger PC, Vincent AL. Hemagglutinin inhibition assay with swine sera. *Methods Mol Biol*. 2014;1161:295–301. [http://dx.doi.org/10.1007/978-1-4939-0758-8\\_24](http://dx.doi.org/10.1007/978-1-4939-0758-8_24)
26. Nelson MI, Wentworth DE, Culhane MR, Vincent AL, Viboud C, LaPointe MP, et al. Introductions and evolution of human-origin seasonal influenza A viruses in multinational swine populations. *J Virol*. 2014;88:10110–9. <http://dx.doi.org/10.1128/JVI.01080-14>
27. Abente EJ, Santos J, Lewis NS, Gauger PC, Stratton J, Skepner E, et al. The molecular determinants of antibody recognition and antigenic drift in the H3 hemagglutinin of swine influenza A virus. *J Virol*. 2016;90:8266–80. <http://dx.doi.org/10.1128/JVI.01002-16>
28. Beaudoin A, Johnson S, Davies P, Bender J, Gramer M. Characterization of influenza A outbreaks in Minnesota swine herds and measures taken to reduce the risk of zoonotic transmission. *Zoonoses Public Health*. 2012;59:96–106. <http://dx.doi.org/10.1111/j.1863-2378.2011.01423.x>
29. Sandbulte MR, Spickler AR, Zaabel PK, Roth JA. Optimal use of vaccines for control of influenza A virus in swine. *Vaccines (Basel)*. 2015;3:22–73. <http://dx.doi.org/10.3390/vaccines3010022>
30. Vincent AL, Perez DR, Rajao D, Anderson TK, Abente EJ, Walia RR, et al. Influenza A virus vaccines for swine. *Vet Microbiol*. 2017;206:35–44. <http://dx.doi.org/10.1016/j.vetmic.2016.11.026>
31. Lewis NS, Anderson TK, Kitikoon P, Skepner E, Burke DF, Vincent AL. Substitutions near the hemagglutinin receptor-binding site determine the antigenic evolution of influenza A H3N2 viruses in U.S. swine. *J Virol*. 2014;88:4752–63. <http://dx.doi.org/10.1128/JVI.03805-13>
32. Vincent A, Awada L, Brown I, Chen H, Claes F, Dauphin G, et al. Review of influenza A virus in swine worldwide: a call for increased surveillance and research. *Zoonoses Public Health*. 2014;61:4–17. <http://dx.doi.org/10.1111/zph.12049>
33. Viboud C, Bjørnstad ON, Smith DL, Simonsen L, Miller MA, Grenfell BT. Synchrony, waves, and spatial hierarchies in the spread of influenza. *Science*. 2006;312:447–51. <http://dx.doi.org/10.1126/science.1125237>
34. Lam TT-Y, Ip HS, Ghedin E, Wentworth DE, Halpin RA, Stockwell TB, et al. Migratory flyway and geographical distance are barriers to the gene flow of influenza virus among North American birds. *Ecol Lett*. 2012;15:24–33. <http://dx.doi.org/10.1111/j.1461-0248.2011.01703.x>
35. Petry M, Paarlberg PL, Lee JG. PRRS and the North American swine trade: a trade barrier analysis. *Journal of Agricultural and Applied Economics*. 1999;33:425–36. <http://dx.doi.org/10.1017/S1074070800008749>
36. Escalera-Zamudio M, Cobián-Güemes G, de los Dolores Soto-del Río M, Isa P, Sánchez-Betancourt I, Parissi-Crivelli A, et al. Characterization of an influenza A virus in Mexican swine that is related to the A/H1N1/2009 pandemic clade. *Virology*. 2012;433:176–82. <http://dx.doi.org/10.1016/j.virol.2012.08.003>

---

Address for correspondence: Martha I. Nelson, National Institutes of Health, 16 Center Dr, Bethesda, MD 20892, USA; email: [nelsonma@mail.nih.gov](mailto:nelsonma@mail.nih.gov)

# *Staphylococcus aureus* Bacteremia in Children of Rural Areas of The Gambia, 2008–2015

Aderonke Odotola, Christian Bottomley, Syed A. Zaman, Jodi Lindsay, Muhammed Shah, Ilias Hossain, Malick Ndiaye, Chidebere D.I. Osuorah, Yekini Olatunji, Henry Badji, Usman N.A. Ikumapayi, Ahmad Manjang, Rasheed Salaudeen, Lamin Ceesay, Momodou Jasseh, Richard A. Adegbola, Tumani Corrah, Philip C. Hill, Brian M. Greenwood, Grant A. Mackenzie

*Staphylococcus aureus* bacteremia is a substantial cause of childhood disease and death, but few studies have described its epidemiology in developing countries. Using a population-based surveillance system for pneumonia, sepsis, and meningitis, we estimated *S. aureus* bacteremia incidence and the case-fatality ratio in children <5 years of age in 2 regions in the eastern part of The Gambia during 2008–2015. Among 33,060 children with suspected pneumonia, sepsis, or meningitis, we performed blood culture for 27,851; of 1,130 patients with bacteremia, 198 (17.5%) were positive for *S. aureus*. *S. aureus* bacteremia incidence was 78 (95% CI 67–91) cases/100,000 person-years in children <5 years of age and 2,080 (95% CI 1,621–2,627) cases/100,000 person-years in neonates. Incidence did not change after introduction of the pneumococcal conjugate vaccine. The case-fatality ratio was 14.1% (95% CI 9.6%–19.8%). Interventions are needed to reduce the *S. aureus* bacteremia burden in The Gambia, particularly among neonates.

In 2016, invasive bacterial diseases accounted for one quarter of the 5.6 million childhood deaths worldwide (1). Most invasive bacterial diseases occur in sub-Saharan Africa and other low- and middle-income countries (2). Deaths caused by these diseases outnumber those caused

by malaria among children <5 years of age (3). The main bacteria implicated in invasive bacterial diseases has been *Streptococcus pneumoniae* and *Haemophilus influenzae* (4). However, after the widespread use of conjugate vaccines against *H. influenzae* type b (Hib) and *S. pneumoniae*, Hib disease has decreased considerably (5), and vaccine-serotype pneumococcal disease is declining (6). The decreased disease incidence associated with these pathogens has led to *Staphylococcus aureus* becoming a relatively more common cause of invasive bacterial disease (7). The clinical spectrum of *S. aureus* disease ranges from life-threatening invasive diseases, such as septicemia, pneumonia, osteomyelitis, endocarditis, meningitis, and brain abscess, to less severe skin and soft tissue infections. *S. aureus* bacteremia is often used as a marker of invasive *S. aureus* disease (8).

In high-income countries, *S. aureus* bacteremia is the second most common cause of neonatal sepsis, after group B *Streptococcus* (9). From the 1970s through the 2000s, the incidence of *S. aureus* bacteremia among children <16 years of age increased in several countries (10), probably because of the increased use of central venous catheters and other factors (10). In the 2010s, the incidence of *S. aureus* bacteremia remained stable (11) or decreased (10).

In Africa, *S. aureus* bacteremia is a common cause of invasive bacterial disease in children. Before the introduction of the Hib vaccine and pneumococcal conjugate vaccine (PCV), population-based studies in Kenya and Mozambique showed that *S. aureus* was the most common gram-positive pathogen among neonates with sepsis (4,12). Also, hospital-based studies showed *S. aureus* to be the most common cause of invasive bacterial disease in children <3 months of age in The Gambia (13) and one of the main causes of invasive bacterial disease in children <5 years of age in Nigeria (14).

Few population-based studies have been conducted in sub-Saharan Africa on the incidence of *S. aureus* bacteremia. In South Africa, a population-based study of children <13 years of age in an area with a high HIV prevalence

Author affiliations: London School of Hygiene and Tropical Medicine, London, UK (A. Odotola, C. Bottomley, S.A. Zaman, B.M. Greenwood, G.A. Mackenzie); Medical Research Council Unit The Gambia at the London School of Hygiene and Tropical Medicine, Banjul, The Gambia (A. Odotola, S.A. Zaman, M. Shah, I. Hossain, M. Ndiaye, C.D.I. Osuorah, Y. Olatunji, H. Badji, U.N.A. Ikumapayi, A. Manjang, R. Salaudeen, M. Jasseh, R.A. Adegbola, T. Corrah, G.A. Mackenzie); St. George's University of London, London (J. Lindsay); King Fahad Medical City, Riyadh, Saudi Arabia (A. Manjang); Ministry of Health and Social Welfare, Banjul (L. Ceesay); University of Otago, Dunedin, New Zealand (P.C. Hill); Murdoch Children's Research Institute, Parkville, Victoria, Australia (G.A. Mackenzie)

DOI: <https://doi.org/10.3201/eid2504.180935>

indicated an incidence of 26 cases/100,000 person-years (15). A study in Kenya involving children admitted to a secondary healthcare facility showed an incidence of 27 cases/100,000 person-years in children <5 years of age; the highest incidence was in infants (89 cases/100,000 person-years) (4). However, variation in the age groups studied and methods used preclude direct comparison of these studies (4,12,13,15). After introduction of the Hib vaccine and before the introduction of PCV, a hospital-based study in The Gambia reported that *S. aureus* was the most common cause of bacteremia (16).

Given the paucity of population-based data on the epidemiology of *S. aureus* bacteremia in sub-Saharan Africa, we studied the incidence, clinical characteristics, case-fatality rate, and risk factors for *S. aureus* bacteremia in young children in a rural region of The Gambia. We also explored the association of *S. aureus* bacteremia with the introduction of PCV.

## Methods

### Study Site and Population

Surveillance for septicemia, pneumonia, and meningitis was performed among children  $\geq 2$  months of age residing in Basse in the Upper River Region of The Gambia through the Basse Health and Demographic Surveillance System (BHDSS) (Figure 1). We established the BHDSS in 2007, and the population in this surveillance area ( $\approx 179,000$  persons in 2015, 19% <5 years of age) is enumerated every 4 months. The BHDSS is served by 5 satellite clinics and the Basse Health Centre (Basse, The Gambia), a primary and secondary healthcare facility with 25 beds to care for children. During 2011–2015, surveillance was extended to include all residents <5 years of age, and a similar surveillance

was set up in the adjacent district of Fuladu West for all residents <5 years of age during a similar time range (2012–2014) through the Fuladu West Health and Demographic Surveillance System (FWHDSS; Figure 1). The population in Fuladu West is enumerated annually (population 92,464 in 2014, 18% <5 years of age). The FWHDSS is served by Bansang Hospital (Bansang, The Gambia) and 2 satellite clinics. Every resident in the areas surveilled by the BHDSS and FWHDSS was assigned a unique identifier.

The conjugate vaccine for Hib was introduced into the Gambian National Programme on Immunization in 1997, and the vaccine for pneumococcus was introduced in 2009. The 7-valent PCV (PCV7) was replaced by the 13-valent vaccine (PCV13) in 2011. In 2012, vaccine coverage for the third dose of the diphtheria-pertussis-tetanus vaccine in these regions surveilled was 81.7% (17). In The Gambia, transmission of *Plasmodium falciparum* is largely restricted to the short rainy season during July–November (18).

### Surveillance Procedures

During May 12, 2008–December 31, 2015, nurses screened all children 2–59 months of age who arrived at a health center participating in the surveillance and who had a unique identifier for septicemia, pneumonia, and meningitis, according to standardized criteria (also referred to as referral surveillance) (19). Children who were admitted and children who were treated as outpatients were screened. Children who screened positive were referred to clinicians who used standardized criteria for assessment and investigation (19). Data collected included age, sex, anthropometric measurements, signs and symptoms, and suspected diagnosis. Blood was collected for culturing, and depending on clinical presentation, cerebrospinal fluid, lung aspirate, or pleural fluid samples were have also been collected for conventional microbiological

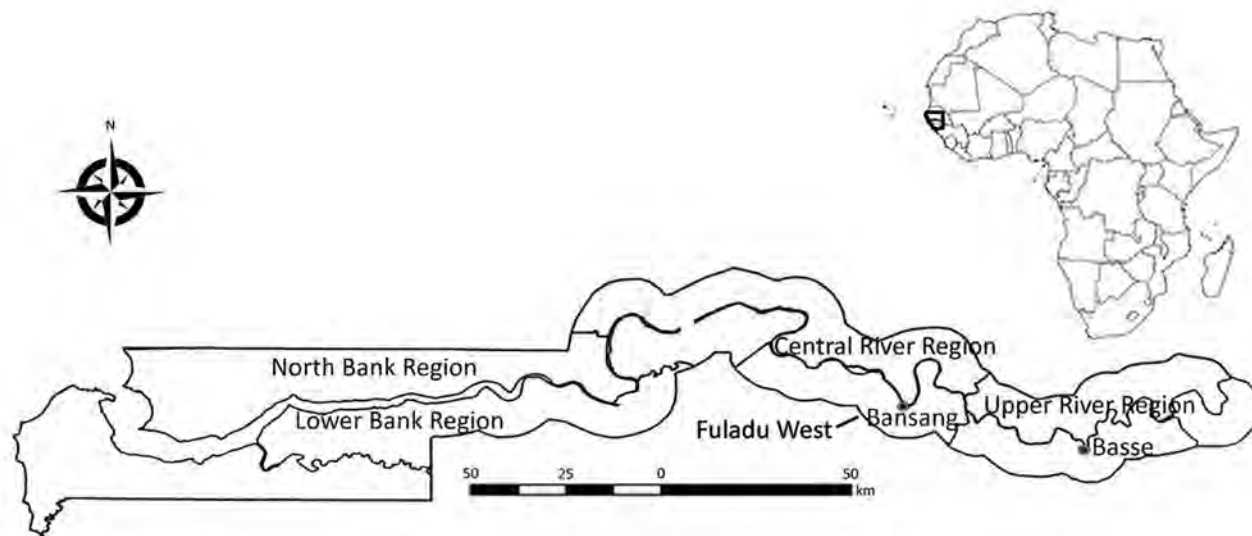


**Figure 1.** Regions surveilled for *Staphylococcus aureus* bacteremia among children <5 years of age through the Basse and Fuladu West Health and Demographic Surveillance Systems, The Gambia, 2008–2015. Inset indicates location of The Gambia in Africa.



tests (6). Rapid diagnostic tests for malaria (ICT Malaria *P.f.* Antigen; ICT Diagnostics, <http://www.ictdiagnostics.co.za>) were routinely performed during the rainy season and at other times at the discretion of the clinician.

During March 1, 2011–December 31, 2015, surveillance was expanded in the BHDSS to include all children 0–59 months of age who were admitted with an acute medical problem from whom a blood sample was collected for culture (also referred to as admission surveillance). During September 12, 2011–December 31, 2014, a similar admission surveillance was conducted for children 0–59 months of age admitted with an acute medical problem using the FWHSS. All *S. aureus* bacteremia cases were linked to the Health and Demographic Surveillance System databases by using the unique identifier.

### Laboratory Methods

We collected 1–3-mL blood samples from all patients with suspected septicemia, pneumonia, or meningitis; inoculated blood samples into BACTEC bottles (Becton Dickinson, <https://www.bd.com>); and incubated them in an automated BACTEC 9050 Blood Culture System (Becton Dickinson) for a maximum of 5 days. We subcultured positive cultures on blood agar plates and confirmed isolates as *S. aureus* by using catalase and coagulase tests. We classified cultures that grew *Bacillus* spp., *Corynebacterium* spp., and coagulase-negative *Staphylococcus* as contaminated. We used standard methods to investigate other body fluid samples collected for microbiological tests (20). We used disc diffusion methods to determine antimicrobial drug susceptibility according to the Clinical and Laboratory Standards Institute guidelines (21). We categorized all *S. aureus* isolates resistant to cefoxitin as methicillin-resistant.

We defined *S. aureus* bacteremia cases as clinically suspected cases of septicemia, pneumonia, meningitis, osteomyelitis, septic arthritis, pyomyositis, or abscess identified by using standardized criteria (19) in patients from whom *S. aureus* was isolated from their blood.

### Statistical Methods

We used referral and admission surveillance data for statistical analyses. The unique identifier assigned to every patient enabled us to avoid duplication of data in our data set. We used the referral surveillance data to investigate trends in incidence because these data covered a longer period (2008–2015) than the admissions surveillance data (2011–2015). We used both the admission and referral surveillance data to estimate age-specific incidence and the case-fatality ratio (CFR).

We obtained incidence estimates by dividing the number of *S. aureus* bacteremia cases by the number of person-years at risk using the estimated midyear population. To account for the shorter period of observation in 2008 (May 12–

December 31), we calculated person-years at risk as the midyear population multiplied by 234/365. We calculated incidence in neonates using 2 methods, first as cases per 1,000 live births and second as cases per 100,000 person-years. We defined the neonatal period as the time from birth to 28 days of age.

With the referral surveillance data, we assessed trends in incidence over time and variation in incidence before (pre-PCV period, May 12, 2008–May 11, 2010) and after (PCV13 period, January 1, 2013–December 31, 2015) the introduction of PCV7 using Poisson regression with robust error variance to allow for overdispersion. To account for the increased rate of eligible patients requiring blood culture over time, we adjusted the number of *S. aureus* bacteremia cases of each age group and year by multiplying by the ratio of the annual rate of eligible children enrolled over the mean rate of eligible children enrolled during the entire study period (6). For the denominators of the pre-PCV and PCV13 periods, we used the average of the corresponding midyear populations indicated by the BHDSS.

We defined CFR as the number of patients with *S. aureus* bacteremia who died before discharge divided by the total number of patients with *S. aureus* bacteremia. We identified potential risk factors for death before discharge using logistic regression, although surveillance was not designed to assess risk factors. We generated weight-for-age and weight-for-height z-scores using the 2006 World Health Organization child growth standards ([https://www.who.int/childgrowth/standards/technical\\_report](https://www.who.int/childgrowth/standards/technical_report)). We considered children with weight-for-age z-scores <3 SDs from the median weight-for-age as severely underweight and weight-for-height z-scores <3 SDs from the median weight-for-height as severely stunted. We performed analyses using Stata 14.0 (<https://www.stata.com/stata14>) and considered p values <0.05 as the criterion for statistical significance.

### Ethics Statement

Ethics approval for this study was granted by The Gambia Government/Medical Research Council Joint Ethics Committee and the London School of Hygiene and Tropical Medicine Ethics Committee. We obtained written informed consent from the parents or guardians of all patients.

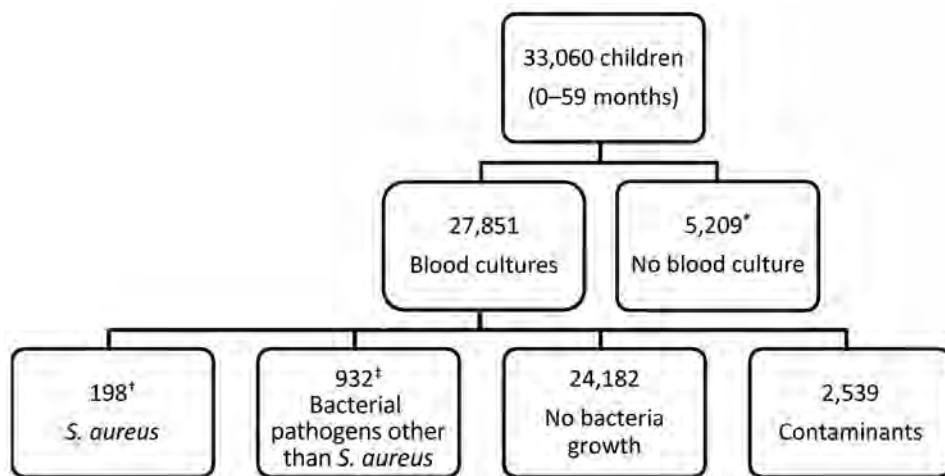
### Results

In total, 33,060 children met the criteria for investigation, and 27,851 (84.2%) blood samples were collected and cultured (Figure 2). Contaminants grew in the cultures of 2,539 (9.1%) blood samples; these samples were excluded from analysis because contamination can mask an *S. aureus* bacteremia diagnosis.

### Bacteremia

Bacteremia was identified in 1,130 children 0–59 months of age (Table 1). *S. aureus* was isolated in 198 (17.5%)

**Figure 2.** Flowchart of participants included and excluded in study of *Staphylococcus aureus* bacteremia incidence in children <5 years of age, The Gambia, 2008–2015. Participants were identified through the Basse and Fuladu West Health and Demographic Surveillance Systems. In total, 521 cases were identified through referral surveillance and 418 through admission surveillance.



\*Reasons for not having blood culture done included unsuccessful venipuncture (n = 487), declined consent for venipuncture (n = 416), declined consent to join study (n = 249), and unknown (n = 4,057). †In total, 76 children were identified through referral surveillance and 122 through admission surveillance. ‡Seven patients had polymicrobial bacteremia (*S. aureus* and a second bacterial pathogen).

‡Seven patients had polymicrobial bacteremia (*S. aureus* and a second bacterial pathogen).

children with bacteremia (76 identified through referral surveillance and 122 admission surveillance) and was the most common cause of bacteremia in neonates (46.4%, 84/181). Pathogens other than *S. aureus* were isolated from 932 children: *S. pneumoniae* (35.0%, n = 326), *Salmonella* spp. (15.1%, n = 141), and *Escherichia* spp. (10.7%, n = 100). In 7 children with bacteremia, *S. aureus* and a second bacterial pathogen were isolated.

### Patient Characteristics

Using the combined admission and referral surveillance data, we found that 18.2% (4,541/24,885) of all patients were severely underweight and 10.9% (2,658/24,405) were severely stunted; 18.3% (4,183/22,902) of patients were admitted in the 2 weeks before disease onset. Antimicrobial drug use in the week before onset of signs and symptoms was uncommon. Most patients had fever ( $\geq 37.5^{\circ}\text{C}$ ) and tachypnea (Table 1).

Among patients with *S. aureus* bacteremia, a diagnosis of suspected septicemia was made in 56.2%, suspected pneumonia in 28.4%, and suspected meningitis in 6.7%. The median duration of hospital stay was 5 (interquartile range 2–6) days (Table 1).

Cough and difficult breathing were experienced more often by patients without bacteremia or with bacteremia caused by other pathogens than by patients with *S. aureus* bacteremia (Table 1). *S. aureus* bacteremia patients were more likely to have a diagnosis of suspected septicemia or other focal sepsis and less likely to have a diagnosis of suspected pneumonia than patients without bacteremia or with bacteremia caused by other pathogens (Table 1).

### Incidence and Risk Factors for *S. aureus* Bacteremia

Using the combined referral and admission surveillance data (2011–2015 in BDHSS and 2012–2014 in FWDHSS),

we found the incidence of *S. aureus* bacteremia to be 78 (95% CI 67–91) cases/100,000 person-years in children 0–59 months of age. The incidence was highest among neonates (2,080 [95% CI 1,621–2,627] cases/100,000 person-years, 3.5 [95% CI 2.9–4.7] cases/1,000 live births) and decreased in older age groups (Table 2). Incidence of *S. aureus* bacteremia in the 1–11-month age group was 133 (95% CI 99–174) cases/100,000 person-years, and incidence in the 1–4-year age group was 27 (95% CI 20–36) cases/100,000 person-years. Among the 84 *S. aureus* bacteremia cases in neonates, 13 (15.5%) presented in the first week of life and 35 (41.7%) in the second. The incidence of *S. aureus* bacteremia was higher in the wet season than in the dry season (Table 2).

### Trends in Incidence of *S. aureus* Bacteremia

Using referral surveillance data (2008–2015 in BDHSS), we found the mean annual incidence of *S. aureus* bacteremia in children 2–59 months of age to be 22.3 (95% CI 16.7–29.2) cases/100,000 person-years. The incidence did not change over this period (p value for trend = 0.28), although PCV vaccination coverage increased during this period (Figure 3).

Using the referral surveillance data, we observed that 9 cases (10 cases after enrollment rate adjustment) of *S. aureus* bacteremia occurred in the pre-PCV period and 26 cases (23 cases after enrollment rate adjustment) in the PCV13 period. The crude *S. aureus* bacteremia incidence was 16 cases/100,000 person-years in the pre-PCV period and 26 cases/100,000 person-years in the PCV13 period (incidence rate ratio 1.6, 95% CI 0.8–3.5; p = 0.19). With the increasing size of the population and after adjusting for increased enrollment of eligible children over time, no significant increase in *S. aureus* bacteremia incidence

**Table 1.** Characteristics of patients <5 years of age with suspected pneumonia, septicemia, or meningitis with or without *Staphylococcus aureus* bacteremia identified through 2 surveillance systems, The Gambia, 2008–2015\*

Patient characteristic	Patients with <i>S. aureus</i> bacteremia, n = 198	Patients with bacteremia caused by other pathogen, n = 932	Patients without bacteremia, n = 24,182
Age, mo			
<1	84/198 (42.4)	97/932 (10.4)	1,911/24,177 (7.9)
1–11	61/198 (30.8)	310/932 (33.3)	8,675/24,177 (35.9)
12–23	33/198 (16.7)	265/932 (28.4)	7,505/24,177 (31.0)
24–59	20/198 (10.1)	260/932 (27.9)	6,086/24,177 (25.2)
Sex			
M	97/198 (49.0)	532/932 (57.1)	13,740/24,177 (56.8)
F	101/198 (51.0)	400/932 (42.9)	10,437/24,177 (43.2)
Severely stunted†	20/109 (18.3)	216/884 (24.4)	3,425/21,736 (15.8)
Mid-upper arm circumference <11 cm	81/198 (40.9)	184/932 (19.7)	3,080/24,182 (12.7)
Admitted in previous 2 weeks	31/162 (19.1)	157/843 (18.6)	3,995/21,897 (18.2)
Hospital stay, d, median (IQR)	5 (2–6)	4 (3–6)	3 (2–4)
Disease onset during wet season‡	97/198 (49.0)	335/932 (35.9)	10,335/24,171 (42.8)
Died	28/198 (14.1)	161/932 (17.3)	860/24,182 (3.6)
Symptoms			
Cough	103/198 (52.0)	675/928 (72.7)	19,523/24,148 (80.8)
Difficult breathing	89/197 (45.2)	535/927 (57.7)	14,280/24,102 (59.2)
Prostration	29/197 (14.7)	147/918 (16.0)	1,602/23,906 (6.7)
Diarrhea	38/190 (20.0)	271/861 (31.5)	5,798/22,772 (25.5)
Convulsion	8/198 (4.0)	72/927 (7.8)	1,174/24,127 (4.9)
Signs			
Lower chest wall in-drawing	164/198 (82.8)	732/927 (79.0)	17,856/24,129 (74.0)
Meningism	1/192 (0.5)	34/867 (3.9)	174/22,841 (0.8)
Altered level of consciousness	124/193 (64.2)	407/873 (46.6)	9,590/23,518 (40.8)
Axillary temperature			
<36.5°C	18/198 (9.1)	79/932 (8.5)	2,405/24,182 (9.9)
36.5°C–37.5°C	40/198 (20.2)	147/932 (15.8)	6,819/24,182 (28.2)
>37.5°C	140/198 (70.7)	706/932 (75.7)	14,958/24,182 (61.9)
Pulse rate, beats/min§			
Increased for age	84/198 (42.4)	621/932 (66.6)	15,107/24,182 (62.5)
Respiratory rate, breaths/min¶			
Increased for age	128/198 (64.6)	682/932 (73.2)	17,157/24,177 (71.0)
Oxygen saturation <92%	33/198 (16.7)	116/932 (12.4)	2,140/24,182 (8.8)
Suspected diagnosis#			
Septicemia	109/194 (56.2)	434/896 (48.4)	8,549/23,068 (37.1)
Pneumonia	55/194 (28.4)	347/896 (38.8)	13,244/23,068 (57.4)
Meningitis	13/194 (6.7)	96/896 (10.7)	718/23,068 (3.1)
Other focal sepsis	17/194 (8.8)	19/896 (2.1)	557/23,068 (2.4)
Malaria positivity**	14/131 (10.7)	84/723 (11.6)	3,276/21,626 (15.1)

\*Values are no. patients/total no. in category (%) except as indicated. Surveillance data are from the Basse Health and Demographic Surveillance System and the Fuladu West Health and Demographic Surveillance System. IQR, interquartile range.

†Defined as weight-for-height z-score <3 SDs from median weight-for-height for the corresponding age group. We calculated weight-for-height using z-scores from the 2006 World Health Organization child growth standards in Stata 14.0 (<https://www.stata.com/stata14>). Neonates were not included in weight-for-height measurements.

‡The wet season occurs during July–November and the dry season during December–June.

§The reference ranges for pulse rates were 70–190 beats/min for children <1 month of age, 80–160 beats/min for children 1–11 months of age, 80–130 beats/min for children 1–2 years of age, 80–120 beats/min for children 3–4 years of age, 75–115 beats/min for children 5–6 years of age, 70–110 beats/min for children 7–9 years of age, and 60–100 beats/min for children >10 years of age.

¶Increased respiratory rate was defined as >60 breaths/min for children <2 months of age, >50 breaths/min for children 2–12 months of age, >40 breaths/min for children >1–5 years of age.

#Surveillance diagnosis was categorized into mutually exclusive groups in order of severity; meningitis was considered more severe than septicemia, which was considered more severe than pneumonia.

\*\*Malaria was tested using a rapid diagnostic test (ICT Malaria *P.f.* Antigen, ICT Diagnostics, <http://www.ictdiagnostics.co.za>).

was found between the pre-PCV (18 cases/100,000 person-years) and the PCV13 (23 cases/100,000 person-years) periods (incidence rate ratio 1.3, 95% CI 0.6–2.7; *p* = 0.49).

### CFRs and Risk Factors Associated with Fatality

In total, 28 deaths occurred among 198 *S. aureus* bacteremia patients before discharge (CFR 14.1%, 95% CI 9.4%–20.4%) (Table 1). In comparison, the CFR among patients without bacteremia was 3.6% (95% CI 3.3%–3.8%) and

among patients with bacteremia with other pathogens 17.2% (95% CI 14.7%–20.1%). The *S. aureus* bacteremia CFR did not vary by year (*p* value for trend = 0.75) or age group (*p* value for trend = 0.99). Deaths associated with *S. aureus* bacteremia most often occurred on the day of admission (71.4%, 20/28). During 2011–2015, *S. aureus* bacteremia deaths accounted for 7.0% (12/171) of all deaths in neonates and 3.6% (24/662) of all deaths in children <5 years of age. The risk factors associated with death from *S. aureus* bacteremia



**Table 2.** Factors associated with *Staphylococcus aureus* bacteremia in children <5 years of age identified through 2 surveillance systems, The Gambia, 2011–2015\*

Variable	No. cases/no. person-years at risk	Incidence, cases/100,000 person-years	Incidence rate ratio (95% CI)	p value
Age, mo				
24–59	18/128,994	14.0	1	
12–23	29/44,433	65.3	4.70 (2.6–8.4)	
1–11	53/39,969	132.6	9.50 (5.6–16.2)	
<1	70/3,367	2079.0	148.99 (88.8–250.1)	<0.001
Sex				
M	82/107,515	76.3	1	
F	88/109,248	80.6	1.06 (0.8–1.4)	0.72
Season				
Dry	85/144,508	58.8	1	
Wet	85/72,255	117.6	2.00 (1.5–2.7)	<0.001

\*Surveillance data are from the Basse Health and Demographic Surveillance System and the Fuladu West Health and Demographic Surveillance System

were prostration at clinical presentation and musculoskeletal swelling with or without tenderness (Table 3).

### Treatment and Susceptibility of Isolates

Among *S. aureus* bacteremia patients identified through referral surveillance, 17.1% (13/76) received initial empiric therapy with cloxacillin, 23.7% (18/76) ampicillin, 31.6% (24/76) penicillin, and 50.0% (38/76) gentamicin; 50 (65.8%) of these patients received >1 antimicrobial drug. The mortality rate did not differ by empiric therapy. Among the 193 *S. aureus* isolates tested, 3.1% were methicillin-resistant (Table 4).

### Discussion

We estimated the incidence and CFR of *S. aureus* bacteremia in a rural part of The Gambia using surveillance data over a 5-year period and evaluated trends in incidence over an 8-year period. The incidence was high, particularly among neonates (3.5 cases/1,000 live births), but did not increase with time (Figure 3). The CFR (14.1%) was substantial (Table 1).

The observed incidence of *S. aureus* bacteremia in The Gambia among children 0–59 months of age (78.4 cases/100,000 person-years) was higher than that for industrialized countries (6.5–42.0 cases/100,000 person-years) (22,23) and some countries of Africa (4) and Asia (24,25), although lower than that reported for Mozambique (12). *S. aureus* bacteremia incidence was reported to be 27 cases/100,000 person-years in children <5 years in Kenya (4) and 101 cases/100,000 person-years in Mozambique (12). In Thailand, a study that reviewed national hospital-based data on bacteremia reported a *S. aureus* bacteremia incidence of 2.5 cases/100,000 person-years (24), whereas a population-based study in Bangladesh that focused on children 1–59 months of age with respiratory symptoms reported an incidence of 9.9 cases/100,000 person-years (25). The differences in incidence among studies are likely related to the different selection criteria used in the various studies, nutritional status of the

patients, presence of concurrent medical conditions, or high levels of antimicrobial drug use without a prescription, especially in Asia (26).

During 2008–2015, we found no trend in *S. aureus* bacteremia incidence in The Gambia. Researchers in industrialized countries have shown an increase in the proportion of all bacteremia cases caused by *S. aureus* after the introduction of PCV (27). However, our data do not support an association between *S. aureus* bacteremia incidence and the introduction of PCV. Further studies in different settings could help confirm this finding.

The incidence of *S. aureus* bacteremia was highest in neonates, 8 times that reported in Kenya (4), and *S. aureus* was the most common cause of bacteremia in this age group. This finding is similar to those of other studies conducted in Africa (12,14), where *S. aureus* was responsible for 39.0%–56.2% of isolates recovered from neonates. *S. aureus* carriage, which is likely a prerequisite for disease, is also highest during the neonatal period, higher than the carriage of *S. pneumoniae* and *H. influenzae* (28). In addition to high rates of acquisition of *S. aureus*

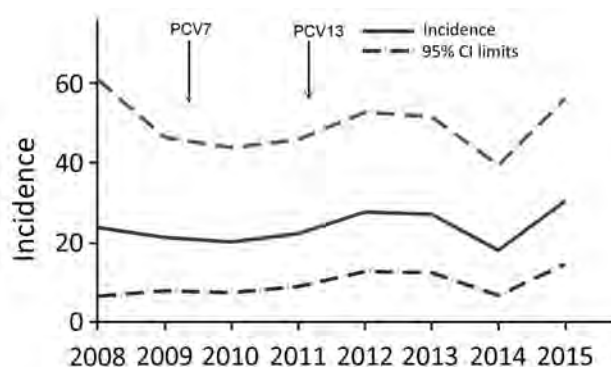


**Figure 3.** Unadjusted annual incidence of *Staphylococcus aureus* bacteremia (cases/100,000 person-years) in children 2–59 months of age, Basse, The Gambia, 2008–2015. Cases were identified by referral surveillance through the Basse Health and Demographic Surveillance System. Arrows indicate introduction of PCV7 and PCV13. PCV7, 7-valent pneumococcal conjugate vaccine; PCV13, 13-valent pneumococcal conjugate vaccine.

**Table 3.** Sociodemographic and clinical parameters associated with death from *Staphylococcus aureus* bacteremia among children <5 years of age identified through 2 surveillance systems, The Gambia, 2008–2015\*

Parameter	Deaths/persons at risk (%)	Unadjusted OR (95% CI)	p value	Adjusted OR (95% CI)†	p value
Age, mo					
<1	13/84 (15.5)	Referent		Referent	
1–11	8/61 (13.1)	0.8 (0.3–2.1)		0.9 (0.4–2.6)	
12–23	4/33 (12.1)	0.8 (0.2–2.5)		1.3 (0.4–4.6)	
24–59	3/20 (15.0)	1.0 (0.3–3.8)	0.96‡	1.1 (0.3–4.6)	0.96
Sex					
M	16/97 (16.5)	Referent			
F	12/101 (11.9)	0.7 (0.3–1.5)	0.35		
Severely stunted§					
No	20/150 (13.3)	Referent			
Yes	5/41 (12.2)	0.9 (0.3–2.6)	0.85		
Axillary temperature					
36.5°C–37.5°C	4/18 (22.2)	Referent			
<36.5°C	4/40 (10.0)	0.4 (0.1–1.8)			
>37.5°C	20/140 (14.3)	0.6 (0.2–2.0)	0.48		
Pulse rate, beats/min¶					
Within reference ranges	13/114 (11.4)	Referent			
Increased for age	15/84 (17.9)	1.7 (0.8–3.8)	0.20		
Respiratory rate, breaths/min#					
Within reference ranges	8/70 (11.4)	Referent			
Increased for age	20/128 (15.6)	1.4 (0.6–3.5)	0.41		
Need for oxygen supplementation					
No	21/165 (12.7)	Referent			
Yes	7/33 (21.2)	1.9 (0.7–4.8)	0.22		
Season					
Dry	18/101 (17.8)	Referent			
Wet	10/97 (10.3)	0.5 (0.2–1.2)	0.13		
Cough					
No	13/95 (13.7)	Referent			
Yes	15/103 (14.6)	1.1 (0.5–2.4)	0.86		
Difficult breathing					
No	14/108 (13.0)	Referent			
Yes	14/89 (15.7)	1.3 (0.6–2.8)	0.58		
Prostration					
No	17/168 (10.1)	Referent		Referent	
Yes	11/29 (37.9)	5.4 (2.2–13.4)	0.0004	5.7 (2.2–14.8)	0.01
Admitted in previous 2 weeks					
No	20/131 (15.3)	Referent			
Yes	2/31 (6.5)	0.4 (0.1–1.7)	0.16		

\*Surveillance data are from the Basse Health and Demographic Surveillance System and the Fuladu West Health and Demographic Surveillance System. OR, odds ratio.

†Adjusted for age only.

‡p value for trend.

§Defined as weight-for-height z-score <3 SDs from median weight-for-height for the corresponding age group. We calculated weight-for-height using z-scores from the 2006 World Health Organization child growth standards in Stata 14.0 (<https://www.stata.com/stata14>). Neonates were not included in weight-for-height measurements.

¶The reference ranges for pulse rates were 70–190 beats/min for children <1 month of age, 80–160 beats/min for children 1–11 months of age, 80–130 beats/min for children 1–2 years of age, 80–120 beats/min for children 3–4 years of age, 75–115 beats/min for children 5–6 years of age, 70–110 beats/min for children 7–9 years of age, and 60–100 beats/min for children >10 years of age.

#Increased respiratory rate was defined as >60 breaths/min for children <2 months of age, >50 breaths/min for children 2–12 months of age, >40 breaths/min for children >1–5 years of age.

during the neonatal period, other reasons for the high risk for *S. aureus* bacteremia might include an immature immune system (29).

In our study, only 16% of the *S. aureus* bacteremia cases in neonates presented within the first week of life, unlike for group B *Streptococcus* disease, where 80% of parents seek treatment for their neonates within this period (30). Reasons for the difference in timing of treatment might relate to the age at and source of *S. aureus* acquisition.

We found *S. aureus* bacteremia to be more common during the wet season. This seasonal variation might

relate to *S. aureus* colonization (a prerequisite for disease), which is highest during the wet season (31), or seasonal differences in the incidence of viral infections, which are known to disrupt mucosal epithelium, thereby encouraging *S. aureus* invasion (32). In a study of US adults (33), the peak incidence of *S. aureus* infection occurred during the winter months and coincided with the peak incidence of viral infections. In Africa, the incidence of viral infections usually peaks during the wet season (34), coinciding with the peak *S. aureus* bacteremia incidence.

**Table 4.** Antimicrobial drug susceptibility of *Staphylococcus aureus* isolates from children <5 years of age identified through 2 surveillance systems, The Gambia, 2008–2015\*

Antimicrobial drug	No. isolates tested	No. (%) sensitive	No. (%) intermediate	No. (%) resistant
Cefoxitin†	193	187 (96.9)	0	6 (3.1)
Chloramphenicol	186	176 (94.6)	2 (1.1)	8 (4.3)
Cotrimoxazole	180	119 (66.1)	21 (11.7)	40 (22.2)
Erythromycin	173	141 (81.5)	24 (13.9)	8 (4.6)
Gentamicin	177	174 (98.3)	0	3 (1.7)
Oxacillin	194	170 (87.6)	24 (12.4)	0
Tetracycline	180	128 (71.1)	2 (1.1)	50 (27.8)

\*Surveillance data are from the Basse Health and Demographic Surveillance System and the Fuladu West Health and Demographic Surveillance System. †Cefoxitin was used as a surrogate for methicillin-resistant isolates as recommended by the Clinical and Laboratory Standards Institute (21).

The CFR in our study was similar to (10) or greater than that reported by others (12,23). Variation in CFRs could be explained by differences between study populations in terms of age, quality of and access to healthcare, focus of infection, antimicrobial drug resistance rates, severity of *S. aureus* bacteremia, or presence of concurrent medical conditions. In our study, 71.4% of deaths occurred on the day of admission, which might be a reflection of severity of disease when care was sought. Even though age is strongly associated with *S. aureus* bacteremia–related death (10,11), in our study CFR did not vary with age.

The strengths of our study were that the surveillance was population-based and uninterrupted and that blood culture was performed on >84% of eligible patients. However, the study also had some limitations. First, incidence might have been underestimated because some persons with *S. aureus* bacteremia never seek treatment at hospitals and the sensitivity of blood culture is <100%. Second, an increasing rate of enrollment and investigation over time required adjustment of annual case counts. Third, prior use of antimicrobial drugs, although uncommon in our study area, might have reduced the detection of *S. aureus* bacteremia by blood culture. Last, our study was not specifically designed to evaluate risk factors for *S. aureus* bacteremia. For example, *S. aureus* nasal carriage, hospitalization in the previous 6 months, and HIV status were not systematically assessed.

In conclusion, we demonstrated that the incidence of *S. aureus* bacteremia is high in rural Gambia, especially in neonates and infants. Strategies are urgently needed to reduce the burden of *S. aureus* bacteremia and should target children in their first month of life.

### Acknowledgments

We thank the staffs of Basse District Hospital (formerly known as Basse Health Centre), Bansang Hospital, and the health facilities in Demba Kunda, Fatoto, Gambissara, Garawol, Koina, Brikama Ba, and Jakhaly. We also thank the staff of the Expanded Programme on Immunisation of The Gambia and the government of The Gambia for their ongoing collaboration with the Medical Research Council Unit The Gambia. We appreciate all staff at the Medical Research Council Unit The Gambia Basse Field Station (especially the staff who worked on the

Pneumococcal Surveillance Project and the BHDSS and FWHSS) for their support and the residents living in the regions surveilled by the BHDSS and FWHSS for participating in the study staff. We are particularly grateful to the parents and guardians who allowed their children to participate in this study.

The work was supported by GAVI's Pneumococcal Vaccines Accelerated Development and Introduction Plan (Bloomberg School of Public Health, Johns Hopkins University, Baltimore, MD, USA), the Bill & Melinda Gates Foundation (OPP 1020372), and the UK Medical Research Council.

### About the Author

Dr. Odotola is a PhD student working at the Medical Research Council Unit The Gambia at the London School of Hygiene and Tropical Medicine, London, UK. Her research interests include epidemiology and *S. aureus* diseases.

### References

1. United Nations Inter-agency Group for Child Mortality Estimation. Levels & trends in child mortality report 2017. New York: United Nations Children's Fund; 2017.
2. Liu L, Johnson HL, Cousens S, Perin J, Scott S, Lawn JE, et al.; Child Health Epidemiology Reference Group of WHO and UNICEF. Global, regional, and national causes of child mortality: an updated systematic analysis for 2010 with time trends since 2000. *Lancet*. 2012;379:2151–61. [http://dx.doi.org/10.1016/S0140-6736\(12\)60560-1](http://dx.doi.org/10.1016/S0140-6736(12)60560-1)
3. Blomberg B, Manji KP, Urassa WK, Tamim BS, Mwakagile DS, Jureen R, et al. Antimicrobial resistance predicts death in Tanzanian children with bloodstream infections: a prospective cohort study. *BMC Infect Dis*. 2007;7:43. <http://dx.doi.org/10.1186/1471-2334-7-43>
4. Berkley JA, Lowe BS, Mwangi I, Williams T, Bauni E, Mwarumba S, et al. Bacteremia among children admitted to a rural hospital in Kenya. *N Engl J Med*. 2005;352:39–47. <http://dx.doi.org/10.1056/NEJMoa040275>
5. Oluwalana C, Howie SR, Secka O, Ideh RC, Ebruke B, Sambou S, et al. Incidence of *Haemophilus influenzae* type b disease in The Gambia 14 years after introduction of routine *Haemophilus influenzae* type b conjugate vaccine immunization. *J Pediatr*. 2013;163(Suppl):S4–7. <http://dx.doi.org/10.1016/j.jpeds.2013.03.023>
6. Mackenzie GA, Hill PC, Jeffries DJ, Hossain I, Uchendu U, Ameh D, et al. Effect of the introduction of pneumococcal conjugate vaccination on invasive pneumococcal disease in The Gambia: a population-based surveillance study. *Lancet Infect Dis*. 2016;16:703–11. [http://dx.doi.org/10.1016/S1473-3099\(16\)00054-2](http://dx.doi.org/10.1016/S1473-3099(16)00054-2)



7. Waters D, Jawad I, Ahmad A, Lukšić I, Nair H, Zgaga L, et al. Aetiology of community-acquired neonatal sepsis in low and middle income countries. *J Glob Health*. 2011;1:154–70.
8. Johnson AP, Pearson A, Duckworth G. Surveillance and epidemiology of MRSA bacteraemia in the UK. *J Antimicrob Chemother*. 2005;56:455–62. <http://dx.doi.org/10.1093/jac/dki266>
9. Stoll BJ, Hansen NI, Sánchez PJ, Faix RG, Poindexter BB, Van Meurs KP, et al.; Eunice Kennedy Shriver National Institute of Child Health and Human Development Neonatal Research Network. Early onset neonatal sepsis: the burden of group B streptococcal and *E. coli* disease continues. *Pediatrics*. 2011;127:817–26. <http://dx.doi.org/10.1542/peds.2010-2217>
10. Cobos-Carrascosa E, Soler-Palacín P, Nieves Larrosa M, Bartolomé R, Martín-Nalda A, Antoinette Frick M, et al. *Staphylococcus aureus* bacteremia in Children: changes during eighteen years. *Pediatr Infect Dis J*. 2015;34:1329–34. <http://dx.doi.org/10.1097/INF.0000000000000907>
11. Mejer N, Westh H, Schönheyder HC, Jensen AG, Larsen AR, Skov R, et al.; Danish Staphylococcal Bacteraemia Study Group. Stable incidence and continued improvement in short term mortality of *Staphylococcus aureus* bacteraemia between 1995 and 2008. *BMC Infect Dis*. 2012;12:260. <http://dx.doi.org/10.1186/1471-2334-12-260>
12. Sigaúque B, Roca A, Mandomando I, Morais L, Quintó L, Sacarlal J, et al. Community-acquired bacteremia among children admitted to a rural hospital in Mozambique. *Pediatr Infect Dis J*. 2009;28:108–13. <http://dx.doi.org/10.1097/INF.0b013e318187a87d>
13. Mulholland EK, Ogunlesi OO, Adegbola RA, Weber M, Sam BE, Palmer A, et al. Etiology of serious infections in young Gambian infants. *Pediatr Infect Dis J*. 1999;18(Suppl):S35–41. <http://dx.doi.org/10.1097/00006454-199910001-00007>
14. Uzodimma CC, Njokanna F, Ojo O, Falase M, Ojo T. Bacterial isolates from blood cultures of children with suspected sepsis in an urban hospital in Lagos: a prospective study using BACTEC blood culture system. *Internet J Pediatr Neonatol*. 2013;16:1623.
15. Groome MJ, Albrich WC, Wadula J, Khoosal M, Madhi SA. Community-onset *Staphylococcus aureus* bacteraemia in hospitalised African children: high incidence in HIV-infected children and high prevalence of multidrug resistance. *Paediatr Int Child Health*. 2012;32:140–6. <http://dx.doi.org/10.1179/1465328111Y.00000000044>
16. Hill PC, Onyema CO, Ikumapayi UN, Secka O, Ameyaw S, Simmonds N, et al. Bacteraemia in patients admitted to an urban hospital in West Africa. *BMC Infect Dis*. 2007;7:2. <http://dx.doi.org/10.1186/1471-2334-7-2>
17. Scott S, Odutola A, Mackenzie G, Fulford T, Afolabi MO, Jallow YL, et al. Coverage and timing of children's vaccination: an evaluation of the expanded programme on immunisation in The Gambia. *PLoS One*. 2014;9:e107280. <http://dx.doi.org/10.1371/journal.pone.0107280>
18. Mwesigwa J, Okebe J, Affara M, Di Tanna GL, Nwakanma D, Janha O, et al. On-going malaria transmission in The Gambia despite high coverage of control interventions: a nationwide cross-sectional survey. *Malar J*. 2015;14:314. <http://dx.doi.org/10.1186/s12936-015-0829-6>
19. Mackenzie GA, Plumb ID, Sambou S, Saha D, Uchendu U, Akinsola B, et al. Monitoring the introduction of pneumococcal conjugate vaccines into West Africa: design and implementation of a population-based surveillance system. *PLoS Med*. 2012;9:e1001161. <http://dx.doi.org/10.1371/journal.pmed.1001161>
20. Adegbola RA, Falade AG, Sam BE, Aidoo M, Baldeh I, Hazlett D, et al. The etiology of pneumonia in malnourished and well-nourished Gambian children. *Pediatr Infect Dis J*. 1994;13:975–82. <http://dx.doi.org/10.1097/00006454-199411000-00008>
21. Clinical and Laboratory Standards Institute. Performance standards for antimicrobial disk susceptibility tests; approved standard—twelfth edition (M02-A12). Wayne (PA): The Institute; 2015.
22. Frederiksen MS, Espersen F, Frimodt-Møller N, Jensen AG, Larsen AR, Pallesen LV, et al. Changing epidemiology of pediatric *Staphylococcus aureus* bacteremia in Denmark from 1971 through 2000. *Pediatr Infect Dis J*. 2007;26:398–405. <http://dx.doi.org/10.1097/01.inf.0000261112.53035.4c>
23. Asgeirsson H, Gudlaugsson O, Kristinsson KG, Vilbergsson GR, Heiddal S, Haraldsson A, et al. Low mortality of *Staphylococcus aureus* bacteremia in Icelandic children: nationwide study on incidence and outcome. *Pediatr Infect Dis J*. 2015;34:140–4. <http://dx.doi.org/10.1097/INF.0000000000000485>
24. Kanoksil M, Jatapai A, Peacock SJ, Limmathurotsakul D. Epidemiology, microbiology and mortality associated with community-acquired bacteremia in northeast Thailand: a multicenter surveillance study. *PLoS One*. 2013;8:e54714. <http://dx.doi.org/10.1371/journal.pone.0054714>
25. Arifeen SE, Saha SK, Rahman S, Rahman KM, Rahman SM, Bari S, et al. Invasive pneumococcal disease among children in rural Bangladesh: results from a population-based surveillance. *Clin Infect Dis*. 2009;48(Suppl 2):S103–13. <http://dx.doi.org/10.1086/596543>
26. Zellweger RM, Carrique-Mas J, Limmathurotsakul D, Day NPJ, Thwaites GE, Baker S, et al.; Southeast Asia Antimicrobial Resistance Network. A current perspective on antimicrobial resistance in Southeast Asia. *J Antimicrob Chemother*. 2017; 72:2963–72. <http://dx.doi.org/10.1093/jac/dkx260>
27. Greenhow TL, Hung YY, Herz A. Bacteremia in Children 3 to 36 months old after introduction of conjugated pneumococcal vaccines. *Pediatrics*. 2017;139:e20162098. <http://dx.doi.org/10.1542/peds.2016-2098>
28. Peacock SJ, Justice A, Griffiths D, de Silva GD, Kantzanou MN, Crook D, et al. Determinants of acquisition and carriage of *Staphylococcus aureus* in infancy. *J Clin Microbiol*. 2003; 41:5718–25. <http://dx.doi.org/10.1128/JCM.41.12.5718-5725.2003>
29. Power Coombs MR, Kronforst K, Levy O. Neonatal host defense against Staphylococcal infections. *Clin Dev Immunol*. 2013;2013:826303. <http://dx.doi.org/10.1155/2013/826303>
30. Trijbels-Smeulders M, de Jonge GA, Pasker-de Jong PC, Gerards LJ, Adriaanse AH, van Lingen RA, et al. Epidemiology of neonatal group B streptococcal disease in the Netherlands before and after introduction of guidelines for prevention. *Arch Dis Child Fetal Neonatal Ed*. 2007;92:F271–6. <http://dx.doi.org/10.1136/adc.2005.088799>
31. Bojang A, Kendall L, Usuf E, Egere U, Mulwa S, Antonio M, et al. Prevalence and risk factors for *Staphylococcus aureus* nasopharyngeal carriage during a PCV trial. *BMC Infect Dis*. 2017;17:588. <http://dx.doi.org/10.1186/s12879-017-2685-1>
32. Wang X, Zhang N, Glorieux S, Holtappels G, Vanechoutte M, Krysko O, et al. Herpes simplex virus type 1 infection facilitates invasion of *Staphylococcus aureus* into the nasal mucosa and nasal polyp tissue. *PLoS One*. 2012;7:e39875. <http://dx.doi.org/10.1371/journal.pone.0039875>
33. Lewis SS, Walker VJ, Lee MS, Chen L, Moehring RW, Cox CE, et al. Epidemiology of methicillin-resistant *Staphylococcus aureus* pneumonia in community hospitals. *Infect Control Hosp Epidemiol*. 2014;35:1452–7. <http://dx.doi.org/10.1086/678594>
34. Breiman RF, Cosmas L, Njenga M, Williamson J, Mott JA, Katz MA, et al. Severe acute respiratory infection in children in a densely populated urban slum in Kenya, 2007–2011. *BMC Infect Dis*. 2015;15:95. <http://dx.doi.org/10.1186/s12879-015-0827-x>

---

Address for correspondence: Aderonke Odutola, Medical Research Council Unit The Gambia at the London School of Hygiene and Tropical Medicine, Disease Control and Elimination Theme, 20 Atlantic Rd, Fajara, PO Box 273, Banjul, The Gambia; email: ceeme10@yahoo.ca

# Pneumonia-Specific *Escherichia coli* with Distinct Phylogenetic and Virulence Profiles, France, 2012–2014

Béatrice La Combe, Olivier Clermont, Jonathan Messika, Matthieu Eveillard, Achille Kouatchet, Sigismond Lasocki, Stéphane Corvec, Karim Lakhal, Typhaine Billard-Pomares, Romain Fernandes, Laurence Armand-Lefevre, Sandra Bourdon, Jean Reignier, Vincent Fihman, Nicolas de Prost, Julien Bador, Julien Goret, Frederic Wallet, Erick Denamur, Jean-Damien Ricard, on behalf of the COLOCOLI group<sup>1</sup>

In a prospective, nationwide study in France of *Escherichia coli* responsible for pneumonia in patients receiving mechanical ventilation, we determined *E. coli* antimicrobial susceptibility, phylotype, O-type, and virulence factor gene content. We compared 260 isolates with those of 2 published collections containing commensal and bacteremia isolates. The preponderant phylogenetic group was B2 (59.6%), and the predominant sequence type complex (STc) was STc73. STc127 and STc141 were overrepresented and STc95 underrepresented in pneumonia isolates compared with bacteremia isolates. Pneumonia isolates carried higher proportions of virulence genes *sfa/foc*, *papGIII*, *hlyC*, *cnf1*, and *iroN* compared with bacteremia isolates. Virulence factor gene content and antimicrobial drug resistance were higher in pneumonia than in commensal isolates. Genomic

and phylogenetic characteristics of *E. coli* pneumonia isolates from critically ill patients indicate that they belong to the extraintestinal pathogenic *E. coli* pathovar but have distinguishable lung-specific traits.

Nosocomial infections remain a major threat for patients and a burden on healthcare institutions, hampering the public health economy. In intensive care units (ICUs), the most common life-threatening nosocomial infection is ventilator-associated pneumonia; the attributable mortality rate is ≈13%, partly because of increased durations of mechanical ventilation and ICU stays (1,2), all of which generate considerable additional costs (3).

Until the early 2000s, *Enterobacteriaceae* were not considered as major pathogens responsible for ventilator-assisted pneumonia (2); as such, pathophysiological studies focused mainly on *Pseudomonas aeruginosa*, *Staphylococcus aureus*, and *Acinetobacter baumannii*. However, recent data have consistently shown that *Enterobacteriaceae* are now frequent etiologic agents of ventilator-assisted pneumonia, more frequent than *P. aeruginosa* and *S. aureus* (4–6). According to the World Health Organization, *Enterobacteriaceae*, including *Escherichia coli*, are among the critical priority antibiotic-resistant bacteria (7). Therefore, to optimize patient management, in-depth epidemiologic knowledge of the phenotypic and genotypic characteristics of these bacteria is warranted. Although most *E. coli* responsible for symptomatic extraintestinal infections (8), including the urinary tract (9), bloodstream (10,11), cerebral spinal fluid (12,13), and peritoneum (14), have been extensively studied, less is known about *E. coli* strains responsible for pneumonia (15), especially in the context of highly virulent and resistant clones such as sequence type (ST) 69 and ST131 (16).

Author affiliations: Infection, Antimicrobiens, Modélisation, Évolution, Paris, France (B. La Combe, O. Clermont, J. Messika, T. Billard-Pomares, R. Fernandes, L. Armand-Lefevre, E. Denamur, J.-D. Ricard); Université Paris Diderot, Paris (B. La Combe, O. Clermont, J. Messika, T. Billard-Pomares, R. Fernandes, L. Armand-Lefevre, E. Denamur, J.-D. Ricard); Hôpital Louis Mourier, Colombes, France (B. La Combe, J. Messika, T. Billard-Pomares, R. Fernandes, J.-D. Ricard); Centre Hospitalier Universitaire, Angers, France (M. Eveillard, A. Kouatchet, S. Lasocki); Centre Hospitalier Universitaire, Nantes, France (S. Corvec, J. Reignier); Hôpital Laënnec, Nantes (K. Lakhal); Hôpital Bichat, AP-HP, Paris (L. Armand-Lefevre, E. Denamur); Centre Hospitalier Départemental Vendée, La Roche-sur-Yon, France (S. Bourdon); Hôpital Henri Mondor, AP-HP, Créteil, France (V. Fihman, N. de Prost); Centre Hospitalier Universitaire Bocage Central, Dijon, France (J. Bador); Centre Hospitalier Universitaire Pellegrin, Bordeaux, France (J. Goret); Centre Hospitalier Régional Universitaire, Lille, France (F. Wallet)

DOI: <https://doi.org/10.3201/eid2504.180944>

<sup>1</sup>Group members are listed at the end of this article.

Our previous monocentric prospective study in France found a predominance of B2 phylogenetic group (66%) among *E. coli* pneumonia isolates, one third of which belonging to ST complex (STc) 127 (15). To obtain further insights in the physiopathology of ventilator-assisted pneumonia, we conducted a multicentric prospective epidemiologic study of genomic and phylogenetic characteristics of *E. coli* strains responsible for pneumonia across France.

## Materials and Methods

### Patients and *E. coli* Isolates

We conducted this prospective study in 14 ICUs throughout France, in collaboration with their hospital laboratories. We selected these ICUs to guarantee appropriate geographic coverage of metropolitan France. The same geographic selection was also applied to the ICUs in the Paris area. The ethics committee of the French Intensive Care Society approved the study (SRLF-CE 12-388), which was registered at ClinicalTrials.gov (NCT03303937). Formal consent was not required because of the observational, noninterventional study design (no change in practices, and all procedures already routinely performed). Patients or family/relatives were informed of the nature of the study and its purpose and objectives and had the option of declining participation.

During a 38-month period (2012–2014), any *E. coli* isolate responsible for pneumonia in a mechanically ventilated patient was collected, regardless of the method of sampling (quantitative cultures of tracheal suctioning, bronchoalveolar lavage, or protected telescoping catheter). Demographic and clinical data for the patient were recorded. We defined ventilator-assisted pneumonia as pneumonia occurring  $\geq 48$  hours after initiation of invasive ventilation, hospital-acquired pneumonia as pneumonia occurring  $\geq 48$  hours after hospital admission but within the first 48 hours of invasive ventilation, and community-acquired pneumonia as pneumonia that occurred either before or within the first 48 hours of hospitalization (17). Each *E. coli* isolate was stored at  $-80^{\circ}\text{C}$  in brain-heart infusion broth containing glycerol 20% (the COLOCOLI collection).

### *E. coli* Phylotyping, O-Typing, and Virulence Factor Gene Content Determination

We used quadruplex PCR to determine the *E. coli* phylogenetic group (A, B1, B2, C, D, E, F) or belonging to clade I (18). Among the strains, we determined the B1 clonal complex 87 (CC87) (Institut Pasteur MLST schema nomenclature corresponding to the ST58 and 155 in the Achtman schema [19]), the 10 main B2 subgroups (20), and the clonal group A (clonal group A) from the D phylogroup (21). The exhaustive correspondence between this typing

approach and STc membership according to the currently used Achtman MLST schema is available in (22).

We used PCR to determine the most anticipated serotypes in isolates from patients with extraintestinal infections (Table 1) (23). Multiplex PCR was used to detect genes encoding for 11 frequently encountered extraintestinal virulence factors (*sfa/foc*, *papC*, *papGII*, *papGIII*, *fyuA*, *iroN*, *aer*, *traT*, *neuC*, *hlyC*, and *cnf1*), which belong to the main classes of virulence factors (adhesins, toxins, iron acquisition systems, and protectins) (11). For each isolate, we calculated the virulence score, which was defined by the number of virulence factors present among the 11 tested.

### Antimicrobial Resistance Phenotypes

We determined the antimicrobial susceptibility of each isolate by using the disk-diffusion method according to the French Society of Microbiology (<https://www.sfm-microbiologie.org>) (Table 2). Resistance score was defined as the sum of inactive in vitro antimicrobial agents for each isolate. A score of 1 indicates resistant; 0.5, intermediary; and 0, sensitive. A higher score indicates a more resistant isolate. Detection of gene sequences coding for the TEM, SHV, and CTX-M enzymes was performed by PCR with genomic DNA. The oligonucleotide primer sets specific for the  $\beta$ -lactamase genes used in the PCR assays have been published (24,25).

### Characteristics of Other *E. coli* Strain Collections

To learn more about *E. coli* pneumonia strains, we compared the isolates from the COLOCOLI collection with

**Table 1.** Characterization of the main *Escherichia coli* B2 phylogroup clones, by combination of subgroup and O-type, among patients with extraintestinal infections, France, 2012–2014\*

Subgroup and O-type	B2 clones, no. (%), n = 155
I-O25b	15 (62.5)
I-O6a	2 (8.3)
I-O16	3 (12.5)
II-O22	2 (5)
II-O2b	4 (10)
II-O6a	26 (65)
III-O6a	16 (100)
IV-O2b	19 (95)
VI-O4	13 (92.9)
VII-O18	2 (66.6)
VII-O75	1 (33.3)
IX-O1	7 (50)
IX-O18	3 (21.4)
IX-O2a	3 (21.4)

\*Data are presented as no. (%) of each clone within the corresponding subgroup. Roman numerals correspond to the B2 subgroup. The correspondence with the Achtman multilocus sequence type schema is as follows: subgroup I, sequence type complex (STc) 131; subgroup II, STc73; subgroup III, STc127; subgroup IV, STc141; subgroup VI, STc12; subgroup VII, STc14; subgroup IX, STc95 (22). The most anticipated serotypes in extraintestinal infections were searched by PCR: O1, O2a, O2b, O4, O6, O7, O12, O15, O16, O17, O18, O22, O25a, O25b, O45a, O75, O78.



**Table 2.** Resistance and virulence traits of the 260 *Escherichia coli* isolates responsible for pneumonia in patients receiving mechanical ventilation, according to phylogenetic group, France, 2012–2014\*

Trait	Phylogenetic group			Phylogenetic group				
	B2, n = 155	Non-B2, n = 105	p value	A, n = 22	B1, n = 26	C, n = 20	D, n = 25	F, n = 11
<i>iroN</i>	130 (83.9)	52 (49.5)	<0.0001	10 (45.4)	13 (50)	16 (80)	6 (24)	6 (54.5)
<i>sfa/foc</i>	109 (70.3)	0	<0.0001	0	0	0	0	0
<i>neuC</i>	41 (26.4)	0	<0.0001	0	0	0	0	0
<i>fyuA</i>	152 (98.1)	51 (48.6)	<0.0001	7 (31.8)	9 (34.6)	16 (80)	10 (40)	8 (72.7)
<i>hlyC</i>	98 (63.2)	2 (1.9)	<0.0001	0	2 (7.7)	0	0	0
<i>cnf1</i>	91 (58.7)	1 (1)	<0.0001	0	1 (3.8)	0	0	0
<i>aer</i>	65 (41.9)	67 (63.8)	0.0006	14 (63.6)	15 (57.7)	14 (70)	15 (60)	8 (72.7)
<i>papC</i>	100 (64.5)	27 (25.7)	<0.0001	7 (31.8)	3 (11.5)	8 (40)	8 (32)	1 (9.1)
<i>papGII</i>	27 (17.4)	4 (3.8)	0.0007	0	0	0	4 (16)	0
<i>papGIII</i>	64 (41.3)	0	<0.0001	0	0	0	0	0
<i>traT</i>	70 (45.2)	82 (78.1)	<0.0001	15 (68.2)	20 (76.9)	17 (85)	20 (80)	9 (81.8)
Virulence score, median (IQR)†	7 (5–7)	3 (2–4)	<0.0001	2.5 (2–4)	3 (1–4)	4 (3–5)	3 (2–3)	3 (2.5–3)
Antimicrobial resistance								
Amoxicillin	75 (48.4)	83 (79)	<0.0001	19 (86.4)	19 (73)	16 (80)	19 (76)	10 (90.9)
Amoxicillin/clavulanic acid	66 (42.6)	68 (64.8)	0.0006	18 (81.8)	13 (50)	15 (75)	14 (56)	8 (72.7)
Piperacillin/tazobactam	21 (13.5)	27 (25.7)	0.02	6 (27.3)	6 (23.1)	7 (35)	3 (12)	5 (45.4)
Cefotaxime	11 (7.1)	17 (16.2)	0.02	4 (18.2)	4 (15.4)	2 (10)	3 (12)	4 (36.4)
Ceftazidime	12 (7.7)	17 (16.2)	0.04	4 (18.2)	4 (15.4)	2 (10)	3 (12)	4 (36.4)
Imipenem	0	1 (1)	0.4	0	1 (3.8)	0	0	0
Gentamicin	4 (2.6)	10 (9.5)	0.02	3 (13.6)	1 (3.8)	2 (10)	1 (4)	3 (27.3)
Amikacin	3 (1.9)	1 (1)	0.6	0	0	0	0	1 (9.1)
Ofloxacin	15 (9.7)	28 (26.7)	0.0005	7 (31.8)	6 (23.1)	6 (30)	2 (8)	6 (54.5)
Ciprofloxacin	13 (8.4)	24 (22.9)	0.002	7 (31.8)	5 (19.2)	6 (30)	2 (8)	4 (36.4)
Resistance score, median (IQR)‡	1.5 (0–4)	4.5 (2.5–7)	<0.0001	5 (3.5–8)	4 (1–6)	4.5 (3.5–7.5)	4 (1.5–5.5)	7.5 (5–9)
ESBL phenotype	10 (6.4)	12 (11.4)	0.2	4 (18.2)	1 (3.8)	1 (4)	2 (8)	3 (27.3)
WT phenotype	84 (54.2)	24 (22.9)	<0.0001	4 (18.2)	7 (26.9)	6 (24)	7 (28)	1 (9.1)

\*Values are no. (%) except as indicated. ESBL, extended-spectrum beta-lactamase; IQR, interquartile range; WT, wild type (susceptible to all tested antimicrobials).

†Virulence score was calculated, defined by the number of present virulence factors among the 11 tested.

‡Resistance score was defined as the sum of inactive in vitro antimicrobial agents for each isolate. Tested antimicrobials were gentamicin, amikacin, minocycline, nalidixic acid, ofloxacin, ciprofloxacin, fosfomycin, furans, trimethoprim, amoxicillin, amoxicillin-clavulanic acid, ticarcillin, piperacillin, piperacillin-tazobactam, imipenem, cefotaxime, and ceftazidime. A score of 1 was attributed for a resistant, 0.5 for an intermediary, and 0 for a sensitive isolate; a higher score thus indicated a more resistant isolate. For each antimicrobial, resistance is defined by the sum of resistant or intermediary isolates.

those of 2 published collections, originating from the Paris area in France. In 2010, a total of 280 *E. coli* strains were isolated from fecal samples from community adults and can be considered as commensal strains (COLIVILLE collection) (26). In 2005, a total of 373 *E. coli* strains were isolated from the blood of 373 in-patients in 14 hospitals during the course of bacteremia (COLIBAFI collection) (27). Of note, 20.6% of isolates from patients with bacteremia were nosocomial and 57% were of urinary origin. Among patients with bacteremia, the portal of entry was pulmonary for <2% (most patients were not in an ICU).

For these strains, we determined the phylogroup/subgroup membership, the presence of the 11 virulence factors cited above, and the susceptibility to 6 antimicrobial drugs (amoxicillin, amoxicillin/clavulanic acid, cefotaxime, amikacin, ofloxacin, and ceftazidime). For all strains, we calculated a virulence score.

### Statistical Analyses

For our analyses we used GraphPad Prism7 software (<https://www.graphpad.com>). For quantitative variables, results are presented as the median and range, and for

categorical variables, as frequency and proportion. Variables were compared according to whether they were nosocomial or community isolates and whether they were of phylogenetic group B2 or not B2. As we compared the virulence factor gene content of the 3 collections, we also compared the proportion of phylogenetic groups and subgroups and of resistant strains. We used the Student *t* test to compare continuous variables and the Fisher exact test to compare categorical variables. Because of the observational design of the study and its exploratory aim, we did not adjust for multiple testing (28). We considered  $p < 0.05$  to be significant.

## Results

### Host Characteristics

During the study period, we collected 260 *E. coli* isolates from 243 patients with a median age of 64 years (interquartile range 52–73 years) (Table 3). Of these isolates, 117 were responsible for ventilator-assisted pneumonia, 61 for hospital-acquired pneumonia, and 82 for community-acquired pneumonia. The main reasons for ICU admission

**Table 3.** Demographics and clinical characteristics of 243 pneumonia patients requiring mechanical ventilation, from whom *Escherichia coli* was isolated, France, 2012–2014\*

Characteristic	Value
Age, y, median (IQR)	64 (52–73)
Sex	
M	183 (75.3)
F	60 (24.7)
SAPS II at admission, median (IQR)	57 (42–69)
Comorbid conditions	
Chronic alcohol consumption	56 (23)
Diabetes mellitus	45 (18.5)
Neoplastic disease	43 (17.7)
Immunosuppression†	77 (31.7)
Cirrhosis	12 (4.9)
Chronic kidney disease	18 (7.4)
Dialysis	5 (2.1)
Chronic respiratory disease	33 (13.6)
Chronic heart failure	43 (17.7)
Reason for ICU admission	
Acute respiratory failure	61 (25.1)
Coma	48 (19.8)
Septic shock	44 (18.1)
Cardiac arrest	28 (11.5)
Cardiogenic shock	14 (5.8)
Polytrauma	22 (9.1)
Postoperative care	8 (3.3)
Hemorrhagic shock	5 (2.1)
Exposure to antimicrobial drug therapy in previous 3 mo	98 (40.3)
Amoxicillin	6 (2.5)
Amoxicillin/clavulanic acid	38 (15.6)
Third-generation cephalosporin	19 (7.8)
Aminoglycosides	29 (11.9)
Piperacillin/tazobactam	24 (9.9)
Quinolone	10 (4.1)
Carbapenem	11 (4.5)
Polymicrobial sampling	57 (23.5)
ICU length of stay, d (IQR)	17 (7–33)
Hospital length of stay, d (IQR)	24 (10–45)
Death	
While in ICU	90 (37)
While in hospital	99 (40.7)
Associated with <i>E. coli</i>	27 (11.1)

\*Values are no. (%) except as indicated. ICU, intensive care unit; IQR, interquartile range; SAPS II, Simplified Acute Physiology Score II.

†Defined by  $\geq 1$  immunosuppression factor among neoplastic disease, hematologic malignancy, HIV infection, immunosuppressive therapy, corticosteroids therapy.

were acute respiratory failure ( $n = 61$ , 25.1%), coma ( $n = 48$ , 19.8%), and septic shock ( $n = 44$ , 18.1%). A total of 98 (40.3%) patients had received antimicrobial drugs in the previous 3 months.

### *E. coli* Characteristics

*E. coli* alone was isolated from 76.5% of the respiratory samples, whereas 23.5% of the samples were polymicrobial. The monomicrobial and polymicrobial samples did not differ in terms of phylogroup, virulence factor content, or antimicrobial resistance. We compiled classifications of the different phylogenetic groups/subgroups (Table 4) and details about their community or nosocomial status (Appendix Table 1, <https://wwwnc.cdc.gov/EID/>

article/25/4/18-0944-App1.pdf). The main phylogenetic groups were B2 ( $n = 155$ , 59.6%), B1 ( $n = 26$ , 10%), and D ( $n = 25$ , 9.6%). The most commonly identified lineages were STc73 (subgroup II,  $n = 40$ , 25.8% of B2 isolates), STc131 (subgroup I,  $n = 24$ , including 18 ST131), STc69 (clonal group A [29],  $n = 20$ ), STc141 (subgroup IV,  $n = 20$ ), and STc127 (subgroup III,  $n = 16$ ). STc95 (subgroup IX) encompassed 14 strains (9% of B2 isolates). Community and nosocomial isolates did not differ in terms of phylogenetic group, except for C phylogroup isolates, which had a community predisposition (14.6% community vs. 4.5% nosocomial;  $p = 0.01$ ).

We identified the O-type of 163 strains. We identified B2 phylogroup strains at the clonal level as having a combination of subgroup and O-type, as previously described (27) (Table 1). Among B2 strains, clones II-O6a were predominant, followed by IV-O2b, I-O25b (which belongs to ST131), III-O6a (which belongs to the highly virulent archetypal strain 536 [30]), and VI-O4.

Resistance and virulence traits of the 260 strains are detailed in Table 2 and Appendix Table 2. B2 phylogroup strains carried more virulence factor genes (virulence score 7 [5–7]) than non-B2 phylogroup strains (3 [2–4];  $p < 0.0001$ ). However, *traT* genes were significantly more present in non-B2 (78.1%) than B2 phylogroup (45.2%) isolates ( $p < 0.0001$ ), as were *aer* genes (non-B2 63.8% and B2 41.9%;  $p = 0.0006$ ). In nearly three quarters of strains, mainly B2 strains, we found *iroN* (70%) and *fyuA* (78.1%). Community and nosocomial isolates did not differ in terms of virulence and resistance scores. A total of 22 (8.5%) isolates were producers of extended-spectrum  $\beta$ -lactamases, including 13 CTX-M-1 group, 6 CTX-M-9 group, and 3 TEM. One isolate produced an OXA-48 carbapenemase, 28 (10.8%) isolates were resistant to cefotaxime, and 48 (18.5%) strains were resistant to piperacillin-tazobactam. B2 phylogroup strains were more sensitive to antimicrobials (resistance score 1.5 [0–4]) than were non-B2 phylogroup strains (resistance score 4.5 [2.5–7];  $p < 0.0001$ ).

### General Comparisons of the COLOCOLI, COLIBAFI, and COLIVILLE Collections

When comparing the pneumonia *E. coli* isolates with those from the 2 other collections, we found strong differences (Table 5; Figure). The B2 phylogroup was overrepresented in pneumonia strains (59.6%) compared with commensal strains (32.1%;  $p < 0.0001$ ) but not with bacteremia strains (52%;  $p = 0.06$ ). Among B2 phylogroup pneumonia strains, subgroup III (STc127) was significantly overrepresented (10.3%) compared with the 2 other collections (bacteremia 4.1%,  $p = 0.03$ ; commensal 2.2%,  $p = 0.02$ ). The proportion of subgroup IV (STc141) isolates was significantly higher among pneumonia strains (12.9%) than bacteremia strains (2.6%;  $p = 0.0002$ ), whereas subgroup IX (STc95) isolates

(9%) were underrepresented compared with the bacteremia B2 phylogroup strains (29.4%;  $p < 0.0001$ ). Within the D phylogenetic group, the proportions of clonal group A pneumonia isolates (80%) were greater than those of commensal isolates (40%;  $p = 0.001$ ).

Virulence scores of pneumonia isolates (5 [3–7]) were significantly higher than those of commensal isolates (3 [1–5];  $p < 0.0001$ ) but not different from those of the bacteremia isolates (4 [2–7];  $p = 0.3$ ). However, some adhesins (*sfa/foc*, *papGIII*), some toxins (*hlyC*, *cnfI*), and *iroN* were significantly overrepresented in pneumonia *E. coli* strains compared with strains in the 2 other collections.

Pneumonia *E. coli* isolates were more resistant than commensal isolates to all tested antimicrobial drugs except amikacin. Pneumonia isolates and bacteremia isolates did not differ in terms of antimicrobial drug susceptibility, except for resistance to cefotaxime (pneumonia isolate resistance 10.8%) and ceftazidime (pneumonia isolate resistance 11.5%) compared with bacteremia isolates (5.1%;  $p = 0.009$  for cefotaxime,  $p = 0.004$  for ceftazidime). Of note, when the 260 pneumonia isolates were compared with the 220 bacteremia strains of urinary tract origin, they were still distinguishable in terms of phylogroups/subgroups and virulence factor content (Appendix).

## Discussion

This prospective nationwide study provides data on *E. coli* pneumonia isolates in critically ill patients. With regard to the characteristics of *E. coli* pneumonia isolates, we found the following: 1) a preponderance of phylogenetic group B2 (59.6%); 2) a predominant STc73 (subgroup II) lineage and threatening emergence of ST131 (within subgroup I), STc69 (clonal group A), and STc127 (subgroup III), along with STc141 (subgroup IV); 3) a much lower proportion of STc95 (subgroup IX) in B2 pneumonia than in bacteremia isolates; 4) a specific virulence factor gene content in pneumonia versus bacteremia strains. Taken together, these epidemiologic, phylogenetic, genotypic, and experimental data argue for inclusion of *E. coli* pneumonia isolates in the extraintestinal pathogenic *E. coli* (ExPEC) pathovar but with distinguishable lung-specific traits.

In 2010, Croxen and Finlay reviewed the molecular mechanisms of *E. coli* pathogenicity (31). Among ExPEC, numerous pathovars were listed, including uropathogenic and neonatal meningitis pathogenic *E. coli*, but none concerned the lungs. Pneumonia was not even cited as a possible disease caused by *E. coli*.

The situation is now clearly different. In 2012, Hamet et al. reported that *Enterobacteriaceae* accounted for a quarter of the 323 episodes of ventilator-assisted pneumonia occurring in their ICU (6). Our group showed that over a 5-year analysis of ventilator-assisted pneumonia episodes, finding *Enterobacteriaceae* as the responsible

**Table 4.** Phylogenetic groups/subgroups of *Escherichia coli* isolated from 260 pneumonia patients requiring mechanical ventilation, France, 2012–2014\*

Phylogroup	No. (%)
A	22 (8.5)
B1	26 (10)
CC87†	11 (42.3)
Non-CC87	15 (57.7)
B2	155 (59.6)
I ST131†	18 (11.6)
I non-ST131	6 (3.9)
II	40 (25.8)
III	16 (10.3)
IV	20 (12.9)
V	1 (0.6)
VI	14 (9)
VII	3 (1.9)
IX	14 (9)
Unassigned	23 (14.8)
C	20 (7.7)
D	25 (9.6)
CGA†	20 (80)
Non-CGA	5 (20)
F	11 (4.2)
Clade I	1 (0.4)

\*Nosocomial isolates encompass ventilator-associated pneumonia and hospital-acquired pneumonia isolates. CC87, clonal complex 87 (sequence type complex [STc] 155) (19); CGA, clonal group A (STc69) (21); ST131, sequence type 131.  
The correspondence with the Achtman MLST schema is as follows: subgroup I, STc131; subgroup II, STc73; subgroup III, STc127; subgroup IV, STc141; subgroup V, STc144; subgroup VI, STc12; subgroup VII, STc14; subgroup IX, STc95. No isolate belonged to subgroup VIII (STc452), X (STc372), or E phylogroup (22).  
†Proportions of subgroups are reported as fractions of the respective phylogroups.

pathogen increased significantly (5). In an international multicenter study, Kollef et al. also confirmed that *Enterobacteriaceae* were the leading pathogens of ventilator-assisted pneumonia in the ICU (4). Among them, *E. coli* is a major threat, recently highlighted by the World Health Organization, because of its ever-increasing resistance to antimicrobial drugs (7).

ExPEC are characterized by pathogenic virulence factor genes coding for various combinations of adhesins, toxins, iron-acquisition systems, capsule production, and toxins that enable them to cause disease once outside the host gut reservoir (32). ExPEC virulence factors are encoded on the bacterial chromosome, where they are usually located within pathogenicity-associated islands (PAIs) or plasmids. Most ExPEC isolates belong to the B2 phylogroup and, to a lesser extent, the D phylogroup. More in-depth analysis of ExPEC strains has enabled characterization of particular STs of ExPEC isolates including ST131, ST73, and ST127 (33). Our most striking finding was the specificity of pneumonia *E. coli* strains, compared with bacteremia ones, within the ExPEC family (Table 5). First, although B2 phylogroup strains are preponderant in ExPEC (15,34), we found a trend toward an even greater proportion of B2 isolates among pneumonia isolates (59.6%) than among bacteremia isolates, whatever the origin (52%;  $p = 0.06$ ).



**Table 5.** Proportion of phylogenetic groups, B2 subgroups, D CGA, and B1 CC87 among pneumonia, bacteremia, or commensal isolates\*

Phylogenetic characteristics	Pneumonia isolates	Bacteremia isolates	Commensal isolates
A	–	+	++
B1	+	–	+
CC87†	+++	+++	+
B2	++++	++++	+++
I	+	+	+
II	++	++	++
III	+	–	–
IV	+	–	+
IX	–	++	+
C	–	–	–
D	–	+	+
CGA*	++++	++++	+++
E	–	–	–
F	–	–	–

\*CGA, clonal group A (sequence type complex [STc] 69) (21); CC87, clonal complex 87 (STc155) (19); –, <10%; +, 10%–20%; ++, 20%–30%; +++ 30–50%; +++++, >50% of isolates. Correspondence with the Achtman multilocus sequence typing schema is subgroup I = STc131; subgroup II = STc73; subgroup III = STc127; subgroup IV = STc141; and subgroup IX = STc95 (22).

†Proportions of subgroups are calculated within each respective phylogroup.

(Table 3; Figure). This finding is in the range of what is observed in urosepsis isolates (62%) (11) but a little less than in neonatal meningitis strains (68%) (13). Then, among B2 phylogroup isolates (Table 4), if the predominance of subgroup II (STc73) was expected, we found high proportions of specific phylogenetic group B2 clones among other lineages, which could be worrisome (Table 1). The ST131 O25b:H4 clone represented 9.7% of the B2 phylogroup isolates, 53.3% of them producing an extended-spectrum  $\beta$ -lactamase. Subgroup IV (STc141) was significantly more present among pneumonia strains than among bacteremia strains. Challenging the hypothesis of a commensal character, with a low level of human invasiveness (27), this finding indicates that subgroup IV isolates may have a high affinity for the respiratory tract. Last, we must highlight the greater proportion of subgroup III among pneumonia isolates (namely STc127) compared with bacteremia and commensal isolates, in agreement with previous findings from our group (15). Contrary to isolates from the other 2 collections, pneumonia isolates were composed of fewer IX subgroup strains (STc95). Whereas subgroup IX is usually well represented among commensal and other pathogenic *E. coli* strains (26,27,35), these data suggest that the respiratory tract is less suitable than other tissues for subgroup IX implantation, a finding in agreement with our previous report in which subgroup IX was not represented (15).

Among D phylogroup strains, the higher prevalence of clonal group A (STc69) in pneumonia isolates than in bacteremia and commensal isolates was unexpected. Among 571 D phylogroup *E. coli* responsible for extraintestinal infection, Johnson et al. reported only 144 clonal group A *E. coli* (25.2%) (29). The multidrug-resistant nature of these pathogens is of increasing concern (29,36).

Regarding virulence factor gene content, the literature suggests that PAIs involved in ExPEC causing pneumonia differ from those involved in urinary tract and blood-

stream infections (37,38). Using PAI deletion mutants in a rat model of pneumonia, Phillips-Houlbracq et al. related pneumonia pathogenicity to the presence of PAIs I and III (37). In our study (Figure 1), pneumonia isolates differed from bacteremia isolates because they significantly more often carried *sfa/foc*, *iroN* (both belonging to PAI III), *papGIII* and *cnfI* (belonging to PAI II), and *hlyC* (belonging to PAI I and II). The role of  $\alpha$ -hemolysin in experimentally induced pneumonia in rats has been reported (15,39). Of note, the virulence factor content of the pneumonia strains still differs when we consider only the urosepsis isolates (Appendix). Although additional studies are required to confirm, these findings do suggest a coherent molecular trait for the isolates' lung specificity.

Consistent with data in the literature (15), we found that pneumonia B2 isolates were less resistant to antimicrobial drugs (B2 resistance score 1.5 [0–4] vs. non-B2 resistance score 4.5 [2.5–7];  $p < 0.0001$ ) but carried more virulence factor genes (B2 virulence score 7 [5–7] vs. non-B2 virulence score 3 [2–4];  $p < 0.0001$ ) (Table 2). However, contrary to an old belief, this trade-off does not mean that antimicrobial drug resistance decreases with increasing virulence (40). Indeed, virulence and antimicrobial-drug resistance were both higher in pneumonia isolates than in commensal isolates and the following were more highly represented: *sfa/foc*, *papC*, *papGIII*, *fyuA*, *iroN*, *hlyC*, and *cnfI*.

Our study should be interpreted within the context of its limitations. First, although our collection of *E. coli* pneumonia isolates is large, results regarding some subgroup analyses will require confirmation because of their sample size. Our choice of PCR rather than whole-genome characterization was governed by our wish to compare the 2 other collections with the same type of data. Despite these limitations, our analysis based on 14 centers representing France on a population and geographic level, its prospective design, and the comparison of our large number of isolates

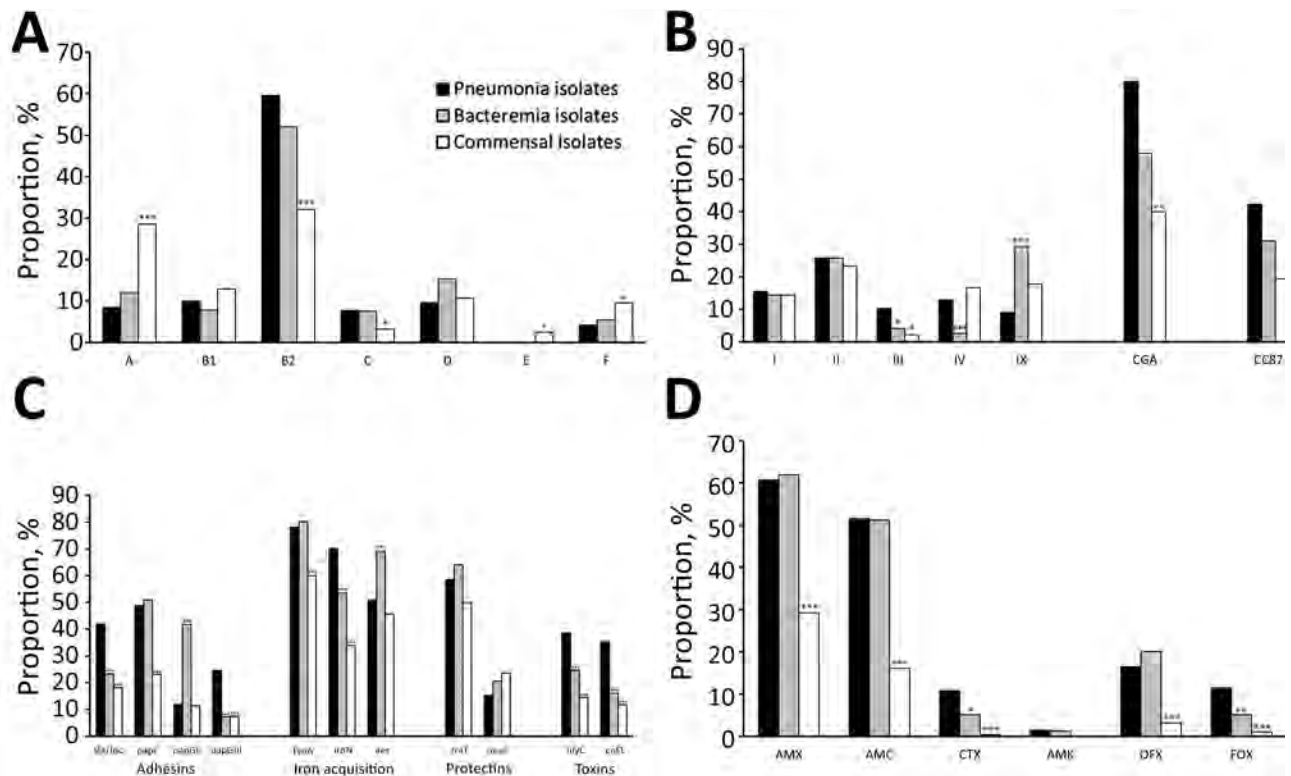


**Figure.** Comparison of *Escherichia coli* isolates among pneumonia patients with extraintestinal infections, France, 2012–2014, with commensal *E. coli* (COLIVILLE collection) and *E. coli* bacteremia isolates (COLIBAFI collection). A) Proportions of *E. coli* phylogenetic groups and subgroups; B) B2 subgroups, D CGA, and B1 CC87; C) virulence factors; and D) antimicrobial drug resistance. Roman numerals correspond to the B2 subgroup. Correspondence with the Achtman multilocus sequence typing schema is as follows: subgroup I, STc131; subgroup II, STc73; subgroup III, STc127; subgroup IV, STc141; subgroup VI, STc12; subgroup VII, STc14; subgroup IX, STc95 (22). Proportions of subgroups are reported as fractions of the respective phylogroups. Asterisks indicate a significant difference between respiratory isolates and strains responsible for bacteremia (COLIBAFI collection) or commensal strains (COLIVILLE collection): \* $p < 0.05$ ; \*\* $p < 0.005$ ; \*\*\* $p < 0.0005$ . AMC, amoxicillin/clavulanic acid; AMK, amikacin; AMX, amoxicillin; CTX, cefotaxime; FOX, cefoxitin; OFX, ofloxacin; STc, sequence type complex.

with those from recently published collections enable us to draw valid conclusions. We did not assess the functionality and expression of the encoded virulence factors in these isolates. Our team has consistently demonstrated these features in several murine models of infection (including pneumonia) and observed a strong correlation between the presence of these genes and death (15,34,37).

Our data raise the question of why certain clonal lineages were overrepresented in patients with respiratory tract infection. Patients acquire *E. coli* infection from their own digestive tract (41). This event implies an upward retrograde motion of the bacterial cells to reach the oropharynx and the lung parenchyma and suggests particular metabolic-adaptation and response-to-stress characteristics (e.g., to overcome the acidity of the stomach). We have previously shown that some *E. coli* strains are capable of high growth capacities in relation to metabolic pathways (42) while others are highly resistant to stress (43). For both studies, however, no link to specific clones could be

established. The specific organ tropism therefore more probably results from a combination of genetic background and virulence factors.

In summary, we identified emerging pneumonia-causing pathogenic *E. coli* whose main characteristics define them as ExPEC. Their specificities include a very strong proportion of B2 phylogroup isolates; a high proportion of subgroups II (STc73), I (STc131), IV (STc141), and III (STc127); and consequent proportions of clonal group A (STc69) isolates within the D phylogroup. Virulence factor gene content of pneumonia isolates also appeared to be singular compared with that of bacteremia isolates, among them urosepsis isolates. These epidemiologic data underline the specificity of pneumonia *E. coli* populations and may help with the design of more targeted therapies.

#### Acknowledgments

We are indebted to the physicians (microbiologists and intensivists) who took part in the COLOCOLI Study. We are

also grateful to the patients and their families, and we gratefully acknowledge Dominique Poignard and Marie-Claire Hipeaux for technical assistance and all the nurses and assistant nurses of the ICU for their help in obtaining the microbiological samples.

Collaborators for the COLOCOLI group: Catherine Branger, Luce Landraud, Alexandre Bleibtreu, Françoise Jauréguy (Infection, Antimicrobiens, Modélisation, Évolution, Paris, France); Pierre Asfar (Centre Hospitalier Universitaire, Angers, France); Didier Dreyfuss, Guilène Barnaud, Fatma Magdoud (Hôpital Louis Mourier, AP-HP, Colombes, France); Michel Wolff, Jean-François Timsit (Hôpital Bichat, AP-HP, Paris, France); Stéphanie Martin (Centre Hospitalier Départemental Vendée, La Roche-sur-Yon, France); Pierre-Emmanuel Charles (Centre Hospitalier Universitaire Bocage Central, Dijon, France); Alexandre Boyer (Centre Hospitalier Universitaire Pellegrin, Bordeaux, France); Emmanuelle Jaillette, Saad Nseir (Centre Hospitalier Régional Universitaire, Lille, France); Raymond Ruimy, Pierre-Eric Danin, Jean Dellamonica (Centre Hospitalier Universitaire, Nice, France); Julie Cremniter, Jean-Pierre Frat (Centre Hospitalier Universitaire, Poitiers, France); Christophe Clec'h (Hôpital Avicenne, AP-HP, Bobigny, France), Dominique Decré, Eric Maury (Hôpital Saint-Antoine, AP-HP, Paris, France).

This work was supported by a grant from the Fonds de Dotation Recherche en Santé Respiratoire/Fondation du Souffle to (B.L.C.). This work was partly supported by a grant from the Fondation pour la Recherche Médicale (to E.D., Équipe FRM 2016, grant no. DEQ20161136698).

## About the Author

Dr. La Combe is an intensive care physician who works at the Infection, Antimicrobials, Modelling, Evolution laboratory of the French Institute for Medical Research in Paris. Her work focuses on the virulence and antimicrobial resistance of respiratory *E. coli* isolates and the pharmacodynamics and genetics of chlorhexidine resistance of oropharyngeal isolates in patients receiving mechanical ventilation.

## References

- Melsen WG, Rovers MM, Groenwold RHH, Bergmans DCJJ, Camus C, Bauer TT, et al. Attributable mortality of ventilator-associated pneumonia: a meta-analysis of individual patient data from randomised prevention studies. *Lancet Infect Dis*. 2013;13:665–71. [http://dx.doi.org/10.1016/S1473-3099\(13\)70081-1](http://dx.doi.org/10.1016/S1473-3099(13)70081-1)
- Chastre J, Fagon J-Y. Ventilator-associated pneumonia. *Am J Respir Crit Care Med*. 2002;165:867–903. <http://dx.doi.org/10.1164/ajrcm.165.7.2105078>
- Russo TA, Johnson JR. Medical and economic impact of extraintestinal infections due to *Escherichia coli*: focus on an increasingly important endemic problem. *Microbes Infect*. 2003;5:449–56. [http://dx.doi.org/10.1016/S1286-4579\(03\)00049-2](http://dx.doi.org/10.1016/S1286-4579(03)00049-2)
- Kollef MH, Ricard J-D, Roux D, Francois B, Ischaki E, Rozgonyi Z, et al. A randomized trial of the amikacin fosfomicin inhalation system for the adjunctive therapy of gram-negative ventilator-associated pneumonia: IASIS Trial. *Chest*. 2017;151:1239–46. <http://dx.doi.org/10.1016/j.chest.2016.11.026>
- Fihman V, Messika J, Hajage D, Tourmier V, Gaudry S, Magdoud F, et al. Five-year trends for ventilator-associated pneumonia: correlation between microbiological findings and antimicrobial drug consumption. *Int J Antimicrob Agents*. 2015;46:518–25. <http://dx.doi.org/10.1016/j.ijantimicag.2015.07.010>
- Hamet M, Pavon A, Dalle F, Pechinot A, Prin S, Quenot J-P, et al. *Candida* spp. airway colonization could promote antibiotic-resistant bacteria selection in patients with suspected ventilator-associated pneumonia. *Intensive Care Med*. 2012;38:1272–9. <http://dx.doi.org/10.1007/s00134-012-2584-2>
- World Health Organization. Global priority list of antibiotic-resistant bacteria to guide research, discovery, and development of new antibiotics [cited 2017 Sep 29]. <http://www.who.int/medicines/publications/global-priority-list-antibiotic-resistant-bacteria/en/>
- Johnson JR, Russo TA. Extraintestinal pathogenic *Escherichia coli*: “the other bad *E. coli*.” *J Lab Clin Med*. 2002;139:155–62. <http://dx.doi.org/10.1067/mlc.2002.121550>
- Johnson JR, Kuskowski MA, Gajewski A, Soto S, Horcajada JP, Jimenez de Anta MT, et al. Extended virulence genotypes and phylogenetic background of *Escherichia coli* isolates from patients with cystitis, pyelonephritis, or prostatitis. *J Infect Dis*. 2005;191:46–50. <http://dx.doi.org/10.1086/426450>
- Johnson JR, Kuskowski MA, O'Bryan TT, Maslow JN. Epidemiological correlates of virulence genotype and phylogenetic background among *Escherichia coli* blood isolates from adults with diverse-source bacteremia. *J Infect Dis*. 2002;185:1439–47. <http://dx.doi.org/10.1086/340506>
- Lefort A, Panhard X, Clermont O, Woerther P-L, Branger C, Mentré F, et al.; COLIBAFI Group. Host factors and portal of entry outweigh bacterial determinants to predict the severity of *Escherichia coli* bacteremia. *J Clin Microbiol*. 2011;49:777–83. <http://dx.doi.org/10.1128/JCM.01902-10>
- Bidet P, Mahjoub-Messai F, Blanco J, Dehem M, Aujard Y, et al. Combined multilocus sequence typing and O serogrouping distinguishes *Escherichia coli* subtypes associated with infant urosepsis and/or meningitis. *J Infect Dis*. 2007;196:297–303. <http://dx.doi.org/10.1086/518897>
- Bingen E, Picard B, Brahim N, Mathy S, Desjardins P, Elion J, et al. Phylogenetic analysis of *Escherichia coli* strains causing neonatal meningitis suggests horizontal gene transfer from a predominant pool of highly virulent B2 group strains. *J Infect Dis*. 1998;177:642–50. <http://dx.doi.org/10.1086/514217>
- Bert F, Johnson JR, Ouattara B, Leflon-Guibout V, Johnston B, Marcon E, et al. Genetic diversity and virulence profiles of *Escherichia coli* isolates causing spontaneous bacterial peritonitis and bacteremia in patients with cirrhosis. *J Clin Microbiol*. 2010;48:2709–14. <http://dx.doi.org/10.1128/JCM.00516-10>
- Messika J, Magdoud F, Clermont O, Margetis D, Gaudry S, Roux D, et al. Pathophysiology of *Escherichia coli* ventilator-associated pneumonia: implication of highly virulent extraintestinal pathogenic strains. *Intensive Care Med*. 2012;38:2007–16. <http://dx.doi.org/10.1007/s00134-012-2699-5>
- Blanco J, Mora A, Mamani R, López C, Blanco M, Dahbi G, et al. National survey of *Escherichia coli* causing extraintestinal infections reveals the spread of drug-resistant clonal groups O25b:H4-B2-ST131, O15:H1-D-ST393 and CGA-D-ST69 with high virulence gene content in Spain. *J Antimicrob Chemother*. 2011;66:2011–21. <http://dx.doi.org/10.1093/jac/dkr235>
- American Thoracic Society, Infectious Diseases Society of America. Guidelines for the management of adults with



- hospital-acquired, ventilator-associated, and healthcare-associated pneumonia. *Am J Respir Crit Care Med.* 2005;171:388–416. <http://dx.doi.org/10.1164/rccm.200405-644ST>
18. Clermont O, Christenson JK, Denamur E, Gordon DM. The Clermont *Escherichia coli* phylo-typing method revisited: improvement of specificity and detection of new phylo-groups. *Environ Microbiol Rep.* 2013;5:58–65. <http://dx.doi.org/10.1111/1758-2229.12019>
  19. Skurnik D, Clermont O, Guillard T, Launay A, Danilchanka O, Pons S, et al. Emergence of antimicrobial-resistant *Escherichia coli* of animal origin spreading in humans. *Mol Biol Evol.* 2016;33:898–914. <http://dx.doi.org/10.1093/molbev/msv280>
  20. Clermont O, Christenson JK, Daubié A-S, Gordon DM, Denamur E. Development of an allele-specific PCR for *Escherichia coli* B2 sub-typing, a rapid and easy to perform substitute of multilocus sequence typing. *J Microbiol Methods.* 2014;101:24–7. <http://dx.doi.org/10.1016/j.mimet.2014.03.008>
  21. Johnson JR, Owens K, Manges AR, Riley LW. Rapid and specific detection of *Escherichia coli* clonal group A by gene-specific PCR. *J Clin Microbiol.* 2004;42:2618–22. <http://dx.doi.org/10.1128/JCM.42.6.2618-2622.2004>
  22. Clermont O, Gordon D, Denamur E. Guide to the various phylogenetic classification schemes for *Escherichia coli* and the correspondence among schemes. *Microbiology.* 2015;161:980–8. <http://dx.doi.org/10.1099/mic.0.000063>
  23. Clermont O, Johnson JR, Menard M, Denamur E. Determination of *Escherichia coli* O types by allele-specific polymerase chain reaction: application to the O types involved in human septicemia. *Diagn Microbiol Infect Dis.* 2007;57:129–36. <http://dx.doi.org/10.1016/j.diagmicrobio.2006.08.007>
  24. Eckert C, Gautier V, Saladin-Allard M, Hidri N, Verdet C, Ould-Hocine Z, et al. Dissemination of CTX-M-type beta-lactamases among clinical isolates of *Enterobacteriaceae* in Paris, France. *Antimicrob Agents Chemother.* 2004;48:1249–55. <http://dx.doi.org/10.1128/AAC.48.4.1249-1255.2004>
  25. Rasheed JK, Jay C, Metchock B, Berkowitz F, Weigel L, Crellin J, et al. Evolution of extended-spectrum beta-lactam resistance (SHV-8) in a strain of *Escherichia coli* during multiple episodes of bacteremia. *Antimicrob Agents Chemother.* 1997;41:647–53. <http://dx.doi.org/10.1128/AAC.41.3.647>
  26. Massot M, Daubié A-S, Clermont O, Jauréguy F, Couffignal C, Dahbi G, et al.; The COLIVILLE Group. Phylogenetic, virulence and antibiotic resistance characteristics of commensal strain populations of *Escherichia coli* from community subjects in the Paris area in 2010 and evolution over 30 years. *Microbiology.* 2016;162:642–50. <http://dx.doi.org/10.1099/mic.0.000242>
  27. Clermont O, Couffignal C, Blanco J, Mentré F, Picard B, Denamur E; COLIVILLE and COLIBAFI groups. Two levels of specialization in bacteraemic *Escherichia coli* strains revealed by their comparison with commensal strains. *Epidemiol Infect.* 2017;145:872–82. <http://dx.doi.org/10.1017/S0950268816003010>
  28. Bender R, Lange S. Adjusting for multiple testing—when and how? *J Clin Epidemiol.* 2001;54:343–9. [http://dx.doi.org/10.1016/S0895-4356\(00\)00314-0](http://dx.doi.org/10.1016/S0895-4356(00)00314-0)
  29. Johnson JR, Menard ME, Lauderdale T-L, Kosmidis C, Gordon D, Collignon P, et al.; Trans-Global Initiative for Antimicrobial Resistance Analysis Investigators. Global distribution and epidemiologic associations of *Escherichia coli* clonal group A, 1998–2007. *Emerg Infect Dis.* 2011;17:2001–9. <http://dx.doi.org/10.3201/eid1711.110488>
  30. Brzuszkiewicz E, Brüggemann H, Liesegang H, Emmerth M, Olschläger T, Nagy G, et al. How to become a uropathogen: comparative genomic analysis of extraintestinal pathogenic *Escherichia coli* strains. *Proc Natl Acad Sci U S A.* 2006;103:12879–84. <http://dx.doi.org/10.1073/pnas.0603038103>
  31. Croxen MA, Finlay BB. Molecular mechanisms of *Escherichia coli* pathogenicity. *Nat Rev Microbiol.* 2010;8:26–38. <http://dx.doi.org/10.1038/nrmicro2265>
  32. Russo TA, Johnson JR. Proposal for a new inclusive designation for extraintestinal pathogenic isolates of *Escherichia coli*: ExPEC. *J Infect Dis.* 2000;181:1753–4. <http://dx.doi.org/10.1086/315418>
  33. Dale AP, Woodford N. Extra-intestinal pathogenic *Escherichia coli* (ExPEC): disease, carriage and clones. *J Infect.* 2015;71:615–26. <http://dx.doi.org/10.1016/j.jinf.2015.09.009>
  34. Picard B, Garcia JS, Gouriou S, Duriez P, Brahimi N, Bingen E, et al. The link between phylogeny and virulence in *Escherichia coli* extraintestinal infection. *Infect Immun.* 1999;67:546–53.
  35. Ciesielczuk H, Jenkins C, Chattaway M, Doumith M, Hope R, Woodford N, et al. Trends in ExPEC serogroups in the UK and their significance. *Eur J Clin Microbiol Infect Dis.* 2016;35:1661–6. <http://dx.doi.org/10.1007/s10096-016-2707-8>
  36. Kallonen T, Brodrick HJ, Harris SR, Corander J, Brown NM, Martin V, et al. Systematic longitudinal survey of invasive *Escherichia coli* in England demonstrates a stable population structure only transiently disturbed by the emergence of ST131. *Genome Res.* 2017;27:1437–49. <http://dx.doi.org/10.1101/gr.216606.116>
  37. Phillips-Houlbracq M, Ricard J-D, Fourcier A, Yoder-Himes D, Gaudry S, Bex J, et al. Pathophysiology of *Escherichia coli* pneumonia: respective contribution of pathogenicity islands to virulence. *Int J Med Microbiol.* 2018;308:290–6. <http://dx.doi.org/10.1016/j.ijmm.2018.01.003>
  38. Turret J, Diard M, Garry L, Matic I, Denamur E. Effects of single and multiple pathogenicity island deletions on uropathogenic *Escherichia coli* strain 536 intrinsic extra-intestinal virulence. *Int J Med Microbiol.* 2010;300:435–9. <http://dx.doi.org/10.1016/j.ijmm.2010.04.013>
  39. Russo TA, Davidson BA, Genagon SA, Warholc NM, Macdonald U, Pawlicki PD, et al. *E. coli* virulence factor hemolysin induces neutrophil apoptosis and necrosis/lysis in vitro and necrosis/lysis and lung injury in a rat pneumonia model. *Am J Physiol Lung Cell Mol Physiol.* 2005;289:L207–16. <http://dx.doi.org/10.1152/ajplung.00482.2004>
  40. Roux D, Danilchanka O, Guillard T, Cattoir V, Aschard H, Fu Y, et al. Fitness cost of antibiotic susceptibility during bacterial infection. *Sci Transl Med.* 2015;7:297ra114. <http://dx.doi.org/10.1126/scitranslmed.aab1621>
  41. Garrouste-Orgeas M, Chevret S, Arlet G, Marie O, Rouveau M, Popoff N, et al. Oropharyngeal or gastric colonization and nosocomial pneumonia in adult intensive care unit patients. A prospective study based on genomic DNA analysis. *Am J Respir Crit Care Med.* 1997;156:1647–55. <http://dx.doi.org/10.1164/ajrccm.156.5.96-04076>
  42. Sabarly V, Bouvet O, Glodt J, Clermont O, Skurnik D, Diancourt L, et al. The decoupling between genetic structure and metabolic phenotypes in *Escherichia coli* leads to continuous phenotypic diversity. *J Evol Biol.* 2011;24:1559–71. <http://dx.doi.org/10.1111/j.1420-9101.2011.02287.x>
  43. Bleibtreu A, Gros P-A, Laouénan C, Clermont O, Le Nagard H, Picard B, et al. Fitness, stress resistance, and extraintestinal virulence in *Escherichia coli*. *Infect Immun.* 2013;81:2733–42. <http://dx.doi.org/10.1128/IAI.01329-12>

---

Address for correspondence: Jean-Damien Ricard, Service de Réanimation Médicale, Hôpital Louis Mourier, 92700 Colombes, France; email: jean-damien.ricard@aphp.fr

---

# Symptoms, Sites, and Significance of *Mycoplasma genitalium* in Men Who Have Sex with Men

Tim R.H. Read, Gerald L. Murray, Jennifer A. Danielewski, Christopher K. Fairley, Michelle Doyle, Karen Worthington, Jenny Su, Elisa Mokany, L.T. Tan, David Lee, Lenka A. Vodstrcil, Eric P.F. Chow, Suzanne M. Garland, Marcus Y. Chen, Catriona S. Bradshaw

During 2016–2017, we tested asymptomatic men who have sex with men (MSM) in Melbourne, Australia, for *Mycoplasma genitalium* and macrolide resistance mutations in urine and anorectal swab specimens by using PCR. We compared *M. genitalium* detection rates for those asymptomatic men to those for MSM with proctitis and nongonococcal urethritis (NGU) over the same period. Of 1,001 asymptomatic MSM, 95 had *M. genitalium*; 84.2% were macrolide resistant, and 17% were co-infected with *Neisseria gonorrhoeae* or *Chlamydia trachomatis*. Rectal positivity for *M. genitalium* was 7.0% and urine positivity was 2.7%. *M. genitalium* was not more commonly detected in the rectums of MSM (n = 355, 5.6%) with symptoms of proctitis over the same period but was more commonly detected in MSM (n = 1,019, 8.1%) with NGU. *M. genitalium* is common and predominantly macrolide-resistant in asymptomatic MSM. *M. genitalium* is not associated with proctitis in this population.

*Mycoplasma genitalium* causes nongonococcal urethritis (NGU) in men and is associated with pelvic inflammatory disease (PID), spontaneous abortion, and premature labor in women (1,2). Most guidelines recommend azithromycin as a first-line treatment;

however, macrolide resistance is widespread and increasing in many countries (3–5). In a recent study of *M. genitalium* urethritis in Melbourne, Victoria, Australia, 39% of cases were in men who have sex with men (MSM); macrolide resistance was detected almost twice as often in MSM as in women or heterosexual men (76% of MSM vs. 39% for women and heterosexual men combined;  $p = 0.005$ ) (6). We hypothesized that this difference may have arisen from frequent treatment of MSM for *Chlamydia trachomatis* and *Neisseria gonorrhoeae* infections, resulting in exposure of asymptomatic *M. genitalium* infections to azithromycin.

*M. genitalium* has been proposed as a cause of proctitis in MSM, but few studies have examined this association. Soni et al. found *M. genitalium* in 4.4% of rectal swabs from 438 MSM in England and found no association with rectal symptoms (7). Francis et al. found *M. genitalium* in 5.4% of rectal swabs from 500 MSM in the United States but found only a weak association with rectal symptoms (8). Bissessor et al. reported that bacterial load of rectal *M. genitalium* was higher in MSM with proctitis compared with those with asymptomatic infection, and detection was more common in HIV-positive than HIV-negative MSM (21% vs. 8%;  $p = 0.006$ ) (9). A meta-analysis in 2009 of 19 mostly cross-sectional or case–control studies found an association between *M. genitalium* and HIV infection, particularly in studies from sub-Saharan Africa (10). Subsequently, *M. genitalium* was detected twice as commonly in women who seroconverted to HIV in a prospective study in Africa (11), but no equivalent studies in MSM are available.

We aimed to determine the proportion of asymptomatic MSM who had *M. genitalium* in the urethra or rectum and the prevalence of macrolide resistance and risk factors for infection. We compared these data with the proportion of tests positive for *M. genitalium* in MSM with symptoms of proctitis and nongonococcal urethritis to further examine the contribution of *M. genitalium* to these syndromes in MSM.

---

Author affiliations: Melbourne Sexual Health Centre, Carlton, Victoria, Australia (T.R.H. Read, C.K. Fairley, M. Doyle, K. Worthington, D. Lee, L.A. Vodstrcil, E.P.F. Chow, M.Y. Chen, C.S. Bradshaw); Monash University, Melbourne, Victoria, Australia (T.R.H. Read, C.K. Fairley, L.A. Vodstrcil, E.P.F. Chow, M.Y. Chen, C.S. Bradshaw); Monash Biomedicine Discovery Institute, Melbourne (G.L. Murray); Murdoch Children's Research Institute, Parkville, Victoria, Australia (G.L. Murray, J.A. Danielewski, J. Su, S.M. Garland); Royal Women's Hospital, Melbourne (G.L. Murray, J.A. Danielewski, S.M. Garland); Royal Children's Hospital, Melbourne (G.L. Murray, S.M. Garland); SpeeDx Pty Ltd, Eveleigh, Sydney, New South Wales, Australia (E. Mokany, L.T. Tan); University of Melbourne, Melbourne (S.M. Garland)

DOI: <https://doi.org/10.3201/eid2504.181258>

## Methods

This cross-sectional study was undertaken during August 23, 2016–September 27, 2017, at Melbourne Sexual Health Centre (MSHC), the only public sexual health clinic in Melbourne, a city of 4.5 million. MSM  $\geq 18$  years of age who were asymptomatic at both triage and clinician consultations and reported receptive anal sex within the preceding year were eligible to participate. To minimize the impact of this study on clinical and laboratory services, recruitment was restricted to 8 of 49 clinical staff members, who offered the study to consecutive eligible clients. To determine how representative participants were of all asymptomatic MSM attending MSHC, we compared positivity for rectal *C. trachomatis* and *N. gonorrhoeae* in recruited and nonrecruited MSM. We asked participants to complete a questionnaire about recent sexual risk practices and to record any anogenital symptoms experienced in the preceding week. Participants provided urine and a rectal swab specimen (self- or clinician-collected) for *M. genitalium* screening.

We agitated the rectal swabs in 0.6 mL of phosphate-buffered saline to release cellular material, vortexed them briefly, and centrifuged them at low speed (8,000 rcf, 10 min) to remove PCR inhibitors. This step was required to reduce inhibition that differentially affected rectal samples; in early evaluations, the internal control failed in 9 (20.5%) of 44 uncentrifuged rectal samples but in none of 106 samples subjected to centrifugation. We transferred 0.2 mL of supernatant for nucleic acid isolation using the MagNA Pure 96 DNA and viral small volume kit on the automated MagNA Pure 96 system (Roche Diagnostics, <https://www.roche.com>). We prepared urine samples as described previously (12). We detected *M. genitalium* and macrolide resistance mutations in the 23S rRNA gene using the ResistancePlus MG test (Speedx Pty Ltd, Australia, <https://plexpcr.com>). Published evaluations of this assay report specificity for the detection of *M. genitalium* of 100% and sensitivities of 94.9%, 98.5%, and 98.9% (13–15).

Participants provided additional samples for *C. trachomatis* and *N. gonorrhoeae* screening of the throat, urethra, and rectum; we performed serologic testing for syphilis and HIV as indicated. We tested samples for *N. gonorrhoeae* and *C. trachomatis* by transcription-mediated amplification (Aptima Combo 2, Hologic, <https://www.hologic.com>).

MSM who were recalled for treatment of *M. genitalium* completed another questionnaire about antimicrobial drug use. We also collected throat swab specimens from men with rectal *M. genitalium* infection so we could perform pharyngeal *M. genitalium* testing. Resources were not available for testing all participants, particularly since published studies have rarely detected *M. genitalium* at this site. However, we hypothesized that *M. genitalium* may be more common in the pharynx in men with rectal *M. genitalium*. We agitated the throat swabs in 0.6 mL of phosphate-

buffered saline to release cellular material and performed nucleic acid isolation as described for the other samples.

## Statistical Methods

With a sample size of 1,000, a prevalence of *M. genitalium* of 10% would provide 80% power ( $\alpha = 0.05$ ) to detect an odds ratio of  $\geq 1.9$  for a characteristic present in 30% of those who did not have *M. genitalium*. We assessed associations between *M. genitalium*, *C. trachomatis*, and *N. gonorrhoeae* and risk factors, as well as mild urethral and anorectal symptoms reported in the questionnaire, using logistic regression.

All patients attending MSHC who have symptoms of nongonococcal urethritis or proctitis are tested for *M. genitalium*. During the 13-month study period, we also extracted test results from the clinic database for *M. genitalium*, *C. trachomatis*, and *N. gonorrhoeae* from MSM who received diagnoses of proctitis or urethritis (based on symptoms and signs, not microscopic criteria). Using univariate logistic regression, we then used corresponding test results from the asymptomatic study population as controls to assess any association between detection of each organism in the rectum and urine and diagnoses of proctitis and urethritis. For men with *M. genitalium* detected, we compared risk factors for macrolide resistance mutations using  $\chi^2$  or Fisher exact tests, where appropriate. We also recorded the proportions of *M. genitalium* patients co-infected with *C. trachomatis* or *N. gonorrhoeae* in the urethra and rectum. We compared associations between the detection of *M. genitalium* and that of *C. trachomatis* or *N. gonorrhoeae* in the rectum or urine in the asymptomatic study population using logistic regression, as we did with associations between *M. genitalium* and *C. trachomatis* in cases of nongonococcal urethritis diagnosed during the same period.

This project was approved by the ethics committee of the Alfred Hospital in Melbourne (project no. 278/16). All participants gave written informed consent.

## Results

During August 23, 2016–September 27, 2017, a total of 1,028 MSM were triaged as asymptomatic and invited to participate in the study. Of these, 17 declined: 3 declined the additional rectal swab specimen collection, and 14 declined for reasons unrelated to the study (distress or being unable to return to the clinic). Of the remaining 1,011, a total of 6 rectal swabs were unassessable (internal control failed), and 4 did not provide a urine sample. These 10 patients were excluded from the analysis, leaving 1,001 men with assessable samples from both collection sites.

Participants had a median age of 28.8 (interquartile range 24.3–34.1). A total of 107 (10.7%) were HIV positive, and 142 (15.9%) of the HIV-negative men were taking or commencing HIV preexposure prophylaxis medication (PrEP) (Table 1).



**Table 1.** Characteristics associated with urethral or rectal *Mycoplasma genitalium* in asymptomatic men who have sex with men, Australia\*

Characteristic	All patients	<i>M. genitalium</i> not detected	<i>M. genitalium</i> detected†	Crude OR (95% CI)	p value
Detected in urine, rectum, or both					
Prevalence	1,001	906 (90.5)	95 (9.5, 7.7–11.5)		
Median age, y (IQR)	28.8 (24.3–34.1)	28.9 (24.5–34.3)	27.4 (23.3–32.3)	0.96 (0.93–0.99)	0.006
HIV status‡					
Negative	894	804 (88.7)	90 (94.7)		
Positive	107	102 (11.3)	5 (5.3, 1.7–11.9)	0.44 (0.17–1.10)	0.08
On/commencing PrEP§					
No	752	678 (84.3)	74 (82.2)		
Yes	142	126 (15.7)	16 (17.8, 10.5–27.3)	1.16 (0.66–2.06)	0.60
Detected in urine only					
Urine prevalence		974 (97.3)	27 (2.7, 1.8–3.9)		
Insertive oral sex partners in previous 3 mo, n = 984¶					
<4	431	421 (44.0)	10 (37.0)		
≥4	553	536 (56.0)	17 (63.0)	1.34 (0.61–2.95)	0.47
Insertive anal sex partners in previous 3 months, n = 941#					
<2	428	418 (45.7)	10 (38.5)		
≥2	513	497 (54.3)	16 (61.5)	1.34 (0.60–3.0)	0.47
Condom use insertive anal sex in previous 3 mo					
Always	287	280 (38.7)	7 (29.2)		
Not always	460	443 (61.3)	17 (70.8)	1.53 (0.63–3.75)	0.35
Detected in rectum only					
Rectal prevalence		931 (93.0)	70 (7.0, 5.5–8.8)		
Receptive anal sex partners in previous 3 mo, n = 945#					
<2	367	349 (39.8)	18 (26.1)		
≥2	578	527 (60.2)	51 (73.9)	1.88 (1.08–3.3)	0.026
Condom use receptive anal sex in previous 3 mo					
Always	301	288 (37.1)	13 (20.0)		
Not always	540	488 (62.9)	52 (80.0)	2.36 (1.24–4.81)	0.006

\*Values are no. (%; 95% CI) except as indicated. This table should be viewed in conjunction with Table 2. IQR, interquartile range; OR, odds ratio; PrEP, preexposure prophylaxis.  
 †In 2 of 97 infected men, *M. genitalium* was detected in both the urine and the rectum.  
 ‡Includes 5 men with unknown HIV infection status. *M. genitalium* was detected in 4.7% of HIV-positive men vs. 10.1% of HIV-negative men (p = 0.08).  
 §HIV-negative men only.  
 ¶Median 4.  
 #Median 2.

Of the 1,001 men, 95 (9.5% [95% CI 7.7%–11.5%]) had *M. genitalium* detected at any site. Twenty-seven (2.7% [95% CI: 1.8%–3.9%]) had *M. genitalium* detected in the urine and 70 (7.0% [95% CI 5.5%–8.8%]) in the rectum; 2 men were infected at both sites. *C. trachomatis* was detected in 91 (9.6% [95% CI 7.8%–11.7%]) of 948 men tested at both sites, and *N. gonorrhoeae* was detected in 64 (6.7% [95% CI 5.2%–8.5%]) of 952 men tested at both sites (Table 2). For urine samples, *M. genitalium* was detected in 2.7%, *C. trachomatis* in 1.7%, and *N. gonorrhoeae* in 0.7%. For rectal samples, *M. genitalium* was detected in 7.0%, *C. trachomatis* in 8.5%, and *N. gonorrhoeae* in 6.2%.

During the study period, 4,228 MSM were triaged as asymptomatic at MSHC and not offered the study but were tested for rectal *C. trachomatis* and *N. gonorrhoeae* at least once. After excluding repeat tests, positivity for *C. trachomatis* did not differ between nonrecruited (7.4%) and recruited (8.5%) MSM (p = 0.25), but *N. gonorrhoeae* was lower in nonrecruited (4.2%) than in recruited (6.2%) MSM (p = 0.006).

Detection of *M. genitalium* was significantly associated with younger age (odds ratio [OR] 0.96 [95% CI

0.93–0.99]) per year of increasing age. Detection of *M. genitalium* in the rectum was significantly associated with receptive anal sex with ≥2 partners within the past 3 months (OR 1.88 [95% CI 1.08–3.3]) and inconsistent condom use for receptive anal sex (OR 2.36 [95%CI 1.24–4.81]). *M. genitalium* was less common in HIV-infected men than in uninfected men (4.7% vs 10.1%, p = 0.08) but was not associated with taking or commencing PrEP.

The study population of 1,001 asymptomatic MSM completed a questionnaire about the presence of any anogenital or urethral symptoms in the week before presentation (all participants were asymptomatic at recruitment). Of these, 8.7% reported any recent symptoms in the urethra (itch, discomfort, discharge, or dysuria) and 25.5% in the anorectum (itch, discomfort, pain, or bleeding). Recent symptoms were not associated with detection of *M. genitalium*, *C. trachomatis*, or *N. gonorrhoeae* at either site (p>0.5 for all symptoms, individually or combined; Table 3).

We compared rectal test positivity for *M. genitalium*, *C. trachomatis*, and *N. gonorrhoeae* in the asymptomatic study population (n = 1,001) with rectal positivity in MSM who had symptoms of proctitis (n = 355) during the study

**Table 2.** Detection of urethral or rectal *Chlamydia trachomatis* or *Neisseria gonorrhoeae* in asymptomatic men who have sex with men, Australia\*

Characteristic	All patients	<i>C. trachomatis</i> not detected	<i>C. trachomatis</i> detected†	<i>N. gonorrhoeae</i> not detected	<i>N. gonorrhoeae</i> detected‡
Detected in urine, rectum, or both					
STI prevalence	1,001	857 (90.4)	91 (9.6, 7.8–11.7)	888 (93.3)	64 (6.7, 5.2–8.5)
Median age, y (IQR)	28.8 (24.3–34.1)	28.8 (24.3–34.0)	27.6 (23.8–35.2)	28.8 (24.3–34.1)	27.2 (24.1–33.1)
HIV status					
Negative‡	894	782 (91.3)	72 (79.1)	801 (90.2)	55 (85.9)
Positive	107	75 (8.8)	19 (20.9)	87 (9.8)	9 (14.1)
On/commencing PrEP§					
No	752	666 (85.2)	57 (79.2)	683 (85.3)	39 (70.9)
Yes	142	116 (14.8)	15 (20.8)	118 (14.7)	16 (29.1)
Detected in urine only					
Urine prevalence	958	942 (98.3)	16 (1.7, 1.0–2.7)	951 (99.3)	7 (0.7, 0.3–1.4)
Insertive oral sex partners in previous 3 mo, n = 984¶					
<4	431	407 (44.0)	4 (25.0)	408 (43.6)	2 (28.6)
≥4	553	519 (56.0)	12 (75.0)	527 (56.4)	5 (71.4)
Insertive anal sex partners in previous 3 mo, n = 941#					
<2	428	406 (45.9)	4 (25.0)	409 (45.8)	0
≥2	513	479 (54.1)	12 (75.0)	485 (54.2)	7 (100)
Condom use insertive anal sex in previous 3 mo					
Always	287	273 (39.1)	5 (31.3)	273 (38.6)	4 (57.1)
Not always	460	425 (60.9)	11 (68.7)	434 (61.4)	3 (42.9)
Detected in rectum only					
Rectal prevalence	958–963	877 (91.5)	81 (8.5, 6.8–10.4)	903 (93.8)	60 (6.2, 4.8–7.9)
Receptive anal sex partners in previous 3 mo, n = 945#					
<2	367	336 (40.8)	20 (24.7)	342 (40.1)	15 (26.3)
≥2	578	488 (59.2)	61 (75.3)	511 (59.9)	42 (73.7)
Condom use receptive anal sex in previous 3 mo					
Always	301	270 (37.1)	18 (23.4)	277 (36.7)	11 (20.0)
Not always	540	458 (62.9)	59 (76.6)	477 (63.3)	44 (80.0)

\*Values are no. (%) or no. (%), 95% CI except as indicated. This table should be viewed in conjunction with Table 1. All 1,001 men had urine and rectal swabs tested for *Mycoplasma genitalium*, but only 948 were tested at both sites for *C. trachomatis* and 952 for *N. gonorrhoeae*. IQR, interquartile range; PrEP, preexposure prophylaxis.

†Denominators varied based on numbers tested; 958 men had urine tests for both infections; 948 men were screened at both sites and 958 men had rectal tests for *C. trachomatis*; and 952 men were screened at both sites and 963 men had rectal tests for *N. gonorrhoeae*.

‡Includes 5 men of unknown HIV infection status. *M. genitalium* was detected in 4.7% of HIV-positive men vs. 10.1% of HIV-negative men ( $p = 0.08$ ).

§HIV-negative men only.

¶Median 4.

#Median 2.

period (Table 4). *M. genitalium* detection was similar in MSM with proctitis and asymptomatic MSM (5.6% for proctitis vs. 7.0% for asymptomatic; OR 0.79 [95% CI 0.45–1.35];  $p = 0.38$ ). However, rectal detection of both *C. trachomatis* (21.3% vs. 8.5%, OR 2.93 [95% CI 2.05–4.18]) and *N. gonorrhoeae* (28.4% vs. 6.2%, OR 5.97 [95% CI 4.15–8.61]) was significantly more common in MSM with symptoms of proctitis than in asymptomatic MSM.

We compared the urine test positivity for *M. genitalium* and *C. trachomatis* in the asymptomatic study population ( $n = 1,001$ ) with the positivity in 1,019 MSM presenting with symptoms of NGU during the study period. Both *M. genitalium* (8.1% vs. 2.7%; OR 3.20 [95% CI 2.03–5.18]) and *C. trachomatis* (14.5% vs. 1.7%, OR 9.99 [95% CI 5.89–18.07]) were more commonly detected in MSM with symptoms of NGU than in asymptomatic MSM (Table 4).

We detected macrolide resistance mutations in 80 (84.2% [95% CI 75.3%–90.9%]) of 95 men who had positive *M. genitalium* tests (Table 5). We found no significant association between resistance and site of infection, and

although these mutations were more common in MSM reporting recent use of antimicrobial drugs, particularly azithromycin, this difference was not significant. Macrolide resistance mutations were found in all HIV-negative men taking or commencing PrEP ( $p = 0.06$ ).

Table 6 shows the proportion of asymptomatic MSM with *M. genitalium* who were co-infected with *C. trachomatis* and *N. gonorrhoeae*, by anatomic site. Rectal *C. trachomatis* and rectal *N. gonorrhoeae* were detected with similar frequency in MSM with rectal *M. genitalium* compared with men without rectal *M. genitalium* (*C. trachomatis*, 9.2% vs. 8.4%,  $p = 0.82$ ; *N. gonorrhoeae*, 6.1% vs. 6.2%;  $p = 0.98$ ). However, *C. trachomatis* and *N. gonorrhoeae* were detected significantly more often in the urine of asymptomatic men with *M. genitalium* compared with men without urethral *M. genitalium* (*C. trachomatis*, 7.4% vs. 1.5%,  $p = 0.03$ ; *N. gonorrhoeae*, 7.4% vs. 0.5%,  $p = 0.002$ ).

In contrast, in MSM with NGU, detection of *C. trachomatis* was uncommon in men with urethral *M. genitalium* (2.5%) compared with men without urethral *M. genitalium*

**Table 3.** Detection of *Mycoplasma genitalium*, *Chlamydia trachomatis*, and *Neisseria gonorrhoeae* in asymptomatic men who have sex with men according to reports of symptoms during the preceding week, Australia\*

Characteristic	Urethral symptoms†				Anorectal symptoms‡			
	None, no. (%)	Mild, no. (%)	Odds ratio (95% CI)	p value	None, no. (%)	Mild, no. (%)	Odds ratio (95% CI)	p value
<i>M. genitalium</i> , n = 1,001								
Not detected	889 (97.3)	85 (97.7)	0.84 (0.19–3.59)	0.81	692 (92.7)	239 (93.7)	0.86 (0.48–1.53)	0.60
Detected	25 (2.7)	2 (2.3)			54 (7.2)	16 (6.3)		
<i>C. trachomatis</i> , n = 958								
Not detected	861 (98.4)	81 (97.6)	1.52 (0.34–6.80)	0.59	657 (91.4)	220 (92.1)	0.92 (0.54–1.56)	0.75
Detected	14 (1.6)	2 (2.4)			62 (8.6)	19 (7.9)		
<i>Neisseria gonorrhoeae</i> , n = 958								
Not detected	868 (99.3)	83 (98.8)	1.74 (0.21–14.65)	0.61	675 (93.8)	228 (93.8)	0.99 (0.54–1.80)	0.97
Detected	6 (0.7)	1 (1.2)			45 (6.3)	15 (6.2)		

\*All participants were triaged as asymptomatic. This table reports answers to a questionnaire about “any symptoms (even if mild) in the past week.”

†Urethral symptoms were any of the following: dysuria, discharge, urethral itch, or discomfort. No individual symptom was significantly associated with any organism.

‡Anorectal symptoms were any of the following: anal pain, bleeding, itch, or discomfort. No individual symptom was significantly associated with any organism.

(15.5%; p = 0.001). Overall, of 89 MSM with *M. genitalium* infection detected at any site and tested for all 3 infections, 15 (16.9% [95% CI 9.7–26.3]) were co-infected with either *C. trachomatis* or *N. gonorrhoeae*. Of 143 MSM with either *C. trachomatis* or *N. gonorrhoeae*, 15 (10.5% [95% CI 5.9%–16.7%]) were co-infected with *M. genitalium*.

Throat swabs were collected from 54 (77.1%) of 70 MSM with rectal *M. genitalium*, all 60 MSM with rectal *N. gonorrhoeae*, and 37 (45.7%) of 81 MSM with rectal *C. trachomatis* (routine clinic testing for pharyngeal *C. trachomatis* commenced halfway through the study). Only 1 (1.9% [95% CI 0.05–9.9]) of 54 MSM with rectal *M. genitalium* had pharyngeal *M. genitalium*. In contrast, 8 (21.6% [95% CI 9.8–38.2]) of 37 MSM with rectal chlamydia had pharyngeal chlamydia, and 21 (35% [95% CI 23.1–48.4]) of 60 MSM with rectal gonorrhea had pharyngeal gonorrhea. Thus, dual pharyngeal and rectal infection with *M. genitalium* was significantly less common than was observed for *C. trachomatis* (p = 0.002) and *N. gonorrhoeae* (p < 0.001). Of

all men tested, 12 (3.0%) of 407 had pharyngeal chlamydia and 62 (6.4%) of 963 had pharyngeal gonorrhea.

### Discussion

Almost 1 in 10 asymptomatic MSM attending a sexual health center in Melbourne, Victoria, Australia, during a 13-month period were infected with *M. genitalium*, and 84% of these infections were macrolide resistant. *M. genitalium* was detected in 7% of asymptomatic MSM at the rectum, 2.7% at the urethra, and only 0.2% at both sites. Overall, *M. genitalium* was as common as chlamydia and more common than gonorrhea in asymptomatic MSM. The proportion of asymptomatic MSM with *M. genitalium* in the rectum was no different from that in MSM with symptoms of proctitis during the same period. Co-infection with *C. trachomatis* or *N. gonorrhoeae* was common and present in 17% of *M. genitalium* infections. Screening MSM for *C. trachomatis* and *N. gonorrhoeae* will identify these infections, but if they are treated, asymptomatic *M. genitalium* infections,

**Table 4.** Detection of *Mycoplasma genitalium*, *Chlamydia trachomatis*, and *Neisseria gonorrhoeae* in asymptomatic men who have sex with men compared with clinic attendees diagnosed with proctitis or NGU, Australia\*

Characteristic	Asymptomatic men tested at the rectum for STIs	Clinic attendees with symptoms of proctitis	Odds ratio (95% CI)	p value	Asymptomatic men tested at the urethra for STIs	Clinic attendees with symptoms of NGU	Odds ratio (95% CI)	p value
	<i>M. genitalium</i>							
Not detected	931 (93.0)	335 (94.4)	0.79 (0.45–1.35)	0.38	974 (97.3)	936 (91.9)	3.20 (2.03–5.18)	<0.0001
Detected	70 (7.0)	20 (5.6)			27 (2.7)	83 (8.1)		
<i>C. trachomatis</i>								
Not detected	877 (91.5)	277 (78.7)	2.93 (2.05–4.18)	<0.0001	942 (98.3)	878 (85.5)	9.99 (5.89–18.07)	<0.0001
Detected	81 (8.5)	75 (21.3)			16 (1.7)	149 (14.5)		
<i>N. gonorrhoeae</i>								
Not detected	903 (93.8)	252 (71.6)	5.97 (4.15–8.61)	<0.0001				
Detected	60 (6.2)	100 (28.4)						

\*Treated as NGU but not confirmed by urethral Gram stain. NGU, nongonococcal urethritis; STI, sexually transmitted infection.





data. MSHC has been using the same resistance assay for *M. genitalium* since June 20, 2016; by March 27, 2018, a total of 943 patients with NGU, cervicitis, PID, proctitis, or contacts of infection had *M. genitalium* detected. Macrolide resistance mutations were routinely detected in 265 (51.5% [95% CI 47.0–55.9]) of 515 heterosexual men and women compared with 349 (81.5% [95% CI 77.5–85.1]) of 428 MSM ( $p < 0.0001$ ). This difference between MSM and heterosexuals was also seen in a recent study in Spain, which reported macrolide resistance in 71% of MSM compared with 13% of heterosexuals ( $p < 0.001$ ); prior azithromycin exposure was a significant risk factor for resistance (20). Other recent studies in MSM report macrolide resistance in 74%–80% of *M. genitalium* infections (17,21). The high proportion of cases with resistance reduced our ability to identify risk factors; we detected resistance in 90% of infected men who recalled taking any antimicrobial drug within the previous 3 months and 100% of those who recalled taking azithromycin, but this difference was not significant.

Asymptomatic urethral co-infections with *C. trachomatis* and *N. gonorrhoeae* were significantly associated with detection of *M. genitalium*, but this association was not seen with rectal co-infections. Although the association between *M. genitalium* and urethral co-infections was significant, we found only 4 cases of co-infection. Specific host factors might possibly lead some men to tolerate, and therefore accumulate, urethral infections. The proportion of asymptomatic men with *M. genitalium* detected in their urine was higher than for *C. trachomatis* and for *N. gonorrhoeae*, again consistent with the hypothesis that *M. genitalium* might be less pathogenic than *C. trachomatis* or *N. gonorrhoeae*.

Pharyngeal *M. genitalium* is reported as rare (22–26), so to optimize detection, we limited pharyngeal testing to MSM with rectal infection because other pharyngeal sexually transmitted infections (STIs) are commonly concurrent with rectal infections. Of patients with rectal *M. genitalium*, only 1.9% had pharyngeal *M. genitalium*, which was much lower than for pharyngeal *C. trachomatis* (22%) and *N. gonorrhoeae* (35%) in MSM with these rectal infections. However, *C. trachomatis* and *N. gonorrhoeae* were detected by transcription mediated amplification. A recent Sydney study using the ResistancePlus PCR assay also found no pharyngeal *M. genitalium* infections in 508 MSM (rectal prevalence 8.9%), providing further evidence that *M. genitalium* is rarely detected in pharyngeal specimens (17).

Of concern, 17% of MSM with *M. genitalium* were co-infected with *C. trachomatis* or *N. gonorrhoeae*, predominantly reflecting rectal infections. The rectum appears likely to be a reservoir for asymptomatic *M. genitalium*, and treatment of concurrent STIs promotes macrolide

resistance, which is estimated to develop de novo in 12% of wild-type cases exposed to single-dose azithromycin (6). The high proportion of macrolide-resistant *M. genitalium* in MSM may be caused by the combination of a high background prevalence of asymptomatic rectal *M. genitalium*, a high frequency of concurrent chlamydia or gonorrhea, and the resulting use of azithromycin in this population.

This study has limitations, including reliance on recall of antimicrobial drug exposure, recruitment from a sexual health center where findings may not reflect MSM elsewhere, and restricted testing for pharyngeal *M. genitalium*. Centrifugation to remove PCR inhibitors was undertaken on rectal samples because of higher levels of inhibition, which could have reduced the sensitivity of rectal *M. genitalium* detection. Furthermore, we were unable to approach all MSM attending the clinic. The study population had a higher proportion with rectal gonorrhea, but not chlamydia, compared with those who were not recruited, possibly because our inclusion criteria required receptive anal sex in the previous year and the nonrecruited group included MSM attending an express service for lower-risk men. This difference suggests that the study population may have had a slightly elevated risk of infection, which should be considered alongside our findings. Diagnoses of nongonococcal urethritis and proctitis were predominantly clinical, based on symptoms and sexual risk, which is likely to lead to a lower prevalence of STIs in these groups compared with studies that required microscopic criteria for case definitions. However, clinical diagnoses are commonly used in primary care and are supported by the strong associations we observed between detection of *C. trachomatis* and *N. gonorrhoeae* and the symptom-based definitions of proctitis and urethritis.

We detected *M. genitalium* in 9.5% of asymptomatic MSM; although it was as common as chlamydia or gonorrhoea, 84% of these infections were macrolide resistant. The high proportion of MSM with macrolide-resistant *M. genitalium* might be considered a reason to screen for this infection but would not meet the criteria for screening established by Wilson and Jungner (27). For example, the natural history of *M. genitalium* infection, particularly in the rectum, is poorly understood. Testing is not widely available and the high prevalence of antimicrobial drug resistance also limits the availability of treatment. If we screened this population, 8% of MSM (84% of 9.5%) would require moxifloxacin or a similar agent. Moxifloxacin is expensive, difficult to obtain in many parts of the world, and associated with uncommon but concerning toxicities. Resistance to quinolone antimicrobial drugs is now detected in 16% of patients coming to MSHC (mixed heterosexual and MSM population) in ongoing unpublished work (G.L. Murray, unpub. data). Increasing the

use of moxifloxacin as a result of screening would be expected to generate more resistance.

Rectal *M. genitalium* infection may not warrant treatment. It was not associated with current anorectal symptoms in this study; most published literature suggests no association or only a weak association. No prospective studies have associated *M. genitalium* with increased risk for HIV infection in MSM, in contrast to women; such an association may become less critical when HIV PrEP and treatment are widely used. Therefore, screening asymptomatic MSM for *M. genitalium* would result in considerable expense and adverse events for uncertain benefit. Although *M. genitalium* has been identified in cases of proctitis, it is predominantly asymptomatic in the rectum, and there appears to be insufficient evidence to suggest that *M. genitalium* is a cause of proctitis.

### Acknowledgments

We thank Micken Grant, Colin Denver, the staff at MSHC, and the study participants for their important contributions to this study.

T.R.H.R. and E.P.F.C. are funded by Australian National Health and Medical Research Council early career fellowships (nos. 1091536 and 1091226).

### About the Author

Dr. Read was a sexual health physician at Melbourne Sexual Health Centre and a research fellow at Monash University, Melbourne, Victoria, Australia. He was elected to the Parliament of Victoria in 2018 and no longer works in medical research.

### References

1. Horner PJ, Martin DH. *Mycoplasma genitalium* infection in men. *J Infect Dis*. 2017;216(suppl2):S396–405. <http://dx.doi.org/10.1093/infdis/jix145>
2. Lis R, Rowhani-Rahbar A, Manhart LE. *Mycoplasma genitalium* infection and female reproductive tract disease: a meta-analysis. *Clin Infect Dis*. 2015;61:418–26. <http://dx.doi.org/10.1093/cid/civ312>
3. Jensen JS, Bradshaw C. Management of *Mycoplasma genitalium* infections—can we hit a moving target? *BMC Infect Dis*. 2015;15:343. <http://dx.doi.org/10.1186/s12879-015-1041-6>
4. Antibiotic Expert Groups, editor. Therapeutic guidelines: antibiotic. 15 ed. Melbourne: Therapeutic Guidelines Limited; 2014.
5. Workowski KA, Bolan GA; Centers for Disease Control and Prevention. Sexually transmitted diseases treatment guidelines, 2015. *MMWR Recomm Rep*. 2015;64(RR-03):1–137.
6. Read TRH, Fairley CK, Tabrizi S, Bissessor M, Vodstrcil L, Chow EPF, et al. Azithromycin 1.5g over 5 days compared to 1g single dose in urethral *Mycoplasma genitalium*: impact on treatment outcome and resistance. *Clin Infect Dis*. 2017;64:250–6. <http://dx.doi.org/10.1093/cid/ciw719>
7. Soni S, Alexander S, Verlander N, Saunders P, Richardson D, Fisher M, et al. The prevalence of urethral and rectal *Mycoplasma genitalium* and its associations in men who have sex with men attending a genitourinary medicine clinic. *Sex Transm Infect*. 2010;86:21–4. <http://dx.doi.org/10.1136/sti.2009.038190>
8. Francis SC, Kent CK, Klausner JD, Rauch L, Kohn R, Hardick A, et al. Prevalence of rectal *Trichomonas vaginalis* and *Mycoplasma genitalium* in male patients at the San Francisco STD clinic, 2005–2006. *Sex Transm Dis*. 2008;35:797–800. <http://dx.doi.org/10.1097/OLQ.0b013e318177ec39>
9. Bissessor M, Tabrizi SN, Bradshaw CS, Fairley CK, Hocking JS, Garland SM, et al. The contribution of *Mycoplasma genitalium* to the aetiology of sexually acquired infectious proctitis in men who have sex with men. *Clin Microbiol Infect*. 2016;22:260–5. <http://dx.doi.org/10.1016/j.cmi.2015.11.016>
10. Napierala Mavedzenge S, Weiss HA. Association of *Mycoplasma genitalium* *Mycoplasma genitalium* and HIV infection: a systematic review and meta-analysis. *AIDS*. 2009;23:611–20. <http://dx.doi.org/10.1097/QAD.0b013e328323da3e>
11. Napierala Mavedzenge S, Van Der Pol B, Weiss HA, Kwok C, Mambo F, Chipato T, et al. The association between *Mycoplasma genitalium* and HIV-1 acquisition in African women. *AIDS*. 2012;26:617–24. <http://dx.doi.org/10.1097/QAD.0b013e32834ff690>
12. Read TRH, Jensen JS, Fairley CK, Grant M, Danielewski JA, Su J, et al. Use of pristinamycin for macrolide-resistant *Mycoplasma genitalium* infection. *Emerg Infect Dis*. 2018;24:328–35. <http://dx.doi.org/10.3201/eid2402.170902>
13. Le Roy C, Hénin N, Bébéc C, Pereyre S. Evaluation of a commercial multiplex quantitative PCR (qPCR) assay for simultaneous detection of *Mycoplasma genitalium* and macrolide resistance-associated mutations in clinical specimens. *J Clin Microbiol*. 2017;55:978–9. <http://dx.doi.org/10.1128/JCM.02168-16>
14. Pitt R, Cole MJ, Fifer H, Woodford N. Evaluation of the *Mycoplasma genitalium* Resistance Plus kit for the detection of *M. genitalium* and mutations associated with macrolide resistance. *Sex Transm Infect*. 2018;94:565–7. <http://dx.doi.org/10.1136/sextrans-2017-053366>
15. Tabrizi SN, Su J, Bradshaw CS, Fairley CK, Walker S, Tan LY, et al. Prospective evaluation of ResistancePlus MG, a new multiplex quantitative PCR assay for detection of *Mycoplasma genitalium* and macrolide resistance. *J Clin Microbiol*. 2017;55:1915–9. <http://dx.doi.org/10.1128/JCM.02312-16>
16. Baumann L, Cina M, Egli-Gany D, Goutaki M, Halbeisen FS, Lohrer GR, et al. Prevalence of *Mycoplasma genitalium* in different population groups: systematic review and meta-analysis. *Sex Transm Infect*. 2018;94:255–62. <http://dx.doi.org/10.1136/sextrans-2017-053384>
17. Couldwell DL, Jalocon D, Power M, Jeffreys NJ, Chen SC, Lewis DA. *Mycoplasma genitalium*: high prevalence of resistance to macrolides and frequent anorectal infection in men who have sex with men in western Sydney. *Sex Transm Infect*. 2018;94:406–10. <http://dx.doi.org/10.1136/sextrans-2017-053480>
18. Bissessor M, Tabrizi SN, Bradshaw CS, Fairley CK, Hocking JS, Garland SM, et al. The contribution of *Mycoplasma genitalium* to the aetiology of sexually acquired infectious proctitis in men who have sex with men. *Clin Microbiol Infect*. 2016;22:260–5. <http://dx.doi.org/10.1016/j.cmi.2015.11.016>
19. Ong JJ, Aung E, Read TRH, Fairley CK, Garland SM, Murray G, et al. Clinical characteristics of anorectal *Mycoplasma genitalium* infection and microbial cure in men who have sex with men. *Sex Transm Dis*. 2018;45:522–6.
20. Barberá MJ, Fernández-Huerta M, Jensen JS, Caballero E, Andreu A. *Mycoplasma genitalium* macrolide and fluoroquinolone resistance: prevalence and risk factors among a 2013–2014 cohort of patients in Barcelona, Spain. *Sex Transm Dis*. 2017;44:457–62. <http://dx.doi.org/10.1097/OLQ.0000000000000631>
21. Dionne-Odom J, Geisler WM, Aaron KJ, Waites KB, Westfall AO, Van Der Pol B, et al. High prevalence of multidrug-resistant *Mycoplasma genitalium* in human immunodeficiency



- virus-infected men who have sex with men in Alabama. *Clin Infect Dis*. 2018;66:796–8. <http://dx.doi.org/10.1093/cid/cix8853>
22. Bradshaw CS, Fairley CK, Lister NA, Chen SJ, Garland SM, Tabrizi SN. *Mycoplasma genitalium* in men who have sex with men at male-only saunas. *Sex Transm Infect*. 2009;85:432–5. <http://dx.doi.org/10.1136/sti.2008.035535>
23. Deguchi T, Yasuda M, Yokoi S, Nakano M, Ito S, Ohkusu K, et al. Failure to detect *Mycoplasma genitalium* in the pharynxes of female sex workers in Japan. *J Infect Chemother*. 2009;15:410–3. <http://dx.doi.org/10.1007/s10156-009-0726-4>
24. Munson E, Wenten D, Jhansale S, Schuknecht MK, Pantuso N, Gerrits J, et al. Expansion of comprehensive screening of male sexually transmitted infection clinic attendees with *Mycoplasma genitalium* and *Trichomonas vaginalis* molecular assessment: a retrospective analysis. *J Clin Microbiol*. 2016;55:321–5. <http://dx.doi.org/10.1128/JCM.01625-16>
25. Nakashima K, Shigehara K, Kawaguchi S, Wakatsuki A, Kobori Y, Nakashima K, et al. Prevalence of human papillomavirus infection in the oropharynx and urine among sexually active men: a comparative study of infection by papillomavirus and other organisms, including *Neisseria gonorrhoeae*, *Chlamydia trachomatis*, *Mycoplasma* spp., and *Ureaplasma* spp. *BMC Infect Dis*. 2014;14:43. <http://dx.doi.org/10.1186/1471-2334-14-43>
26. Philibert P, Khiri H, Pénaranda G, Camus C, Drogoul MP, Halfon P. High prevalence of asymptomatic sexually transmitted infections among men who have sex with men. *J Clin Med*. 2014;3:1386–91. <http://dx.doi.org/10.3390/jcm3041386>
27. Wilson JWG, Jungner G. Principles and practice of screening for disease. Geneva: World Health Organization; 1968.

Address for correspondence: Catriona S. Bradshaw, Melbourne Sexual Health Centre, 580 Swanston St, Carlton, VIC 3053, Australia; email: [cbradshaw@mshc.org.au](mailto:cbradshaw@mshc.org.au)



**EID**  
journal

@CDC\_EIDjournal

Follow the EID journal on Twitter and get the most current information from Emerging Infectious Diseases.

# Differences in Neuropathogenesis of Encephalitic California Serogroup Viruses

Alyssa B. Evans, Clayton W. Winkler, Karin E. Peterson

The California serogroup of orthobunyaviruses comprises a group of mosquito-borne viruses, including La Crosse (LACV), snowshoe hare (SSHV), Tahyna (TAHV), Jamestown Canyon (JCV), and Inkoo (INKV) viruses, that cause neurologic disease in humans of differing ages with varying incidences. To determine how the pathogenesis of these viruses differs, we compared their ability to induce disease in mice and replicate and induce cell death in vitro. In mice, LACV, TAHV, and SSHV induced neurologic disease after intraperitoneal and intranasal inoculation, and JCV induced disease only after intranasal inoculation. INKV rarely induced disease, which correlated with less viral antigen in the brain than the other viruses. In vitro, all viruses replicated to high titers; however, LACV, SSHV, and TAHV induced high cell death, whereas JCV and INKV did not. Results demonstrated that CSG viruses differ in neuropathogenesis in vitro and in vivo, which correlates with the differences in pathogenesis reported in humans.

The California serogroup (CSG) of orthobunyaviruses comprises a large group of closely related mosquito-borne, trisegmented, negative-sense RNA viruses in the family *Peribunyaviridae* of the order *Bunyvirales*. La Crosse virus (LACV), snowshoe hare virus (SSHV), Tahyna virus (TAHV), Jamestown Canyon virus (JCV), and Inkoo virus (INKV) are members of the CSG that have been reported to cause neurologic disease in humans. LACV, SSHV, TAHV, and INKV primarily cause neuroinvasive disease in children; however, the incidence differs for each virus (1–3). LACV is the leading cause of pediatric viral encephalitis in the United States, responsible for ≈50–100 reported cases per year. SSHV and TAHV only cause several reported cases of neuroinvasive disease annually (1,2,4–6), and TAHV disease most often manifests as influenza-like symptoms and only rarely leads to encephalitis (2,7). INKV has caused the fewest cases of human disease. However, several confirmed neuroinvasive cases have occurred in Finland, and children had more severe disease

than adults (3). In contrast, JCV appears to preferentially cause neuroinvasive disease in adults, and several cases occur every year in the United States and Canada (1,8). Because the number of reported cases increased substantially in the 2010s, JCV is considered a potentially emerging arboviral disease (9).

The number of actual cases caused by these CSG viruses is likely underreported because of the difficulty of diagnosing these viral infections. Patients who do not seek medical treatment and those with less severe disease might not be included in case reports. All 5 viruses have high reported seroprevalence rates in endemic regions: ≈1%–27% for LACV, JCV, and SSHV; ≈24%–51% for INKV; and up to 80% for TAHV (1,2,10–12).

These CSG viruses have differing but overlapping geographic distributions (Figure 1, panel A). LACV, JCV, and SSHV are all found in the United States; JCV and SSHV extend into Canada; and SSHV extends into Russia (1,2,4,8,10,13–28). Although TAHV and INKV are primarily found in Europe, TAHV extends into Africa and Asia, and INKV is limited to northern Europe and Russia (2,3,12,29,34–36). These CSG viruses use a variety of mosquito vectors, primarily in the *Aedes* and *Ochlerotatus* genera, and mammalian host species, including small rodents (SSHV, LACV, and TAHV), hares (SSHV, TAHV, and INKV), and deer (JCV) (Figure 1, panel B) (1,2,12,22,29,31–33).

Despite their differing and widespread geographical distributions, the CSG viruses are genetically closely related. The large segment encodes the viral RNA-dependent RNA polymerase, the medium segment encodes 2 envelope glycoproteins and a nonstructural protein, and the small segment encodes the nucleocapsid and a second nonstructural protein (NSs), which in LACV is a type I interferon antagonist (37,38). Across all 3 segments, JCV and INKV are the most closely related to each other, with 84%–92.4% nucleotide identity, followed by LACV and SSHV with 79.4%–89.1% nucleotide identity (30). TAHV has ≈72.5%–84.7% nucleotide identity with LACV and SSHV and 69.2%–80.3% with JCV and INKV (30).

Author affiliation: National Institute of Allergy and Infectious Diseases, National Institutes of Health, Hamilton, Montana, USA

DOI: <https://doi.org/10.3201/eid2504.181016>



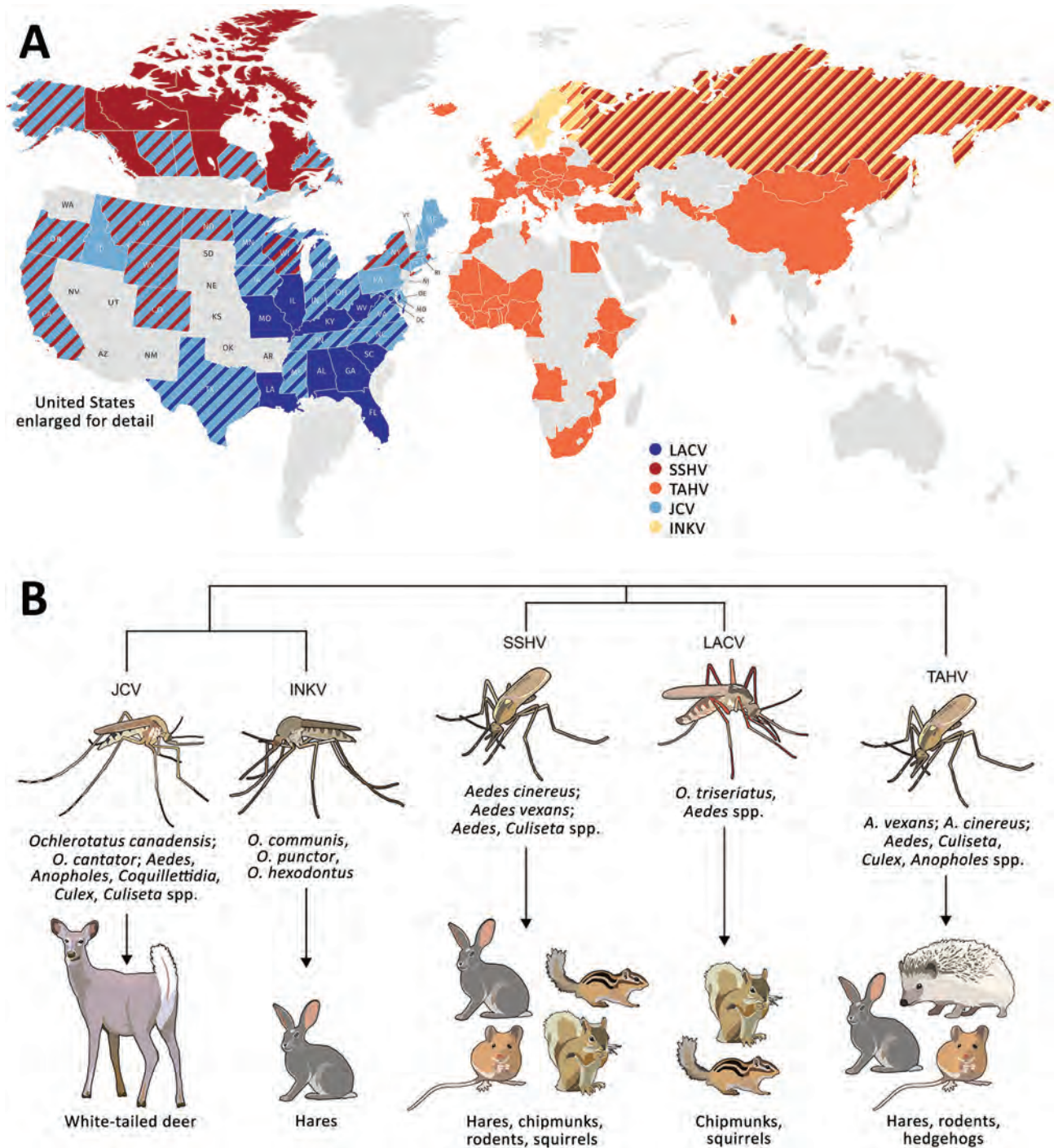


**Figure 1.** Global distribution, phylogenetic relationship, and vectors and hosts of the 5 California serogroup (CSG) viruses included in study of neuropathogenesis. A) These viruses are found across the globe, primarily throughout North America, Europe, Asia, and Africa (1,4,8,10,12–29). Several of these viruses have overlapping regions of distribution (as indicated by diagonal patterns), including in the United States, where LACV, SSHV, and JCV are all present, and Europe, where TAHV and INKV are present. States and countries indicated have evidence of these viruses from reported human cases, serologic surveys of humans and animals, or isolation of virus from mosquitoes. B) Within these closely related CSG viruses, JCV and INKV are the most closely related, followed by LACV and SSHV, and then TAHV (30). The CSG viruses use a variety of mosquito vectors, primarily in the *Aedes* and *Ochlerotatus* genera. Listed are the most prominent vectors and additional genera the virus has been found in. Mammals implicated as reservoir or amplifying hosts are listed for each virus; some hosts are shared among several CSG viruses (1,2,12,22,31–33). INKV, Inkoo virus; JCV, Jamestown Canyon virus; LACV, La Crosse virus; SSHV, snowshoe hare virus; TAHV, Tahyna virus.



In mouse studies of LACV, weanling C57BL/6 mice were susceptible to neurologic disease after intraperitoneal inoculation, but adult mice were not, demonstrating age-dependent susceptibility to disease that mimics clinical disease in humans (39). Certain strains of TAHV, but not JCV, have been shown to cause neurologic disease in weanling Swiss Webster mice after intraperitoneal inoculation, although both viruses were capable of replicating in the brain after intracranial inoculation (40,41). In these studies, only weanling mice were used, and thus, age-dependent susceptibility was not evaluated.

Determining how LACV, SSHV, TAHV, JCV, and INKV differ in pathogenesis in animal and cell culture models could help explain their differing disease outcomes in humans. However, a direct comparison between these viruses in their ability to invade the central nervous system (CNS) and induce neuronal damage has not been investigated. In this study, we investigated age-related differences in pathogenesis of LACV, SSHV, TAHV, JCV, and INKV. We examined the ability of these viruses to enter the CNS and cause disease in mice and their ability to replicate in neurons and induce cell death *in vitro*.

## Materials and Methods

### Cells and Viruses

All cell culture reagents were from Gibco (<http://www.biosciences.ie/gibco>) unless otherwise specified. We maintained Vero cells in Dulbecco modified Eagle medium supplemented with 10% fetal bovine serum (Atlas Biologicals, <https://atlasbio.com>) and 1% penicillin/streptomycin solution; C6/36 cells in minimum essential medium supplemented with 10% fetal bovine serum, 2 mM glutamine, 1× nonessential amino acids, and 1% penicillin/streptomycin; the neuroblastoma cell line SH-SY5Y (American Type Culture Collection [ATCC], <https://www.atcc.org>) in a 1:1 ratio of Eagle minimum essential medium (ATCC) and F-12K (ATCC) supplemented with 10% fetal bovine serum and 1% penicillin/streptomycin; and H9 human embryonic stem cell-derived human neural stem cells (hNSCs; Gibco, <https://www.fishersci.com>) in KnockOut DMEM/F-12 supplemented with 1× GlutaMAX-I Supplement, 20 ng/mL basic fibroblast growth factor, 20 ng/mL epidermal growth factor, 2% StemPro neural supplement, and 1% penicillin/streptomycin. We seeded hNSCs on plates or flasks treated with 20 µg/mL fibronectin in Dulbecco phosphate-buffered saline for 1 h at 37°C. We passaged stocks of LACV (human 1978 strain), JCV (strain 61V2235), TAHV (strain 92 Bardos), SSHV (1976), and INKV (SW AR 83-161), all kindly provided by Stephen Whitehead (Laboratory of Infectious Diseases, National Institute of Allergy and Infectious Diseases, National Institutes of Health, Bethesda, MD, USA), in Vero or C6/36 cells up to 3 times.

### Inoculation of Mice

All mouse experiments were approved by the Rocky Mountain Laboratories Animal Care and Use Committee (Hamilton, Montana, USA) and performed in accordance with National Institutes of Health guidelines under protocol 2016-061-E. We used C57BL/6 mice for all experiments.

We inoculated weanlings at 21–23 days of age, adults at 6–8 weeks of age, and aged mice at 19–34 weeks of age. We diluted the viruses in phosphate-buffered saline (PBS). For intraperitoneal inoculations, we injected mice with  $10^5$  or  $10^3$  PFU of virus in a volume of 200 µL. For intranasal inoculations, we inoculated mice with  $10^4$  or  $10^2$  PFU of virus in a volume of 20 µL. We anesthetized mice with isoflurane before inoculation. After inoculation, we checked mice twice daily for clinical signs of neurologic disease, which primarily included ataxia, circling, limb paralysis and weakness, twitching, and seizures. Mice displaying signs of neurologic disease were perfused transcardially with 100 U/mL heparin saline before removal of tissues. We humanely euthanized mice that did not display any signs of neurologic disease by 30 days postinoculation (dpi).

### RNA Isolation and Quantitative Reverse Transcription PCR

For RNA analysis, we flash-froze spleens and brain tissue from infected mice in liquid nitrogen, then stored them at  $-80^{\circ}\text{C}$ . We performed mRNA analysis as previously described (42). We amplified viral RNA from mouse tissues using the following virus-specific primers: LACV forward (5'-ATTCTACCCGCTGACCATTG-3') and reverse (5'-GTGAGAGTGCCATAGCGTTG-3'), SSHV forward (5'-AGCATGATCAAAACGGAGGC-3') and reverse (5'-CATGCCAATCAGACACCAGC-3'), TAHV forward (5'-AGGTCTACATTGCCGTTCA-3') and reverse (5'-TGGTCTACAGGTGCTAGCTC-3'), JCV forward (5'-TATGGTCCCCGGTAGTGTG-3') and reverse (5'-TAACATGGTGCTTCTCGTGC-3'), and INKV forward (5'-AGTCCAAGATAAAGCCCCAGA-3') and reverse (5'-TCATGTTAGCCTGGCATCCA-3'). We subjected primer sequences to BLAST analysis (<https://blast.ncbi.nlm.nih.gov/Blast.cgi>) and tested each primer set on RNA from brains of mice infected with the 5 CSG viruses that had neurologic disease to verify virus-specific amplification by each primer set.

### Immunohistochemistry

For immunohistochemistry studies, we transcardially perfused mice, removed tissues, and placed them in 10% neutral buffered formalin. After fixation, we cryoprotected tissues in 30% sucrose in PBS, embedded them in Tissue-Tek O.C.T. Compound (Sakura, <https://www.sakura.eu>) and froze them on dry ice; then, 10-µm sections were cut on a cryostat

and mounted on slides. We washed sections with PBS and blocked for 30 minutes in blocking buffer (PBS with 5% normal donkey serum, 0.1% triton-X, and 0.3 M glycine). We diluted the primary antibody against viral antigens (in-house polyclonal antibody raised in rabbits in response to LACV infection, 1:100) and microtubule-associated protein 2 (mouse monoclonal antibody MAB3418, 1:200; Millipore, <http://www.emdmillipore.com>) in blocking buffer, applied these solutions to tissues, and incubated them overnight at 4°C. We washed tissue sections with PBS and incubated for 1 hour at room temperature with donkey anti-rabbit Alexa Fluor 647 (1:1,000, Life Technologies, <https://www.thermofisher.com>) and donkey anti-mouse Alexa Fluor 594 (1:500, Life Technologies). After washing sections again with PBS, we stained with Hoechst (1:1,000) and mounted on slides with ProLong Gold (Invitrogen, <https://www.thermofisher.com>). We imaged entire brain sections using the Zeiss Axio Scan.Z1 (<https://www.zeiss.com>) with the 40× objective lens. We acquired high-resolution images on the Zeiss 710 laser scanning microscope with the 63× objective and processed images in Imaris version 8.4.1 (<https://imaris.oxinst.com>) or Fiji (<http://fiji.sc>).

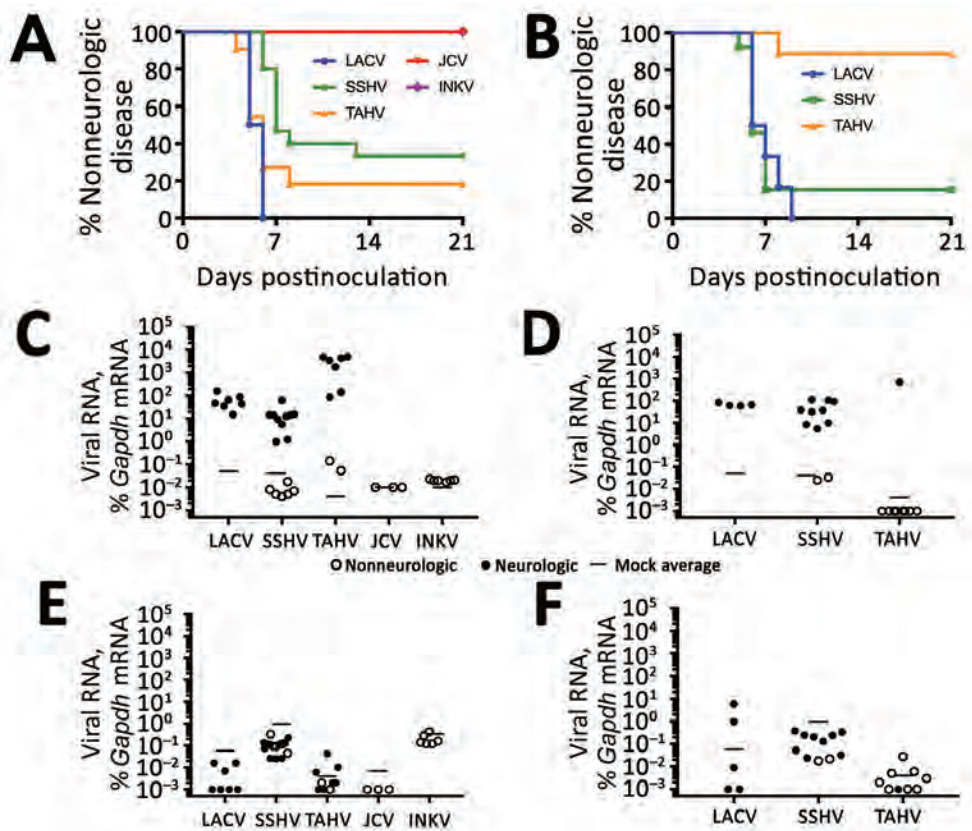
**Cytotoxicity Assays**

We coated 96-well plates with fibronectin as previously described and seeded  $5 \times 10^4$  SH-SY5Y cells or  $2 \times 10^4$  hNSCs per well. The next day, cells were inoculated with each virus in triplicate at multiplicities of infection (MOIs) of 0.1 and 0.01 for SH-SY5Y cells and 0.01 and 0.001 for hNSCs. We added Cytotox Green (Essen Bioscience, <https://www.essenbioscience.com>) for a final well volume of 100  $\mu$ L and a final concentration of 250 nM. Cells were then imaged with an IncuCyte (Essen Bioscience) by taking 3 images per well with the 20× objective every 3 hours during a 97-hour time course. We measured confluence and fluorescent intensity using IncuCyte S3 software. We performed all statistical analyses using Prism 7.0c (<https://www.graphpad.com>).

**Replication Kinetics**

We plated and inoculated cells as described in the previous section, except that plates seeded with SH-SY5Y cells were not treated with fibronectin. We collected supernatants at 1, 6, 12, 24, 48, 72, and 96 hours

**Figure 2.** Neuroinvasiveness of California serogroup (CSG) viruses in weanling C57BL/6 mice after intraperitoneal inoculation in study of neuropathogenesis. We inoculated 5–15 mice per group with  $10^5$  PFU of each virus (A) and 6–13 mice per group with  $10^3$  PFU of LACV, SSHV, or TAHV (B). Brains and spleens of mice were collected at the experimental endpoint and evaluated for viral RNA by quantitative reverse transcription PCR with virus-specific primers. The average of 3 mock controls is reported for each primer set. The viral RNA level in each sample was calculated as the difference in the percentage in cycle threshold ( $C_i$ ):  $C_i$  for *Gapdh* mRNA minus  $C_i$  for viral mRNA. Viral RNA was plotted as the percentage of gene expression relative to that of the *Gapdh* gene. Viral RNA in brains of mice inoculated with  $10^5$  PFU of each virus (C) or  $10^3$  PFU of LACV, SSHV, and TAHV (D). Viral RNA in spleens of mice inoculated with  $10^5$  PFU of each virus (E) or  $10^3$  PFU of LACV, SSHV, and TAHV (F). *Gapdh*, glyceraldehyde 3-phosphate dehydrogenase; INKV, Inkoo virus; JCV, Jamestown Canyon virus; LACV, La Crosse virus; SSHV, snowshoe hare virus; TAHV, Tahyna virus.





postinoculation. We determined virus titers of supernatants by plaque assay using Vero cells as described previously (43). We counted LACV, TAHV, and JCV plaques at 5 dpi and SSHV and INKV plaques at 3 dpi. We performed all statistical analyses using Prism 7.0c (<https://www.graphpad.com>).

**Results**

**Assessment of Neuroinvasive Disease in Mice after Intraperitoneal Inoculation with CSG Viruses**

To determine if these 5 CSG viruses differed in their ability to enter the CNS and cause neurologic disease (i.e.,

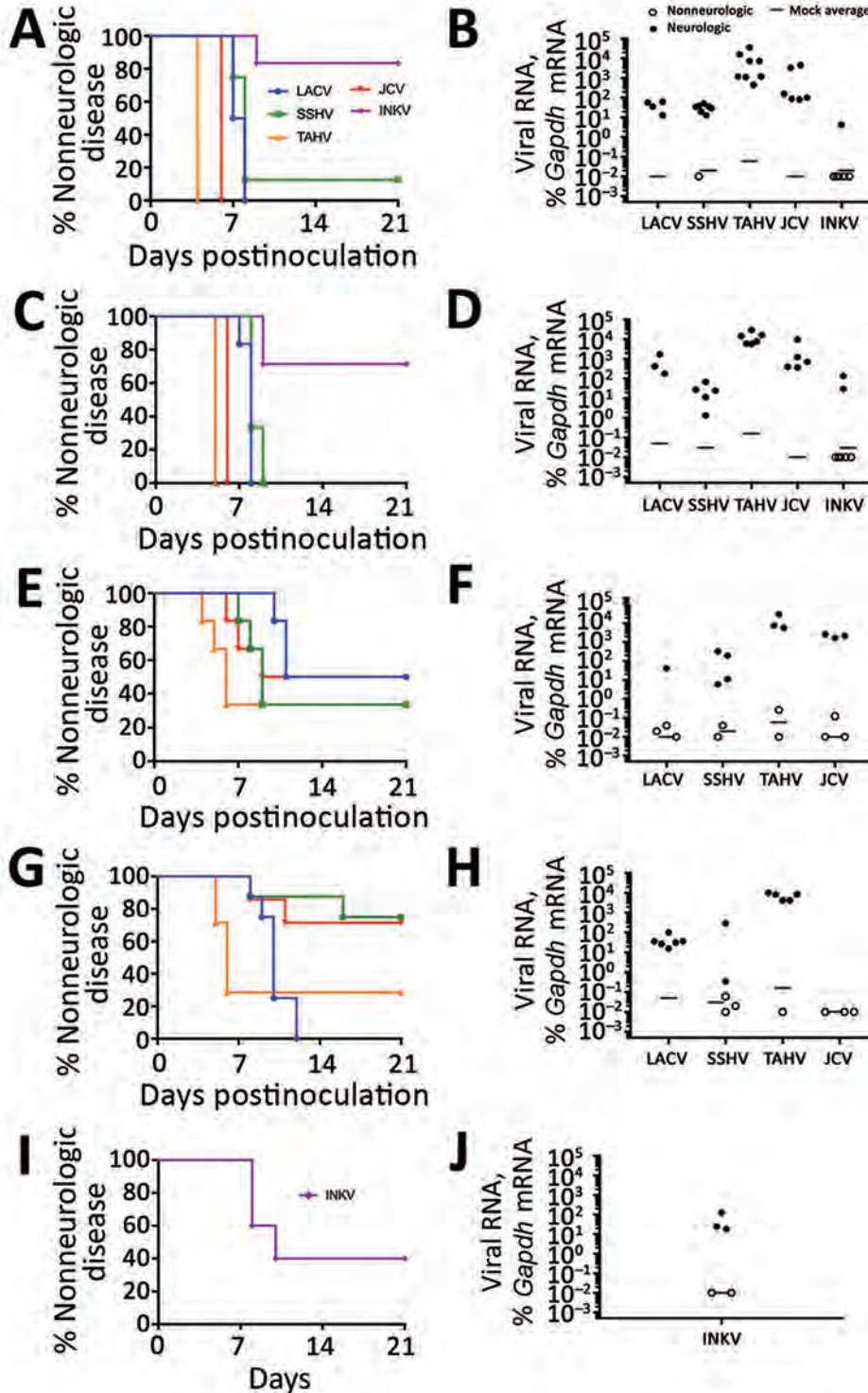
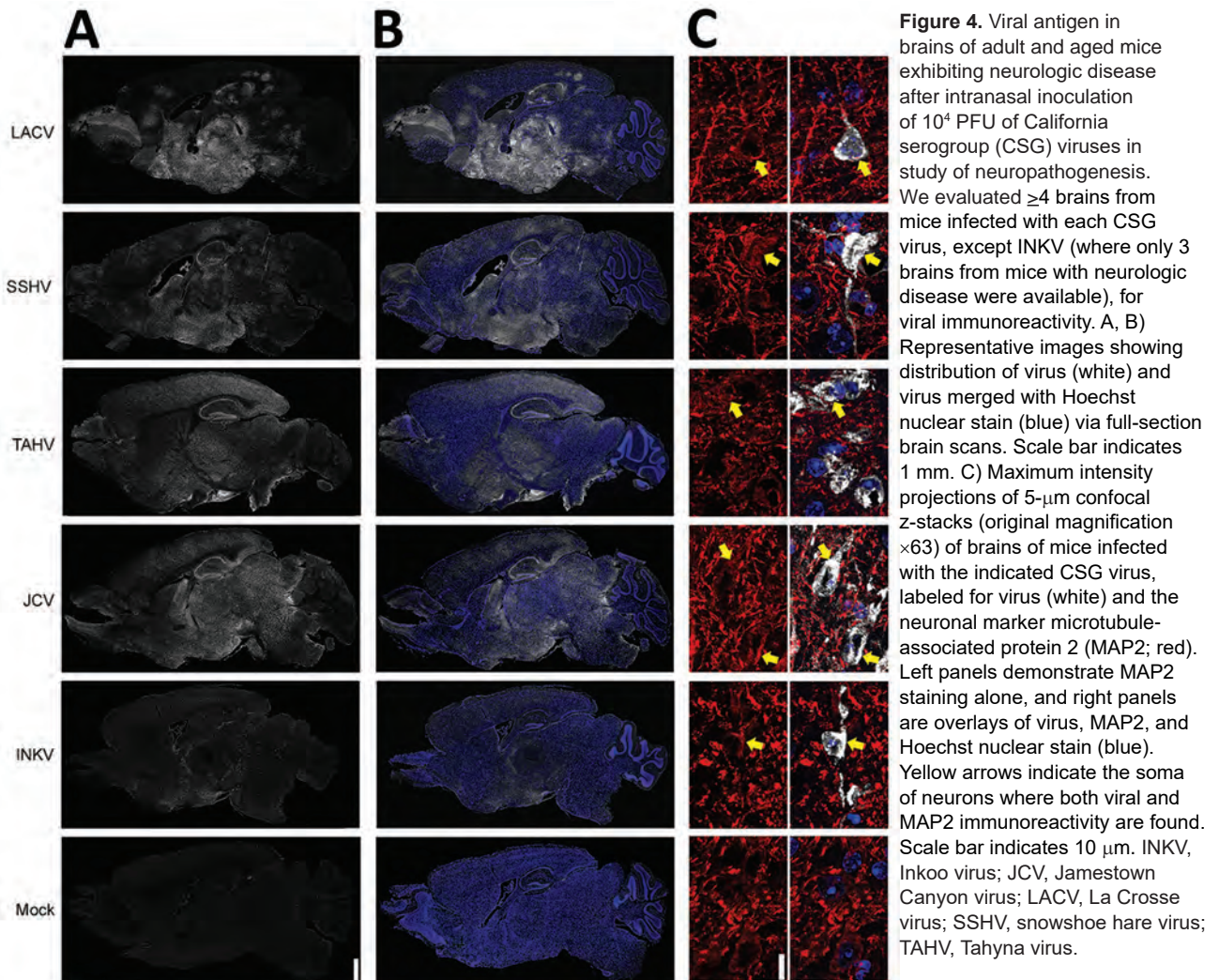


**Figure 3.** Neurovirulence of California serogroup (CSG) viruses in adult, aged, and weanling mice after intranasal inoculation in study of neuropathogenesis. Groups of adult (A, B) and aged (C, D) mice (6–8 mice per group) were inoculated with  $10^4$  PFU of each virus; groups of adult (E, F) and aged (G, H) mice (6–8 mice per group) were inoculated with  $10^2$  PFU of LACV, SSHV, TAHV, and JCV; and 5 weanling mice were inoculated with  $10^4$  PFU of INKV (I, J). E, G) Survival rate differences between adult and aged mice infected with  $10^2$  PFU of virus were calculated for each virus by using the Gehan-Breslow-Wilcoxon test. LACV was the only virus with a significant difference ( $p = 0.035$ ). B, D, F, H, J) Viral RNA in mouse brains was analyzed by quantitative reverse transcription PCR with virus-specific primers. The average of 3 mock controls is reported for each primer set. The viral RNA level in each sample was calculated as the difference in the percentage in cycle threshold ( $C_t$ );  $C_t$  for *Gapdh* mRNA minus  $C_t$  for viral mRNA. Viral RNA was plotted as the percentage of gene expression relative to that of the *Gapdh* gene. *Gapdh*, glyceraldehyde 3-phosphate dehydrogenase; INKV, Inkoo virus; JCV, Jamestown Canyon virus; LACV, La Crosse virus; SSHV, snowshoe hare virus; TAHV, Tahyna virus. A color version of this figure is available online (<http://wwwnc.cdc.gov/EID/article/25/4/18-1016-F3.htm>).





neuroinvasive disease), C57BL/6 mice were inoculated intraperitoneally with a high dose ( $10^5$  PFU) of each virus. Because previous studies of LACV infection showed clear age-dependent differences in disease susceptibility between weanling and adult mice, we inoculated weanling, adult, and aged mice with each virus and followed them for the development of clinical signs of neurologic disease. None of the viruses induced neuroinvasive disease in adult or aged mice after intraperitoneal inoculation (data not shown). However, neuroinvasive disease developed by 5–6 dpi in all weanling mice inoculated with  $10^5$  PFU of LACV (Figure 2, panel A), consistent with previous reports (39,44). SSHV induced neuroinvasive disease in  $\approx 70\%$  of weanling mice and TAHV in  $\approx 80\%$  of weanling mice. Neurologic signs were primarily observed at 6–7 dpi for SSHV and 5–6 dpi for TAHV. Neurologic signs were similar for LACV, SSHV, and TAHV and included ataxia, circling, limb paralysis and weakness, twitching, and seizures. JCV and INKV did not induce neuroinvasive disease in any weanling mice.

In previous studies with LACV, nearly 100% of weanling mice were susceptible to neuroinvasive disease after intraperitoneal inoculation at a dose of  $10^3$  PFU (39). To determine if TAHV and SSHV also maintain their pathogenicity at this low dose, we inoculated weanling mice intraperitoneally with  $10^3$  PFU of LACV, SSHV, or TAHV. JCV and INKV were not included in this experiment because they did not induce neuroinvasive disease at the high dose. Consistent with previous studies,  $10^3$  PFU of LACV caused disease in 100% of mice but with a slight delay in the onset of neurologic signs compared with the  $10^5$  PFU dose (Figure 2, panel B). At the low dose, SSHV induced disease in a similar percentage of mice as the high dose, whereas TAHV caused disease in only 1 of 9 mice at the low dose (Figure 2, panel B).

All weanling mice with neurologic disease had detectable viral RNA in the brain, whereas weanling, adult, and aged mice without neurologic disease had no detectable virus in the brain compared with mock controls (Figure 2, panels C, D; data not shown). Regardless of disease

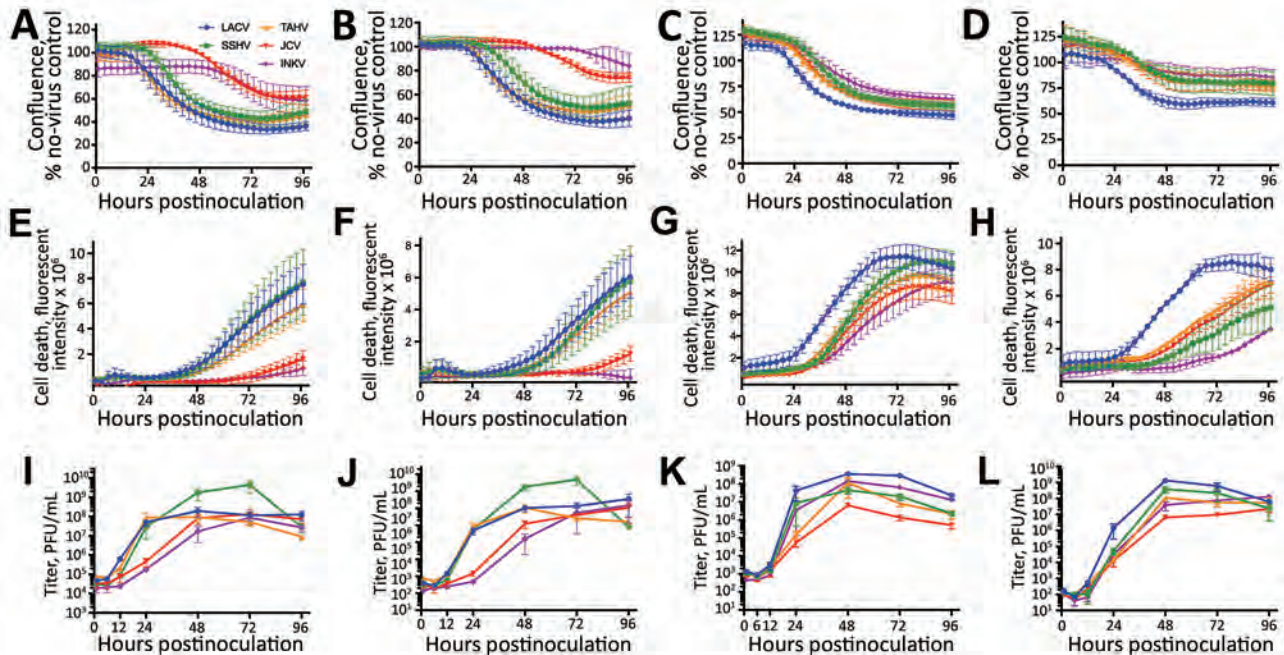


**Figure 5.** Cytotoxicity and viral replication kinetics assays of California serogroup (CSG) viruses in SH-SY5Y cells and human neural stem cells (hNSCs) for up to 96 hours postinoculation in study of neuropathogenesis. SH-SY5Y cells were infected at a multiplicity of infection of 0.1 (A, E, I) or 0.01 (B, F, J), and hNSCs were infected at a multiplicity of infection of 0.01 (C, G, K) or 0.001 (D, H, L). A–D) Confluence was measured over time on the InCuCyte (Essen Bioscience, <https://www.essenbioscience.com>) as the percentage of the image covered by cells. Graphs show the percentage of confluence compared with that of uninfected control wells. E–H) Cell death was measured over time with the InCuCyte and reported as the total integrated fluorescent intensity of the Cytotox Green (Essen Bioscience) reagent. I–L) Supernatants were harvested from SH-SY5Y cells and hNSCs at 1, 6, 12, 24, 48, 72, and 96 hours postinfection and titered on Vero cells by plaque assay. All error bars indicate SEM. PFU, plaque-forming units.

outcome, mice had little to no detectable viral RNA in the spleen (Figure 2, panels E, F; data not shown), suggesting clearance of virus from the periphery.

Overall, these results indicate that LACV, SSHV, and TAHV can induce neuroinvasive disease in weanling mice after intraperitoneal inoculation, whereas JCV and INKV cannot. None of the CSG viruses caused neurologic signs in adult or aged mice after intraperitoneal inoculation, suggesting an age-related susceptibility of mice to LACV-, SSHV-, and TAHV-induced neuroinvasive disease.

#### Assessment of Neurovirulence of CSG Viruses after Intranasal Inoculation of Mice

The inability of a virus to cause neuroinvasive disease after intraperitoneal inoculation could be due to a lack of virus replication in the periphery or an inability of the virus to gain access to the CNS. These barriers can be bypassed by intracranial or intranasal inoculation. For example, LACV is not neuroinvasive in adult mice after intraperitoneal inoculation but does cause disease in adult mice when inoculated intracranially or intranasally (39,44,45). Because none of these CSG viruses caused disease in older mice after intraperitoneal inoculation, adult and aged

mice were inoculated intranasally with each virus to determine if they were neurovirulent (i.e., could replicate in the brain) and neuropathogenic (i.e., could cause disease in the brain) after a more direct inoculation route and to determine if neuropathogenesis was restricted by age. Because of the low stock concentration of some viruses, we could not inoculate mice with  $10^5$  PFU intranasally; therefore, we used a high dose of  $10^4$  PFU and a low dose of  $10^2$  PFU. At a dose of  $10^4$  PFU per mouse, all viruses except INKV induced neurologic disease in nearly all adult and aged mice (Figure 3, panels A, C). INKV was less neuropathogenic than the other CSG viruses, inducing disease in only 1 of 6 adult mice and 2 of 7 aged mice. Compared with the high dose, the low dose induced neurologic disease in a reduced percentage of mice for all viruses, except LACV in aged mice (Figure 3, panels E, G). Viral RNA was readily detectable in the brains (Figure 3, panels B, D, F, H) but not spleens (data not shown) of all mice with neurologic disease.

Because INKV induced limited disease in adult mice, we inoculated weanling mice intranasally with INKV to determine if neuropathogenicity was age dependent. Neurologic disease developed in 3 (60%) of 5 mice and was associated with viral RNA in the brain (Figure 3, panels A,



**Table 1.** Cell death and replication kinetics of 5 encephalitic California serogroup viruses in SH-SY5Y cells\*

Virus	MOI 0.1					MOI 0.01				
	Difference in cell death†		Virus replication			Difference in cell death†		Virus replication		
	Range, hpi	p value range	Replication rate p value‡	Peak titer, PFU/mL	hpi§	Range, hpi	p value range	Replication rate p value‡	Peak titer, PFU/mL	hpi§
LACV	Ref	Ref	Ref	$1.93 \times 10^8$	48	Ref	Ref	Ref	$3.51 \times 10^8$	96
SSHV	NS	NS	<b>0.041</b>	$4.36 \times 10^9$	72	NS	NS	<b>0.038</b>	$4.82 \times 10^9$	72
TAHV	NS	NS	<b>0.110</b>	$9.13 \times 10^7$	48	NS	NS	<b>0.995</b>	$1.05 \times 10^8$	48
JCV	61–96	0.047–0.0001	<b>0.033</b>	$1.33 \times 10^8$	72	67–96	0.022–0.0001	<b>0.034</b>	$1.09 \times 10^8$	96
INKV	64–96	0.024–0.0001	<b>0.002</b>	$8.72 \times 10^7$	72	67–96	0.023–0.0001	<b>0.023</b>	$1.55 \times 10^8$	96

\*All statistical comparisons were made with LACV used as the reference. hpi, hour postinoculation; INKV, Inkoo virus; JCV, Jamestown Canyon virus; LACV, La Crosse virus; MOI, multiplicity of infection; NS, not significant; Ref, referent; SSHV, snowshoe hare virus; TAHV, Tahyna virus.  
†Cell death for  $\geq 3$  independent experiments analyzed by 2-way analysis of variance.  
‡Replication rates from 3 independent experiments were analyzed via linear regression analysis of slopes during the log phase of viral growth (6–48 hpi). Significant p values (<0.05) are in boldface.  
§Time point at which the sampled peak titer was observed.

I). Thus, with a high dose and direct intranasal route to the CNS, INKV was more neuropathogenic in young mice than in adults (Figure 3, panels B, J).

Next, we examined the distribution of the CSG viruses in the brain using immunohistochemistry. In mice inoculated intranasally with  $10^4$  PFU of LACV, SSHV, TAHV, or JCV that had neurologic disease, virus was widespread throughout the brains regardless of the day after inoculation or severity of neurologic disease (Figure 4, panels A, B). In contrast, the brains of adults and aged mice displaying neurologic disease after intranasal inoculation of INKV showed only small, sporadic patches of virus (Figure 4, panels A, B). All viruses co-localized with the neuronal marker microtubule-associated protein 2, indicating that all CSG viruses primarily infected neurons within the CNS (Figure 4, panel C). Overall, these results demonstrate that LACV, SSHV, TAHV, and JCV are neurovirulent in mice when inoculated intranasally, whereas INKV appears to be less neurovirulent and infects fewer neurons within the CNS.

#### Ability of CSG Viruses to Replicate in and Kill Neurons in vitro

The differences in pathogenicity among the CSG viruses observed in mice and humans could be related to differences in their ability to infect and kill neurons. Therefore, we analyzed the ability of these viruses to replicate in and

kill neurons using the human neuroblastoma cell line SH-SY5Y and hNSCs. We inoculated cells with each virus at MOIs predetermined to provide a sufficient time frame to measure virus replication before the onset of substantial cell death with LACV (MOIs of 0.1 and 0.01 for SH-SY5Y cells and MOIs of 0.01 and 0.001 for hNSCs). In SH-SY5Y cells, LACV, SSHV, and TAHV induced substantial cell death at both MOIs, whereas JCV and INKV induced little cell death (Figure 5, panels A, B, E, F). However, JCV and INKV replicated to similar titers as LACV (Table 1), albeit with a delay in replication (Table 1; Figure 5, panels I, J). In hNSCs, all 5 viruses induced cell death at both MOIs (Figure 5, panels C, D, G, H); however, LACV had a more pronounced cell death rate than the other viruses, indicating that LACV may be more neurotoxic to hNSCs than the other 4 CSG viruses, most notably INKV (Table 2; Figure 5, panels G, H). All viruses rapidly replicated to high titers at both MOIs in hNSCs; however, JCV appeared to replicate slower and reached a lower peak titer than the other CSG viruses (Table 2; Figure 5, panels K, L). All CSG viruses had significantly slower rates of growth in hNSCs with 1 or both MOIs compared with LACV (Table 2).

Together, these results suggest that LACV, SSHV, and TAHV are capable of replicating quickly to high titers in neurons and inducing substantial cell death. In contrast, INKV and JCV replicated more slowly but to similar titers. INKV and JCV also induced less cell death than the other

**Table 2.** Cell death and replication kinetics of 5 encephalitic California serogroup viruses in human neural stem cells\*

Virus	MOI 0.01					MOI 0.001				
	Difference in cell death†		Virus replication			Difference in cell death†		Virus replication		
	Range, hpi	p value range	Replication rate p value‡	Peak titer, PFU/mL	hpi§	Range, hpi	p value range	Replication rate p value‡	Peak titer, PFU/mL	hpi§
LACV	Ref	Ref	Ref	$3.63 \times 10^8$	48	Ref	Ref	Ref	$1.34 \times 10^9$	48
SSHV	34–49	0.042–0.013	<b>0.018</b>	$4.48 \times 10^7$	48	49–94	0.044–0.001	0.091	$3.82 \times 10^8$	48
TAHV	43–61	0.043–0.025	0.050	$1.16 \times 10^8$	48	64–70	0.047–0.044	<b>0.042</b>	$1.08 \times 10^8$	48
JCV	34–73	0.027–0.003	<b>0.012</b>	$6.42 \times 10^6$	48	58–76	0.037–0.015	<b>0.033</b>	$2.21 \times 10^7$	96
INKV	34–79	0.026–0.0001	0.075	$1.43 \times 10^8$	48	46–96	0.045–0.0001	<b>0.035</b>	$1.30 \times 10^8$	96

\*All statistical comparisons were made with LACV used as the reference. hpi, hour postinoculation; INKV, Inkoo virus; JCV, Jamestown Canyon virus; LACV, La Crosse virus; MOI, multiplicity of infection; NS, not significant; Ref, referent; SSHV, snowshoe hare virus; TAHV, Tahyna virus.  
†Cell death for  $\geq 3$  independent experiments analyzed by 2-way analysis of variance.  
‡Replication rates from 3 independent experiments were analyzed via linear regression analysis of slopes during the log phase of viral growth (6–48 hpi). Significant p values (<0.05) are in boldface.  
§Time point at which the sampled peak titer was observed.



CSG viruses, although the level of cell death varied by cell type. The lower cell death associated with INKV infection *in vitro* correlates with the low level of INKV infection within the CNS *in vivo*.

## Discussion

In our study, the CSG viruses differed in pathogenesis both in mice and *in vitro*. Overall, LACV showed the highest neuropathogenicity and neurovirulence *in vitro* and *in vivo*, whereas INKV was the least pathogenic. These results appear to be consistent with disease patterns observed in humans, with LACV reported to cause the most neuroinvasive cases, and INKV only infrequent cases (3,4,14). Only LACV, TAHV, and SSHV were capable of causing neuroinvasive disease, a finding only observed in weanling mice. The lack of disease in adult animals is consistent with previous findings with LACV, where an age-dependent immune response in adult mice protects them from virus-induced neurologic disease (39,46).

LACV and SSHV maintained similar levels of neuroinvasiveness down to a dose of  $10^3$  PFU, whereas TAHV's ability to induce neuroinvasive disease was greatly diminished at this low dose (Figure 2, panels A, B). The difference in dose-dependent disease susceptibility suggests that TAHV might be less virulent than LACV or SSHV. The lower virulence of TAHV than LACV or SSHV correlates with the low number of TAHV-induced neuroinvasive cases in humans, despite TAHV's larger geographic distribution and higher rates of seroprevalence than LACV (1,2,4).

When the peripheral immune system was bypassed and adult and aged mice were inoculated intranasally, all viruses except INKV replicated extensively throughout the brain and caused neurologic disease (Figure 4). However, INKV did cause disease in a few adult and aged mice and 60% of weanling mice after intranasal inoculation, indicating INKV can be neuropathogenic under certain conditions, particularly in younger animals. These results are consistent with human case reports showing that INKV causes more severe disease in children than adults (3).

Less viral antigen was found in the brains of the 3 adult and aged INKV-inoculated mice that developed neurologic disease than in the brains from mice infected with the other CSG viruses (Figure 4). INKV induced less cell death than LACV in SH-SY5Y cells, suggesting that the lack of neuropathogenicity observed with INKV *in vivo* could be due to low levels of INKV-induced neuronal cell death. In addition, INKV also replicated slower than LACV in SH-SY5Y cells, suggesting the limited spread of INKV in the brains of mice might be due to inefficient replication of INKV in neurons. Further studies are needed to determine why INKV has a reduced ability to induce neuronal death compared with other CSG viruses.

In humans, JCV appears to be distinct from the other CSG viruses in that JCV preferentially causes neuroinvasive disease in adults rather than in children. Although we did not observe a similar age-dependent difference in neuroinvasion of JCV in mice, this virus did differ from the other CSG viruses. JCV (like INKV) was unable to invade the CNS, yet JCV (like LACV, SSHV, and TAHV) was highly neurovirulent in brains of mice when inoculated intranasally. However, the same high level of neurovirulence was not observed *in vitro*. In both SH-SY5Y cells and hNSCs, JCV induced less cell death and replicated slower than LACV. These findings suggest there might be underlying genetic differences or complexities in JCV pathogenesis not shared by any of the other CSGs.

Given that genetic variation exists within and between these encephalitic CSG viruses (30), additional differences in pathogenicity might exist for different isolates not tested in our studies. However, overall these results show that, despite being closely related, these CSG viruses differ substantially in their abilities to induce neurologic disease in mice and replicate in neurons *in vitro* and *in vivo*. Further characterization of the host and viral factors that contribute to the differences in CSG virus pathogenesis will help determine why INKV is less neurovirulent than the other CSG viruses and elucidate potential targets for CSG virus encephalitis therapies.

## Acknowledgments

We thank Stephen Whitehead for providing the CSG viruses, Paul Policastro for assistance with SH-SY5Y cells and hNSC cultures, and Tyson Woods for LACV stock preparation and technical assistance. We thank Austin Athman and Ryan Kissinger for the preparation of Figure 1. We thank Leonard Evans, Stefano Boi, Emmie de Wit, and Carrie Long for critical review of the manuscript. We thank the staff of the Rocky Mountain Veterinary Branch, in particular Malea Higgins and Maarit Culbert, for excellent care of the animals used in this study.

This work was supported by the National Institutes of Allergy and Infectious Diseases Division of Intramural Research, National Institutes of Health.

## About the Author

Dr. Evans is a postdoctoral fellow in the Laboratory of Persistent Viral Diseases at Rocky Mountain Laboratories in Hamilton, Montana, USA. Her primary research interests are in comparative viral genetics and viral-host interactions.

## References

1. Drebot MA. Emerging mosquito-borne bunyaviruses in Canada. *Can Commun Dis Rep*. 2015;41:117–23. <http://dx.doi.org/10.14745/ccdr.v41i06a01>

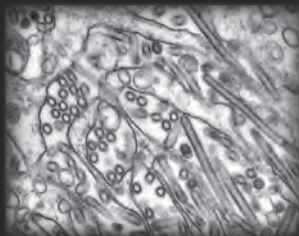
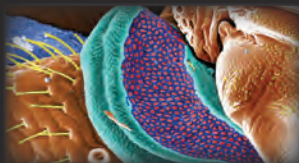
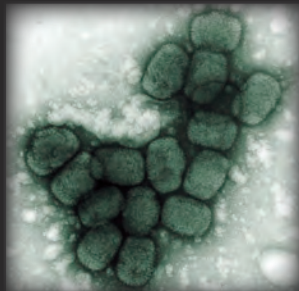
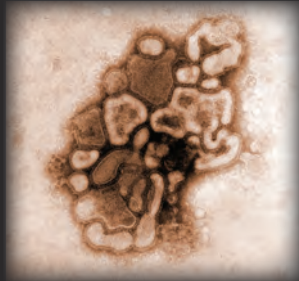
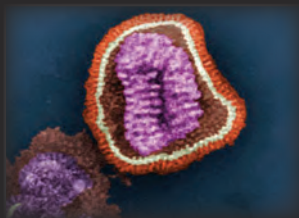
2. Hubálek Z. Mosquito-borne viruses in Europe. *Parasitol Res.* 2008; 103(Suppl 1):29–43. <http://dx.doi.org/10.1007/s00436-008-1064-7>
3. Putkuri N, Kantele A, Levanov L, Kivistö I, Brummer-Korvenkontio M, Vaheri A, et al. Acute human Inkoo and Chatanga virus infections, Finland. *Emerg Infect Dis.* 2016;22:810–7. <http://dx.doi.org/10.3201/eid2205.151015>
4. Centers for Disease Control and Prevention. La Crosse encephalitis. Epidemiology and geographic distribution. 2018 Jan 25 [cited 2018 May 22]. <https://www.cdc.gov/lac/tech/epi.html>
5. Gaensbauer JT, Lindsey NP, Messacar K, Staples JE, Fischer M. Neuroinvasive arboviral disease in the United States: 2003 to 2012. *Pediatrics.* 2014;134:e642–50. <http://dx.doi.org/10.1542/peds.2014-0498>
6. Lau L, Wudel B, Kadkhoda K, Keynan Y. Snowshoe hare virus causing meningoencephalitis in a young adult from northern Manitoba, Canada. *Open Forum Infect Dis.* 2017;4:ofx150. <http://dx.doi.org/10.1093/ofid/ofx150>
7. Kilian P, Růžek D, Danielová V, Hypsa V, Grubhoffer L. Nucleotide variability of Tahyna virus (*Bunyaviridae*, *Orthobunyavirus*) small (S) and medium (M) genomic segments in field strains differing in biological properties. *Virus Res.* 2010;149:119–23. <http://dx.doi.org/10.1016/j.virusres.2010.01.005>
8. Pastula DM, Hoang Johnson DK, White JL, Dupuis AP II, Fischer M, Staples JE. Jamestown Canyon virus disease in the United States—2000–2013. *Am J Trop Med Hyg.* 2015;93:384–9. <http://dx.doi.org/10.4269/ajtmh.15-0196>
9. Pastula DM, Smith DE, Beckham JD, Tyler KL. Four emerging arboviral diseases in North America: Jamestown Canyon, Powassan, chikungunya, and Zika virus diseases. *J Neurovirol.* 2016;22:257–60. <http://dx.doi.org/10.1007/s13365-016-0428-5>
10. Kosoy O, Rabe I, Geissler A, Adjemian J, Panella A, Laven J, et al. Serological survey for antibodies to mosquito-borne bunyaviruses among US National Park Service and US Forest Service employees. *Vector Borne Zoonotic Dis.* 2016;16:191–8. <http://dx.doi.org/10.1089/vbz.2015.1865>
11. Monath TP, Nuckolls JG, Berall, Bauer H, Chappell WA, Coleman PH. Studies on California encephalitis in Minnesota. *Am J Epidemiol.* 1970;92:40–50. <http://dx.doi.org/10.1093/oxfordjournals.aje.a121178>
12. Putkuri N, Vaheri A, Vapalahti O. Prevalence and protein specificity of human antibodies to Inkoo virus infection. *Clin Vaccine Immunol.* 2007;14:1555–62. <http://dx.doi.org/10.1128/CVI.00288-07>
13. Walters LL, Tirrell SJ, Shope RE. Seroepidemiology of California and Bunyamwera serogroup (*Bunyaviridae*) virus infections in native populations of Alaska. *Am J Trop Med Hyg.* 1999;60:806–21. <http://dx.doi.org/10.4269/ajtmh.1999.60.806>
14. Haddow AD, Odoi A. The incidence risk, clustering, and clinical presentation of La Crosse virus infections in the eastern United States, 2003–2007. *PLoS One.* 2009;4:e6145. <http://dx.doi.org/10.1371/journal.pone.0006145>
15. Clark GG, Crabbs CL, Watts DM, Bailey CL. An ecological study of Jamestown Canyon virus on the Delmarva Peninsula, with emphasis on its possible vector. *J Med Entomol.* 1986;23:588–99. <http://dx.doi.org/10.1093/jmedent/23.6.588>
16. Boromisa RD, Grimstad PR. Virus-vector-host relationships of *Aedes stimulans* and Jamestown Canyon virus in a northern Indiana enzootic focus. *Am J Trop Med Hyg.* 1986;35:1285–95. <http://dx.doi.org/10.4269/ajtmh.1986.35.1285>
17. Pinger RR, Rowley WA, Wong YW, Dorsey DC. Trivittatus virus infections in wild mammals and sentinel rabbits in central Iowa. *Am J Trop Med Hyg.* 1975;24:1006–9. <http://dx.doi.org/10.4269/ajtmh.1975.24.1006>
18. Heard PB, Zhang MB, Grimstad PR. Isolation of Jamestown Canyon virus (California serogroup) from *Aedes* mosquitoes in an enzootic focus in Michigan. *J Am Mosq Control Assoc.* 1990; 6:461–8.
19. Anderson JF, Main AJ, Armstrong PM, Andreadis TG, Ferrandino FJ. Arboviruses in North Dakota, 2003–2006. *Am J Trop Med Hyg.* 2015;92:377–93. <http://dx.doi.org/10.4269/ajtmh.14-0291>
20. McFarlane BL, Embil JA, Artsob H, Spence L, Rozee KR. Antibodies to the California group of arboviruses in the moose (*Alces alces americana* Clinton) population of Nova Scotia. *Can J Microbiol.* 1981;27:1219–23. <http://dx.doi.org/10.1139/m81-187>
21. Berry RL, Weigert BJL, Calisher CH, Parsons MA, Bear GT. Evidence for transovarial transmission of Jamestown Canyon virus in Ohio. *Mosq News.* 1977;37:494–6.
22. Issel CJ, Hoff GL, Trainer DO. Serologic evidence of infection of white-tailed deer in Texas with three California group arboviruses, (Jamestown Canyon, San Angelo, and Keystone). *J Wildl Dis.* 1973;9:245–8. <http://dx.doi.org/10.7589/0090-3558-9.3.245>
23. Tyers D, Zimmer J, Lewandowski K, Hennager S, Young J, Pappert R, et al. Serologic survey of snowshoe hares (*Lepus americanus*) in the Greater Yellowstone Area for brucellosis, tularemia, and snowshoe hare virus. *J Wildl Dis.* 2015;51:769–73. <http://dx.doi.org/10.7589/2015-01-021>
24. Campbell GL, Eldridge BF, Hardy JL, Reeves WC, Jessup DA, Presser SB. Prevalence of neutralizing antibodies against California and Bunyamwera serogroup viruses in deer from mountainous areas of California. *Am J Trop Med Hyg.* 1989;40:428–37. <http://dx.doi.org/10.4269/ajtmh.1989.40.428>
25. Eldridge BF, Calisher CH, Fryer JL, Bright L, Hobbs DJ. Serological evidence of California serogroup virus activity in Oregon. *J Wildl Dis.* 1987;23:199–204. <http://dx.doi.org/10.7589/0090-3558-23.2.199>
26. Issel CJ, Trainer DO, Thompson WH. Serologic evidence of infections of white-tailed deer in Wisconsin with three California group arboviruses (La Crosse, trivittatus, and Jamestown Canyon). *Am J Trop Med Hyg.* 1972;21:985–8. <http://dx.doi.org/10.4269/ajtmh.1972.21.985>
27. Srihongse S, Grayson MA, Deibel R. California serogroup viruses in New York state: the role of subtypes in human infections. *Am J Trop Med Hyg.* 1984;33:1218–27. <http://dx.doi.org/10.4269/ajtmh.1984.33.1218>
28. Walker ED, Grayson MA, Edman JD. Isolation of Jamestown Canyon and snowshoe hare viruses (California serogroup) from *Aedes* mosquitoes in western Massachusetts. *J Am Mosq Control Assoc.* 1993;9:131–4.
29. Jentes ES, Robinson J, Johnson BW, Conde I, Sakouvougui Y, Iverson J, et al. Acute arboviral infections in Guinea, West Africa, 2006. *Am J Trop Med Hyg.* 2010;83:388–94. <http://dx.doi.org/10.4269/ajtmh.2010.09-0688>
30. Hughes HR, Lanciotti RS, Blair CD, Lambert AJ. Full genomic characterization of California serogroup viruses, genus *Orthobunyavirus*, family *Peribunyaviridae* including phylogenetic relationships. *Virology.* 2017;512:201–10. <http://dx.doi.org/10.1016/j.virol.2017.09.022>
31. Pantuwatana S, Thompson WH, Watts DM, Hanson RP. Experimental infection of chipmunks and squirrels with La Crosse and trivittatus viruses and biological transmission of La Crosse virus by *Aedes triseriatus*. *Am J Trop Med Hyg.* 1972;21:476–81. <http://dx.doi.org/10.4269/ajtmh.1972.21.476>
32. Artsob H. Distribution of California serogroup viruses and virus infections in Canada. *Prog Clin Biol Res.* 1983;123:277–90.
33. Andreadis TG, Anderson JF, Armstrong PM, Main AJ. Isolations of Jamestown Canyon virus (*Bunyaviridae*: *Orthobunyavirus*) from field-collected mosquitoes (Diptera: *Culicidae*) in Connecticut, USA: a ten-year analysis, 1997–2006. *Vector Borne Zoonotic Dis.* 2008;8:175–88. <http://dx.doi.org/10.1089/vbz.2007.0169>

## RESEARCH

34. Kunz C, Buckley SM, Casals J. Antibodies in man against Tahyna and Lumbo viruses determined by hemagglutination-inhibition and tissue-culture neutralization tests. *Am J Trop Med Hyg.* 1964;13:738–41. <http://dx.doi.org/10.4269/ajtmh.1964.13.738>
35. Sonnleitner ST, Lundström J, Baumgartner R, Simeoni J, Schennach H, Zelger R, et al. Investigations on California serogroup orthobunyaviruses in the Tyrols: first description of Tahyna virus in the Alps. *Vector Borne Zoonotic Dis.* 2014; 14:272–7. <http://dx.doi.org/10.1089/vbz.2013.1360>
36. Kuniholm MH, Wolfe ND, Huang CYH, Mpoudi-Ngole E, Tamoufe U, LeBreton M, et al. Seroprevalence and distribution of *Flaviviridae*, *Togaviridae*, and *Bunyaviridae* arboviral infections in rural Cameroonian adults. *Am J Trop Med Hyg.* 2006;74:1078–83. <http://dx.doi.org/10.4269/ajtmh.2006.74.1078>
37. Elliott RM. Orthobunyaviruses: recent genetic and structural insights. *Nat Rev Microbiol.* 2014;12:673–85. <http://dx.doi.org/10.1038/nrmicro3332>
38. Blakqori G, Delhaye S, Habjan M, Blair CD, Sánchez-Vargas I, Olson KE, et al. La Crosse bunyavirus nonstructural protein NSs serves to suppress the type I interferon system of mammalian hosts. *J Virol.* 2007;81:4991–9. <http://dx.doi.org/10.1128/JVI.01933-06>
39. Taylor KG, Woods TA, Winkler CW, Carmody AB, Peterson KE. Age-dependent myeloid dendritic cell responses mediate resistance to La Crosse virus-induced neurological disease. *J Virol.* 2014;88:11070–9. <http://dx.doi.org/10.1128/JVI.01866-14>
40. Bennett RS, Gresko AK, Murphy BR, Whitehead SS. Tahyna virus genetics, infectivity, and immunogenicity in mice and monkeys. *Viol J.* 2011;8:135. <http://dx.doi.org/10.1186/1743-422X-8-135>
41. Bennett RS, Nelson JT, Gresko AK, Murphy BR, Whitehead SS. The full genome sequence of three strains of Jamestown Canyon virus and their pathogenesis in mice or monkeys. *Viol J.* 2011;8:136. <http://dx.doi.org/10.1186/1743-422X-8-136>
42. Butchi NB, Woods T, Du M, Morgan TW, Peterson KE. TLR7 and TLR9 trigger distinct neuroinflammatory responses in the CNS. *Am J Pathol.* 2011;179:783–94. <http://dx.doi.org/10.1016/j.ajpath.2011.04.011>
43. Winkler CW, Myers LM, Woods TA, Messer RJ, Carmody AB, McNally KL, et al. Adaptive immune responses to Zika virus are important for controlling virus infection and preventing infection in brain and testes. *J Immunol.* 2017;198:3526–35. <http://dx.doi.org/10.4049/jimmunol.1601949>
44. Bennett RS, Cress CM, Ward JM, Firestone CY, Murphy BR, Whitehead SS. La Crosse virus infectivity, pathogenesis, and immunogenicity in mice and monkeys. *Viol J.* 2008;5:25. <http://dx.doi.org/10.1186/1743-422X-5-25>
45. Winkler CW, Race B, Phillips K, Peterson KE. Capillaries in the olfactory bulb but not the cortex are highly susceptible to virus-induced vascular leak and promote viral neuroinvasion. *Acta Neuropathol.* 2015;130:233–45. <http://dx.doi.org/10.1007/s00401-015-1433-0>
46. Winkler CW, Myers LM, Woods TA, Carmody AB, Taylor KG, Peterson KE. Lymphocytes have a role in protection, but not in pathogenesis, during La Crosse virus infection in mice. *J Neuroinflammation.* 2017;14:62. <http://dx.doi.org/10.1186/s12974-017-0836-3>

Address for correspondence: Karin E. Peterson, National Institutes of Health, National Institute of Allergy and Infectious Diseases, Laboratory of Persistent Viral Diseases, Rocky Mountain Laboratories, 903 S 4th St, Hamilton, MT 59840, USA; email: [petersonka@niaid.nih.gov](mailto:petersonka@niaid.nih.gov)

## The Public Health Image Library (PHIL)



The Public Health Image Library (PHIL), Centers for Disease Control and Prevention, contains thousands of public health–related images, including high-resolution (print quality) photographs, illustrations, and videos.

PHIL collections illustrate current events and articles, supply visual content for health promotion brochures, document the effects of disease, and enhance instructional media.

PHIL images, accessible to PC and Macintosh users, are in the public domain and available without charge.

Visit PHIL at <http://phil.cdc.gov/phil>



# *Klebsiella pneumoniae* ST307 with *bla*<sub>OXA-181</sub>, South Africa, 2014–2016

Michelle Lowe,<sup>1</sup> Marleen M. Kock, Jennifer Coetzee, Ebrahim Hoosien, Gisele Peirano, Kathy-Ann Strydom, Marthie M. Ehlers, Nontombi M. Mbelle, Elena Shashkina, David B. Haslam, Puneet Dhawan, Robert J. Donnelly, Liang Chen,<sup>1</sup> Barry N. Kreiswirth, Johann D.D. Pitout

*Klebsiella pneumoniae* sequence type (ST) 307 is an emerging global antimicrobial drug-resistant clone. We used whole-genome sequencing and PCR to characterize *K. pneumoniae* ST307 with oxacillinase (OXA) 181 carbapenemase across several private hospitals in South Africa during 2014–2016. The South Africa ST307 belonged to a different clade (clade VI) with unique genomic characteristics when compared with global ST307 (clades I–V). Bayesian evolution analysis showed that clade VI emerged around March 2013 in Gauteng Province, South Africa, and then evolved during 2014 into 2 distinct lineages. *K. pneumoniae* ST307 clade VI with OXA-181 disseminated over a 15-month period within 42 hospitals in 23 cities across 6 northeastern provinces, affecting 350 patients. The rapid expansion of ST307 was most likely due to intrahospital, interhospital, intercity, and interprovince movements of patients. This study highlights the importance of molecular surveillance for tracking emerging antimicrobial clones.

The World Health Organization recently identified global spread of antimicrobial resistance (AMR) as one of the most serious recent threats to human health (1). The emergence and spread of carbapenem resistance is a substantial public health concern, because these agents are regarded as one of the last effective therapies available for treating serious infections caused by gram-negative bacteria. Carbapenemases, the predominant cause of carbapenem resistance, are commonly harbored on plasmids that are able to transfer between members of the family *Enterobacteriaceae* (2). The

most common carbapenemases among clinical *Enterobacteriaceae* are the *Klebsiella pneumoniae* carbapenemases (KPCs; Ambler class A); the metallo- $\beta$ -lactamases (IMPs, VIMs, NDMs; Ambler class B); and oxacillinase 48 (OXA-48)-like (Ambler class D) enzymes.

The OXA-48-like carbapenemases are identified mostly in *K. pneumoniae* and *Escherichia coli* and include the following enzymes: OXA-48, OXA-162, OXA-181, OXA-204, OXA-232, OXA-244, OXA-245, and OXA-247 (3). They are active against penicillins and weakly hydrolyze carbapenems, with limited activities against broad-spectrum cephalosporins and most  $\beta$ -lactam inhibitors.

The earliest reported case in South Africa of a *K. pneumoniae* that contained *bla*<sub>OXA-48</sub> occurred in Johannesburg in 2011; the case-patient had previously been hospitalized in Egypt (4). The report also described OXA-181-producing *K. pneumoniae* from different Johannesburg and Cape Town private hospitals. Laboratory surveillance reports showed that OXA-48-like enzymes are the second most common carbapenemase (after NDMs) in various health-care centers across South Africa (5).

The molecular diagnostic reference center at Ampath Laboratories (Amphath-MDRC) in Pretoria, Gauteng Province, South Africa, experienced a substantial increase of *K. pneumoniae* with *bla*<sub>OXA-48-like</sub> during 2014–2016 from different private hospitals across northeastern South Africa. We designed a study to investigate the underlying molecular mechanisms associated with the increase of *K. pneumoniae* with OXA-48-like enzymes. We obtained ethics approval from the Conjoint Health Research Ethics Board at the University of Calgary (REB17-1010) and from the Research Ethics Committee (REC), Faculty of Health Sciences, University of Pretoria (protocol nos. 240/2016 and 104/2017).

## Materials and Methods

### Setting and Workflow

We described South Africa's health system and the role of Amphath-MDRC (Appendix, <https://wwwnc.cdc.gov/EID/>

Author affiliations: University of Pretoria, Pretoria, South Africa (M. Lowe, M.M. Kock, K.-A. Strydom, M.M. Ehlers, N.M. Mbelle, J.D.D. Pitout); National Health Laboratory Service, Pretoria (M. Lowe, M.M. Kock, K.-A. Strydom, M.M. Ehlers, N.M. Mbelle); Amphath Laboratories, Pretoria (J. Coetzee, E. Hoosien); Calgary Laboratory Services, Calgary, Alberta, Canada (G. Peirano, J.D.D. Pitout); University of Calgary, Calgary (G. Peirano, J.D.D. Pitout); Rutgers University, Newark, New Jersey, USA (E. Shashkina, L. Chen, B.N. Kreiswirth); Cincinnati Children's Hospital Medical Center, Cincinnati, Ohio, USA (D.B. Haslam); New Jersey Medical School, Newark (P. Dhawan, R.J. Donnelly)

DOI: <https://doi.org/10.3201/eid2504.181482>

<sup>1</sup>These authors contributed equally to this article.

article/25/4/18-1482-App1.pdf). We also summarized the study workflow (Appendix Figure 1).

We screened all carbapenem-nonsusceptible *K. pneumoniae* at Ampath-MDRC using a PCR for *bla*<sub>NDM</sub>, *bla*<sub>KPC</sub>, *bla*<sub>OXA-48</sub>-like, *bla*<sub>IMP</sub>, *bla*<sub>VIM</sub>, and *bla*<sub>GES</sub>. We performed pulsed-field gel electrophoresis (PFGE) on 471 *K. pneumoniae* isolates positive for OXA-48-like enzyme to determine if some of the isolates were genetically related. We identified 1 dominant pulsotype (pulsotype A) and a related pulsotype (AR) and selected isolates representing them from different geographic sites over various time periods. We used these isolates for initial Illumina short-read sequencing (n = 28) (Illumina, <http://www.illumina.com>) and PacBio long-read sequencing (n = 1) (Pacific Biosciences, <http://www.pacb.com>) to determine if they belong to the same sequence type and to identify the OXA-48-like enzyme.

We identified the pulsotypes as sequence type (ST) 307 containing OXA-181 on IncX3 plasmids. We then compared this whole-genome sequencing (WGS) data with the sequences from the US National Center for Biotechnology Information (NCBI) genome database (<ftp://ftp.ncbi.nih.gov/genomes>) to design PCR primers for the detection of ST307, IncX3, and OXA-181-IS3000 mobile genetic element (MGE). We used previously characterized *K. pneumoniae* STs with different plasmid replicons to verify these primers (Appendix Table 1). We screened *K. pneumoniae* producing OXA-48-like enzyme (n = 471) with PCR primers to identify ST307, IncX3 plasmids, and OXA-181-IS3000 MGE. We selected additional *K. pneumoniae* ST307 isolates (n = 60) from different geographic locations, time points, and specimens to undergo Illumina short-read WGS to elucidate the evolution of ST307 in South Africa.

### Bacterial Isolates

During January 2014–December 2016, various Ampath regional clinical laboratories referred 1,247 unique clinical, carbapenem (i.e., ertapenem, meropenem, or imipenem) nonsusceptible *K. pneumoniae* isolates to Ampath-MDRC for PCR confirmation of carbapenemases (Appendix Figure 1). We performed PCR screening for *bla*<sub>NDM</sub>, *bla*<sub>KPC</sub>, *bla*<sub>OXA-48</sub>-like, *bla*<sub>IMP</sub>, *bla*<sub>VIM</sub>, and *bla*<sub>GES</sub> using LightMix modular carbapenemase kits (TIB Molbiol, <https://www.tib-molbiol.com>) on a LightCycler 480 II instrument (Roche Diagnostics, <https://www.roche.com>). Details on the identification and susceptibility testing of the bacterial isolates are provided in the Appendix.

### PFGE

We performed PFGE on the *K. pneumoniae* isolates with OXA-48-like enzymes (n = 471) to determine if there was a dominant pulsotype among them. The Appendix describes the methodology used and results obtained with PFGE.

### PCR

We designed 3 sets of PCR primers for the detection of ST307, IncX3 plasmid, and the IS3000-OXA MGE. We screened *K. pneumoniae* isolates with OXA-48-like enzymes (n = 471) using different primer sequences (Appendix Table 1).

### WGS and Data Analysis

We sequenced the *K. pneumoniae* isolates that tested positive by PCR for ST307 (n = 88) using the Illumina NextSeq platform (Appendix). We prepared libraries with the Illumina Nextera XT kit to produce paired end reads of 150 bp for a predicted coverage of  $\geq 75\times$ . We chose *K. pneumoniae* I72 (isolated from urine obtained in Benoni, Gauteng Province, during December 2014) that was positive for *bla*<sub>OXA-181</sub> and *bla*<sub>OXA-48</sub> for long-read WGS using the RSII platform (Pacific Biosciences) to characterize plasmids.

We compared the South Africa genomes sequenced in this study (deposited in the NCBI Bioproject database [<https://www.ncbi.nlm.nih.gov/bioproject>] under accession no. PRJ-NA488070) with 620 ST307 genomes previously deposited in the NCBI Sequence Read Archive (<https://www.ncbi.nlm.nih.gov/sra>) and the genome database. The global ST307 genomes were from the United States (n = 488), the United Kingdom (n = 45), Norway (n = 30), Italy (n = 10), Thailand (n = 9), Australia (n = 6), Brazil (n = 3), Colombia (n = 3), China (n = 3), Nepal (n = 3), Cambodia (n = 2), France (n = 2), Nigeria (n = 2), Cameroon (n = 1), Guinea (n = 1), Iran (n = 1), Netherlands (n = 1), Pakistan (n = 1), and other unspecified regions (n = 9).

We mapped all genomes to the ST307 reference genome NR5632 (GenBank accession no. CP025143) using Snippy (<https://github.com/tseemann/snippy>). We predicted prophages using PHASTER (6), examined repeated regions using MUMmer (7), and predicted putative regions of recombination with Gubbins (8), followed by filtering using vcftools. We generated a recombination-free single-nucleotide polymorphism phylogenetic tree, using a general time-reversible model of nucleotide substitution with a gamma model of rate heterogeneity and 4 rate categories, by using RAXML version 8.2.4 (9). We conducted hierarchical Bayesian analysis of population structure with 3 nested levels and 10 independent runs of the stochastic optimization algorithm with the a priori upper bound of 10–30 clusters varying across the runs to identify phylogenetic clades. We defined clades using the first level of clustering (10) and annotated the phylogenetic tree in iTOL (11).

We used BEAST version 2.4.7 (12) to estimate a timed phylogeny with concatenated recombination-free core single-nucleotide polymorphism alignment. To increase the accuracy of the time to most recent common ancestor, we included 17 additional ST307 isolates from a Pretoria academic hospital in this analysis. We identified the *bla*<sub>OXA181</sub> harboring IncX3 plasmids by de novo assembly using plasmidSPAdes (13) and manually investigated the findings

using Bandage assembly graph viewer (14) and blastn (<https://blast.ncbi.nlm.nih.gov/Blast.cgi>), as well as S1-PFGE in combination with Southern blotting (Appendix).

## Results

### Overview

Ampath-MDRC experienced an increase in OXA-48–like *K. pneumoniae* isolates during July 2015–June 2016, especially from private hospitals in Gauteng Province. We identified by PFGE a dominant pulsotype named A (and a related pulsotype AR) among the OXA-48–like collection. Initial WGS on 28 isolates that belong to pulsotypes A and AR identified them as ST307 with OXA-181 on IncX3 plasmid that was shown using PacBio long-read sequencing. Using WGS, we used PCR primers specific to ST307, IncX3, and OXA-181-IS3000 MGE to screen the OXA-48–like *K. pneumoniae* and showed that 74% belonged to ST307 containing IncX3 plasmids.

WGS of an additional 60 PCR-positive ST307 illustrated, when compared with ST307 from other countries, that the South Africa ST307 belonged to a different clade. The South Africa clade emerged around March 2013 in Gauteng Province, then evolved during 2014 into 2 distinct lineages that spread across northeastern South Africa, affecting 350 patients.

### Increase of OXA-48–Like Positive *K. pneumoniae* across Northeastern South Africa

Overall, 574 carbapenemase gene PCR-positive *K. pneumoniae* were detected at Ampath-MDRC during January 2014–December 2016; the total included NDM (n = 58), KPC (n = 10), VIM (n = 35), and OXA-48–like (n = 471) carbapenemases (Appendix Table 2). The OXA-48–like isolates from 2014 came mainly from different private hospitals in Johannesburg and Alberton, Gauteng Province. The numbers of OXA-48–like *K. pneumoniae* increased exponentially toward the end of 2015 and peaked during the first 6 months of 2016 (e.g., we detected 349/471 [74%] of OXA-48–like *K. pneumoniae* during July 2015–June 2016). This increase was especially evident in various hospitals across the province. Private hospitals from other areas in northern and eastern South Africa also experienced increases during 2015–2016 (Appendix Table 2). Throughout the study period, the numbers of *K. pneumoniae* with KPC, NDM, and VIM remained relatively low and stable compared with OXA-48–like *K. pneumoniae*. PCR testing did not detect IMP or GES during this period.

We obtained OXA-48–like *K. pneumoniae* from intraabdominal specimens (n = 78), urine (n = 196), skin and soft tissues (n = 11), blood (n = 76), central venous catheter tips (n = 8), respiratory specimens (n = 99), and rectal specimens (n = 3). The isolates tested nonsusceptible

(intermediate or full resistance) to ampicillin, amoxicillin/clavulanic acid, piperacillin/tazobactam, cefotaxime, ceftazidime, cefepime, and ertapenem. Most isolates were also nonsusceptible to trimethoprim/sulfamethoxazole (98%), gentamicin (98%), ciprofloxacin (92%), and meropenem (52%), whereas 44% of isolates were nonsusceptible to imipenem and 11% to amikacin. The tigecycline (TGC) and colistin MICs were each  $\leq 1$   $\mu\text{g/mL}$ , except for 4 isolates that had TGC MICs of 2, 4, 4, and 8  $\mu\text{g/mL}$ .

### Dissemination of ST307 across Private Hospitals

PCR screening of OXA-48–like *K. pneumoniae* showed that 350/471 (74%) isolates were positive for ST307, IncX3, and IS3000-OXA-181 (cited as ST307\_X3-OXA-181). ST307\_X3-OXA-181 appeared in different private hospitals in Johannesburg and Alberton during January–June 2014 (Figures 1, 2). During July 2014–June 2016, ST307\_X3-OXA-181 subsequently spread to other private hospitals in Gauteng Province, especially in Pretoria, and to Mpumalanga, North West, Limpopo, Free State, and Eastern Cape Provinces (Figures 1, 2). Gauteng Province was the epicenter of the dissemination of ST307\_X3-OXA-181, showing a substantial increase in numbers from 2014 (n = 18) to 2015 (n = 138) (Figure 1).

We isolated ST307\_X3-OXA-181 mostly from urine (41%), respiratory (20%), intraabdominal (18%), and blood (16%) specimens; 96% of specimens were submitted from hospital settings. Ampath-MDRC receives  $\approx 80\%$  of community, nursing home, and hospital specimens from the private sector in Gauteng, Mpumalanga, North West, Limpopo, Free State, and Eastern Cape Provinces. We isolated ST307\_X3-OXA-181 exclusively from hospital

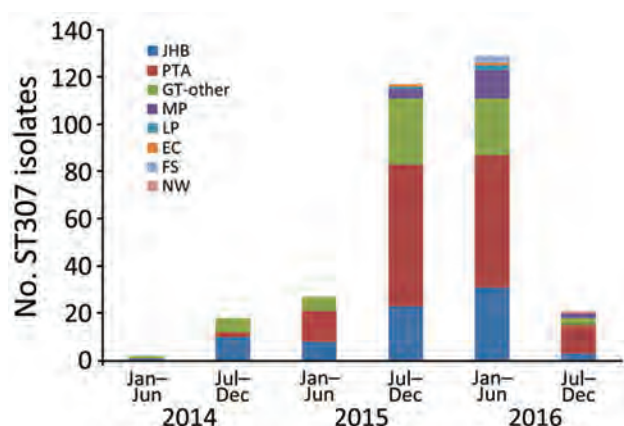


**Figure 1.** Locations of *Klebsiella pneumoniae* with ST307 oxacillinase 48–like in South Africa during January 2014–December 2016, as identified at Ampath Molecular Diagnostic Reference Center (PTA). EC, Eastern Cape Province; FS, Free State Province; GT-other, other cities in Gauteng Province; JHB, Johannesburg, Gauteng Province; LP, Limpopo Province; MP, Mpumalanga Province; NW, North West Province; PTA, Pretoria, Gauteng Province; ST, sequence type.



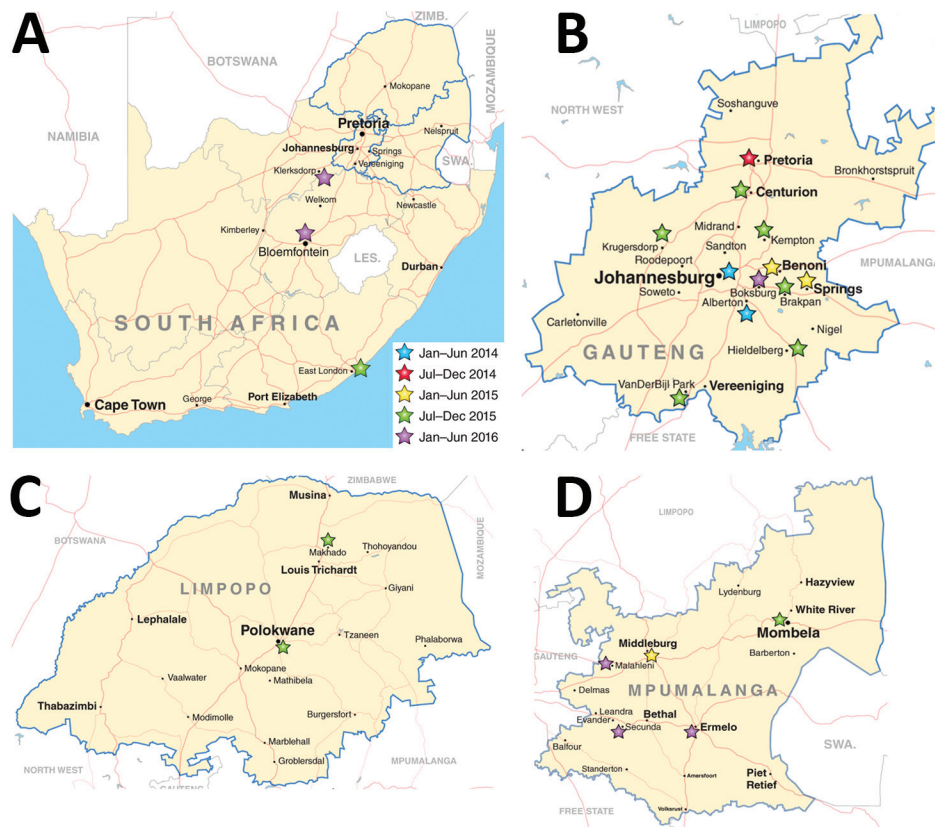


**Figure 2.** Geographic distribution of *Klebsiella pneumoniae* sequence type 307 with oxacillinase 181 in northeastern South Africa, January 2014–December 2016. A) South Africa; B) Gauteng Province; C) Limpopo Province; D) Mpumalanga Province. Map source: <http://d-maps.com>.

specimens; therefore, it is unlikely that the community or nursing home sectors were important reservoirs of ST307.

### South Africa *K. pneumoniae* ST307 Clade

The overall characteristics of the ST307 sequences from this study ( $n = 88$ ) were similar to ST307 with  $bla_{KPC}$  and  $bla_{CTX-M-15}$  sequences obtained previously in Colombia, Italy, and the United Kingdom, and those in this study contained the capsular loci  $wzi-173$ , capsule 2,  $\pi$ -fimbrial cluster, Type IV secretion system (15). The hierarchical Bayesian clustering analysis of 88 South Africa ST307 and additional 620 genomes from publicly available databases divided ST307 into 6 distinct clades: clades I–IV, from the United States (mainly Texas) (16); clade V, from various countries (Australia, Brazil, Cambodia, Cameroon, China, Colombia, France, Guinea, Iran, Italy, Nepal, Netherlands, Nigeria, Norway, Pakistan, Thailand, the United Kingdom, and the United States); and clade VI, which consisted of the isolates from South Africa (Figure 3). Clade V also includes a subset of isolates from Texas. Sequence analysis of the mutations in the quinolone resistance-determining regions in chromosomal  $gyrA$  and  $parC$  indicated that most of the isolates from clades V and VI contained the ParC-80I and GyrA-83I mutations, whereas isolates from clades I–IV harbored an additional GyrA-87N mutation (Figure 3).

Genomic analysis revealed that clade VI isolates contained some unique characteristics when compared with clades I–V. All of clade VI harbored the plasmid  $p72\_X3\_OXA181$  with  $bla_{OXA-181}$  that contained the IncX3 and truncated ColKp3 replicons (Appendix Figure 2). Approximately 30% of isolates in clades I–V contained various carbapenemase genes, namely  $bla_{KPC-2}$  ( $n = 184$ ),  $bla_{KPC-3}$  ( $n = 4$ ),  $bla_{NDM-1}$  ( $n = 3$ ),  $bla_{NDM-5}$  ( $n = 2$ ), and  $bla_{OXA-48}$  ( $n = 2$ ). KPC-2 was distributed within clades I–V, whereas KPC-3, NDM-1, NDM-5, and OXA-48 were restricted to clade V (Figure 3). Most ST307 isolates in clades I–VI contained the extended-spectrum  $\beta$ -lactamase gene  $bla_{CTX-M-15}$  (684/708, 96.6%) that was adjacent to  $ISEcp1$  (682/684, 99.7%) situated on a FIB-like plasmid and showed high similarities to the previously described  $pKPN3-307\_type\ A$  plasmid (15).

We identified 5 prophages (72\_page 1–5) and 1 novel integrative conjugative element (72\_ICE) within the 88 sequenced ST307 that belonged to clade VI (Figure 3); the 72\_pages 2, 3, and 4 correlated with the previously described ST307 phages 1, 3, and 4 (15). The 72\_page1, 72\_page5, and 72\_ICE were mainly restricted in clade VI; 72\_ICE was unique to clade VI, whereas 72\_page1 was also present in 5 isolates and 72\_page5 in 23 isolates from clade V. The 72\_page3 and 72\_page4 were found in clade VI and a subset of clade V, and the 72\_page2 was part of ST307 isolates from clusters I–VI (Figure 3).

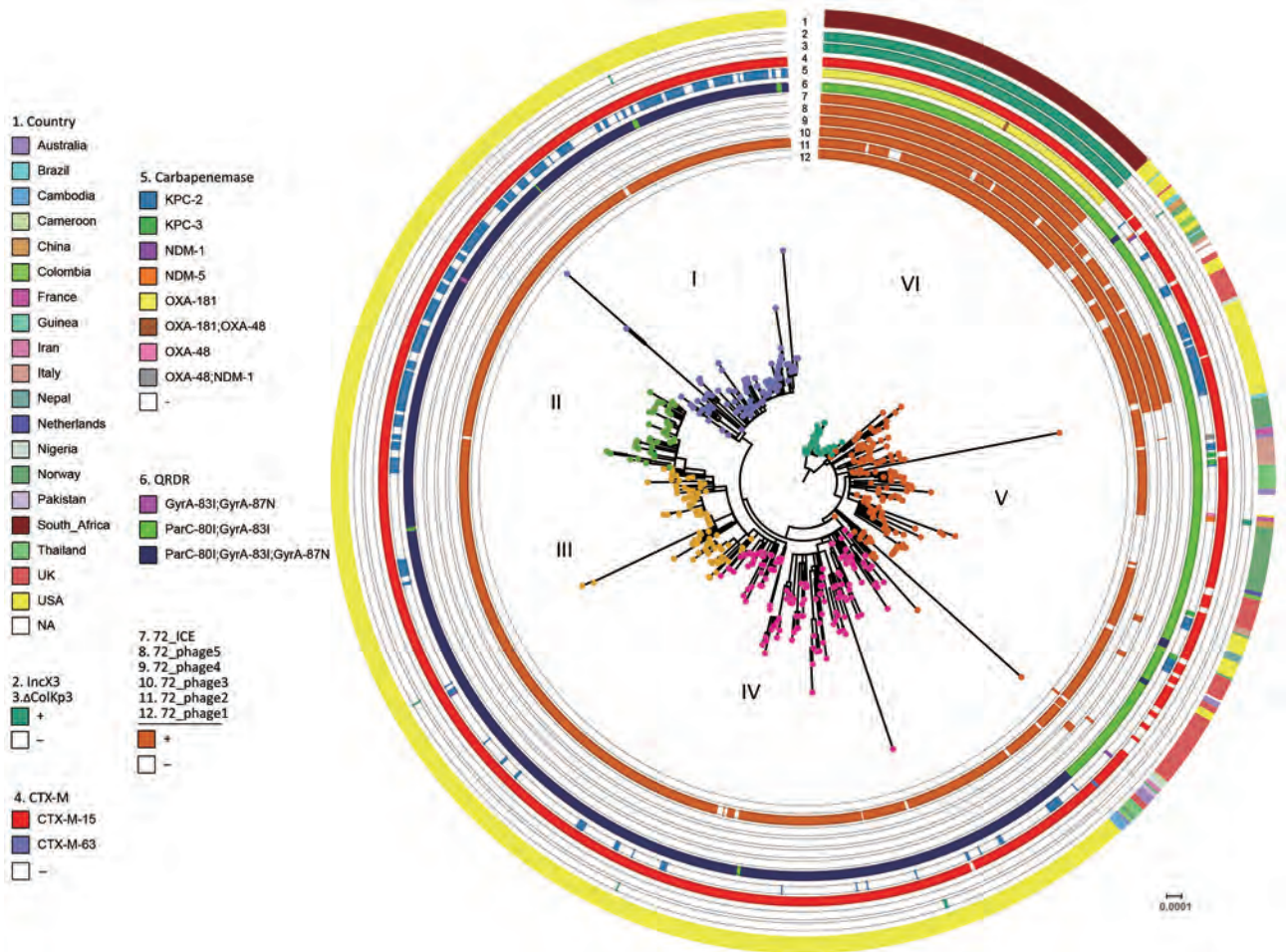


**Figure 3.** Bayesian phylogenetic analysis of global *Klebsiella pneumoniae* sequence type (ST) 307 isolates. The ST307 genomes included 88 from South Africa (this study) and 620 international isolates from 19 countries (downloaded from the US National Center for Biotechnology Information whole genome shotgun database). ST307 has 6 distinct clades, as indicated on branches. CTX-M, active on cefotaxime first isolated in Munich; KPC, *Klebsiella pneumoniae* carbapenemase; NDM, New Delhi metallo-β-lactamases; OXA, active on oxacillin; QRDR, quinolone resistance determinants.

### Origin of ST307 Clade VI

Bayesian evolution analysis conducted with BEAST estimated the time to most recent common ancestor of clade VI around March 2013, ≈2 months before the first isolate (C6) that was collected in May 2013 from a Johannesburg hospital, J1 (Figure 4). We estimated the mean evolutionary rate as  $1.16 \times 10^{-6}$  substitutions/site/year (95% highest posterior density  $7.7 \times 10^{-7}$  to  $1.6 \times 10^{-6}$  substitutions/site/year), corresponding to 5.7 substitutions/genome/year among clade VI. This analysis placed the outbreak node, from which all outbreak isolates were derived, at April 2014 (95% highest posterior density September 2013–September 2014).

Two distinct lineages evolved within Gauteng Province from the outbreak node. Lineage A originated in Johannesburg and lineage B in Alberton, and they spread to different hospitals across Gauteng (both lineages), Mpumalanga (both lineages), Free State (lineage A), Eastern Cape

(lineage A), Limpopo (lineage A), and North West Provinces (lineage B) (Figure 4).

### Dissemination by Movement of Patients

Genomics, combined with admission, discharge, and transfer data, showed evidence of intrahospital spread. For example, patient I51 in hospital P5 was transferred during December 2015 from the medical intensive care unit to the high-risk unit. Subsequently a highly related ST307 was isolated during January 2016 from patient I68 in the high-risk unit (Figure 4). We also observed interhospital spread when patient I14 was transferred from the surgical intensive care unit at hospital P1 to hospital P4 during September 2016. In December 2016, a highly related ST307 was isolated at hospital P4 from patient K43 (Figure 4). Intercity and interprovince spread were illustrated by patient I2 from the city of Springs, patient K61 from the town of Heidelberg, and patient K22



from the North West Province, all with highly related ST307 isolates, having previously received medical care at hospital J2 in Johannesburg (Figure 4).

**Discussion**

*K. pneumoniae* producing OXA-181 was first described as isolated in hospitals in India during 2006–2007 (17),

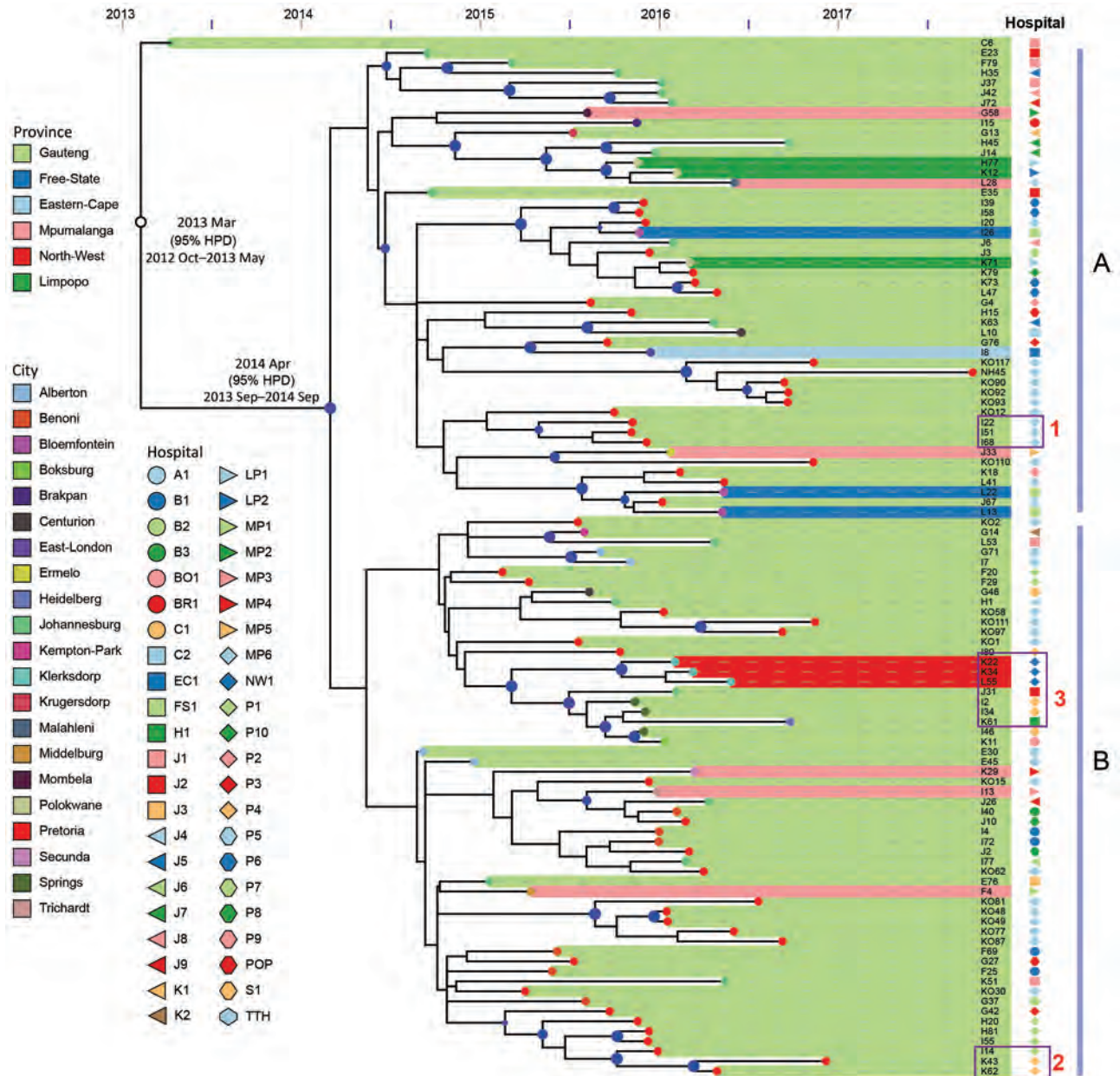


**Figure 4.** Bayesian evolution analysis of *Klebsiella pneumoniae* sequence type (ST) 307 in South Africa hospitals, January 2014–December 2016. A and B indicate the 2 distinct lineages that evolved within Gauteng Province. Highlighted areas depict the provinces from which isolates were obtained, and colored dots at the tips of areas represent the cities from which the isolates were obtained (e.g., for Gauteng Province, Pretoria is red, Johannesburg is green). Dark blue dots at branch points indicate posterior probability >70%, and dot size is proportional to posterior probability values. Hospital locations are indicated as follows; all are private except for Tshwane tertiary hospital: A1, Alberton; J1–J10, Johannesburg; P1–P8, Pretoria; B1–3, Benoni; BO1, Boksburg; BR1, Brakpan; C1–C2, Centurion; EC1, Eastern Cape Province; FS1, Free State Province; K1, Krugersdorp; K2, Kempton Park; LP1–2, Limpopo Province; MP1–6, Mpumalanga Province; NW1, North West Province; S1, Springs; TTH, Tshwane (tertiary hospital). Box 1 shows intrahospital spread: highly related ST307 isolates were obtained from patient I51 and patient I68 in hospital P5. Box 2 shows interhospital spread: patient I14 was transferred from hospital P1 to hospital P4; 3 months later, highly related ST307 was isolated from patient K43 at hospital P4. Box 3 shows intercity and interprovince spread: patient I2 from Springs, patient K61 from Heidelberg, and patient K22 from North West Province, all with highly related ST307 isolates, had previously received medical care at hospital J2 in Johannesburg. HPD, highest posterior density interval; POP, outpatient.



with a subsequent report from Oman (18). OXA-181 has a global distribution, is the second most common OXA-48 derivative, and differs from OXA-48 by 4 amino acid substitutions, while retaining the same spectrum of activity (3). Various *K. pneumoniae* clones with OXA-48–like carbapenemases have been described from several localized hospital outbreaks in Africa, Europe, and the Middle East (3). Previous studies have shown that bla<sub>OXA-181</sub> are present on ColE2-type (18), IncT (19), IncN (20), and IncX3 (21) plasmids.

We describe the dissemination of a carbapenemase-producing clone, *K. pneumoniae* ST307 containing an IncX3 plasmid with bla<sub>OXA-181</sub>, across 23 cities and towns within 6 provinces in South Africa. The plasmid (p72\_X3\_OXA181) was identical to other IncX3 plasmids with bla<sub>OXA-181</sub> previously reported from China (21) and Angola (22). We tracked (with PCR) and confirmed (with WGS) the presence of ST307 within Gauteng, Mpumalanga, North West, Limpopo, Free State, and Eastern Cape provinces. Genomics combined with admission, discharge, and transfer data showed intra-hospital, interhospital, intercity, and interprovince spread to involve 350 patients in 42 private hospitals.

*K. pneumoniae* ST307 is a superclone that emerged during the mid-1990s and was responsible for several worldwide nosocomial outbreaks (23). The earliest published report was in 2013 from hospitals in Texas, USA (24), and it has since been reported globally (23). ST307 is associated with several antimicrobial resistance determinants, including CTX-M-15 (25), KPC (26), OXA-48 (27), NDM-1 (28), and *mcr-1* (29). Recent reports from Texas (16), Colombia (26), and Italy (30) have shown that ST307 is replacing ST258 as the most prevalent clone associated with multidrug resistance. Certain characteristics of ST307 may lead to increased fitness, persistence, and adaptation to the hospital environment and the human host (15).

*K. pneumoniae* ST307 belongs to 6 distinct clades: US clades I–IV; an international clade, V; and South Africa clade VI. The presence of 72\_ICE, p72\_X3\_OXA181 is unique to clade VI and, with other genetic changes, may have played a role in the success of this clade. Bayesian evolution analysis showed that clade VI emerged around March 2013 and evolved during 2014 into 2 distinct lineages that spread across northeastern South Africa over a 15-month period.

In 2014, the World Health Organization reported that key tools to tackle AMR, such as basic surveillance systems to track and monitor the problem, do not exist in many countries (1). This study highlighted the public health and clinical utility of using WGS data to develop rapid, reliable, and user-friendly molecular surveillance methods such as PCR for tracking emerging AMR clones and plasmids during outbreaks. We designed PCR primers for tracking ST307 and p72\_X3\_OXA181 across northeastern South

Africa. From a global perspective, this study is an example of a productive collaboration between resource-limited and industrialized countries that rapidly generated cost-effective PCR methodologies to track an emerging AMR clone.

*K. pneumoniae* ST307 clade VI spread rapidly between various private hospitals across South Africa. The reasons for this are unclear, but the medical community needs to know how and why this happened. The increase in OXA-48–like bacteria occurred during a period of high carbapenem usage in the private sector (J. Coetzee, unpub. data). Patients often visit various private hospitals during their treatment. Our results suggest that the intrahospital, interhospital, intercity, and interprovince movements of patients were responsible for the dissemination of ST307.

It is imperative that the medical community continues to explore the reasons for the spread of ST307. Studies investigating the pathogenicity, fitness, adaptiveness, and evolution of ST307 clade VI are currently in progress. The South Africa clade VI has the potential to be introduced to other countries and the ability to cause devastating country-wide outbreaks associated with substantial healthcare costs. A recent report from the United Kingdom highlighted the economic implications associated with a 10-month outbreak of carbapenemase-producing *K. pneumoniae* affecting 40 patients from 5 hospitals across London, costing around €1.1 million (31). Clinical studies are also urgently required to investigate the reasons for the high transmission rates of *K. pneumoniae* ST307. Such projects will serve as models to predict what could happen with the continuing emergence of successful clones among clinically relevant bacteria (32).

### Acknowledgments

We thank the Department of Medical Microbiology of Ampath Laboratories and the National Health Laboratory Service for the use of their facilities and for providing isolates. We also thank Anthony Smith for the donation of the *Salmonella enterica* subsp. *enterica* serovar Braenderup isolate (ATCC BAA-664).

This work was supported in part by research grants from Calgary Laboratory Services (10015169; J.D.D.P.), National Institutes of Health grants R01AI090155 (B.N.K.) and R21AI117338 (L.C.), and the NHLS Research Trust (M.M.K.); and RESCOM, University of Pretoria (M.M.K.). M.L. was supported by a National Research Foundation grant. Opinions expressed and conclusions arrived at are those of the authors and are not necessarily to be attributed to the NRF. The funders of the study had no role in the study design, data collection, data analysis, interpretation, or writing of the report. The corresponding author had full access to all the data and takes final responsibility for this publication.

Declaration of interest: J.D.D.P. had previously received research funds from Merck and Astra Zeneca. Other authors have nothing to declare.

## About the Author

Ms. Lowe is a PhD student at the University of Pretoria. Her research interests include the molecular epidemiology of antimicrobial-resistant organisms.

## References

- World Health Organization. Antimicrobial resistance: global report on surveillance 2014. Geneva: The Organization; 2014 [cited 2019 Feb 8]. <https://www.who.int/drugresistance/documents/surveillance-report/en>
- Pitout JD, Nordmann P, Poirel L. Carbapenemase-producing *Klebsiella pneumoniae*, a key pathogen set for global nosocomial dominance. *Antimicrob Agents Chemother*. 2015;59:5873–84. <http://dx.doi.org/10.1128/AAC.01019-15>
- Mairi A, Pantel A, Sotto A, Lavigne JP, Touati A. OXA-48-like carbapenemases producing *Enterobacteriaceae* in different niches. *Eur J Clin Microbiol Infect Dis*. 2018;37:587–604. <http://dx.doi.org/10.1007/s10096-017-3112-7>
- Brink AJ, Coetzee J, Corcoran C, Clay CG, Hari-Makkan D, Jacobson RK, et al. Emergence of OXA-48 and OXA-181 carbapenemases among *Enterobacteriaceae* in South Africa and evidence of in vivo selection of colistin resistance as a consequence of selective decontamination of the gastrointestinal tract. *J Clin Microbiol*. 2013;51:369–72. <http://dx.doi.org/10.1128/JCM.02234-12>
- Perovic O, Britz E, Chetty V, Singh-Moodley A. Molecular detection of carbapenemase-producing genes in referral *Enterobacteriaceae* in South Africa: a short report. *S Afr Med J*. 2016; 106:975–7. <http://dx.doi.org/10.7196/SAMJ.2016.v106i10.11300>
- Arndt D, Grant JR, Marcu A, Sajed T, Pon A, Liang Y, et al. PHASTER: a better, faster version of the PHAST phage search tool. *Nucleic Acids Res*. 2016;44(W1):W16–21. <http://dx.doi.org/10.1093/nar/gkw387>
- Kurtz S, Phillippy A, Delcher AL, Smoot M, Shumway M, Antonescu C, et al. Versatile and open software for comparing large genomes. *Genome Biol*. 2004;5:R12. <http://dx.doi.org/10.1186/gb-2004-5-2-r12>
- Croucher NJ, Page AJ, Connor TR, Delaney AJ, Keane JA, Bentley SD, et al. Rapid phylogenetic analysis of large samples of recombinant bacterial whole-genome sequences using Gubbins. *Nucleic Acids Res*. 2014;43:e15. <https://doi.org/10.1093/nar/gku1196>
- Stamatakis A. RAxML version 8: a tool for phylogenetic analysis and post-analysis of large phylogenies. *Bioinformatics*. 2014;30:1312–3. <http://dx.doi.org/10.1093/bioinformatics/btu033>
- Cheng L, Connor TR, Sirén J, Aanensen DM, Corander J. Hierarchical and spatially explicit clustering of DNA sequences with BAPS software. *Mol Biol Evol*. 2013;30:1224–8. <http://dx.doi.org/10.1093/molbev/mst028>
- Letunic I, Bork P. Interactive tree of life (iTOL) v3: an online tool for the display and annotation of phylogenetic and other trees. *Nucleic Acids Res*. 2016;44(W1):W242–5. <http://dx.doi.org/10.1093/nar/gkw290>
- Bouckaert R, Heled J, Kühnert D, Vaughan T, Wu CH, Xie D, et al. BEAST 2: a software platform for Bayesian evolutionary analysis. *PLOS Comput Biol*. 2014;10:e1003537. <http://dx.doi.org/10.1371/journal.pcbi.1003537>
- Antipov D, Hartwick N, Shen M, Raiko M, Lapidus A, Pevzner PA. plasmidSPAdes: assembling plasmids from whole genome sequencing data. *Bioinformatics*. 2016;32:3380–7.
- Wick RR, Schultz MB, Zobel J, Holt KE. Bandage: interactive visualization of de novo genome assemblies. *Bioinformatics*. 2015;31:3350–2. <http://dx.doi.org/10.1093/bioinformatics/btv383>
- Villa L, Feudi C, Fortini D, Brisse S, Passet V, Bonura C, et al. Diversity, virulence, and antimicrobial resistance of the KPC-producing *Klebsiella pneumoniae* ST307 clone. *Microb Genom*. 2017;3:e000110. <http://dx.doi.org/10.1099/mgen.0.000110>
- Long SW, Olsen RJ, Eagar TN, Beres SB, Zhao P, Davis JJ, et al. Population genomic analysis of 1,777 extended-spectrum beta-lactamase-producing *Klebsiella pneumoniae* isolates, Houston, Texas: unexpected abundance of clonal group 307. *MBio*. 2017;8:e00489-17. <http://dx.doi.org/10.1128/mBio.00489-17>
- Castanheira M, Deshpande LM, Mathai D, Bell JM, Jones RN, Mendes RE. Early dissemination of NDM-1- and OXA-181-producing *Enterobacteriaceae* in Indian hospitals: report from the SENTRY Antimicrobial Surveillance Program, 2006–2007. *Antimicrob Agents Chemother*. 2011;55:1274–8. <http://dx.doi.org/10.1128/AAC.01497-10>
- Potron A, Nordmann P, Lafeuille E, Al Maskari Z, Al Rashdi F, Poirel L. Characterization of OXA-181, a carbapenem-hydrolyzing class D beta-lactamase from *Klebsiella pneumoniae*. *Antimicrob Agents Chemother*. 2011;55:4896–9. <http://dx.doi.org/10.1128/AAC.00481-11>
- Villa L, Carattoli A, Nordmann P, Carta C, Poirel L. Complete sequence of the IncT-type plasmid pT-OXA-181 carrying the *bla*<sub>OXA-181</sub> carbapenemase gene from *Citrobacter freundii*. *Antimicrob Agents Chemother*. 2013;57:1965–7. <http://dx.doi.org/10.1128/AAC.01297-12>
- McGann P, Snesrud E, Ong AC, Appalla L, Koren M, Kwak YI, et al. War wound treatment complications due to transfer of an IncN plasmid harboring *bla*<sub>OXA-181</sub> from *Morganella morganii* to CTX-M-27-producing sequence type 131 *Escherichia coli*. *Antimicrob Agents Chemother*. 2015;59:3556–62. <http://dx.doi.org/10.1128/AAC.04442-14>
- Liu Y, Feng Y, Wu W, Xie Y, Wang X, Zhang X, et al. First report of OXA-181-producing *Escherichia coli* in China and characterization of the isolate using whole-genome sequencing. *Antimicrob Agents Chemother*. 2015;59:5022–5. <http://dx.doi.org/10.1128/AAC.00442-15>
- Kieffer N, Nordmann P, Aires-de-Sousa M, Poirel L. High prevalence of carbapenemase-producing *Enterobacteriaceae* among hospitalized children in Luanda, Angola. *Antimicrob Agents Chemother*. 2016;60:6189–92. <http://dx.doi.org/10.1128/AAC.01201-16>
- Wyres KL, Hawkey J, Hetland MAK, Fostervold A, Wick RR, Judd LM, et al. Emergence and rapid global dissemination of CTX-M-15-associated *Klebsiella pneumoniae* strain ST307. *J Antimicrob Chemother*. 2018. <http://dx.doi.org/10.1093/jac/dky492>
- Castanheira M, Farrell SE, Wanger A, Rolston KV, Jones RN, Mendes RE. Rapid expansion of KPC-2-producing *Klebsiella pneumoniae* isolates in two Texas hospitals due to clonal spread of ST258 and ST307 lineages. *Microb Drug Resist*. 2013;19:295–7. <http://dx.doi.org/10.1089/mdr.2012.0238>
- Habeeb MA, Haque A, Nematzadeh S, Iversen E, Giske CG. High prevalence of 16S rRNA methylase RmtB among CTX-M extended-spectrum β-lactamase-producing *Klebsiella pneumoniae* from Islamabad, Pakistan. *Int J Antimicrob Agents*. 2013;41:524–6. <http://dx.doi.org/10.1016/j.ijantimicag.2013.02.017>
- Ocampo AM, Chen L, Cienfuegos AV, Roncancio G, Chavda KD, Kreiswirth BN, et al. A two-year surveillance in five Colombian tertiary care hospitals reveals high frequency of non-CG258 clones of carbapenem-resistant *Klebsiella pneumoniae* with distinct clinical characteristics. *Antimicrob Agents Chemother*. 2016; 60:332–42. <http://dx.doi.org/10.1128/AAC.01775-15>
- Novović K, Trudić A, Brkić S, Vasiljević Z, Kojić M, Medić D, et al. Molecular epidemiology of colistin-resistant, carbapenemase-producing *Klebsiella pneumoniae* in Serbia from 2013 to 2016. *Antimicrob Agents Chemother*. 2017;61:e02550-16. <http://dx.doi.org/10.1128/AAC.02550-16>

28. Bocanegra-Ibarias P, Garza-González E, Morfin-Otero R, Barrios H, Villarreal-Treviño L, Rodríguez-Noriega E, et al. Molecular and microbiological report of a hospital outbreak of NDM-1-carrying *Enterobacteriaceae* in Mexico. PLoS One. 2017;12:e0179651. <http://dx.doi.org/10.1371/journal.pone.0179651>
29. Saavedra SY, Diaz L, Wiesner M, Correa A, Arévalo SA, Reyes J, et al. Genomic and molecular characterization of clinical isolates of *Enterobacteriaceae* harboring *mcr-1* in Colombia, 2002 to 2016. Antimicrob Agents Chemother. 2017;61:e00841-17. <http://dx.doi.org/10.1128/AAC.00841-17>
30. Bonura C, Giuffrè M, Aleo A, Fasciana T, Di Bernardo F, Stampone T, et al.; MDR-GN Working Group. An update of the evolving epidemic of *bla*<sub>KPC</sub>-carrying *Klebsiella pneumoniae* in Sicily, Italy, 2014: emergence of multiple non-ST258 clones. PLoS One. 2015;10:e0132936. <http://dx.doi.org/10.1371/journal.pone.0132936>
31. Otter JA, Burgess P, Davies F, Mookerjee S, Singleton J, Gilchrist M, et al. Counting the cost of an outbreak of carbapenemase-producing *Enterobacteriaceae*: an economic evaluation from a hospital perspective. Clin Microbiol Infect. 2017;23:188–96. <http://dx.doi.org/10.1016/j.cmi.2016.10.005>
32. Mathers AJ, Peirano G, Pitout JD. The role of epidemic resistance plasmids and international high-risk clones in the spread of multidrug-resistant *Enterobacteriaceae*. Clin Microbiol Rev. 2015;28:565–91. <http://dx.doi.org/10.1128/CMR.00116-14>

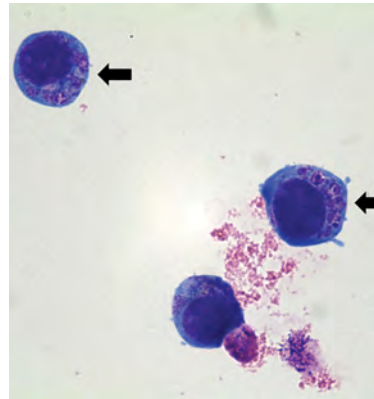
Address for correspondence: Johann D.D. Pitout, Calgary Laboratory Services, #9, 3535 Research Rd NW, Calgary, Alberta, Canada; email: [johann.pitout@cls.ab.ca](mailto:johann.pitout@cls.ab.ca)

# etymologia

## *Anaplasma phagocytophilum* [an"ə-plaz'mə fa'go-sīt"o-fī-lum]

Ronnie Henry

A species of tickborne bacteria that causes human agranulocytic anaplasmosis, *Anaplasma* (from the Greek *an-* ["without?"] + *plasma* ["shape"]) *phagocytophilum* (named for its affinity for growing in neutrophils: phagocyte + Latin *phile* ["loving?"]) has gone by many names. First it was named *Rickettsia* (for Howard Taylor Ricketts) *phagocytophilum*, then *Cytoecetes* (for its similarity to *Cytoecetes microti phagocytophilum*, and then *Ehrlichia* (for Paul Ehrlich) *phagocytophilum*. More recently, *E. equi* and the agent of human granulocytic ehrlichiosis (now anaplasmosis) were combined with *E. phagocytophilum* as *A. phagocytophilum*.



*Anaplasma phagocytophilum* cultured in human promyelocytic cells, showing morulae as basophilic and intracytoplasmic inclusions (arrows). Wright-Giemsa stain. Original magnification x1,000. Image: Emerg Infect Dis. 2014;20:1708–11.

### Source

1. Kim K-H, Yi J, Oh WS, Kim N-K, Choi SJ, Choe PG, et al. Human granulocytic anaplasmosis, South Korea, 2013. Emerg Infect Dis. 2014;20:1708–11. <http://dx.doi.org/10.1016/j.vetpar.2009.09.013>
2. Woldehiwet Z. The natural history of *Anaplasma phagocytophilum*. Vet Parasitol. 2010;167:108–22. <http://dx.doi.org/10.3201/eid2010.131680>

Address for correspondence: Ronnie Henry, Centers for Disease Control and Prevention, 1600 Clifton Rd NE, Mailstop E28, Atlanta, GA 30329-4027, USA; email: [boq3@cdc.gov](mailto:boq3@cdc.gov)

DOI: <https://doi.org/10.3201/eid2504.ET2504>



# Co-infections in Persons with Early Lyme Disease, New York, USA

Gary P. Wormser, Donna McKenna, Carol Scavarda, Denise Cooper, Marc Y. El Khoury, John Nowakowski, Praveen Sudhindra, Alexander Ladenheim, Guiqing Wang, Carol L. Karmen, Valerie Demarest, Alan P. Dupuis II, Susan J. Wong

In certain regions of New York state, USA, *Ixodes scapularis* ticks can potentially transmit 4 pathogens in addition to *Borrelia burgdorferi*: *Anaplasma phagocytophilum*, *Babesia microti*, *Borrelia miyamotoi*, and the deer tick virus subtype of Powassan virus. In a prospective study, we systematically evaluated 52 adult patients with erythema migrans, the most common clinical manifestation of *B. burgdorferi* infection (Lyme disease), who had not received treatment for Lyme disease. We used serologic testing to evaluate these patients for evidence of co-infection with any of the 4 other tickborne pathogens. Evidence of co-infection was found for *B. microti* only; 4–6 patients were co-infected with *Babesia microti*. Nearly 90% of the patients evaluated had no evidence of co-infection. Our finding of *B. microti* co-infection documents the increasing clinical relevance of this emerging infection.

Lyme disease, caused by *Borrelia burgdorferi*, is the most common tickborne infection in North America (1,2). The Lower Hudson Valley, in the US state of New York, is a region of high risk for bites from *Ixodes scapularis* ticks (3). *I. scapularis* ticks in this region, and in certain other geographic areas in New York and the northeastern United States, are responsible for transmission of 4 other pathogens besides *B. burgdorferi*: *Anaplasma phagocytophilum*, the cause of human granulocytic anaplasmosis; *Babesia microti*; *Borrelia miyamotoi*; and the deer tick virus subtype of Powassan virus (POWV) (4–9). The earliest and most common clinical manifestation of Lyme disease is the lesion erythema migrans. To look for evidence of co-infection with these 4 tickborne pathogens, we tested the serum of 52 adult patients with erythema migrans who had not received treatment for Lyme disease.

Author affiliations: New York Medical College, Valhalla, New York, USA (G.P. Wormser, D. McKenna, C. Scavarda, D. Cooper, M.Y. El Khoury, J. Nowakowski, P. Sudhindra, A. Ladenheim, G. Wang, C.L. Karmen); New York State Department of Health, Albany, New York, USA (V. Demarest, A.P. Dupuis II, S.J. Wong)

DOI: <https://doi.org/10.3201/eid2504.181509>

## Methods

### Patient Cohort

We enrolled adult patients with Lyme disease in a prospective study at the Lyme Disease Diagnostic Center, in Westchester County in the Lower Hudson Valley region of New York, to assess the outcome of this infection over 1 year, as described elsewhere (10). The Lower Hudson Valley region of New York is defined as Westchester, Putnam, Dutchess, Rockland, Orange, Ulster, and Sullivan Counties. This report focuses on 52 persons who at the time of study entry had erythema migrans but no treatment for Lyme disease and no clinical evidence of a concomitant extracutaneous manifestation of Lyme disease. Each patient had  $\geq 1$  expanding erythematous skin lesion that was  $\geq 5$  cm in diameter (11,12).

For each of the 52 persons with erythema migrans, baseline visits occurred from June 2, 2011, through July 30, 2015; blood was collected before antimicrobial drug treatment began (baseline) and at the next follow-up visit. The study was approved by the institutional review board at New York Medical College.

### Testing and Confirmation of Infection

Serologic testing to document co-infection was performed retrospectively. Testing for antibodies to *A. phagocytophilum* was conducted by immunofluorescent assay at Focus Diagnostics, Inc. (Cypress, CA, USA) (10). Testing for antibodies to *B. microti* was done by immunofluorescent assay at either Focus Diagnostics, Inc., or at the New York State Department of Health Wadsworth Center (Albany, NY, USA) (10).

Testing for antibodies to the glycerophosphodiester phosphodiesterase (GlpQ) protein of *B. miyamotoi* was performed at the Wadsworth Center by using a microsphere immunoassay that detects total antibodies (IgG + IgA + IgM) to recombinant GlpQ of *B. miyamotoi*. The recombinant GlpQ was kindly provided by Sukanya Narasimhan and Erol Fikrig of Yale University (New Haven, CT, USA).

Testing for antibodies to POWV was also performed at the Wadsworth Center (8). Serologic testing for POWV

infection included a microsphere immunoassay to detect total antibodies (IgG + IgA + IgM) to recombinant deer tick virus envelope protein and an IgM capture enzyme immunoassay to the LB strain of POWV (8). When the microsphere immunoassay and the IgM capture enzyme immunoassay were both reactive on acute- or convalescent-phase serum specimens, plaque reduction testing for neutralization antibodies against the LB strain of POWV was also performed.

Serologic evidence of *A. phagocytophilum* co-infection required a 4-fold rise in IgG titer between the acute- and convalescent-phase samples to  $\geq 1:512$  (13). Serologic evidence of *B. microti* infection required a 4-fold rise in IgG titers between the acute- and convalescent-phase serum samples. Patients who had clinical evidence of *A. phagocytophilum* or *B. microti* infections (e.g., new onset of fever, characteristic hematologic abnormalities, or both), or in whom such clinical evidence developed, were also tested when these findings were observed, by blood smear, PCR, or both, to detect these microorganisms, as described elsewhere (13,14). Because a positive result on the acute-phase sample is atypical for acute *B. miyamotoi* infection, serologic evidence of *B. miyamotoi* infection required seroconversion in the convalescent-phase sample for antibody to GlpQ (15). A diagnosis of possible POWV co-infection required a finding of positive IgM and neutralizing antibodies to POWV for the same serum sample. A confirmed diagnosis of POWV co-infection, however, required a 4-fold rise in neutralizing antibodies between the acute- and convalescent-phase serum samples; in addition, the neutralizing titer value had to exceed by >4-fold the neutralizing antibody titers found by using the patient's serum under the same test conditions but using other flaviviruses, such as West Nile virus.

### Other Assessments

At each patient's baseline visit, we collected demographic and clinical data, including data on 12 somatic symptoms (e.g., fatigue, headache, joint pain, muscle pain, and cognitive complaints), as described elsewhere (10,16). We performed serologic testing for Lyme disease at both the baseline and convalescent visits by using the C6 Lyme ELISA kit (Immunitics, Inc., <http://www.oxfordimmunotec.com>) according to the manufacturer's recommendations.

### Statistical Methods

For comparison of categorical variables, we used the Fisher exact test or the exact McNemar test; for continuous variables, we used the Student *t*-test. All testing was 2-tailed. We considered  $p < 0.05$  to be significant.

### Results

At the time of the baseline visit, none of the 52 patients with erythema migrans had received antimicrobial drugs;

31 (59.6%) patients had 1 erythema migrans lesion, and 21 (40.4%) patients had multiple erythema migrans lesions (Table 1). Thirty-four (65.4%) patients were male, mean age  $\pm$  SD was  $50.2 \pm 15.7$  years (range 20–86 years), and 39 (75.0%) patients had concomitant subjective symptoms such as fatigue. All but 4 patients had been exposed to ticks while in areas that included the Lower Hudson Valley (Table 1).

Convalescent-phase blood samples, which were obtained at a mean of 16.7 days (range 7–30 days) after the baseline visit, were screened for antibodies to the C6 peptide of *B. burgdorferi* and for antibodies to *A. phagocytophilum*, *B. microti*, GlpQ protein of *B. miyamotoi*, and POWV. A total of 46 (88.5%) patients were seropositive by the C6 Lyme ELISA, 32 (69.6%) on both the baseline and convalescent-phase blood samples, and 14 (30.4%) on the convalescent-phase sample only.

None of the 52 patients had evidence of *A. phagocytophilum* co-infection, although 4 had an IgG titer of 1:64 on the convalescent-phase blood sample, which is regarded as a nonspecific finding (13,17,18). Titers <1:64 were considered to be negative by the performing laboratory and thus were not reported.

Of the 52 patients, 4 (7.7%, 95% CI 3%–18%) had convincing evidence of *B. microti* co-infection (Table 2), and active babesiosis was clinically suspected for 3 of these patients. For 1 of the 3 patients who had clinical evidence of active babesiosis and a single erythema migrans lesion, fever developed on day 4 of amoxicillin therapy. Another of these patients underwent diagnostic testing for babesiosis because of fever before development of a single erythema migrans lesion. The third patient, who was afebrile, was tested for babesiosis 2 days after beginning antimicrobial drug treatment for a single erythema migrans lesion because of thrombocytopenia and anemia that were documented at the time of study entry. These 3 patients were positive for *B. microti* DNA by PCR, and 1 of the 3 also had a positive blood smear. All 3 patients received a course of treatment for babesiosis.

**Table 1.** Demographics and sites of potential tick exposure for 52 participants in study of co-infections in persons with Lyme disease, New York, USA, June 2, 2011, through July 30, 2015\*

Variable	No. (%)
Sex	
M	34 (65.4)
F	18 (34.6)
Multiple erythema migrans skin lesions	21 (40.4)
Tick exposure	
Potential exposure in at least LHV	48 (92.3)
Potential tick exposure in LHV alone	32 (61.5)
No tick exposure in LHV†	4 (7.7)

\*Mean age  $50.2 \pm 15.7$  y, range 20–86 y. LHV, Lower Hudson Valley of New York state, USA (includes Westchester, Putnam, Dutchess, Rockland, Orange, Ulster, and Sullivan Counties).

†Two participants were exposed to ticks in Long Island, New York, and 2 in Connecticut.

**Table 2.** Participants with evidence of *Babesia microti* co-infection in study of co-infections in persons with Lyme disease, New York, USA, June 2, 2011, through July 30, 2015\*

Age, y	Fever	No. symptoms at baseline visit	Tick exposure in LHV	Tick exposure outside LHV	Baseline <i>B. microti</i> antibody titer	Convalescent-phase <i>B. microti</i> antibody titer (timing, d)†	Blood smear	PCR for <i>Babesia</i> DNA
69	Yes, but began 4 d after baseline visit while taking amoxicillin for treatment of Lyme disease	1	Yes	No	≥1:1,024	≥1:1,024 (12)	+	+
58	Yes, began 1 or 2 d before the baseline visit	10	Yes	Yes	<1:64	≥1:1,024 (14)	–	+
61	No	2	Yes	No	≥1:1024	≥1:1,024 (21)	–	+
45	No	1	Yes	No	<1:64	1:512 (18)	ND	ND
54	No	2	No	Yes	≥1:1024	≥1:1,024 (19)	ND	ND
32	No	4	Yes	No	≥1:1024	≥1:1,024 (14)	ND	ND

\*LHV, Lower Hudson Valley of New York state, USA (includes Westchester, Putnam, Dutchess, Rockland, Orange, Ulster, and Sullivan Counties); ND, not done; +, positive; –, negative.

†Time from baseline visit.

A fourth patient without a febrile illness had a convalescent-phase IgG titer of 1:512 and an acute-phase titer of <1:64, consistent with co-infection with *B. microti*. In addition, 2 patients without clinical evidence of a febrile illness had acute- and convalescent-phase IgG titers of ≥1,024 (Table 2). Because the exact titer for these serum specimens was not determined, it was not possible to determine if the convalescent-phase sample demonstrated a 4-fold increase in titer. Although none of these 3 patients received anti-*Babesia* drug therapy, all recovered fully from Lyme disease during the 1-year follow-up period.

Therefore, up to 6 (11.5%; 95% CI 5%–23%) of the 52 patients may have been co-infected with *Babesia*; 3 of these patients were known to have had fever, hematologic findings consistent with active *Babesia* infection, or both. All 6 had ≥1 nonspecific symptoms at study entry; mean ± SD was 3.3 ± 3.4 symptoms (range 1–10 symptoms). In comparison, the mean number of symptoms for the other 46 patients at the baseline visit was 3.1 ± 3.3 (range 0–12 symptoms;  $p = 0.88$ ). One additional patient had a convalescent-phase IgG titer of 1:128 and an acute-phase IgG titer of 1:256, possibly indicative of a prior *Babesia* infection antedating the onset of Lyme disease.

None of the 52 patients met criteria for serologic evidence of *B. miyamotoi* co-infection, although 4 (7.7%) were seropositive for antibodies to GlpQ on acute- and convalescent-phase serum samples but without a discernible increase in values on the convalescent-phase sample. In addition, none of the 52 patients met criteria for serologic evidence for possible or confirmed POWV co-infection; 1 serum sample was positive for IgM to the LB strain of POWV but negative for neutralization antibodies to both the LB strain and a deer tick virus subtype strain of POWV. Therefore, more patients had laboratory evidence of co-infection with *Babesia* than with *A. phagocytophilum*, *B. miyamotoi*, or POWV (possibly as high as 6

[11.5%] for *Babesia* vs. 0 for the other pathogens tested;  $p = 0.031$ ).

## Discussion

In this study of 52 adult patients who had erythema migrans but had not been treated for Lyme disease, conducted in the Lower Hudson Valley of New York, the only documented *B. burgdorferi* co-infection was with *B. microti*. Several prior studies that used PCR have evaluated *I. scapularis* ticks found in this region for co-infection with *B. burgdorferi*; these studies found values of up to 30% for co-infection with *A. phagocytophilum* (4,5,9,19), up to 24% for *B. microti* (4,5,9,19), 1% for *B. miyamotoi* (4), and up to 3.9% for POWV (4,9). In general, lower rates of co-infection were associated with *I. scapularis* ticks in the nymphal stage than in the adult stage; this finding is relevant to our study because most cases of early Lyme disease in this region result from bites of ticks in the nymphal stage (20).

Extrapolating data on the rate of co-infections by PCR testing of ticks to human co-infection rates should be done cautiously. Confounding factors are the possible existence of nonpathogenic strains of *Anaplasma* or *Babesia* in ticks and whether these organisms may have contributed to a portion of the positive PCR results for *A. phagocytophilum* (21) or *B. microti*. For example, *B. odocoilei* is found in *I. scapularis* ticks but is not regarded as a human pathogen (22). In addition, the potential tick exposure locations of participants in our study were not restricted to the Lower Hudson Valley region of New York. Indeed, tick exposure for 4 of the 52 study participants occurred exclusively in Long Island or Connecticut (Table 1), and 1 of these 4 participants was among the 6 participants with laboratory evidence of *B. microti* co-infection (Table 2). This participant had no clinical evidence of a febrile illness but had acute- and convalescent-phase *B. microti* IgG titers ≥1,024.



We systematically evaluated adult patients with erythema migrans for co-infection with 4 *I. scapularis* tick-transmitted pathogens. We used well-defined and highly rigorous criteria for defining co-infection and focused on consecutively enrolled patients with the most certain clinical marker of early Lyme disease; namely, an erythema migrans lesion (12). Studies using less stringent case definitions may potentially detect higher numbers of putative co-infections but with less certain validity and less clarity for differentiating sequential from simultaneous infections (13,23). Unlike a previous study of untreated *Babesia* co-infections in patients considered to have Lyme disease (24), patients in our study with evidence of *Babesia* co-infection at baseline evaluation were not more symptomatic than those without this co-infection.

Limitations of our study are the relatively small sample size and the assumption that the convalescent-phase serum samples were obtained at the appropriate time to reliably identify the co-infections assessed (mean time from baseline visit to collection of the convalescent-phase blood sample was 16.7 days [range 7–30 days]). Most (75%) of the 52 patients in our study had received doxycycline, raising the question of whether this treatment may have affected the likelihood of seroconversion for antibodies to *A. phagocytophilum*. However, patients with culture-confirmed human granulocytic anaplasmosis regularly produce high antibody titers within 2 weeks of symptom onset despite receipt of doxycycline (17). Thus, the only theoretical concern about whether doxycycline might have reduced the observed frequency of *A. phagocytophilum* co-infection would have been for cases of incubating infection that might have been prevented from becoming active.

Another possibility, however, is that we excluded patients whose fever or systemic symptoms were primarily caused by human granulocytic anaplasmosis, rather than Lyme disease, and thus had started antimicrobial drug therapy before study entry. To address this question, we separately looked at acute- and convalescent-phase antibody titers to *A. phagocytophilum* in 38 patients with erythema migrans who were enrolled into the same study but for whom antimicrobial drug therapy had been initiated before enrollment. For 1 (2.6%) of the 38 patients, we found a 4-fold rise in antibody titers to *A. phagocytophilum* between the acute- and convalescent-phase serum samples. However, this finding did not differ significantly from what we found for the 52 patients with erythema migrans (1/38 vs. 0/52;  $p = 0.42$ ).

Another study limitation is our use of serologic testing assays that were not approved by the US Food and Drug Administration; consequently, their performance characteristics are uncertain. Last, our results pertain to a particular geographic area over a discrete time frame and may not pertain to other locations or other periods.

In conclusion, we systematically and rigorously evaluated consecutively enrolled adult patients with erythema migrans for co-infection with the 4 other *I. scapularis* tick-transmitted pathogens found in parts of New York and in other geographic areas in the northeastern United States. Nearly 90% of the patients evaluated had no serologic evidence of co-infection. *B. microti* was the only co-infection found, further documenting the clinical relevance of this emerging infection. Similar studies in other geographic areas, in addition to testing acute- and convalescent-phase serum, should include direct diagnostic testing by use of reliable PCR assays to detect potential co-infecting pathogens (particularly for *A. phagocytophilum*, *B. microti*, and *B. miyamotoi*) at the baseline visit.

### Acknowledgments

We thank Paul Visintainer, Julia Singer, Sophia Less, Artemio Zavala, Shana Warner, Lisa Giarratano, and Anne Payne for their assistance.

G.P.W. received funding from the Centers for Disease Control and Prevention (RO1 CK 000152) and research grants from Immunetics, Inc., Institute for Systems Biology, Rarecyte, Inc., and Quidel Corporation. He owns equity in Abbott/AbbVie, has been an expert witness in malpractice cases involving Lyme disease, and is an unpaid board member of the American Lyme Disease Foundation.

### About the Author

Dr. Wormser is chief of infectious diseases and vice chairman of medicine at New York Medical College and the founder and medical director of the Lyme Disease Diagnostic Center. His research interest is tickborne infections.

### References

1. Hinckley AF, Connally NP, Meek JI, Johnson BJ, Kemperman MM, Feldman KA, et al. Lyme disease testing by large commercial laboratories in the United States. *Clin Infect Dis*. 2014;59:676–81. <http://dx.doi.org/10.1093/cid/ciu397>
2. Nelson CA, Saha S, Kugeler KJ, Delorey MJ, Shankar MB, Hinckley AF, et al. Incidence of clinician-diagnosed Lyme disease, United States, 2005–2010. *Emerg Infect Dis*. 2015;21:1625–31. <http://dx.doi.org/10.3201/eid2109.150417>
3. Falco RC, Daniels TJ, Vinci V, McKenna D, Scavarda C, Wormser GP. Assessment of duration of tick feeding by the scutal index reduces need for antibiotic prophylaxis after *Ixodes scapularis* tick bites. *Clin Infect Dis*. 2018;67:614–6. <http://dx.doi.org/10.1093/cid/ciy221>
4. Tokarz R, Jain K, Bennett A, Briese T, Lipkin WI. Assessment of polymicrobial infections in ticks in New York state. *Vector Borne Zoonotic Dis*. 2010;10:217–21. <http://dx.doi.org/10.1089/vbz.2009.0036>
5. Prusinski MA, Kokas JE, Hukey KT, Kogut SJ, Lee J, Backenson PB. Prevalence of *Borrelia burgdorferi* (Spirochaetales: Spirochaetaceae), *Anaplasma phagocytophilum* (Rickettsiales: Anaplasmataceae), and *Babesia microti* (Piropalmsida: Babesiidae) in *Ixodes scapularis* (Acari: Ixodidae) collected from recreational

- lands in the Hudson Valley Region, New York State. *J Med Entomol*. 2014;51:226–36. <http://dx.doi.org/10.1603/ME13101>
6. Schaubert EM, Gertz SJ, Maple WT, Ostfeld RS. Coinfection of blacklegged ticks (Acari: Ixodidae) in Dutchess County, New York, with the agents of Lyme disease and human granulocytic ehrlichiosis. *J Med Entomol*. 1998;35:901–3. <http://dx.doi.org/10.1093/jmedent/35.5.901>
  7. Dupuis AP II, Peters RJ, Prusinski MA, Falco RC, Ostfeld RS, Kramer LD. Isolation of deer tick virus (Powassan virus, lineage II) from *Ixodes scapularis* and detection of antibody in vertebrate hosts sampled in the Hudson Valley, New York State. *Parasit Vectors*. 2013;6:185. <http://dx.doi.org/10.1186/1756-3305-6-185>
  8. El Khoury MY, Camargo JF, White JL, Backenson BP, Dupuis AP II, Escuyer KL, et al. Potential role of deer tick virus in Powassan encephalitis cases in Lyme disease–endemic areas of New York, USA. *Emerg Infect Dis*. 2013;19:1926–33. <http://dx.doi.org/10.3201/eid1912.130903>
  9. Aliota MT, Dupuis AP II, Wilczek MP, Peters RJ, Ostfeld RS, Kramer LD. The prevalence of zoonotic tick-borne pathogens in *Ixodes scapularis* collected in the Hudson Valley, New York State. *Vector Borne Zoonotic Dis*. 2014;14:245–50. <http://dx.doi.org/10.1089/vbz.2013.1475>
  10. Wormser GP, Sudhinda P, Lopez E, Patel L, Reza S, Brumbaugh AD, et al. Fatigue in patients with erythema migrans. *Diagn Microbiol Infect Dis*. 2016;86:322–6. <http://dx.doi.org/10.1016/j.diagmicrobio.2016.07.026>
  11. Tibbles CD, Edlow JA. Does this patient have erythema migrans? *JAMA*. 2007;297:2617–27. <http://dx.doi.org/10.1001/jama.297.23.2617>
  12. Wormser GP, Dattwyler RJ, Shapiro ED, Halperin JJ, Steere AC, Klemperer MS, et al. The clinical assessment, treatment, and prevention of Lyme disease, human granulocytic anaplasmosis, and babesiosis: clinical practice guidelines by the Infectious Diseases Society of America. *Clin Infect Dis*. 2006;43:1089–134. <http://dx.doi.org/10.1086/508667>
  13. Horowitz HW, Aguero-Rosenfeld ME, Holmgren D, McKenna D, Schwartz I, Cox ME, et al. Lyme disease and human granulocytic anaplasmosis coinfection: impact of case definition on coinfection rates and illness severity. *Clin Infect Dis*. 2013;56:93–9. <http://dx.doi.org/10.1093/cid/cis852>
  14. Wang G, Wormser GP, Zhuge J, Villafuerte P, Ip D, Zeren C, et al. Utilization of a real-time PCR assay for diagnosis of *Babesia microti* infection in clinical practice. *Ticks Tick Borne Dis*. 2015;6:376–82. <http://dx.doi.org/10.1016/j.ttbdis.2015.03.001>
  15. Molloy PJ, Weeks KE, Todd B, Wormser GP. Seroreactivity to the C6 peptide in *Borrelia miyamotoi* infections occurring in the northeastern United States. *Clin Infect Dis*. 2018;66:1407–10. <http://dx.doi.org/10.1093/cid/cix1023>
  16. Weitzner E, McKenna D, Nowakowski J, Scavarda C, Dornbush R, Bittker S, et al. Long-term assessment of post-treatment symptoms in patients with culture-confirmed early Lyme disease. *Clin Infect Dis*. 2015;61:1800–6. <http://dx.doi.org/10.1093/cid/civ735>
  17. Aguero-Rosenfeld ME, Kalantarpour F, Baluch M, Horowitz HW, McKenna DF, Raffalli JT, et al. Serology of culture-confirmed cases of human granulocytic ehrlichiosis. *J Clin Microbiol*. 2000;38:635–8.
  18. Aguero-Rosenfeld ME, Donnarumma L, Zentmaier L, Jacob J, Frey M, Noto R, et al. Seroprevalence of antibodies that react with *Anaplasma phagocytophila*, the agent of human granulocytic ehrlichiosis, in different populations in Westchester County, New York. *J Clin Microbiol*. 2002;40:2612–5. <http://dx.doi.org/10.1128/JCM.40.7.2612-2615.2002>
  19. Hersh MH, Ostfeld RS, McHenry DJ, Tibbetts M, Brunner JL, Killilea ME, et al. Co-infection of blacklegged ticks with *Babesia microti* and *Borrelia burgdorferi* is higher than expected and acquired from small mammal hosts. *PLoS One*. 2014;9:e99348. <http://dx.doi.org/10.1371/journal.pone.0099348>
  20. Falco RC, McKenna DF, Daniels TJ, Nadelman RB, Nowakowski J, Fish D, et al. Temporal relation between *Ixodes scapularis* abundance and risk for Lyme disease associated with erythema migrans. *Am J Epidemiol*. 1999;149:771–6. <http://dx.doi.org/10.1093/oxfordjournals.aje.a009886>
  21. Morissette E, Massung RF, Foley JE, Alleman AR, Foley P, Barbet AF. Diversity of *Anaplasma phagocytophilum* strains, USA. *Emerg Infect Dis*. 2009;15:928–31. <http://dx.doi.org/10.3201/eid1506.081610>
  22. Armstrong PM, Katavolos P, Caporale DA, Smith RP, Spielman A, Telford SR III. Diversity of *Babesia* infecting deer ticks (*Ixodes dammini*). *Am J Trop Med Hyg*. 1998;58:739–42. <http://dx.doi.org/10.4269/ajtmh.1998.58.739>
  23. Krause PJ, McKay K, Thompson CA, Sikand VK, Lentz R, Lepore T, et al.; Deer-Associated Infection Study Group. Disease-specific diagnosis of coinfecting tickborne zoonoses: babesiosis, human granulocytic ehrlichiosis, and Lyme disease. *Clin Infect Dis*. 2002;34:1184–91. <http://dx.doi.org/10.1086/339813>
  24. Krause PJ, Telford SR III, Spielman A, Sikand V, Ryan R, Christianson D, et al. Concurrent Lyme disease and babesiosis. Evidence for increased severity and duration of illness. *JAMA*. 1996;275:1657–60. <http://dx.doi.org/10.1001/jama.1996.03530450047031>

---

Address for correspondence: Gary P. Wormser, Wadsworth Center, New York Medical College, Division of Infectious Diseases, 40 Sunshine Cottage Rd, Skyline Office #2N-E14, Valhalla, NY 10595, USA; email: gwormser@nysc.edu

---

# Middle East Respiratory Syndrome Coronavirus Infection Dynamics and Antibody Responses among Clinically Diverse Patients, Saudi Arabia

Hail M. Al-Abdely,<sup>1</sup> Claire M. Midgley,<sup>1</sup> Abdulrahim M. Alkhamis, Glen R. Abedi, Xiaoyan Lu, Alison M. Binder, Khalid H. Alanazi, Azaibi Tamin, Weam M. Banjar, Sandra Lester, Osman Abdalla, Rebecca M. Dahl, Mutaz Mohammed, Suvang Trivedi, Homoud S. Algarni, Senthilkumar K. Sakthivel, Abdullah Algwizani, Fahad Bafaqeeh, Abdullah Alzahrani, Ali Abraheem Alsharef, Raafat F. Alhakeem, Hani A. Aziz Jokhdar, Sameeh S. Ghazal, Natalie J. Thornburg, Dean D. Erdman, Abdullah M. Assiri, John T. Watson, Susan I. Gerber

Middle East respiratory syndrome coronavirus (MERS-CoV) shedding and antibody responses are not fully understood, particularly in relation to underlying medical conditions, clinical manifestations, and mortality. We enrolled MERS-CoV-positive patients at a hospital in Saudi Arabia and periodically collected specimens from multiple sites for real-time reverse transcription PCR and serologic testing. We conducted interviews and chart abstractions to collect clinical, epidemiologic, and laboratory information. We found that diabetes mellitus among survivors was associated with prolonged MERS-CoV RNA detection in the respiratory tract. Among case-patients who died, development of robust neutralizing serum antibody responses during the second and third weeks of illness was not sufficient for patient recovery or virus clearance. Fever and cough among mildly ill patients typically aligned with RNA detection in the upper respiratory tract; RNA levels peaked during the first week of illness. These findings should be considered in the development of infection control policies, vaccines, and antibody therapeutics.

---

Author affiliations: Ministry of Health, Riyadh, Saudi Arabia (H.M. Al-Abdely, A.M. Alkhamis, K.H. Alanazi, W.M. Banjar, O. Abdalla, M. Mohammed, H.S. Algarni, A. Alzahrani, A.A. Alsharef, R.F. Alhakeem, H.A.A. Jokhdar, A.M. Assiri); Centers for Disease Control and Prevention, Atlanta, Georgia, USA (C.M. Midgley, G.R. Abedi, X. Lu, A.M. Binder, A. Tamin, S. Lester, R.M. Dahl, S.K. Sakthivel, N.J. Thornburg, D.D. Erdman, J.T. Watson, S.I. Gerber); Princess Nourah Bint Abdulrahman University, Riyadh (W.M. Banjar); Prince Mohammed Bin Abdulaziz Hospital, Riyadh (A. Algwizani, F. Bafaqeeh, S.S. Ghazal)

DOI: <https://doi.org/10.3201/eid2504.181595>

Infection with Middle East respiratory syndrome (MERS) coronavirus (MERS-CoV) results in a wide range of clinical manifestations, from mild or asymptomatic illness to severe respiratory failure (1–8); infection has a reported mortality rate of 35% (9). Most MERS cases have been reported in older adults with underlying medical conditions (4,7). Asymptomatic or mild infections are typically reported in younger, healthy adults, including healthcare personnel (2,4). MERS-CoV transmission is commonly associated with exposure to symptomatic patients in health-care (1,2,10,11) or household (12) settings or with direct exposure to dromedary camels (13).

Infection prevention and control guidance for MERS-CoV in humans is partially based on severe acute respiratory syndrome (SARS) coronavirus infection dynamics (14,15); MERS-specific recommendations are incomplete. Investigations of virus shedding in MERS patients have demonstrated that MERS-CoV RNA can be detected in the respiratory tract for >1 month from illness onset (16,17); lower respiratory tract (LRT) specimens have higher (18–23) and often more prolonged RNA levels (17,18) than upper respiratory tract (URT) specimens; more severely ill patients typically have higher (18,21) and more prolonged (18) RNA levels; and MERS-CoV RNA is detected in the blood (17,22,24), serum (18,19,24), plasma (22,25,26), stool (19,23,27), and urine (17,19,23) of some patients. However, important knowledge gaps remain, particularly regarding shedding in association with clinical manifestations and host factors (4).

Serologic responses among MERS patients are incompletely understood; such data are critical for the development

---

<sup>1</sup>These first authors contributed equally to this article.



of vaccines, antibody therapeutics, and diagnostics. Investigations of MERS survivors have demonstrated that antibody titers are higher and longer-lived in more severely ill patients than in mildly ill patients (28), some of whom do not develop a detectable response (28,29). Antibodies are usually detected by day 21 after illness onset (30,31) and can persist for  $\geq 34$  months after infection (32). Data on case-patients who died, however, are limited (19,25,29).

To address gaps in viral and antibody kinetics, we longitudinally assessed 33 hospitalized MERS-CoV-infected patients. Our aim was to characterize MERS-CoV infection dynamics and antibody responses in relation to outcome, clinical manifestations, underlying medical conditions, and preillness exposures.

## Methods

### Patient Enrollment

The study population was drawn from a MERS referral hospital in Riyadh, Saudi Arabia. All patients testing positive for MERS-CoV locally by real-time reverse transcription PCR (rRT-PCR) assay and admitted to this hospital during August 1, 2015–August 31, 2016, were eligible for participation. All enrolled patients provided informed written consent.

### Data Collection

We reviewed epidemiologic interviews conducted at the time of case identification to include patient demographics, symptom history, and relevant exposures during the 2 weeks before onset. After patient death or discharge, we performed comprehensive medical chart reviews to collect medical history; symptoms before hospitalization; and daily information regarding symptoms during hospitalization, clinical course, treatments, medications, patient vital signs, diagnostic tests, and clinical outcome.

To assess MERS-CoV infection status, we retrospectively reviewed 3 data sources (as available) containing information on clinical diagnostic testing: 1) rRT-PCR request forms submitted to a regional testing facility; 2) hospital copies of corresponding results; and 3) if the hospital's clinical series was incomplete, rRT-PCR results from the Health Electronic Surveillance Network (33), a national platform for reporting notifiable diseases in Saudi Arabia. MERS-CoV clinical diagnostic testing had been performed on URT or LRT specimens typically collected every other day throughout hospitalization. Healthcare personnel collected LRT specimens from intubated patients and URT specimens otherwise. MERS-CoV results were positive, probable, or negative and, if available, cycle threshold ( $C_t$ ) values for MERS-CoV upstream of the envelope E (upE) or open reading frame (ORF) 1a (34); a probable finding indicated that only 1 of these 2 targets was detected.

### Laboratory Investigation

In addition to retrospectively reviewing clinical MERS-CoV test results, we periodically collected specimens throughout hospitalization for molecular and serologic testing at the US Centers for Disease Control and Prevention (CDC). Specimens were collected from respiratory and nonrespiratory sites, frozen at  $< -70^\circ\text{C}$ , and shipped on dry ice. Available specimens were URT (nasopharyngeal, oropharyngeal swab, or combined), LRT (sputum or tracheal aspirate), whole blood, serum, stool, and urine. Specimens were collected during days 1–42 postenrollment and additionally at 1 year for serum.

### Molecular Assays

Specimens were processed and screened by upE and N2 rRT-PCR. Specimens positive by only 1 RT-PCR were confirmed by N3 assay as previously described (35). MERS-CoV isolation was performed as previously described (36). We attempted full genome sequencing, as previously described (36), on the earliest available respiratory specimen (or serum, if not available) for each patient.

### Serologic Assays

Serum specimens with sufficient volume were tested using 4 CDC serologic assays: 1) microneutralization (MN) assay (37); 2) spike (S)-specific pseudoparticle neutralization assay (VSV-MERS-S); 3) S ELISA (Ig-specific) (38); and 4) nucleocapsid (N) ELISA (Ig-specific) (37,38). Additional description is available in Appendix 1 (<https://wwwnc.cdc.gov/EID/article/25/4/18-1595-App1.pdf>).

### Data Analysis

#### Definitions

We defined illness onset as the first day of reported symptoms consistent with MERS; for asymptomatic patients identified through routine contact investigations, we used the date of the first positive MERS-CoV test. We analyzed data relative to the date of illness onset (day 0). Patients were classified as having diabetes mellitus (DM) if there was a documented medical history of DM. Patients with multiple periods of hyperglycemia during hospitalization (random glucose readings  $> 200$  mg/dL), but with no documented medical history of DM, were considered as possible DM status.

Cardiac disease included congestive heart failure, coronary artery disease, or a history of myocardial infarction; reports of isolated hypertension were not included. Pulmonary disease included chronic obstructive pulmonary disease, asthma or reactive airway disease, or use of supplemental oxygen at home. Renal disease included reports of chronic kidney disease. Secondary exposure was defined as contact with MERS-CoV-infected persons in the 2 weeks

before illness onset. Primary exposure was defined as either reported direct camel contact or no known contact with MERS-CoV–infected persons.

### Illness Severity

We retrospectively categorized patients into 3 groups on the basis of the need for supplemental oxygen, ventilation, and clinical outcome. Group 1 (G1) received room air throughout hospitalization; group 2 (G2) required ventilator support (mechanical or nonmechanical) and survived; and group 3 (G3) required ventilator support and died.

### MERS-CoV Detection Period

To analyze duration of detectable MERS-CoV among survivors, we assessed the number of days from illness onset to negativity in clinical respiratory specimens tested at the regional testing facility, based on reports from the hospital or the Health Electronic Surveillance Network. We defined the day of MERS-CoV negativity as the first of  $\geq 2$  consecutive negative tests before discharge. These variables were based

on either URT or LRT specimens. Because mildly ill patients did not provide LRT specimens, we only assessed detection in URT specimens when comparing severity groups.

### Prolonged MERS-CoV Detection

To assess prolonged MERS-CoV detection, we expressed time to negativity as a binary variable: patients with time to negativity  $\leq 11$  versus  $>11$  days. We chose this cutoff to reflect the median time to negativity among survivors. Given the low numbers of patients in our cohort, we also assessed 2 additional cut-offs for prolonged shedding to strengthen statistically significant findings:  $\leq 14$  versus  $>14$  days and  $\leq 21$  versus  $>21$  days.

### Viral Load

To approximate viral load in clinical results, we assessed MERS-CoV upE rRT-PCR  $C_t$  values determined at the regional testing facility. We used  $C_t$  values from LRT specimens to assess mechanically ventilated patients. We were able to identify the minimum  $C_t$  value (or peak RNA level)

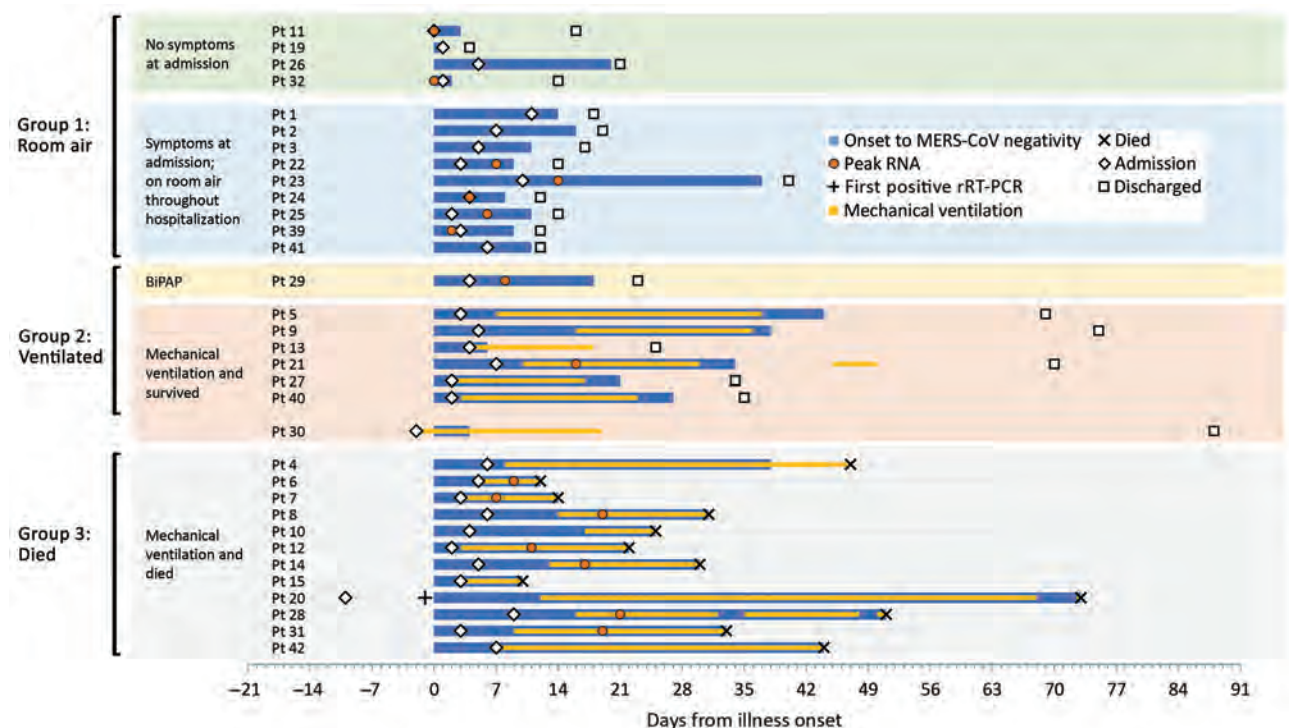


**Figure 1.** Timeline of clinical course and MERS-CoV detection, by patient, Saudi Arabia, August 1, 2015–August 31, 2016. Findings are presented by time since illness onset (day 0). Patients are grouped by illness severity and outcome. For each patient, day of admission, discharge or death, period of mechanical ventilation (if applicable), and MERS-CoV detection are depicted. For a subset of patients with sufficient data, the peak RNA level (or the minimum upstream of the envelope cycle threshold value) is depicted. Peak RNA was based on upper respiratory tract specimen results among group 1 patients and Pt 29, and lower respiratory tract specimen results in group 2 and group 3 patients. The date of death is shown for group 3 patients. Pt 11 and Pt 32 did not report any symptoms throughout their hospitalization. Pt 30 was hospitalized and mechanically ventilated before MERS onset because of a road traffic accident; this patient was excluded from severity and clinical course analyses. Pt 23 has been described previously (36). The first positive MERS-CoV rRT-PCR for Pt 20 was collected 1 day before symptom onset. BiPAP, bilevel positive airway pressure; CoV, coronavirus; MERS, Middle East respiratory syndrome; Pt, patient; rRT-PCR, real-time reverse transcription PCR.

**Table 1.** Characteristics of MERS-CoV–infected patients, by clinical severity outcome, Saudi Arabia, August 1, 2015–August 31, 2016\*

Characteristic	No. (%) patients			p value†	
	Group 1, n = 13	Group 2, n = 7	Group 3, n = 12	Mortality, G1 and G2 vs. G3	Ventilation support, G1 vs. G2
<b>Demographics</b>					
<b>Sex</b>					
M	7 (54)	6 (86)	7 (58)	0.724	0.329
F	6 (46)	1 (14)	5 (42)		
<b>Nationality</b>					
Saudi	5 (38)	6 (86)	10 (83)	0.139	0.070
Non-Saudi	8 (62)	1 (14)	2 (17)		
<b>Age group, y</b>					
25–44	10 (77)	4 (57)	0	<0.001	0.548
45–64	3 (23)	2 (29)	7 (58)		
≥65	0	1 (14)	5 (42)		
Median age (range), y	33 (26–62)	41 (30–73)	62 (55–78)	<0.001	0.047
<b>Underlying conditions</b>					
None reported	10 (77)	0	0	0.004	0.003
Any reported underlying condition	3 (23)	7 (100)	11 (92)		
Unknown underlying condition	0	0	1 (8)		
DM‡	3 (23)	4 (80)	11 (100)	0.001	0.047
DM and possible DM§	3 (23)	6 (86)	12 (100)	0.002	0.047
Hypertension	1 (8)	2 (29)	11 (100)	<0.001	0.270
Cardiac disease¶	0	0	6 (55)	0.001	NA
Pulmonary disease#	0	2 (29)	2 (18)	0.602	0.111
On oxygen at home**	0	1 (14)	1 (9)	1.000	0.350
Renal disease††	0	0	3 (27)	0.001	NA
Cardiac, pulmonary, or renal disease	0	2 (29)	9 (82)	<0.001	0.111
History of cerebrovascular accident	1 (8)	0	3 (27)	0.318	1.000
Cancer in previous 12 mo	0	0	1 (9)	0.355	NA
<b>Possible preillness exposure</b>					
Secondary,‡‡ healthcare personnel	5 (38)	0	0	NA	NA
Secondary, household contact	4 (31)	1 (14)	1 (8)	NA	NA
Secondary, hospital visitor	2 (15)	1 (14)	2 (17)	NA	NA
Secondary, hospital inpatient	0	0	3 (25)	NA	NA
Any secondary exposure	11 (85)	2 (29)	6 (50)	0.249	0.022
Direct camel contact	0	0	2 (17)		
Multiple possible exposures	0	1 (14)	0		
No recognized risks§§	2 (15)	4 (57)	4 (33)		
<b>Primary vs. secondary exposure¶¶</b>					
Primary###	2 (15)	4 (67)	6 (50)	0.452	0.046
Secondary	11 (85)	2 (33)	6 (50)		
<b>Symptoms before admission</b>					
Absence of symptoms	4 (31)	0	0	NA	NA
Any reported symptom	9 (69)	7 (100)	12 (100)	NA	NA
Fever	8 (62)	6 (86)	11 (92)	0.212	0.354
Cough	7 (54)	6 (86)	10 (83)	0.422	0.329
Dyspnea	1 (8)	7 (100)	11 (92)	0.008	<0.001
Vomiting	4 (31)	2 (29)	2 (17)	0.676	1.000
Diarrhea	2 (15)	1 (14)	4 (33)	0.379	1.000
Sore throat	2 (15)	1 (14)	1 (8)	1.000	1.000
Rhinorrhea	1 (8)	1 (14)	1 (8)	1.000	1.000

\*Group 1, on room air; group 2, ventilated but survived; group 3, died. CoV, coronavirus; DM, diabetes mellitus; MERS, Middle East respiratory syndrome; NA, not applicable.

†p values are for Fisher exact or Kruskal–Wallis tests comparing long-term and short-term.

‡Based on documented medical history of DM; comparison excludes 3 patients with possible DM status; group 1, n = 13; group 2, n = 5; group 3, n = 11.

§Includes 18 patients with a documented history of DM and 3 patients with possible DM status who exhibited multiple periods of hyperglycemia (random glucose readings >395 mg/dL) but who had no documented history of DM.

¶Cardiac disease includes congestive heart failure, coronary artery disease, a history of coronary artery bypass, or a history of myocardial infarction. Reports of isolated hypertension were not included.

#Pulmonary disease includes chronic obstructive pulmonary disease, asthma or reactive airway disease, or use of supplemental oxygen at home.

\*\*Patients who were on supplemental oxygen at home (both patients were on bilevel positive airway pressure) required mechanical ventilation when hospitalized.

††Renal disease includes reports of chronic kidney disease.

‡‡Secondary exposure defined as reported contact with a known MERS case-patient.

§§No recognized risks defined as no reported contact with a known MERS case-patient or camel (direct or indirect contact).

¶¶Comparison excludes 1 patient with multiple exposures; group 2, n = 6.

###Primary exposure defined as no reported contact with a known MERS case-patient; includes direct camel contact and patients with no recognized risks.



**Table 2.** Demographic and exposure characteristics of survivors with prolonged MERS-CoV detection, Saudi Arabia, August 1, 2015–August 31, 2016\*

Characteristic	Total, N = 19	Days to negativity		p value†
		≤11 d, n = 11	>11 d, n = 8	
<b>Demographics</b>				
Sex				
M	13/19 (68)	6/11 (55)	7/8 (88)	0.177
F	6/19 (32)	5/11 (45)	1/8 (12)	
Nationality				
Saudi	10/19 (53)	5/11 (45)	5/8 (63)	0.650
Non-Saudi	9/19 (47)	6/11 (55)	3/8 (37)	
Age group, y				
25–44	14/19 (74)	9/11 (82)	5/8 (63)	0.262
45–64	4/19 (21)	1/11 (9)	3/8 (38)	
≥65	1/19 (5)	1/11 (9)	0/8	
Median age, y (range)	36 (26–73)	30 (26–73)	40 (27–62)	0.083
<b>Underlying conditions</b>				
None reported	10/19 (53)	8/11 (73)	2/8 (25)	0.070
Any reported underlying condition	9/19 (47)	3/11 (27)	6/8 (75)	
DM‡	7/18 (39)	2/11 (20)	5/7 (71)	0.049
DM and possible DM§	8/19 (42)	2/11 (20)	6/8 (75)	0.024
Hypertension	3/19 (16)	1/11 (9)	2/8 (25)	0.546
Cardiac disease¶	1/19 (5)	1/11 (9)	0/8	1.000
Pulmonary disease#	1/19 (5)	1/11 (9)	0/8	1.000
On oxygen at home**	1/19 (5)	1/11 (9)	0/8	1.000
<b>Possible preillness exposure</b>				
Secondary, †† healthcare personnel	5/19 (26)	4/11 (36)	1/8 (13)	NA
Secondary, household contact	5/19 (26)	3/11 (27)	2/8 (25)	NA
Secondary, hospital visitor	3/19 (16)	0/11	3/8 (38)	NA
Secondary, hospital inpatient	0/19	0/11	0/8	NA
Any secondary exposure	13/19 (68)	7/11 (64)	6/8 (75)	0.796
Direct camel contact	0/19	0/11	0/8	
Multiple possible exposures	2/19 (11)	1/11 (9)	1/8 (13)	
No recognized risks‡‡	4/19 (21)	3/11 (27)	1/8 (13)	
Primary vs. secondary exposure§§				
Primary¶¶	4/17 (24)	3/10 (30)	1/7 (14)	0.603
Secondary	13/17 (78)	7/10 (70)	6/7 (86)	

\*Values are no. (%) patients except as indicated. CoV, coronavirus; DM, diabetes mellitus; MERS, Middle East respiratory syndrome; NA, not applicable.

†p values are for Fisher exact or Kruskal–Wallis tests comparing long-term and short-term.

‡Based on documented medical history of DM; comparison excludes 1 patient with possible DM status; total, N = 18; prolonged shedding >11 days, n = 7.

§Includes 7 patients with a documented history of DM and 1 patient (of possible DM status) who had no documented history of DM but exhibited multiple periods of hyperglycemia (>200 mg/dL) during hospitalization, with a maximum random glucose reading of 404 mg/dL.

¶Cardiac disease includes congestive heart failure, coronary artery disease, a history of coronary artery bypass, or a history of myocardial infarction.

Reports of isolated hypertension were not included.

#Pulmonary disease includes chronic obstructive pulmonary disease, asthma or reactive airway disease, or use of supplemental oxygen at home.

\*\*Patient who was on supplemental oxygen (bilevel positive airway pressure) at home required mechanical ventilation when hospitalized.

††Secondary exposure defined as reported contact with a known MERS case-patient.

‡‡No recognized risks defined as no reported contact with a known MERS case-patient or camel (direct or indirect contact).

§§Comparison excludes 2 patients with multiple exposures; total, N = 17; shed ≤11 days, n = 10; shed >11 days, n = 7.

¶¶Primary exposure defined as no reported contact with a known MERS case-patient; includes direct camel contact and patients with no recognized risks.

in a subset of patients. For specimens submitted to CDC, we estimated viral load on the basis of the upE  $C_t$  value (or N2  $C_t$  value if upE testing was negative and N3 was positive).

### Antibody Responses

We compared the proportion of serum specimens with detectable antibody responses between survivors and patients who died. We assessed specimens collected <14, <21, and <28 days after illness onset; during 28–56 days after onset; and then at 1 year.

### Statistical Analyses

We summarized patient characteristics by illness severity and, among survivors, by time to MERS-CoV negativity.

We used Fisher exact, Kruskal–Wallis, or log rank tests to compare groups and exact logistic regression for multivariable analysis. We compared antibody titers with estimated viral load in different specimen types by using the Spearman test for correlation. All data were analyzed using Microsoft Excel 2016 (<https://products.office.com>) and SAS version 9.4 (<https://www.sas.com>).

## Results

### Cohort Description

During August 1, 2015–August 31, 2016, a total of 33 MERS-CoV–infected patients were enrolled. Among these, 4 were classified as asymptomatic on admission, and

**Table 3.** Clinical features of survivors with prolonged MERS-CoV detection, Saudi Arabia, August 1, 2015–August 31, 2016\*

Clinical feature	Total, N = 19	Days to negativity		p value†
		≤11 d, n = 11	>11 d, n = 8	
<b>Symptoms before admission‡</b>				
No symptoms	4/18 (21)	3/10 (30)	1/8 (13)	0.603
Fever	13/18 (72)	7/10 (70)	6/8 (75)	1.000
Cough	11/18 (61)	5/10 (50)	6/8 (75)	0.367
Dyspnea	6/18 (33)	2/10 (20)	4/8 (50)	0.321
Vomiting	5/18 (28)	2/10 (20)	3/8 (38)	0.608
Diarrhea	3/18 (17)	0/10	3/8 (38)	0.069
<b>Clinical course‡</b>				
Room air	13/18 (72)	9/10 (90)	4/8 (50)	0.118
Ventilator support§	5/18 (28)	1/10 (10)	4/8 (50)	
Abnormal chest radiograph	9/18 (50)	4/10 (40)	5/8 (63)	0.637
<b>Medications¶</b>				
Ribavirin plus peg-IFN $\alpha$	2/19 (11)	0/11	2/8 (25)	0.164
Oseltamivir	12/19 (63)	6/11 (55)	6/8 (75)	0.633
Antibiotics	15/19 (79)	8/11 (73)	7/8 (88)	0.603
Parenteral steroids	3/19 (16)	0/11	3/8 (38)	0.058
Group 2 only#	3/5 (60)	0/1	3/4 (75)	0.400
Inhaled steroids	2/19 (11)	0/11	2/8 (25)	0.164
Group 2 only#	2/5 (40)	0/1	2/4 (50)	1.000
Bronchodilators	5/19 (26)	2/11 (18)	3/8 (38)	0.603
Antipyretics	9/19 (47)	6/11 (55)	3/8 (38)	0.650

\*Values are no. (%) patients except as indicated. Group 2, ventilated but survived; MERS-CoV, Middle East respiratory syndrome coronavirus.

†p values are for Fisher exact or Kruskal–Wallis tests comparing long-term and short-term.

‡Excludes patient no. 30, who was admitted and intubated before onset because of injuries sustained in a road traffic accident (N = 18).

§Includes mechanical or nonmechanical (i.e., bilevel positive airway pressure) ventilation.

¶Medication given during MERS-CoV detection period (on the basis of diagnostic testing in respiratory specimens).

#Assessing steroid use among G2 patients only.

9 reported symptoms but remained on room air during hospitalization (Figure 1; Appendix 1 Figure 1; Appendix 2 Table 1, <https://wwwnc.cdc.gov/EID/article/25/4/18-1595-App1.xlsx>); 10 of these 13 patients were identified through contact tracing (5 were healthcare personnel) and were hospitalized to ensure isolation. Twenty patients required ventilator support (1 bilevel positive airway pressure [BiPAP] and 19 mechanical ventilation), 12 of whom died. We grouped 13 patients into G1, 7 into G2, and 12 into G3; 1 patient (patient [Pt] 30) was initially hospitalized and intubated after a road traffic accident, before MERS onset, and was excluded from analyses regarding severity and clinical course resulting from MERS-CoV infection.

Patient ages ranged from 26 to 78 years, and 63% were male (Appendix 2 Table 1). Twenty-three (70%) patients had  $\geq 1$  underlying medical condition, 19 of whom had documented DM; an additional 3 patients were considered of possible DM status because they exhibited multiple periods of hyperglycemia (random glucose readings  $>395$  mg/dL) but had no documented history of DM. Death was associated with older age ( $p < 0.001$ ), DM ( $p = 0.001$ ), hypertension ( $p < 0.001$ ), cardiac disease ( $p = 0.001$ ), or renal disease ( $p = 0.001$ ) (Table 1). Among survivors, ventilator support was associated with DM ( $p = 0.047$ ), older age ( $p = 0.047$ ), or preillness primary exposure ( $p = 0.046$ ) (Table 1). Among the 12 patients with a primary exposure, 8 had DM (Appendix 2 Table 1).

Clinical course and time to MERS-CoV negativity (in clinical respiratory specimens) is depicted according

to date of illness onset (Figure 1; Appendix 2 Table 2). Time to admission (median 4 days) did not differ between groups. Time to MERS-CoV negativity among survivors ranged from day 1 to day 44 after illness onset and was typically longer among G2 than G1 patients. Twelve of 13 patients in G1 were discharged by day 21 after onset; the mildly ill patient who was in the hospital until day 40 after onset (Pt 23) has been described previously (36). Duration of hospitalization for G2 patients was 19–70 days, and duration of intubation was 14–31 days. G3 patients died 10–73 days after onset.

### Daily Symptoms

Common symptoms before admission were fever (78%), cough (72%), and dyspnea (59%) (Table 1). Dyspnea before admission was associated with a more severe outcome ( $p < 0.001$ ). Among the 4 patients who reported no symptoms on admission, 2 were mildly symptomatic during hospitalization (Appendix 2 Table 3).

Among G1 patients, fever and cough were commonly reported, and the proportion of patients with either symptom appeared to align with the proportion who concurrently had detectable MERS-CoV in clinical respiratory specimens (Figure 2, panel A). Cough persisted in 5 G1 patients for  $\leq 4$  days after MERS-CoV negativity (Figure 2, panel B). Chest radiographs of 4 G1 patients were described as abnormal, typically with unilateral findings (Appendix 2 Table 4). Oxygen saturation remained  $>92\%$  in G1 patients. Among G2 patients,

the proportion of patients mechanically ventilated appeared to align with the proportion who had detectable MERS-CoV in the LRT (Figure 2, panel C); only 1 G2 patient (Pt 13, who had underlying pulmonary disease) was MERS-CoV–positive for a short period but required extended mechanical ventilation. Among the 12 G3 patients, 11 were MERS-CoV RNA–positive until death (Figure 2, panel D).

### MERS-CoV RNA in Respiratory Specimens

MERS-CoV upE  $C_t$  values from clinical diagnostic reports are depicted in Figure 3. MERS-CoV RNA levels in the URT of most G1 patients peaked in the first week after onset (Figure 3, panel D). Among patients who died, RNA levels peaked in the LRT during weeks 2 and 3 (Figure 3, panel E), after which RNA levels typically began to decrease (Figure 3, panel C); 4 patients died with negative or probable rRT-PCR results.

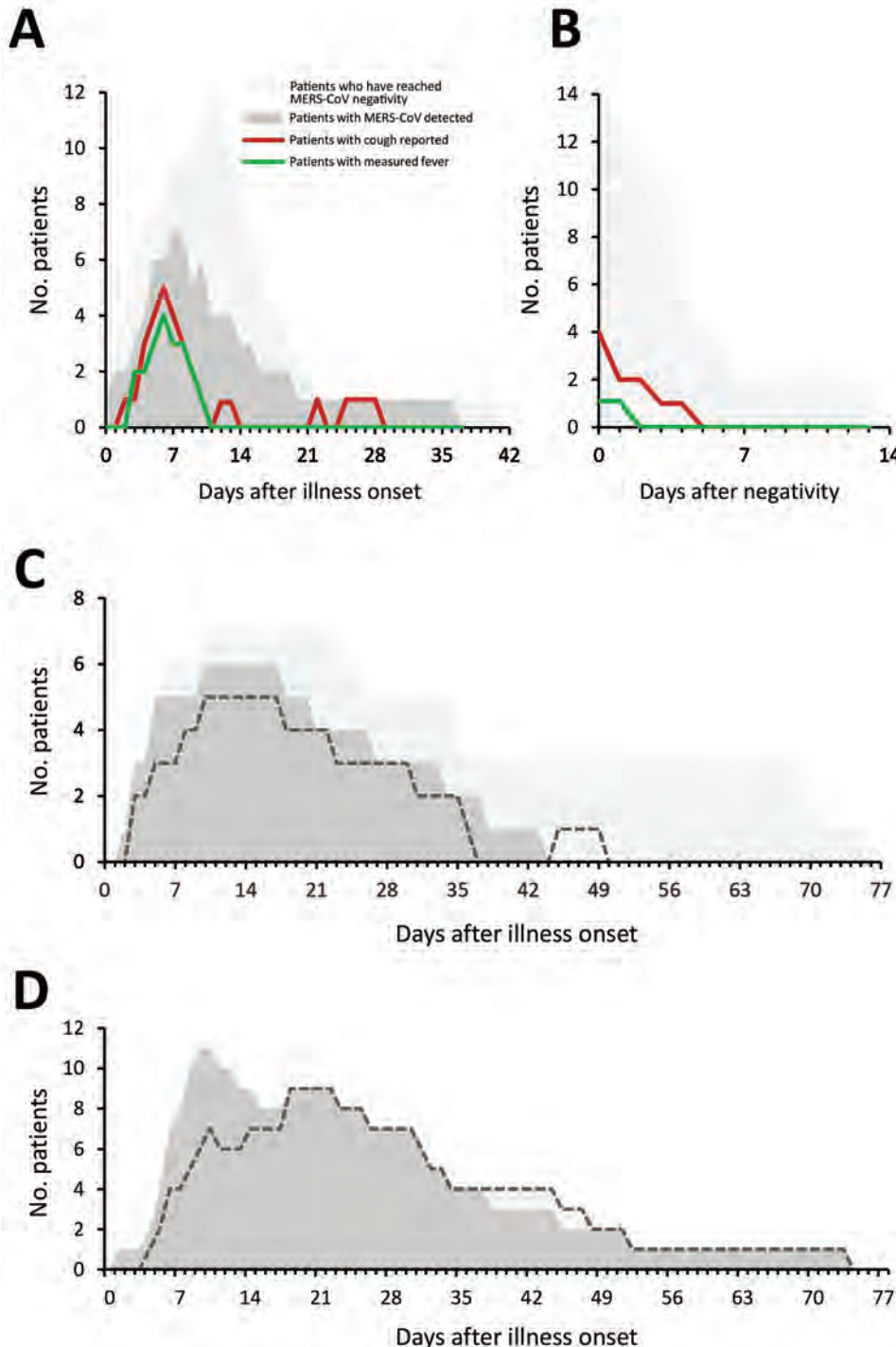


**Figure 2.** Symptom progression and MERS-CoV detection during hospitalization at a MERS referral hospital, Saudi Arabia, August 1, 2015–August 31, 2016. Each panel depicts the number of patients hospitalized on a given day for each category shown; MERS-CoV detection is based on the clinical diagnostic reports in the upper or lower respiratory tract. A, B) Number of group 1 patients with fever (measured oral temperature  $>38.0^{\circ}\text{C}$  or measured axillary temperature  $>37.5^{\circ}\text{C}$ ) and reported cough during (A) and after (B) the MERS-CoV detection period. C, D) Number of patients intubated (dashed lines) and the number of patients who were positive for MERS-CoV on a given day for group 2 (C) and group 3 (D). MERS, Middle East respiratory syndrome; MERS-CoV, Middle East respiratory syndrome coronavirus. Group 1, on room air; group 2, ventilated but survived; group 3, died.



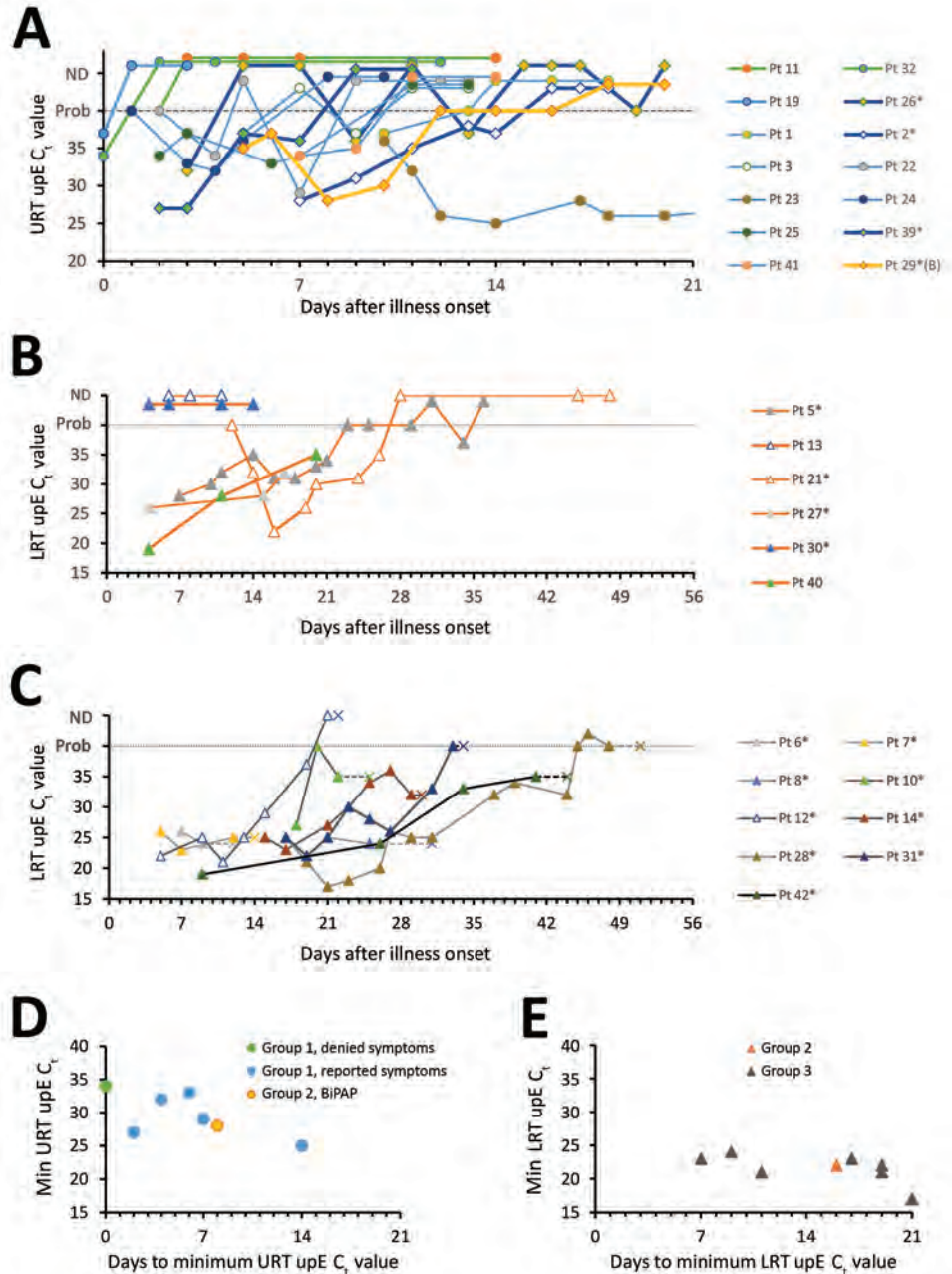
We next assessed characteristics of survivors with prolonged MERS-CoV detection periods (on the basis of clinical diagnostic reports of URT specimens) (Tables 2, 3; Appendix 2 Tables 5, 6). Patients who reached negativity >11 days after onset were more likely to have DM than patients who cleared the virus earlier ( $p = 0.049$ ; when adjusting for severity group,  $p = 0.061$ ) (Tables 2, 3). This association was also observed in patients who reached negativity >14 days after onset ( $p = 0.013$ ) and when adjusting for severity group ( $p = 0.030$ ) (Appendix

2 Table 5). Evidence for this association was stronger when patients with DM and possible DM were combined (Tables 2, 3; Appendix 2 Table 5). No other underlying medical conditions were associated with prolonged detection. Survivors with prolonged detection (>14 or >21 days) were also more likely to require ventilator support (Appendix 2 Table 5), but this was not significant when adjusting for DM.

Based on respiratory specimens submitted to CDC (Appendix 1 Figures 2, 3), full-genome sequences from 13

**Figure 3.** MERS-CoV RNA detection in the respiratory tract, based on clinical diagnostic reports, among MERS-CoV patients, Saudi Arabia, August 1, 2015–August 31, 2016.

A–C) UpE real-time reverse transcription PCR  $C_t$  values of group 1 (A), 2 (B), and 3 (C) patients, by days since illness onset (day 0). Panel A depicts URT specimens, and panels B and C depict LRT specimens collected during MV; Pt 29 (a G2 patient who received BiPAP ventilation) is depicted in panel A because only URT specimens were collected for this patient. The dashed line represents the limit of detection, above which specimens were considered MERS-CoV–negative or not detected. Probable results, meaning that only 1 of 2 real-time reverse transcription PCR assays were positive, are depicted on the dashed line for graphing purposes. Patients with limited  $C_t$  values or unknown specimen types are not depicted. Patients 11 and 32 did not report any symptoms throughout their illness. Pt 30 is depicted alongside G2 patients. Pt 23 reached negativity 37 days after illness onset, as described previously (36). \*Indicates patients with a documented history of diabetes mellitus. D, E) Minimum  $C_t$  values reported, which was determined for a subset of patients with sufficient data. Panel D depicts URT specimen results among group 1 patients and Pt 29; panel E depicts LRT specimen results in group 2 and 3 patients, collected from the LRT during MV. Group 1, on room air; group 2, ventilated but survived; group 3, died. BiPAP, bilevel positive airway pressure;  $C_t$ , cycle threshold; CoV, coronavirus; LRT, lower respiratory tract; MERS, Middle East respiratory syndrome; min, minimum; MV, mechanical ventilation; Pt, patient; URT, upper respiratory tract; upE, upstream of the envelope.



patients belonged to the NRC-2015 (39) clade (or lineage 5 [40]) (GenBank accession nos. MG520075 and MG757593–MG757605). Viable MERS-CoV was isolated from 3 of 37 URT specimens; 2 specimens were from a mildly ill patient (Pt 23) collected on days 13 and 15 after onset (described previously [36]), and 1 specimen was collected on day 13 from a patient who subsequently died (Pt 8).

### MERS-CoV RNA in Nonrespiratory Specimens

CDC received 252 nonrespiratory specimens for MERS-CoV testing, collected from 31 patients <3 months after

onset; 7 patients (21 specimens, all MERS-CoV–negative) were excluded because specimens were only collected after the virus had been cleared from the respiratory tract. Fourteen of 24 patients had MERS-CoV RNA detected in whole blood, 9/20 in serum, 5/10 in stool, and 3/16 in urine (Figure 4; Appendix 2 Table 2). In G1, MERS-CoV RNA was detected in the whole blood or serum of 4/8 patients ( $\leq 2.3 \times 10^3$  copies/mL) for  $\leq 13$  days and in the stool of 3/5 patients ( $\leq 7.5 \times 10^3$  copies/mL) for  $\leq 15$  days; only 1 patient with RNA-positive stool had concurrent gastrointestinal symptoms. Specimens were limited in G2, but MERS-CoV RNA

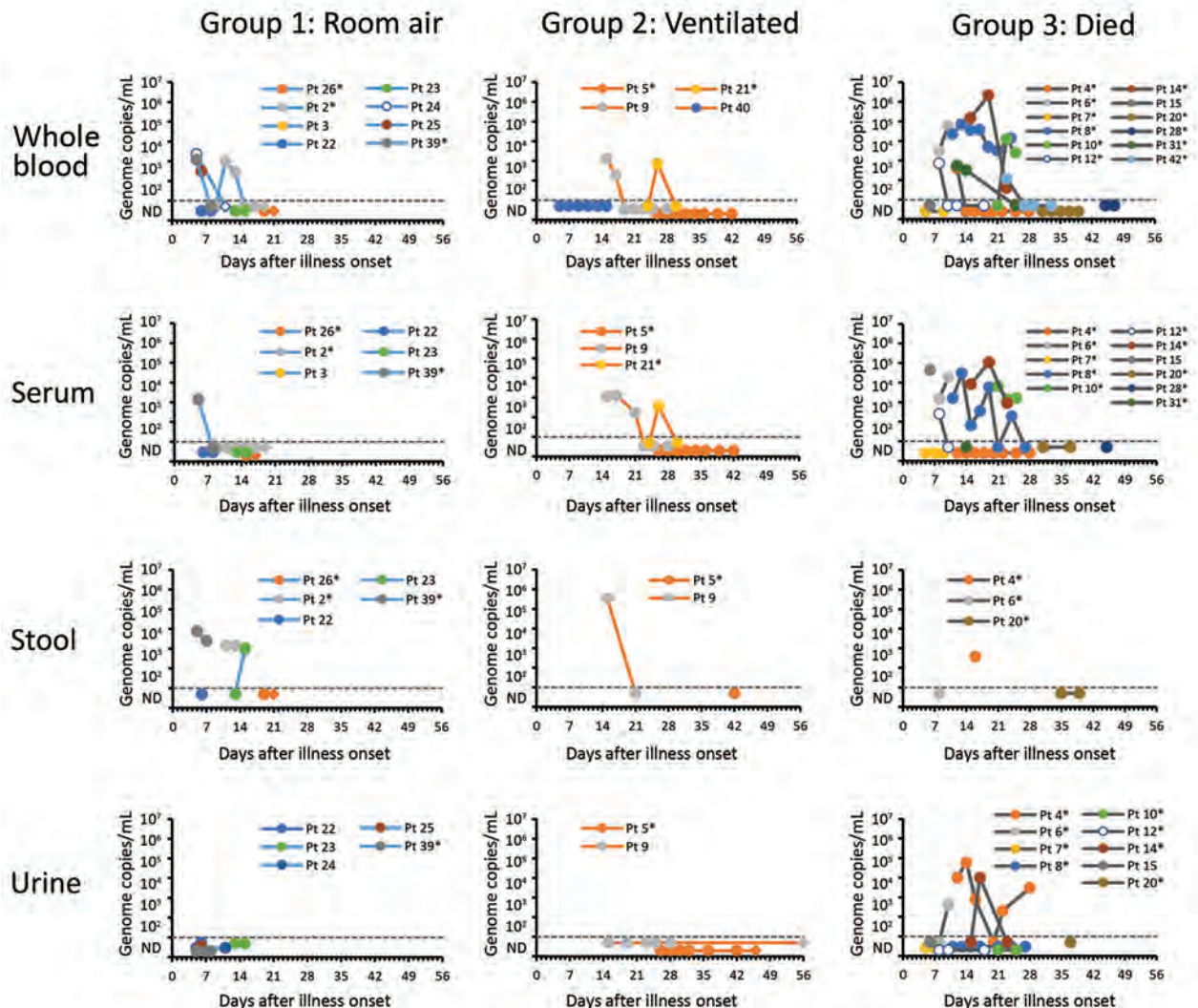


**Figure 4.** Estimated viral loads in non–respiratory tract specimens collected from hospitalized MERS-CoV patients, Saudi Arabia, August 1, 2015–August 31, 2016, and submitted to the US Centers for Disease Control and Prevention. Specimen types are shown by severity group. Estimated viral loads are based on upstream of the envelope (upE) real-time reverse transcription PCR cycle threshold values, or N2 cycle threshold values if the upE real-time reverse transcription PCR was negative. The dashed line represents the limit of detection, below which specimens were considered MERS-CoV–negative or not detected. Round data points represent specimens collected during the MERS-CoV detection period (defined by clinical results from respiratory specimens). Diamond data points represent specimens collected after the MERS-CoV detection period (defined by clinical results from respiratory specimens); no specimens were positive for MERS-CoV after the detection period. \*Patients with a documented history of diabetes mellitus. MERS-CoV, Middle East respiratory syndrome coronavirus; Pt, patient.







**Table 4.** Specimens and MERS-CoV–infected patients with detectable Abs, by time since illness onset and outcome, Saudi Arabia, August 1, 2015–August 31, 2016\*

Outcome	Days since onset	No. specimens with Abs detected/no. tested				No. patients† with Abs detected/no. tested			
		MN	VSV-MERS-S	S ELISA	N ELISA	MN	VSV-MERS-S	S ELISA	N ELISA
Survived	<14	3/17	4/16	5/17	7/17	3/11	4/10	4/11	5/11
	14–20	4/8	4/8	4/8	6/8	3/5	3/5	3/5	4/5
	21–27	6/6	5/5	6/6	6/6	3/3	3/3	3/3	3/3
	28–55	10/10	10/10	10/10	10/10	4/4	4/4	4/4	4/4
	1 y	4/4	4/4	4/4	4/4	4/4	4/4	4/4	2/4
Died	<14	9/11	8/11	5/11	8/11	5/6	5/6	3/6	4/6
	14–20	9/9	6/8	7/9	9/9	4/4	2/3	4/4	4/4
	21–27	9/9	8/9	8/9	9/9	4/4	4/4	4/4	4/4
	28–55	4/4	4/4	4/4	4/4	3/3	3/3	3/3	3/3
	1 y	NA	NA	NA	NA	NA	NA	NA	NA

\*Abs, antibodies; MERS-CoV, Middle East respiratory syndrome coronavirus; MN, microneutralization assay; N ELISA, nucleocapsid ELISA; S ELISA, spike ELISA; VSV-MERS-S, pseudoparticle neutralization assay; NA, not available.

†Number of patients represents those with available specimens for a given period. Specimens were not available from all patients during all periods. Some specimens were not tested by VSV-MERS-S pseudoparticle assay because of insufficient volume.

from South Korea (5,45–47) in 2015, and its association with increased severity in that setting was less clear (5,45). In our investigation, factors affecting DM management before infection were unknown.

Information about MERS-CoV detection and antibody responses in case-patients who died has been limited (19,24–26,29). In our study, patients who died had robust neutralizing antibody responses during the second and third weeks of illness, but this response was not sufficient for patient recovery. During this same period (weeks 2–3), RNA levels peaked in the LRT of these case-patients, suggesting that antibodies might not be sufficient for virus clearance. Antibodies were more often co-detected with viral RNA in the serum and URT of case-patients who died compared with survivors. Co-detection of antibodies and RNA has been described previously but not by patient outcome (19,25). Six patients who died had MERS-CoV RNA in their serum, despite the presence of neutralizing antibodies, and 3 had RNA in urine. Detection of MERS-CoV in blood or serum has previously been associated with need for supplemental oxygen (18), the need for mechanical ventilation (24), and death (24,26). Although we detected RNA in the blood or serum of all severity groups, estimated viral loads might have been higher in patients who died than survivors; this was difficult to assess statistically because of limited specimen collection and variability in timing of collection. In 4/12 patients who died, RNA levels in the LRT decreased to low or undetectable before death, suggesting that viral replication in the respiratory tract might variably or indirectly contribute to outcome.

Previous studies using MN tests (19) or S-specific assays (25,31) have suggested that some case-patients who die might exhibit a delayed MERS-CoV–specific antibody response. Although most patients in our study developed early and concomitant MN and VSV-MERS-S (pseudoparticle assays) responses, 1 case-patient who died exhibited a prominent delay in detectable VSV-MERS-S and S ELISA responses compared with MN. This finding warrants

further investigation and might suggest that the MN assay targets antibodies functioning beyond S-specific viral entry. Although our neutralizing assays targeted 2 different MERS-CoV strains, no variations exist within the receptor binding sites of these viruses (Appendix 1 Figure 10). Compared with these 2 viruses, the virus strain used in our S ELISA (EMC) differs in S by 2–3 aa, which is unlikely to confer a notable difference in binding during a polyclonal antibody response.

We further characterized virus shedding among mildly ill patients (i.e., those who did not require supplemental oxygen while hospitalized and who might typically be isolated at home) and found that RNA levels in the URT peaked during the first week of illness among this group, not in the second week as previously suggested (18), although LRT specimens were not available for included patients. Similar to previous descriptions, we detected MERS-CoV RNA in the blood or serum of some mildly ill patients (18,25), but we also detected RNA in stool up to 15 days after illness onset; viable virus was not isolated from these specimen types. MERS-CoV RNA has been reported in stool previously (19), but the severity of illness and the time since illness onset in these patients were unknown. Replication in the intestinal tract has been postulated (27), but its role in pathogenesis or transmission remains unclear.

We characterized symptom progression in mildly symptomatic patients and found that fever and cough (when present) typically aligned with MERS-CoV detection. However, some patients remained febrile or reported cough even after virus clearance from the URT. Given the variability we observed in symptom progression during the MERS-CoV detection period, testing for viral shedding should continue to inform patient management, as stated in current World Health Organization guidance (14).

Our investigation has several limitations. First, the number of patients enrolled might have been insufficient to detect some associations, especially when adjusting for other variables. Second, testing data were not

available before onset for all but 1 patients, and so we used days from onset to MERS-CoV negativity to assess shedding duration; we also excluded fatal cases from such analyses because time to death was not reflective of shedding duration, meaning that factors associated predominantly with mortality were not assessed for prolonged shedding. Third, the presence of MERS-CoV RNA does not necessarily represent viable

virus. Fourth, serum specimen collection was deemed too sparse to reliably assess antibody kinetics at the patient level.

Prolonged shedding in those with DM and the detection of MERS-CoV RNA from nonrespiratory specimens, including RNA-positive stool in mildly ill patients, should be considered in infection prevention and control and when determining whether home isolation is appropriate. The

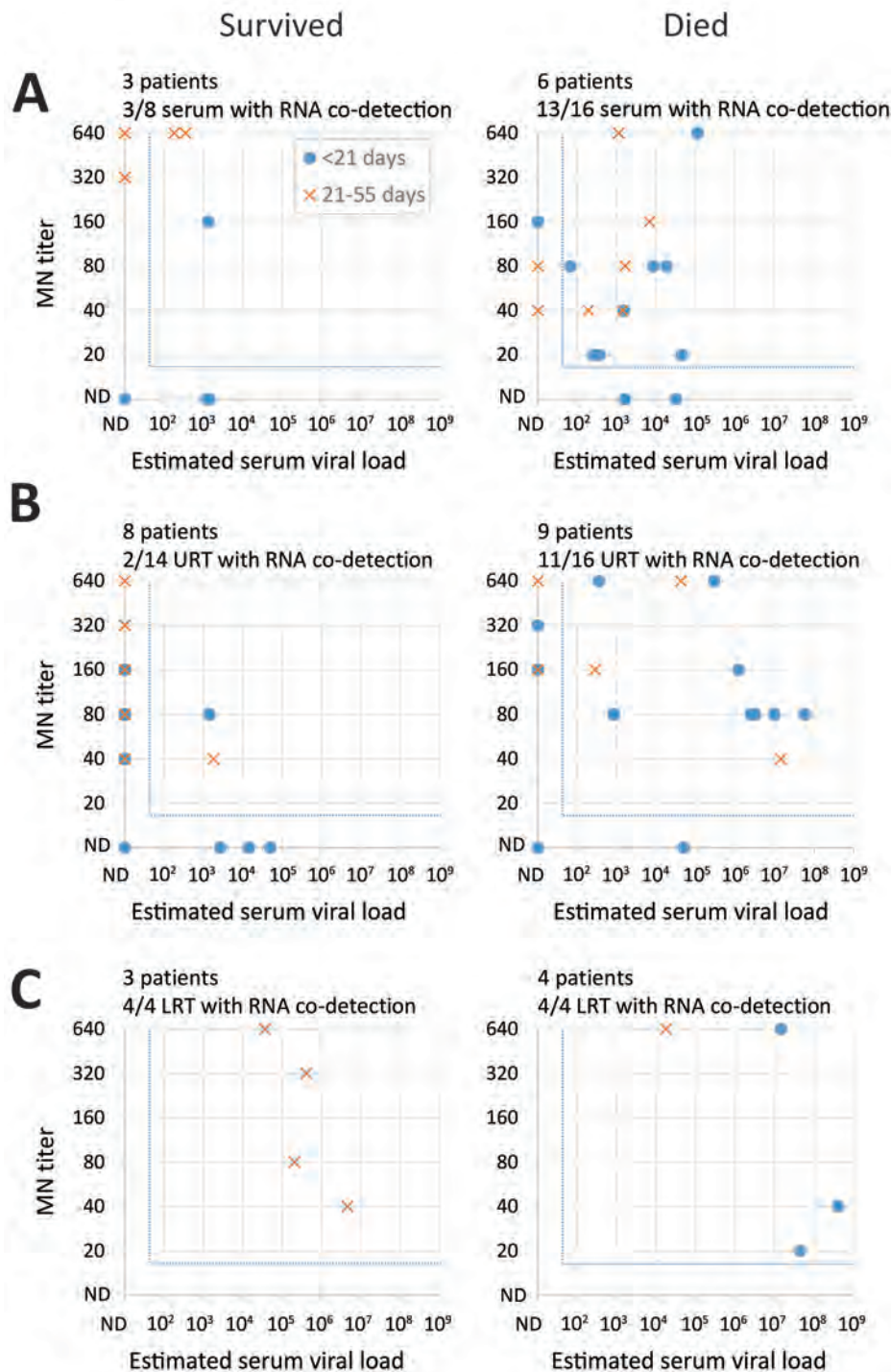


**Figure 6.** Co-detection of neutralizing serum antibodies with RNA found in serum and the upper and lower respiratory tracts among Middle East respiratory syndrome patients, by clinical outcome, Saudi Arabia, August 1, 2015–August 31, 2016. For each patient and specimen, MN titers of serum specimens were compared with estimated viral loads in the same serum specimen (A) or in URT (B) and LRT (C) specimens collected on the same day from the same patient. We defined RNA co-detection as the detection of both RNA and neutralizing antibodies (MN) in the same specimen or in respiratory specimens collected on the same day from a given patient. We only included specimens from patients who were known to develop neutralizing antibodies at any point during or after their illness. For the comparison in serum specimens, we only included specimens from patients who were known to have RNA detected in serum, at any point during their illness. For each panel, the number of patients included are indicated above the panel. The number of specimens with RNA co-detection (indicated by X) among those with detectable antibodies (indicated by Y) are also indicated by numbers (X/Y) above each panel. The blue dotted lines indicate the detection cut-offs for each assay. LRT, lower respiratory tract; ND, not detected; MN, microneutralization assay; URT, upper respiratory tract.

presence of detectable antibodies in case-patients who died and the co-detection of antibodies with viral RNA might also have implications for the development of vaccines and antibody therapeutics. Our findings broaden our understanding of MERS-CoV natural history and provide evidence to inform surveillance strategies, diagnostics, therapeutic and vaccine development, and clinical and public health management guidelines for MERS patients.

### Acknowledgments

We thank Holly M. Biggs for critical review of the manuscript, Shifaq Kamili for specimen coordination, and Melvina Girvan for assistance with data collection.

This work was funded by the Ministry of Health in Saudi Arabia, and the US Centers for Disease Control and Prevention.

The study was reviewed and approved by the Saudi Arabia Ministry of Health institutional review board. Because CDC only had access to deidentified data for secondary analyses, it was determined this project was not human subjects research, and therefore CDC's institutional review board approval was not required.

### About the Author

During this investigation, Dr. Al-Abdely was general director of Infection Prevention and Control, Ministry of Health, Saudi Arabia. He currently is professor of medicine at Alfaisal University, Saudi Arabia, and a consultant in infectious diseases for King Faisal Specialist Hospital and Research Centre, Saudi Arabia. His research interests include infection prevention and control, medical mycology, and microbial resistance.

### References

- Assiri A, McGeer A, Perl TM, Price CS, Al Rabeeah AA, Cummings DA, et al.; KSA MERS-CoV Investigation Team. Hospital outbreak of Middle East respiratory syndrome coronavirus. *N Engl J Med*. 2013;369:407–16. <http://dx.doi.org/10.1056/NEJMoa1306742>
- Oboho IK, Tomczyk SM, Al-Asmari AM, Banjar AA, Al-Mugti H, Aloraini MS, et al. 2014 MERS-CoV outbreak in Jeddah—a link to health care facilities. *N Engl J Med*. 2015;372:846–54. <http://dx.doi.org/10.1056/NEJMoa1408636>
- Arabi YM, Al-Omari A, Mandourah Y, Al-Hameed F, Sindi AA, Alraddadi B, et al.; Saudi Critical Care Trial Group. Critically ill patients with the Middle East respiratory syndrome: a multicenter retrospective cohort study. *Crit Care Med*. 2017;45:1683–95. <http://dx.doi.org/10.1097/CCM.0000000000002621>
- Arabi YM, Balkhy HH, Hayden FG, Bouchama A, Luke T, Baillie JK, et al. Middle East respiratory syndrome. *N Engl J Med*. 2017;376:584–94. <http://dx.doi.org/10.1056/NEJMsr1408795>
- Ko JH, Park GE, Lee JY, Lee JY, Cho SY, Ha YE, et al. Predictive factors for pneumonia development and progression to respiratory failure in MERS-CoV infected patients. *J Infect*. 2016;73:468–75. <http://dx.doi.org/10.1016/j.jinf.2016.08.005>
- Senga M, Arabi YM, Fowler RA. Clinical spectrum of the Middle East respiratory syndrome coronavirus (MERS-CoV). *J Infect Public Health*. 2017;10:191–4. <http://dx.doi.org/10.1016/j.jiph.2016.04.008>
- Assiri A, Al-Tawfiq JA, Al-Rabeeah AA, Al-Rabiah FA, Al-Hajjar S, Al-Barrak A, et al. Epidemiological, demographic, and clinical characteristics of 47 cases of Middle East respiratory syndrome coronavirus disease from Saudi Arabia: a descriptive study. *Lancet Infect Dis*. 2013;13:752–61. [http://dx.doi.org/10.1016/S1473-3099\(13\)70204-4](http://dx.doi.org/10.1016/S1473-3099(13)70204-4)
- Saad M, Omrani AS, Baig K, Bahloul A, Elzein F, Matin MA, et al. Clinical aspects and outcomes of 70 patients with Middle East respiratory syndrome coronavirus infection: a single-center experience in Saudi Arabia. *Int J Infect Dis*. 2014;29:301–6. <http://dx.doi.org/10.1016/j.ijid.2014.09.003>
- World Health Organization. Middle East respiratory syndrome coronavirus (MERS-CoV) fact sheet [cited 2017 Oct 30]. [https://www.who.int/en/news-room/fact-sheets/detail/middle-east-respiratory-syndrome-coronavirus-\(mers-cov\)](https://www.who.int/en/news-room/fact-sheets/detail/middle-east-respiratory-syndrome-coronavirus-(mers-cov))
- Assiri AM, Biggs HM, Abedi GR, Lu X, Bin Saeed A, Abdalla O, et al. Increase in Middle East Respiratory syndrome-coronavirus cases in Saudi Arabia linked to hospital outbreak with continued circulation of recombinant virus, July 1–August 31, 2015. *Open Forum Infect Dis*. 2016;3:ofw165.
- Assiri A, Abedi GR, Bin Saeed AA, Abdalla MA, al-Masry M, Choudhry AJ, et al. Multifacility outbreak of Middle East respiratory syndrome in Taif, Saudi Arabia. *Emerg Infect Dis*. 2016;22:32–40. <http://dx.doi.org/10.3201/eid2201.151370>
- Drosten C, Meyer B, Müller MA, Corman VM, Al-Masry M, Hossain R, et al. Transmission of MERS-coronavirus in household contacts. *N Engl J Med*. 2014;371:828–35. <http://dx.doi.org/10.1056/NEJMoa1405858>
- Alraddadi BM, Watson JT, Almarashi A, Abedi GR, Turkistani A, Sadran M, et al. Risk factors for primary Middle East respiratory syndrome coronavirus illness in humans, Saudi Arabia, 2014. *Emerg Infect Dis*. 2016;22:49–55. <http://dx.doi.org/10.3201/eid2201.151340>
- World Health Organization. Infection prevention and control during health care for probable or confirmed cases of Middle East respiratory syndrome coronavirus (MERS-CoV) infection—interim guidance [cited 2017 Oct 30]. [https://www.who.int/csr/disease/coronavirus\\_infections/ipc-mers-cov/en](https://www.who.int/csr/disease/coronavirus_infections/ipc-mers-cov/en)
- World Health Organization. Management of asymptomatic persons who are RT-PCR positive for Middle East respiratory syndrome coronavirus (MERS-CoV) [cited 2018 Sep 20]. [https://www.who.int/csr/disease/coronavirus\\_infections/management\\_of\\_asymptomatic\\_patients/en](https://www.who.int/csr/disease/coronavirus_infections/management_of_asymptomatic_patients/en)
- Memish ZA, Assiri AM, Al-Tawfiq JA. Middle East respiratory syndrome coronavirus (MERS-CoV) viral shedding in the respiratory tract: an observational analysis with infection control implications. *Int J Infect Dis*. 2014;29:307–8. <http://dx.doi.org/10.1016/j.ijid.2014.10.002>
- Poissy J, Goffard A, Parmentier-Decrucq E, Favory R, Kaut M, Kipnis E, et al.; MERS-CoV Biology Group. Kinetics and pattern of viral excretion in biological specimens of two MERS-CoV cases. *J Clin Virol*. 2014;61:275–8. <http://dx.doi.org/10.1016/j.jcv.2014.07.002>
- Oh MD, Park WB, Choe PG, Choi SJ, Kim JI, Chae J, et al. Viral load kinetics of MERS coronavirus infection. *N Engl J Med*. 2016;375:1303–5. <http://dx.doi.org/10.1056/NEJMc1511695>
- Corman VM, Albarrak AM, Omrani AS, Albarrak MM, Farah ME, Almasri M, et al. Viral shedding and antibody response in 37 patients with Middle East respiratory syndrome coronavirus infection. *Clin Infect Dis*. 2016;62:477–83.
- Memish ZA, Al-Tawfiq JA, Makhdoom HQ, Assiri A, Alhakeem RF, Albarrak A, et al. Respiratory tract samples, viral load, and genome fraction yield in patients with Middle East respiratory syndrome. *J Infect Dis*. 2014;210:1590–4. <http://dx.doi.org/10.1093/infdis/jiu292>



21. Feikin DR, Alraddadi B, Qutub M, Shabouni O, Curns A, Oboho IK, et al. Association of higher MERS-CoV virus load with severe disease and death, Saudi Arabia, 2014. *Emerg Infect Dis*. 2015;21:2029–35. <http://dx.doi.org/10.3201/eid2111.150764>
22. Guery B, Poissy J, el Mansouf L, Séjourné C, Ettahar N, Lemaire X, et al.; MERS-CoV study group. Clinical features and viral diagnosis of two cases of infection with Middle East respiratory syndrome coronavirus: a report of nosocomial transmission. *Lancet*. 2013;381:2265–72. [http://dx.doi.org/10.1016/S0140-6736\(13\)60982-4](http://dx.doi.org/10.1016/S0140-6736(13)60982-4)
23. Drosten C, Seilmaier M, Corman VM, Hartmann W, Scheible G, Sack S, et al. Clinical features and virological analysis of a case of Middle East respiratory syndrome coronavirus infection. *Lancet Infect Dis*. 2013;13:745–51. [http://dx.doi.org/10.1016/S1473-3099\(13\)70154-3](http://dx.doi.org/10.1016/S1473-3099(13)70154-3)
24. Kim SY, Park SJ, Cho SY, Cha RH, Jee HG, Kim G, et al. Viral RNA in blood as indicator of severe outcome in Middle East respiratory syndrome coronavirus infection. *Emerg Infect Dis*. 2016;22:1813–6. <http://dx.doi.org/10.3201/eid2210.160218>
25. Min CK, Cheon S, Ha NY, Sohn KM, Kim Y, Aigerim A, et al. Comparative and kinetic analysis of viral shedding and immunological responses in MERS patients representing a broad spectrum of disease severity. *Sci Rep*. 2016;6:25359. <http://dx.doi.org/10.1038/srep25359>
26. Shalhoub S, Farahat F, Al-Jiffri A, Simhairi R, Shamma O, Siddiqi N, et al. IFN- $\alpha$ 2a or IFN- $\beta$ 1a in combination with ribavirin to treat Middle East respiratory syndrome coronavirus pneumonia: a retrospective study. *J Antimicrob Chemother*. 2015;70:2129–32. <http://dx.doi.org/10.1093/jac/dkv085>
27. Zhou J, Li C, Zhao G, Chu H, Wang D, Yan HH, et al. Human intestinal tract serves as an alternative infection route for Middle East respiratory syndrome coronavirus. *Sci Adv*. 2017;3:eaa04966.
28. Choe PG, Perera RAPM, Park WB, Song KH, Bang JH, Kim ES, et al. MERS-CoV antibody responses 1 year after symptom onset, South Korea, 2015. *Emerg Infect Dis*. 2017;23:1079–84. <http://dx.doi.org/10.3201/eid2307.170310>
29. Shin HS, Kim Y, Kim G, Lee JY, Jeong I, Joh JS, et al. Immune responses to MERS coronavirus during the acute and convalescent phases of human infection. *Clin Infect Dis*. 2018. <http://dx.doi.org/10.1093/cid/ciy595>
30. Park WB, Perera RA, Choe PG, Lau EH, Choi SJ, Chun JY, et al. Kinetics of serologic responses to MERS coronavirus infection in humans, South Korea. *Emerg Infect Dis*. 2015;21:2186–9. <http://dx.doi.org/10.3201/eid2112.151421>
31. Ko JH, Müller MA, Seok H, Park GE, Lee JY, Cho SY, et al. Serologic responses of 42 MERS-coronavirus-infected patients according to the disease severity. *Diagn Microbiol Infect Dis*. 2017;89:106–11. <http://dx.doi.org/10.1016/j.diagmicrobio.2017.07.006>
32. Payne DC, Iblan I, Rha B, Alqasrawi S, Haddadin A, Al Nsour M, et al. Persistence of antibodies against Middle East respiratory syndrome coronavirus. *Emerg Infect Dis*. 2016;22:1824–6. <http://dx.doi.org/10.3201/eid2210.160706>
33. Saeed AA, Abedi GR, Alzahrani AG, Salameh I, Abdirizak F, Alhakeem R, et al. Surveillance and testing for Middle East respiratory syndrome coronavirus, Saudi Arabia, April 2015–February 2016. *Emerg Infect Dis*. 2017;23:682–5. <http://dx.doi.org/10.3201/eid2304.161793>
34. Corman VM, Ölschläger S, Wendtner CM, Drexler JF, Hess M, Drosten C. Performance and clinical validation of the RealStar MERS-CoV kit for detection of Middle East respiratory syndrome coronavirus RNA. *J Clin Virol*. 2014;60:168–71. <http://dx.doi.org/10.1016/j.jcv.2014.03.012>
35. Lu X, Whitaker B, Sakthivel SK, Kamili S, Rose LE, Lowe L, et al. Real-time reverse transcription-PCR assay panel for Middle East respiratory syndrome coronavirus. *J Clin Microbiol*. 2014;52:67–75. <http://dx.doi.org/10.1128/JCM.02533-13>
36. Al-Abdely HM, Midgley CM, Alkhamis AM, Abedi GR, Tamin A, Binder AM, et al. Infectious MERS-CoV isolated from a mildly ill patient, Saudi Arabia. *Open Forum Infect Dis*. 2018;5:ofy111. <http://dx.doi.org/10.1093/ofid/ofy111>
37. Al-Abdallat MM, Payne DC, Alqasrawi S, Rha B, Tohme RA, Abedi GR, et al.; Jordan MERS-CoV Investigation Team. Hospital-associated outbreak of Middle East respiratory syndrome coronavirus: a serologic, epidemiologic, and clinical description. *Clin Infect Dis*. 2014;59:1225–33. <http://dx.doi.org/10.1093/cid/ciu359>
38. Trivedi S, Miao C, Al-Abdallat MM, Haddadin A, Alqasrawi S, Iblan I, et al. Inclusion of MERS-spike protein ELISA in algorithm to determine serologic evidence of MERS-CoV infection. *J Med Virol*. 2018;90:367–71. <http://dx.doi.org/10.1002/jmv.24948>
39. Assiri AM, Midgley CM, Abedi GR, Bin Saeed A, Almasri MM, Lu X, et al. Epidemiology of a novel recombinant Middle East respiratory syndrome coronavirus in humans in Saudi Arabia. *J Infect Dis*. 2016;214:712–21. <http://dx.doi.org/10.1093/infdis/jiw236>
40. Sabir JS, Lam TT, Ahmed MM, Li L, Shen Y, Abo-Aba SE, et al. Co-circulation of three camel coronavirus species and recombination of MERS-CoVs in Saudi Arabia. *Science*. 2016;351:81–4. <http://dx.doi.org/10.1126/science.aac8608>
41. World Health Organization. Diabetes country profile, Saudi Arabia [cited 2017 Dec 26]. [https://www.who.int/diabetes/country-profiles/sau\\_en.pdf](https://www.who.int/diabetes/country-profiles/sau_en.pdf)
42. International Diabetes Federation. Age-adjusted prevalence of diabetes (20–79), Saudi Arabia, 2017 [cited 2017 Dec 26]. <http://www.diabetesatlas.org/across-the-globe.html>
43. Badawi A, Ryoo SG. Prevalence of diabetes in the 2009 influenza A (H1N1) and the Middle East respiratory syndrome coronavirus: a systematic review and meta-analysis. *J Public Health Res*. 2016;5:733. <http://dx.doi.org/10.4081/jphr.2016.733>
44. Banik GR, Alqahtani AS, Booy R, Rashid H. Risk factors for severity and mortality in patients with MERS-CoV: analysis of publicly available data from Saudi Arabia. *Virol Sin*. 2016;31:81–4. <http://dx.doi.org/10.1007/s12250-015-3679-z>
45. Choi WS, Kang CI, Kim Y, Choi JP, Joh JS, Shin HS, et al.; Korean Society of Infectious Diseases. Clinical presentation and outcomes of Middle East respiratory syndrome in the Republic of Korea. *Infect Chemother*. 2016;48:118–26. <http://dx.doi.org/10.3947/ic.2016.48.2.118>
46. Kim ES, Choe PG, Park WB, Oh HS, Kim EJ, Nam EY, et al. Clinical progression and cytokine profiles of Middle East respiratory syndrome coronavirus infection. *J Korean Med Sci*. 2016;31:1717–25. <http://dx.doi.org/10.3346/jkms.2016.31.11.1717>
47. Kim KH, Tandil TE, Choi JW, Moon JM, Kim MS. Middle East respiratory syndrome coronavirus (MERS-CoV) outbreak in South Korea, 2015: epidemiology, characteristics and public health implications. *J Hosp Infect*. 2017;95:207–13. <http://dx.doi.org/10.1016/j.jhin.2016.10.008>

---

Address for correspondence: Claire M. Midgley or John T. Watson, Centers for Disease Control and Prevention, 1600 Clifton Road NE, Atlanta, GA, 30329-4027; email: ydk5@cdc.gov or acq4@cdc.gov

---

# *Francisella tularensis* Transmission by Solid Organ Transplantation, 2017<sup>1</sup>

Christina A. Nelson, Christian Murua, Jefferson M. Jones, Kelli Mohler, Ying Zhang, Landon Wiggins, Natalie A. Kwit,<sup>2</sup> Laurel Respicio-Kingry, Luke C. Kingry, Jeannine M. Petersen, Jennifer Brown, Saima Aslam, Melissa Krafft, Shadaba Asad, Hikmat N. Dagher, John Ham, Luis H. Medina-Garcia, Kevin Burns, Walter E. Kelley, Alison F. Hinckley, Pallavi Annambhotla, Karen Carifo, Anthony Gonzalez, Elizabeth Helsel, Joseph Iser, Michael Johnson, Curtis L. Fritz, Sridhar V. Basavaraju, and the Tularemia in Transplant Recipients Investigation Team<sup>3</sup>

In July 2017, fever and sepsis developed in 3 recipients of solid organs (1 heart and 2 kidneys) from a common donor in the United States; 1 of the kidney recipients died. Tularemia was suspected only after blood cultures from the surviving kidney recipient grew *Francisella* species. The organ donor, a middle-aged man from the southwestern United States, had been hospitalized for acute alcohol withdrawal syndrome, pneumonia, and multiorgan failure. *F. tularensis* subsp. *tularensis* (clade A2) was cultured from archived spleen tissue from the donor and blood from both kidney recipients. Whole-genome multilocus sequence typing indicated that the isolated strains were indistinguishable. The heart recipient remained seronegative with negative blood cultures but had been receiving antimicrobial drugs for a medical device infection before transplant. Two lagomorph

carcasses collected near the donor's residence were positive by PCR for *F. tularensis* subsp. *tularensis* (clade A2). This investigation documents *F. tularensis* transmission by solid organ transplantation.

---

Tularemia, also known as rabbit fever, is a zoonotic disease caused by the gram-negative bacterium *Francisella tularensis*. Natural transmission to humans occurs through a variety of routes, including tick and deerfly bites, direct handling of infected tissues, ingestion of contaminated water or tissues, or inhalation of infective materials (1). Tularemia occurs throughout the northern hemisphere in every US state except Hawaii. Each year in the United States, ≈120 cases are reported (2).

*F. tularensis* is a Tier 1 bioterrorism threat because of its low infective dose, ability to aerosolize, and history of development as a bioterrorism agent. Several countries have studied this organism or developed it as a bioweapon (3,4). *F. tularensis* has also caused laboratory-acquired infections (5); therefore, laboratory personnel must take specific precautionary measures when handling clinical isolates (6).

Clinical manifestations of *F. tularensis* infection depend on route of exposure. Ulceroglandular and glandular tularemia, characterized by fever and tender regional lymphadenopathy, are the most common forms and typically follow inoculation of the skin. Pneumonic tularemia, the most lethal form, results from inhalation of *F. tularensis* or hematogenous spread from local infection. Pneumonic tularemia typically produces fever, chest pain, shortness

---

Author affiliations: Centers for Disease Control and Prevention, Fort Collins, Colorado, USA (C.A. Nelson, N.A. Kwit, L. Respicio-Kingry, L.C. Kingry, J.M. Petersen, A.F. Hinckley); Southern Nevada Health District, Las Vegas, Nevada, USA (C. Murua, Y. Zhang, K. Carifo, J. Iser, M. Johnson); Centers for Disease Control and Prevention, Atlanta, Georgia, USA (J.M. Jones, P. Annambhotla, S.V. Basavaraju); Phoenix Area Indian Health Service, Phoenix, Arizona, USA (K. Mohler, L. Wiggins, E. Helsel); University of California Davis Medical Center, Sacramento, California, USA (J. Brown); University of California, San Diego, California, USA (S. Aslam, M. Krafft); University Medical Center of Southern Nevada, Las Vegas (S. Asad, J. Ham, L.H. Medina-Garcia); Sunrise Hospital and Medical Center, Las Vegas (H.N. Dagher); Nevada Donor Network, Las Vegas (K. Burns); American Red Cross, Salt Lake City, Utah, USA (W.E. Kelley); University of Arizona College of Medicine, Tucson, Arizona, USA (W.E. Kelley); Sacramento County Public Health Laboratory, Sacramento (A. Gonzalez); California Department of Public Health, Sacramento (C.L. Fritz)

DOI: <https://doi.org/10.3201/eid2504.181807>

---

<sup>1</sup>Results from this investigation were presented at the 9th International Conference on Tularemia; October 16–19, 2018; Montreal, Québec, Canada.

<sup>2</sup>Current affiliation: Vermont Department of Health, Burlington, Vermont, USA.

<sup>3</sup>Members of the team are listed at the end of this article.

of breath, and variable radiographic findings. Oropharyngeal, oculoglandular, and typhoidal tularemia occur less frequently (7). The drugs typically recommended for treatment of tularemia are streptomycin, gentamicin, ciprofloxacin, or doxycycline (4).

In July 2017, the Centers for Disease Control and Prevention (CDC) was notified that blood cultures from 2 solid organ transplant recipients in different US states, both of whom had sepsis, yielded a small, gram-negative organism suspected to be *F. tularensis*. The 2 recipients shared a common organ donor, prompting a collaborative public health investigation to characterize the source of transmission.

## Patients

### Transplant Recipients

In July 2017, septic shock developed in 2 patients who had received a kidney and 1 patient who had received a heart from a common donor. The clinical course of disease, antimicrobial drug regimens, and immunosuppressive medications for these patients are summarized in Figure 1.

#### Kidney Recipient 1

The patient was a middle-aged man who had received a kidney transplant for IgA nephropathy and focal segmental glomerulosclerosis. Four days after transplantation, fever (39.4°C), hypoxemia, and wheezing developed. The next day, despite empiric treatment with vancomycin and meropenem, disseminated intravascular coagulation and septic shock developed, and the patient died. The organ procurement organization was alerted and immediately notified the physicians for the other 2 solid organ recipients.

Three days after the patient's death, small gram-negative bacilli grew from a blood culture that had been collected 4 days after transplantation (Figure 1). Isolate characteristics subsequently suggested that it was a possible organism of bioterrorism (Select Agent); therefore, in accordance with American Society for Microbiology guidelines ([https://www.asm.org/Articles/Policy/Laboratory-Response-Network-\(LRN\)-Sentinel-Level-C](https://www.asm.org/Articles/Policy/Laboratory-Response-Network-(LRN)-Sentinel-Level-C)), the hospital laboratory discontinued identification procedures and referred the isolate to the local public health laboratory, a Laboratory Response Network (LRN) biological facility (8). Using growth characteristics, biochemical testing, and real-time PCR testing, the laboratory presumptively identified the organism as a *Francisella* species, notified CDC, and sent clinical samples to CDC for characterization.

#### Kidney Recipient 2

This patient was a woman in her 60s who had received a kidney transplant for diabetes mellitus-induced end-stage renal disease. Four days after transplantation, she

experienced fever (39.4°C). Clinical samples were collected for culture, and treatment with vancomycin, ceftriaxone, and metronidazole was empirically initiated. She remained febrile, anemia and thrombocytopenia (49,000 platelets/mm<sup>3</sup>) developed, and she required mechanical ventilation and vasopressor support. Six days after transplantation, after the healthcare team was notified that the other kidney recipient had died of sepsis, doxycycline was added to the antimicrobial drug regimen. The patient eventually recovered.

Seven days after transplantation, gram-negative bacilli were isolated from blood and dialysate cultures (Figure 1). Gram-negative bacilli were also subsequently isolated from culture of samples from the peritoneal dialysis catheter tip and biliary fluid. Clinical samples were transferred to the local LRN biological facility and presumptively identified as a *Francisella* species (8). An isolate from the blood sample was sent to CDC for characterization.

#### Heart Recipient

The heart recipient was a middle-aged man with a history of nonischemic cardiomyopathy. Before transplantation, he had received ciprofloxacin and ceftriaxone for recurrent *Serratia marcescens* bacteremia related to an infected ventricular assist device. Ciprofloxacin was discontinued 1 day before transplantation and ceftriaxone the day of transplantation. Several hours after transplantation, fever (39.1°C), hypotension, and septic shock developed. He received vancomycin, meropenem, and cefepime, and fever resolved 5 days after transplantation. Results for cultures of blood collected during the septic episode, when the patient was receiving systemic antimicrobial drugs, were negative. Eleven days after transplantation, the clinical team was notified that the organ donor possibly had tularemia. The patient was empirically administered a 10-day course of oral ciprofloxacin and discharged home 27 days after transplantation.

#### Organ Donor

In June 2017, a middle-aged alcoholic man was evaluated at an emergency department for obtundation, bloody emesis, fever (39.6°C), and respiratory distress. He had abruptly ceased alcohol intake 5 days before admission and experienced a nonproductive cough, nausea, headache, and conjunctivitis 3 days before admission. Chest radiographs revealed right upper and lower lobe infiltrates (Figure 2). Platelet count was low (108,000/mm<sup>3</sup>). Soon thereafter, the patient became hypoxic but did not require mechanical ventilation.

The patient was admitted for presumed aspiration pneumonia, sepsis, and alcohol withdrawal and administered piperacillin/tazobactam, vancomycin, and benzodiazepine. Five days later, his fever and mental status temporarily



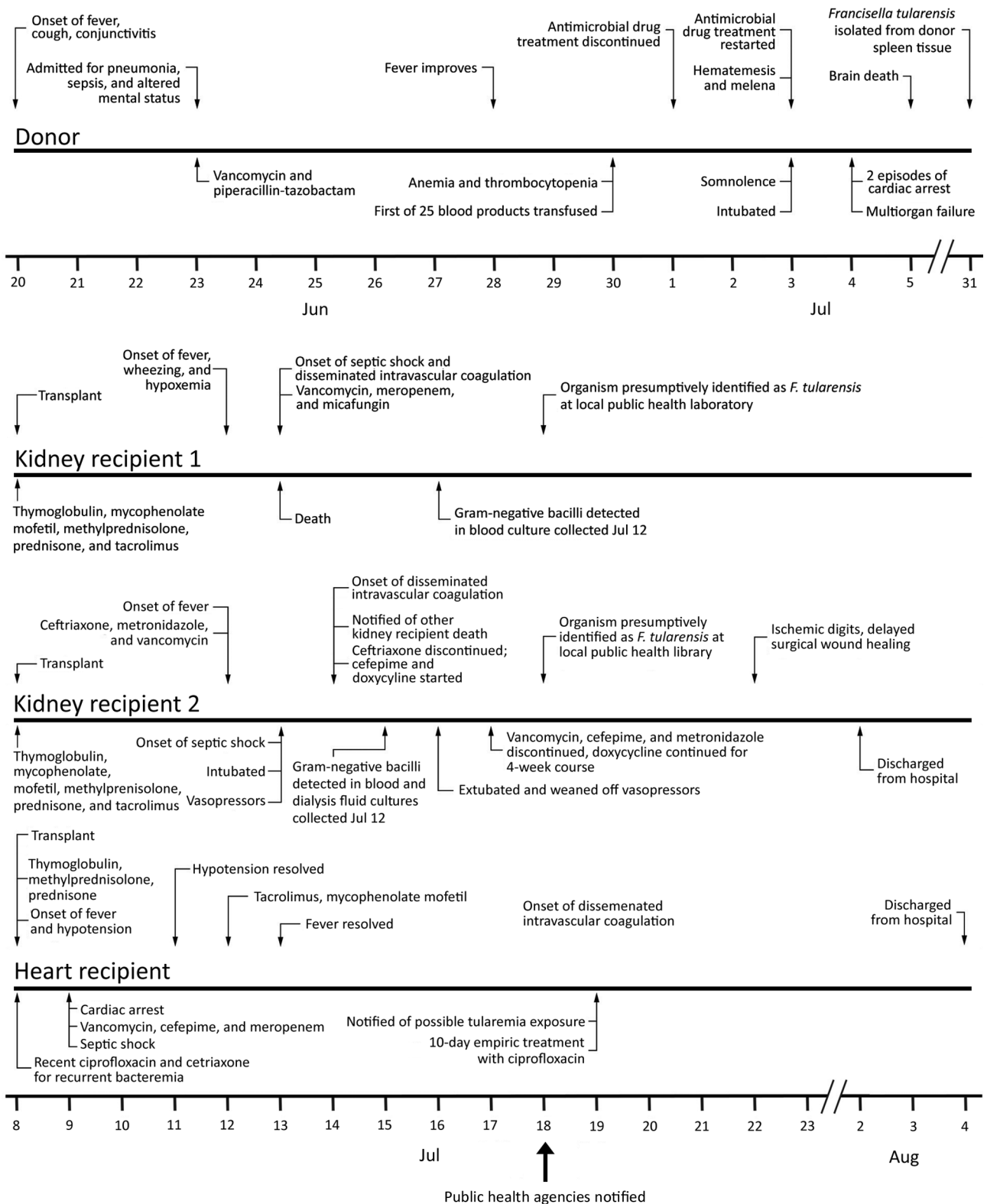
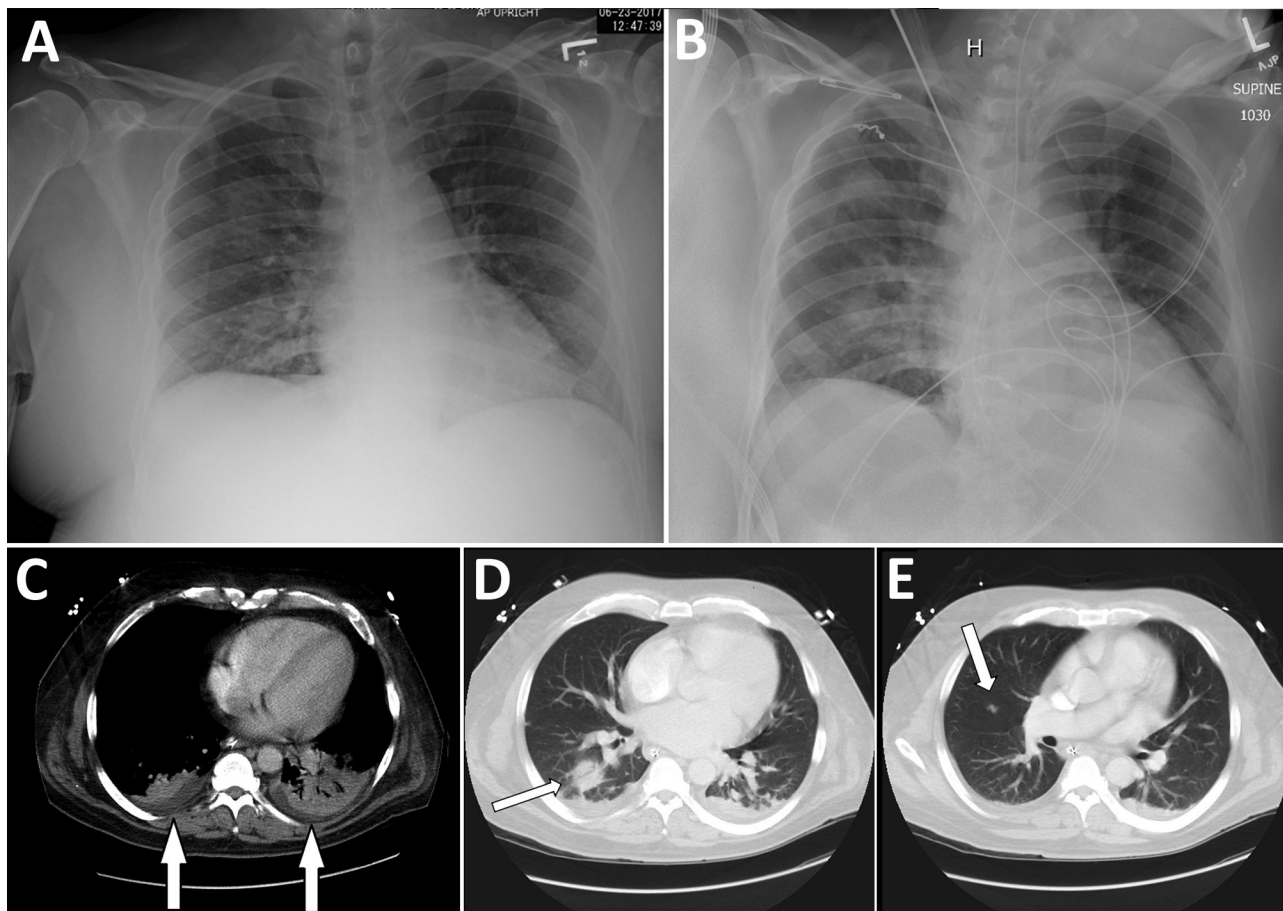


Figure 1. Clinical disease course for *Francisella tularensis*-infected organ donor and organ recipients, United States, 2017.



**Figure 2.** Radiographs (A, B) and computed tomography (C–E) images of chest of organ donor with *Francisella tularensis* infection, United States, 2017. Computed tomography images were taken after brain death. A) Anteroposterior view with patient in upright position, taken on day of admission; B) anteroposterior view with patient in supine position, taken on hospital day 10. C) Small bibasilar pleural effusions with adjacent subsegmental atelectasis versus pneumonia in the lower lobes (arrows); D) 3-cm round focus of pneumonia in the right lower lobe (arrow); E) 1-cm ill-defined nodule in the inferior right upper lobe (arrow).

improved, but thrombocytopenia (range 1,000–26,000 platelets/mm<sup>3</sup>), bloody emesis, and melena progressively worsened. Over 7 days, he received 25 blood product transfusions. Chest radiographs demonstrated worsening interstitial opacities (Figure 2). During the next day, he experienced multiorgan failure and 2 cardiac arrests; 12 days after admission, he was declared brain dead.

Results of cultures of the donor's blood (collected in blood culture bottles multiple times during hospitalization), urine, endotracheal aspirate, and bronchoalveolar lavage were all negative. Computed tomography of the chest performed after brain death revealed focal consolidation and a 1-cm nodule in the right perihilar region (Figure 2). Bronchoscopy indicated no abnormalities in the gross appearance of the lungs. An autopsy was not performed. Results of standard infectious disease testing for organ donor eligibility were negative (9). Both kidneys and the heart were procured for transplantation.

## Methods

We reviewed medical records of the organ donor and recipients and interviewed families and the 2 surviving patients about potential exposures to tularemia. In addition, we asked the organ donor's family about the donor's course of illness before hospitalization and illnesses of anyone who had been in close contact with him.

## Laboratory Testing

Recovered isolates were cultured at CDC on cysteine heart agar with 9% chocolate sheep blood and confirmed as *F. tularensis* by direct fluorescent antibody (DFA) testing. DNA was extracted from organ donor and kidney recipient cultures and lagomorph bone marrow by using the QIAamp DNA MiniKit (QIAGEN, <https://www.qiagen.com>) and tested with real-time TaqMan PCR by using *F. tularensis* multitarget type A and type B assays, then A1 and A2 subtyping assays (10,11). Serum samples were tested for

antibodies to *F. tularensis* by using the microagglutination assay (6); we considered a titer of  $\geq 1:128$  to be positive.

Pulsed-field gel electrophoresis (PFGE) typing of isolates was performed with the *PmeI* restriction enzyme (12) and clustered by using BioNumerics 6.64, Dice coefficient, and UPGMA (unweighted pair group method with arithmetic mean; Applied Maths, <http://www.applied-maths.com>). Whole-genome sequencing was performed by using Illumina V2 300 cycle reagents (13,14). The genome of each isolate was sequenced to an average depth of 311 $\times$  coverage. To compare the isolated strains, we used whole-genome multilocus sequence typing (wgMLST) with the *F. tularensis* A2 strain WY96-3418 as a reference (GenBank accession no. NC\_009257.1) (15). In brief, we mapped paired-end reads from each isolate to the WY96-3418 genome sequence and scanned 1,637 gene sequences (1,505,638 bp) representing 79% of the whole WY96-3418 genome (1,898,476 bp) for nucleotide differences by using CLC Genomics 10.0 (QIAGEN). Cluster analysis of alleles was performed in BioNumerics 7.5 (Applied Maths) by using categorical coefficient and UPGMA.

**Blood Donor Traceback**

To determine whether infection may have been transmitted from an asymptomatic blood donor to the organ donor, we investigated the sources of all blood products transfused to the organ donor. Blood donors were asked about any potential exposures to tularemia and whether they had experienced febrile illness during the 2-week period after

blood donation. Donors who reported potential exposures or febrile illness were tested for *F. tularensis* by serology.

**Environmental Assessment**

We investigated the organ donor’s community—including the vicinity of the donor’s residence, neighboring homes, nearby fields, and a river swimming area—to identify animal carcasses or other evidence of recent rodent or lagomorph die-off. Presence of potential arthropod vectors such as deer flies was noted informally during the assessment; however, arthropods were not systematically collected as part of the investigation.

We also evaluated the residential water supply as a possible source of infection. Records from standard municipal water testing results were reviewed, and the source well for the donor’s residence was examined for evidence of compromise or animal contamination.

**Results**

**Laboratory Tests**

**Culture, DFA, and PCR**

Testing of archived organ donor blood (collected in acid citrate dextrose and EDTA tubes 13 days after admission and stored at room temperature) and frozen spleen and lymph node tissues (collected 14 days after admission) produced the following results. Blood samples were negative for *F. tularensis* by PCR and culture (Table). *F. tularensis* was cultured from the spleen tissue; PCR genotyping of

**Table.** Culture and serology results for samples from *Francisella tularensis*-infected organ donor and organ recipients, United States, 2017

Patient, outcome, samples tested	Results
<b>Donor</b>	
Blood	Culture negative
Endotracheal aspirate	Culture negative
Urine	Culture negative
Bilateral bronchial washes	Culture negative
Lymph node, after brain death	Culture negative
Spleen tissue, after brain death	Culture positive for <i>Francisella tularensis</i>
Serum, after brain death	Serology positive (titer 1:128)*
<b>Kidney recipient 1, died</b>	
Blood	Culture positive for <i>F. tularensis</i>
Cerebrospinal fluid, postmortem	Culture positive for <i>F. tularensis</i>
Kidney tissue, postmortem	Culture positive for <i>F. tularensis</i>
Bone marrow, postmortem	Culture positive for <i>F. tularensis</i>
<b>Kidney recipient 2, discharged</b>	
Blood	Culture positive for <i>F. tularensis</i>
Dialysate	Culture positive for <i>F. tularensis</i>
Biliary fluid	Culture positive for <i>F. tularensis</i>
Peritoneal dialysis catheter tip	Culture positive for <i>F. tularensis</i>
<b>Heart recipient, discharged</b>	
Blood	Culture negative†
Serum	Serology negative

\*Antibody titer may be artificially low because of the large volume of blood products and other fluids that the patient received. Presence of a mounted immune response, as evidenced by seropositivity, might have contributed to negative culture results in all specimens other than spleen tissue.

†Before transplantation, the patient received ciprofloxacin and ceftriaxone for bacteremia related to a colonized ventricular assist device. At the time of sample collection, the patient had received a final dose of ciprofloxacin the previous day and a final dose of ceftriaxone that morning. Subsequent blood cultures were collected while the patient was receiving antimicrobial drugs for presumed sepsis and were negative.



the isolate revealed that it was *F. tularensis* subsp. *tularensis* (clade A2). Results of DFA and direct PCR testing of spleen tissue were negative. No isolate was recovered from lymph node tissue. Isolates from kidney recipients 1 and 2 were confirmed as *F. tularensis* by DFA testing and determined to be *F. tularensis* subsp. *tularensis* (clade A2) by PCR genotyping.

### Serologic Findings

Organ donor plasma from the archived EDTA blood specimen collected 13 days after admission was positive for antibodies to *F. tularensis* (titer 1:128). A serum sample from the heart recipient collected 11 days after transplant was negative for *F. tularensis* antibodies (titer <1:4).

### Strain Types

Molecular typing of the *F. tularensis* A2 strains from the donor and both kidney recipients found all 3 to be indistinguishable from one another by 2 methods (Figure 3). *PmeI* PFGE banding patterns for the 3 strains were the same. Comparison of this banding pattern to a larger PFGE database of *PmeI* patterns for A2 strains from throughout the western United States ( $n = 30$ ) demonstrated that the pattern was unique. Genome sequencing followed by wgMLST analysis revealed no nucleotide differences across 1.5 megabases of compared genome sequences between the 3 strains.

### Blood Donor Traceback Findings

Two blood suppliers provided the blood products transfused to the organ donor. Further blood donation by the donors who provided these products was temporarily deferred until the traceback and further serologic testing were completed. We identified and interviewed 43 of the blood donors. A review of blood supplier records confirmed that all blood donors met applicable regulations and standards at the time of donation. Telephone interviews of donors asked 9 questions specific to *F. tularensis* risk. One donor reported right-sided cervical lymphadenopathy; follow-up commercial laboratory testing of blood from this donor was negative for antibodies to *F. tularensis*.

### Environmental Assessment Findings

Interviews and medical record reviews of the organ recipients and their families revealed no known risk factors for tularemia. The organ donor resided on tribal lands in the southwestern United States. Family interviews revealed no known contact with sick animals, arthropod bites, household pets, or other noteworthy exposures. One family member reported observing groundhogs and rabbits near the donor's residence but denied any apparent animal die-offs. The donor was unemployed and had not traveled outside the region for several months before his death.

No deer flies or other arthropod vectors were observed near the organ donor's residence. Two lagomorph carcasses were found and collected  $\approx 150$  feet and 500 feet from the donor's residence. No organs or soft tissue from the carcasses were available for testing; however, PCR testing of DNA from femur bone marrow followed by genotyping indicated that both lagomorphs were positive for *F. tularensis* subsp. *tularensis* (clade A2).

Maintenance records of the community water source, a municipal well and spring, did not indicate a breakdown of the chlorination process. Investigation of the well site revealed an intact well cover and functioning system with no evidence of animal entry.

### Discussion

We report human-to-human transmission of tularemia by solid organ transplantation. All 3 recipients of organs from a common donor with unrecognized tularemia became ill; 1 recipient died. *F. tularensis* infection in the donor and both kidney recipients was confirmed. Use of PFGE and wgMLST demonstrated that the *F. tularensis* isolates recovered from the donor and both kidney recipients were indiscernible from each other and distinct from other A2 strains, thereby corroborating transmission of *F. tularensis* A2 by solid organ transplant. Clinicians and organ procurement organizations evaluating potential organ donors who died of an unknown febrile illness should carefully assess risk factors for organ transplant-transmissible infectious diseases, including tularemia, and consider additional diagnostic testing if indicated (6,16).

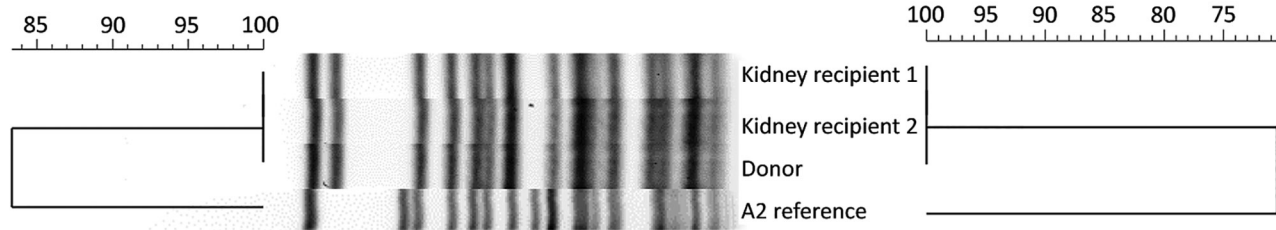


**Figure 3.** Pulsed-field gel electrophoresis (PFGE) and whole-genome multilocus sequence typing (wgMLST) comparisons of *Francisella tularensis* A2 strains. PFGE banding patterns and PFGE and wgMLST cluster analysis are shown for isolates from the organ donor and kidney recipients in relation to the *F. tularensis* A2 reference (strain WY96-3418). Dendrograms indicate percentage strain similarity for *PmeI* PFGE (left) and wgMLST (right).

The incubation period for naturally acquired tularemia is typically 3 to 5 days but can range from 1 to 21 days (7). For both kidney recipients, signs of infection developed 4 days after transplant, and the patients experienced rapidly progressive illness. Kidney recipient 2 might have survived because of empirically initiated ceftriaxone treatment. Ceftriaxone in vitro activity against *F. tularensis* has been demonstrated (17); however, in some cases ceftriaxone has been associated with treatment failure (18).

Although sepsis developed in the heart recipient several hours after transplantation, *F. tularensis* infection was not identified by culture or serology and would not be consistent with such a short incubation period. The episode of septic shock shortly after transplant might have been related to manipulation and removal of the infected medical device. It is possible that pretransplant ciprofloxacin for *Serratia marcescens* or posttransplant cefepime either prevented isolation of the organism or prevented *F. tularensis* infection altogether.

Human-to-human transmission of tularemia has been clearly documented just one time, in a medical examiner who accidentally cut her thumb during autopsy of a person who had died of tularemia (19). Another unconfirmed report from 1924 described a mother who contracted glandular tularemia after pricking her thumb while tending a tularemia ulcer on her son's ear (20).

Two subspecies of *F. tularensis* can result in human infection: subspecies *tularensis* (type A) and subspecies *holarctica* (type B) (21). PFGE analyses have further classified type A into 2 clades, A1 and A2, which differ in geographic distribution and case-fatality rate. A2 infections are known to occur only in the western United States, including the arid region from the Rocky Mountains west to the Sierra Nevada Mountains, matching the geographic location of the residence of the organ donor and the *F. tularensis*-positive lagomorph carcasses described in this report (11,12).

The organ donor might have been at increased risk for tularemia because of his residence on tribal lands. Native Americans are disproportionately represented among reported cases of tularemia; during 2001–2010, annual incidence among Native Americans was nearly 10 times higher than that of the general population (0.3 vs. 0.04 cases/100,000 persons) (2). Previous studies have estimated that 7%–17.5% of Native Americans residing in the United States and Canada have detectable *F. tularensis* antibodies (22–26). In addition, several outbreaks of tularemia among Native Americans have been reported, typically ascribed to tickborne infections (26–29).

Clinical and laboratory diagnoses of tularemia pose considerable challenges. Pneumonic tularemia, in particular, has myriad clinical forms and can mimic community-acquired pneumonia or other lung disorders

(1,7). *F. tularensis* is not often isolated from blood cultures because it is fastidious and slow growing (5,12,21,30). For the organ donor reported in this article, blood culture sensitivity was probably further limited by neutralizing antibodies, given his positive tularemia serology results (31). Additional laboratory tests that may aid diagnosis include PCR and DFA, although these tests are not routinely performed unless disease is clinically suspected. Serology may aid diagnosis, although antibody responses are generally not detectable until 1–2 weeks after infection (1,6). Clinical laboratories must promptly report suspected *F. tularensis* infections to public health laboratories, according to LRN guidelines (8).

These findings are subject to limitations. First, the extent to which *F. tularensis* infection contributed to the donor's clinical syndrome or death is unclear. Pulmonary findings may have resulted from aspiration pneumonia; gastrointestinal bleeding is not typically associated with tularemia but could have been precipitated by sepsis-related disseminated intravascular coagulation. In addition, we could not identify a specific-exposure source for the donor. However, identification of lagomorph carcasses near the donor's home suggested a recent tularemia epizootic, and detection of *F. tularensis* A2 in the lagomorph carcasses confirmed presence of this organism near the donor's residence.

Generally speaking, recipients' risks for infection from any pathogen must be balanced with the growing shortage of organs (32). During the past 2 decades, several emerging or uncommon pathogens have been identified as potentially transmissible through solid organ transplantation (33,34), highlighting the challenges of identifying potentially transmissible pathogens in brain-dead organ donors (32). These unusual transplant-transmitted infections have prompted the addition of more questions on standard interviews administered to donors' next of kin (9) and the performance of additional laboratory screening of donors at the discretion of organ procurement organizations. Real-time nucleic acid-based testing and other methods show promise for more rapidly and accurately identifying donor infections (32). All suspected donor-derived diseases should be reported to the Organ Procurement and Transplantation Network (<https://optn.transplant.hrsa.gov>), as was done in this investigation.

*F. tularensis* continues to affect public health because of ongoing naturally acquired infections, potential to cause laboratory-acquired infections, status as a Tier 1 bioterrorism threat, and newly described human-to-human transmission. Clinicians should be aware of the possibility of *F. tularensis* infection in patients receiving organ transplants. When evaluating potential organ donors with febrile illnesses, clinicians should consider risk factors for tularemia such as recent contact with animal carcasses, arthropod bites, landscaping activities, residence in a rural

area, and white or Native American race (2). If tularemia or other infectious diseases are suspected, this suspicion should be clearly conveyed to recipient transplant clinicians so that vigilant posttransplant clinical surveillance can be conducted and timely treatment initiated should a donor-derived infection occur.

Tularemia in Transplant Recipients Investigation Team members: V. Abitria, E. Adler, I. Bautista, W. Bendik, A. Blacker, G. Broeren, E. Buttery, J. Carr, D. Civic, S.H. Cohen, C.J. Conaway, K. Crabtree, R. Eisen, J. Ferreira, K. Gage, L. Gillogly, V.A. Gladden, S. Gujrathi, K. Hertin, K. Hicks, B. Hunter, O. Kasirye, P. Klouse, K. Kugeler, D. Lahrman, S. Landin, S. Larson, F. Leguen, E. McDonald, P. Mead, A. Mehretu, M. Morita, J. Mosely, S. Mott, J. Nash, R. Pappert, M. Paquette-Delcollo, M. Peek-Bullock, A. Perea, C.R. Polage, E. Pond, G. Pretorius, D. Raman, V. Raman, T. Reidhead, J. Reszetar, M. Russell, J. Sageshima, J. Sanguinet, S. Scaccia, M. Schriefer, A. Seifert, D. Slater, A. Stachnik, M. Tonge, J. Ventura, M. Wadsworth, D. Wallis, B.H. Weng, A. Young, and J. Young.

### Acknowledgments

We thank the surviving organ transplant recipients, family members of all recipients, and the family and community members of the organ donor for their support of the investigation. We also thank Katharine Cooley for assistance with the table and references and Shannon Fleck for manuscript review.

### About the Author

Dr. Nelson is a medical epidemiologist in the Bacterial Diseases Branch, Division of Vector-Borne Diseases, National Center for Emerging and Zoonotic Infectious Diseases, Centers for Disease Control and Prevention, Fort Collins, Colorado. Her primary research interests are the epidemiology and clinical manifestations of tularemia, plague, Lyme disease, and *Bartonella* infections.

### References

- Nigrovic LE, Wingerter SL. Tularemia. *Infect Dis Clin North Am*. 2008;22:489–504. <http://dx.doi.org/10.1016/j.idc.2008.03.004>
- Centers for Disease Control and Prevention. Tularemia—United States, 2001–2010. *MMWR Morb Mortal Wkly Rep*. 2013;62:963–6.
- Green MS, LeDuc J, Cohen D, Franz DR. Confronting the threat of bioterrorism: realities, challenges, and defensive strategies. *Lancet Infect Dis*. 2018.
- Dennis DT, Inglesby TV, Henderson DA, Bartlett JG, Ascher MS, Eitzen E, et al.; Working Group on Civilian Biodefense. Tularemia as a biological weapon: medical and public health management. *JAMA*. 2001;285:2763–73. <http://dx.doi.org/10.1001/jama.285.21.2763>
- Overholt EL, Tigertt WD, Kadull PJ, Ward MK, Charkes ND, Rene RM, et al. An analysis of forty-two cases of laboratory-acquired tularemia. Treatment with broad spectrum antibiotics. *Am J Med*. 1961;30:785–806. [http://dx.doi.org/10.1016/0002-9343\(61\)90214-5](http://dx.doi.org/10.1016/0002-9343(61)90214-5)
- Johansson A, Petersen J, Sjöstedt A. Laboratory diagnostics and discrimination of subspecies and strains. In: Tärnvik A, editor. *WHO Guidelines on Tularemia*. Geneva: World Health Organization; 2007. p. 27–34.
- Anda P, Pearson A, Tärnvik A. Clinical expression in humans. In: Tärnvik A, editor. *WHO Guidelines on Tularemia*. Geneva: World Health Organization; 2007. p. 11–19.
- Centers for Disease Control and Prevention. The Laboratory Response Network partners in preparedness [cited 2018 May 4]. <https://emergency.cdc.gov/lrn/index.asp>
- Organ Procurement and Transplantation Network. Organ Procurement and Transplantation Network policies [cited 2018 May 4]. [https://optn.transplant.hrsa.gov/media/1200/optn\\_policies.pdf](https://optn.transplant.hrsa.gov/media/1200/optn_policies.pdf)
- Molins CR, Carlson JK, Coombs J, Petersen JM. Identification of *Francisella tularensis* subsp. *tularensis* A1 and A2 infections by real-time polymerase chain reaction. *Diagn Microbiol Infect Dis*. 2009;64:6–12. <http://dx.doi.org/10.1016/j.diagmicrobio.2009.01.006>
- Kugeler KJ, Pappert R, Zhou Y, Petersen JM. Real-time PCR for *Francisella tularensis* types A and B. *Emerg Infect Dis*. 2006;12:1799–801. <http://dx.doi.org/10.3201/eid1211.060629>
- Staples JE, Kubota KA, Chalcraft LG, Mead PS, Petersen JM. Epidemiologic and molecular analysis of human tularemia, United States, 1964–2004. *Emerg Infect Dis*. 2006;12:1113–8. <http://dx.doi.org/10.3201/eid1207.051504>
- Danforth M, Novak M, Petersen J, Mead P, Kingry L, Weinburke M, et al. Investigation of and response to 2 plague cases, Yosemite National Park, California, USA, 2015. *Emerg Infect Dis*. 2016;22. <http://dx.doi.org/10.3201/eid2212.160560>
- Melman SD, Ettestad PE, VinHatton ES, Ragsdale JM, Takacs N, Onischuk LM, et al. Human case of bubonic plague resulting from the bite of a wild Gunnison's prairie dog during translocation from a plague-endemic area. *Zoonoses Public Health*. 2018;65:e254–8. <http://dx.doi.org/10.1111/zph.12419>
- Kingry LC, Rowe LA, Respicio-Kingry LB, Beard CB, Schriefer ME, Petersen JM. Whole genome multilocus sequence typing as an epidemiologic tool for *Yersinia pestis*. *Diagn Microbiol Infect Dis*. 2016;84:275–80. <http://dx.doi.org/10.1016/j.diagmicrobio.2015.12.003>
- Hepburn MJ, Simpson AJ. Tularemia: current diagnosis and treatment options. *Expert Rev Anti Infect Ther*. 2008;6:231–40. <http://dx.doi.org/10.1586/14787210.6.2.231>
- Hotta A, Fujita O, Uda A, Sharma N, Tanabayashi K, Yamamoto Y, et al. In vitro antibiotic susceptibility of *Francisella tularensis* isolates from Japan. *Jpn J Infect Dis*. 2013;66:534–6. <http://dx.doi.org/10.7883/yoken.66.534>
- Cross JT, Jacobs RF. Tularemia: treatment failures with outpatient use of ceftriaxone. *Clin Infect Dis*. 1993;17:976–80. <http://dx.doi.org/10.1093/clinids/17.6.976>
- Weilbacher JO, Moss ES. Tularemia following injury while performing post-mortem examination of a human case. *J Lab Clin Med*. 1938;24:34–8.
- Harris CE. Tularemia. *Colorado Medicine*. 1924;32:328–34.
- Petersen JM, Schriefer ME. Tularemia: emergence/re-emergence. *Vet Res*. 2005;36:455–67. <http://dx.doi.org/10.1051/vetres/2005006>
- Philip RN, Casper EA, Lackman DB. The skin test in an epidemiologic study of tularemia in Montana trappers. *J Infect Dis*. 1967;117:393–402. <http://dx.doi.org/10.1093/infdis/117.5.393>
- Philip RN, Huntley B, Lackman DB, Comstock GW. Serologic and skin test evidence of tularemia infection among Alaskan Eskimos, Indians and Aleuts. *J Infect Dis*. 1962;110:220–30. <http://dx.doi.org/10.1093/infdis/110.3.220>
- Wood WJ. Tularemia; a study based on the incidence of positive agglutination tests against *P. tularensis* in the Indian population



- of Manitoba and North-Western Ontario. *Manit Med Rev.* 1951;31:641–4.
25. Greenberg L, Blake JD. An immunological study of the Canadian Indian. *Can Med Assoc J.* 1957;77:211–6.
  26. Schmid GP, Kornblatt AN, Connors CA, Patton C, Carney J, Hobbs J, et al. Clinically mild tularemia associated with tick-borne *Francisella tularensis*. *J Infect Dis.* 1983;148:63–7. <http://dx.doi.org/10.1093/infdis/148.1.63>
  27. Markowitz LE, Hynes NA, de la Cruz P, Campos E, Barbaree JM, Plikaytis BD, et al. Tick-borne tularemia. An outbreak of lymphadenopathy in children. *JAMA.* 1985;254:2922–5. <http://dx.doi.org/10.1001/jama.1985.03360200074030>
  28. Centers for Disease Control. Outbreak of tick-borne tularemia—South Dakota. *MMWR Morb Mortal Wkly Rep.* 1984;33:601–2.
  29. Saliba GS, Harmston FC, Diamond BE, Zymet CL, Goldenberg MI, Chin TD. An outbreak of human tularemia associated with the American dog tick, *Dermacentor variabilis*. *Am J Trop Med Hyg.* 1966;15:531–8. <http://dx.doi.org/10.4269/ajtmh.1966.15.531>
  30. Karagöz S, Kiliç S, Berk E, Uzel A, Çelebi B, Çomoğlu Ş, et al. *Francisella tularensis* bacteremia: report of two cases and review of the literature. *New Microbiol.* 2013;36:315–23.
  31. Koskela P, Salminen A. Humoral immunity against *Francisella tularensis* after natural infection. *J Clin Microbiol.* 1985; 22:973–9.
  32. Tullius SG, Rabb H. Improving the supply and quality of deceased-donor organs for transplantation. *N Engl J Med.* 2018;378:1920–9. <http://dx.doi.org/10.1056/NEJMra1507080>
  33. Srinivasan A, Burton EC, Kuehnert MJ, Rupprecht C, Sutker WL, Ksiazek TG, et al.; Rabies in Transplant Recipients Investigation Team. Transmission of rabies virus from an organ donor to four transplant recipients. *N Engl J Med.* 2005;352:1103–11. <http://dx.doi.org/10.1056/NEJMoa043018>
  34. Hocevar SN, Paddock CD, Spak CW, Rosenblatt R, Diaz-Luna H, Castillo I, et al.; Microsporidia Transplant Transmission Investigation Team. Microsporidiosis acquired through solid organ transplantation: a public health investigation. *Ann Intern Med.* 2014;160:213–20. <http://dx.doi.org/10.7326/M13-2226>

Address for correspondence: Christina A. Nelson, Centers for Disease Control and Prevention, 3156 Rampart Rd, Mailstop P02, Fort Collins, CO 80521, USA; email: [wje1@cdc.gov](mailto:wje1@cdc.gov)



## EMERGING INFECTIOUS DISEASES®

May 2018

# Vectorborne Infections

- History of Mosquitoborne Diseases in the United States and Implications for New Pathogens
- Surveillance for Mosquitoborne Transmission of Zika Virus, New York City, NY, USA, 2016
- Two Cases of Israeli Spotted Fever with Purpura Fulminans, Sharon District, Israel
- Antimicrobial Resistance in Invasive Bacterial Infections in Hospitalized Children, Cambodia, 2007–2016
- Epidemic Dynamics of *Vibrio parahaemolyticus* Illness in a Hotspot of Disease Emergence, Galicia, Spain
- Dynamics of Spirochetemia and Early PCR Detection of *Borrelia miyamotoi*
- Transmission of Severe Fever with Thrombocytopenia Syndrome Virus by *Haemaphysalis longicornis* Ticks, China
- Seroprevalence of Severe Fever with Thrombocytopenia Syndrome Virus Antibodies in Rural Areas, South Korea
- Human Usutu Virus Infection with Atypical Neurologic Presentation, Montpellier, France, 2016
- Alkhurma Hemorrhagic Fever Virus RNA in *Hyalomma rufipes* Ticks Infesting Migratory Birds, Europe and Asia Minor
- Cholera Epidemic in South Sudan and Uganda and Need for International Collaboration in Cholera Control
- External Quality Assessment for Zika Virus Molecular Diagnostic Testing, Brazil
- Spread of Plague by Respiratory Droplets or Ectoparasites
- A Mental Models Approach to Assessing Public Understanding of Zika Virus, Guatemala
- Heartland Virus and Hemophagocytic Lymphohistiocytosis in Immunocompromised Patient, Missouri, USA
- Equine Encephalosis Virus in India, 2008 Epizootic Hemorrhagic Disease Virus Serotype 6 Infection in Cattle, Japan, 2015
- Fatal Visceral Leishmaniasis Caused by *Leishmania infantum*, Lebanon
- Second Human Pegivirus in Hepatitis C Virus–Infected and Hepatitis C Virus/HIV-1–Co-infected Persons Who Inject Drugs, China

To revisit the May 2018 issue, go to:

<https://wwwnc.cdc.gov/eid/articles/issue/24/5/table-of-contents>

# *Streptococcus agalactiae* Sequence Type 283 in Farmed Fish, Brazil

Carlos A.G. Leal, Guilherme A. Queiroz,  
Felipe L. Pereira, Guilherme C. Tavares,  
Henrique C.P. Figueiredo

In 2016 and 2017, we characterized outbreaks caused by *Streptococcus agalactiae* serotype III sequence type (ST) 283 in Nile tilapia farms in Brazil. Whole-genome multilocus sequence typing clustered the fish isolates together with the zoonotic ST283 and other STs related to cases in humans, frogs, dogs, cattle, and dolphins.

*Streptococcus agalactiae* (group B *Streptococcus* [GBS]) is a major etiologic agent of diseases in humans and animals (1). Episodes of bacteremia and meningitis in humans associated with raw fish consumption were reported in Singapore (2,3). Two case-control studies determined that GBS serotype III sequence type (ST) 283 was associated with disease in 9 (2) and 19 (3) patients in that country at different times during 2015. This specific ST has been identified as a zoonotic agent to humans and already has been detected in freshwater fish dishes from food stalls in Singapore (1); consumption of such fish dishes led to increased cases during that year. In farmed fish, GBS serotype III ST283 was detected in diseased tilapia (*Oreochromis* sp.) in Thailand (4).

In Brazil, fish-pathogenic GBS has been isolated mainly from farmed Nile tilapia (*Oreochromis niloticus*) since the 2000s. The predominant serotype in Brazil is serotype Ib from ST260, ST927, and a nontypeable ST; all these STs are reported as fish-adapted pathogens (5). Sporadic detection of serotype Ia ST103 also was described in Brazil (6). However, since 2016, a new serotype, serotype III, has emerged in the country. This serotype has been detected in different Nile tilapia farms in the northeastern region (7). The genetic diversity and ST of these isolates have not yet been identified.

Our objective was to evaluate, by molecular and genomic approaches, the GBS serotype III isolates from outbreaks in Nile tilapia farms in Brazil. We also aimed to study the genetic relationship between isolates from farmed fish in Brazil, from foodborne isolates from humans in Asia, and from cases in fish.

## The Study

During July 2016–June of 2017, we followed 6 outbreaks that led to Nile tilapia deaths at commercial farms in 4 Brazilian states: Piauí, Pernambuco, Ceará, and Bahia (Figure 1). Disease outbreaks with high death rates (daily rates >0.2% and total death rates in the herds of 25%–35%) in fish vaccinated with a commercial inactivated vaccine against GBS serotype Ib were reported. Diseased fish showed signs of lethargy, melanosis, and exophthalmia. We sampled 71 diseased fish and transported them on ice to the laboratory (Table), where we immediately performed bacteriologic analyses. Fish tissue sampling and the culture conditions of the analyses were as described previously (8). The isolates obtained from 64 fish were identified up to the species level by matrix-assisted laser desorption ionization time-of-flight mass spectrometry analysis, using a previously published method (9). We confirmed GBS as the principal pathogen associated with the deaths during all the outbreaks (Table).

We performed capsular polysaccharide typing for all GBS isolates using a previously published multiplex PCR (10). In addition, we conducted sequencing of housekeeping genes for multilocus sequence typing (MLST) analysis (11). According to the GBS MLST database (<http://pubmlst.org/sagalactiae>), 59 isolates belonged to serotype III ST283 and 3 to serotype Ib ST260.

For selected GBS isolates from each farm, we performed a PCR-based fingerprinting technique (ERIC-PCR [enterobacterial repetitive intergenic consensus PCR]) described by Costa et al. (12) to evaluate genetic diversity in comparison with MLST results. We observed nondistinguishable banding patterns between all GBS serotype III ST283 isolates, regardless of their geographic origin (data not shown), suggesting the possibility of a genetically close relation.

To determine the genomic relationship between GBS serotype III ST283 isolates from fish in Brazil and Asia and foodborne cases in humans, we conducted whole-genome sequencing and whole-genome MLST (wgMLST) analyses. In brief, 8 isolates (SA01AQUAVET, SA06AQUAVET, SA12AQUAVET, SA22AQUAVET, SA90AQUAVET, SA98AQUAVET, SApx2AQUAVET, and SApx7AQUAVET), representing each outbreak case, and 3 isolates from outbreak 2, because the isolates of outbreak 2 were obtained from 3 different farms, were selected

Author affiliation: Federal University of Minas Gerais, Belo Horizonte, Brazil

DOI: <https://doi.org/10.3201/eid2504.180543>

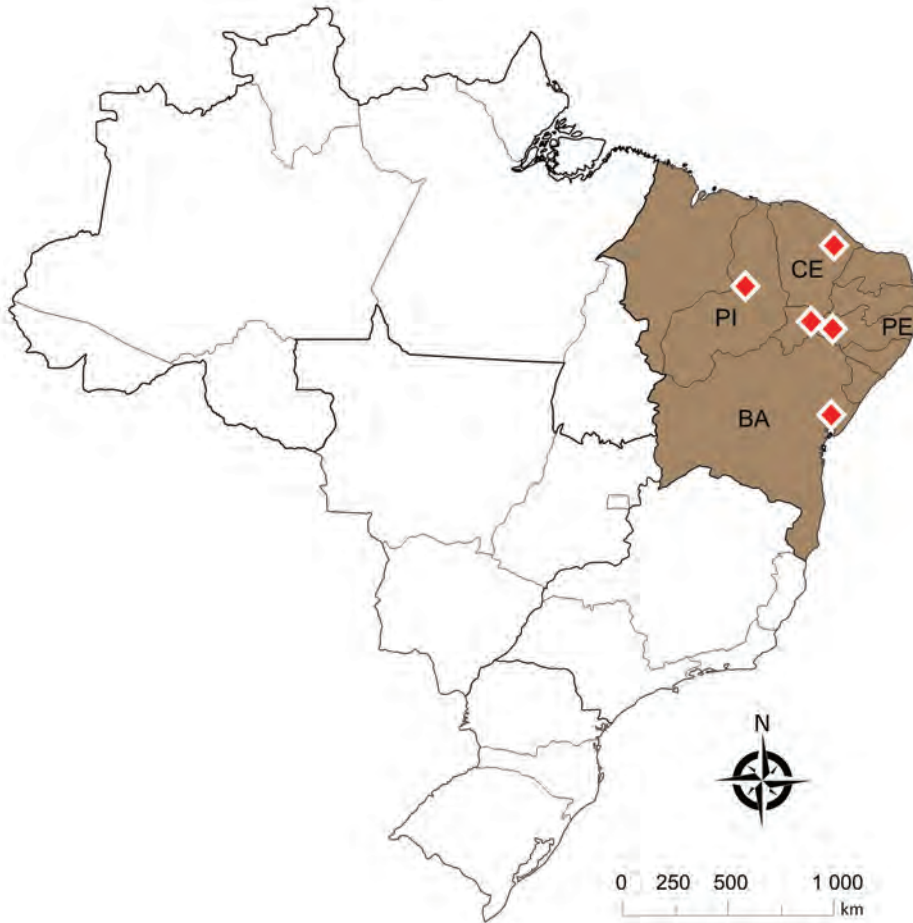


**Figure 1.** Location of the deaths of farmed Nile tilapia (*Oreochromis niloticus*) (shaded area) caused by *Streptococcus agalactiae* serotype III sequence type 283 (red diamonds), Brazil. BA, Bahia state; CE, Ceará state; PE, Pernambuco state; PI, Piauí state; ST, sequence type.

(Appendix, <https://wwwnc.cdc.gov/EID/article/25/4/18-0543-App1.pdf>).

In the wgMLST analysis, GBS serotype III ST283 isolates formed 1 phylogenomic related group (Figure 2, panel A). We compared 3,539 loci of the analyzed GBS isolates based on pairwise comparisons of the numbers of homologous loci with distinct allele sequences and found that all ST283 isolates (from fish and humans) displayed up to 505 distinct allele sequences. When we compared isolates from Brazil with fish strains from Asia, we observed variations ranging from 136 to 505 (3.84%–14.26%) (Figure 2, panel B) in loci. Among isolates from humans and fish in Asia, the variations were 31–240 (0.87%–6.78%), whereas for

isolates from humans in Asia compared with from fish in Brazil, the variations were 272–415 (7.68%–11.72%). GBS ST283 from Brazil showed loci variations ranging from 71 to 256 between each other. These levels of local diversities within an ST were reported in a previous study that evaluated distinct STs obtained from fish in Brazil (5).

Finally, we conducted a phylogenetic analysis with MLST loci concatenated (Figure 2, panels C, D). The 7 loci (i.e., *adhP*, *pheS*, *atr*, *glnA*, *sdhA*, *glcK*, and *tkt*) of each of 1,193 STs, available in GBS MLST database) were concatenated and aligned using CLC Genomics Workbench (QIAGEN, <https://www.qiagen.com>). From the alignment results, we generated a phylogenetic tree

**Table.** Characteristics of *Streptococcus agalactiae* outbreaks in Nile tilapia (*Oreochromis niloticus*), Brazil\*

Outbreak	Date	State	No. fish tested	Diagnosis (no. fish)	Serotype	MLST
1	2016 Jul	Piauí	8	<i>S. agalactiae</i> (7)	III	283
2	2017 Mar	Pernambuco	21	<i>S. agalactiae</i> (18) <i>S. agalactiae</i> (3)	III Ib	283 260
3	2017 Mar	Bahia	13	<i>S. agalactiae</i> (12), <i>S. dysgalactiae</i> (1)	III	283
4	2017 May	Ceará	7	<i>S. agalactiae</i> (4)	III	283
5	2017 May	Piauí	6	<i>S. agalactiae</i> (2) <i>S. dysgalactiae</i> (1)	III	283
6	2017 Jun	Bahia	16	<i>S. agalactiae</i> (16)	III	283

\*Capsular serotyping and MLST analyses were performed only for *S. agalactiae* isolates. MLST, multilocus sequence typing.



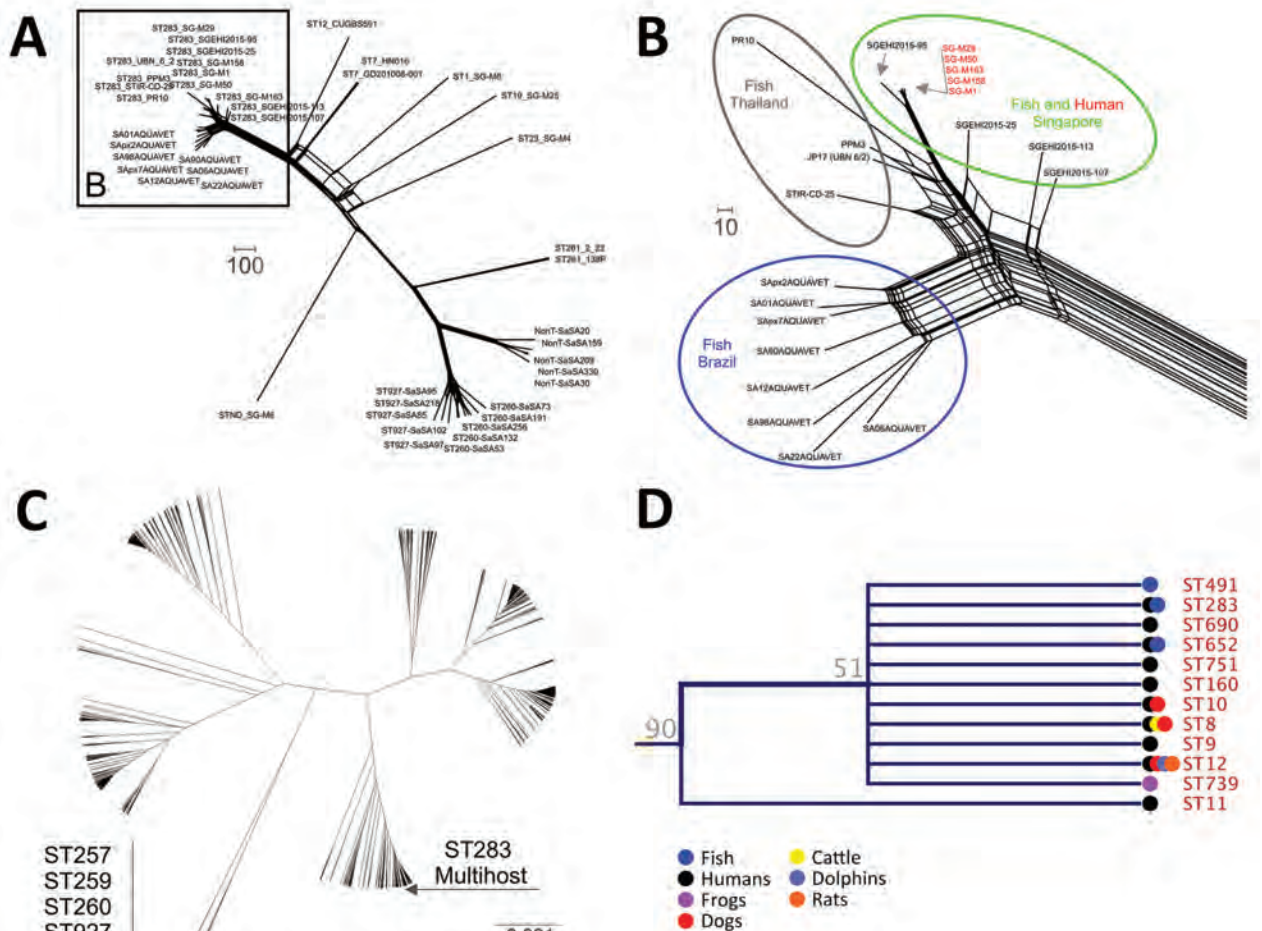


**Figure 2.** Phylogenetic analyses of *Streptococcus agalactiae* strains. A) Phylogenomic neighbor network of whole-genome multilocus sequence typing data of 45 group B *Streptococcus* (GBS) strains. Scale bar measures 100 different alleles between the isolates. B) Magnified image from panel A showing GBS ST283 phylogenomic splits. Isolates obtained from clinical cases of diseased fish in Brazil (blue circle) and Thailand (gray circle) and isolates from foodborne outbreaks in Singapore (green circle). Scale bar measures 10 different alleles between the isolates. C) Phylogenetic relationship of all GBS STs concatenated using CLC Genomics Workbench (QIAGEN, <https://www.qiagen.com>) and generated using UPGMA (unweighted pair group method with arithmetic mean). GBS strains isolated exclusively from fish are genetically distant from ST283 cluster. Scale bar measures nucleotide substitutions per site. D) ST283 clade comprises multihost strains. ST, sequence type.

in the CLC Genomics Workbench using the UPGMA (unweighted pair group method with arithmetic mean) construction method, Jukes-Cantor as the nucleotide distance measure, and 1,000 replicates on bootstrap analysis. ST283 formed a consistent (bootstrap 90%) clade with other STs with different hosts other than fish (Figure 2, panel D), such as humans, fish, and frogs, including some with multihost range, among them humans, fish, cattle, dolphins, dogs, and frogs.

## Conclusions

We described the emergence of GBS ST (GBS serotype III ST283) associated with the Nile tilapia infection in Brazil. ST283 had been previously detected in fish (with and

without clinical disease) only in Southeast Asia countries (1,4). This report in Brazil indicates possible spread of this pathogen genotype around the world. Based on import records of live Nile tilapia from Singapore to Brazil in 2014 and our analyses (ERIC-PCR, MLST, and wgMLST), it is possible that this genotype was introduced into the country with the recently imported fish.

GBS serotype III ST283 caused severe foodborne outbreaks in Singapore in 2015, and these outbreaks have been linked to raw fish consumption (2), indicating a zoonotic lineage for this serotype. Our results demonstrate that GBS serotype III ST283 isolates from Brazil clustered in the same network branch with GBS isolates from Asia, from fish and human hosts; however, we observed genomic

diversity that depicted a clonal expansion of this genotype. The genomic diversity among GBS isolates from human and fish hosts was also observed in a previous study (1), which further reinforces the concept of a lineage that is adapted to >1 host. This previous study on GBS suggested that ST283 might not be pathogenic for fish (1). However, a previous study (4) found that it was associated with disease in fish. After evaluating isolates of tilapia clinical disease cases, we confirmed that this ST283 is associated with multiple outbreaks in commercial tilapia farms. Thus, it demonstrates the clear pathogenic behavior of this ST to fish. Moreover, genomic analysis indicates it belongs to a cluster with other STs from multiple susceptible hosts (Figure 2, panel D), such as the ST12, which was isolated from humans, dogs, dolphins, and rats, corroborating the suggestion that the member of this clade affects multiple host species. ST283 was only isolated from diseased tilapia, which cannot be used for human consumption. Future longitudinal noncasuistic study is needed to identify the occurrence and prevalence of GBS infection by the ST283 lineage also in asymptomatic fish before and after the outbreaks. In this context, asymptomatic tilapia carriers might represent a serious public health concern.

Fundação de Amparo à Pesquisa do Estado de Minas Gerais (FAPEMIG) and Coordenação de Aperfeiçoamento de Pessoal de Nível Superior (CAPES) provided student fellowships, and the Ministry of Agriculture, Livestock and Food Supply financially supported this project.

### About the Author

Dr. Leal is a veterinarian and adjunct professor at the Federal University of Minas Gerais, Brazil. His primary research interest is infectious diseases in aquatic animals, especially bacterial diseases, and the immunology of these animals.

### References

1. Chau ML, Chen SL, Yap M, Hartantyo SHP, Chiew PKT, Fernandez CJ, et al. Group B streptococcus infections caused by improper sourcing and handling of fish for raw consumption, Singapore, 2015–2016. *Emerg Infect Dis.* 2017;23:2002. <http://dx.doi.org/10.3201/eid2312.170596>
2. Rajendram P, Mar Kyaw W, Leo YS, Ho H, Chen WK, Lin R, et al. Group B streptococcus sequence type 283 disease linked to consumption of raw fish, Singapore. *Emerg Infect Dis.* 2016;22:1974–7. <http://dx.doi.org/10.3201/eid2211.160252>
3. Tan S, Lin Y, Foo K, Koh HF, Tow C, Zhang Y, et al. Group B streptococcus serotype III sequence type 283 bacteremia associated with consumption of raw fish, Singapore. *Emerg Infect Dis.* 2016;22:1970–3. <http://dx.doi.org/10.3201/eid2211.160210>
4. Delannoy CM, Cruimlish M, Fontaine MC, Pollock J, Foster G, Dagleish MP, et al. Human *Streptococcus agalactiae* strains in aquatic mammals and fish. *BMC Microbiol.* 2013;13:41. <http://dx.doi.org/10.1186/1471-2180-13-41>
5. Barony GM, Tavares GC, Pereira FL, Carvalho AF, Dorella FA, Leal CAG, et al. Large-scale genomic analyses reveal the population structure and evolutionary trends of *Streptococcus agalactiae* strains in Brazilian fish farms. *Sci Rep.* 2017;7:13538. <http://dx.doi.org/10.1038/s41598-017-13228-z>
6. Godoy DT, Carvalho-Castro GA, Leal CAG, Pereira UP, Leite RC, Figueiredo HCP. Genetic diversity and new genotyping scheme for fish pathogenic *Streptococcus agalactiae*. *Lett Appl Microbiol.* 2013;57:476–83. <http://dx.doi.org/10.1111/lam.12138>
7. Chideroli RT, Amoroso N, Mainardi RM, Suphoronski SA, de Padua SB, Alfieri AF, et al. Emergence of a new multidrug-resistant and highly virulent serotype of *Streptococcus agalactiae* in fish farms from Brazil. *Aquaculture.* 2017;479:45–51. <http://dx.doi.org/10.1016/j.aquaculture.2017.05.013>
8. Mian GF, Godoy DT, Leal CAG, Yuhara TY, Costa GM, Figueiredo HCP. Aspects of the natural history and virulence of *S. agalactiae* infection in Nile tilapia. *Vet Microbiol.* 2009;136:180–3. <http://dx.doi.org/10.1016/j.vetmic.2008.10.016>
9. Assis GBN, Pereira FL, Zegarra AU, Tavares GC, Leal CAG, Figueiredo HCP. Use of MALDI-TOF mass spectrometry for the fast identification of gram-positive fish pathogens. *Front Microbiol.* 2017;8:1492. <http://dx.doi.org/10.3389/fmicb.2017.01492>
10. Poyart C, Tazi A, Réglie-Poupet H, Billoët A, Tavares N, Raymond J, et al. Multiplex PCR assay for rapid and accurate capsular typing of group B streptococci. *J Clin Microbiol.* 2007;45:1985–8. <http://dx.doi.org/10.1128/JCM.00159-07>
11. Jones N, Bohnsack JF, Takahashi S, Oliver KA, Chan M-S, Kunst F, et al. Multilocus sequence typing system for group B streptococcus. *J Clin Microbiol.* 2003;41:2530–6. <http://dx.doi.org/10.1128/JCM.41.6.2530-2536.2003>
12. Costa FAA, Leal CAG, Leite RC, Figueiredo HCP. Genotyping of *Streptococcus dysgalactiae* strains isolated from Nile tilapia, *Oreochromis niloticus* (L.). *J Fish Dis.* 2014;37:463–9. <http://dx.doi.org/10.1111/jfd.12125>

---

Address for correspondence: Carlos A.G. Leal, Veterinary School, Department of Preventive Veterinary Medicine, Federal University of Minas Gerais, Av. Antônio Carlos 6627, Pampulha 31270-901, Belo Horizonte, Minas Gerais, Brazil; email: carlosleal@vet.ufmg.br

# Genomic Survey of *Bordetella pertussis* Diversity, United States, 2000–2013

Michael R. Weigand, Margaret M. Williams,  
Yanhui Peng, Dane Kania, Lucia C. Pawloski,  
Maria L. Tondella, CDC Pertussis Working Group<sup>1</sup>

We characterized 170 complete genome assemblies from clinical *Bordetella pertussis* isolates representing geographic and temporal diversity in the United States. These data capture genotypic shifts, including increased pertactin deficiency, occurring amid the current pertussis disease resurgence and provide a foundation for needed research to direct future public health control strategies.

Whooping cough (pertussis) remains a public health challenge in the United States where, despite high vaccine coverage, an increased number of cases have been reported since the late 1980s. This resurgence has included >48,000 cases reported in 2012 and notable recent statewide epidemics (1). Likely causes of the increase in reporting include heightened awareness, expanded surveillance, improved laboratory diagnostics, and waning protection conferred by acellular pertussis (aP) vaccine formulations (1,2).

The United States exclusively uses aP vaccines composed of inactivated *Bordetella pertussis* immunogenic proteins pertussis toxin (Pt), pertactin (Prn), and filamentous hemagglutinin (Fha), either with or without fimbria (Fim) types 2 and 3. Genetic divergence of circulating *B. pertussis* away from vaccine reference strains has led to allelic mismatch and the rapid emergence of Prn deficiency (3). Although such recent genetic changes may be ascribed to vaccine-driven immune selection (4), aP vaccines remain effective (5).

The chromosome of *B. pertussis* also undergoes frequent structural rearrangement (6) that presents unique challenges to thorough investigation of genetic contributions to disease resurgence, limiting assessment of public health strategies. Until recently, genomic data with sufficient resolution to study sequence and structural variation were available only for vaccine and laboratory reference strains. However, pathogen evolution must be explored through multinomic characterization of circulating

genotypes. To address this gap, we developed a dataset of complete, reference-quality genome sequence assemblies from isolates representing the geographic and temporal diversity of *B. pertussis* circulating in the United States during 2000–2013.

## The Study

The Centers for Disease Control and Prevention (CDC) maintains a collection of *B. pertussis* isolates recovered by state public health laboratories through routine surveillance and outbreaks or the Enhanced Pertussis Surveillance/Emerging Infections Program Network (7). We selected a subset of isolates ( $n = 170$ ) to account for potential geographic diversity. We stratified all isolates in the collection by state and time period (2000–2002, 2003–2009, 2010, 2011, 2012, and 2013) chosen according to diversity indices reported previously (8), with additional emphasis on more recent sampling. We then randomly sampled the stratified collection to maximize the number of source states ( $n = 34$ ) during each period with equal weighting (Figure 1, panel A, B). Most isolates were characterized by existing molecular approaches, multilocus variable-number tandem-repeat analysis (MLVA), and pulsed-field gel electrophoresis (PFGE), as described previously (9). The selected isolates included 17 MLVA types, with type 27 the most prevalent, and 33 PFGE profiles, with profile CDC013 the most prevalent (Appendix Table 1, <https://wwwnc.cdc.gov/EID/article/25/4/18-0812-App1.pdf>).

We performed whole-genome shotgun sequencing and assembly as described previously (10) (Appendix). Genome assembly yielded a single circular contig for all isolates, and we performed sequence-based molecular typing (Appendix). Nearly all isolates (96%) were of the predominant type *prn2-ptxP3-ptxA1* with either *fimH1* or *fimH2*, and few harbored alternate types such as *prn1-ptxP1-ptxA2-fimH1* (Figure 1, panel C). Prn deficiency has been observed in  $\geq 16$  independent mutations to *prn* (6); we observed 10 deficient alleles among 57/170 isolates in our study, including missense substitutions, deletions, promoter disruption, and various IS481 insertions. The proportion of isolates with Prn-deficient alleles increased rapidly beginning in 2010 (Figure 1, panel C), consistent with a larger

Author affiliation: Centers for Disease Control and Prevention, Atlanta, Georgia, USA

DOI: <https://doi.org/10.3201/eid2504.180812>

<sup>1</sup>Additional members of the CDC Pertussis Working Group are listed at the end of this article.



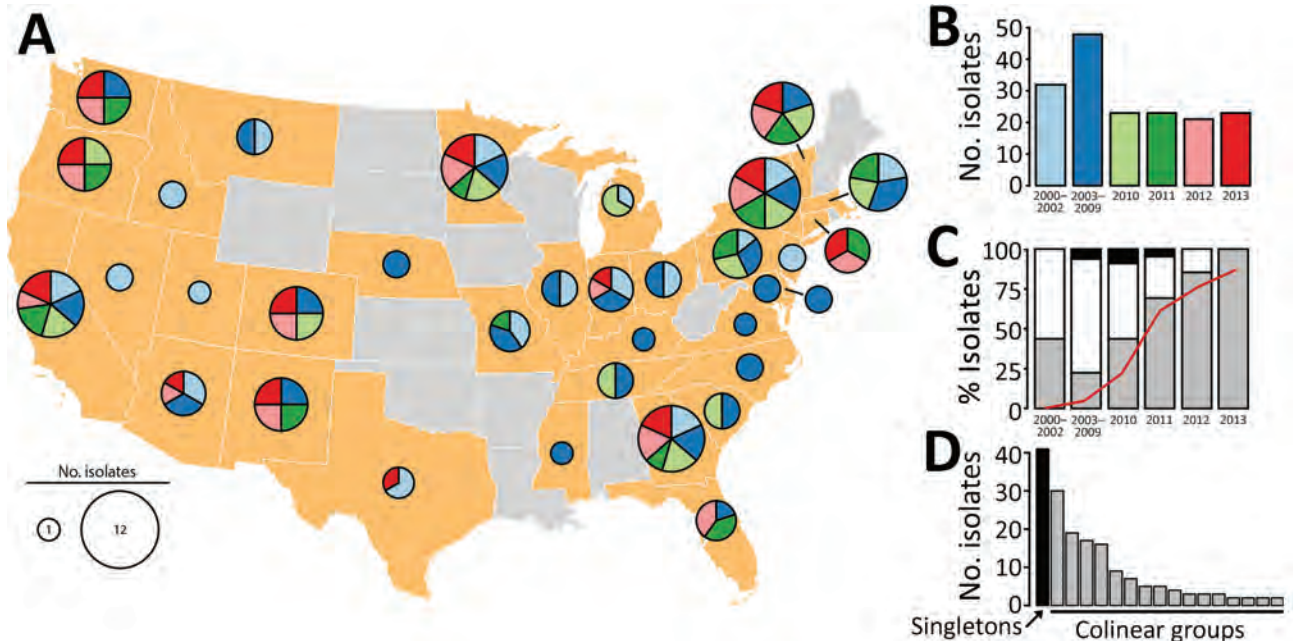


**Figure 1.** *Bordetella pertussis* diversity, United States, 2000–2013. A) Geographic origin of *B. pertussis* isolates selected to maximize the number of source states from each of 6 time periods. Pie chart diameter represents the number of isolates, as detailed in the key, and colors indicate time periods, as shown in panel B. B) Isolate frequency by time period. C) Relative abundance of MLST types *prn2-ptxP3-ptxA1-fimH1* (gray), *prn2-ptxP3-ptxA1-fimH2* (white), and other (black). Red line indicates frequency of pertactin-deficient alleles. D) Abundance distribution of genome structures. Black bar indicates unique structures (singletons) and gray bars the 16 colinear groups. MLST, multilocus sequence typing.

molecular survey of US isolates conducted previously that included some used in this study (3). We also determined MLVA type from genome assemblies using a custom bioinformatics pipeline (wgsMLVA) based on traditional PCR primer sequences (11) (Appendix). None of the genomes encoded known 23S ribosomal RNA mutation associated with erythromycin resistance (12).

To determine variation in chromosome structure, we performed exhaustive pairwise alignment of assembled genomes as previously described (6). Of the 170 assemblies, 129 clustered into 16 groups of  $\geq 2$  colinear genomes (lacking observable rearrangement or deletion  $>1,500$  bp), whereas 41 assemblies (singletons) exhibited unique structures not shared with any others in the dataset. Observed structures largely correlated with PFGE, a proxy for chromosome structure, clustering isolates with shared PFGE profiles. The abundance of common structures reflected predominant PFGE profiles, and the largest cluster corresponded to profile CDC013 (Figure 1, panel D). Differences between many common structures could be attributed to large inversions flanked by insertions of the multicopy *IS481*. Select singleton structures resulted from tandem duplication of large regions (15.5–190 kbp) in the genomes of 5 isolates (D236, D665, H624, J085, and J139) that were also flanked by copies of *IS481*.

We reconstructed a maximum-likelihood phylogeny of the isolate genomes from 840 core variable single-nucleotide polymorphisms (SNPs) determined from the reference Tohama I (GenBank accession no. CP010964) (Appendix). The resulting tree topology revealed deep divergence of lineages bearing alleles *ptxP1* and *ptxP3*, as well as clear distinctions between clades of *prn2-ptxP3-ptxA1-fimH1* and *prn2-ptxP3-ptxA1-fimH2* (Figure 2). Only certain *prn*-disrupting mutations (e.g., nonsense C1273T, promoter disruption) and chromosome structures (e.g., cluster-4, cluster-6, cluster-7, cluster-9) appeared phylogenetically linked, meaning isolates sharing them were also related according to their SNP patterns. However, each group of related isolates was recovered across multiple states and time periods, suggesting that genotypes, whether defined by gene sequence or chromosome structure, were stable enough to be widely circulated. *Prn* deficiency due to *IS481* disruption has resulted from  $\geq 7$  independent events among the isolates in this dataset, but related isolates with these mutations were likewise geographically and temporally distributed. These results are consistent with phylogenies of circulating *B. pertussis* reported elsewhere (6,13).

## Conclusions

We have developed a representative dataset of complete genome sequence assemblies derived from *B. pertussis* clinical isolates recovered in the United States that captures

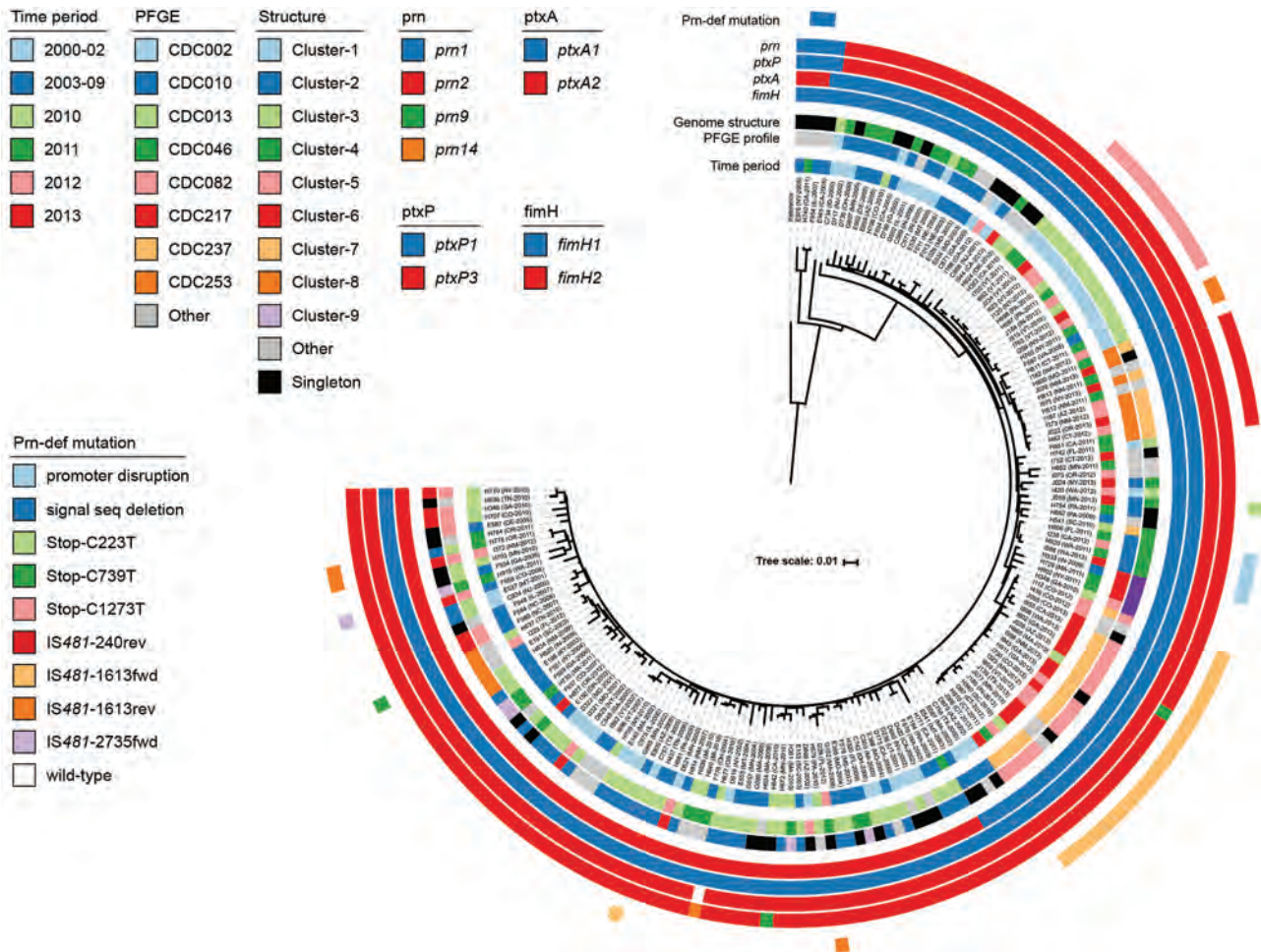


**Figure 2.** Phylogenetic reconstruction of all 170 isolates and the reference Tohama I (GenBank accession no. CP010964). Isolate metadata and molecular characteristics are color coded, as detailed in the key. Scale bar indicates substitutions per site. CDC, Centers for Disease Control and Prevention; fim, fimbria; fwd, forward insertion; rev, reverse insertion; PFGE, pulsed-field gel electrophoresis; prn, pertactin; ptx, pertussis toxin.

shifting population genetics concurrent with disease resurgence. We selected isolates to maximize the geographic diversity of circulating *B. pertussis* across 6 time periods during 2000–2013 and to span the time period in which Prn deficiency emerged as the predominant molecular type. Although the sparse sampling of individual states and regions prohibited detailed analyses of geographic distribution, we did recover isolates with shared SNP patterns and chromosome structures from disparate states. Our results illustrate underlying challenges to the molecular study of pertussis resurgence, including a circulating mixture of gene sequence (SNP) and chromosome structure variants.

The genomic data we provide will aid open research toward improved vaccine development and disease control strategies. Because little to no such high-quality data existed previously, the contribution of genome evolution to pertussis resurgence has not been fully appreciated. A subset of

these data has already helped elucidate historical patterns of chromosome rearrangement (6). However, comparative genomics alone is not sufficient to understand the resurgence in pertussis. Further laboratory experimentation using *in vitro* and *in vivo* infection models is needed to link outcomes with novel, bioinformatically determined genetic variation, such as discrete rearrangements and tandem duplications. Potential differences in antigen expression resulting from these changes in gene organization, which may influence the burden of disease, remain untested. Our results provide needed context to guide such investigations by highlighting representative, circulating genotypes as they continue their divergence from existing laboratory and vaccine reference strains. Data such as those presented here critically establish the necessary foundation for collaborative development of advanced diagnostics, novel molecular typing methods, and improved vaccine formulations.

Additional members of the CDC Pertussis Working Group: Dhvani Batra, Katherine E. Bowden, Mark Burroughs, Pamela K. Cassidy, Jamie K. Davis, Taccara Johnson, Hong Ju, Phalasy Juieng, Kristen Knipe, Vladimir N. Loparev, Stacey W. Martin, Christine Miner, Lori A. Rowe, Tami H. Skoff, Mili Sheth, Kevin Tang.

This work was made possible through support from the Advanced Molecular Detection program at the US Centers for Disease Control and Prevention.

### About the Author

Dr. Weigand is a bioinformatics research scientist in the Pertussis and Diphtheria Laboratory, Division of Bacterial Diseases, National Center for Immunization and Respiratory Diseases, CDC, Atlanta. His primary research interest is comparative genomics of bacterial pathogens, with a current focus on *Bordetella pertussis*.

### References

- Clark TA. Changing pertussis epidemiology: everything old is new again. *J Infect Dis*. 2014;209:978–81. <http://dx.doi.org/10.1093/infdis/jiu001>
- Ausiello CM, Cassone A. Acellular pertussis vaccines and pertussis resurgence: revise or replace? *MBio*. 2014;5:e01339–14. <http://dx.doi.org/10.1128/mBio.01339-14>
- Pawloski LC, Queenan AM, Cassidy PK, Lynch AS, Harrison MJ, Shang W, et al. Prevalence and molecular characterization of pertactin-deficient *Bordetella pertussis* in the United States. *Clin Vaccine Immunol*. 2014;21:119–25. <http://dx.doi.org/10.1128/CVI.00717-13>
- Martin SW, Pawloski L, Williams M, Weening K, DeBolt C, Qin X, et al. Pertactin-negative *Bordetella pertussis* strains: evidence for a possible selective advantage. *Clin Infect Dis*. 2015;60:223–7. <http://dx.doi.org/10.1093/cid/ciu788>
- Breakwell L, Kelso P, Finley C, Schoenfeld S, Goode B, Misegades LK, et al. Pertussis vaccine effectiveness in the setting of pertactin-deficient pertussis. *Pediatrics*. 2016;137:e20153973. <http://dx.doi.org/10.1542/peds.2015-3973>
- Weigand MR, Peng Y, Loparev V, Batra D, Bowden KE, Burroughs M, et al. The history of *Bordetella pertussis* genome evolution includes structural rearrangement. *J Bacteriol*. 2017;199:e00806–16. <http://dx.doi.org/10.1128/JB.00806-16>
- Skoff TH, Baumbach J, Cieslak PR. Tracking pertussis and evaluating control measures through enhanced pertussis surveillance, Emerging Infections Program, United States. *Emerg Infect Dis*. 2015;21:1568–73. <http://dx.doi.org/10.3201/eid2109.150023>
- Schmidtke AJ, Boney KO, Martin SW, Skoff TH, Tondella ML, Tatti KM. Population diversity among *Bordetella pertussis* isolates, United States, 1935–2009. *Emerg Infect Dis*. 2012;18:1248–55. <http://dx.doi.org/10.3201/eid1808.120082>
- Hardwick TH, Cassidy PK, Weyant RS, Bisgard KM, Sanden GN. Changes in predominance and diversity of genomic subtypes of *Bordetella pertussis* isolated in the United States, 1935 to 1999. *Emerg Infect Dis*. 2002;8:44–9. [http://dx.doi.org/10.3201/eid0801.010021\\_article](http://dx.doi.org/10.3201/eid0801.010021_article)
- Bowden KE, Weigand MR, Peng Y, Cassidy PK, Sammons S, Knipe K, et al. Genome structural diversity among 31 *Bordetella pertussis* isolates from two recent U.S. whooping cough statewide epidemics. *mSphere*. 2016;May–Jun:e00036–16. <http://dx.doi.org/10.1128/mSphere.00036-16>
- Schouls LM, van der Heide HG, Vauterin L, Vauterin P, Mooi FR. Multiple-locus variable-number tandem repeat analysis of Dutch *Bordetella pertussis* strains reveals rapid genetic changes with clonal expansion during the late 1990s. *J Bacteriol*. 2004; 186:5496–505. <http://dx.doi.org/10.1128/JB.186.16.5496-5505.2004>
- Bartkus JM, Juni BA, Ehresmann K, Miller CA, Sanden GN, Cassidy PK, et al. Identification of a mutation associated with erythromycin resistance in *Bordetella pertussis*: implications for surveillance of antimicrobial resistance. *J Clin Microbiol*. 2003;41:1167–72. <http://dx.doi.org/10.1128/JCM.41.3.1167-1172.2003>
- Bart MJ, Harris SR, Advani A, Arakawa Y, Bottero D, Bouchez V, et al. Global population structure and evolution of *Bordetella pertussis* and their relationship with vaccination. *MBio*. 2014;5:e01074. <http://dx.doi.org/10.1128/mBio.01074-14>

Address for correspondence: Michael R. Weigand, Centers for Disease Control and Prevention, 1600 Clifton Rd NE, Mailstop H18-B, Atlanta, GA 30329-4027, USA; email: mweigand@cdc.gov



# Early Genomic Detection of Cosmopolitan Genotype of Dengue Virus Serotype 2, Angola, 2018

**Sarah C. Hill, Jocelyne Neto de Vasconcelos,  
Bernardo Gutierrez Granja, Julien Thézé,  
Domingos Jandondo, Zoraima Neto,  
Marinela Mirandela, Cruz dos Santos Sebastião,  
Ana Luísa Micolo Cândido, Carina Clemente,  
Sara Pereira da Silva, Túlio de Oliveira,  
Oliver G. Pybus, Nuno R. Faria,  
Joana Morais Afonso**

We used portable genome sequencing to investigate reported dengue virus transmission in Angola. Our results show that autochthonous transmission of dengue serotype 2 (cosmopolitan genotype) occurred in January 2018.

In Africa, the prevalence of disease caused by *Aedes* mosquito-borne virus infections might be similar to that in the Americas (1,2). However, the transmission and genetic diversity of arthropodborne viruses (arboviruses) in Africa remains poorly understood because of a paucity of systematic surveillance. Moreover, syndromic surveillance might confound symptomatically similar illnesses, and serologic diagnostic tests can be misleading because of cross-reactivity between related circulating flaviviruses (3). Improved viral genomic surveillance can assist in better understanding viral transmission dynamics in Africa.

During 2013, Angola experienced a large dengue outbreak that was concentrated in Luanda Province (4). Cases detected in travelers returning from Angola to other parts of the world showed that the virus rapidly disseminated from Angola to Europe, Asia, and the Americas (5). Although infections were predominantly caused by dengue virus (DENV) serotype 1 (6), all DENV serotypes were reported in returning travelers from Angola (7).

Author affiliations: University of Oxford, Oxford, United Kingdom (S.C. Hill, B. Gutierrez Granja, J. Thézé, O.G. Pybus, N.R. Faria); Instituto Nacional de Investigação em Saúde, Luanda, Angola (J. Neto de Vasconcelos, D. Jandondo, Z. Neto, M. Mirandela, C. dos Santos Sebastião, A.L.M. Cândido, J.M. Afonso); Universidad San Francisco de Quito, Colegio de Ciencias Biológicas y Ambientales, Quito, Ecuador (B. Gutierrez Granja); Cligest, Luanda (C. Clemente, S.P. da Silva); University of KwaZulu-Natal, Durban, South Africa (T. de Oliveira)

DOI: <https://doi.org/10.3201/eid2504.180958>

Although dengue is probably endemic in Angola, patterns of DENV transmission in the country outside the 2013 epidemic are poorly characterized. The lack of genomic characterization restricts our understanding of DENV diversity within Angola and the frequency and directionality with which DENVs are exchanged with other countries. Although enhanced viral genomic sequencing capacity can improve outbreak detection and response, acquiring this tool remains challenging for many public health laboratories because of the high startup costs of traditional benchtop sequencing (8). Recent technologic advances now permit more affordable sequencing using the MinION portable sequencer (Oxford Nanopore Technologies, <https://nanoporetech.com>). We used a combination of portable sequencing and genetic analysis to characterize the causative lineage of a DENV outbreak in Luanda.

## The Study

To investigate the timing and frequency of dengue occurrence in Angola, we conducted rapid diagnostic tests by using the SD Bioline Dengue Duo kit (Alere, <https://www.alere.com>) to detect the presence of dengue-specific IgM, IgG, and, since January 2017, nonstructural protein 1 (NS1) (Appendix Figure, <https://wwwnc.cdc.gov/EID/article/25/4/18-0958-App1.pdf>). During January 1, 2016–May 15, 2018, we collected samples from 6,839 patients (3,276 male, 3,563 female) in central Luanda for whom a physician suspected dengue as the cause of an illness with symptoms consistent with DENV infection. Samples were originally obtained for routine diagnostic purposes from persons visiting local clinics. Thus, we used residual samples without informed consent, with ethics approval from the National Ethical Committee of the Angola Ministry of Health.

We identified 80 DENV NS1-positive cases among the tested samples (Appendix Figure). The first confirmed infections were detected in May 2017, and the number of cases appeared to peak around May 2018 (Figure, panel A).

We tested 153 randomly selected serum samples (IgG, IgM, or NS1-positive) collected during July 21, 2017–January 31, 2018, for DENV RNA by using real-time quantitative reverse transcription PCR (qRT-PCR) at the Instituto Nacional de Investigação em Saúde (INIS) in Luanda, Angola. We used the US Centers for Disease Control and

Prevention's DENV1–4 Real-Time RT-PCR assay kit on an Applied Biosystems 7500 Fast Real-Time PCR System (<https://www.thermofisher.com>), according to the manufacturer's instructions (7). Of these 153 samples, 1 (isolate AO-1) yielded a qRT-PCR cycle threshold of 22.5 for DENV serotype 2 (DENV-2). This sample was obtained from a 48-year-old man living in Luanda who visited a clinic on January 18, 2018. The patient reported traveling

to Mussulo Island, a resort 30 km from Luanda, during December 24, 2017–January 2, 2018.

We subjected the qRT-PCR–positive sample to viral genomic amplification and sequencing by using a multiplex PCR primer scheme designed to amplify the entire coding region of DENV-2. We aligned published genomes of non-sylvatic DENV-2 and used them to generate a 90% consensus sequence that formed the target for primer design. We

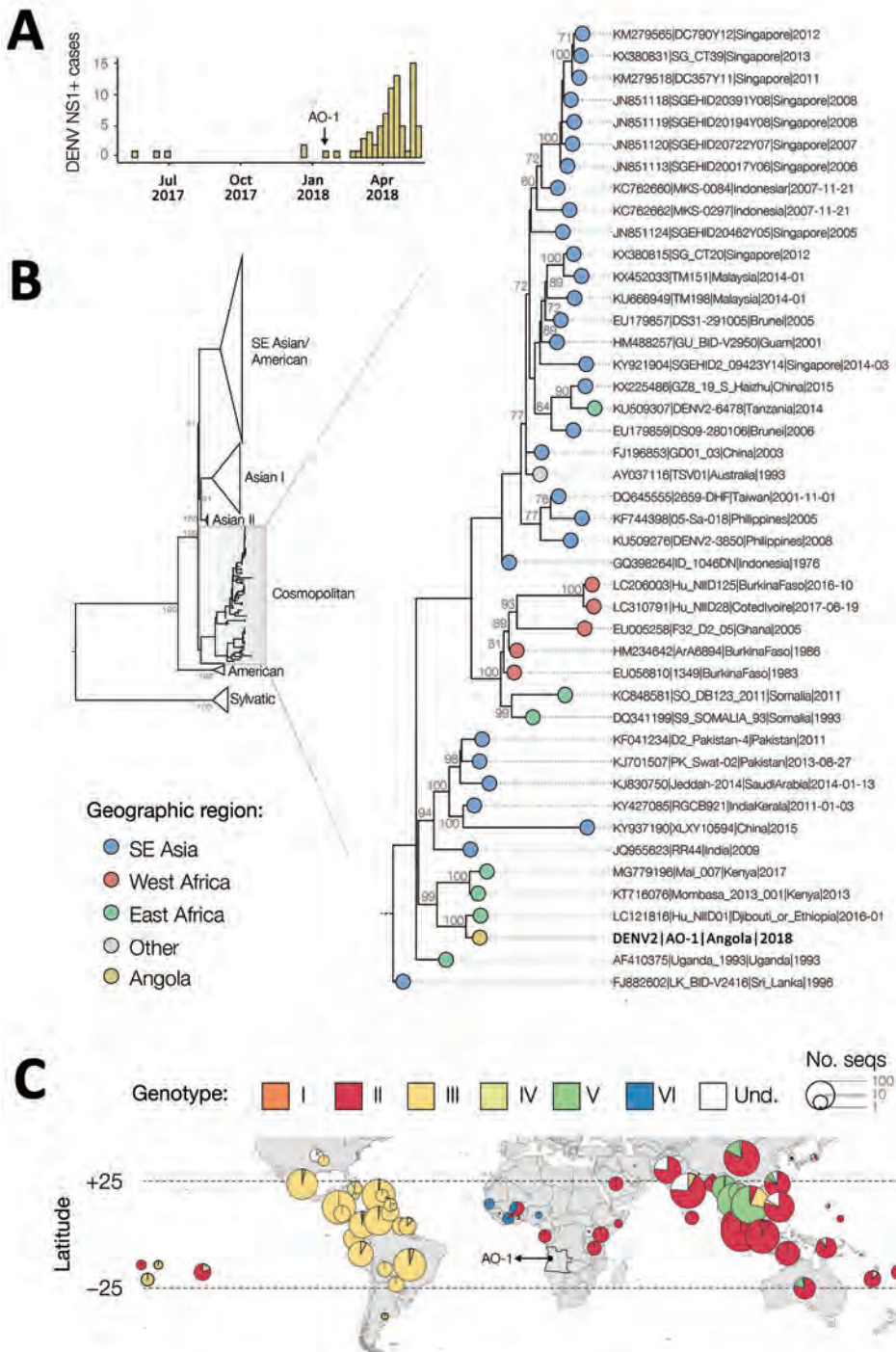


**Figure.** Investigation of DENV infections in Luanda, Angola, January 1, 2016–May 15, 2018. A) Number of DENV infections (i.e., cases positive for DENV NS1), Luanda, Angola, May 1, 2017–May 15, 2018. B) Midpoint rooted maximum-likelihood phylogeny of DENV-2 whole genomes. Support for branching structure is shown by bootstrap values at nodes. On the right side, the cosmopolitan genotype clade containing the Angola DENV-2 sequence is expanded. Colors indicate geographic location of sampling. The Angola DENV-2 is shown in bold. Support for branching structure is shown by bootstrap values at nodes (bootstrap scores >70 shown). C) Geographic distribution of available DENV-2 sequence data (>100 bp). Pie chart radii are log-proportional to the number of sequences available in each country and are colored according to genotype DENV, dengue virus; DENV-2, dengue virus serotype 2; NS1, nonstructural protein 1; SE, Southeast; seq, sequences; und, undefined.

designed primers that generated overlapping amplicons 980 bp in length with an overlap of 20 bp as previously described (9; Appendix Table). Details of cDNA synthesis, multiplex PCRs, library preparation, sequencing, and generation of consensus sequences are described in the Appendix.

We originally used the 90% consensus sequence as a reference genome for mapping sequencing reads, but we later refined this reference to a more appropriate reference genome (GenBank accession no. LC121816) by using BLAST (<http://www.ncbi.nlm.nih.gov/BLAST>) to identify DENV sequences with high identity to the provisionally mapped data. The median sequencing depth was 11,448 reads, and 75% of the genome had a depth of at least 2,419 reads. In total, we sequenced 96% of the coding region of DENV-2 (isolate AO-1; GenBank accession no. MH460898). Raw and processed data are available on GitHub (Appendix).

We constructed phylogenetic trees to explore the relationship of the sequenced AO-1 genome to those of other isolates. We retrieved 1,395 DENV-2 genome sequences with associated date and country of collection from GenBank. From this dataset, we generated a subset that included all 35 identified sequences from Africa, 200 globally sampled sequences (randomly sampled from the remaining 1,360 sequences), and the novel AO-1 sequence. We aligned these sequences by using MUSCLE, as implemented in Geneious 9.0.5 (10). We constructed a maximum-likelihood phylogenetic tree by using a general time-reversible model with gamma distributed among site rate heterogeneity (4 categories) in RAXML version 8.2.10 (11). We performed 500 nonparametric bootstrap replicates to evaluate statistical support for phylogenetic nodes. We also constructed a phylogeny that includes additional partial gene sequences (Appendix).

Phylogenetic estimation strongly supports placement of the isolate from Angola in the cosmopolitan genotype of DENV-2 (Figure, panel B). The Angola strain forms part of a well-supported monophyletic clade that comprises genomes sampled in East Africa and is most closely related to DENV isolated from a returning traveler from this region. Viruses from this clade have been present in East Africa since at least 2013 (Figure, panel B).

To explore the global distribution of the DENV-2 cosmopolitan genotype and identify geographic gaps in DENV genomic surveillance that might bias phylogenetic interpretation, we generated maps of the distribution of currently available DENV sequence data. We downloaded from GenBank all DENV sequences >100 bp of any serotype with known location of sampling (including those from returning travelers). We genotyped DENV-2 sequences by using the Genome Detective online classification tool (<http://www.genomedetective.com>). Most sequenced DENVs in Africa belong to DENV-2 (49%), of which 70%

belong to the cosmopolitan genotype (Figure, panel C). We found that although 16% of all global clinically apparent dengue infections have been estimated to occur in Africa (2), DENV serotype 1–4 sequences from Africa currently represent <1% of the available global DENV sequence data. No data exist from the Democratic Republic of the Congo, which has been epidemiologically linked with Angola during past arbovirus outbreaks (12). Additional data will help to address transmission dynamics of DENV-2 in Angola and identify common routes of virus importation into the country.

## Conclusions

The DENV-2 portable sequencing approach we describe represents a useful tool for genomic characterization and molecular epidemiology of outbreaks in Africa and elsewhere. On the basis of phylogenetic evidence and the geographic distribution of detected genotypes, the DENV-2 cosmopolitan genotype detected in Angola is probably endemic in Africa. The AO-1 genome we analyzed probably represents an early transmission event from an ongoing DENV-2 epidemic in Luanda. Further sequencing of DENV in the region is required to determine whether the cosmopolitan genotype is endemic to Angola or if it represents a more recent introduction from elsewhere (e.g., East Africa or other unsampled locations).

## Acknowledgments

We would like to thank all the patients involved and the staff who assisted with sample collection.

This study was made possible by funding from the Wellcome Trust and Royal Society Sir Henry Dale Fellowship (grant no. 204311/Z/16/Z), the Higher Education Funding Council for England's Global Challenges Research Fund (grant no. 005073), and the John Fell Research Fund (grant no. 005166). Travel to Angola by S.C.H. and N.R.F. was supported by Africa–Oxford Travel Grants (grant nos. AfiOx-48 and AfiOx-60).

This work forms part of the ArboSPREAD project.

## About the Author

Dr. Hill is a postdoctoral researcher at the University of Oxford, United Kingdom. She studies the genomic epidemiology of mosquito-borne viruses, including yellow fever virus, Zika virus, and dengue virus.

## References

1. Gubler DJ. Dengue and dengue hemorrhagic fever. *Clin Microbiol Rev.* 1998;11:480–96. <http://dx.doi.org/10.1128/CMR.11.3.480>
2. Bhatt S, Gething PW, Brady OJ, Messina JP, Farlow AW, Moyes CL, et al. The global distribution and burden of dengue. *Nature.* 2013;496:504–7. <http://dx.doi.org/10.1038/nature12060>
3. Rabe IB, Staples JE, Villanueva J, Hummel KB, Johnson JA, Rose L, et al. Interim guidance for interpretation of Zika virus



- antibody test results. *MMWR Morb Mortal Wkly Rep.* 2016; 65:543–6.
4. Centers for Disease Control and Prevention (CDC). Ongoing dengue epidemic—Angola, June 2013. *MMWR Morb Mortal Wkly Rep.* 2013;62:504–7.
  5. Schwartz E, Meltzer E, Mendelson M, Tooke A, Steiner F, Gautret P, et al. Detection on four continents of dengue fever cases related to an ongoing outbreak in Luanda, Angola, March to May 2013. *Euro Surveill.* 2013;18:20488.
  6. Parreira R, Centeno-Lima S, Lopes A, Portugal-Calisto D, Constantino A, Nina J. Dengue virus serotype 4 and chikungunya virus coinfection in a traveller returning from Luanda, Angola, January 2014. *Euro Surveill.* 2014;19:20730. <http://dx.doi.org/10.2807/1560-7917.ES2014.19.10.20730>
  7. Abreu C, Silva-Pinto A, Lazzara D, Sobrinho-Simões J, Guimarães JT, Sarmento A. Imported dengue from 2013 Angola outbreak: not just serotype 1 was detected. *J Clin Virol.* 2016;79:77–9. <http://dx.doi.org/10.1016/j.jcv.2016.04.011>
  8. Gardy JL, Loman NJ. Towards a genomics-informed, real-time, global pathogen surveillance system. *Nat Rev Genet.* 2018;19:9–20. <http://dx.doi.org/10.1038/nrg.2017.88>
  9. Quick J, Grubaugh ND, Pullan ST, Claro IM, Smith AD, Gangavarapu K, et al. Multiplex PCR method for MinION and Illumina sequencing of Zika and other virus genomes directly from clinical samples. *Nat Protoc.* 2017;12:1261–76. <http://dx.doi.org/10.1038/nprot.2017.066>
  10. Kearse M, Moir R, Wilson A, Stones-Havas S, Cheung M, Sturrock S, et al. Geneious Basic: an integrated and extendable desktop software platform for the organization and analysis of sequence data. *Bioinformatics.* 2012;28:1647–9. <http://dx.doi.org/10.1093/bioinformatics/bts199>
  11. Stamatakis A. RAxML version 8: a tool for phylogenetic analysis and post-analysis of large phylogenies. *Bioinformatics.* 2014;30:1312–3. <http://dx.doi.org/10.1093/bioinformatics/btu033>
  12. Kraemer MUG, Faria NR, Reiner RC Jr, Golding N, Nikolay B, Stasse S, et al. Spread of yellow fever virus outbreak in Angola and the Democratic Republic of the Congo 2015–16: a modelling study. *Lancet Infect Dis.* 2017;17:330–8. [http://dx.doi.org/10.1016/S1473-3099\(16\)30513-8](http://dx.doi.org/10.1016/S1473-3099(16)30513-8)

Address for correspondence: Joana M. Afonso, Instituto Nacional de Investigação em Saúde Luanda, Angola; email: [jmafonso.7@gmail.com](mailto:jmafonso.7@gmail.com); Nuno R. Faria, University of Oxford, Department of Zoology, Peter Medawar Building, Oxford OX1 3SY, UK; email: [nuno.faria@zoo.ox.ac.uk](mailto:nuno.faria@zoo.ox.ac.uk)



**EMERGING  
INFECTIOUS DISEASES®**

**August 2017**

## Vectorborne Infections

- Added Value of Next-Generation Sequencing for Multilocus Sequence Typing Analysis of a *Pneumocystis jirovecii* Pneumonia Outbreak
- *Bartonella quintana*, an Unrecognized Cause of Infective Endocarditis in Children in Ethiopia
- Characteristics of Dysphagia in Infants with Microcephaly Caused by Congenital Zika Virus Infection, Brazil, 2015
- Zika Virus Infection in Patient with No Known Risk Factors, Utah, USA, 2016
- Acute Febrile Illness and Complications Due to Murine Typhus, Texas, USA
- High Infection Rates for Adult Macaques after Intravaginal or Intrarectal Inoculation with Zika Virus
- Lyme Borreliosis in Finland, 1995–2014
- Characterization of Fitzroy River Virus and Serologic Evidence of Human and Animal Infection
- Genomic Characterization of Recrudescence *Plasmodium malariae* after Treatment with Artemether/Lumefantrine
- Molecular Characterization of *Corynebacterium diphtheriae* Outbreak Isolates, South Africa, March–June 2015
- Clinical Laboratory Values as Early Indicators of Ebola Virus Infection in Nonhuman Primates
- Maguari Virus Associated with Human Disease
- Human Infection with Highly Pathogenic Avian Influenza A(H7N9) Virus, China
- Human Metapneumovirus and Other Respiratory Viral Infections during Pregnancy and Birth, Nepal
- Global Spread of Norovirus GII.17 Kawasaki 308, 2014–2016
- Preliminary Epidemiology of Human Infections with Highly Pathogenic Avian Influenza A(H7N9) Virus, China, 2017
- Real-Time Evolution of Zika Virus Disease Outbreak, Roatán, Honduras

To revisit the August 2017 issue, go to:

<https://wwwnc.cdc.gov/eid/articles/issue/23/8/table-of-contents>

# Enterovirus A71 Phenotypes Causing Hand, Foot and Mouth Disease, Vietnam

**Hoang Minh Tu Van, Nguyen To Anh, Nguyen Thi Thu Hong, Le Nguyen Truc Nhu, Lam Anh Nguyet, Tran Tan Thanh, Nguyen Thi Han Ny, Vu Thi Ty Hang, Truong Huu Khanh, Ho Lu Viet, Do Chau Viet, Ha Manh Tuan, Nguyen Thanh Hung, Du Tuan Quy, Do Quang Ha, Phan Tu Qui, Le Nguyen Thanh Nhan, Guy Thwaites, Nguyen Van Vinh Chau, Louise Thwaites, H. Rogier van Doorn, Le Van Tan**

We investigated enterovirus A71–associated hand, foot and mouth disease in Vietnam and found that, after replacing subgenogroup C4 in 2013, B5 remained the leading cause of this disease. In contrast with previous observations, this switch did not result in an explosive outbreak, and B5 evolution was driven by negative selection.

Enterovirus A71 (EV-A71)–associated hand, foot and mouth disease (HFMD) is a major problem in Asia. With >1 million cases reported across the region annually, HFMD is attributed to large numbers of hospitalized cases (1). In addition, EV-A71 often is associated with high case-fatality rates for those with severe HFMD disease (2,3).

EV-A71 outbreaks are usually associated with predominant subgenogroup switches (4). In Vietnam, a switch from subgenogroup C5 to C4 in 2011 coincided with an explosive outbreak, resulting 174,677 hospitalizations and 200 deaths (2). More recently, EV-A71 subgenogroup C4 was replaced by subgenogroup B5 in 2013, and subgenogroup C5 was sporadically detected (5–7). Yet, no comprehensive report about subgenogroup circulation, evolution, and associated clinical phenotypes of EV-A71 in Vietnam

has been generated since 2013. We investigated these subgenogroups to inform development of intervention strategies and guide public health authorities in response to HFMD outbreaks.

## The Study

We used clinical samples derived from patients enrolled in a concurrent HFMD research program in southern Vietnam. In that program, patients with suspected HFMD of all severities are enrolled from 3 major referral hospitals in Ho Chi Minh City: Children’s Hospital 1, Children’s Hospital 2, and the Hospital for Tropical Diseases (8). This study was approved by the hospital institutional review boards (document no. 73/BB-BVND1, Children’s Hospital 1; document no. 03EI/BVND2, Children’s Hospital 2; and document no. 150/BVBND-KH, Hospital for Tropical Diseases) and the Oxford Tropical Research Ethics Committee (document no. OxtREC reference 1005-13).

During July 2013–July 2015, we enrolled 1,547 patients. We performed PCR and identified EV-A71 as the most common cause of HFMD (24.5%, 379). Of patients with EV-A71, 91 (24%) had grade 2b1 HFMD or above (Table 1), accounting for most (47.4%) of the 192 enrolled patients who had severe HFMD.

We performed whole-genome sequencing on representatives of EV-A71–positive throat and rectal swab specimens with sufficient viral load (9). We obtained 146 EV-A71 complete genomes spanning the sampling period from July 2013 through April 2015. We removed 1 recombinant, a result of a recombination between 2 parental subgenogroup B5 strains, from our analysis (data not shown). Phylogenetically, 136 isolates belonged to the B5 subgenogroup and 10 belonged to the C4 subgenogroup (Appendix Figure 1, <http://wwwnc.cdc.gov/EID/article/25/4/18-1367-App1.pdf>). The C4 subgenogroup was sporadically detected from September 2014 onward (Table 2).

To unravel the evolutionary history of subgenogroup B5 in Vietnam, we used BEAST version 1.8.3 (10). The results of our analyses for main discrete geographic locations in Vietnam showed high fluidity within southern Vietnam, with Ho Chi Minh City being a likely source of viral circulation (Figure 1; Appendix Figure 2), supporting previously observed phylogeographic patterns of EV-A71 and other HFMD pathogens (8). Bayesian skyline analyses indicated that the relative genetic diversity of

Author affiliations: Oxford University Clinical Research Unit, Ho Chi Minh City, Vietnam (H.M.T. Van, N.T. Anh, N.T.T. Hong, L.N.T. Nhu, L.A. Nguyet, T.T. Thanh, N.T.H. Ny, V.T.T. Hang, D.Q. Ha, G. Thwaites, L. Thwaites, H.R. van Doorn, L.V. Tan); Children’s Hospital 2, Ho Chi Minh City (H.M.T. Van, H.L. Viet, D.C. Viet, H.M. Tuan); Children’s Hospital 1, Ho Chi Minh City (T.H. Khanh, N.T. Hung, D.T. Quy, L.N.T. Nhan); University of Oxford, Oxford, UK (P.T. Qui, G. Thwaites, L. Thwaites, H.R. van Doorn); Hospital for Tropical Diseases, Ho Chi Minh City (N.V.V. Chau)

DOI: <https://doi.org/10.3201/eid2504.181367>

**Table 1.** Demographics and clinical severities of enterovirus A71 in patients with hand, foot and mouth disease, Vietnam, July 2013–July 2015\*

Characteristic	Total EV-A71 cases enrolled, n = 379	EV-A71 cases included for phylogenetic analysis, n = 146	Subgenogroup C4 cases, n = 10	Subgenogroup B5 cases, n = 136
Sex				
M	213 (56.2)	89 (61)	8 (80)	81 (59.6)
F	166 (43.8)	57 (39)	2 (20)	55 (40.4)
Median age, mo (range)	21.9 (14.3–32.1)	19.4 (13.2–30.8)	13.9 (15.5–23.5)	19.6 (13–31.2)
Discharge grade†				
1	168 (44.3)	78 (53.4)	0	78 (57.4)
2a	120 (31.7)	42 (28.8)	3 (30)	39 (28.7)
2b1	30 (7.9)	13 (8.9)	4 (40)	9 (6.6)
2b2	16 (4.2)	10 (6.8)	2 (20)	8 (5.9)
3	43 (11.3)	3 (2.1)	1 (10)	2 (1.5)
4	2 (0.5)	0	0	0
Death	0	0	0	0

\*Values are no. (%) except as indicated. EV-A71, enterovirus A71.

†Grade 1, mouth ulcers or vesicles or papules on hands, feet, or buttocks, with or without mild fever (temperature <39°C). Grade 2a, central nervous system involvement (myoclonus reported by parents or caregivers only, temperature >39°C or ataxia). Grade 2b1, myoclonus observed by medical staff or history of myoclonus and lethargy or pulse >130 bpm. Grade 2b2, ataxia, nystagmus, limb weakness, cranial nerve palsies, persistent high fever, or pulse >150 bpm. Grade 3, autonomic dysfunction with sweating, hypertension, tachycardia, and tachypnea. Grade 4, additional cardiopulmonary compromise with pulmonary edema or shock syndrome.

subgenogroup B5 increased sharply in 2012. This diversity was then maintained at a high level with slight fluctuations from 2013 to 2015, coinciding with a complete switch from subgenogroup C4 to B5 in 2013 (6) (Figure 2; Appendix Figure 3).

To estimate the rate of nonsynonymous (dN) and synonymous (dS) substitution, we used estimate selection for each codon, Z-test of selection, and Fisher exact test of selection methods available in MEGA5 (11). We estimated the nucleotide substitution rates among whole-genome sequences of EV-A71 subgenogroup B5 at 3.9

$\times 10^{-3}$  substitutions/site/year and for viral protein (VP) 1 sequences at  $5.12 \times 10^{-3}$  substitutions/site/year. Whereas no data exist for nucleotide substitution rates of EV-A71 whole-genome sequences, the substitution rate we estimated for VP1 sequences is slightly higher than that from previous reports (6,12).

Maximum-likelihood-based analysis revealed the estimates of mean dN:dS values were 0.0465 for VP1 and 0.0428 for complete coding regions, suggesting that EV-A71 subgenogroup B5 evolution was driven by strong negative selection, which supports previous reports (6,12). In contrast with findings from previous studies (6,12), our investigation for dN:dS ratios of individual codons did not reveal any sites, including VP1 residues 43 and 145, that underwent positive selection pressure. Because of the small number of subgenogroup C4 sequenced in our study, in-depth C4 phylogenetic analysis and comparison of associated clinical phenotypes between C4 and B5 were deemed uninformative.

## Conclusions

Because others have extensively described the evolutionary history of EV-A71 on a global scale, including subgenogroup B5 (5,6), we focused our analysis on EV-A71 obtained from a comprehensive HFMD research program in Vietnam during July 2013–July 2015 (8) and the associated clinical phenotypes.

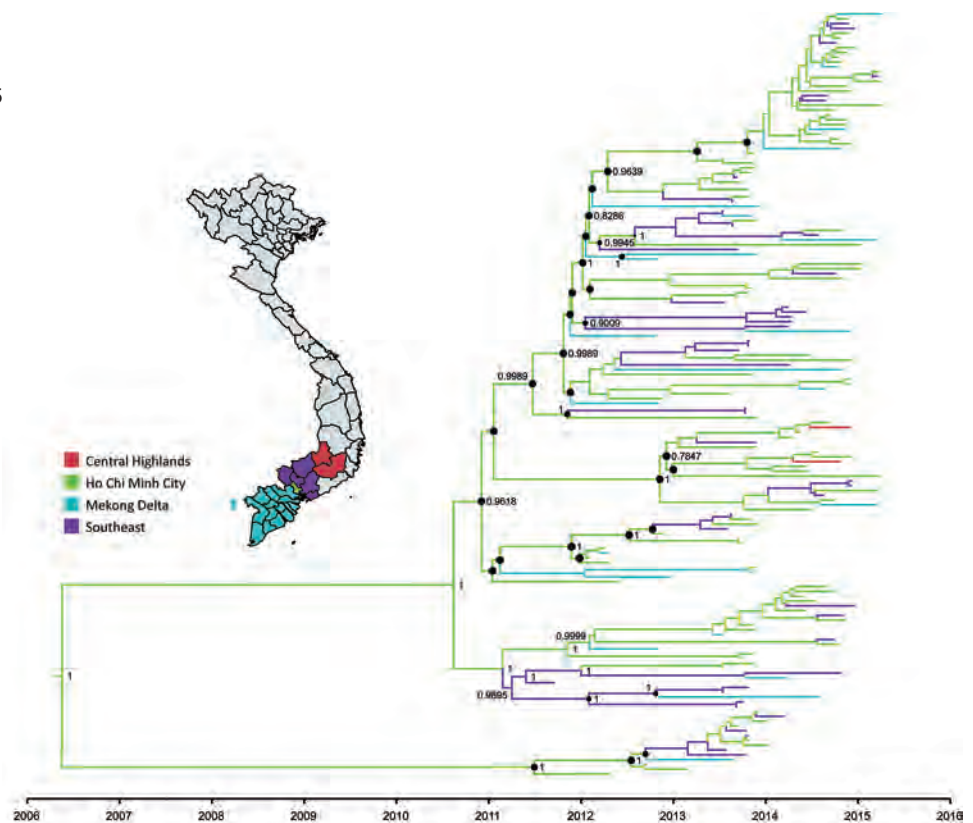
We showed that, after replacing subgenogroup C4 in 2013, subgenogroup B5 continued to circulate at a high level of endemicity and transmissibility, as reflected in our skyline plots (Figure 2; Appendix Figure 3) and phylogeographic patterns (Figure 1; Appendix Figures 1, 2), and was the major cause of HFMD in Vietnam, including cases with severe disease. However, compared with the 2011–2012 period, when subgenogroup C4 was circulating after replacing C5, the numbers of reported cases

**Table 2.** Distribution of enterovirus A71 subgenogroups detected by month, Vietnam, July 2013–April 2015

Year and month	Subgenogroup		Total
	B5	C4	
2013			
Jul	5	0	5
Aug	6	0	6
Sep	9	0	9
Oct	10	0	10
Nov	15	0	15
Dec	3	0	3
2014			
Jan	2	0	2
Feb	0	0	0
Mar	3	0	3
Apr	6	0	6
May	2	0	2
Jun	5	0	5
Jul	4	0	4
Aug	6	0	6
Sep	5	2	7
Oct	16	4	20
Nov	16	1	17
Dec	11	1	12
2015			
Jan	3	0	3
Feb	0	0	0
Mar	6	2	8
Apr	3	0	3



**Figure 1.** Maximum-clade credibility tree illustrating results of phylogeographic analysis of enterovirus A71 subgenogroup B5 coding sequences, Vietnam, July 2013–April 2015. Black circles indicate posterior probabilities  $\geq 70\%$  and state probabilities  $\geq 70\%$  at all nodes. Branch colors represent sampling locations from 5 discrete states in Vietnam (inset map; <https://mapchart.net>). Small sample sizes from individual provinces precluded phylogeographic analyses at a finer spatial scale. Except for Ho Chi Minh City, we grouped provinces in Vietnam from which we sampled viruses into discrete locations, including southeast (Ba Ria, Binh Duong, Binh Phuoc, Dong Nai, Tay Ninh, and Vung Tau Provinces), Mekong Delta (Can Tho, Dong Thap, Hau Giang, Kien Giang, Long An, and Tien Giang Provinces), and Central Highlands (Dac Nong and Lam Dong Provinces). We analyzed whole-genome sequence data using general time-reversible plus gamma 4 nt substitution models suggested by IQ-TREE version 1.4.3 (<http://www.iqtree.org>). Viral protein 1–based analysis yielded similar results (Appendix Figure 2, <https://wwwnc.cdc.gov/EID/article/25/4/18-1367-App1.pdf>). Enterovirus A71 sequences generated in this study were submitted to GenBank under accession nos. MH\_716248–6393 and KP\_691643–66.



decreased during July 2013–July 2015, as did the proportion of fatalities attributed to HFMD in Vietnam (<http://iris.wpro.who.int/handle/10665.1/14188>). Of note, subgenogroup B5 exclusively circulates in the Asia-Pacific region and has been responsible for large HFMD outbreaks in Malaysia, Brunei, Taiwan (13,14), and, more recently, Thailand (15), whereas C4 has been circulating in China since 2008 and annually causes >1 million reported cases. Epidemiologically, subgenogroup switches often accompany large EV-A71–associated HFMD outbreaks (4,6). However, existing evidence fails to demonstrate the differences in terms of virulence and transmissibility between EV-A71 subgenogroups. Collectively, the underlying mechanism and factor determining pathogen emergence and the scale and severity of HFMD outbreaks, especially in specific localities, remains unknown, which might be a consequence of a complex interplay between cross-immunity, pathogen evolution, herd immunity, and public health responses.

The extent to which EV-A71 may adapt to in vitro cell culture systems remains unknown. We did not observe any specific amino acid residue that underwent positive selection in our analysis of subgenogroup B5

sequences from Vietnam. However, a recent study of subgenogroup B5 sequences from Vietnam generated by VP1 sequencing of B5 culture isolates recovered in RD and Vero cell lines worldwide showed that amino acid

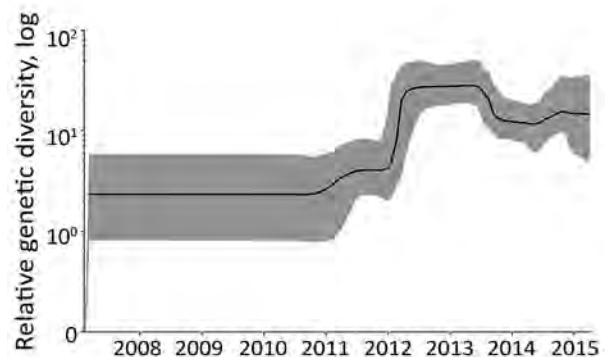


**Figure 2.** Complete coding sequence–based Bayesian skyline plot illustrating the relative genetic diversity of enterovirus A71 subgenogroup B5 in Vietnam over time. Black line indicates the mean; gray shading shows the upper and lower 95% highest posterior density values. Viral protein 1–based analysis yielded similar results (Appendix Figure 3, <https://wwwnc.cdc.gov/EID/article/25/4/18-1367-App1.pdf>).

residues 43 and 145 of the VP1 protein are under positive selection (6). Because we obtained all EV-A71 genomes directly from clinical samples, our results could more accurately reflect the genetic diversity of EV-A71 in human populations, which might explain a slight difference in the estimated nucleotide substitution rate for VP1 sequences between our study and a recent report (6). Research to explore the potential biases introduced by the cell culture step on the observed genetic diversity of EV-A71 is urgently needed. Information obtained through such work could have profound implications for disease surveillance, which might also inform vaccine development and implementation.

Our study has some limitations. Because we based our surveillance only in southern Vietnam, the circulating viruses in the northern and central parts were not well represented. In addition, only EV-A71 samples with real-time PCR crossing point values  $\leq 30$  were subjected to sequencing, which might have resulted in an underestimation of EV-A71 diversity.

In summary, after replacing subgenogroup C4 in 2013, subgenogroup B5 EV-A71 continued to circulate at a high level of endemicity and transmissibility and remained the leading cause of HFMD in Vietnam, including cases with severe disease, during 2013–2015. However, this subgenogroup replacement event did not result in an explosive HFMD outbreak during the study period, and subgenogroup B5 evolution was entirely driven by negative selection. The underlying mechanisms and factors determining pathogen emergence, the scale and severity of outbreaks, and the extent to which EV-A71 may adapt to in vitro cell culture systems remain to be clarified.

### Acknowledgments

We are indebted to the patients and their parents for their participation in this study and all the nursing and medical staff of the pediatric intensive care unit, infectious diseases wards, and outpatient clinics at Children's Hospital 1, Children's Hospital 2, and the Hospital for Tropical Diseases who provided care for the patients and helped collect clinical data. We thank Le Kim Thanh for her logistic support.

This work was supported by the Wellcome Trust, UK (101104/Z/13/Z, 106680/B/14/Z, and 204904/Z/16/Z).

### About the Author

Dr. Van is a postdoctoral researcher at the Oxford University Clinical Research Unit, Ho Chi Minh City, Vietnam. Her research interests are emerging infections and novel approaches to improving outcomes of critically ill patients in low- and middle-income countries.

### References

1. Yang B, Liu F, Liao Q, Wu P, Chang Z, Huang J, et al. Epidemiology of hand, foot and mouth disease in China, 2008 to 2015 prior to the introduction of EV-A71 vaccine. *Euro Surveill*. 2017;22:pii=16-00824. <http://dx.doi.org/10.2807/1560-7917.ES.2017.22.50.16-00824>
2. Khanh TH, Sabanathan S, Thanh TT, Thoa LPK, Thuong TC, Hang VtT, et al. Enterovirus 71-associated hand, foot, and mouth disease, southern Vietnam, 2011. *Emerg Infect Dis*. 2012;18:2002–5. <http://dx.doi.org/10.3201/eid1812.120929>
3. Ooi MH, Wong SC, Lewthwaite P, Cardoso MJ, Solomon T. Clinical features, diagnosis, and management of enterovirus 71. *Lancet Neurol*. 2010;9:1097–105. [http://dx.doi.org/10.1016/S1474-4422\(10\)70209-X](http://dx.doi.org/10.1016/S1474-4422(10)70209-X)
4. Solomon T, Lewthwaite P, Perera D, Cardoso MJ, McMin P, Ooi MH. Virology, epidemiology, pathogenesis, and control of enterovirus 71. *Lancet Infect Dis*. 2010;10:778–90. [http://dx.doi.org/10.1016/S1473-3099\(10\)70194-8](http://dx.doi.org/10.1016/S1473-3099(10)70194-8)
5. Geoghegan JL, Tan LV, Kühnert D, Halpin RA, Lin X, Simenauer A, et al. Phylodynamics of enterovirus A71-associated hand, foot, and mouth disease in Viet Nam. *J Virol*. 2015;89:8871–9. <http://dx.doi.org/10.1128/JVI.00706-15>
6. Thao NTT, Donato C, Trang VTH, Kien NT, Trang PMMT, Khanh TQ, et al. Evolution and spatiotemporal dynamics of enterovirus A71 subgenogroups in Vietnam. *J Infect Dis*. 2017;216:1371–9. <http://dx.doi.org/10.1093/infdis/jix500>
7. Le TV, Nguyen VTT, Nguyen QH, Pham DT. Molecular epidemiology analysis of enterovirus 71 strains isolated in Dak Lak, Vietnam, 2011–2016. *J Med Virol*. 2019;91:56–64. <http://dx.doi.org/10.1002/jmv.25286>
8. Anh NT, Nhu LNT, Van HMT, Hong NTT, Thanh TT, Hang VTT, et al. Emerging coxsackievirus A6 causing hand, foot and mouth disease, Vietnam. *Emerg Infect Dis*. 2018;24:654–62. <http://dx.doi.org/10.3201/eid2404.171298>
9. Tan LV, Tuyen NTK, Thanh TT, Ngan TT, Van HMT, Sabanathan S, et al. A generic assay for whole-genome amplification and deep sequencing of enterovirus A71. *J Virol Methods*. 2015;215–216:30–6. <http://dx.doi.org/10.1016/j.jviromet.2015.02.011>
10. Drummond AJ, Suchard MA, Xie D, Rambaut A. Bayesian phylogenetics with BEAUti and the BEAST 1.7. *Mol Biol Evol*. 2012;29:1969–73. <http://dx.doi.org/10.1093/molbev/mss075>
11. Tamura K, Peterson D, Peterson N, Stecher G, Nei M, Kumar S. MEGA5: molecular evolutionary genetics analysis using maximum likelihood, evolutionary distance, and maximum parsimony methods. *Mol Biol Evol*. 2011;28:2731–9. <http://dx.doi.org/10.1093/molbev/msr121>
12. Tee KK, Lam TT-Y, Chan YF, Bible JM, Kamarulzaman A, Tong CYW, et al. Evolutionary genetics of human enterovirus 71: origin, population dynamics, natural selection, and seasonal periodicity of the VP1 gene. *J Virol*. 2010;84:3339–50. <http://dx.doi.org/10.1128/JVI.01019-09>
13. AbuBakar S, Sam I-C, Yusof J, Lim MK, Misbah S, Hooi P-S, et al. Enterovirus 71 outbreak, Brunei. *Emerg Infect Dis*. 2009;15:79–82. <http://dx.doi.org/10.3201/eid1501.080264>
14. Huang S-W, Hsu Y-W, Smith DJ, Kiang D, Tsai H-P, Lin K-H, et al. Reemergence of enterovirus 71 in 2008 in Taiwan: dynamics of genetic and antigenic evolution from 1998 to 2008. *J Clin Microbiol*. 2009;47:3653–62. <http://dx.doi.org/10.1128/JCM.00630-09>
15. Puenpa J, Auphimai C, Korkong S, Vongpunsawad S, Poovorawan Y. Enterovirus A71 infection, Thailand, 2017. *Emerg Infect Dis*. 2018;24:1386–7. <http://dx.doi.org/10.3201/eid2407.171923>

Address for correspondence: Hoang Minh Tu Van or Le Van Tan, Oxford University Clinical Research Unit, Ho Chi Minh City, Vietnam; email: vanhmt@oucru.org or tanlv@oucru.org

# Distribution, Host-Seeking Phenology, and Host and Habitat Associations of *Haemaphysalis longicornis* Ticks, Staten Island, New York, USA

Danielle M. Tufts,<sup>1</sup> Meredith C. VanAcker,<sup>1</sup>  
Maria P. Fernandez, Anthony DeNicola,  
Andrea Egizi, Maria A. Diuk-Wasser

*Haemaphysalis longicornis*, an invasive Ixodid tick, was recently reported in the eastern United States. The emergence of these ticks represents a potential threat for livestock, wildlife, and human health. We describe the distribution, host-seeking phenology, and host and habitat associations of these ticks on Staten Island, New York, a borough of New York City.

The invasive Asian longhorned tick, *Haemaphysalis longicornis*, is rapidly becoming an agricultural and epidemiologic concern in the United States. Native to eastern Asia, this tick is a major pest of domestic livestock throughout its invasive range in Australia, New Zealand, and surrounding islands (1,2) and also parasitizes wildlife and humans (2,3). The Asian longhorned tick is a vector of various pathogens infectious to humans (3,4), including severe fever with thrombocytopenia syndrome virus in China, which can be transmitted transstadially and transovarially to other ticks and mice (5). It is unknown whether these ticks also transmit pathogens endemic to the United States, or could contribute to the galactose- $\alpha$ -1,3-galactose meat allergy currently associated with *Amblyomma* and *Ixodes* tick species (6).

Although *H. longicornis* ticks have been detected by the US Department of Agriculture on quarantined horses and livestock for several years, it only recently became a health concern when high densities were found feeding on a nonimported domestic sheep in New Jersey (7) and in field collections in New York, New York (W. Bajwa, pers. comm.). These ticks have also been detected in eastern and

southern US states including New York, Pennsylvania, Connecticut, New Jersey, Maryland, West Virginia, Virginia, North Carolina, and Arkansas (3).

Rapid emergence of *H. longicornis* ticks might be facilitated by their ability to reproduce parthenogenetically (3,4,7,8) and tolerate a wide range of environmental temperatures ( $-2^{\circ}\text{C}$  to  $40^{\circ}\text{C}$ ), although they are most successful in moist, warm-temperate conditions (9). *H. longicornis* ticks are a 3-host tick, similar to other Ixodid ticks (9), and have variable phenology depending on latitude (9,10). The phenology of *H. longicornis* ticks in the United States has not been characterized.

*H. longicornis* ticks might feed on a wide range of mammalian and avian hosts, which enables rapid geographic expansion (2,9). In New Zealand, *H. longicornis* ticks prefer habitat with Dallas grass (*Paspalum dilatatum*) and rushes (*Juncus* spp.) (9), plants abundant throughout the Midwestern and southern United States that could provide suitable habitat. In New Jersey, *H. longicornis* ticks were found in areas with unmowed grass (7), suggesting that these ticks might occupy wider habitat ranges than *Amblyomma* and *Ixodes* ticks.

We aimed to assess the ability of *H. longicornis* ticks to establish in the United States, their potential to acquire endemic human pathogens, and possible exposure risk to humans. We investigated the questing phenology and host and habitat associations in public parks and peridomestic environments of an emerging population of *H. longicornis* ticks on Staten Island, New York, during 2017–2018.

## The Study

All protocols and procedures were approved by the Institutional Review Board of Columbia University (protocol AAAR3750) and an Institutional Animal Care and Use Committee (protocols AC-AAAX4454 and AC-AAAS6470). Sampling efforts on public lands began in June 2017 when 13 forest sites were surveyed for questing ticks. During June 30–August 10, 2017, we removed avian-derived ticks from mist-netted birds at Freshkills Park on Staten Island. During June 3–August 24, 2018, we

Author affiliations: Columbia University, New York, New York, USA (D.M. Tufts, M.C. VanAcker, M.P. Fernandez, M.A. Diuk-Wasser); White Buffalo Inc., Moodus, Connecticut, USA (A. DeNicola); Rutgers University, New Brunswick, New Jersey, USA (A. Egizi); Monmouth County Mosquito Control Division, Tinton Falls, New Jersey, USA (A. Egizi)

DOI: <https://doi.org/10.3201/eid2504.181541>

<sup>1</sup>These authors contributed equally to this article.



**Table 1.** Sites surveyed for *Haemaphysalis longicornis* ticks, Staten Island, New York, USA, 2017 and 2018\*

Year and location	Surveyed	Habitat	Density/1,000 m <sup>2</sup>	Adult	Nymph	Larvae
2017						
Bloomington Park	Questing	Forest	3.1 (2)	0	5	0
Blue Heron Park	Questing	Forest	0.9 (2)	0	0	1
Clay Pit Ponds State Park Preserve	Questing	Forest	61.5 (2)	5	89	0
Clove Lakes Park	Questing	Forest	0.0 (2)	0	0	0
Conference House Park	Questing	Forest	7.4 (2)	7	78	0
Freshkills Park	Questing; host	Grassland	0.0 (2)	0	0	0
Great Kills Park	Questing	Grassland	0.0 (2)	0	0	0
High Rock Park	Questing	Forest	0.0 (2)	0	0	0
Latourette Park	Questing	Forest	1.3 (3)	0	3	0
Lemon Creek Park	Questing	Grassland	0.0 (2)	0	0	0
Silver Lake Park	Questing	Grassland	0.3 (2)	0	1	0
Willowbrook Park	Questing	Forest	0.8 (2)	0	1	0
Wolfe's Pond Park	Questing	Forest	0.0 (2)	0	0	0
2018						
Arden Woods Park	Questing; host	Forest	2.7 (6)	2	4	2
Bloomington Park	Questing	Forest	5.9 (3)	0	13	0
Blueberry Park	Questing	Forest	0.0 (1)	0	0	0
Blue Heron Park	Questing; host	Forest	0.3 (6)	0	1	0
Bunker Pond Park	Questing	Forest	1.4 (1)	1	0	0
Clay Pit Ponds State Park Preserve	Questing; host	Forest	146.2 (3)	26	280	70
Clove Lakes Park	Questing; host	Forest	0.0 (6)	0	0	0
College of Staten Island	Questing; host	Grassland	676.0 (1)	0	0	169
Conference House Park	Questing; host	Forest	509.7 (6)	128	1,058	343
Deere Park	Questing	Forest	0.0 (1)	0	0	0
Freshkills Park	Questing; host	Grassland	11.0 (1)	4	7	0
Goodhue Park	Questing; host	Forest	0.3 (6)	0	1	0
Great Kills Park	Questing	Grassland	0.0 (1)	0	0	0
High Rock Park	Questing	Forest	3.3 (1)	0	2	0
Hybrid Oak Woods Park	Questing	Forest	13.6 (3)	6	18	1
Ingram Woods Park	Questing	Forest	0.0 (1)	0	0	0
Jones Woods Park	Questing	Forest	0.0 (1)	0	0	0
King Fisher Park	Questing; host	Forest	0.0 (6)	0	0	0
Latourette Park	Questing; host	Forest	5.3 (6)	3	3	10
Lemon Creek Park	Questing	Grassland	0.0 (1)	0	0	0
Midland Field Park	Questing	Forest	0.0 (1)	0	0	0
Miller Field Park	Questing	Forest	0.0 (1)	0	0	0
Mount Loretto State Forest	Questing; host	Grassland	675.0 (1)	2	1	78
Ocean Breeze Park	Questing	Grassland	0.0 (1)	0	0	0
Reed's Basket Willow Swamp Park	Questing	Forest	0.0 (2)	0	0	0
Seidenberg Park	Questing	Forest	0.0 (1)	0	0	0
Silver Lake Park	Questing	Grassland	0.0 (1)	0	0	0
Wegener Park	Questing	Forest	0.0 (1)	0	0	0
Westwood Park	Questing	Forest	0.7 (1)	1	0	0
Willowbrook Park	Questing; host	Forest	1.0 (6)	0	2	1
Wolfe's Pond Park	Questing	Forest	0.0 (1)	0	0	0
Woodhull Park	Questing	Forest	1.7 (1)	0	1	0

\*Adult, nymph, and larval counts include questing ticks only. Values in parentheses indicate no. visits per site.

surveyed 24 forest and grassland sites for questing ticks and 8 forested grid sites for questing and mammal-derived ticks. Questing ticks were obtained by dragging a 1-m<sup>2</sup> corduroy cloth over the leaf litter, which was checked every 10 m or 20 m and all attached ticks were removed. White-footed mice (*Peromyscus leucopus*) were trapped biweekly for 2 consecutive nights in Sherman live traps (<https://www.shermantraps.com>) separated by 10 m in 10 × 5 trap grids.

During August 5–21, 2018, we anesthetized 16 male white-tailed deer (*Odocoileus virginianus*) and groomed them for ticks from 4 locations: College of Staten Island, Clay Pit Ponds, Mount Loretto State Forest, and Freshkills

Park. Mount Loretto State Forest, and Freshkills Park are dominated by grassland and wetland ecosystems, and Clay Pit Ponds is characterized by dense forest. College of Staten Island has manicured landscaping with grass and forest (separated by fencing) along the perimeter. While deer were anesthetized, we checked antlers, ears/head, front legs, hind legs, and body for ticks. Each animal was screened for 15 min to minimize time spent under anesthesia. Ticks were removed with forceps and stored in 100% ethanol for later identification.

During June 6–July 13, 2018, tick sampling was conducted on residential properties, which were selected by using a random cluster sampling strategy within areas

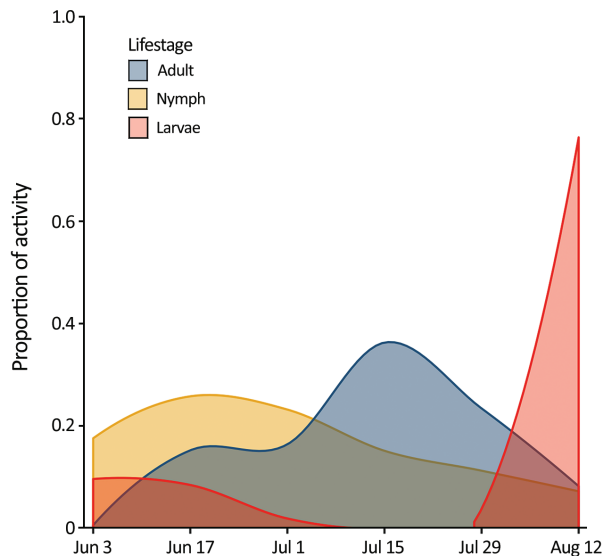


**Figure 1.** Seasonal activity of *Haemaphysalis longicornis* ticks (adults, nymphs, and larvae), Staten Island, New York, USA. Questing ticks were pooled by 2-week collection sessions during June 3–August 23, 2018.

previously identified as high risk given their proximity to parks (within 100 m). Houses were visited once, and questing ticks were collected along property edges by using the same method as in public parks.

We found questing *H. longicornis* ticks at 7 of 13 parks surveyed in 2017 and 16 of 32 parks surveyed in 2018 (Table 1). Adult ticks were most active in late July and nymphs were active from mid-June to mid-July, similar to findings in South Korea (11). Larvae showed highest proportional activity in late August (Figure 1). We identified ticks primarily by morphology; a representative sample of specimens from deer and drag collections ( $n = 63$ ) were confirmed as *H. longicornis* ticks by DNA barcoding using the cytochrome c oxidase I locus (12).

In 2017, we processed 39 birds: 11 American robins (*Turdus migratorius*), 1 common yellowthroat (*Geothlypis trichas*), 20 gray catbirds (*Dumetella carolinensis*), 2 house wrens (*Troglodytes aedon*), 1 indigo bunting (*Passerina cyanea*), 3 northern cardinals (*Cardinalis cardinalis*), and 1 American yellow warbler (*Setophaga petechia*). We found no *H. longicornis* ticks of any life stage. We found no *H. longicornis* ticks on 87 uniquely

tagged *P. leucopus* mice (190 individual captures), 2 eastern chipmunks (*Tamias striatus*), 14 northern short-tailed shrews (*Blarina brevicauda*), and 1 brown rat (*Rattus norvegicus*). All life stages were recovered from deer at all 4 locations, and larvae were the most prevalent stage collected (Table 2). These findings indicate that immature stages of these ticks might feed exclusively on white-tailed deer or unsampled medium-sized animals. The high proportion of larvae on deer was probably caused by sampling during peak larval activity.

We surveyed 135 residential properties (average size 1,455 m<sup>2</sup>) (total visited = 505), of which 80% were located adjacent to parks in south and central Staten Island (Figure 2). Ticks were present at 34.1% of inspected properties. *H. longicornis* nymphs ( $n = 16$ ) were found at 5 properties (in tall grass and shaded lawns), all located in the southern section of the island; no other life stages were found.

## Conclusions

The ability of *H. longicornis* ticks to feed on a wide range of domestic and wildlife hosts, reproduce asexually, and survive various environmental conditions likely contributed to their establishment throughout the eastern United States. All 3 life stages were found feeding on white-tailed deer in August, together with 2 other established tick species (*A. americanum* and *I. scapularis*). Pathogen transmission by co-feeding has been documented in field and laboratory studies (13,14) and could be a potential mechanism for *H. longicornis* ticks acquiring pathogens when feeding alongside infected *A. americanum* or *I. scapularis* ticks.

We found no *H. longicornis* ticks on *P. leucopus* mice or avian hosts even in sites with high densities of questing ticks, limiting the potential for this tick to acquire human pathogens. In New Zealand, immature life stages were commonly found on hares and goats, and adults were frequently found on larger mammals; the brown hare (*Lepus europaeus*) was touted as a major disseminator (9,15). These findings indicate the need for extensive sampling of other mammalian hosts. Finding *H. longicornis* ticks on residential properties is a human health concern because its potential as a vector of human pathogens in the United States is unknown. The combination of suitable habitat types, a plethora of host species, and high humidity make most regions of the United States suitable for *H. longicornis* tick establishment and proliferation.

**Table 2.** Number of *Haemaphysalis longicornis* ticks removed from 16 deer on Staten Island, New York, USA

Location*	Adult	Nymph	Larvae	Total
City University of New York College of Staten Island, $n = 10$	7	1	193	201
Clay Pit Ponds State Park Reserve, $n = 3$	56	63	217	336
Mount Loretto State Forest, $n = 2$	90	4	63	157
Freshkills Park, $n = 1$	15	6	140	161
Total, $n = 16$	168	74	613	855

\*Values indicate no. deer screened at each location.

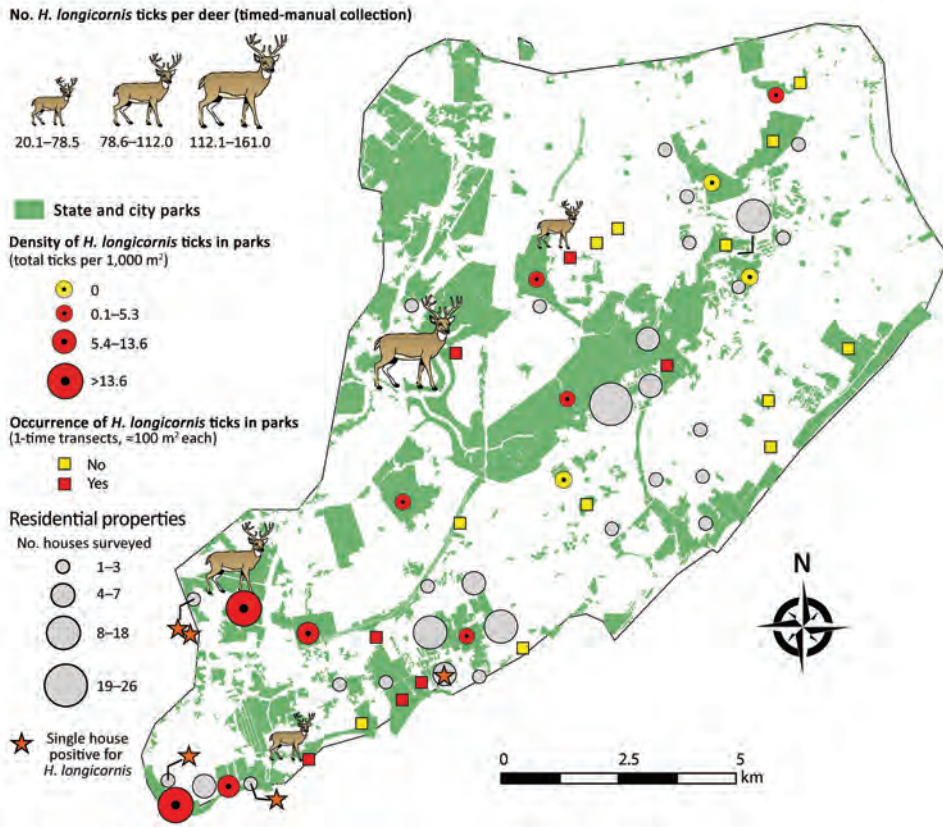


**Figure 2.** Sampling site locations and number of *Haemaphysalis longicornis* ticks collected on deer, in parks (grids and transects), and during household visits on Staten Island, New York, USA.

**Acknowledgments**

We thank the anonymous reviewers for their helpful comments and Staten Island summer field assistants and household survey assistants for participating in this study.

This study was supported by Cooperative Agreement No. U01CK000509-01 from the Centers for Disease Control and Prevention.

**About the Author**

Dr. Tufts is a geneticist and disease ecologist at Columbia University, New York, NY. Her research interests include infectious diseases, tickborne pathogens, ecology, and evolutionary genetics.

**References**

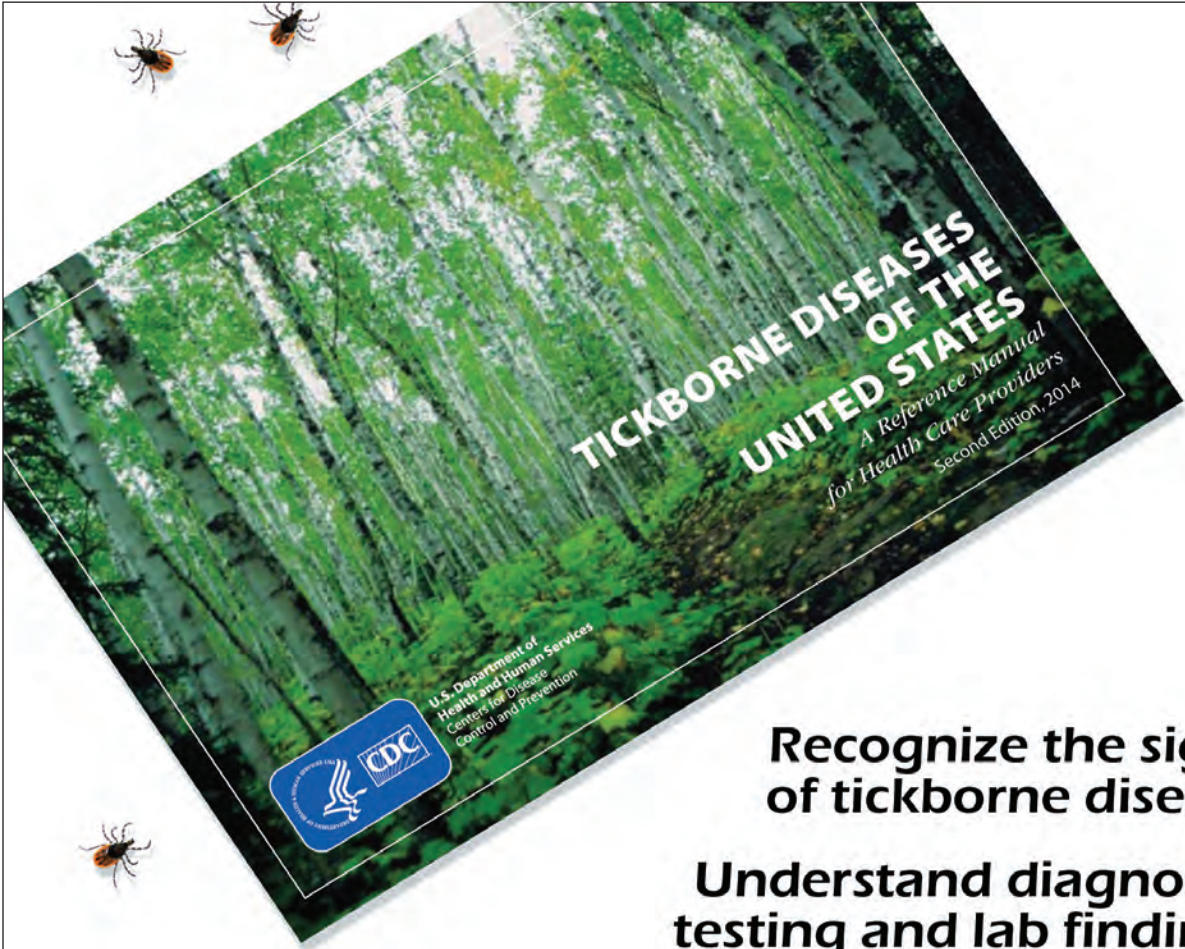
1. Heath AC, Palma RL, Cane RP, Hardwick S. Checklist of New Zealand ticks (Acari: Ixodidae, Argasidae). *Zootaxa*. 2011; 2995:55–63.
2. Hoogstraal H, Roberts FH, Kohls GM, Tipton VJ. Review of *Haemaphysalis (kaiseriana) Longicornis* Neumann (resurrected) of Australia, New Zealand, New Caledonia, Fiji, Japan, Korea, and northeastern China and USSR, and its parthenogenetic and bisexual populations (Ixodoidea, Ixodidae). *J Parasitol*. 1968;54:1197–213. <http://dx.doi.org/10.2307/3276992>
3. Beard CB, Occi J, Bonilla DL, Egizi AM, Fonseca DM, Mertins JW, et al. Multistate infestation with the exotic disease-vector tick *Haemaphysalis longicornis*—United States,

- August 2017–September 2018. *MMWR Morb Mortal Wkly Rep*. 2018;67:1310–3. <http://dx.doi.org/10.15585/mmwr.mm6747a3>
4. Chen Z, Yang X, Bu F, Yang X, Liu J. Morphological, biological and molecular characteristics of bisexual and parthenogenetic *Haemaphysalis longicornis*. *Vet Parasitol*. 2012;189:344–52. <http://dx.doi.org/10.1016/j.vetpar.2012.04.021>
5. Luo L-M, Zhao L, Wen H-L, Zhang Z-T, Liu J-W, Fang L-Z, et al. *Haemaphysalis longicornis* ticks as reservoir and vector of severe fever with thrombocytopenia syndrome virus in China. *Emerg Infect Dis*. 2015;21:1770–6. <http://dx.doi.org/10.3201/eid2110.150126>
6. Chinuki Y, Ishiwata K, Yamaji K, Takahashi H, Morita E. *Haemaphysalis longicornis* tick bites are a possible cause of red meat allergy in Japan. *Allergy*. 2016;71:421–5. <http://dx.doi.org/10.1111/all.12804>
7. Rainey T, Occi JL, Robbins RG, Egizi A. Discovery of *Haemaphysalis longicornis* (Ixodida: Ixodidae) parasitizing a sheep in New Jersey, United States. *J Med Entomol*. 2018;55:757–9. <http://dx.doi.org/10.1093/jme/tjy006>
8. Oliver JH Jr. Parthenogenesis in mites and ticks (Arachnida: Acari). *American Zoologist*. 1971;11:283–99. <http://dx.doi.org/10.1093/icb/11.2.283>
9. Heath A. Biology, ecology and distribution of the tick, *Haemaphysalis longicornis* Neumann (Acari: Ixodidae) in New Zealand. *N Z Vet J*. 2016;64:10–20. <http://dx.doi.org/10.1080/00480169.2015.1035769>
10. Sutherst RW, Moorhouse DE. The seasonal incidence of Ixodid ticks on cattle in an elevated area of South-Eastern Queensland. *Australian Journal of Agricultural Research*. 1972;23:195–204. <http://dx.doi.org/10.1071/AR9720195>
11. Johnson JL, Kim HC, Coburn JM, Chong ST, Chang NW, Robbins RG, et al. Tick surveillance in two southeastern provinces, including three metropolitan areas, of the Republic of Korea during



2014. Systematic and Applied Acarology. 2017;22:271–88. <http://dx.doi.org/10.11158/saa.22.2.10>
12. Chitimia L, Lin RQ, Cosoroaba I, Wu XY, Song HQ, Yuan ZG, et al. Genetic characterization of ticks from southwestern Romania by sequences of mitochondrial *cox1* and *nad5* genes. *Exp Appl Acarol*. 2010;52:305–11. <http://dx.doi.org/10.1007/s10493-010-9365-9>
  13. Lee JK, Stokes JV, Moraru GM, Harper AB, Smith CL, Wills RW, et al. Transmission of *Amblyomma maculatum*-associated *Rickettsia* spp. during cofeeding on cattle. *Vector Borne Zoonotic Dis*. 2018;18:511–8. <http://dx.doi.org/10.1089/vbz.2017.2228>
  14. States SL, Huang CI, Davis S, Tufts DM, Diuk-Wasser MA. Co-feeding transmission facilitates strain coexistence in *Borrelia burgdorferi*, the Lyme disease agent. *Epidemics*. 2017;19:33–42. <http://dx.doi.org/10.1016/j.epidem.2016.12.002>
  15. Heath ACG, Tenquist JD, Bishop DM. Goats, hares, and rabbits as hosts for the New Zealand cattle tick, *Haemaphysalis longicornis*. *New Zealand Journal of Zoology*. 1987;14:549–55. <http://dx.doi.org/10.1080/03014223.1987.10423028>

Address for correspondence: Danielle M. Tufts, Columbia University, E3B, 1102 Schermerhorn Extension Bldg, 1200 Amsterdam Ave, New York, NY 10027, USA; email: dt2503@columbia.edu



**TICKBORNE DISEASES OF THE UNITED STATES**  
A Reference Manual  
for Health Care Providers  
Second Edition, 2014

U.S. Department of Health and Human Services  
Centers for Disease Control and Prevention  
CDC

**Recognize the signs of tickborne disease**

**Understand diagnostic testing and lab findings**

**Quickly find treatment recommendations**

**Order or download at**  
**[www.cdc.gov/pubs](http://www.cdc.gov/pubs)**

# Aerosol Transmission of *Aspergillus fumigatus* in Cystic Fibrosis Patients in the Netherlands

Tobias G.P. Engel, Ellen Erren,  
Koen S.J. Vanden Driessche,  
Willem J.G. Melchers, Monique H. Reijers,  
Peter Merkus, Paul E. Verweij

We collected sputum samples and cough plates from 15 cystic fibrosis patients in the Netherlands who were colonized with *Aspergillus fumigatus*; we recovered *A. fumigatus* of the same genotype in cough aerosols and sputum samples from 2 patients. The belief that transmission of *A. fumigatus* from cystic fibrosis patients does not occur should be reconsidered.

**P**rogressive lung injury in cystic fibrosis (CF) patients can lead to chronic colonization with bacteria and fungi (1,2). Different routes of patient-to-patient transmission have been identified for various microorganisms (3). For saprophytic molds, such as *Aspergillus fumigatus*, exposure to aerosolized conidia in the environment is believed to be the primary route leading to colonization of the airways (3). Secretion of these fungi from the human lung into the environment is thought not to occur, and the general view is that humans are dead-end hosts of filamentous fungi. However, some reports have provided information suggesting that this belief might need to be revised (4). We set out to examine whether aerosol formation of *A. fumigatus* occurs in CF patients during coughing.

## The Study

During 2017–2018, we invited 15 adult CF patients in the Netherlands who were colonized with *A. fumigatus* to participate in a cough plate experiment. We defined *A. fumigatus* colonization as the recovery of *A. fumigatus* from >50% of sputum samples collected over the course of the 2 previous years. To enable genetic comparisons among study samples, we stored cultured fungal isolates from included patients in the Radboud University Medical Center Medical Microbiology Department (Nijmegen, the Netherlands)

Author affiliations: Radboud University Medical Center, Nijmegen, the Netherlands (T.G.P. Engel, E. Erren, K.S.J. Vanden Driessche, W.J.G. Melchers, M.H. Reijers, P. Merkus, P.E. Verweij); Center of Expertise in Mycology Radboud UMC/CWZ, Nijmegen (T.G.P. Engel, W.J.G. Melchers, M.H. Reijers, P.E. Verweij)

DOI: <https://doi.org/10.3201/eid2504.181110>

fungal species bank. We performed sample collection during 2 routine quarterly visits before or after routinely performed spirometry. We instructed participants to take a maximal inspiration and cough twice on each of 2 different agar plates, Sabouraud dextrose agar and Columbia blood agar, held at a 5-cm distance from the participant's mouth. In addition, we collected a sputum sample on the same day or alternatively within a month if the participant was unable to produce sputum during the visit. We incubated Sabouraud dextrose agar cough plates at 28°C and Columbia blood agar cough plates at 36°C for 3 weeks and inspected daily for bacterial and fungal growth. We processed sputum samples according to CF guidelines (3). We collected individual CFUs (up to a maximum of 20 CFUs per sample) from cough plates and sputum cultures and genotyped *A. fumigatus* CFUs using microsatellite genotyping (5). We considered the detection of identical *A. fumigatus* genotypes from cough plates and sputum samples as proof of aerosolization of *A. fumigatus* from humans. We genotyped up to 6 sputum cultures of stored *A. fumigatus* isolates from each participant.

This study was reviewed by the institutional review board, which considered the study exempt from further institutional review board oversight in accordance with the law in the Netherlands on research with humans. All participants provided informed consent.

We cultured *A. fumigatus* from 18 (60%) sputum samples collected from 11 different participants (Table). *A. fumigatus* was also recovered from 3 (17%) of the 18 corresponding cough plate samples; these 3 samples were from 2 different participants. In both cases, cough plates had been acquired after the participant had undergone spirometry. Genotyping of the *A. fumigatus* isolates from sputum samples and cough plates from both participants showed identical genotypes. One participant was colonized with at least 10 different *A. fumigatus* genotypes (Figure). In this participant, the genotype recovered from the cough plate was not found in the sputum sample collected at the same visit but in the sputum sample recovered at the next visit. The second participant was colonized with a single genotype, which was recovered from multiple cough plates and sputum samples.

We also assessed for bacterial species present on cough plates and in sputum samples to enable comparison of transmission frequencies among pathogens. The cough



**Table.** Characteristics of and growth of *Aspergillus fumigatus*, *Pseudomonas aeruginosa*, *Staphylococcus aureus*, and *Stenotrophomonas maltophilia* in sputum samples and on cough plates from 15 cystic fibrosis patients, the Netherlands, 2017–2018\*

Pt. no.	Age, y/sex	FEV1, L (% predicted)	Peak flow, L/s	AB/AF use	Growth on first/second cough plates				Cultured from first/second sputum sample			
					A. <i>fumigatus</i>	P. <i>aeruginosa</i>	S. <i>aureus</i>	S. <i>maltophilia</i>	A. <i>fumigatus</i>	P. <i>aeruginosa</i>	S. <i>aureus</i>	S. <i>maltophilia</i>
1	23/F	2.7 (85)	7.9	Yes/no	-/-	+/-	-/-	-/-	-/-	+/+	+/+	+/-
2	20/F	4.0 (101)	8.6	Yes/no	-/-	-/-	-/-	-/+	-/ND	-/ND	+/ND	+/ND
3	22/F	2.3 (74)	7.9	Yes/no	-/-	-/-	-/+	-/-	+/+	-/-	+/+	-/-
4	20/M	3.2 (61)	7.4	Yes/no	+/-	-/-	-/-	-/-	+/+	-/-	+/+	-/-
5	49/F	2.3 (74)	7.7	No/no	-/-	-/-	-/-	-/-	+/-	-/-	+/+	-/-
6	43/F	2.7 (82)	7.2	Yes/no	-/-	-/-	-/-	-/-	+/+	+/+	-/-	-/-
7	26/M	4.6 (106)	10.9	Yes/no	-/-	-/-	+/+	-/-	+/ND	-/ND	+/ND	-/ND
8	39/F	1.0 (33)	5.7	Yes/no	-/-	-/-	-/+	-/-	+/+	-/-	-/-	+/+
9	49/M	1.2 (31)	3.4	Yes/no	-/-	+/+	-/-	-/-	+/+	+/+	-/-	-/-
10	22/M	2.0 (41)	7.8	Yes/no	-/-	+/+	-/-	-/-	+/-	+/+	+/+	-/-
11	58/F	2.2 (79)	5.1	Yes/no	-/-	-/-	-/-	-/-	-/-	+/+	+/-	-/-
12	31/M	2.0 (41)	5.3	Yes/no	-/-	+/+	+/+	-/-	-/+	-/+	-/+	-/-
13	51/F	0.7 (26)	3.5	Yes/no	-/-	+/+	-/-	-/-	-/-	+/+	+/+	-/-
14	30/M	2.5 (50)	8.7	Yes/no	-/-	+/+	-/-	-/-	+/+	+/+	-/-	-/+
15	27/F	3.8 (102)	8.4	Yes/no	+/+	-/-	-/-	-/-	+/+	-/-	-/-	-/-

\*AB, antibiotic; AF, antifungal; FEV1, forced expiratory volume in 1 second; ND, not done; Pt, patient; +, positive; -, negative.

secretion frequency for *Pseudomonas aeruginosa* was 67% (10/15) and for *Staphylococcus aureus* was 19% (3/16) (Table). No growth of *Stenotrophomonas maltophilia* on cough plates was observed.

Our study demonstrates that *A. fumigatus* can be recovered from cough aerosols from colonized CF patients with a similar frequency as *S. aureus*. This aerosolization is strikingly occurring in CF outpatients without any cavitory lesions or other serious complications. Cavitory lesions can facilitate sporulation of *A. fumigatus* inside patient lungs and thereby aids in fungal secretion.

By continuously monitoring indoor airborne fungal contamination with electrostatic dustfall collectors, Lemaire et al. identified patient airways as the source of

*A. fumigatus* contamination in an intensive care unit (4). Microsatellite genotyping showed that the airborne *A. fumigatus* and isolates from the patient's respiratory samples were identical. That observation and our study results indicate that the current consensus that transmission of *A. fumigatus* from colonized or infected patients does not occur should be reconsidered.

Although CF patients are typically colonized with unique *A. fumigatus* genotypes, several studies report the recovery of identical *A. fumigatus* genotypes from different CF patients (6). These genotypes could not be linked to a common environmental source and thus remained unexplained, but identical genotypes in different patients might point toward patient-to-patient transmission (6). Patient-derived

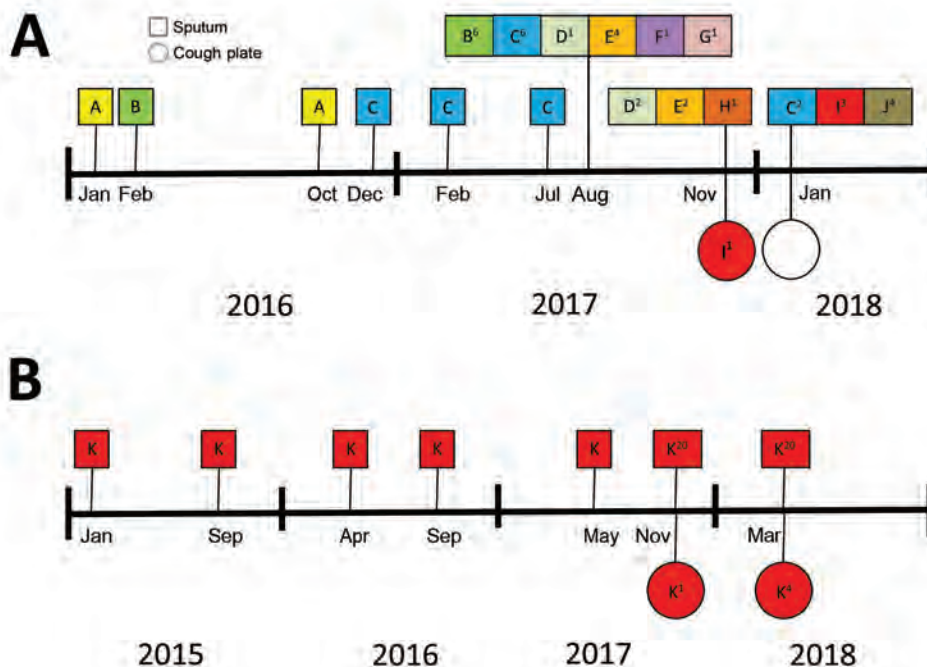


**Figure.** Genotyping results of *Aspergillus fumigatus* isolates in sputum cultures and on cough plates obtained from 2 participants with cystic fibrosis demonstrating aerosol formation of *A. fumigatus*, the Netherlands, 2015–2018. For samples collected after August 2017, a maximum of 20 isolates per sputum culture were saved. For samples collected earlier, only 1 sputum sample isolate was saved. Genotypes of the isolates collected from patient 4 (A) and 15 (B) are indicated. The superscript number indicates the number of isolates of that same genotype cultured from the collected sample.



azole resistance mutations have been reported in CF patient (7) and environmental (8) isolates. The mechanism for acquisition of azole resistance is unknown for environmental isolates, but resistance might have developed in isolates during human infection or colonization and then subsequently spread into the environment. Our observation of *A. fumigatus* in cough aerosols suggests droplet or airborne transmission as potential routes of patient to patient transmission. Traits such as azole resistance might spread through cough aerosols from patient to patient or from patient to environment. Both participants with positive cough plates had undergone spirometry before coughing, indicating that maximal inspiration and expiration might facilitate the release of *A. fumigatus*.

Aerosolized *A. fumigatus* conidia from environmental sources could represent a greater and more continuous burden for CF patients than potentially aerosolized conidia from patients. However, some studies suggest that *A. fumigatus* in chronically infected patients undergoes an evolutionary trajectory resulting in strains with specific traits that are better adapted to the lung environment (9,10). Endogenous and exogenous stress factors, such as host immunity or exposure to antifungal azoles, might result in the selection of traits that are better able to resist these stress factors (11). Isolates that are better adapted to the lung environment might have a greater propensity than environmental isolates to successfully colonize and persist in the airways of CF patients. In CF, 42% of azole resistance is derived through in-host selection and is thought to be associated with prolonged (prophylactic) use of anti-*Aspergillus* azoles (12,13). Passaging through the lungs of CF patients conceivably could provide *A. fumigatus* isolates the opportunity to acquire specific traits that increase their ability to survive in different environments. Evolution experiments have confirmed the potential of *A. fumigatus* to rapidly adapt to various environments (9).

## Conclusions

In summary, our results show that *A. fumigatus* can be recovered from cough aerosols of colonized CF patients. These findings underscore the need for additional studies to further elaborate transmission dynamics of *A. fumigatus*, evaluate if patient-to-patient transmission occurs, and determine if additional infection prevention measures are required.

## About the Author

Mr. Engel is a resident in clinical microbiology and a doctoral candidate in the Radboud University Medical Center, Nijmegen, the Netherlands. His primary research interest is in mycology, especially fungal colonization in CF patients.

## References

1. Elborn JS. Cystic fibrosis. *Lancet*. 2016;388:2519–31. [http://dx.doi.org/10.1016/S0140-6736\(16\)00576-6](http://dx.doi.org/10.1016/S0140-6736(16)00576-6)
2. Schwarz C, Bouchara JP, Buzina W, Chrenkova V, Dmeńska H, de la Pedrosa EGG, et al. Organization of patient management and fungal epidemiology in cystic fibrosis. *Mycopathologia*. 2018;183:7–19. <http://dx.doi.org/10.1007/s11046-017-0205-x>
3. Saiman L, Siegel JD, LiPuma JJ, Brown RF, Bryson EA, Chambers MJ, et al.; Cystic Fibrosis Foundation; Society for Healthcare Epidemiology of America. Infection prevention and control guideline for cystic fibrosis: 2013 update. *Infect Control Hosp Epidemiol*. 2014;35(Suppl 1):S1–67. <http://dx.doi.org/10.1086/676882>
4. Lemaire B, Normand A-C, Forel J-M, Cassir N, Piarroux R, Ranque S. Hospitalized patient as source of *Aspergillus fumigatus*, 2015. *Emerg Infect Dis*. 2018;24:1524–7. <http://dx.doi.org/10.3201/eid2408.171865>
5. de Valk HA, Meis JF, Curfs IM, Muehlethaler K, Mouton JW, Klaassen CH. Use of a novel panel of nine short tandem repeats for exact and high-resolution fingerprinting of *Aspergillus fumigatus* isolates. *J Clin Microbiol*. 2005;43:4112–20. <http://dx.doi.org/10.1128/JCM.43.8.4112-4120.2005>
6. de Valk HA, Klaassen CHW, Yntema JB, Hebestreit A, Seidler M, Haase G, et al. Molecular typing and colonization patterns of *Aspergillus fumigatus* in patients with cystic fibrosis. *J Cyst Fibros*. 2009;8:110–4. <http://dx.doi.org/10.1016/j.jcf.2008.10.003>
7. Morio F, Aubin GG, Danner-Boucher I, Haloun A, Sacchetto E, Garcia-Hermoso D, et al. High prevalence of triazole resistance in *Aspergillus fumigatus*, especially mediated by TR/L98H, in a French cohort of patients with cystic fibrosis. *J Antimicrob Chemother*. 2012;67:1870–3. <http://dx.doi.org/10.1093/jac/dks160>
8. Bader O, Tünnermann J, Dudakova A, Tangwattanaachuleeporn M, Weig M, Groß U. Environmental isolates of azole-resistant *Aspergillus fumigatus* in Germany. *Antimicrob Agents Chemother*. 2015;59:4356–9. <http://dx.doi.org/10.1128/AAC.00100-15>
9. Verweij PE, Zhang J, Debets AJM, Meis JF, van de Veerdonk FL, Schoustra SE, et al. In-host adaptation and acquired triazole resistance in *Aspergillus fumigatus*: a dilemma for clinical management. *Lancet Infect Dis*. 2016;16:e251–60. [http://dx.doi.org/10.1016/S1473-3099\(16\)30138-4](http://dx.doi.org/10.1016/S1473-3099(16)30138-4)
10. Ballard E, Melchers WJG, Zoll J, Brown AJP, Verweij PE, Warris A. In-host microevolution of *Aspergillus fumigatus*: a phenotypic and genotypic analysis. *Fungal Genet Biol*. 2018;113:1–13. <http://dx.doi.org/10.1016/j.fgb.2018.02.003>
11. Zelante T, Iannitti RG, De Luca A, Arroyo J, Blanco N, Servillo G, et al. Sensing of mammalian IL-17A regulates fungal adaptation and virulence. *Nat Commun*. 2012;3:683. <http://dx.doi.org/10.1038/ncomms1685>
12. Mortensen KL, Jensen RH, Johansen HK, Skov M, Pressler T, Howard SJ, et al. *Aspergillus* species and other molds in respiratory samples from patients with cystic fibrosis: a laboratory-based study with focus on *Aspergillus fumigatus* azole resistance. *J Clin Microbiol*. 2011;49:2243–51. <http://dx.doi.org/10.1128/JCM.00213-11>
13. Hamprecht A, Morio F, Bader O, Le Pape P, Steinmann J, Dannaoui E. Azole resistance in *Aspergillus fumigatus* in patients with cystic fibrosis: a matter of concern? *Mycopathologia*. 2018;183:151–60. <http://dx.doi.org/10.1007/s11046-017-0162-4>

Address for correspondence: Tobias G.P. Engel, Radboud University Medical Center, Department of Medical Microbiology, Route 777, Geert Grooteplein Zuid 10, 6500 HB Nijmegen, the Netherlands; email: tobias.engel@radboudumc.nl

# Pneumonic Plague in a Dog and Widespread Potential Human Exposure in a Veterinary Hospital, United States

Paula A. Schaffer,<sup>1</sup> Stephanie A. Brault,<sup>1</sup> Connor Hershkowitz,<sup>1</sup> Lauren Harris, Kristy Dowers, Jennifer House, Tawfik A. Aboellail, Paul S. Morley, Joshua B. Daniels

In December 2017, a dog that had pneumonic plague was brought to a veterinary teaching hospital in northern Colorado, USA. Several factors, including signalment, season, imaging, and laboratory findings, contributed to delayed diagnosis and resulted in potential exposure of  $\geq 116$  persons and 46 concurrently hospitalized animals to *Yersinia pestis*.

Plague is rare in dogs, even in areas to which *Yersinia pestis* is endemic (1,2). We describe a case of canine pneumonic plague that resulted in  $\geq 116$  potential human exposures.

## The Study

A 3-year-old mixed-breed dog was brought to a veterinarian in Colorado, USA, during December 2017 for evaluation of lethargy and fever 4 days after the dog was observed sniffing a dead prairie dog. Treatment with amoxicillin/clavulanic acid was initiated before referral the next day to the Colorado State University Veterinary Teaching Hospital (CSU-VTH; Fort Collins, CO, USA) because of progressive illness and development of hemoptysis. Imaging demonstrated unilateral lung lobar consolidation and small foci of parenchymal density in other lobes and intrathoracic lymphadenopathy (Figure 1).

Plague was considered unlikely because of the animal species, season, lack of peripheral lymphadenopathy, and unilateral lobar imaging pattern consistent with an aspirated foreign body, which is common in dogs (3). Treatment with ampicillin/sulbactam and enrofloxacin was initiated, and accessory lung lobectomy was performed to remove the presumed source of sepsis. Consolidation of the



**Figure 1.** Transverse computed tomography of dog with pneumonic plague on day 2 of hospitalization, Colorado, USA. Image shows accessory lung lobar consolidation.

accessory lobe and scattered dark red foci in other lung lobes were noted intraoperatively. Histologically, the excised lobe was effaced by severe necrosuppurative pneumonia with hemorrhage and fibrinous pleuritis but no intralobular bacteria (Figure 2).

After 48 hours of aerobic incubation, a swab specimen of lung parenchyma yielded light and pure growth of bacteria that we identified by using matrix-assisted laser desorption/ionization time-of-flight mass spectrometry (Vitek-MS, <https://www.biomerieux.com>) with 91.1% confidence as *Yersinia pseudotuberculosis*, although the database of the instrument contained mass spectra for 5 *Y. pestis* strains. Because signs were not consistent with *Y. pseudotuberculosis*, there was concern about misidentification. We performed PCR of the isolate the next day (5 days after admission) by using a Centers for Disease Control and Prevention (Atlanta, GA, USA) Laboratory Response Network protocol for *Y. pestis* (<https://www.epa.gov/homeland-security-research/sam-and-us-centers-disease-control-and-prevention-cdc-laboratory-response>).

Author affiliations: Colorado State University, Fort Collins, Colorado, USA (P.A. Schaffer, S.A. Brault, C. Hershkowitz, L. Harris, K. Dowers, T.A. Aboellail, P.S. Morley, J.B. Daniels); Colorado Department of Public Health and Environment, Denver, Colorado, USA (J. House)

DOI: <https://doi.org/10.3201/eid2504.181195>

<sup>1</sup>These authors contributed equally to this article.

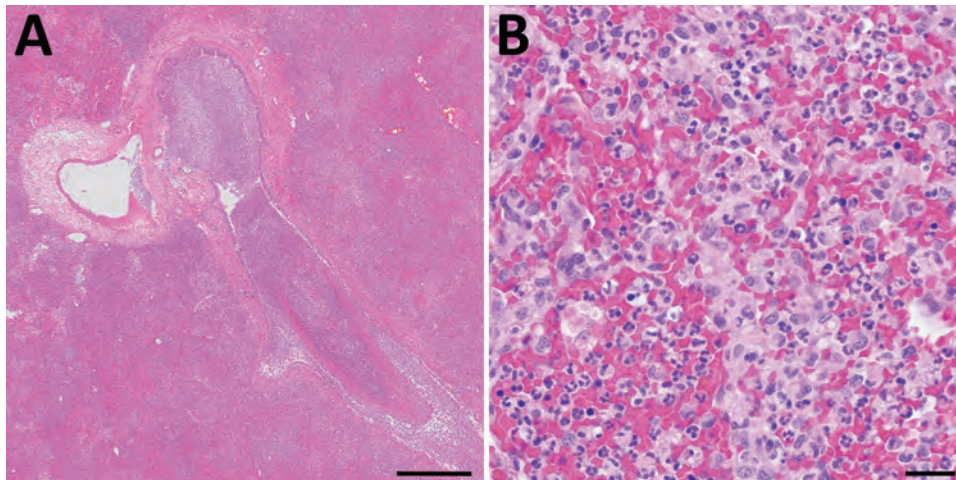


**Figure 2.** Histopathologic analysis of accessory lung lobe of dog with pneumonic plague (hematoxylin and eosin stain), Colorado, USA. A) Parenchyma, which is diffusely effaced by necrohemorrhagic pneumonia. Scale bar indicates 500  $\mu\text{m}$ . B) Alveolar detail, which is obscured by necrosis, hemorrhage, and suppurative inflammation without intralveolar bacteria. Scale bar indicates 20  $\mu\text{m}$ .

The dog was humanely killed the same day because of progression of pneumonia and poor prognosis. A limited necropsy was performed by informed personnel and found diffuse necrosuppurative and hemorrhagic pneumonia and severe necrotizing tonsillitis. Only liver tissue was positive for *Y. pestis* by PCR.

The dog had been transported throughout the hospital and housed in an oxygen cage vented to the room, potentially exposing personnel from multiple clinical services. Those handling specimens in the diagnostic laboratory were also considered exposed to *Y. pestis*. Exposures during the first 2 days of hospitalization were considered most critical because fluoroquinolone treatment was initiated after admission, and guidelines from the Colorado Department of Public Health and Environment (CDPHE) state that veterinary patients with *Y. pestis* have limited contagious risk after 48 hours of appropriate therapy (4).

While PCR results were pending, paper sheets were circulated to personnel to record contact with the dog. After the positive PCR result, emails were sent to these persons, followed by emails to all personnel. The delay between suspicion and diagnosis of *Y. pestis* resulted in word of mouth traveling faster than official communication, which caused anxiety among personnel. Many expressed frustration that suspicion and diagnosis of plague did not occur earlier. Two hospital-wide meetings were held for questions, discussion, and feedback. An online postincident survey was conducted, and 52 respondents indicated that they were aware of their potential exposure within 48 hours of the diagnosis.

We found 116 documented potential human exposures (Table 1). CDPHE recommendations were based on risk assessments, and interventions were decided by potentially exposed persons in consultation with healthcare providers (Table 2). In addition, 46 hospitalized animals co-housed in the same room were classified as potentially exposed. Prophylactic antimicrobial drugs were recommended

because most of these animals were critically ill and had decreased immune status. To our knowledge, there were no cases of *Y. pestis* infection in potentially exposed humans or animals. A fever developed in 1 person, but this fever was not determined to be caused by *Y. pestis* infection. One survey respondent reported adverse effects from antimicrobial drugs.

## Conclusions

Several factors delayed the diagnosis of pneumonic plague, resulting in many potential exposures. Pneumonic plague is uncommon in dogs; most dogs with plague have bubonic or septicemic plague and signs of fever, lethargy, and peripheral lymphadenopathy (1). The occurrence of this case during December was outside the predominant period of plague transmission in the Northern Hemisphere (April–October) (5). Of 89 animals with plague reported to CDPHE during 2008–2017, only 1 case (in a wild lynx) occurred in December. The mild winter in Colorado during 2017 might have prolonged activity of flea vectors, consistent with climate models that predict altered plague seasonality (6). In humans, radiographic abnormalities typically include bilateral lobar changes (7); in this dog, the accessory lung lobe was primarily affected on initial imaging, and this finding was interpreted as aspiration pneumonia. Histologically, pneumonic plague usually results in acute necrosuppurative, hemorrhagic pneumonia with obvious colonies of bacteria (8). In this case, antibiotics might have resulted in the histologic absence of bacteria.

**Table 1.** Number of potentially exposed persons by occupation to dog with pneumonic plague, Colorado, USA\*

Occupation	No. (%) persons
CSU-VTH employees	64 (55)
Veterinary students	35 (30)
Laboratory personnel	17 (15)
Total	116 (100)

\*CSU-VTH, Colorado State University Veterinary Teaching Hospital.



**Table 2.** Public health risk–based recommendations and interventions for persons exposed to dog with pneumonic plague, Colorado, USA\*

Level of interaction with dog	Recommended intervention	No. (%) contacts reporting intervention
Exposure ( $\leq 6$ feet) to dog with pneumonic plague; exposure to exudates, blood, or tissue without barrier precautions; bite or scratch from infected dog or flea	Antimicrobial drug prophylaxis	68 (59)†
Presence in critical care ward where dog was housed; exposure or contact after 48 h of appropriate patient antimicrobial drug treatment	Fever and symptom watch	38 (33)
Persons who did not meet the above criteria	No action (awareness education only)	Remainder of employees, staff, and students

\*Ten (8%) of 116 listed contacts did not report chosen intervention.  
†Of respondents who specified type of antimicrobial drug therapy received, 37 received doxycycline only, 2 doxycycline and gentamicin, 1 doxycycline and ciprofloxacin, 1 doxycycline and trimethoprim/sulfamethoxazole, and 1 ciprofloxacin only.

Matrix-assisted laser desorption/ionization time-of-flight mass spectrometry identified the isolate as *Y. pseudotuberculosis* with a high confidence score, but the species-level identification was considered suspicious. *Y. pestis* has been previously misidentified as *Y. pseudotuberculosis*, *Pseudomonas luteola*, and *Acinetobacter lwoffii* by automated systems (9) even when information for *Y. pestis* is present in databases. This isolate produced a strong peak at 3,061 m/z, which was present in spectra of the 5 *Y. pestis* isolates in the database and absent from *Y. pseudotuberculosis* spectra, likely corresponding to a *Y. pestis* biomarker previously described at 3,065 m/z (10).

At the time of this incident, CSU-VTH infection control standard operating procedures stressed suspicion of plague in cats and minimized the presence of this disease in dogs. Criteria for designating patients as high-risk plague suspects were opportunity for exposure (including geography and season), fever, and enlarged peripheral lymph nodes. Although the dog was febrile and had interacted with a prairie dog, the species, lack of peripheral lymphadenopathy, and nonseasonal presentation resulted in low-risk designation. Standard operating procedures are being updated to emphasize that dogs might be affected with plague year round and that lymphadenopathy might not be present. Isolation and plague testing for all dogs with pneumonia is not feasible, but increased suspicion of patients with hemoptysis might be appropriate. A relatively rare finding in dogs (11), hemoptysis was present in this dog, as well as in 2 other previously reported cases of canine pneumonic plague (12,13).

This unique case highlights the public health response challenges in a large teaching institution. Veterinary workers are at increased risk for infection with zoonotic diseases (14), and exposure to infectious agents is an occupational stressor with potential emotional toll (15). Veterinary hospital administrations should educate staff about zoonotic hazards, mitigate exposures, and communicate rapidly to personnel when potential exposures occur. The communication process in place at the CSU-VTH for zoonotic exposures has historically been used in small-scale events. The

extensive potential exposures in this instance highlighted the shortcomings of the process for reaching large numbers of persons. These problems are being addressed through development of frequently updated email listservs and telephone lists. Computerized logs may also be useful for documenting contact with patients with historical and syndromic factors consistent with potential zoonoses.

In summary, pneumonic plague, although rare, should be considered in dogs that have fever and respiratory signs with potential exposure in disease-endemic areas, regardless of season and lobar distribution. Efficient zoonotic disease communication and response plans should be prepared for large-scale events.

### About the Author

Dr. Schaffer is an anatomic pathologist in the Veterinary Diagnostic Laboratory and an assistant professor in the Department of Microbiology, Immunology, and Pathology, Colorado State University, Fort Collins, CO. Her research interests are identification and characterization of new pathologic entities in domestic and aquatic animal species.

### References

- Nichols MC, Ettestad PJ, Vinhatton ES, Melman SD, Onischuk L, Pierce EA, et al. *Yersinia pestis* infection in dogs: 62 cases (2003–2011). *J Am Vet Med Assoc*. 2014;244:1176–80. <http://dx.doi.org/10.2460/javma.244.10.1176>
- Orloski KA, Eidson M. *Yersinia pestis* infection in three dogs. *J Am Vet Med Assoc*. 1995;207:316–8.
- Lotti U, Niebauer GW. Tracheobronchial foreign bodies of plant origin in 153 hunting dogs. *J Am Anim Hosp Assoc*. 1992;1992:900–4.
- Colorado Department of Health and Environment. Animal plague in Colorado [cited 2018 Feb 26]. <https://www.colorado.gov/pacific/cdphe/plague>
- Colorado Department of Health and Environment. Communicable disease manual, 2015 [cited 2018 Jun 27]. <https://www.colorado.gov/pacific/cdphe/communicable-disease-manual>
- Nakazawa Y, Williams R, Peterson AT, Mead P, Staples E, Gage KL. Climate change effects on plague and tularemia in the United States. *Vector Borne Zoonotic Dis*. 2007;7:529–40. <http://dx.doi.org/10.1089/vbz.2007.0125>
- Kool JL. Risk of person-to-person transmission of pneumonic plague. *Clin Infect Dis*. 2005;40:1166–72. <http://dx.doi.org/10.1086/428617>

8. Robbins SL, Kumar V, Cotran RS. Robbins and Cotran pathologic basis of disease. 8th ed. Philadelphia: Saunders/Elsevier; 2010.
9. Tourdjman M, Ibraheem M, Brett M, Debess E, Progulskje B, Ettetstad P, et al. Misidentification of *Yersinia pestis* by automated systems, resulting in delayed diagnoses of human plague infections—Oregon and New Mexico, 2010–2011. *Clin Infect Dis*. 2012;55:e58–60. <http://dx.doi.org/10.1093/cid/cis578>
10. Lasch P, Drevinek M, Nattermann H, Grunow R, Stämmler M, Dieckmann R, et al. Characterization of *Yersinia* using MALDI-TOF mass spectrometry and chemometrics. *Anal Chem*. 2010;82:8464–75. <http://dx.doi.org/10.1021/ac101036s>
11. Bailiff NL, Norris CR. Clinical signs, clinicopathological findings, etiology, and outcome associated with hemoptysis in dogs: 36 cases (1990–1999). *J Am Anim Hosp Assoc*. 2002;38:125–33. <http://dx.doi.org/10.5326/0380125>
12. Runfola JK, House J, Miller L, Colton L, Hite D, Hawley A, et al.; Centers for Disease Control and Prevention. Outbreak of human pneumonic plague with dog-to-human and possible human-to-human transmission—Colorado, June–July 2014. *MMWR Morb Mortal Wkly Rep*. 2015;64:429–34.
13. Wang H, Cui Y, Wang Z, Wang X, Guo Z, Yan Y, et al. A dog-associated primary pneumonic plague in Qinghai Province, China. *Clin Infect Dis*. 2011;52:185–90. <http://dx.doi.org/10.1093/cid/ciq107>
14. Baker WS, Gray GC. A review of published reports regarding zoonotic pathogen infection in veterinarians. *J Am Vet Med Assoc*. 2009;234:1271–8. <http://dx.doi.org/10.2460/javma.234.10.1271>
15. Centers for Disease Control and Prevention. Exposure to stress: occupational hazards in hospitals, 2008 [cited 2018 Jun 27]. <https://www.cdc.gov/niosh/docs/2008-136/pdfs/2008-136.pdf>

Address for correspondence: Joshua B. Daniels, Veterinary Diagnostic Laboratory, Colorado State University, 200 W. Lake St, 1644 Campus Delivery, Fort Collins, CO 80523, USA; email: [josh.daniels@colostate.edu](mailto:josh.daniels@colostate.edu)



## EMERGING INFECTIOUS DISEASES®

September 2017

# Zoonoses

- Bioinformatic Analyses of Whole-Genome Sequence Data in a Public Health Laboratory
- Convergence of Humans, Bats, Trees, and Culture in Nipah Virus Transmission, Bangladesh
- Processes Underlying Rabies Virus Incursions across US–Canada Border as Revealed by Whole-Genome Phylogeography
- Real-Time Whole-Genome Sequencing for Surveillance of *Listeria monocytogenes*, France
- Role of Food Insecurity in Outbreak of Anthrax Infections among Humans and Hippopotamuses Living in a Game Reserve Area, Rural Zambia
- Molecular Antimicrobial Resistance Surveillance for *Neisseria gonorrhoeae*, Northern Territory, Australia
- Estimated Annual Numbers of Foodborne Pathogen–Associated Illnesses, Hospitalizations, and Deaths, France, 2008–2013
- Epidemiology of *Salmonella enterica* Serotype Dublin Infections among Humans, United States, 1968–2013
- Prevalence of *Yersinia enterocolitica* Bioserotype 3/O:3 among Children with Diarrhea, China, 2010–2015
- Risk for Low Pathogenicity Avian Influenza Virus on Poultry Farms, the Netherlands, 2007–2013
- Patterns of Human Plague in Uganda, 2008–2016
- Serologic Evidence for Influenza C and D Virus among Ruminants and Camelids, Africa, 1991–2015
- Norovirus in Bottled Water Associated with Gastroenteritis Outbreak, Spain, 2016
- Group A Rotavirus Associated with Encephalitis in Red Fox
- Protective Effect of Val<sub>129</sub>-PrP against Bovine Spongiform Encephalopathy but not Variant Creutzfeldt-Jakob Disease
- Imported Infections with *Mansonella perstans* Nematodes, Italy
- Genetic Diversity of Highly Pathogenic Avian Influenza A(H5N8/H5N5) Viruses in Italy, 2016–17
- Microcephaly Caused by Lymphocytic Choriomeningitis Virus
- Influenza A(H3N2) Virus in Swine at Agricultural Fairs and Transmission to Humans, Michigan and Ohio, USA, 2016
- Use of Blood Donor Screening to Monitor Prevalence of HIV and Hepatitis B and C Viruses, South Africa
- Emergence of Plasmid-Mediated Fosfomycin-Resistance Genes among *Escherichia coli* Isolates, France

To revisit the September 2017 issue, go to:

<https://wwwnc.cdc.gov/eid/articles/issue/23/9/table-of-contents>

# Seroprevalence of *Borrelia burgdorferi*, *B. miyamotoi*, and Powassan Virus in Residents Bitten by *Ixodes* Ticks, Maine, USA

Robert P. Smith, Jr., Susan P. Elias,  
Catherine E. Cavanaugh, Charles B. Lubelczyk,  
Eleanor H. Lacombe, Janna Brancato,  
Hester Doyle, Peter W. Rand,  
Gregory D. Ebel, Peter J. Krause

We conducted a serosurvey of 230 persons in Maine, USA, who had been bitten by *Ixodes scapularis* or *I. cookei* ticks. We documented seropositivity for *Borrelia burgdorferi* (13.9%) and *B. miyamotoi* (2.6%), as well as a single equivocal result (0.4%) for Powassan encephalitis virus.

Reports of Lyme disease in Maine, USA, have increased from a few cases in the late 1980s to 1,848 cases in 2017 (1), coinciding with range expansion of *Ixodes scapularis* ticks over the past 3 decades (2). The Maine Center for Disease Control reported the first 2 cases of hard-tick relapsing fever caused by *Borrelia miyamotoi* during 2016 and an additional 6 cases during 2017 (1). Hard-tick relapsing fever typically manifests as a nonspecific febrile illness (3,4). Han et al. (5) found a *B. miyamotoi* infection prevalence of 3.7% in adult *I. scapularis* ticks in Maine, ≈10-fold less than that for *B. burgdorferi* infection (50%, range 32%–65%) (6).

Powassan virus (POWV) encephalitis can have devastating complications and has infected 10 residents of Maine during 2000–2017. There are 2 variants of POWV with distinct enzootic cycles and tick vectors. Lineage 1 is transmitted by *I. cookei* ticks and lineage 2, sometimes referred to as deer tick virus, is transmitted by *I. scapularis* ticks (7). Both lineages are present in Maine (7), but lineage 1 has a lesser risk for transmission because human bites by *I. cookei* ticks are infrequent (8). One fatal Maine

case was demonstrated to be caused by lineage 2 POWV (7). Although POWV infection prevalence in Maine *I. scapularis* ticks is low (0.7%–1.8%) (9), frequent exposure to *I. scapularis* bites (8) and rapidity of POWV transmission (i.e., POWV can be transmitted to vertebrates after only 15 min from onset of the tick bite) (10) raise concern.

Our objective was to determine the seroprevalence of *B. burgdorferi*, *B. miyamotoi*, and POWV to clarify the frequency of exposure to each of these pathogens in residents of Maine, USA, who had been bitten by *I. scapularis* or *I. cookei* ticks. We also anticipated that a serosurvey might provide evidence of asymptomatic POWV infection or self-limited illness in a few persons, as reported elsewhere (11,12).

## The Study

The Vector-Borne Disease Laboratory of the Maine Medical Center Research Institute provided a free, statewide tick identification service during 1989–2013 to monitor exposure to *I. scapularis* ticks during range expansion of this invasive vector of human and animal disease. Persons submitted ticks that they had removed from themselves, family members, and pets. As of 2014, 33,332 ticks representing 14 species were identified in Maine; *I. scapularis* ticks were predominant.

During 2014, we used our tick identification service database (2) to identify persons who had removed ≥1 attached *I. scapularis* or *I. cookei* tick(s) in the previous 5 years (2009–2013). We invited these persons to participate in a serosurvey to assess past exposure to *B. burgdorferi*, *B. miyamotoi*, and POWV. Family members who attended the clinic with these persons and who reported being bitten by ticks were also invited to participate. The study was approved by Maine Medical Center Institutional Review Board (Protocol #4222). Participants provided informed consent (assent for minors) and submitted 30 mL of blood. Blood was centrifuged at 3,500 rpm for 15 min. Serum aliquots were stored at –20°C and then shipped to testing laboratories.

Serologic testing for antibodies to *B. miyamotoi* was conducted at the laboratory of one of the authors (P.J.K.). An ELISA and confirmatory Western blot assay were used

Author affiliations: Maine Medical Center Research Institute, Scarborough, Maine, USA (R.P. Smith, Jr., S.P. Elias, C.B. Lubelczyk, E.H. Lacombe, P.W. Rand); Lincoln Health, Damariscotta, Maine, USA (C.E. Cavanaugh); Colorado State University, Fort Collins, Colorado, USA (G.D. Ebel); Yale School of Public Health, New Haven, Connecticut, USA (J. Brancato, P.J. Krause); Yale School of Medicine, New Haven (H. Doyle, P.J. Krause)

DOI: <https://doi.org/10.3201/eid2504.180202>



to detect serum reactivity to *B. miyamotoi* G1pQ protein (13). For the ELISA, serum samples were diluted 1:320 and a signal  $\geq 3$  SD above the mean of 3 *B. miyamotoi*-negative serum controls was considered positive for *B. miyamotoi* antibody. Serum samples were considered *B. miyamotoi* seropositive if ELISA IgG and Western blot IgG tests yielded positive results.

Serologic evidence of exposure to *B. burgdorferi* was detected by the standard 2-step ELISA and Western blot assay in the L2 Diagnostic Laboratory at Yale School of Medicine by one of the authors (H.D.). A reactive serum was defined as one that reacted to a dilution  $\geq 1:100$ . All

borderline or reactive serum was further characterized by Western blot immunoassay. Specimens were considered positive for *B. burgdorferi* exposure if the IgG immunoblot contained  $\geq 5$  of the 10 most common *B. burgdorferi*-associated bands (14).

Serologic testing for POWV was conducted by one of the authors (G.D.E.) by using a plaque-reduction neutralization test (PRNT) and a POWV–West Nile virus (WNV) chimeric virus (POWV–premembrane–envelope [prME]/WNV) assay as described (15). The specificity of the assay was determined by cross-neutralization studies, which demonstrated that antiserum raised against

**Table 1.** Characteristics of residents bitten by blacklegged (deer) ticks (*Ixodes scapularis*) during 2009 and 2013 who participated in a serosurvey for antibodies against *Borrelia burgdorferi*, *B. miyamotoi*, and Powassan virus, Maine, USA, 2014\*

Characteristic	No. (%) residents
<b>Mailings and responses</b>	
No. persons mailed	1,253
No. persons attending a clinic	230
No. database persons	190
No. persons from families of database persons	40
<b>Clinic information</b>	
Location	
Biddeford clinics: April 23 and 26, 21 towns	31 (13.5)
Ellsworth clinics: Apr 18 and 19, 34 towns	94 (40.9)
Rockland clinics: Apr 5 and 18, 21 towns	32 (13.9)
Scarborough clinics: Apr 10 and 12, 36 towns	73 (31.7)
<b>Tick bite history and demographics of persons in database</b>	
Year tick submitted	
2009	27 (14.2)
2010	41 (21.6)
2011	47 (24.7)
2012	37 (19.5)
2013	38 (20.0)
Tick species/stage	
<i>Ixodes cookei</i> nymph	1 (0.5)
<i>Ix. scapularis</i> female	164 (86.3)
<i>Ix. scapularis</i> nymph	25 (13.2)
Tick engorgement	
Slight	82 (43.2)
Moderate	73 (38.4)
Heavy	35 (18.4)
Age, y, at time of bite	
Adults, range 19–84	168 (88.4)
Children, range 6–18	22 (11.6)
Sex	
M	88 (46.3)
F	102 (53.7)
<b>Demographics of all persons at time of clinic visit</b>	
Age, y	
Adults, range 18–90	215 (93.0)
Children, range 8–17	15 (7.0)
Race	
Not reporting	3 (1.3)
American Indian/Alaska Native	0 (0.0)
Asian	2 (0.9)
Black or African American	0 (0.0)
Hispanic or Latino	1 (0.4)
Native Hawaiian/Pacific Islander	0 (0.0)
White	224 (98.7)
Sex	
M	107 (46.5)
F	123 (53.5)

\*Database persons refers to tick-bitten persons who had submitted their ticks to a tick identification program in Maine. Family of database persons were database person family members who reported being bitten by a blacklegged tick during 2009–2013.

**Table 2.** Seropositivity of tick-bitten persons for *Borrelia burgdorferi*, *B. miyamotoi*, and Powassan virus, Maine, USA, 2014\*

Pathogen, antibody test result	No. (%) database persons, n = 190	No. (%) family of database persons, n = 40	No. (%) total, n = 230
<i>B. burgdorferi</i>			
Positive	26 (13.7)	6 (15.0)	32 (13.9)
Negative	164 (86.3)	34 (85.0)	198 (86.1)
<i>B. miyamotoi</i>			
Positive	4 (2.1)	2 (5.0)	6 (2.6)
Negative	186 (97.9)	38 (95.0)	224 (97.4)
<i>B. burgdorferi/B. miyamotoi</i>			
Positive	2 (1.1)	0	2 (0.9)
Negative	188 (98.9)	40 (100.0)	228 (99.1)
Powassan virus			
Positive	0	1 (2.5)	1 (0.4)
Negative	190 (100.0)	39 (97.5)	229 (99.6)

\*Database persons refers to tick-bitten persons who had submitted their ticks to a tick identification program in Maine. Family of database persons were database person family members who reported being bitten by a blacklegged tick during 2009–2013.

POWV efficiently neutralized chimeric POWV–prME/WNV but not WNV and that antiserum raised against WNV did not neutralize POWV–prME/WNV (15). Use of the chimeric POWV–prME/WNV assay virus enabled PRNT testing to be conducted on African green monkey kidney (Vero) cells according to standard procedures by using a 90% neutralization cutoff to be considered positive (15).

Of 230 enrolled persons, 190 were in our tick identification program database, and 40 were family members (Table 1). Among the 190 persons, 1 tick bite was from an *I. cookei* nymph, 13% of bites were from *I. scapularis* nymphs, and 86% of bites were from *I. scapularis* adult females. Engorgement of ticks ranged from slight (43%) to moderate (38%) to high (18%). Among the study population, 32 (13.9%) were seropositive for *B. burgdorferi*, 6 (2.6%) were seropositive for *B. miyamotoi*, and 2 (0.9%) were seropositive for both pathogens (Table 2). The serum of 1 person (0.4%) neutralized POWV at a titer of 1:20 and WNV at a titer of 1:10. We designated this serum as flavivirus positive. This person reported a history of neurologic illness for >1 year and a tick bite within the study year.

## Conclusions

Among residents of southern Maine with a history of *I. scapularis* tick bites, the percentage who were seropositive for *B. burgdorferi* was 5 times greater than that for *B. miyamotoi* (13.9% vs. 2.6%) and 35 times greater than the percentage of deer ticks infected with POWV (0.4%). Because our study population consisted of persons bitten by *I. scapularis* ticks (with engorgement ranging from slight to high), we expect seroprevalence to be greater in this group than in that of the general population. The *B. burgdorferi* seroprevalence of 13.9% in our study population was  $\approx$ 1.5 times higher than the seroprevalence of 9.4% reported by Krause et al. (13) in healthy residents of southern New England. In contrast, the *B. miyamotoi* seroprevalence of 2.6% was comparable to the seroprevalence of 1%–3.9% reported by Krause et al. (4,13).

Of 1,854 cases of infection with *Borrelia* spp. reported in Maine in 2017, a total of 1,848 were attributed to Lyme disease and only 6 (0.3%) were attributed to *B. miyamotoi* (1). On the basis of a seroprevalence of  $\approx$ 2% in this study and that *B. miyamotoi* might be transmitted by all tick stages, we believe that this disease is underdiagnosed in Maine (5). Our population was identified by history of tick exposure, rather than by symptoms. Our results therefore represent the relative frequency of exposure to these different agents rather than risk for illness.

Although the sensitivity and specificity of the 2-tier antibody assay for *B. burgdorferi* is better validated than those of the *B. miyamotoi* and POWV assays, the sensitivity and specificity of these assays are good (13–15). Nonetheless, our findings might represent overestimates or underestimates of actual exposure to these agents because of false-positive or false-negative results. These data provide evidence that humans are exposed to *B. burgdorferi*, *B. miyamotoi*, and POWV in Maine and help define the prevalence of human infection caused by each of these tickborne pathogens.

## Acknowledgments

We thank Thomas Courtney and his Biddeford office staff; Cheryl Liechty, Mark Eggena, and staff of Pen Bay Medical Center (Rockport, ME); Robert Pinsky and staff of Ellsworth Internal Medicine (Ellsworth, ME); and staff of the Maine Medical Center Research Institute (Scarborough, ME) for providing space and administrative support for the serosurvey clinics. We also thank the staff at the Maine Medical Center Research Institute Vector-Borne Disease Laboratory for processing samples.

This study was supported by National Institute of Health grant 1R56AI114859-01 (P.J.K.), a generous gift from the Gordon and Llura Gund Foundation (P.J.K.), and the Maine Medical Center Neuroscience Institute Research Grant Program. Study data were managed by using REDCap electronic data capture, hosted at Tufts University (<https://www.tuftsctsi.org/research-services/informatics/redcap-research-electronic-data-capture/>).

## About the Author

Dr. Smith is director of the Division of Infectious Diseases, Maine Medical Center Research Institute, Scarborough, ME; professor of medicine at Tufts University School of Medicine, Boston, MA; and principal investigator at the Vector-Borne Disease Laboratory, Maine Medical Center. His major research interests include epidemiology and ecology of emerging vectorborne diseases (Lyme disease, babesiosis, anaplasmosis, and infections with POWV and Eastern equine encephalitis virus) and clinical recognition and diagnosis of emerging vectorborne diseases.

## References

1. Maine Center for Disease Control. Reportable infectious diseases in Maine, 2017 summary; 2018. [cited 2018 Sep 18]. <https://www.maine.gov/dhhs/mecdc/infectious-disease/epi/publications/#annualreports>
2. Rand PW, Lacombe EH, Dearborn R, Cahill B, Elias S, Lubelczyk CB, et al. Passive surveillance in Maine, an area emergent for tick-borne diseases. *J Med Entomol.* 2007;44:1118–29. <http://dx.doi.org/10.1093/jmedent/44.6.1118>
3. Platonov AE, Karan LS, Kolyasnikova NM, Makhneva NA, Toporkova MG, Maleev VV, et al. Humans infected with relapsing fever spirochete *Borrelia miyamotoi*, Russia. *Emerg Infect Dis.* 2011;17:1816–23. <http://dx.doi.org/10.3201/eid1710.101474>
4. Krause PJ, Fish D, Narasimhan S, Barbour AG. *Borrelia miyamotoi* infection in nature and in humans. *Clin Microbiol Infect.* 2015;21:631–9. <http://dx.doi.org/10.1016/j.cmi.2015.02.006>
5. Han S, Lubelczyk C, Hickling GJ, Belperron AA, Bockenstedt LK, Tsao JI. Vertical transmission rates of *Borrelia miyamotoi* in *Ixodes scapularis* collected from white-tailed deer. *Ticks and Tick-borne Diseases.* 2019 Feb 26 [Epub ahead of print]. <http://dx.doi.org/10.1016/j.ttbdis.2019.02.014>
6. Smith RP, Elias SP, Borelli TJ, Missaghi B, York BJ, Kessler RA, et al. Human babesiosis, 1995–2011, Maine, USA. *Emerg Infect Dis.* 2014;20:1727–30. <http://dx.doi.org/10.3201/eid2010.130938>
7. Cavanaugh CE, Muscat PL, Telford SR III, Goethert H, Pendlebury W, Elias SP, et al. Fatal deer tick virus infection in Maine. *Clin Infect Dis.* 2017;65:1043–6. <http://dx.doi.org/10.1093/cid/cix435>
8. Smith RP Jr, Lacombe EH, Rand PW, Dearborn R. Diversity of tick species biting humans in an emerging area for Lyme disease. *Am J Public Health.* 1992;82:66–9. <http://dx.doi.org/10.2105/AJPH.82.1.66>
9. Robich RM, Lubelczyk C, Welch M, Henderson E, Smith RP Jr. Detection of Powassan virus (lineage II) from *Ixodes scapularis* collected from four counties in Maine. Poster LB-5175. Presented at: 66th Annual Meeting of the American Society of Tropical Medicine and Hygiene; Baltimore, MD, USA; November 5–9, 2017.
10. Ebel GD, Kramer LD. Short report: duration of tick attachment required for transmission of Powassan virus by deer ticks. *Am J Trop Med Hyg.* 2004;71:268–71. <http://dx.doi.org/10.4269/ajtmh.2004.71.3.0700268>
11. Frost HM, Schotthoefer AM, Thomm AM, Dupuis AP II, Kehl SC, Kramer LD, et al. Serologic evidence of Powassan virus infection in patients with suspected Lyme disease. *Emerg Infect Dis.* 2017;23:1384–8. <http://dx.doi.org/10.3201/eid2308.161971>
12. El Khoury MY, Camargo JF, White JL, Backenson BP, Dupuis AP II, Escuyer KL, et al. Potential role of deer tick virus in Powassan encephalitis cases in Lyme disease-endemic areas of New York, USA. *Emerg Infect Dis.* 2013;19:1926–33. <http://dx.doi.org/10.3201/eid1912.130903>
13. Krause PJ, Narasimhan S, Wormser GP, Barbour AG, Platonov AE, Brancato J, et al.; Tick Borne Diseases Group. *Borrelia miyamotoi* sensu lato seroreactivity and seroprevalence in the northeastern United States. *Emerg Infect Dis.* 2014;20:1183–90. <http://dx.doi.org/10.3201/eid2007.131587>
14. Centers for Disease Control and Prevention. Recommendations for test performance and interpretation from the second national conference on serologic diagnosis of Lyme disease. *MMWR Morb Mortal Wkly Rep.* 1995;44:590–1.
15. Nofchissey RA, Deardorff ER, Blevins TM, Anishchenko M, Bosco-Lauth A, Berl E, et al. Seroprevalence of Powassan virus in New England deer, 1979–2010. *Am J Trop Med Hyg.* 2013;88:1159–62. <http://dx.doi.org/10.4269/ajtmh.12-0586>

---

Address for correspondence: Susan P. Elias, Vector-Borne Disease Research Laboratory, Maine Medical Center Research Institute, 81 Research Dr, Scarborough, ME 04106, USA; email: [susan.elias@maine.edu](mailto:susan.elias@maine.edu)



# Prolonged Shedding of Zika Virus RNA in Vaginal Secretions, Nicaragua

Yaoska Reyes,<sup>1</sup> Natalie M. Bowman,<sup>1</sup>  
Sylvia Becker-Dreps, Edwing Centeno,  
Matthew H. Collins, Guei-Jiun Alice Liou,  
Filemón Bucardo

Zika virus, an arthropodborne flavivirus pathogen in humans, is unusual because it can be sexually transmitted and can be shed for prolonged periods in semen. We report viral shedding in vaginal secretions for up to 6 months, indicating the potential for sexual and vertical transmission by infected women.

Zika virus swept through the Americas beginning in 2014, with >1 million cases reported through December 2017 (Pan American Health Organization, [https://www.paho.org/hq/index.php?option=com\\_docman&task=doc\\_view&Itemid=270&gid=43297&lang=en](https://www.paho.org/hq/index.php?option=com_docman&task=doc_view&Itemid=270&gid=43297&lang=en)). Zika virus had been considered relatively benign, but during the Americas epidemic, several new pathogenic features were identified: association with severe birth defects in infants born to women infected during pregnancy, transmission by sexual contact, prolonged shedding in semen, and Guillain-Barré syndrome (1–3). Shedding in the female genitourinary tract has not been widely reported and remains a serious question because of the potential for sexual transmission or ascending fetal infection in a pregnant woman (4).

## The Study

During October 2016–November 2017, we recruited women ≥18 years of age with symptomatic Zika virus infection (any combination of rash, fever, and conjunctivitis for ≤7 days) at a public health center and Hospital Escuela Oscar Danilo Rosales Argüello in León, Nicaragua. We enrolled 5 women in a prospective cohort to characterize duration of viral shedding in the genital tract. We collected blood by venipuncture, and each woman provided urine and saliva samples.

We tested whole blood, urine, and saliva from each woman for Zika virus RNA at enrollment with quantitative reverse transcription PCR (qRT-PCR). If we detected Zika

virus RNA in any fluid, we asked women to provide blood, urine, saliva, and vaginal secretions at 7, 14, 21, 28, 60, 90, and 180 days postonset (dpo) of initial symptoms. We collected vaginal fluid using the BBL Culture Swab Collection and Transport System (Becton Dickinson, <http://www.bd.com>). Vaginal swabs were self-collected by the woman, who inserted the swab ≈5 cm into the vagina, left it in place for 5 minutes, removed it, and placed it into swab transport media. Women did not provide samples during menstruation to avoid contamination with blood. Study staff transported the swab specimens at 4°C within 3 hours to the Universidad Nacional Autónoma de Nicaragua-León microbiology laboratory, where it was stored at 4°C for up to 4 months until RNA extraction.

To elute Zika virus RNA, we incubated vaginal swabs in 140 μL of phosphate-buffered saline at room temperature for 10 min. We extracted Zika virus RNA from the eluent using the QIAamp Viral RNA Mini Kit (QIAGEN, <https://www.qiagen.com>) according to manufacturer instructions. We detected Zika virus RNA by qPCR (AgPath-ID, Applied Biosystems, <https://www.thermofisher.com>) on an ABI 7500 RT-PCR system (Applied Biosystems) using published primers that detect all known Zika virus genotypes (Zika1087/1108FAM/1163c) and those that are specific to the Asian genotype (Zika4481/4507cFAM/4552c) (5,6). We added 8 μL RNA to 12 μL 2X RT-PCR buffer, 1 μL (10 pmol) each forward and reverse primers, 1 μL (10 pmol) probe, 1 μL 25X RT-PCR enzyme mix, and 1.7 μL detection enhancer to a final volume of 25 μL. We amplified Zika virus RNA at 50°C for 30 min and 95°C for 15 min, followed by 44 cycles of 95°C for 15 s and 60°C for 1 min. We used QIAGEN AVE buffer as negative RNA purification control and DEPC water as no-template control. The positive control was cell culture supernatant of the FP/2013 strain. We defined a positive sample as a cycle threshold (C<sub>t</sub>) <38 in either reaction.

The study was approved by the institutional review boards of Universidad Nacional Autónoma de Nicaragua-León (acta no. 86, 2016) and University of North Carolina at Chapel Hill (protocol no. 16–0541). All subjects provided written informed consent at enrollment.

Five women with acute Zika virus infection provided ≥1 sample of vaginal secretions. The median age of these

Author affiliations: Universidad Nacional Autónoma de Nicaragua, León, Nicaragua (Y. Reyes, E. Centeno, F. Bucardo); University of North Carolina, Chapel Hill, North Carolina, USA (N.M. Bowman, S. Becker-Dreps, M.H. Collins, G.-J.A. Liou)

DOI: <https://doi.org/10.3201/eid2504.180977>

<sup>1</sup>These authors contributed equally to this article.

participants was 25 years (range 18–54 years). Four women were pregnant; gestational age at enrollment was 1–8 months. Infants of all 4 women were healthy at birth with no obvious congenital anomalies. The 54-year-old subject had hypertension; no other participants reported chronic medical conditions. Symptoms started a median of 4 days before enrollment (range 1–6 days).

No woman provided samples at all time points because of menstruation or lack of follow-up. Of 18 vaginal fluid specimens examined, 10 (56%) were Zika virus positive by qRT-PCR with  $\geq 1$  of the primer sets, and 3 were positive by both. Neither sample collected at 7 dpo was qRT-PCR positive, but 2/3 (67%) were Zika virus positive at 14 dpo, 3/4 (75%) at 21 dpo, 1/3 (33%) at 28 dpo, 2/2 (100%) at 60 dpo, 1/2 (50%) at 90 dpo, and 1/2 (50%) at 180 dpo. Three women had only 1 vaginal fluid sample positive for Zika virus by qRT-PCR; 1 had 2 of 3 positive; and 1 woman, who shed through 180 dpo, had Zika virus in 5 of 6 samples tested (Table).

## Conclusions

Detection of Zika virus RNA in vaginal secretions 60–180 days after the onset of symptoms is a novel observation; the presence of Zika virus in vaginal secretions for  $\leq 6$  months has crucial implications for couples planning pregnancy and for sexual transmission. In contrast to our results, in a population-based study of patients with symptomatic acute Zika virus infection followed for 6 months, only 1 of 50 women had Zika virus detectable in vaginal secretions, in a single specimen collected 3 dpo (4). The longest previously reported persistence of Zika virus RNA in vaginal secretions was 37 dpo (7); no other studies have detected Zika virus RNA in the reproductive

tract for  $>14$  dpo (8). Shedding was intermittent in several patients in our study, so 1 negative specimen does not necessarily signify viral clearance.

Most of our subjects were pregnant at enrollment; pregnant women are known to shed Zika virus in blood for up to 3 times longer than nonpregnant women, possibly because of fetal infection (9). Another study reported detection of Zika virus RNA in cervical cytology samples of 32 of 59 pregnant women compared with 18 of 109 nonpregnant women (10). Fetal tissue may act as a reservoir for long-term infection, or pregnancy-related immunosuppression might delay viral clearance. One patient in our study (A018) shed Zika virus RNA in the reproductive tract after delivery, suggesting that there may be reservoirs of viral replication in the female reproductive tract.

Our findings have implications for future pregnancies. Persistent Zika virus shedding in the reproductive tract could be a source of fetal infection. Vaginal shedding of Zika virus could result in ascending infection, as occurs with vaginal cervical herpesvirus 2 infections (11), or transmission during delivery, as seen with other viral infections such as human immunodeficiency virus and hepatitis B. Alternatively, transplacental infection may occur during viremia occurring after sexual transmission. Although the role of vaginal replication of Zika virus in fetal infection is not well characterized, mouse models suggest that fetal infection from vaginal sources of Zika virus replication can occur (12,13).

Our findings also suggest that sexual transmission of Zika virus from women to their sexual partners may be possible for up to 6 months after infection. Infectivity studies are warranted to investigate whether Zika virus shed in vagina secretions is capable of replication and infection.

**Table.** Clinical characteristics and viral shedding in 5 women with acute Zika virus infection, Nicaragua, 2016–2017\*

Characteristic	A013	A018	A020	A024	A039
Age, y	54	18	25	19	25
Duration of symptoms at enrollment, d	1	3	4	6	5
Pregnant at enrollment	No	Yes	Yes	Yes	Yes
Estimated gestational age at enrollment, mo	NA	7	7	5	1
Timing of delivery, days after symptom onset	NA	39	61	149	305
Hematocrit, %, reference range 36–45	36	32	35	37	40
Leukocytes, cells/mm <sup>3</sup> , reference range 5,000–10,000	4,230	5,410	3,510	17,430	8,050
Sexual contact in the last 3 mo†	No	Yes	Yes	Yes	Yes
Previous infection with dengue virus†	Yes	No	No	No	No
Previous infection with chikungunya virus†	Yes	Yes	No	No	Yes
Fluid Zika-positive by qRT-PCR at baseline	Saliva	Blood, urine	Blood	Urine	Blood, saliva
Vaginal fluid PCR results, C <sub>1</sub> /C <sub>2</sub> ‡ at approximate days after symptom onset					
7	NS	NS	NS	0/0	0/0
14	NS	31/0	32/33	NS	0/0
21	NS	35/0	34/36	0/0	37/0
28	33/0	0/0	NS	0/0	NS
60	NS	34/36	NS	36/0	NS
90	NS	35/0	NS	0/0	NS
180	NS	37/0	0/0	NS	NS

\*C<sub>1</sub>, cycle threshold; NA, not applicable; NS, no sample; qRT-PCR, quantitative reverse transcription PCR.

†By participant report.

‡C<sub>1</sub> refers to pan-Zika primers; C<sub>2</sub> refers to Asian-specific primers.

Sexually acquired Zika virus, mainly by male-to-female transmission, has been reported in  $\geq 18$  articles; however, there is evidence of infectious Zika virus particles in vaginal fluids (14). We lacked sufficient sample volumes to perform viral culture to distinguish between vaginal shedding of viral RNA and replication-competent virions, a limitation of our study. Only 1 report has documented the presence of culture-confirmed live Zika virus in vaginal secretions from an HIV-infected woman 3 dpo (14), and there is 1 reported case of likely female-to-male sexual transmission (15). Larger studies are needed to clarify the potential of the female reproductive tract to transmit Zika virus.

### Acknowledgments

We thank Xiomara Obando for her clinical support and Aravinda de Silva for his laboratory support for serological testing.

This work was funded by US National Institute of Allergy and Infectious Diseases grant no. R21 AI129532 and an Emerging Challenges in Biomedical Research award from the University of North Carolina at Chapel Hill.

### About the Author

Dr. Reyes is a medical microbiologist and junior faculty member at the Universidad Nacional Autónoma de Nicaragua-León, Nicaragua. Her main area of expertise is the molecular epidemiology of viruses of public health importance in Nicaragua, in particular gastrointestinal viruses and arboviruses. Dr. Bowman is an assistant professor in the Division of Infectious Diseases at the University of North Carolina School of Medicine. Her research focuses on vectorborne diseases in the Americas.

### References

- Paploski IAD, Prates APPB, Cardoso CW, Kikuti M, Silva MMO, Waller LA, et al. Time lags between exanthematous illness attributed to Zika virus, Guillain-Barré syndrome, and microcephaly, Salvador, Brazil. *Emerg Infect Dis*. 2016;22:1438–44. <http://dx.doi.org/10.3201/eid2208.160496>
- Hills SL, Russell K, Hennessey M, Williams C, Oster AM, Fischer M, et al. Transmission of Zika virus through sexual contact with travelers to areas of ongoing transmission—continental United States, 2016. *MMWR Morb Mortal Wkly Rep*. 2016;65:215–6. <http://dx.doi.org/10.15585/mmwr.mm6508e2>
- Brasil P, Pereira JP, Moreira ME, Ribeiro Nogueira RM, Damasceno L, Wakimoto M, et al. Zika virus infection in pregnant women in Rio de Janeiro. *N Engl J Med*. 2016;375:2321–34.
- Paz-Bailey G, Rosenberg ES, Doyle K, Munoz-Jordan J, Santiago GA, Klein L, et al. Persistence of Zika virus in body fluids—final report. *N Engl J Med*. 2017;379:1234–43. <http://dx.doi.org/10.1056/NEJMoa1613108>
- Lanciotti RS, Kosoy OL, Laven JJ, Velez JO, Lambert AJ, Johnson AJ, et al. Genetic and serologic properties of Zika virus associated with an epidemic, Yap State, Micronesia, 2007. *Emerg Infect Dis*. 2008;14:1232–9. <http://dx.doi.org/10.3201/eid1408.080287>
- Bingham AM, Cone M, Mock V, Heberlein-Larson L, Stanek D, Blackmore C, et al. Comparison of test results for Zika virus RNA in urine, serum, and saliva specimens from persons with travel-associated Zika virus disease—Florida, 2016. *MMWR Morb Mortal Wkly Rep*. 2016;65:475–8. <http://dx.doi.org/10.15585/mmwr.mm6518e2>
- Sánchez-Montalvá A, Pou D, Sulleiro E, Salvador F, Bocanegra C, Treviño B, et al. Zika virus dynamics in body fluids and risk of sexual transmission in a non-endemic area. *Trop Med Int Health*. 2018;23:92–100. <http://dx.doi.org/10.1111/tmi.13019>
- Murray KO, Gorchakov R, Carlson AR, Berry R, Lai L, Natrajan M, et al. Prolonged detection of Zika virus in vaginal secretions and whole blood. *Emerg Infect Dis*. 2017;23:99–101. <http://dx.doi.org/10.3201/eid2301.161394>
- Lozier MJ, Rosenberg ES, Doyle K, Adams L, Klein L, Muñoz-Jordan J, et al. Prolonged detection of Zika virus nucleic acid among symptomatic pregnant women: a cohort study. *Clin Infect Dis*. 2018;67:624–7. <http://dx.doi.org/10.1093/cid/ciy209>
- Zambrano H, Waggoner J, León K, Pinsky B, Vera K, Schettino M, et al. High incidence of Zika virus infection detected in plasma and cervical cytology specimens from pregnant women in Guayaquil, Ecuador. *Am J Reprod Immunol*. 2017;77:12630. <http://dx.doi.org/10.1111/aji.12630>
- McGee D, Smith A, Poncil S, Patterson A, Bernstein AI, Racicot K. Cervical HSV-2 infection causes cervical remodeling and increases risk for ascending infection and preterm birth. *PLoS One*. 2017;12:e0188645. <http://dx.doi.org/10.1371/journal.pone.0188645>
- Yockey LJ, Varela L, Rakib T, Khoury-Hanold W, Fink SL, Stutz B, et al. Vaginal exposure to Zika virus during pregnancy leads to fetal brain infection. *Cell*. 2016;166:1247–1256.e4. <http://dx.doi.org/10.1016/j.cell.2016.08.004>
- Winkler CW, Woods TA, Rosenke R, Scott DP, Best SM, Peterson KE. Sexual and vertical transmission of Zika virus in anti-interferon receptor-treated Rag1-deficient mice. *Sci Rep*. 2017;7:7176. <http://dx.doi.org/10.1038/s41598-017-07099-7>
- Penot P, Brichler S, Guilleminot J, Lascoux-Combe C, Taulera O, Gordien E, et al. Infectious Zika virus in vaginal secretions from an HIV-infected woman, France, August 2016. *Euro Surveill*. 2017;22:30444. <http://dx.doi.org/10.2807/1560-7917.ES.2017.22.3.30444>
- Davidson A, Slavinski S, Komoto K, Rakeman J, Weiss D. Suspected female-to-male sexual transmission of Zika virus—New York City, 2016. *MMWR Morb Mortal Wkly Rep*. 2016;65:716–7. <http://dx.doi.org/10.15585/mmwr.mm6528e2>

Address for correspondence: Natalie M. Bowman, University of North Carolina at Chapel Hill School of Medicine, CB#7030, Bioinformatics Building, 2nd Fl, 130 Mason Farm Rd, Chapel Hill, NC 27999-7030, USA; email: nbowman@med.unc.edu



# Self-Flagellation as Possible Route of Human T-Cell Lymphotropic Virus Type 1 Transmission

Alice R. Tang, Graham P. Taylor, Divya Dhasmana

We report human T-cell lymphotropic virus type 1 infection associated with self-flagellation in 10 UK residents. These persons were heterosexual men from Pakistan, India, and Iraq. One person showed seroconversion in adulthood; 1 was co-infected with hepatitis C virus. No other risk factors for bloodborne virus acquisition were identified. Onward sexual transmission has occurred.

Human T-cell lymphotropic virus type 1 (HTLV-1) is transmitted sexually, by contaminated blood products, by organ transplantation, or from mother to child. The estimate of 5–10 million global infections excludes 85% of the general population, for which testing has not occurred, and is probably an underestimate (1). Disease occurs in <10% of carriers. In 2%–6%, adult T-cell leukemia/lymphoma develops; this condition has a high mortality rate and a median survival of 8–10 months despite therapy (2). In 0.25%–3.8%, HTLV-1–associated myelopathy develops; this condition has a high morbidity rate, and many other inflammatory conditions have been reported (3).

Self-flagellation, one of several practices in which piercing of the body occurs as part of religious practice, typically involves beating the back with implements attached to ropes or chains, resulting in skin lacerations, as part of a public or private religious practice. The implements might be knives or blades, as used by the Pakistani Shia community, in which the practice is referred to as *zanjeer*, or may involve whips or rods. Alternatively, in *tatbir*, practiced predominantly by Shia communities in the Middle East, the forehead is struck with a knife.

Self-flagellation has been practiced throughout history by different religious groups, usually only by men. It is a controversial practice, even among some of the Shia Islamic and Catholic communities that continue it. It occurs worldwide but notably in Iraq, Lebanon, Afghanistan, and India. Self-flagellation has also been documented to occur

in Catholic communities (4). Although self-flagellation is widely reported by the media, there are no statistics regarding its prevalence. We report HTLV-1 infection associated with self-flagellation in 10 UK residents.

## The Study

Case-patient A was given a diagnosis of HTLV-1 infection during screening before he and his wife undertook in vitro fertilization (IVF). The patient was of Indian origin and had lived in the United Kingdom since early adulthood. He provided no history of receiving blood products, tattoos, or injection drug use. No family history was suggestive of HTLV-1 infection. In 2008, he donated blood in the United Kingdom that was tested for HTLV-1; he was seronegative. His wife of 10 years was also negative for HTLV-1. He had engaged in *zanjeer* voluntarily during childhood outside the United Kingdom and continued this practice. In the United Kingdom, the blades were soaked in a bucket containing an over-the-counter antiseptic solution, along with the blades of other men conducting the practice simultaneously. In the previous few years, his practice had also involved striking his forehead with a knife, which was subsequently shared by other men. Physical examination showed widespread scarring on his back (Figure) and the superior aspect of his scalp associated with self-flagellation.

We provide epidemiologic findings and HTLV-1 proviral load (HTLV-1 DNA copies/100 peripheral blood mononuclear cells) for this case-patient and 9 other asymptomatic HTLV-1 carriers of similar demography who reported a history of self-flagellation in Iraq, Pakistan, India, or the United Kingdom (Table). Most reported sharing of blades. Some had required sutures abroad. Eight patients had single lifetime sexual partners and no other risk factors for acquisition of bloodborne viruses. One man was co-infected with hepatitis C virus (HCV); all others were negative for HIV, hepatitis B virus, and HCV.

All 10 patients were given a diagnosis of infection with HTLV-1 through screening programs since 2013. Nine patients had strongly positive Western blot results and positive PCR results. One patient had indeterminate Western blot results and negative PCR results but an HTLV-1/2 enzyme immunoassay sample/cutoff ratio >80, which is consistent with HTLV infection (5). HTLV-1 proviral load is routinely measured in our center to monitor

---

Author affiliations: Imperial College London, London, UK (A.R. Tang, G.P. Taylor); St. Mary's Hospital, London (G.P. Taylor, D. Dhasmana)

DOI: <https://doi.org/10.3201/eid2504.180984>



**Figure.** Back of case-patient A showing scarring from self-flagellation, United Kingdom.

HTLV-1–infected carriers. Eight of the 10 patients had a low HTLV proviral load (<1%), which is typical of asymptomatic HTLV-1 infection and suggests a low risk for development of HTLV-1–associated disease. Two of the men had an HTLV-1 proviral load >1%, which is associated with a higher risk for complications.

## Conclusions

We describe 10 cases of HTLV-1 infection in men in whom the practice of self-flagellation was the only identifiable risk factor. In 1 patient, co-infection with HCV was also found. Mother-to-child transmission is difficult to exclude without testing all mothers of the case-patient, not all of whom are in the United Kingdom. However, the 1 screened mother was seronegative for HTLV-1, and case-patient A was

uninfected when he donated blood 9 years earlier, which excludes maternal transmission. It is likely that either sharing blood-stained blades, reusing personal equipment after inadequate cleaning with a shared disinfectant, contact of infected blood with open wounds, or contact with infected medical equipment resulted in HTLV-1 transmission.

Self-flagellation has also been noted to result in pneumothorax (6). In addition, Ashura, the period during which it is practiced, has been associated with increased medically reported injuries (7).

The contribution of self-flagellation to the transmission of bloodborne viruses is unknown. In the United Kingdom, clinics that screen for these viruses (antenatal and sexual health settings) do not ask about the practice and do not screen for HTLV. We propose that self-flagellation be added to the list of risk factors that result in testing for bloodborne viruses, including HTLV-1. Blood transfusion services might screen for this practice when assessing potential blood donors; for 6 men in this study, blood donation was the route of diagnosis. However, screening blood donors for HTLV-1 infection is not universal. Absence of screening, particularly in regions where self-flagellation is practiced, could accelerate dissemination of this infection. The seroprevalence of HTLV in Pakistan is unknown, but a recent study reported a prevalence of 0.19% among low-risk blood donors (8).

Four men were given diagnoses of infection with HTLV-1 as a result of Human Fertilization and Embryology Authority licensing regulations (9) on the basis of a 2015 European Union directive. The directive requires facilities storing and processing human reproductive tissue

**Table.** Characteristics of 10 case-patients infected with HTLV-1 who practice self-flagellation, United Kingdom\*

Case-patient	Age at diagnosis, y	Country of birth or ethnicity	HTLV-1 proviral load %	Route of diagnosis	HTLV-1 status		Characteristic
					of regular sexual partner	Sharing of equipment	
A	34	Indian	0.8	Screening for IVF	Negative	Yes	Blood donor in UK 9 y earlier, documented HTLV negative
B	40	Pakistan	0.7	Cord blood donor (partner)	Positive	Yes	Hepatitis C virus co-infection now cured
C	47	Pakistan	0.8	Screening for IVF	Negative	Yes	Multiple previous blood donations in Pakistan
D	25	Pakistan	0.79	UK blood donor	No current partner	Yes	Previous blood donor in Pakistan
E	37	Pakistan	2.11	Cord blood donor (partner)	Positive	Yes	None
F	31	UK, Indian	0.14	UK blood donor	Negative	Yes	None
G	22	UK, Pakistani	0.4	UK blood donor	Positive	No	Received sutures in Iraq; wife seroconverted and became pregnant
H	33	UK, Indian	2.69	UK blood donor	Negative	Yes	None
I	37	Pakistan	Undetectable	UK blood donor	Negative	No	Sample/cutoff ratio >80†
J	38	Iraq	0.001	UK blood donor	Unknown	Yes	None

\*All case-patients were male. HTLV-1, human T-cell lymphotropic virus type 1; IVF, in vitro fertilization.

†For an enzyme immunoassay assay.

to test for HTLV-1 in persons from areas of high prevalence, or with partners or parents from areas of high prevalence; that is, where infection is present in >1% of the general population or >1 case/10,000 persons for first-time blood donors (10).

Of the 7 couples for whom each partner's diagnosis was known, 4 couples were serodiscordant, despite unprotected sex over many years. Sexual transmission has been associated with proviral load and duration of the relationship (11). One study reported an ≈1% per year risk for infection among serodiscordant couples (12), although further data are needed to quantify sexual transmission risk in new relationships. During the 4 years since the first of these 10 cases was diagnosed, there has been 1 case of sexual transmission (case-patient G) (Table), and the affected woman is in her first pregnancy. She had negative results for HTLV-1 on 2 previous occasions.

All 10 men had asymptomatic HTLV-1 infections, but 2 men had a high proviral load (>1%), which places them at risk for HTLV-associated disease. In all but 1 case-patient, HTLV-1 was the only bloodborne virus detected. Within heterosexual populations, transmission of HCV is commonly associated with using contaminated injection equipment. HTLV-1 predominance in our cohort suggests the presence of a pool of monoinfected persons and spread within this international community.

All patients have been advised by medical practitioners not to share implements during self-flagellation and to encourage fellow practitioners of flagellation to be tested for bloodborne viruses. Our visits to communities in which these practices occur to discuss risk elimination, raise awareness, and promote testing facilities have been favorably received, and risk reduction has been implemented.

### Acknowledgments

We thank Meg Boothby, Ruby Christdoss, and Alec Bonington for their contributions to this study.

A.R.T. performed a literature search, collated data, and wrote the original draft of the manuscript; G.P.T. documented clinical findings, contributed to study design, and edited the manuscript for publication; and D.D. designed the study, documented clinical findings, collated data, performed a literature search, contributed to and edited the manuscript for publication.

### About the Author

Ms. Tang is a final-year medical student at Imperial College London, London, UK. Her research interests include the neurologic manifestations of infectious diseases.

### References

1. European Centre for Disease Prevention and Control. Geographical distribution of areas with a 140 high prevalence of HTLV-1 infection. Stockholm: ECDC; 2015 [cited 2018 Jun 11]. <https://ecdc.europa.eu/sites/portal/files/media/en/publications/Publications/geographical-distribution-areas-high-prevalence-HTLV1.pdf>
2. Katsuya H, Ishitsuka K, Utsunomiya A, Hanada S, Eto T, Moriuchi Y, et al.; ATL-Prognostic Index Project. Treatment and survival among 1594 patients with ATL. *Blood*. 2015;126:2570–7. <http://dx.doi.org/10.1182/blood-2015-03-632489>
3. Martin F, Taylor GP, Jacobson S. Inflammatory manifestations of HTLV-1 and their therapeutic options. *Expert Rev Clin Immunol*. 2014;10:1531–46. <http://dx.doi.org/10.1586/1744666X.2014.966690>
4. Why do some Catholics self-flagellate? BBC News Magazine. November 24, 2009 [cited 2018 Mar 7]. [http://news.bbc.co.uk/2/hi/uk\\_news/magazine/8375174.stm](http://news.bbc.co.uk/2/hi/uk_news/magazine/8375174.stm)
5. Tosswill JH, Taylor GP. Interpretation of low reactivity in the Abbott Architect rHTLV I/II assay. *Transfus Med*. 2017;28:326–30. <http://dx.doi.org/10.1111/tme.12482>
6. Akhtar A, Bhattacharjee C, Khan S, Bradley PA, Shenton AF. Flagellation: a rare cause of pneumothorax. *Emerg Med J*. 2002;19:463. <http://dx.doi.org/10.1136/emj.19.5.463>
7. Al-Lami F, Al-Fatlawi A, Bloland P, Nawwar A, Jetheer A, Hantooosh H, et al. Pattern of morbidity and mortality in Karbala hospitals during Ashura mass gathering at Karbala, Iraq, 2010. *East Mediterr Health J*. 2013;19(Suppl 2):S13–8. <http://dx.doi.org/10.26719/2013.19.Supp2.S13>
8. Niazi SK, Bhatti FA, Salamat N. Seroprevalence of human T-cell lymphotropic virus-1/2 in blood donors in northern Pakistan: implications for blood donor screening. *J Coll Physicians Surg Pak*. 2015;25:874–7.
9. Human Fertilisation and Embryology Authority. Code of practice, 8th ed. [cited 2018 Jun 11]. <https://www.hfea.gov.uk/media/2062/2017-10-02-code-of-practice-8th-edition-full-version-11th-revision-final-clean.pdf>
10. European Centre for Disease Prevention and Control. Risk assessment of HTLV-1/2 transmission 159 by tissue/cell transplantation. Part 1: epidemiological review. Stockholm; March 3, 2011 [cited 2018 Jun 11]. <https://ecdc.europa.eu/sites/portal/files/media/en/publications/Publications/120403-RA-Human-T-lymphotropic-Virus-transmission.pdf>
11. Kaplan JE, Khabbaz RF, Murphy EL, Hermansen S, Roberts C, Lal R, et al.; The Retrovirus Epidemiology Donor Study Group. Male-to-female transmission of human T-cell lymphotropic virus types I and II: association with viral load. *J Acquir Immune Defic Syndr Hum Retrovirol*. 1996;12:193–201. <http://dx.doi.org/10.1097/00042560-199606010-00014>
12. Stuver SO, Tachibana N, Okayama A, Shioiri S, Tsunetoshi Y, Tsuda K, et al. Heterosexual transmission of human T cell leukemia/lymphoma virus type I among married couples in southwestern Japan: an initial report from the Miyazaki Cohort Study. *J Infect Dis*. 1993;167:57–65. <http://dx.doi.org/10.1093/infdis/167.1.57>

Address for correspondence: Divya Dhasmana, National Centre for Human Retrovirology, Imperial College Healthcare National Health Service Trust, St. Mary's Hospital, Praed St, London W2 1NY, UK; email: [divya.dhasmana@nhs.net](mailto:divya.dhasmana@nhs.net)



# Seroprevalence of Zika and Dengue Virus Antibodies among Migrant Workers, Taiwan, 2017

Guey Chuen Perng, Tzu-Chuan Ho, Hsin-I Shih,  
Chia-Hua Lee, Pei-Wen Huang,  
Chih-Huan Chung, Nai-Ying Ko,  
Wen-Chien Ko, Yu-Wen Chien

A serosurvey of 600 workers newly arrived in Taiwan from 4 Southeast Asia countries showed that 18 (3%) were positive for Zika virus IgM; 6 (1%) fulfilled the World Health Organization criteria for laboratory-confirmed recent Zika virus infection. The incidence of Zika virus infection in Southeast Asia might be underestimated.

Approximately 690,000 migrant workers live in Taiwan; most are from 4 countries in Southeast Asia: Indonesia, the Philippines, Thailand, and Vietnam. Although these migrants are valuable to the workforce, they may also bring the risk of spreading mosquito-borne diseases. Most imported cases of Zika virus and dengue virus (DENV) infections in Taiwan come from Southeast Asia. Although screening for fever at international airports was implemented in Taiwan in 2003 (1), most Zika virus and DENV infections are inapparent and cannot be detected.

For assessing the true disease burden of flavivirus infections, seroprevalence studies are effective. Recently, several serosurveys of Zika virus infections were conducted in Africa, Oceania, Latin America, and the Caribbean (2). Although small outbreaks of Zika virus infection have been reported in Singapore, Vietnam, and Thailand (3–5), seroprevalence in Southeast Asia countries remains largely unknown. To estimate the incidence of Zika virus and DENV infections in Southeast Asia and to evaluate the risk of importing these viruses into Taiwan, we investigated seroprevalence of IgM and IgG against these viruses among newly arrived migrant workers in Taiwan.

## The Study

Migrant workers are required by law to undergo preemployment health examinations within 3 days of arrival in Taiwan. For this study, we recruited 600 newly arrived migrant workers from Indonesia, the Philippines, Thailand, and Vietnam (150 workers from each country) who received preemployment examinations at a regional hospital in Tainan, Taiwan, during June–August 2017. Workers who were >20 years of age and willing to participate were eligible without specific exclusion criteria. We used commercial ELISAs (<https://focusdx.com>) to test for IgM and IgG against dengue virus, anti-Zika virus IgG ELISA (Euroimmun AG, <https://www.euroimmun.com>) to test for IgG against Zika virus, and InBios Zika Detect IgM Capture ELISA (<http://www.inbios.com>) to test for IgM against Zika virus (because this assay seems to have higher sensitivity) (6). All tests were performed and interpreted according to manufacturers' instructions. We performed plaque reduction neutralization tests (PRNTs) on a subgroup of samples to detect neutralizing antibodies against 4 DENV serotypes (DENV-1, strain Hawaii; DENV-2, strain 16681; DENV-3, strain H87; DENV-4, strain H241) and 2 Zika virus strains (strain MR766 and 1 clinical isolate from a patient who acquired infection in Thailand). We calculated titers required to reduce dengue and Zika viral plaques by 50% (PRNT<sub>50</sub>) and 90% (PRNT<sub>90</sub>) (Appendix, <https://wwwnc.cdc.gov/EID/article/25/4/18-1449-App1.pdf>). For persons positive for Zika virus IgM, we used the interim case definition of laboratory-confirmed cases of recent Zika virus infection defined by the World Health Organization to see whether they fulfilled these criteria: IgM antibody against ZIKV positive and PRNT<sub>90</sub> for ZIKV with titer  $\geq 20$  and ZIKV PRNT<sub>90</sub> titer ratio  $\geq 4$  compared to other flaviviruses (7). This study was approved by the institutional review board of National Cheng Kung University Hospital (approval no. A-ER-106-045).

Most migrant workers were young adults 20–39 years of age (Appendix Table 1). Of the 600 workers, 18 (3.0%) were positive for Zika virus IgM and 233 (38.8%) were positive for Zika virus IgG. Only 3 (0.5%) workers had detectable DENV IgM, but 484 (80.7%) had DENV IgG. Seroprevalence of IgG against Zika virus and DENV was much lower in Vietnam than in the other 3 countries (Appendix Tables 2, 3).

Author affiliations: National Cheng Kung University College of Medicine, Tainan, Taiwan (G.C. Perng, T.-C. Ho, H.-I. Shih, C.-H. Lee, P.-W. Huang, N.-Y. Ko, W.-C. Ko, Y.-W. Chien); National Cheng Kung University Hospital, Tainan (H.-I. Shih, N.-Y. Ko, W.-C. Ko, Y.-W. Chien); Kuo General Hospital, Tainan (C.-H. Chung)

DOI: <https://doi.org/10.3201/eid2504.181449>

**Table 1.** Zika virus and DENV serostatus for 600 migrant workers from Southeast Asia, Taiwan, 2017\*

Serostatus	No. (%) workers				Total
	Zika virus IgG+		Zika virus IgG-		
	Zika virus IgM+	Zika virus IgM-	Zika virus IgM+	Zika virus IgM-	
DENV IgG+					
DENV IgM+	0	3 (0.5)	0	0	3 (0.5)
DENV IgM-	11 (1.8)	213 (35.5)	6 (1.0)	251 (41.8)	481 (80.2)
DENV IgG-					
DENV IgM+	0	0	0	0	0
DENV IgM-	0	6 (1.0)	1 (0.2)	109 (18.2)	116 (19.3)
Total	11 (1.8)	222 (37.0)	7 (1.2)	360 (60.0)	600 (100)

\*DENV, dengue virus; +, positive; -, negative.

Among all workers, 227 (37.8%) had IgG against both Zika virus and DENV, 6 (1.0%) had only Zika virus IgG, 257 (42.8%) had only DENV IgG, and 110 (18.3%) were negative for both (Table 1). All 18 workers positive for Zika virus IgM were negative for DENV IgM, indicating that false-positive results from cross-reactivity with DENV IgM or polyclonal B cell stimulation were unlikely. We found that 6 (1%) workers positive for Zika virus IgM had Zika virus PRNT<sub>90</sub> titers ≥20, and their Zika virus PRNT<sub>90</sub> titer ratio was ≥4 compared with that of 4 serotypes of DENV (Table 2; Appendix Table 4). Although we did not perform PRNT for flaviviruses other than Zika virus and DENV, we assumed that these 6 workers fulfilled the World Health Organization criteria of confirmed Zika virus infection. All 3 workers with positive DENV IgM had detectable PRNT<sub>50</sub> and PRNT<sub>90</sub> titers against single or multiple DENV serotypes; thus, the positive ELISA results for DENV IgM were considered true positives. Among 6 participants with positive Zika virus IgG but negative DENV IgG, 5 had a high PRNT<sub>50</sub> titer against Zika virus (Appendix Table 4).

**Conclusions**

Zika virus IgM persists for ≈12 weeks (8); therefore, our results suggest that 1% of the workers had confirmed Zika virus infection within 3 months before blood collection,

implying that the incidence of Zika virus infection in Southeast Asia might be severely underestimated. The median duration of viremia is 2 weeks (9); thus, some workers might have entered Taiwan during their viremia period and had the potential to spread Zika virus through *Aedes* mosquitoes in Taiwan. In addition, Zika virus can be detected in semen up to 6 months after symptom onset (10); thus, Zika virus transmission through sexual contact with these workers, who are at a sexually active age, is also possible. Furthermore, 3 female workers with confirmed Zika virus infection were of childbearing age, raising concerns about the risk for congenital infection.

The infectiousness of persons with asymptomatic Zika virus infection remains unknown. However, a recent study of DENV showed that asymptomatic persons could infect mosquitoes despite their lower average level of viremia (11). A recent modeling analysis estimated that 84% of DENV transmission is attributable to persons with inapparent infections because these persons are more mobile (12). If the infection characteristics of Zika virus are similar to those of DENV, the ability of fever screening programs at international airports and ports to prevent importation of Zika virus from migrant workers and travelers will be limited.

In this study, we may have overestimated Zika virus IgG seroprevalence (38.8%) because of false positivity resulting from cross-reactivity; nevertheless, the observed

**Table 2.** Serostatus and neutralizing antibody titers for Zika virus and DENV among 11 migrant workers from Southeast Asia who were IgM and IgG positive for Zika virus, Taiwan, 2017\*

Worker no., age, y/sex	ELISA				90% PRNT titer					
	Zika virus IgM	Zika virus IgG	DENV IgM	DENV IgG	DENV-1	DENV-2	DENV-3	DENV-4	Thai	MR766
	ID01, 21/F†	+	+	-	+	10	10	<10	<10	149
ID02, 37/F	+	+	-	+	609	1,401	40	<10	10	<10
ID03, 28/M	+	+	-	+	138	505	11	149	438	<10
VN01, 34/M†	+	+	-	+	<10	40	<10	<10	40	160
PH01, 28/F†	+	+	-	+	124	440	147	<10	1486	>2,560
PH02, 24/M†	+	+	-	+	<10	10	<10	<10	227	639
PH03, 24/F†	+	+	-	+	<10	<10	<10	<10	800	1279
TH01, 42/M	+	+	-	+	<10	40	<10	<10	107	143
TH02, 46/M†	+	+	-	+	<10	513	<10	<10	593	>2,560
TH03, 43/F	+	+	-	+	405	310	40	40	10	1,215
TH04, 31/M	+	+	-	+	>2,560	1,360	1,600	10	1,468	1,599

\*DENV, dengue virus; DENV-1-4, DENV serotypes 1-4; MR766, African Zika virus strain MR766; PRNT, plaque reduction neutralization test; Thai, 1 Zika virus isolate from a worker with an imported case acquired in Thailand.

†Six persons positive for Zika virus IgM fulfilled the criteria for laboratory confirmation of recent Zika virus infection adopted with definition according to the World Health Organization (7).

seroprevalence is comparable with that in Martinique (42.2%) and French Polynesia (49%) but lower than that in Brazil (63.3%) and Micronesia (73%) (2). It remains unclear why only very few cases of Zika virus–related microcephaly have been reported in Southeast Asia (13) despite such high seroprevalence. Possible explanations are differences in virus strains, differences in host factors, and limitations of the surveillance system (14).

To our surprise, seroprevalence of DENV IgM was lower than that of Zika virus IgM. In DENV-hyperendemic countries, children may have been exposed to multiple DENV serotypes and then acquired immunity; therefore, the incidence of dengue in adults is relatively low. Also of note, we observed much lower seroprevalences of Zika virus and DENV among workers in Taiwan from Vietnam, which may be because most of these workers originally came from rural areas in subtropical northern Vietnam, where the population density and climate are not suitable for establishing endemic transmission cycles of mosquito-borne viruses (15).

Our finding that 1% of migrant workers from Southeast Asia had laboratory-confirmed recent Zika virus infection suggests that the incidence of Zika virus infection in this region is underestimated. Given the convenience of flight for global travel, the risk for international dissemination of Zika virus by workers and travelers originating from Southeast Asia cannot be neglected.

This work was partially supported by the Taiwan National Health Research Institutes (grant no. NHRI-106A1-MRCO-0517171 to Y.-W.C.), Ministry of Health and Welfare (MOHW104-CDC-C-114-114901-H105002 to G.C.P.), Taiwan Ministry of Science and Technology (MOST 106-2320-B-006-036 to Y.-W.C. and MOST-105-2321-B-006-024 to G.C.P.), and National Cheng Kung University Hospital (NCKUH-10702020 to Y.-W.C.).

### About the Author

Dr. Perng is a professor at the Department of Microbiology and Immunology, College of Medicine, National Cheng Kung University, Tainan, Taiwan. His primary research interests are the role and fate of stem and progenitor cells during the acute stages of DENV infection, their development in asymptomatic and persistent DENV infection, and the epidemiology of Zika virus and DENV infections.

### References

1. Kuan MM, Chang FY. Airport sentinel surveillance and entry quarantine for dengue infections following a fever screening program in Taiwan. *BMC Infect Dis.* 2012;12:182. <http://dx.doi.org/10.1186/1471-2334-12-182>

2. Fritzell C, Rousset D, Adde A, Kazanji M, Van Kerkhove MD, Flamand C. Current challenges and implications for dengue, chikungunya and Zika seroprevalence studies worldwide: a scoping review. *PLoS Negl Trop Dis.* 2018;12:e0006533. <http://dx.doi.org/10.1371/journal.pntd.0006533>
3. Ho ZJM, Hapuarachchi HC, Barkham T, Chow A, Ng LC, Lee JMV, et al.; Singapore Zika Study Group. Outbreak of Zika virus infection in Singapore: an epidemiological, entomological, virological, and clinical analysis. *Lancet Infect Dis.* 2017;17:813–21. [http://dx.doi.org/10.1016/S1473-3099\(17\)30249-9](http://dx.doi.org/10.1016/S1473-3099(17)30249-9)
4. Chu DT, Ngoc VTN, Tao Y. Zika virus infection in Vietnam: current epidemic, strain origin, spreading risk, and perspective. *Eur J Clin Microbiol Infect Dis.* 2017;36:2041–2. <http://dx.doi.org/10.1007/s10096-017-3030-8>
5. Khongwichit S, Wikan N, Auewarakul P, Smith DR. Zika virus in Thailand. *Microbes Infect.* 2018;20:670–5.
6. Granger D, Hilgart H, Misner L, Christensen J, Bistodeau S, Palm J, et al. Serologic testing for Zika virus: comparison of three Zika virus IgM-screening enzyme-linked immunosorbent assays and initial laboratory experiences. *J Clin Microbiol.* 2017;55:2127–36. <http://dx.doi.org/10.1128/JCM.00580-17>
7. Ward MJ, Alger J, Berrueta M, Bock H, Buekens P, Cafferata ML, et al. Zika virus and the World Health Organization criteria for determining recent infection using plaque reduction neutralization testing. *Am J Trop Med Hyg.* 2018;99:780–2. <http://dx.doi.org/10.4269/ajtmh.18-0237>
8. Landry ML, St George K. Laboratory diagnosis of Zika virus infection. *Arch Pathol Lab Med.* 2017;141:60–7. <http://dx.doi.org/10.5858/arpa.2016-0406-SA>
9. Paz-Bailey G, Rosenberg ES, Doyle K, Munoz-Jordan J, Santiago GA, Klein L, et al. Persistence of Zika virus in body fluids—preliminary report. *N Engl J Med.* 2017;379. <http://dx.doi.org/10.1056/NEJMoa1613108>
10. Nicastrì E, Castilletti C, Liuzzi G, Iannetta M, Capobianchi MR, Ippolito G. Persistent detection of Zika virus RNA in semen for six months after symptom onset in a traveller returning from Haiti to Italy, February 2016. *Euro Surveill.* 2016;21:pii:30314. <http://dx.doi.org/10.2807/1560-7917.ES.2016.21.32.30314>
11. Duong V, Lambrechts L, Paul RE, Ly S, Lay RS, Long KC, et al. Asymptomatic humans transmit dengue virus to mosquitoes. *Proc Natl Acad Sci U S A.* 2015;112:14688–93. <http://dx.doi.org/10.1073/pnas.1508114112>
12. Ten Bosch QA, Clapham HE, Lambrechts L, Duong V, Buchy P, Althouse BM, et al. Contributions from the silent majority dominate dengue virus transmission. *PLoS Pathog.* 2018;14:e1006965. <http://dx.doi.org/10.1371/journal.ppat.1006965>
13. Wongsurawat T, Athipanyasilp N, Jenjaroenpun P, Jun SR, Kaewnapan B, Wassenaar TM, et al. Case of microcephaly after congenital infection with Asian lineage Zika virus, Thailand. *Emerg Infect Dis.* 2018;24:1758–61. <http://dx.doi.org/10.3201/eid2409.180416>
14. Lim SK, Lim JK, Yoon IK. An update on Zika virus in Asia. *Infect Chemother.* 2017;49:91–100. <http://dx.doi.org/10.3947/ic.2017.49.2.91>
15. Rabaa MA, Simmons CP, Fox A, Le MQ, Nguyen TTT, Le HY, et al. Dengue virus in sub-tropical northern and central Viet Nam: population immunity and climate shape patterns of viral invasion and maintenance. *PLoS Negl Trop Dis.* 2013;7:e2581. <http://dx.doi.org/10.1371/journal.pntd.0002581>

Address for correspondence: Yu-Wen Chien, Department of Public Health, College of Medicine, National Cheng Kung University, No. 1, University Rd, Tainan 70101, Taiwan; email: yuwenchien@mail.ncku.edu.tw



# *Anopheles sundaicus* Mosquitoes as Vector for *Plasmodium knowlesi*, Andaman and Nicobar Islands, India

Pachalil Thiruvoth Vidhya, Ittoop Pulikkottil Sunish, Anwesh Maile, Ali Khan Zahid

Using PCR and sequencing, we found *Plasmodium knowlesi* in the malaria vector *Anopheles sundaicus* mosquito collected from Katchal Island in the Andaman and Nicobar Islands, India. We cannot rule out natural transmission of this parasite to humans through this mosquito species. An in-depth investigation is needed to prevent disease outbreaks.

*Plasmodium knowlesi* is a simian malaria parasite and is recognized as the fifth human malaria parasite (1). Natural infection in humans by *P. knowlesi* was first reported in Malaysian Borneo (2). Mosquitoes belonging to Leucosphyrus group were reported as vectors of *P. knowlesi* in Southeast Asia countries. Among this group, *Anopheles latens* mosquitoes were identified as a vector of *P. knowlesi* in Malaysian Borneo (3). Similar vectors have been reported elsewhere, including *An. dirus* mosquitoes in Vietnam (4); *An. balabacensis* mosquitoes in Sabah, Malaysia (5); *An. hackeri* mosquitoes in Malaya (now Peninsular Malaysia) (6); and *An. cracens* mosquitoes in Kuala Lipis and *An. introlatus* mosquitoes in Selangor, Malaysia (7). Experimental studies on the H strain of *P. knowlesi* showed that *An. balabacensis* mosquitoes were the most competent vector, followed by *An. stephensi*, *An. maculatus*, and *An. freeborni* mosquitoes (8). However, no studies record isolation of *P. knowlesi* from *An. sundaicus* mosquitoes of the Pyretophorus series. This anopheline species is a known vector of malaria parasites in the Andaman and Nicobar Islands, India.

In 1980, a simian malaria and *P. vivax*-like parasite, *P. cynomolgi*, was isolated from *An. sundaicus* mosquitoes and from a subspecies of macaque, *Macaca umbrosus*, at Great Nicobar (9). In a later study, researchers sequenced 445 archival blood samples from human malaria cases from the Andaman and Nicobar Islands and found 11.9% (53) were positive for *P. knowlesi*, both mono- and

co-infections. (10). Investigators also suspected earlier research might have mistakenly identified *P. knowlesi* as *P. cynomolgi* because the species are difficult to distinguish by light microscopy. In view of these findings, we conducted an entomologic and parasitologic survey in selected islands of Nicobar district to identify the role of anophelines in the transmission of *P. knowlesi*.

## The Study

The Nicobar district is an endemic area for malaria; annual parasitic incidence was 7.04–16.07/1,000 population/year during 2013–2017. In the Nicobar district, Katchal and Great Nicobar Islands are known for high malaria case counts and for macaques that frequently come close to human habitations. Long-tailed macaques, *Macaca fascicularis umbrosa*, are the only nonhuman primates found on Nicobar Islands (11). As yet, the malaria surveillance program has not reported human infection with *P. knowlesi* in the district.

During 2016–2018, we selected 3 villages on Katchal Island (Mildera, Japan Tickrey, and Meenakshi Ram Nagar) and 3 villages on Great Nicobar Island (Rajiv Nagar, Govindnagar, and Sastrinagar). Our selection was based on high numbers of malaria cases and prevalence of macaques. Katchal Island, population 2,658, has a hilly terrain with an area of 146.5 km<sup>2</sup> and has dense tropical rain forest (Indian Census data, <http://www.censusindia.gov.in/2011>). Great Nicobar, population 3,500, has both plains and hilly terrain and is the largest island of Nicobar district at 921 km<sup>2</sup>.

We collected adult mosquitoes by night landing and light trap collections for 8 nights in each village from 5:30 PM through 5:30 AM. We also collected adult mosquitoes by indoor resting collection from 5:00 AM to 8:00 AM. We conducted night landing collections using human, bovine, and caprine baits. We conducted resting collections with oral aspirators in and around 16 sites in each village, including human shelters and animal sheds. We installed 8 light traps in each village. We used standard taxonomic keys for morphological identification (12). We collected blood slides of microscopically confirmed *P. falciparum* and *P. vivax* (n = 55) from the local primary health centers and conducted

Author affiliation: ICMR Regional Medical Research Centre, Port Blair, Andaman and Nicobar Islands, India

DOI: <https://doi.org/10.3201/eid2504.181668>

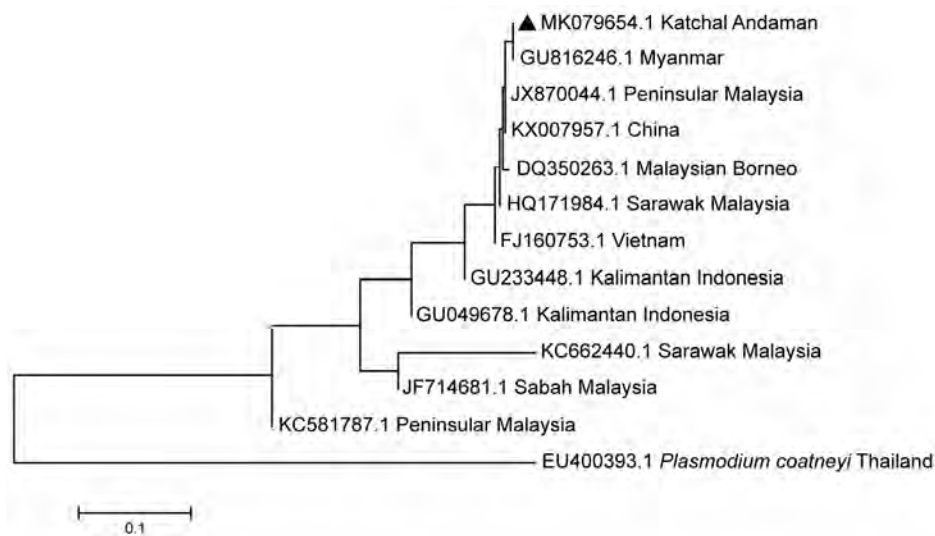


**Figure 1.** Phylogenetic relationship of *Plasmodium knowlesi* from the Andaman and Nicobar Islands, India, to other strains from Southeast Asia countries, inferred by using the neighbor-joining method. Isolates are identified by GenBank accession number and location; *Plasmodium coatneyi* is used as outgroup. Triangle indicates sequence of *P. knowlesi* isolated in this study (accession no. MK079654) that shares a similar clade with a Myanmar sequence (accession no. GU816246). Isolates from Peninsular Malaysia (accession no. JX870044) and China (accession no. KX007957) are also closer to the Andaman isolate. Scale bar indicates nucleotide substitutions per site.

assays for molecular confirmation, including for *P. knowlesi*. In addition, we tested filter paper blood spots (n = 106) that were collected through active fever surveillance and were positive by bivalent rapid diagnostic tests.

We tested 54 pools, 10 mosquitoes per pool, including 35 pools of *An. sundaicus* mosquitoes, 18 pools of *An. maculatus* mosquitoes, and 1 pool with 2 specimens of *An. barbirostris* mosquitoes. We extracted DNA from each pool of anophelines, and from slides and filter paper blood spots, using GeNei Whole Blood DNA Extraction Kit solution (Genie, <http://geneilabs.com>), according to the manufacturer's instructions. We screened the DNA extracts for all 5 malaria parasites by nested PCR, as suggested by Singh et al. (13), amplifying the 18S small subunit ribosomal RNA of *P. knowlesi*. We used Pmk8 and Pmk9 primers to amplify *P. knowlesi*. We used rPLU1 and rPLU5 primers for the first step and other primers, including rFAL1 and rFAL2, rVIV1 and rVIV2, rOVA1 and rOVA2, rMAL1 and rMAL2, for the second step of nested PCR. We obtained positive control *P. knowlesi* blood spots from the National Institute of Malaria Research (New Delhi, India).

Samples were visualized by agarose gel electrophoresis in 2% agarose and we excised bands of 153 bp from the positive samples, then purified these using QIAquick Gel Extraction Kit (QIAGEN, <http://www.qiagen.com>), according to the manufacturer's protocol. We performed sequencing on an ABI 3730 DNA Analyzer (Applied

Biosystems, <https://www.thermofisher.com>). We checked sequence identity with reference sequences obtained from the NCBI database and submitted processed sequences to GenBank (accession no. MK079654). We constructed the phylogenetic tree with closely similar sequences using the neighbor-joining method in MEGA7 (<https://www.megasoftware.net>) (Figure 1).

Of 855 mosquitoes captured, 532 were anophelines and 323 were culicines. Among anophelines, the *An. sundaicus* mosquito was the predominant species collected, followed by *An. maculatus* and *An. barbirostris* mosquitoes (Table). One pool of 10 of *An. sundaicus* mosquitoes collected from Mildera village on Katchal Island was found positive for *P. knowlesi* by PCR and sequencing. Five blood slide samples, 1 identified as *P. vivax* and 4 identified as co-infection with *P. falciparum* and *P. vivax* by microscopy, were found positive for *P. knowlesi* by PCR with primers Pmk8 and Pmk9 (Figure 2, panel A), but no sequences were obtained. Subsequently, these samples showed no amplification with a different set of primers, PKF1140 and PKR1550 (14) (Figure 2, panel B). The false amplification may be due to cross-hybridization of primers Pmk8 and Pmk9 with *P. vivax* DNA. Therefore, we could not conclude that those samples were positive for *P. knowlesi*. We found *P. knowlesi* DNA in *An. sundaicus* mosquitoes and confirmed our findings by nucleotide sequence analysis. The nucleotide sequences obtained from our study resembled *P. knowlesi*

**Table.** Adult mosquitoes collected using various methods, Andaman and Nicobar Islands, India

Serial no.	Mosquito species	Light trap		Night landing, human bait		Night landing, animal bait		Total
		Indoor	Outdoor	Indoor	Outdoor	Caprine	Bovine	
1	<i>Anopheles sundaicus</i>	10	52	0	15	150	123	350
2	<i>An. maculatus</i>	0	0	0	10	70	100	180
3	<i>An. barbirostris</i>	2	0	0	0	0	0	2
4	<i>Armigeres</i> sp.	0	2	10	25	15	7	59
5	<i>Culex</i> sp.	2	264	0	0	0	0	264

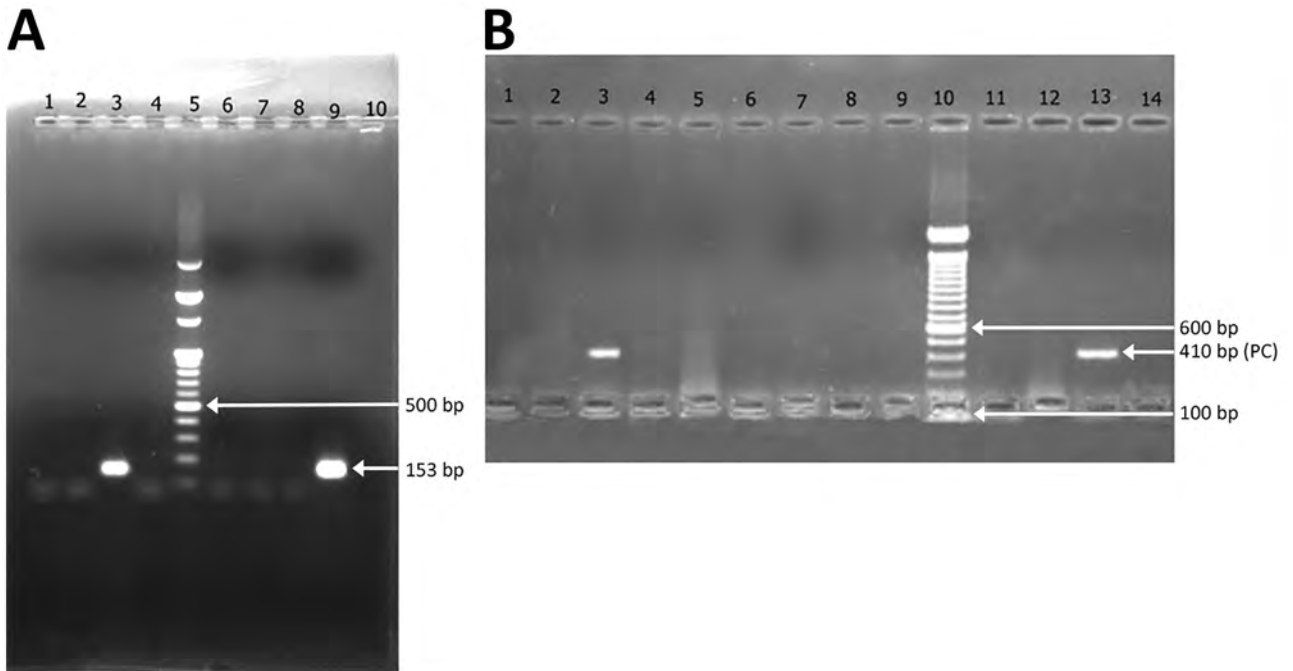


**Figure 2.** Agarose gel (2%) electrophoresis of nested PCR products of amplified *Plasmodium knowlesi* DNA sequences taken from mosquito samples (10 mosquitoes per pool) from Andaman and Nicobar Islands. A) Analysis of PCR products amplified with Pmk8 and Pmk9 primers. Lanes 1–4, pools of *Anopheles sundaicus* mosquitoes; lane 5, size marker DNA (100-bp DNA ladder); lanes 6 and 7, *An. maculatus* mosquito pools; lane 8, *An. barbirostris* mosquito pool (2 mosquitoes); lane 9, positive control; lane 10, negative control. Arrows indicate positive sample from the *An. sundaicus* mosquito pool in lane 3, 500 bp marker in DNA ladder of lane 5, and positive control in lane 9. B) Analysis of nested PCR products amplified with PKF1140 and PKR1550 primers. Lanes 1–5, *An. sundaicus* mosquito pools; lanes 6–9, *An. maculatus* mosquito pools; lane 10, size marker DNA (100-bp DNA ladder); lane 11, *An. maculatus* mosquito pool; lane 12, *An. barbirostris* mosquito pool; lane 13, positive control; lane 14, negative control. Arrows indicate *An. sundaicus* mosquito pool with positive band at 410 bp in lane 3, 600-bp marker in DNA ladder in lane 10, and positive control of 410 bp in lane 13. PC, positive control.

reference sequences retrieved from GenBank (accession nos. GU816246, JX870044, and KX007957). We cannot conclude that *An. sundaicus* mosquitoes are the vector of *P. knowlesi*, but our results suggest the possibility of *An. sundaicus* mosquitoes for transmission of this parasite and indicated that further in-depth investigation is warranted.

### Conclusions

Because *P. knowlesi* is an emerging and potentially lethal malarial parasite, care and safety need to be taken to prevent the spread of infection. As van Hellemond et al. (15) suggest, synergistic use of *P. knowlesi*-specific rapid diagnostic tests and microscopy could identify *P. knowlesi* in health centers in inaccessible areas. An extensive parasitologic survey in humans and macaques could provide a more precise picture on the prevalence of *P. knowlesi* in the Andaman and Nicobar Islands.

### Acknowledgments

We thank the director of the ICMR Regional Medical Research Centre, Port Blair, Andaman and Nicobar Islands, India, for providing facilities. We thank the National Institute of Malaria

Research, New Delhi, India, for providing positive blood spots of *Plasmodium knowlesi*. We also thank medical officers and malaria inspectors of the Directorate of Health Services, Port Blair, for providing human blood filter paper spots collected through active fever surveillance in the islands.

### About the Author

Dr. Vidhya is a research scholar working in the Division of Medical Entomology, ICMR Regional Medical Research Centre, Port Blair, Andaman and Nicobar Islands, India. Her areas of interest are vector biology, ecology, and molecular characterization.

### References

- White NJ. *Plasmodium knowlesi*: the fifth human malaria parasite. Clin Infect Dis. 2008;46:172–3. <http://dx.doi.org/10.1086/524889>
- Singh B, Sung LK, Matusop A, Radhakrishnan A, Shamsul SSG, Cox-Singh J, et al. A large focus of naturally acquired *Plasmodium knowlesi* infections in human beings. Lancet. 2004;363:1017–24. [http://dx.doi.org/10.1016/S0140-6736\(04\)15836-4](http://dx.doi.org/10.1016/S0140-6736(04)15836-4)
- Vythilingam I, Tan CH, Asmad M, Chan ST, Lee KS, Singh B. Natural transmission of *Plasmodium knowlesi* to humans by *Anopheles latens* in Sarawak, Malaysia. Trans R Soc Trop Med Hyg. 2006;100:1087–8. <http://dx.doi.org/10.1016/j.trstmh.2006.02.006>



4. Marchand RP, Culleton R, Maeno Y, Quang NT, Nakazawa S. Co-infections of *Plasmodium knowlesi*, *P. falciparum*, and *P. vivax* among humans and *Anopheles dirus* mosquitoes, southern Vietnam. *Emerg Infect Dis*. 2011;17:1232–9. <http://dx.doi.org/10.3201/eid1707.101551>
5. Wong ML, Chua TH, Leong CS, Khaw LT, Fornace K, Wan-Sulaiman WY, et al. Seasonal and spatial dynamics of the primary vector of *Plasmodium knowlesi* within a major transmission focus in Sabah, Malaysia. *PLoS Negl Trop Dis*. 2015;9:e0004135. <http://dx.doi.org/10.1371/journal.pntd.0004135>
6. Wharton RH, Eyles DE. *Anopheles hackeri*, a vector of *Plasmodium knowlesi* in Malaya. *Science*. 1961;134:279–80. <http://dx.doi.org/10.1126/science.134.3474.279>
7. Vythilingam I, Lim YAL, Venugopalan B, Ngui R, Leong CS, Wong ML, et al. *Plasmodium knowlesi* malaria an emerging public health problem in Hulu Selangor, Selangor, Malaysia (2009–2013): epidemiologic and entomologic analysis. *Parasit Vectors*. 2014;7:436. <http://dx.doi.org/10.1186/1756-3305-7-436>
8. Collins WE, Aikawa M. *Plasmodia* of nonhuman primates. In: Kreier JP, editor. *Parasitic protozoa*, vol. 5. New York: Academic Press; 1993. p. 105e33.
9. Kalra NL. Emergence of malaria zoonosis of simian origin as natural phenomenon in Greater Nicobars, Andaman & Nicobar islands—a preliminary note. *J Commun Dis*. 1980;12:49–54.
10. Tyagi RK, Das MK, Singh SS, Sharma YD. Discordance in drug resistance-associated mutation patterns in marker genes of *Plasmodium falciparum* and *Plasmodium knowlesi* during coinfections. *J Antimicrob Chemother*. 2013;68:1081–8. <http://dx.doi.org/10.1093/jac/dks508>
11. Sivakumar K. Impact of the tsunami (December 2004) on the long tailed macaque of Nicobar Islands, India. *Hystric It J Mamm*. 2010;21:35–42. <https://doi.org/10.4404/hystric-21.1-4484>
12. Christophers SR. The fauna of British India, including Ceylon and Burma. Diptera, Vol. 4, family Culicidae, tribe Anophelini. Sewell BBS, ed. London: Taylor and Francis; 1933.
13. Singh B, Bobogare A, Cox-Singh J, Snounou G, Abdullah MS, Rahman HA. A genus- and species-specific nested polymerase chain reaction malaria detection assay for epidemiologic studies. *Am J Trop Med Hyg*. 1999;60:687–92. <http://dx.doi.org/10.4269/ajtmh.1999.60.687>
14. Imwong M, Tanomsing N, Pukrittayakamee S, Day NP, White NJ, Snounou G. Spurious amplification of a *Plasmodium vivax* small-subunit RNA gene by use of primers currently used to detect *P. knowlesi*. *J Clin Microbiol*. 2009;47:4173–5. <http://dx.doi.org/10.1128/JCM.00811-09>
15. van Hellemond JJ, Rutten M, Koelewijn R, Zeeman AM, Verweij JJ, Wismans PJ, et al. Human *Plasmodium knowlesi* infection detected by rapid diagnostic tests for malaria. *Emerg Infect Dis*. 2009;15:1478–80. <http://dx.doi.org/10.3201/eid1509.090358>

Address for correspondence: Ittoop Pulikkottil Sunish, ICMR Regional Medical Research Centre, Division of Medical Entomology, Post Bag No 13, Port Blair 744 101, Andaman and Nicobar Islands, India; email: [sunish67@gmail.com](mailto:sunish67@gmail.com)

# Discover the world...



[www.cdc.gov/travel](http://www.cdc.gov/travel)

Visit the CDC Travelers' Health website for up-to-date information on global disease activity and international travel health recommendations.

Department of Health and Human Services  
Centers for Disease Control and Prevention

## Prior Vaccination and Effectiveness of Communication Strategies Used to Describe Infectious Diseases

Thomas S. Valley, Aaron M. Scherer, Megan Knaus, Brian J. Zikmund-Fisher, Enny Das, Angela Fagerlin

Author affiliations: University of Michigan, Ann Arbor, Michigan, USA (T.S. Valley, A.M. Scherer, M. Knaus, B.J. Zikmund-Fisher); University of Iowa, Iowa City, Iowa, USA (A.M. Scherer); Radboud University Nijmegen, Nijmegen, the Netherlands (E. Das); University of Utah School of Medicine, Salt Lake City, Utah, USA (A. Fagerlin); Informatics Decision-Enhancement and Analytic Sciences (IDEAS 2.0) Center for Innovation, Salt Lake City (A. Fagerlin)

DOI: <https://doi.org/10.3201/eid2504.171408>

We tested the effect of prior vaccination on response to communication strategies in a hypothetical news article about an influenza pandemic. Vaccinated were more likely than nonvaccinated participants to plan future vaccination, and future vaccination intent was greater with certain communication strategies. Using these findings to target communication may increase vaccination rates.

Vaccination rates for influenza remain surprisingly low (1). Despite goals to vaccinate 75% of high-risk Europeans by 2010, <50% had been vaccinated in 2013 (2). The reluctance of at-risk persons to receive vaccinations highlights the challenge of broadly vaccinating the general public.

Improving communication strategies that clinicians and healthcare organizations use to increase vaccination rates is cost-effective (3). Yet randomized trials to improve influenza vaccination rates by improving physicians' communication skills (4) or by using various public health messages (5) have not succeeded. Several studies have examined the effect of various communication strategies to improve vaccination rates for influenza (6–9). However, the greatest predictor of future vaccination is prior vaccination, and these studies assessed participants in aggregate (6). Guided by the Health Belief Model (10), we investigated whether experiences with prior vaccination might affect the effectiveness of certain communication strategies (Appendix, <https://wwwnc.cdc.gov/EID/article/25/4/17-1408-App1.pdf>).

Our study is a secondary analysis of a randomized experiment to test communication strategies and their effects on influenza immunization (6–9). After our study was

deemed exempt from review by the University of Michigan Institutional Review Board, we recruited a stratified random sample of adults from a panel of Internet users through Survey Sampling International (<https://www.surveysampling.com>) (Appendix). We recruited participants from 11 countries: Finland (n = 1,554), Norway (n = 764), Sweden (n = 1,539), Hungary (n = 998), Poland (n = 1,509), Spain (n = 1,604), Italy (n = 1,509), Germany (n = 1,546), the Netherlands (n = 1,938), the United Kingdom (n = 1,762), and the United States (n = 1,787).

Participants read a hypothetical news article that described the spread of influenza in their country. The article directly quoted hypothetical health experts and contained information about the influenza virus, its potential symptoms, and a vaccine in development. Articles were cross-randomized to provide participants with 5 varying communication strategies: 1) graphics (heat map, DOT map, picto-trendline) (6); 2) case severity (severe, typical, both) (9); confident language (scientific certainty, uncertainty, uncertainty with normalizing language) (7); 4) influenza label (H1N3 influenza, horse flu, Yarraman flu) (8); and 5) metaphor use (infectious disease, war, gardening). The Appendix contains more information about communication strategies. Each news article contained all 5 communication strategies. The experiment used a 3 × 3 × 3 × 3 between-subjects factorial design in which participants were randomly assigned to each communication strategy. After reading the newspaper article, participants were asked their vaccination status (whether they had received an influenza vaccination within the past 2 years) and intent to get vaccinated in the future (defined by a discrete visual analog scale ranging from 1 [“Definitely would not get a vaccination”] to 7 [“Definitely would get a vaccination”]).

We were interested in the main effect for an individual communication strategy depending on a participant's prior vaccination status. For each communication strategy, we conducted separate ordinal logistic regression models and included an interaction term of prior vaccination and the communication strategy of interest for each model. The dependent variable was intent to get vaccinated. As covariates, we included the participant's age, sex, and marital status and whether the participant was a healthcare worker. We estimated robust SEs with clustering by the participant's country of residence.

Of 20,138 participants, 16,401 (81%) completed the survey; of these, 4,999 (30%) had received an influenza vaccination within the previous 2 years and 11,402 (70%) had not. The average age was 51.4 (SD ± 16.9) for vaccinated and 44.9 (SD ± 15.4) for nonvaccinated participants. Approximately 44.6% of vaccinated and 52.1% of nonvaccinated participants were female (Appendix Table 1).

**Table.** Effect of communication strategies on intent for future influenza vaccination, by influenza vaccination status

Strategy	Vaccination over previous 2 y, adjusted odds ratio (95% CI)*				p value for interaction†
	No	p value	Yes	p value	
Graph type					<0.001
Picto-trendline	Referent		Referent		
DOT map	1.1 (0.9–1.2)	0.06	1.0 (0.9–1.1)	0.92	
Heat map	1.1 (1.0–1.2)	0.01	1.1 (0.9–1.2)	0.08	
Case severity					<0.001
Both	Referent		Referent		
Typical	1.0 (0.9–1.1)	0.78	0.9 (0.8–1.0)	0.07	
Severe	1.1 (1.0–1.3)	0.02	1.1 (0.9–1.2)	0.43	
Confident language					<0.001
Uncertainty with normalizing language	Referent		Referent		
Uncertainty	1.0 (0.9–1.1)	0.97	1.1 (0.9–1.2)	0.12	
Scientific certainty	1.2 (1.1–1.3)	<0.001	1.3 (1.1–1.4)	<0.001	
Influenza label					<0.001
Horse	Referent		Referent		
H11N3	1.0 (0.9–1.1)	0.62	1.4 (1.1–1.7)	0.001	
Yarraman	1.1 (1.0–1.2)	0.001	1.2 (1.1–1.4)	0.001	
Metaphor use					<0.001
Infectious disease	Referent		Referent		
War	1.0 (0.9–1.1)	0.78	1.0 (0.9–1.1)	0.60	
Gardening	1.0 (0.9–1.1)	0.75	1.0 (0.9–1.1)	0.41	

\*Multivariable ordinal logistic regression adjusted for participant age, sex, marital status, occupation as healthcare worker, and country of residence.

†Interaction between vaccination status and communication strategy.

Our results showed that previously vaccinated participants were more likely than nonvaccinated participants to plan for future vaccinations (adjusted odds ratio 5.8, 95% CI 4.8–7.0;  $p < 0.001$ ). We found significant interaction effects between prior vaccination and each communication strategy ( $p < 0.001$  for each strategy) (Table; Appendix Table 2). However, this effect varied according to the type of communication strategy. Nonvaccinated participants reported greater intent for future vaccination when heat maps, severe cases, confident language, or exotic influenza labels were used (Table). Vaccinated participants reported greater intent for future vaccination when confident language or scientific/exotic influenza labels were used (Table). The use of metaphors had no effect on either group.

This study should be interpreted in the context of certain limitations. For instance, participants reviewed a hypothetical news article, which may be different than direct communication with a healthcare provider or reading an actual article during a pandemic.

Certain communication strategies, such as use of confident language or an exotic influenza label, were effective regardless of prior vaccination status. Yet use of a scientific influenza label was more effective than use of an exotic influenza label among previously vaccinated participants. Other communication strategies, such as use of heat maps or describing severe cases, were effective among nonvaccinated but not previously vaccinated participants. Vaccination rates for influenza may be improved by targeting healthcare communication based on prior vaccination experiences (11,12).

## Acknowledgments

This work was supported by the European Union's Seventh Framework Programme for research, technological development and demonstration under grant agreement #278763 (to A.F.) and the National Institutes of Health, K23HL140165 (to T.S.V.). Funding sources had no role in the study conception, design, conduct, analysis, or manuscript construction.

## About the Author

Dr. Valley is an assistant professor in the Division of Pulmonary and Critical Care Medicine at the University of Michigan. His research focuses on improving clinical decision making in pulmonary disease and critical care.

## References

1. European Centres for Disease Prevention and Control. Seasonal influenza vaccination in Europe—overview of vaccination recommendations and coverage rates in the EU Member States for the 2012–13 influenza season [cited 2017 Aug 2]. <http://dx.doi.org/10.2900/693898>
2. World Health Organization. Influenza (seasonal) fact sheet. Geneva: The Organization; 2014.
3. Goldstein S, MacDonald NE, Guirguis S; SAGE Working Group on Vaccine Hesitancy. Health communication and vaccine hesitancy. *Vaccine*. 2015;33:4212–4. <http://dx.doi.org/10.1016/j.vaccine.2015.04.042>
4. Henrikson NB, Opel DJ, Grothaus L, Nelson J, Scrol A, Dunn J, et al. Physician communication training and parental vaccine hesitancy: a randomized trial. *Pediatrics*. 2015;136:70–9. <http://dx.doi.org/10.1542/peds.2014-3199>
5. Frew PM, Kriss JL, Chamberlain AT, Malik F, Chung Y, Cortés M, et al. A randomized trial of maternal influenza immunization decision-making: a test of persuasive messaging



- models. *Hum Vaccin Immunother*. 2016;12:1989–96. <http://dx.doi.org/10.1080/21645515.2016.1199309>
6. Fagerlin A, Valley TS, Scherer AM, Knaus M, Das E, Zikmund-Fisher BJ. Communicating infectious disease prevalence through graphics: results from an international survey. *Vaccine*. 2017;35:4041–7. <http://dx.doi.org/10.1016/j.vaccine.2017.05.048>
  7. Han PKJ, Zikmund-Fisher BJ, Duarte CW, Knaus M, Black A, Scherer AM, et al. Communication of scientific uncertainty about a novel pandemic health threat: ambiguity aversion and its mechanisms. *J Health Commun*. 2018;23:435–44. <http://dx.doi.org/10.1080/10810730.2018.1461961>
  8. Scherer AM, Knaus M, Zikmund-Fisher BJ, Das E, Fagerlin A. Effects of influenza strain label on worry and behavioral intentions. *Emerg Infect Dis*. 2017;23:1425–6. <http://dx.doi.org/10.3201/eid2308.170364>
  9. Zikmund-Fisher BJ, Scherer AM, Knaus M, Das E, Fagerlin A. Discussion of average versus extreme case severity in pandemic risk communications. *Emerg Infect Dis*. 2017;23:706–8. <http://dx.doi.org/10.3201/eid2304.161600>
  10. Champion V, Skinner C. The health belief model. In: Glanz K, Rimer BK, Viswanath K, editors. *Health behavior and health education: theory, research, and practice*, 4th ed. San Francisco: Jossey-Bass; 2008. p. 45–67.
  11. Noar SM, Benac CN, Harris MS. Does tailoring matter? Meta-analytic review of tailored print health behavior change interventions. *Psychol Bull*. 2007;133:673–93. <http://dx.doi.org/10.1037/0033-2909.133.4.673>
  12. Cappella JN. Integrating message effects and behavior change theories: organizing comments and unanswered questions. *Journal of Communication*. 2006;56(suppl1):S265–79.

Address for correspondence: Thomas S. Valley, University of Michigan, Division of Pulmonary and Critical Care Medicine, 2800 Plymouth Rd, Bldg 16-G028W, Ann Arbor, MI 48109, USA; email: valleyt@umich.edu

## Peripheral Plasma and Semen Cytokine Response to Zika Virus in Humans

Jean-Michel Mansuy,<sup>1</sup> Hicham El Costa,<sup>1</sup> Jordi Gouilly, Catherine Mengelle, Christophe Pasquier, Guillaume Martin-Blondel, Jacques Izopet, Nabila Jabrane-Ferrat

Author affiliations: Centre Hospitalier Universitaire de Toulouse, Toulouse, France (J.-M. Mansuy, H. El Costa, C. Mengelle, C. Pasquier, G. Martin-Blondel, J. Izopet); INSERM U1043-CNRS UMR5282 Université Toulouse III, Toulouse (H. El Costa, J. Gouilly, G. Martin-Blondel, J. Izopet, N. Jabrane-Ferrat)

DOI: <https://doi.org/10.3201/eid2504.171886>

<sup>1</sup>These authors contributed equally to this article.

We assessed Zika virus RNA and select cytokine levels in semen, blood, and plasma samples from an infected patient in South America. Viral RNA was detected in semen >2 months after viremia clearance; cytokine profiles differed in semen and plasma. After viremia, Zika virus appears to become compartmentalized in the male reproductive tract.

Before the 2015–2016 outbreak, Zika virus infection had been associated with only mild symptoms. However, the outbreak revealed infection could cause severe clinical manifestations, particularly for fetuses and newborns (1). Furthermore, detection of replicative virus in semen and sexual transmission of the infection resulted in a paradigm shift in Zika virus virology (2,3). Several animal models were developed to study these phenomena, and studies revealed that Zika virus persistence within the male reproductive tract (MRT) results in diminished testosterone and oligospermia (4). However, because of complex ethics considerations, the consequences of infection on the MRT remain poorly understood (5).

To characterize infection in the MRT further, we conducted a longitudinal 6-month study examining Zika virus load and immunologic profile in blood, plasma, and semen in 1 man. The study patient was a 32-year-old immunocompetent white man with an asymptomatic Zika virus infection acquired in South America in January 2016; the control was a healthy 40-year-old white man without risk factors for acute or chronic infection who lived in the same area. We evaluated the concentrations of a select panel of cytokines, including innate immune mediators (interferon [IFN]- $\gamma$ , interleukin [IL]-15, IFN- $\beta$ ); inflammatory factors (IL-6, IL-18, soluble intercellular adhesion molecule 1 [sICAM-1]); chemokines (CC-motif chemokine ligand [CCL] 3, CCL-4, CXC-motif chemokine ligand [CXCL] 1, CXCL-8, CXCL-10); hematopoietic factors (granulocyte colony-stimulating factor [G-CSF], granulocyte-macrophage colony-stimulating factor); the angiogenic factor vascular endothelial growth factor A (VEGF-A); and proteases (matrix metalloproteinase [MMP]-2, MMP-9). We quantified cytokines using ProcartaPlex Multiplex Assay (ebioscience, <https://www.thermofisher.com>).

At admission, the patient had moderate fever, maculopapular rash, myalgia, and arthralgia and recovered within a few days. He was HIV negative; dengue and chikungunya virus infections were ruled out using ELISA Diapro (Diagnostic Bioprobes Srl, <https://www.diapro.it>) and RealStar Dengue and Chikungunya RT-PCR Kit 2.0 (Altona Diagnostics, <https://www.altona-diagnostics.com>). The patient did not experience other genital or urinary tract infections during the study.

Two days after symptom onset, viral RNA was higher in semen ( $1.04 \times 10^5$  copies/mL) than in blood ( $9.4 \times 10^3$  copies/mL); RNA was detectable for up to 100 days in blood

and 168 days in semen (Figure). Soluble factors secreted in response to infection could be stratified into 3 profiles. The first profile was a surge of proinflammatory cytokines in semen (IL-6, IFN- $\gamma$ , CCL-3, CCL-4) and plasma (CCL-3, CXCL-10, VEGF-A) at early stages of infection. These cytokines returned to basal levels over time. The second profile (mainly observed in semen) involved decreased CXCL-1, CXCL-8, CXCL-10, and VEGF-A production during the first 50 days after infection, followed by a progressive return to reference ranges coinciding with viral clearance. The third profile involved sustained altered levels of factors in semen (IL-18, sICAM-1, G-CSF, MMP-2) and plasma (CCL-3, CXCL-1, sICAM-1, MMP-2, MMP-9), even after complete viral RNA clearance in plasma. Some factors were undetectable in plasma and semen samples (IL-15,

IFN- $\beta$ , granulocyte-macrophage colony-stimulating factor), and others were absent or barely detectable in plasma (IL-6, IFN- $\gamma$ , CCL-4, CXCL-8, G-CSF).

Our data revealed higher amounts of and more prolonged viral RNA shedding in semen than in blood. Zika virus infection altered cytokine secretion and induced distinct profiles in the plasma and semen; changes in the semen were more prominent. The discrepancies in kinetics and concentrations of cytokines and virus titers between semen and plasma suggest virus compartmentalization.

Cytokines produced in the MRT reflect local immune status, organ function, and tissue damage. The high levels of proinflammatory factors in semen samples from this patient illustrate an exacerbated local immune response established to control Zika virus infection. This response

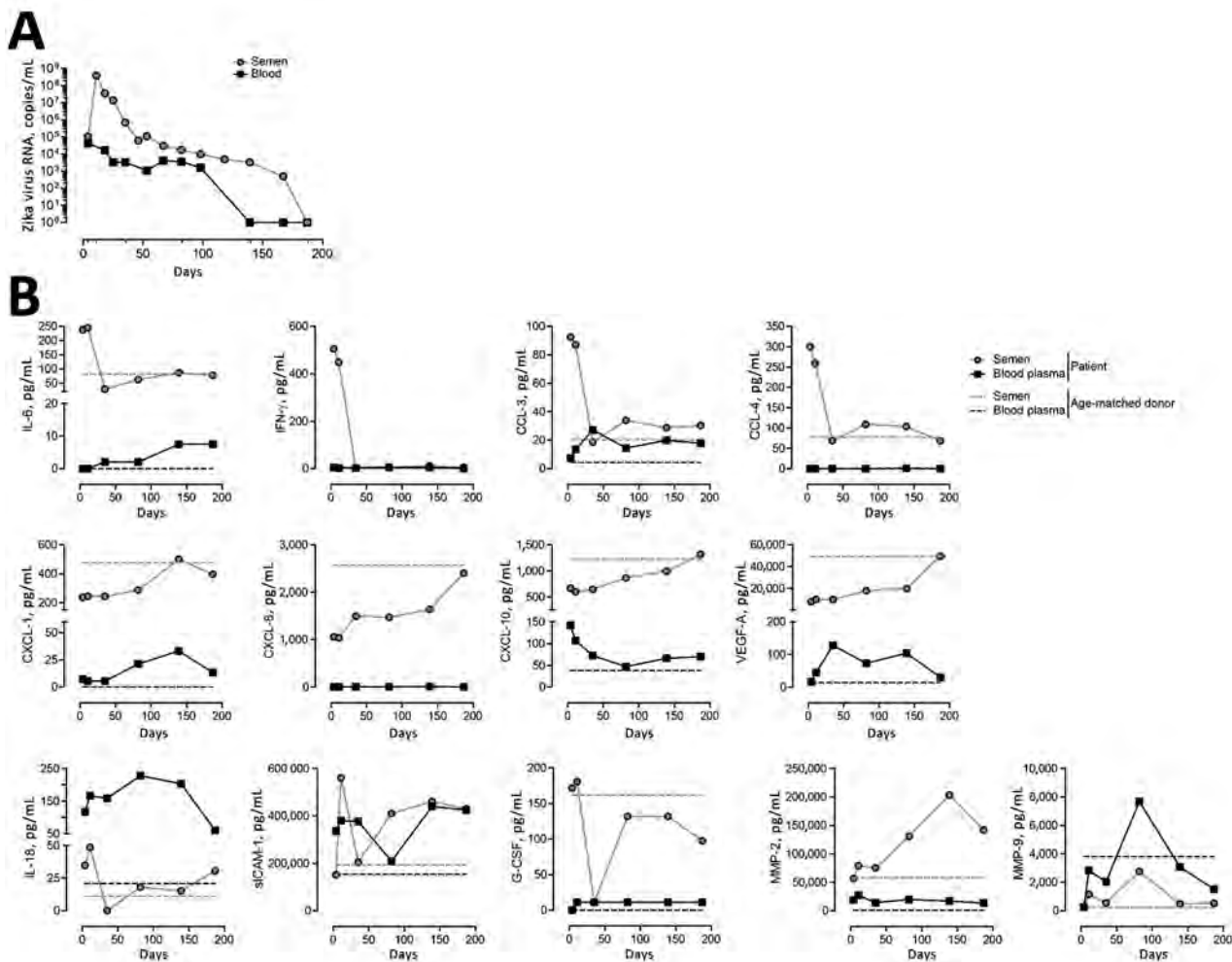


**Figure.** Kinetics of Zika virus replication and cytokine secretion in semen, blood, and plasma samples from a Zika virus–infected patient, France, 2016. A) Kinetics of Zika virus RNA detection in whole blood and semen quantified by real-time reverse transcription PCR. B) Quantification of soluble factors in the blood plasma and semen at 4, 11, 35, 82, 139, and 187 days after symptom onset. Dashed lines represent baseline levels of soluble factors quantified in blood plasma and semen obtained from an age-matched healthy donor. CCL, CC-motif chemokine ligand; CXCL, CXC-motif chemokine ligand; G-CSF, granulocyte colony-stimulating factor; IFN- $\gamma$ , interferon  $\gamma$ ; IL, interleukin; MMP, matrix metalloproteinase; sICAM-1, soluble intercellular adhesion molecule 1; VEGF-A, vascular endothelial growth factor A.

might lead to recruitment of more host and inflammatory cells that further amplify viral replication and organ injury (6). Downregulation of several factors highlights the damage. For instance, the VEGF-A levels mirror the impairment of spermatogonia, primary spermatocytes, and Sertoli cells upon Zika virus infection (4). However, the decrease in CXCL-1, CXCL-8, and CXCL-10 levels in semen during infection could indicate a local immunosuppressive state induced by infection, limiting immune cell infiltration in the MRT and potentially virus dissemination throughout the body.

The different kinetics of virus replication and cytokine secretion in semen samples raises questions about the semen secretome in cases of couples aiming for conception and the necessity to extend the convalescence period beyond Zika disease recovery. In fact, at high concentration, most of these factors might alter the integrity of the mucosal barriers within the female reproductive tract and increase a woman's susceptibility to infection (7). They might also promote peroxidation and affect sperm function, potentially resulting in infertility (8).

The limitations of our study include small sample size. Further investigations with a larger cohort of patients and controls are warranted.

In summary, a profound disruption in the cytokine network is evident in plasma and semen starting at the earliest stage of Zika virus infection and is maintained over time even after viral clearance. Studies to characterize the mechanism involved in the establishment of compartmentalization and develop efficient antiviral therapies that interfere with virus replication in the MRT are needed.

#### Acknowledgment

We thank Isabelle Da Silva for technical assistance.

#### About the Author

Dr. Mansuy is a medical virologist at the University Hospital of Toulouse in Toulouse, France. His research interests include emerging viral diseases and respiratory and enteric diseases.

#### References

1. Brasil P, Pereira JP Jr, Moreira ME, Ribeiro Nogueira RM, Damasceno L, Wakimoto M, et al. Zika virus infection in pregnant women in Rio de Janeiro. *N Engl J Med*. 2016;375:2321–34. <http://dx.doi.org/10.1056/NEJMoa1602412>
2. Baud D, Musso D, Vouga M, Alves MP, Vulliamoz N. Zika virus: a new threat to human reproduction. *Am J Reprod Immunol*. 2017;77:e12614. <http://dx.doi.org/10.1111/aji.12614>
3. Mansuy JM, Suberbielle E, Chapuy-Regaud S, Mengelle C, Bujan L, Marchou B, et al. Zika virus in semen and spermatozoa. *Lancet Infect Dis*. 2016;16:1106–7. [http://dx.doi.org/10.1016/S1473-3099\(16\)30336-X](http://dx.doi.org/10.1016/S1473-3099(16)30336-X)
4. Govero J, Esakky P, Scheaffer SM, Fernandez E, Drury A, Platt DJ, et al. Zika virus infection damages the testes in mice. *Nature*. 2016;540:438–42. <http://dx.doi.org/10.1038/nature20556>
5. Joguet G, Mansuy JM, Matusali G, Hamdi S, Walschaerts M, Pavili L, et al. Effect of acute Zika virus infection on sperm and virus clearance in body fluids: a prospective observational study. *Lancet Infect Dis*. 2017;17:1200–8. [http://dx.doi.org/10.1016/S1473-3099\(17\)30444-9](http://dx.doi.org/10.1016/S1473-3099(17)30444-9)
6. Shi C, Pamer EG. Monocyte recruitment during infection and inflammation. *Nat Rev Immunol*. 2011;11:762–74. <http://dx.doi.org/10.1038/nri3070>
7. Rametse CL, Olivier AJ, Masson L, Barnabas S, McKinnon LR, Ngcapu S, et al. Role of semen in altering the balance between inflammation and tolerance in the female genital tract: does it contribute to HIV risk? *Viral Immunol*. 2014;27:200–6. <http://dx.doi.org/10.1089/vim.2013.0136>
8. Fraczek M, Sanocka D, Kamieniczna M, Kurpisz M. Proinflammatory cytokines as an intermediate factor enhancing lipid sperm membrane peroxidation in vitro conditions. *J Androl*. 2008;29:85–92. <http://dx.doi.org/10.2164/jandrol.107.003319>

Address for correspondence: Jean-Michel Mansuy, Institut Fédératif de Biologie, Laboratoire de Virologie, 330 Avenue de Grande Bretagne, 31059 Toulouse CEDEX, France; email: mansuy.jm@chu-toulouse.fr

## Detection of Epizootic Hemorrhagic Disease Virus Serotype 1, Israel

Natalia Golender,<sup>1</sup> Velizar Y. Bumbarov<sup>1</sup>

Author affiliation: Kimron Veterinary Institute, Beit Dagan, Israel

DOI: <https://doi.org/10.3201/eid2504.180149>

During September 2016–February 2017, we detected epizootic hemorrhagic disease virus (EHDV) in ruminants in Israel. BLAST and phylogenetic analyses of segment 2 in 6 EHDVs isolated from field samples indicated a close relationship to the EHDV serotype 1 strain in Nigeria. Affected cattle had mostly mild or asymptomatic disease.

Epizootic hemorrhagic disease is an infectious, non-contagious viral disease of ruminants, transmitted by insects of the genus *Culicoides*; it mostly affects white-tailed deer and cattle. Epizootic hemorrhagic disease virus (EHDV) belongs to the genus *Orbivirus* within the family *Reoviridae* and is closely related to bluetongue virus (BTV) and African horse-sickness virus. At least

<sup>1</sup>Both authors share first authorship.



7 EHDV serotypes are currently recognized worldwide (1). (EHDV serotype 1 has been isolated from cattle in the Northern Territory of Australia (2), Nigeria, Ecuador, French Guyana, Réunion Island (in the Indian Ocean) (3), and the United States, where it was also isolated from white-tailed deer (4). In cattle in Israel, EHDV serotype 7 first was recognized in 2006, when it manifested in serious clinical signs (5). EHDV serotype 6 caused an outbreak in 2015, when clinical signs were milder than those associated with EHDV serotype 7 (6). However, EHDV serotype 6 RNA was found in placenta and brains of aborted cattle fetuses during the latter outbreak (6).

In the summer and fall of 2016, several arbovirus infections were registered simultaneously in diseased domestic and wild ruminants in Israel. Included were infections with BTV serotypes 2, 3, 4, 8, and 15; Shuni and Akabane viruses, belonging to the Simbu serogroup of genus *Orthobunyavirus* in the *Peribunyaviridae* family; and EHDV. BTV serotype 8 caused a large outbreak that caused heavy losses of livestock in some sheep and cattle farms.

During September 2016–February 2017, we routinely tested 265 field samples by using specific EHDV real-time reverse transcription PCR (rRT-PCR), as described previously (6). The tested field samples included 10 spleen samples from wild and zoo ruminants taken from 4 mountain gazelles, 1 giraffe, 1 Arabian oryx, and 4 Nubian ibexes, as well as 13 spleen samples and 242 whole-blood EDTA samples from diseased cattle. We similarly tested 22 aborted cattle fetuses. We obtained the first EHDV-positive whole-

blood sample from a diseased dairy cow on September 12, 2016, and the most recent one on February 26, 2017.

A total of 81 EHDV-positive field samples originated from northern Israel (the Golan Heights, Galilee, the Sharon Plain, and the Jordan Valley) and central Israel (the Coastal Plain). Positive samples included 1 spleen sample from a wild mountain gazelle that was found dead as a result of a head wound near the Sea of Galilee and 2 spleen samples and 78 whole-blood samples from infected cattle. However, the deaths of EHDV-positive cattle probably were not caused by EHDV. In 1 such case, in an adult dairy cow, *Escherichia coli* from all tested internal organs was isolated, and *Babesia* spp. were found during microscopic examination. In another case, in a 4-month-old calf, we identified BTV by using a BTV-specific rRT-PCR test (Vet-MAX BTV NS3 All Genotypes Kit, LSI; Thermo Fisher Scientific, <https://www.thermofisher.com>), which led to isolation of BTV serotype 8.

Among the EHDV rRT-PCR-positive samples, 18 were also rRT-PCR-positive for BTV and 1 was positive in pan-Simbu rRT-PCR (7), showing Akabane virus infection. All tested aborted cattle fetuses were EHDV-negative by rRT-PCR. We attempted virus isolation on all EHDV- and BTV-positive samples. We isolated 6 EHDV in embryonated chicken eggs, which consequently passed on BHK-21 cells, as previously described (6).

We sequenced 4 partial and 2 complete sequences of segment 2 (encoding viral protein 2) by using the standard Sanger method and submitted them to GenBank (accession

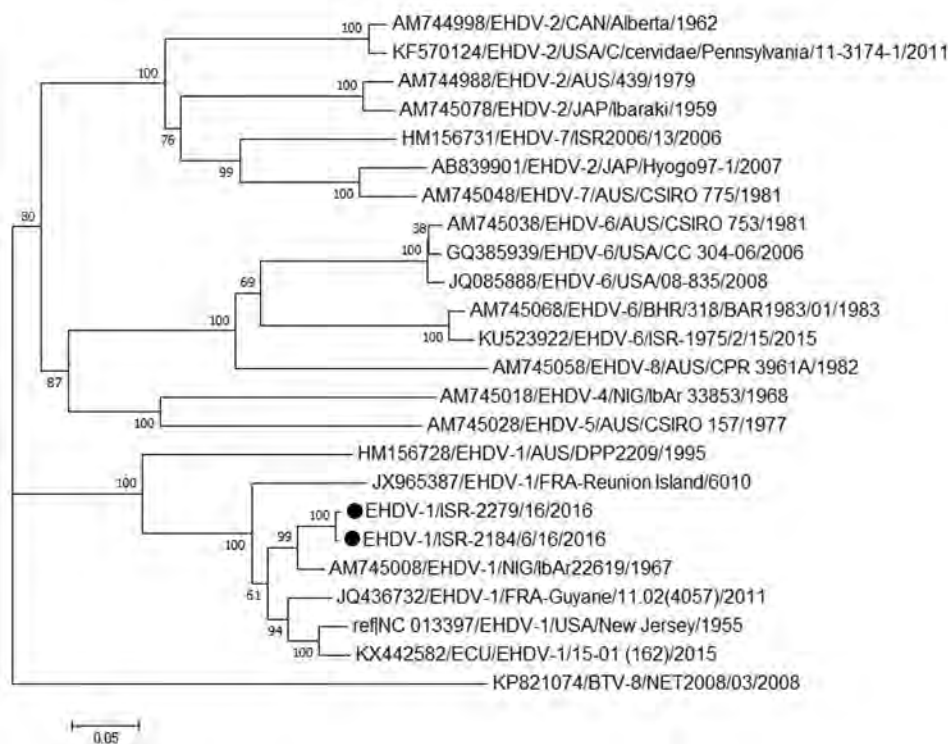


**Figure.** Phylogenetic analysis based on full-length sequences of segment 2 in 2 EHDV serotype 1 isolates from Israel with global EHDVs and BTV-8 from GenBank. We analyzed 24 nucleotide sequences and inferred phylogenetic relationship by using the neighbor-joining method. Numbers below branches indicate bootstrap values. Recent isolates from Israel are marked with black circles. Viruses are identified by GenBank accession number, virus and serotype, 3-letter code of country (and additional information in some cases), isolate identification (in most cases), and year of isolates. Evolutionary analyses were conducted in MEGA7 (8). Scale bar indicates number of nucleotide substitutions per site. BTV, bluetongue virus; EHDV, epizootic hemorrhagic disease virus.

nos. MG808405–MG808410). BLAST (<https://blast.ncbi.nlm.nih.gov/Blast.cgi>) and phylogenetic analyses of the segment 2 sequences showed that the EHDV recently isolated in cattle in Israel belongs to serotype 1 and is closely related to the IbAr22619 strain from Nigeria, with which it shares 95.72%–95.76% identity (Figure).

Retrospective analysis of clinical signs in EHDV-1–infected cattle enabled us to conclude that in many farms EHDV infection was asymptomatic or subclinical; milk-yield reduction, fever, and recumbency were the only prominent clinical signs observed during the outbreak. However, animals with BTV and EHDV co-infections showed more severe clinical signs, including fever, abortion, lameness, subcutaneous emphysema, and death.

During recent years, several new arboviruses have been detected in Israel that were not identified previously. BTV serotype 3 was first identified in 2016 but probably was present in Israel since at least 2013 (9), EHDV serotype 6 was identified in 2015 (6), EHDV serotype 1 was found in 2016, and Shuni virus was detected in 2014 (10). These findings showed that new introductions of arthropodborne viral infections into the Middle East region had occurred. Molecular epidemiologic data indicate the viruses originated in Africa, as ours and other studies (5,6) have shown. Molecular diagnostics, vector-control strategies, and epidemiologic studies should be implemented in Israel to mitigate potential risk for future outbreaks.

### About the Authors

Drs. Golender and Bumbarov are virologists in the Virology Department of the Kimron Veterinary Institute, Beit Dagan, Israel. Their primary research interests include the investigation of arboviral infections caused by viruses of the *Reoviridae* (Orbiviruses) family and the *Peribunyaviridae* (Orthobunyavirus, Simbu serogroup viruses) family, which affect ruminant populations, and developing diagnostic methods to detect these viruses.

### References

- Savini G, Afonso A, Mellor P, Aradaib I, Yadin H, Sanaa M, et al. Epizootic haemorrhagic disease. *Res Vet Sci*. 2011;91:1–17. <http://dx.doi.org/10.1016/j.rvsc.2011.05.004>
- Weir RP, Harmsen MB, Hunt NT, Blacksell SD, Lunt RA, Pritchard LI, et al. EHDV-1, a new Australian serotype of epizootic haemorrhagic disease virus isolated from sentinel cattle in the Northern Territory. *Vet Microbiol*. 1997;58:135–43. [http://dx.doi.org/10.1016/S0378-1135\(97\)00155-7](http://dx.doi.org/10.1016/S0378-1135(97)00155-7)
- Cêtre-Sossah C, Roger M, Sailleau C, Rieau L, Zientara S, Bréard E, et al. Epizootic haemorrhagic disease virus in Reunion Island: evidence for the circulation of a new serotype and associated risk factors. *Vet Microbiol*. 2014;170:383–90. <http://dx.doi.org/10.1016/j.vetmic.2014.02.007>
- Subramaniam K, Lednicky JA, Loeb J, Saylor KA, Wisely SM, Waltzek TB. Genomic sequences of epizootic hemorrhagic disease viruses isolated from Florida white-tailed deer. *Genome Announc*. 2017;5:e01174-17. <http://dx.doi.org/10.1128/genomeA.01174-17>
- Yadin H, Brenner J, Bumbarov V, Oved Z, Stram Y, Klement E, et al. Epizootic haemorrhagic disease virus type 7 infection in cattle in Israel. *Vet Rec*. 2008;162:53–6. <http://dx.doi.org/10.1136/vr.162.2.53>
- Golender N, Khinich Y, Gorohov A, Abramovitz I, Bumbarov V. Epizootic hemorrhagic disease virus serotype 6 outbreak in Israeli cattle in 2015. *J Vet Diagn Invest*. 2017;29:885–8. <http://dx.doi.org/10.1177/1040638717726826>
- Golender N, Bumbarov VY, Erster O, Beer M, Khinich Y, Wernike K. Development and validation of a universal S-segment-based real-time RT-PCR assay for the detection of Simbu serogroup viruses. *J Virol Methods*. 2018;261:80–5. <http://dx.doi.org/10.1016/j.jviromet.2018.08.008>
- Kumar S, Stecher G, Tamura K. MEGA7: Molecular Evolutionary Genetics Analysis version 7.0 for bigger datasets. *Mol Biol Evol*. 2016;33:1870–4. <http://dx.doi.org/10.1093/molbev/msw054>
- Golender N, Eldar A, Khinich Y, Kenigswald G, Bumbarov V. Novel topotypes of bluetongue serotype 3 viruses in the Mediterranean Basin. In: Abstracts of the 11th EPIZONE Annual Meeting, Paris, France, 2017 Sep 19–21. Abstract C1; p. 26.
- Golender N, Brenner J, Valdman M, Khinich Y, Bumbarov V, Panshin A, et al. Malformations caused by Shuni virus in ruminants, Israel, 2014–2015. *Emerg Infect Dis*. 2015;21:2267–8. <http://dx.doi.org/10.3201/eid2112.150804>

Address for correspondence: Natalia Golender, Kimron Veterinary Institute, Beit Dagan 50250, POB 12, Israel; email: [golendern@moag.gov.il](mailto:golendern@moag.gov.il)

## Ross River Virus Antibody Prevalence, Fiji Islands, 2013–2015

**Maite Aubry, Mike Kama, Jessica Vanhomwegen, Anita Teissier, Teheipaura Mariteragi-Helle, Stephane Hue, Martin L. Hibberd, Jean-Claude Manuguerra, Ketan Christi, Conall H. Watson, Eric J. Nilles, Colleen L. Lau, John Aaskov, Didier Musso, Adam J. Kucharski, Van-Mai Cao-Lormeau**

Author affiliations: Institut Louis Malardé, Papeete, French Polynesia (M. Aubry, A. Teissier, T. Mariteragi-Helle, D. Musso, V.-M. Cao-Lormeau); Fiji Centre for Communicable Disease Control, Suva, Fiji (M. Kama); The University of the South Pacific, Suva (M. Kama, K. Christi); Institut Pasteur, Paris, France (J. Vanhomwegen, J.-C. Manuguerra); London School of Hygiene and Tropical Medicine, London, UK (S. Hue, M.L. Hibberd, C.H. Watson, A.J. Kucharski); World Health Organization Division of Pacific Technical Support, Suva (E.J. Nilles); Harvard Medical School and Brigham and Women's Hospital, Boston,

Massachusetts, USA (E.J. Nilles); Harvard Humanitarian Initiative, Cambridge, Massachusetts (E.J. Nilles); Queensland University of Technology, Brisbane, Queensland, Australia (J. Aaskov); Australian National University, Canberra, Australian Capital Territory, Australia (C.L. Lau); Aix Marseille Université, IRD, AP-HM, SSA, VITROME, IHU-Méditerranée Infection, Marseille, France (D. Musso)

DOI: <https://doi.org/10.3201/eid2504.180694>

A unique outbreak of Ross River virus (RRV) infection was reported in Fiji in 1979. In 2013, RRV seroprevalence among residents was 46.5% (362/778). Of the residents who were seronegative in 2013 and retested in 2015, 10.9% (21/192) had seroconverted to RRV, suggesting ongoing endemic circulation of RRV in Fiji.

Ross River virus (RRV) is an *Alphavirus* of the family *Togaviridae* and is transmitted to humans by *Aedes* and *Culex* mosquitoes (1). Marsupials are considered important reservoirs of RRV (1). Clinical manifestations of RRV infections include fever, rash, and arthralgia. RRV is endemic to Australia, where it causes  $\approx 5,000$  cases of epidemic polyarthritis annually (1). Outbreaks of RRV infection were reported during 1979–1980 in Fiji, the Cook Islands, American Samoa, New Caledonia, and Wallis and Futuna (1–3). Subsequently, RRV infections were detected in travelers returning from Fiji during 1997–2009 (3) and in patients with suspected dengue in Fiji in 2005 (4).

The Republic of the Fiji Islands comprises 322 islands distributed among 4 administrative divisions (Central, Western, Eastern, and Northern) and has a population of

$\approx 830,000$ . Apart from RRV, the 4 serotypes of dengue virus were the only mosquito-borne viruses known to circulate in Fiji until the recent emergence of Zika and chikungunya viruses (5). We report evidence of endemic RRV circulation in Fiji on the basis of serologic analysis of blood samples collected in 2013 and 2015.

Our study included 778 participants recruited during September–November 2013 from the Central, Western, and Northern divisions for a community-based serosurvey for leptospirosis and typhoid (6). Among the residents from the Central division who had participated in the 2013 survey, 333 had blood drawn again during October–November 2015, including 311 whose serum sample collected in 2013 was available for testing. We tested all blood samples for RRV IgG by using a recombinant antigen-based microsphere immunoassay (7). We analyzed the data with GraphPad Prism 6.03 using the Fisher or  $\chi^2$  test. We considered  $p$  values  $<0.05$  to be significant.

The prevalence of RRV antibodies among participants in 2013 was 46.5% and was lower in the Central (38.1%) than the Western (58.6%;  $p<0.0001$ ) and Northern (55.9%;  $p = 0.0108$ ) divisions (Table). The prevalence of RRV antibodies among the participants sampled in the Central division in 2015 (37.2%) was similar to results from this division in 2013 (38.1%). In 2013, a total of 37.4% of the participants born after 1982 (postoutbreak) had RRV antibodies, and this rate in 2015 (26.9%) was not significantly different ( $p = 0.0685$ ). The prevalence of RRV antibodies increased with age ( $p<0.0001$  in 2013,  $p = 0.0020$  in 2015) and was higher in rural than in urban ( $p<0.0001$  in 2013,  $p = 0.0197$  in 2015) and periurban areas ( $p = 0.0060$  in 2013). No difference by sex was observed. Among the 311 participants with available serum

**Table.** Prevalence of Ross River virus antibodies in a representative subset of the population of Fiji sampled during September–November 2013 ( $n = 778$ ) and October–November 2015 ( $n = 333$ )\*

Variable	No. seropositive/mo. tested (% [95% CI])	
	2013	2015
Birth year		
<1982	197/336 (58.6 [53.4–63.9])	68/144 (47.2 [39.6–55.7])
$\geq 1982$	165/441 (37.4 [32.9–42.1])	56/189 (29.6 [23.2–36.7])
1982–1990	58/117 (49.6 [41.1–58.9])	17/38 (44.7 [31.4–61.4])
1991–2000	66/146 (45.2 [37.7–53.6])	20/66 (30.3 [21.3–42.9])
2001–2010	40/170 (23.5 [18.1–30.7])	19/83 (22.9 [15.8–33.5])
>2011	1/8 (12.5 [0.3–52.7])	0/2 (0.0 [0.0–84.2])
Sex		
F	195/423 (46.1 [41.5–51.0])	73/190 (38.4 [32.1–45.8])
M	167/354 (47.5 [42.2–52.5])	51/143 (35.7 [28.6–44.1])
Division		
Central	172/451 (38.1 [33.9–42.8])	124/333 (37.2 [32.4–42.7])
Northern	33/59 (55.9 [44.1–68.7])	ND
Western	157/268 (58.6 [52.8–64.5])	ND
Zone		
Rural	189/344 (54.9 [49.8–60.3])	52/113 (46.0 [37.5–55.6])
Periurban	55/135 (40.7 [33.2–49.5])	27/77 (35.1 [26.0–46.8])
Urban	117/298 (39.3 [34.1–45.1])	45/143 (31.5 [24.8–39.8])
Total	362/778† (46.5 [43.1–50.1])	124/333 (37.2 [32.4–42.7])

\*ND, no data (participants were not recruited from the Northern and Western divisions in 2015).

†For 1 participant, information about age and sex were not available; for another participant, information about the zone of residence was not available.



samples collected in both 2013 and 2015, a total of 21 (10.9%) of the 192 participants who had no detectable RRV antibodies in 2013 had seroconverted to RRV by 2015 (data not shown).

A serosurvey conducted after the RRV outbreak in Fiji in 1979 detected RRV antibodies in 92% of the participants from the Western division (2). In our study, which was conducted in 2013, RRV antibody prevalence in the Western, Central, and Northern divisions ranged from 38.1% to 58.6%, and 37.4% of persons born after 1982 had RRV antibodies, suggesting that RRV circulated in all 3 divisions after the 1979 outbreak. The report of RRV infection in travelers or inhabitants from Fiji during 1997–2009 (3,4), the observations that 10.9% of the seronegative participants in our study seroconverted to RRV during 2013–2015, and the increase in the prevalence of RRV antibodies with age, strongly suggest endemic RRV transmission in Fiji.

The finding that RRV seroprevalence was higher in rural than in urban and periurban environments suggests increased transmission risks in the rural areas, potentially because of higher-risk occupations of rural residents (including farming and outdoor work), greater exposure related to rural housing or other environmental factors, greater animal reservoir density, the possibility that non-domestic mosquito species in Fiji such as *Aedes vigilax*, *Ae. polynesiensis*, *Ae. pseudoscutellaris*, *Ae. albopictus*, and *Culex annulirostris* might be more competent vectors of RRV than peridomestic mosquito species such as *Ae. aegypti* (8).

Serosurveys conducted in American Samoa in 2010 (1), in French Polynesia during 2011–2013 (9) and 2014–2015 (7), and our study in Fiji during 2013–2015 suggest that endemic circulation of RRV in the Pacific region continued, or recommenced, after 1979–1980. These data provide further evidence for endemic transmission of RRV in areas where marsupials are absent (10). Because of extensive travel between Australia and the Pacific Islands, it is plausible that RRV is repeatedly seeded into the Pacific region. Whether this plays an important role in perpetuating local transmission in the Pacific Islands is unknown. As previously illustrated with Zika and chikungunya viruses, a risk exists for emerging arboviruses to be imported from the Pacific to other parts of the world, and RRV could be the next unexpected threat.

This work was part of ISID-Pacific and R-ZERO Pacific programs funded by the French Ministry for Europe and Foreign Affairs (Pacific Funds nos. 06314-09/04/14, 12115-02/09/15, 03016-20/05/16, and 04917-19/07/17). The study also received support from the Embassy of France in the Republic of the Fiji Islands. The study was supported by the French Government's Investissement d'Avenir Program (Labex IBEID no.

ANR-10-LABX-62-IBEID). C.L.L. was supported by an Australian National Health and Medical Research Council Fellowship (no. 1109035). Fieldwork in 2013 was funded by the World Health Organization Western Pacific Region and by the Chadwick Trust. C.H.W. was supported by the UK Medical Research Council (grant no. MR/J003999/1). A.J.K. was supported by a Sir Henry Dale Fellowship, jointly funded by the Wellcome Trust and the Royal Society (grant no. 206250/Z/17/Z).

The study was approved by the Fiji National Health Research Ethics Review Committee (FNRRER/no. 2015.114.NW and FNRRER/no. 2015.45.MC), the University of the South Pacific (FSTER/2015/10/Research Proposal Approval), and the London School of Hygiene and Tropical Medicine Observational Research Ethics Committee (approval nos. 6344 and 10207).

### About the Author

Dr. Aubry is a research scientist at the Institut Louis Malardé, Papeete, French Polynesia. Her research interests include the prevalence, epidemiology, and genetic evolution in the Pacific region of various arboviruses, such as dengue, Zika, chikungunya, and Ross River viruses.

### References

1. Lau C, Aubry M, Musso D, Teissier A, Paulous S, Després P, et al. New evidence for endemic circulation of Ross River virus in the Pacific Islands and the potential for emergence. *Int J Infect Dis*. 2017;57:73–6. <http://dx.doi.org/10.1016/j.ijid.2017.01.041>
2. Aaskov JG, Mataika JU, Lawrence GW, Rabukawaqa V, Tucker MM, Miles JA, et al. An epidemic of Ross River virus infection in Fiji, 1979. *Am J Trop Med Hyg*. 1981;30:1053–9. <http://dx.doi.org/10.4269/ajtmh.1981.30.1053>
3. Lau C, Weinstein P, Slaney D. Imported cases of Ross River virus disease in New Zealand—a travel medicine perspective. *Travel Med Infect Dis*. 2012;10:129–34. <http://dx.doi.org/10.1016/j.tmaid.2012.04.001>
4. Ngwe Tun MM, Inoue S, Thant KZ, Talemaitoga N, Aryati A, Dimaano EM, et al. Retrospective seroepidemiological study of chikungunya infection in South Asia, Southeast Asia and the Pacific region. *Epidemiol Infect*. 2016;144:2268–75. <http://dx.doi.org/10.1017/S095026881600056X>
5. Cao-Lormeau V-M, Musso D. Emerging arboviruses in the Pacific. *Lancet*. 2014;384:1571–2. [http://dx.doi.org/10.1016/S0140-6736\(14\)61977-2](http://dx.doi.org/10.1016/S0140-6736(14)61977-2)
6. Lau CL, Watson CH, Lowry JH, David MC, Craig SB, Wynwood SJ, et al. Human leptospirosis infection in Fiji: an eco-epidemiological approach to identifying risk factors and environmental drivers for transmission. *PLoS Negl Trop Dis*. 2016;10:e0004405. <http://dx.doi.org/10.1371/journal.pntd.0004405>
7. Aubry M, Teissier A, Huart M, Merceron S, Vanhomwegen J, Roche C, et al. Ross River virus seroprevalence, French Polynesia, 2014–2015. *Emerg Infect Dis*. 2017;23:1751–3. <http://dx.doi.org/10.3201/eid2310.170583>
8. Mitchell CJ, Gubler DJ. Vector competence of geographic strains of *Aedes albopictus* and *Aedes polynesiensis* and certain other *Aedes* (*Stegomyia*) mosquitoes for Ross River virus. *J Am Mosq Control Assoc*. 1987;3:142–7.

9. Aubry M, Finke J, Teissier A, Roche C, Brout J, Paulous S, et al. Silent circulation of Ross River virus in French Polynesia. *Int J Infect Dis.* 2015;37:19–24. <http://dx.doi.org/10.1016/j.ijid.2015.06.005>
10. Stephenson EB, Peel AJ, Reid SA, Jansen CC, McCallum H. The non-human reservoirs of Ross River virus: a systematic review of the evidence. *Parasit Vectors.* 2018;11:188. <http://dx.doi.org/10.1186/s13071-018-2733-8>

Address for correspondence: Van-Mai Cao-Lormeau, Institut Louis Malardé, PO Box 30, 98713 Papeete, Tahiti, French Polynesia; email: [mlormeau@ilm.pf](mailto:mlormeau@ilm.pf)

## Malignant *Aspergillus flavus* Otitis Externa with Jugular Thrombosis

Maxime Moniot, Marion Montava, Stéphane Ranque, Ugo Scemama, Carole Cassagne, Varoquaux Arthur

Author affiliations: Aix-Marseille University, Marseille, France (M. Moniot, S. Ranque, C. Cassagne); La Conception University Hospital, Marseille (M. Montava, U. Scemama, V. Arthur)

DOI: <https://doi.org/10.3201/eid2504.180710>

We report a case of malignant otitis externa with jugular vein thrombosis caused by *Aspergillus flavus*. Magnetic resonance imaging revealed an unusual ink smudge pattern deep in a cervical abscess. The pattern was consistent with mycetoma and may be important for diagnosing these life-threatening infections.

A 73-year-old male patient sought care from the otorhinolaryngology department at University Hospital, Marseille, France. He had a 5-month history of malignant otitis externa (MOE), which was worsening despite 4 months of treatment with intravenous ceftazidime, oral ciprofloxacin, and topical neomycin, polymyxin B, dexamethasone, and thiomersal combination. The patient had a history of high blood pressure, treated with perindopril and nicardipine, and diabetes mellitus, inadequately controlled (hemoglobin A1c 7.7%) with metformin and sitagliptin.

The patient was admitted, and otoscopic examination found otorrhea, inflammation, and stenosis of the right

external auditory canal; we could not see the tympanic membrane. Examination of the cranial nerve was normal. Pure-tone audiogram showed a right mixed hearing loss with air-bone gap at 15 dB and symmetric bone curve by presbycusis. Laboratory testing showed elevated erythrocyte sedimentation level (42 mm at 1 h, 82 mm at 2 h) and leukocytosis (11 g/L); C-reactive protein results were within reference range. A computed tomography (CT) scan of the head showed thickening of the ear skin; focal tympanic bone osteolysis; partial right mastoid air cells and middle-ear cavity opacification; and osteolysis of the occipital, styloid, and mastoid bones consistent with MOE (Appendix Figure, <https://wwwnc.cdc.gov/EID/article/25/4/18-0710-Appl.pdf>). Magnetic resonance imaging (MRI) with contrast media confirmed skull base osteomyelitis, evidenced by bone lysis and marrow enhancement of the clivus (Figure, panels A–C). Both MRI and CT showed a right jugular vein thrombosis and cellulitis and abscess in the carotid and perivertebral spaces. Abscess content had an unusual aspect: T2-weighted imaging signal void foci surrounded by a hypersignal rim.

We treated the right jugular vein thrombosis with enoxaparin. The patient underwent surgical debridement with facial nerve monitoring; we collected transmastoid biopsy samples and pus for microbiological analysis and inserted a transtympanic aerator. Direct microscopic examination of the samples showed hyaline septate hyphae consistent with hyalohyphomycosis. Biopsy samples grew 2 bacteria, *Corynebacterium striatum* and *Enterococcus faecalis*, and 1 filamentous fungus, *Aspergillus flavus*, that we identified by matrix-assisted laser desorption/ionization time-of-flight mass spectrometry (Microflex LT, <https://www.bruker.com>) against an in-house database described by Normand et al. (1). Etest antifungal susceptibility testing (bioMérieux, <https://www.biomerieux.com>) showed that the *A. flavus* strain was sensitive to voriconazole (MIC 0.380 mg/L) and resistant to amphotericin B (MIC 12 mg/L). We stopped administration of auricular drops, continued intravenous ceftazidime (1.5 g/d) and oral ciprofloxacin (1.5 g/d), and started voriconazole therapy (6 mg/kg/12 h intravenously, followed by 400 mg/d orally). Otagia, otorrhea, and inflammatory external auditory canal symptoms were relieved, and the patient recovered after 6 weeks. No further follow-up was available.

Fungi cause ≈10% of MOE (2). The 3 leading species, by decreasing frequency, are *A. fumigatus*, *A. flavus*, and *A. niger* (3). *A. flavus* is more frequently involved in MOE than is *A. niger* (3,4).

Jugular vein thrombosis (JVT) was previously reported in MOE (5) and other conditions such as Lemierre syndrome, invasive fungal infection, or any inflammatory process including otitis media. Various pathogens can cause JVT, especially *Fusobacterium necrophorum* and zygomycetes.

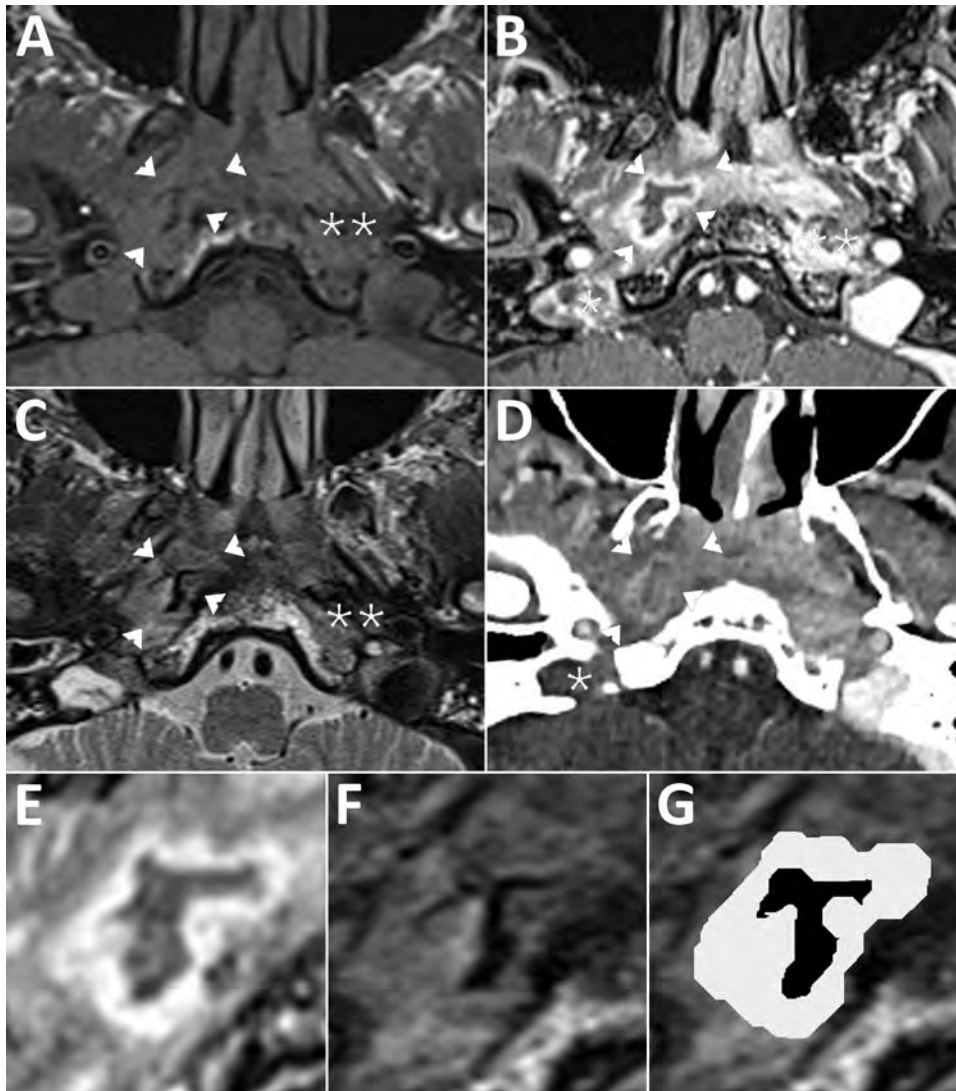


**Figure.** Magnetic resonance imaging (MRI) of a patient with malignant otitis externa, France. Cross-sectional imaging demonstrates a central skull base osteomyelitis in patient's temporal bone. A) T1-weighted imaging; B, E) 3-dimensional T1-weighted imaging with gadolinium enhancement and fat saturation; C, F, G) T2-weighted imaging; and CT with iodine enhancement (D). Single asterisks (\*) indicate jugular bulb thrombosis (panels B, D); double asterisks (\*\*) indicate deep-spaces cellulitis (panels A–C). Arrowheads indicate parapharyngeal abscess at right (panels A–D); parapharyngeal abscess is also visible as a gray layer (panels E, G). The content of the abscess has an unusual “ink smudge” pattern with no signal in T2-weighted imaging, visible as a black layer (panels F, G). This pattern is consistent with a mycetoma surrounded by granulation tissue.

Data on JVT in MOE are scarce; we could find no previously reported case of JVT related to *A. flavus* MOE. Postcontrast CT with soft tissue algorithm is considered the first-line imaging modality to diagnose JVT (5). In our case, both CT and MRI confirmed the diagnosis.

Osteomyelitis and abscess showed on MRI but were hardly visible on CT (Appendix Figure). High-signal T2-weighted imaging is typical in purulent content of abscesses (6). In contrast, this case exhibited an unusual lack of T2-weighted imaging signal. This characteristic pattern is known in various mycetoma locations as paranasal fungus balls (7) or maduromycosis, for which the T2-weighted imaging dot-in-circle sign is specific (8). Most authors explain the signal void as a magnetic susceptibility behavior on T2-weighted imaging resulting from accumulation of iron and other magnetic atoms (9). This case introduced a new T2-weighted imaging signal void pattern we refer to as an “ink smudge” appearance. A bone sequestrum is

a differential diagnosis, yet this lesion lacked calcification in CT. We hypothesize that the ink-smudge sign we identified could be specific to fungal infection. This report should prompt careful assessment by MRI of deep-space abscess in patients with MOE.

The standard treatment for fungal MOE is a combination of surgical debridement, systemic antifungal therapy, and control of concurrent conditions. There is no consensus for the duration of the antifungal treatment; patients usually receive 6–8 weeks of antifungal therapy, more if clinical examination or imaging follow-up supports extending treatment (10).

We highlight the potential use of an MRI ink-smudge pattern to identify fungal infection in MOE. Furthermore, because we saw JVT on both postcontrast CT and MRI scans, our findings and these images may be crucial for improving patient prognosis through timely and adequate treatment.



**About the Author**

Dr. Moniot is a resident at the University Hospital Institute Méditerranée Infection, Marseille, France. His research interests include identification and diagnosis of fungal pathogens and investigation of fungal epidemiology.

**References**

1. Normand A-C, Cassagne C, Gautier M, Becker P, Ranque S, Hendrickx M, et al. Decision criteria for MALDI-TOF MS-based identification of filamentous fungi using commercial and in-house reference databases. *BMC Microbiol.* 2017;17:25. <http://dx.doi.org/10.1186/s12866-017-0937-2>
2. Bhandary S, Karki P, Sinha BK. Malignant otitis externa: a review. *Pac Health Dialog.* 2002;9:64–7.
3. Parize P, Chandesris M-O, Lantermier F, Poirée S, Viard J-P, Bienvenu B, et al. Antifungal therapy of *Aspergillus* invasive otitis externa: efficacy of voriconazole and review. *Antimicrob Agents Chemother.* 2009;53:1048–53. <http://dx.doi.org/10.1128/AAC.01220-08>
4. Gabrielli E, Fothergill AW, Brescini L, Sutton DA, Marchionni E, Orsetti E, et al. Osteomyelitis caused by *Aspergillus* species: a review of 310 reported cases. *Clin Microbiol Infect.* 2014;20:559–65. <http://dx.doi.org/10.1111/1469-0691.12389>
5. Nawas MT, Daruwalla VJ, Spierer D, Micco AG, Nemeth AJ. Complicated necrotizing otitis externa. *Am J Otolaryngol.* 2013;34:706–9. <http://dx.doi.org/10.1016/j.amjoto.2013.07.003>
6. Matt BH, Lusk RP. Delineation of a deep neck abscess with magnetic resonance imaging. *Ann Otol Rhinol Laryngol.* 1987;96:615–7. <http://dx.doi.org/10.1177/000348948709600526>
7. Aribandi M, McCoy VA, Bazan C III. Imaging features of invasive and noninvasive fungal sinusitis: a review. *Radiographics.* 2007;27:1283–96. <http://dx.doi.org/10.1148/rg.275065189>
8. Jain V, Makwana GE, Bahri N, Mathur MK. The “dot in circle” sign on MRI in maduramycosis: a characteristic finding. *J Clin Imaging Sci.* 2012;2:66–66. <http://dx.doi.org/10.4103/2156-7514.103056>
9. Yamada K, Zoarski GH, Rothman MI, Zagardo MT, Nishimura T, Sun CCJ. An intracranial aspergilloma with low signal on T2-weighted images corresponding to iron accumulation. *Neuroradiology.* 2001;43:559–61. <http://dx.doi.org/10.1007/s002340000535>
10. Stodulski D, Kowalska B, Stankiewicz C. Orogenic skull base osteomyelitis caused by invasive fungal infection. *Eur Arch Otorhinolaryngol.* 2006;263:1070–6. <http://dx.doi.org/10.1007/s00405-006-0118-7>

Address for correspondence: Carole Cassagne, IHU Méditerranée Infection, 19-21 Boulevard Jean Moulin, 13005 Marseille, France; email: carole.cassagne@ap-hm.fr

## Epizootic Hemorrhagic Disease in White-Tailed Deer, Canada

Samantha E. Allen, Jamie L. Rothenburger,<sup>1</sup> Claire M. Jardine, Aruna Ambagala, Kathleen Hooper-McGrevy, Nicole Colucci, Tara Furukawa-Stoffer, Stacey Vigil, Mark Ruder, Nicole M. Nemeth<sup>2</sup>

Author affiliations: University of Guelph and Canadian Wildlife Health Cooperative, Guelph, Ontario, Canada (S.E. Allen, J.L. Rothenburger, C.M. Jardine, N.M. Nemeth); Canadian Food Inspection Agency, Winnipeg, Manitoba, Canada (A. Ambagala, K. Hooper-McGrevy); Canadian Food Inspection Agency, Lethbridge, Alberta, Canada (N. Colucci, T. Furukawa-Stoffer); University of Georgia, Athens, Georgia, USA (S. Vigil, M. Ruder, N.M. Nemeth)

DOI: <https://doi.org/10.3201/eid2504.180743>

Epizootic hemorrhagic disease affects wild and domestic ruminants and has recently spread northward within the United States. In September 2017, we detected epizootic hemorrhagic disease virus in wild white-tailed deer, *Odocoileus virginianus*, in east-central Canada. *Culicoides* spp. midges of the subgenus *Avaritia* were the most common potential vectors identified on site.

Epizootic hemorrhagic disease viruses (EHDVs) and bluetongue viruses (BTVs) are *Culicoides* spp. midge-transmitted orbiviruses that represent an imminent threat to the health of ruminant livestock and wildlife. For susceptible ruminants, EHDV and BTV infections can result in high rates of illness and death, leading to severe economic hardship to the agricultural sector (1). These viruses have a historical geographic range of 40°N–50°N and 35°S, following the distribution of the *Culicoides* vectors. However, the epidemiology of these pathogens is changing, with decades of northward expansion into areas of Europe and North America with immunologically naive hosts (1–3).

In Canada, EHDV has rarely and sporadically been detected in the southern portions of British Columbia, Alberta, and Saskatchewan (4). We report the detection of EHDV in white-tailed deer, *Odocoileus virginianus*, in east-central Canada, providing further evidence of the northern range expansion of orbiviruses within North America.

On September 7, 2017, two wild white-tailed deer carcasses were found in a seminatural area adjacent to a

<sup>1</sup>Current affiliation: University of Calgary, Calgary, Alberta, Canada.

<sup>2</sup>Current affiliation: University of Georgia, Athens, Georgia, USA.

river and ravine in London, Ontario, Canada (42.9849°N, 81.2453°W). The carcasses were submitted for diagnostic investigation to the Ontario-Nunavut region of the Canadian Wildlife Health Cooperative. Both deer had gross lesions consistent with epizootic hemorrhagic disease, including multiorgan petechial and ecchymotic hemorrhages on serosal surfaces (5). Spleen, lung, and liver samples from both deer were submitted to the National Centre for Foreign Animal Diseases in Winnipeg. All samples were positive for EHDV genomes by reverse transcription PCR (RT-PCR) (6). The serotype of the virus was identified by serotype-specific conventional RT-PCR followed by Sanger sequencing. EHDV-2 was isolated from spleen samples of both deer. Two additional deer carcasses were identified in the area but were not submitted for diagnostic testing. Tissues from an additional 14 deer carcasses that originated in southern Ontario during September 23–November 28, 2017, showed negative results for EHDV by RT-PCR, as part of enhanced surveillance conducted by the Ontario Ministry of Natural Resources and Forestry and the Canadian Wildlife Health Cooperative.

In addition, we conducted serosurveillance across southern Ontario in the fall of 2017 with samples collected by private veterinarians. All live animal samples were collected by using protocols approved by the Animal Care Committee, University of Guelph (approval no. 3529). Cattle were from Chatham-Kent County, adjacent to Middlesex County, and were born and had lived their whole lives in Canada. Results revealed 15 cattle with antibodies to EHDV-2 by ELISA and serum neutralization tests (S.E. Allen, unpub. data).

We also conducted a targeted survey for adult *Culicoides* midges in the area of the white-tailed deer deaths by using four 2770 UV LED CDC light traps (BioQuip Products, <http://www.bioquip.com>) for 16 trap-nights during September 9–13, 2017. We taxonomically identified 31 individual *Culicoides* spp. midges (7), including subgenus *Avaritia* (n = 22), *C. haematopotus* (n = 5), *C. stellifer* (n = 2), *C. venustus* (n = 1), and *C. crepuscularis* (n = 1) midges.

The northern expansion of EHDV and BTV in the midwestern and northeastern regions of the United States in recent years (1,8) has increased the likelihood of incursion into eastern Canada. The EHDV occurrence in white-tailed deer in Ontario we report supports the need to maintain vigilance. Although this initial occurrence was limited spatially and temporally, future cases may be more widespread in wildlife and livestock. Furthermore, this localized EHDV-2 occurrence was within 72 km of the US border of Michigan and coincided with concurrent and widespread EHDV-2 and EHDV-6 outbreaks across much of the eastern United States during July–October, 2017 (D.E. Stallknecht, University of Georgia, pers. comm, 2018 Jan 10).

EHDV may have been introduced to Ontario through the movement of infected vectors or ruminants, and its detection in Ontario may represent the northern edge of the EHDV outbreak in the eastern United States. Alternatively, low levels of previously undetected EHDV transmission may have been transient or ongoing across a wider region, including Ontario, for an unknown period. In either case, this event may preclude a much more widespread and higher impact EHDV outbreak, such as occurred with BTV in Europe and with EHDV in the United States (2,8).

We identified numerous *Culicoides* spp. midges at the site where the EHDV-infected white-tailed deer carcasses were recovered. However, *C. sonorensis* midges, the only confirmed EHDV vector species in North America (1,9), was not among these. This species was recently identified in Ontario (10), but the density and distribution of this species in the province, as well as its role in regional EHDV transmission, is currently unknown. *Culicoides* spp. composition within areas of past EHDV outbreaks varies widely; therefore, additional *Culicoides* spp. midges may serve as competent EHDV vectors. However, this possibility has not been confirmed (1,9). In addition to vector competence, the climatic limitations for the survival and successful breeding and establishment of current *Culicoides* spp. populations in the region remain to be investigated (1,8). These factors indicate the need for ongoing *Culicoides* spp. midge and deer mortality surveillance in the region.

### Acknowledgments

We thank the submitter for providing information on the deer cases and D. Cristo, C. Embury-Hyatt, and L. Shirose for assistance with sample submission and testing.

This study was funded by the Ontario Ministry of Agriculture, Food and Rural Affairs, University of Guelph Partnership (UofG2015-2212) and the Canadian Foundation for Innovation (RGPIN-2015-04088).

### About the Author

Dr. Allen is a veterinarian and PhD candidate at the University of Guelph, Canada. Her research focuses on wildlife disease, specifically vectorborne viruses and disease at the livestock–wildlife interface.

### References

1. Ruder MG, Lysyk TJ, Stallknecht DE, Foil LD, Johnson DJ, Chase CC, et al. Transmission and epidemiology of bluetongue and epizootic hemorrhagic disease in North America: current perspectives, research gaps, and future directions. *Vector Borne Zoonotic Dis.* 2015;15:348–63. <http://dx.doi.org/10.1089/vbz.2014.1703>
2. Maclachlan NJ. Global implications of the recent emergence of bluetongue virus in Europe. *Vet Clin North Am Food Anim Pract.* 2010;26:163–71. <http://dx.doi.org/10.1016/j.cvfa.2009.10.012>

3. McVey DS, Drolet BS, Ruder MG, Wilson WC, Nayduch D, Pfannenstiel R, et al. Orbiviruses: a North American perspective. *Vector Borne Zoonotic Dis.* 2015;15:335–8. <http://dx.doi.org/10.1089/vbz.2014.1699>
4. Pybus MJ, Ravi M, Pollock C. Epizootic hemorrhagic disease in Alberta, Canada. *J Wildl Dis.* 2014;50:720–2. <http://dx.doi.org/10.7589/2014-02-024>
5. Howerth EW, Stallknecht DE, Kirkland PD. Bluetongue, epizootic hemorrhagic disease, and other orbivirus-related diseases. In: Williams ES, Barker IK, editors. *Infectious diseases of wild mammals.* Ames (IA): Iowa State University Press; 2001. p. 82–9.
6. Pasick J, Handel K, Zhou EM, Clavijo A, Coates J, Robinson Y, et al. Incursion of epizootic hemorrhagic disease into the Okanagan Valley, British Columbia in 1999. *Can Vet J.* 2001;42:207–9.
7. Wirth WW, Dyce AL, Peterson BV. An atlas of wing photographs with a summary of the numerical characters of the Nearctic species of *Culicoides* (Diptera: Ceratopogonidae). *Contrib Am Entomol Inst.* 1985;22:1–46.
8. Stallknecht DE, Allison AB, Park AW, Phillips JE, Goeckjian VH, Nettles VF, et al. Apparent increase of reported hemorrhagic disease in the midwestern and northeastern USA. *J Wildl Dis.* 2015;51:348–61. <http://dx.doi.org/10.7589/2013-12-330>
9. Pfannenstiel RS, Mullens BA, Ruder MG, Zurek L, Cohnstaedt LW, Nayduch D. Management of North American *Culicoides* biting midges: current knowledge and research needs. *Vector Borne Zoonotic Dis.* 2015;15:374–84. <http://dx.doi.org/10.1089/vbz.2014.1705>
10. Jewiss-Gaines A, Barelli L, Hunter FF. First records of *Culicoides sonorensis* (Diptera: Ceratopogonidae), a known vector of bluetongue virus, in southern Ontario. *J Med Entomol.* 2017; 54:757–62.

---

Address for correspondence: Samantha E. Allen, University of Guelph, 50 Stone Rd E, Guelph, ON N1G 2W1, Canada; email: [sallen02@uoguelph.ca](mailto:sallen02@uoguelph.ca)

---

## Effects of Political Instability in Venezuela on Malaria Resurgence at Ecuador–Peru Border, 2018

Robinson Jaramillo-Ochoa,<sup>1</sup> Rachel Sippy,<sup>1</sup> Daniel F. Farrell,<sup>1</sup> Cinthya Cueva-Aponte,<sup>1</sup> Efraín Beltrán-Ayala, Jose L. Gonzaga, Tania Ordoñez-León, Fernando A. Quintana, Sadie J. Ryan, Anna M. Stewart-Ibarra

Author affiliations: Ministerio de Salud Pública del Ecuador, Machala, Ecuador (R. Jaramillo-Ochoa, J.L. Gonzaga, T. Ordoñez-León); State University of New York Upstate Medical

University, Syracuse, New York, USA (R. Sippy, D.F. Farrell, C. Cueva-Aponte, A.M. Stewart-Ibarra); University of Florida, Gainesville, Florida, USA (R. Sippy, S.J. Ryan); Universidad Técnica, Machala (E. Beltrán-Ayala); Ministerio de Salud de Peru, Tumbes, Peru (F.A. Quintana)

DOI: <https://doi.org/10.3201/eid2504.181355>

Mass migration from Venezuela has increased malaria resurgence risk across South America. During 2018, migrants from Venezuela constituted 96% of imported malaria cases along the Ecuador–Peru border. *Plasmodium vivax* predominated (96%). Autochthonous malaria cases emerged in areas previously malaria-free. Heightened malaria control and a response to this humanitarian crisis are imperative.

Malaria is a vectorborne parasitic infection caused by *Plasmodium* spp. and transmitted by *Anopheles* mosquitoes, characterized by fever and hemolysis with chronic and fatal potential (1). Despite substantial strides toward elimination in the Americas, malaria remains a major concern; ≈975,700 cases occurred and 138 million persons were at risk in 2017 (2). Most malaria cases in South America occur in the Amazon region, and *P. vivax* is more common than *P. falciparum* (3).

*P. vivax* and *P. falciparum* malaria were historically endemic to the Ecuador–Peru coastal border region. During 1990–2012, a total of 62,000 malaria cases were reported from El Oro Province, Ecuador, and 85,605 from Tumbes Region, Peru (4). Through vector control and active case surveillance and response, malaria was eliminated from El Oro Province in 2011 and Tumbes Region in 2012 (4). However, malaria cases elsewhere in Ecuador increased from 378 in 2013 (5) to 1,279 in 2017 (6). Peru and other countries in the region also reported increased malaria in 2017, indicating a major risk for re-introduction to elimination areas (2). In 2017, Venezuela alone accounted for more than half of all malaria cases in the Americas (2).

The public health sector in Venezuela is struggling with infectious disease epidemics, including malaria (7), despite a historically successful malaria control program (3). The worsening social and economic crisis has led to large-scale migration from and within Venezuela. The shortage of antimalarial drugs and lax in-country control efforts have exacerbated the situation, affecting countries throughout South America (8). Many people from Venezuela are migrating through Colombia and Ecuador to reach Peru and the southern cone of South America, stopping at various locations along the way (Figure). We report a series of imported malaria cases in migrants from Venezuela and the first autochthonous cases of malaria in the Ecuador–Peru border region since local elimination.

<sup>1</sup>These authors contributed equally to this article.



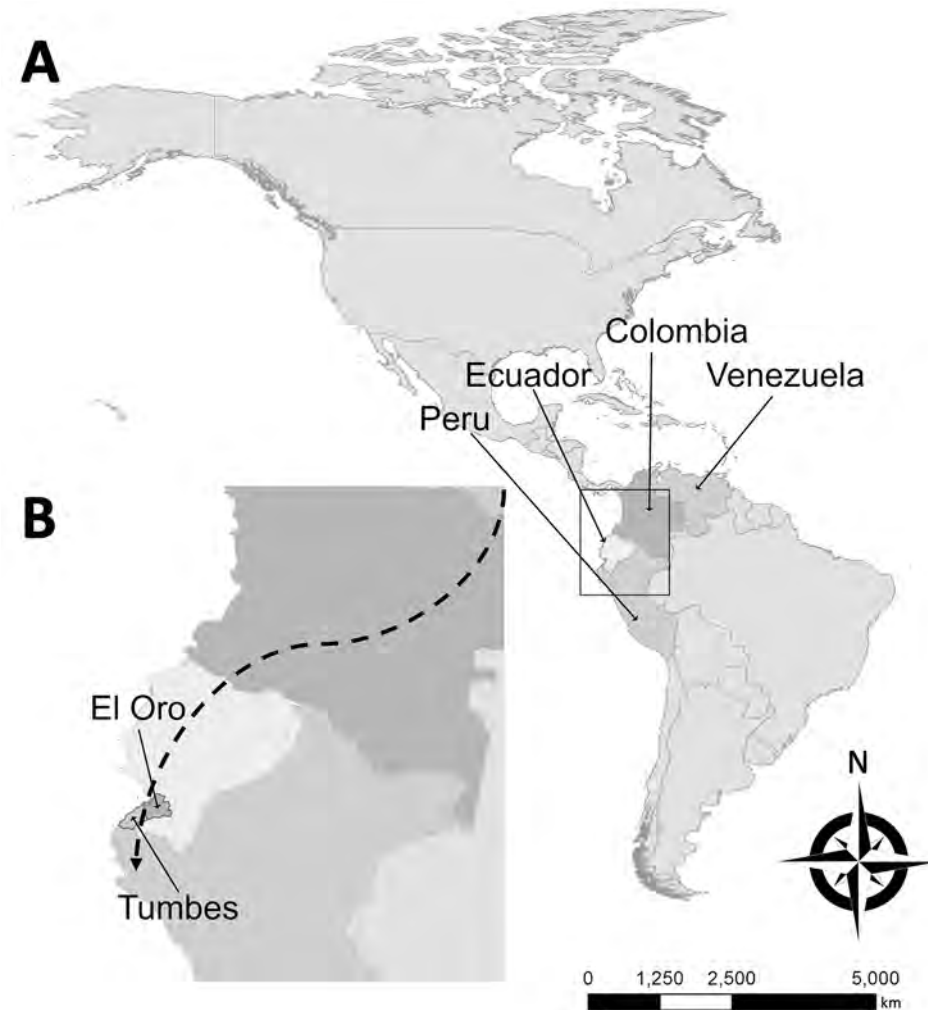


**Figure.** Probable migration route of imported malaria cases described in study of effects of political instability in Venezuela on malaria resurgence at the Ecuador–Peru border, 2018. A) Locations of the 4 countries along the migration route in South America; B) El Oro Province and Tumbes Region on the Ecuador–Peru border. The city of Huaquillas, Ecuador, is 70 km southwest of Machala, the location of the single autochthonous malaria case in this province. Huaquillas is the primary border crossing from Ecuador into Peru. Tumbes, the source of the 3 autochthonous cases in Peru, is the capital of Tumbes Region and is 22 km from the border. Dashed line in panel B broadly denotes the migration route taken from Venezuela through Colombia and Ecuador to Peru. Note the proximity of these countries and additional potential malarial resurgence through migration to Central America, the Caribbean, and the United States.

During February–November 2018, seven malaria cases (6 *P. vivax*, 1 *P. falciparum*) were detected in adults in El Oro Province and reported to the Ecuadorian Ministry of Health (Appendix, <https://wwwnc.cdc.gov/EID/article/25/4/18-1355-App1.pdf>). Five cases occurred in recent migrants from Venezuela, and 1 was imported from Peru. The most recent case (no. 7), reported in November 2018, was autochthonous. *Plasmodium* spp. infection was confirmed at the national reference laboratory in Guayaquil, Ecuador. Active surveillance within 1 km of each case-patient's residence revealed no acute cases, and collateral thick blood smears were negative. Entomologic teams documented *Aedes aegypti* and *Culex* spp. mosquitoes in the homes but no *Anopheles* mosquitoes. The residences all had basic infrastructure and no history of malaria since local elimination in 2011.

During May–October 2018, a total of 20 *P. vivax* malaria cases were detected in adults in Tumbes Region and reported to the Peruvian Ministry of Health (Appendix). Seventeen cases occurred in Venezuelan migrants now

living in the province, and 3 were autochthonous cases in persons residing in Tumbes. An epidemiologic investigation revealed that the autochthonous case-patients had no history of travel outside of Tumbes Region.

We cannot definitively state whether the migrants from Venezuela were exposed to malaria in Venezuela or during transit. Regardless, this population represents a highly vulnerable group with complex treatment issues. Malaria should be considered in the differential diagnosis for febrile patients from Venezuela and for local populations in nearby parts of South America. The transience of the migrant population presents treatment follow-up issues. The incubation period for *P. vivax* malaria is 12–18 days and, for *P. falciparum* malaria, 9–14 days. Case-patients (Appendix) often exhibited inadequately or untreated malaria. Imported cases are the likely source of the locally transmitted cases in Tumbes Region and El Oro Province because the primary mosquito vectors (*An. albimanus* and *An. punctimacula*) remain abundant in this area (9). Another concern is relapse of dormant *P. vivax* hypnozoites, which can occur up to

several years after initial infection (*I*). Issues with primaquine (i.e., *CYP2D6*-poor metabolizers or hemolysis risk in patients with glucose-6-phosphate dehydrogenase deficiency) complicate treatment of dormant hypnozoites that cause relapse (*I*). A new treatment, tafenoquine, which still causes hemolysis in glucose-6-phosphate dehydrogenase deficiency, was recently approved in the United States as a single dose for prevention of *P. vivax* malaria relapse (*10*), although this medication might not reach at-risk groups in South America. Ecuador and Peru currently follow the Pan American Health Organization guidelines regarding primaquine use (<https://www.paho.org/hq/dmdocuments/2011/TreatmentGuidelines-2nd-ed-2010-eng.pdf>).

Local ministries of health responded quickly to these cases and implemented case surveillance. However, reductions in resources after elimination of local malaria transmission in 2011–2012 severely limited malaria control efforts in Ecuador and Peru. Imported cases of malaria at the Ecuador–Peru border region pose a serious threat of continued resurgence in local transmission. We urge international solutions for Venezuela’s humanitarian crisis and augmentation of infectious disease surveillance and control along migration routes and in surrounding regions.

#### About the Author

Dr. Jaramillo-Ochoa is an epidemiologist working for the Ministry of Health for the Health District of the city of Machala, El Oro Province, Ecuador. His primary research interests include the epidemiology of vectorborne diseases and monitoring and evaluating vector-control interventions.

#### References

1. Ashley EA, Pyae Phyo A, Woodrow CJ. Malaria. *Lancet*. 2018; 391:1608–21. [http://dx.doi.org/10.1016/S0140-6736\(18\)30324-6](http://dx.doi.org/10.1016/S0140-6736(18)30324-6)
2. World Health Organization. World malaria report 2018. Geneva: The Organization; 2018.
3. Recht J, Siqueira AM, Monteiro WM, Herrera SM, Herrera S, Lacerda MVG. Malaria in Brazil, Colombia, Peru and Venezuela: current challenges in malaria control and elimination. *Malar J*. 2017;16:273. <http://dx.doi.org/10.1186/s12936-017-1925-6>
4. Krisner LK, Krisner J, Ambuludi M, Arichabala A, Beltrán-Ayala E, Navarrete P, et al. Successful malaria elimination in the Ecuador–Peru border region: epidemiology and lessons learned. *Malar J*. 2016;15:573. <http://dx.doi.org/10.1186/s12936-016-1630-x>
5. World Health Organization. World malaria report 2014: Ecuador. Geneva: The Organization; 2014.
6. Ministerio de Salud Pública de Ecuador. Gaceta Vectorial SE 1–52, 2017. 2018 Jan 3 [cited 2018 Apr 15]. <https://www.salud.gob.ec/wp-content/uploads/2017/07/Gaceta-Vectorial-SE52.pdf>
7. Hotez PJ, Basañez MG, Acosta-Serrano A, Grillet ME. Venezuela and its rising vector-borne neglected diseases. *PLoS Negl Trop Dis*. 2017;11:e0005423. <http://dx.doi.org/10.1371/journal.pntd.0005423>
8. Grillet ME, Villegas L, Oletta JF, Tami A, Conn JE. Malaria in Venezuela requires response. *Science*. 2018;359:528.
9. Ryan SJ, Lippi CA, Boersch-Supan PH, Heydari N, Silva M, Adrian J, et al. Quantifying seasonal and diel variation in

*Anopheline* and *Culex* human biting rates in southern Ecuador.

10. Malar J. 2017;16:479. <http://dx.doi.org/10.1186/s12936-017-2121-4>
10. Frampton JE. Tafenoquine: first global approval. *Drugs*. 2018;78:1517–23. <http://dx.doi.org/10.1007/s40265-018-0979-2>

Address for correspondence: Anna M. Stewart-Ibarra, Institute for Global Health & Translational Science, State University of New York Upstate Medical University, 505 Irving Ave, Syracuse, NY 13210, USA; email: [stewart@upstate.edu](mailto:stewart@upstate.edu)

## ***Rickettsia parkeri* and *Candidatus Rickettsia andeanae* in Ticks of the *Amblyomma maculatum* Group, Mexico**

Jesús Delgado-de la Mora,<sup>1</sup>  
Sokani Sánchez-Montes,<sup>1</sup>  
Jesús D. Licona-Enríquez,<sup>1</sup>  
David Delgado-de la Mora,<sup>1</sup>  
Christopher D. Paddock, Lorenza Beati,  
Pablo Colunga-Salas, Carmen Guzmán-Cornejo,  
María L. Zambrano, Sandor E. Karpathy,  
Andrés M. López-Pérez,  
Gerardo Álvarez-Hernández

Author affiliations: Instituto Nacional de Ciencias Médicas y Nutrición Salvador Zubirán, Mexico City, Mexico (J. Delgado-de la Mora); Universidad Nacional Autónoma de México, Mexico City (S. Sánchez-Montes, P. Colunga-Salas, C. Guzmán-Cornejo, A.M. López-Pérez); Centro Médico Nacional Siglo XXI, Mexico City (J.D. Licona-Enríquez); Instituto Tecnológico de Sonora, Sonora, Mexico (D. Delgado-de la Mora); Centers for Disease Control and Prevention, Atlanta, Georgia, USA (C.D. Paddock, M.L. Zambrano, S.E. Karpathy); Georgia Southern University, Statesboro, Georgia, USA (L. Beati); Universidad de Sonora, Sonora (G. Álvarez-Hernández)

DOI: <https://doi.org/10.3201/eid2504.181507>

We report *Rickettsia parkeri* and *Candidatus Rickettsia andeanae* in ticks of the *Amblyomma maculatum* group collected from dogs in Sonora, Mexico. Molecular characterization of these bacteria was accomplished by DNA amplification and sequence analysis of portions of the rickettsial genes *gltA*, *htrA*, *ompA*, and *ompB*.

<sup>1</sup>These authors contributed equally to this article.

*Rickettsia parkeri*, a member of the spotted fever group *Rickettsia* (SFGR), was initially identified in *Amblyomma maculatum* ticks in 1937, but not until 2004 was the first confirmed human infection reported (1). Through 2018, at least 9 cases of *R. parkeri* rickettsiosis have been identified across several mountainous locations in southern Arizona close to the US–Mexico border, and ticks of the *A. maculatum* group infected with *R. parkeri* have been collected from this region (2).

Epidemic levels of Rocky Mountain spotted fever (RMSF), a severe and frequently fatal spotted fever rickettsiosis, have been identified throughout regions of northern Mexico, including the state of Sonora (3). *R. rickettsii* (the agent of RMSF) is the only SFGR species linked with spotted fever rickettsiosis in Sonora; nonetheless, a unique lineage of *R. parkeri* associated with the *Dermacentor parumapertus* tick was reported recently from northern Mexico (4). Sonora shares an international border with Arizona; the recent identification of *R. parkeri* in *Amblyomma* ticks in southern Arizona (2) prompted our investigation during July 2016 for ticks in northern Sonora to determine whether another pathogenic SFGR species could also exist in Mexico.

The study area comprised 3 localities in Sonora (Yecora, 28°22'16"N, 108°55'32"W; Matarachi, 28°73'54"N, 108°95'87"W; and Mulatos, 28°65'85"N, 108°74'78"W) (Figure), each with a humid subtropical climate situated at ≈1,500 m, with vegetation comprising predominantly oak forests and grasslands (Appendix Figure, panel A, <https://wwwnc.cdc.gov/EID/article/25/4/18-1507-App1.pdf>). During August 2016 and September 2017, we inspected free-roaming dogs (*Canis lupus familiaris*) for attached or crawling ticks (Appendix Figure, panel B). We identified ticks using morphological characteristics (5).

For ticks collected in 2016, we dissected a portion of the posterolateral idiosoma from each specimen and extracted DNA using a DNeasy Blood and Tissue Kit (QIAGEN, <https://www.qiagen.com>). We screened DNA extracts using a *Rickettsia* genus-specific real-time PCR with primers PanR8\_F and PanR8\_R, probe PanR8\_P (6), and 5 μL of DNA template. Samples with cycle threshold values <40 were tested by a PCR targeting a segment of the *ompA* gene using primers Rr190.70p and 190–701 (7). We also tested 1 positive sample using a nested PCR to amplify a segment of the 17-kDa antigen gene with primers R17122 and R17500 (8) in the primary amplification and TZ15 and TZ16 (9) in the nested amplification. Specimens collected in 2017 were processed similarly; however, we screened DNA extracts using a conventional PCR to amplify a segment of the *gltA* gene (4). We subsequently tested positive samples by conventional PCRs targeting fragments of the *ompA* and *ompB*, genes using primers and conditions described elsewhere (4). PCR products were sequenced using an ABI 3500 genetic analyzer with a BigDye Terminator v3.1 Cycle Sequencing Kit (Applied Biosystems, <https://www.thermofisher.com>). Sequences were assembled using Geneious R10 (Biomatters Ltd., <https://www.geneious.com>) and compared with GenBank data using blastn analysis (<http://blast.ncbi.nlm.nih.gov/Blast.cgi>).

We collected a total of 31 *A. maculatum* group ticks from northern Sonora (14 specimens from Yecora in 2016 and 17 from Matarachi and Mulatos in 2017). Three ticks collected in 2017 were deposited as voucher specimens in the Colección del Laboratorio de Acarología, Universidad Nacional Autónoma de México (Mexico City, Mexico).

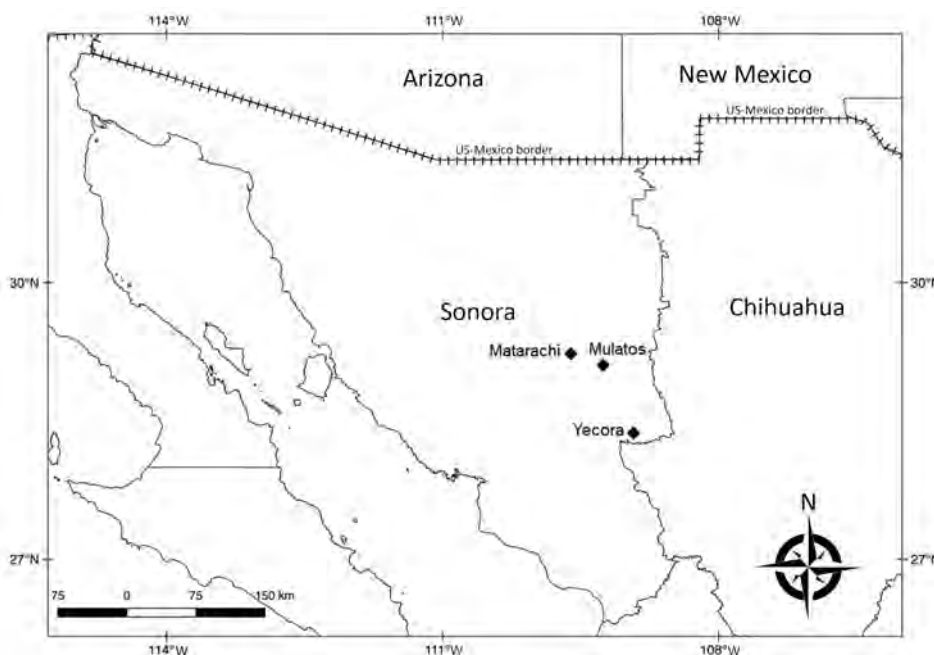


**Figure.** Locations where ticks of the *Amblyomma maculatum* group were collected (diamonds) in a study of *Rickettsia parkeri* and *Candidatus Rickettsia andeanae*, Sonora, Mexico. A layer of Google Maps was used to construct the figure.



We amplified a sequence demonstrating complete identity to the homologous 590-bp segment of the *ompA* gene of *R. parkeri* strain Maculatum 20 (GenBank accession no. U43802) from 1 (7%) of 14 ticks collected in 2016. We further amplified sequences demonstrating complete identities to the homologous segments of the *ompA* (590 bp) and 17-kDa antigen (208 bp) genes of *Candidatus Rickettsia andeanae* (GenBank accession nos. KF179352 and KY402193, respectively) from another tick in this group and sequences revealing complete identity to each other and to the homologous segments of the *gltA* (760 bp), *ompB* (760 bp), and *ompA* (490 bp) genes of *R. parkeri* strain Portsmouth (GenBank accession no. CP003341.1) from 10 (71%) of 14 ticks evaluated from the 2017 collection.

We identified DNA of *R. parkeri* and *Candidatus Rickettsia andeanae* in *A. maculatum* group ticks in northern Sonora. *R. parkeri* causes a disease less severe than RMSF and should be suspected in patients with an eschar, rash, and lymphadenopathy (1). The results of this investigation suggest that *R. parkeri* could contribute to at least some of the cases of spotted fever rickettsiosis described in Sonora and possibly in other regions of Mexico where *A. maculatum* group ticks are found. Differentiation between these 2 diseases is important, principally because there are no reports of fatal disease caused by *R. parkeri*. Nonetheless, clinical suspicion of any SFGR requires immediate treatment with doxycycline. *Candidatus Rickettsia andeanae*, a SFGR of undetermined pathogenicity, has been detected in the United States and Central and South America (2,10). Our findings highlight the need for specific diagnostic tests for SFGR in Mexico that can identify other potential SFGR of public health concern in this country.

#### About the Author

Dr. Delgado-de la Mora is a researcher and resident of Pathology at Instituto Nacional de Ciencias Médicas y Nutrición Salvador Zubirán. His research interests include tickborne diseases, particularly those caused by *Rickettsia* spp.

#### References

- Paddock CD, Sumner JW, Comer JA, Zaki SR, Goldsmith CS, Goddard J, et al. *Rickettsia parkeri*: a newly recognized cause of spotted fever rickettsiosis in the United States. *Clin Infect Dis*. 2004;38:805–11. <http://dx.doi.org/10.1086/381894>
- Allerdice MEJ, Beati L, Yaglom H, Lash RR, Delgado-de la Mora J, Licona-Enriquez JD, et al. *Rickettsia parkeri* (Rickettsiales: Rickettsiaceae) detected in ticks of the *Amblyomma maculatum* (Acari: Ixodidae) group collected from multiple locations in southern Arizona. *J Med Entomol*. 2017;54:1743–9. <http://dx.doi.org/10.1093/jme/tjx138>
- Álvarez-Hernández G, Roldán JFG, Milan NSH, Lash RR, Behravesh CB, Paddock CD. Rocky Mountain spotted fever in Mexico: past, present, and future. *Lancet Infect Dis*. 2017;17:e189–96. [http://dx.doi.org/10.1016/S1473-3099\(17\)30173-1](http://dx.doi.org/10.1016/S1473-3099(17)30173-1)
- Sánchez-Montes S, López-Pérez AM, Guzmán-Cornejo C, Colunga-Salas P, Becker I, Delgado-de la Mora J, et al. *Rickettsia parkeri* in *Dermacentor parumapertus* ticks, Mexico. *Emerg Infect Dis*. 2018;24:1108–11. <http://dx.doi.org/10.3201/eid2406.180058>
- Lado P, Nava S, Mendoza-Urbe L, Caceres AG, Delgado-de la Mora J, Licona-Enriquez JD, et al. The *Amblyomma maculatum* Koch, 1844 (Acari: Ixodidae) group of ticks: phenotypic plasticity or incipient speciation? *Parasites Vectors*. 2018;11:610.
- Kato CY, Chung IH, Robinson LK, Austin AL, Dasch GA, Massung RF. Assessment of real-time PCR assay for detection of *Rickettsia* spp. and *Rickettsia rickettsii* in banked clinical samples. *J Clin Microbiol*. 2013;51:314–7. <http://dx.doi.org/10.1128/JCM.01723-12>
- Regnery RL, Spruill CL, Plikaytis BD. Genotypic identification of rickettsiae and estimation of intraspecies sequence divergence for portions of two rickettsial genes. *J Bacteriol*. 1991;173:1576–89. <http://dx.doi.org/10.1128/jb.173.5.1576-1589.1991>
- Massung RF, Davis LE, Slater K, McKechnie DB, Puerzer M. Epidemic typhus meningitis in the southwestern United States. *Clin Infect Dis*. 2001;32:979–82. <http://dx.doi.org/10.1086/319351>
- Tzianabos T, Anderson BE, McDade JE. Detection of *Rickettsia rickettsii* DNA in clinical specimens by using polymerase chain reaction technology. *J Clin Microbiol*. 1989;27:2866–8.
- Paddock CD, Fournier PE, Sumner JW, Goddard J, Elshenawy Y, Metcalfe MG, et al. Isolation of *Rickettsia parkeri* and identification of a novel spotted fever group *Rickettsia* sp. from Gulf Coast ticks (*Amblyomma maculatum*) in the United States. *Appl Environ Microbiol*. 2010;76:2689–96. <http://dx.doi.org/10.1128/AEM.02737-09>

Address for correspondence: Jesús Delgado-de la Mora, Instituto Nacional de Ciencias Médicas y Nutrición Salvador Zubirán, Departamento de Anatomía Patológica, Avenida Vasco de Quiroga 15, Belisario Domínguez, C.P. 14080, Mexico City, Mexico; email: [jdeldadom1992@gmail.com](mailto:jdeldadom1992@gmail.com)

## Reduced Susceptibility to Neuraminidase Inhibitors in Influenza B Isolate, Canada

Yacine Abed,<sup>1</sup> Clément Fage,<sup>1</sup> Patrick Lagüe,<sup>1</sup> Julie Carbonneau, Jesse Papenburg, Donald C. Vinh, Guy Boivin

Author affiliations: Laval University, Québec City, Québec, Canada (Y. Abed, C. Fage, P. Lagüe, J. Carbonneau, G. Boivin); Montreal Children's Hospital, Montreal, Québec (J. Papenburg); McGill University Health Center, Montreal (D.C. Vinh)

DOI: <https://doi.org/10.3201/eid2504.181554>

<sup>1</sup>These authors contributed equally to this article.

We identified an influenza B isolate harboring a Gly407Ser neuraminidase substitution in an immunocompromised patient in Canada before antiviral therapy. This mutation mediated reduced susceptibility to oseltamivir, zanamivir, and peramivir, most likely by preventing interaction with the catalytic Arg374 residue. The potential emergence of such variants emphasizes the need for new antivirals.

Neuraminidase inhibitors (NAIs) are recommended for the control of severe influenza A and B infections (1). Nevertheless, antiviral resistance may emerge in immunocompromised persons, with major clinical implications (2).

In 2017–18, influenza B/Yamagata/16/88-like strains accounted for 50% of seasonal infections in Canada (3). In March 2018, we identified an influenza B/Yamagata/16/88-like variant containing a Gly407Ser NA substitution conferring reduced susceptibility to various NAIs. This variant was recovered from an immunocompromised patient before NAI therapy.

The 62-year-old woman, who had non-Hodgkin lymphoma, underwent an autologous stem cell transplant in February 2017. In March 2018, she developed therapy-related acute myeloid leukemia that failed to respond to cytarabine treatment. During hospitalization, she had influenza-like symptoms, with confirmed influenza B detection by RT-PCR. Oseltamivir (75 mg 2×/d) was administered during March 27, 2018–April 4, 2018. Because the patient's respiratory symptoms worsened and influenza B persisted despite treatment, we replaced oseltamivir with intravenous zanamivir (600 mg 2×/d) but switched back to oseltamivir because of respiratory distress episodes. Ultimately, the patient opted to stop treatment and died a few days later.

We sequenced the viral hemagglutinin (HA) and NA genes from nasopharyngeal swab specimens using the ABI 3730 analyzer (Thermo Fisher, <https://www.thermofisher.com>). The HA (GenBank accession no. MH450013) and NA (GenBank accession no. MH449670) sequences from the March 27, 2018, specimen (pretherapy: B/Quebec/1182C/2018) were identical

to the April 4, 2018, specimen (day 9 of oseltamivir therapy), sharing 99.5% aa identity with the HA (GenBank accession no. EPI544262) and 98.7% with the NA (GenBank accession no. EPI544263) of the B/Phuket/3073/2013 vaccine strain. Both clinical samples contained a Gly407Ser NA substitution, a marker of NAI resistance (4). We cloned the NA gene from pre- and post-oseltamivir therapy viruses into pJET cloning plasmid and sequenced 15 clones per virus. All NA clones contained the Gly407Ser mutation.

We used an unrelated 2018 isolate (B/Quebec/88855/2018; GenBank accession nos. MH450019 for HA, MH450017 for NA) as a wild-type control for further in vitro characterization. B/Quebec/88855/2018 (wild-type) and B/Quebec/1182C/2018 (Gly407Ser) shared 99.8% aa HA and 99.4% aa NA identities.

We determined NAI 50% inhibitory concentrations ( $IC_{50}$ s) of isolates using fluorometric-based NA inhibition assays (5) and evaluated their NA activity ( $V_{max}$  [maximum velocity of substrate conversion]) by performing enzyme kinetics experiments (6). B/Quebec/1182C/2018 demonstrated reduced inhibition (RI; 5- to 50-fold increases in  $IC_{50}$  over wild-type) (4) to oseltamivir, zanamivir, and peramivir, showing 5.97-, 32.44-, and 38.34-fold increases in  $IC_{50}$ s, respectively, over B/Quebec/88855/2018 WT (Table). The last 2 isolates had similar NA activity ( $V_{max}$ ) (Table). To confirm the role of the Gly407Ser mutation, we expressed the recombinant wild-type and Gly407Ser mutant proteins (obtained by PCR-mediated mutagenesis) in 293T cells (7) and found that Gly407Ser also increased oseltamivir, zanamivir, and peramivir  $IC_{50}$  levels by 4.16-, 10.07- and 16.36-fold, respectively (Table).

We next evaluated replication kinetics of the wild-type and Gly407Ser isolates in ST6Gall-MDCK cells. Mean viral titers obtained with wild-type isolates were higher than the mutant at 24 and 48 h postinfection ( $p < 0.01$ ); comparable titers were obtained at 72 and 96 h postinfection (Appendix Figure 1, <http://wwwnc.cdc.gov/EID/article/25/4/18-1554-App1.pdf>). To assess genetic stability, we sequenced the HA/NA genes after 4 passages in

**Table.** Susceptibility profiles and NA activity of influenza B virus isolates and susceptibility profiles of recombinant influenza B NAs determined by assays using the fluorescent MUNANA substrate, Canada\*

Sample type	$IC_{50}$ in nM $\pm$ SD (fold increase) [phenotype]†			NA activity, $V_{max}$ ‡
	Oseltamivir	Zanamivir	Peramivir	
Clinical isolate				
B/Phuket/3073/2013, vaccine	18.98 $\pm$ 3.89	0.70 $\pm$ 0.17	0.74 $\pm$ 0.02	ND
B/Québec/88855/2018, WT	17.47 $\pm$ 1.43 (1) [NI]	0.85 $\pm$ 0.09 (1) [NI]	0.92 $\pm$ 0.09 (1) [NI]	2.24 $\pm$ 0.3
B/Québec/1182C/2018, Gly407Ser	104 $\pm$ 14.62 (5.97) [RI]	27.58 $\pm$ 2.56 (32.44) [RI]	26.08 $\pm$ 0.1 (38.34) [RI]	2.18 $\pm$ 0.47
Recombinant neuraminidase				
B/Quebec/88855/2018, WT	11.16 $\pm$ 5.25 (1) [NI]	0.97 $\pm$ 0.27 (1) [NI]	0.76 $\pm$ 0.19 (1) [NI]	ND
B/Quebec/88855/2018, Gly407Ser	46.52 $\pm$ 12.58 (4.16) [NI]	9.77 $\pm$ 0.90 (10.07) [RI]	12.44 $\pm$ 5.47 (16.36) [RI]	ND

\*Values are from a representative experiment performed in duplicate.  $IC_{50}$ , 50% inhibitory concentration; MUNANA, 2'-(4-methylumbelliferyl)- $\alpha$ -D-N-acetylneuraminic acid; NA, neuraminidase; NAI, neuraminidase inhibitor; ND, not done; NI, normal inhibition ( $\leq 5$ -fold increase in  $IC_{50}$  over WT); RI, reduced inhibition (5- to 50-fold increase in  $IC_{50}$  over WT);  $V_{max}$ , maximum velocity of substrate conversion; WT, wild type.

†The phenotype of susceptibility to NAI following the World Health Organization guidelines.

‡Numbers indicate mean  $V_{max}$  values (U/sec)  $\pm$  SD of a kinetics experiment performed in triplicate.

ST6GalI-MDCK cells and found that Gly407Ser was conserved with no additional sequence alterations, suggesting genetic stability of the NA mutant.

Finally, we performed molecular dynamics simulations for deciphering the mechanism of cross-RI displayed by Gly407Ser (Appendix). Our model suggests that Gly407Ser affects interaction networks involving a key arginine residue within the NA active site (Arg374) (8) and neighboring residues (Appendix Figure 2). In the wild-type protein, Arg374 forms hydrogen bonds with NAIs (Appendix Figure 2, panels A–C). There is a hydrogen bond between the Gly407 amine and the Arg374 carbonyl, and between the Trp408 amine and the Glu428 carbonyl, in addition to hydrophobic interactions between Trp408 and Val430 side chains. In the Gly407Ser variant, the orientation of Arg374 prevents hydrogen bond formation with NAIs (Appendix Figure 2, panels D–F). A hydrogen bond exists between the Ser407 amine and the Arg374 carbonyl and between the Ser407 side chain hydroxyl and the Glu428 carbonyl, in addition to hydrophobic interactions between the Trp408 and the Arg374 side chains.

In 2007, a Gly407Ser influenza B variant was recovered from a child after 3 days of oseltamivir therapy (9). That variant displayed 4- and 7-fold increases in oseltamivir and zanamivir  $IC_{50}$  levels, respectively, with an unexplained mechanism (9). Here, we identified a contemporary Gly407Ser influenza B variant in a patient before NAI therapy and propose a molecular mechanism for such a cross-RI phenotype. We cannot exclude nosocomial transmission of this virus despite evidence for some alteration in replication kinetics. The Gly407Ser mutation was detected in the absence of NAI constituting 100% of sequenced clones, did not affect NA activity, and was conserved after *in vitro* passages. Thus, such a variant may retain efficient transmissibility. Nevertheless, the effect of this mutation in a suitable animal model (ferrets) remains to be assessed. The potential for emergence of variants with cross-RI to available NAIs in the absence of treatment emphasizes the need for novel antiviral strategies (including combinations) against influenza B viruses.

This work was supported by a Canadian Institutes of Health Research (CIHR) foundation grant to G.B. (grant No. 229733) for a research program on the pathogenesis, treatment, and prevention of respiratory and herpes viruses.

### About the Author

Dr. Abed is an associate professor at the Research Center of Infectious Diseases of the CHU de Québec-Laval University in Québec City, Quebec, Canada. His research interests include influenza A and B infections and mechanisms of antiviral resistance.

### References

1. Samson M, Pizzorno A, Abed Y, Boivin G. Influenza virus resistance to neuraminidase inhibitors. *Antiviral Res.* 2013;98:174–85. <http://dx.doi.org/10.1016/j.antiviral.2013.03.014>
2. Abed Y, Boivin G. A review of clinical influenza A and B infections with reduced susceptibility to both oseltamivir and zanamivir. *Open Forum Infect Dis.* 2017;4:ofx105. <http://dx.doi.org/10.1093/ofid/ofx105>
3. Skowronski DM, Chambers C, De Serres G, Dickinson JA, Winter AL, Hickman R, et al. Early season co-circulation of influenza A(H3N2) and B(Yamagata): interim estimates of 2017/18 vaccine effectiveness, Canada, January 2018. *Euro Surveill.* 2018;23. <http://dx.doi.org/10.2807/1560-7917.ES.2018.23.5.18-00035>
4. WHO. Global monitoring of antiviral resistance in currently circulating human influenza viruses, November 2011. *Wkly Epidemiol Rec.* 2011;86:497–501.
5. Samson M, Abed Y, Desrochers FM, Hamilton S, Luttick A, Tucker SP, et al. Characterization of drug-resistant influenza virus A(H1N1) and A(H3N2) variants selected *in vitro* with laninamivir. *Antimicrob Agents Chemother.* 2014;58:5220–8. <http://dx.doi.org/10.1128/AAC.03313-14>
6. Marathe BM, Lévêque V, Klumpp K, Webster RG, Govorkova EA. Determination of neuraminidase kinetic constants using whole influenza virus preparations and correction for spectroscopic interference by a fluorogenic substrate. *PLoS One.* 2013;8:e71401. <http://dx.doi.org/10.1371/journal.pone.0071401>
7. Abed Y, Baz M, Boivin G. Impact of neuraminidase mutations conferring influenza resistance to neuraminidase inhibitors in the N1 and N2 genetic backgrounds. *Antivir Ther.* 2006;11:971–6.
8. Varghese JN, McKimm-Breschkin JL, Caldwell JB, Kortt AA, Colman PM. The structure of the complex between influenza virus neuraminidase and sialic acid, the viral receptor. *Proteins.* 1992;14:327–32. <http://dx.doi.org/10.1002/prot.340140302>
9. Hatakeyama S, Sugaya N, Ito M, Yamazaki M, Ichikawa M, Kimura K, et al. Emergence of influenza B viruses with reduced sensitivity to neuraminidase inhibitors. *JAMA.* 2007;297:1435–42. <http://dx.doi.org/10.1001/jama.297.13.1435>

Address for correspondence: Guy Boivin, CHU de Québec-Université Laval, CHUL, 2705 blvd Laurier, Sainte-Foy, RC-709, Québec City, QC G1V 4G2, Canada; email: [guy.boivin@crchul.ulaval.ca](mailto:guy.boivin@crchul.ulaval.ca)



## Combination of Clindamycin and Azithromycin as Alternative Treatment for *Toxoplasma gondii* Encephalitis

Daisuke Shiojiri, Ei Kinai, Katsuji Teruya, Yoshimi Kikuchi, Shinichi Oka

Author affiliation: National Centre for Global Health and Medicine, Tokyo, Japan

DOI: <https://doi.org/10.3201/eid2504.181689>

Current standard therapies for toxoplasmic encephalitis often cause severe adverse events. A 57-year-old HIV-positive man in Japan who had toxoplasmic encephalitis but was intolerant to trimethoprim/sulfamethoxazole, pyrimethamine, sulfadiazine, and atovaquone was successfully treated with the combination of clindamycin and azithromycin. This drug combination can be an alternative treatment for this condition.

Current treatment guidelines for toxoplasmic encephalitis (TE) (1) recommend either pyrimethamine plus sulfadiazine or pyrimethamine plus clindamycin; trimethoprim/sulfamethoxazole is also known to have comparable potency (2). However, kidney, liver, and hematologic toxicity, as well as hypersensitivities, often have been reported (2), and few alternatives are available. We report a TE patient who experienced severe toxicity after all standard regimens but was successfully treated with a combination of clindamycin and azithromycin.

A 57-year-old man sought care at the National Centre for Global Health and Medicine (Tokyo, Japan) with fever and mild disorientation. On examination, he was febrile and drowsy with slurred speech. He did not exhibit any apparent focal neurologic deficits.

Blood laboratory test results (reference ranges) were as follows: hemoglobin, 10.4 g/dL (13.7–16.8 g/dL); total leukocyte count,  $6.81 \times 10^3$  cells/L ( $3.3\text{--}8.6 \times 10^3$  cells/L); platelet count,  $2.43 \times 10^5$ /L ( $1.58\text{--}3.48 \times 10^5$ /L);  $\beta$ -D-glucan, 118.4 pg/mL (<20.0 pg/mL); CD4<sup>+</sup> count, 58 cells/ $\mu$ L (500–1,500 cells/ $\mu$ L); and HIV RNA,  $5.1 \times 10^5$  copies/mL (undetected). Brain magnetic resonance imaging results indicated 3 lesions with high intensity on T2-weighted images and irregular ring enhancement. The lesions were in the right frontal lobe (diameter 15.6 mm), left globus pallidus (diameter 17.5 mm), and body of the caudate nucleus extending to the left thalamus (diameter 16.2 mm; Figure, panel A). For cerebrospinal fluid (CSF), laboratory test results (reference ranges) were as follows: leukocyte count 0.3 cells/mm<sup>3</sup> (0–5 cells/mm<sup>3</sup>); protein, 39

mg/dL (15.8–52.6 mg/dL); glucose, 54 mg/dL (47–69 mg/dL); and adenosine deaminase, 2.2 U/L (0–20 U/L). Results of real-time PCR were negative for *Mycobacterium*, Epstein–Barr virus, cytomegalovirus, herpes simplex virus, and JC virus in CSF. Despite mild elevation of  $\beta$ -D-glucan, results of cryptococcal antigen testing were negative. No brain biopsy was performed. Although serum toxoplasma IgM and IgG titers were initially negative, IgG seroconversion was observed in serial tests 6 months (9.2 IU/mL) and 12 months (39.7 IU/mL) later. Toxoplasma nucleic acid in CSF was detected using a loop-mediated isothermal amplification technique (LAMP) with previously validated methods (3).

Trimethoprim/sulfamethoxazole (10 mg/kg/d trimethoprim) was first initiated because of limited availability of pyrimethamine plus sulfadiazine at the time, but acute liver toxicity developed on treatment day 6 (increases in levels of aminotransferase/alanine aminotransferase from 24/20 IU/L to 127/145 IU/L [reference 10–42 IU/L]). Pyrimethamine plus sulfadiazine was started on treatment day 7. However, on day 9, acute renal failure developed because of obstructive urolithiasis caused by sulfadiazine crystals. After the patient was switched to pyrimethamine plus clindamycin, his renal function persistently worsened, and a drug-induced lymphocyte stimulation test suggested that pyrimethamine was responsible for the acute renal failure. A switch to atovaquone on treatment day 12 resulted in thrombocytopenia by day 17.

After switching to the combination of clindamycin (2,400 mg/d) and azithromycin (1,200 mg/d), the patient did not experience any apparent adverse effects or show abnormal laboratory values. He successfully started antiretroviral therapy for his HIV infection during week 6. Repeated brain magnetic resonance imaging performed 1, 3, and 8 months after presentation showed all lesions had substantially decreased, and only a residual nonenhancing lesion was observed 12 months after presentation (Figure, panels B–D). The patient has continued maintenance therapy with the same dose of clindamycin and azithromycin without any symptoms of relapse or immune reconstitution inflammatory syndrome.

Several reports have documented the high prevalence of various adverse events associated with the aforementioned standard therapies for TE (2,4), but little information is available regarding the efficacy of alternative drugs. Although atovaquone is the only safe alternative agent for which efficacy and safety have been relatively well established, it has been proven to be less potent than standard therapies (5).

Clindamycin has in vitro activity against *Toxoplasma gondii*, inhibitory effects in vivo at lower concentrations (6), and the ability to penetrate into CSF (7), suggesting that it is a promising alternative agent for TE treatment. More important,

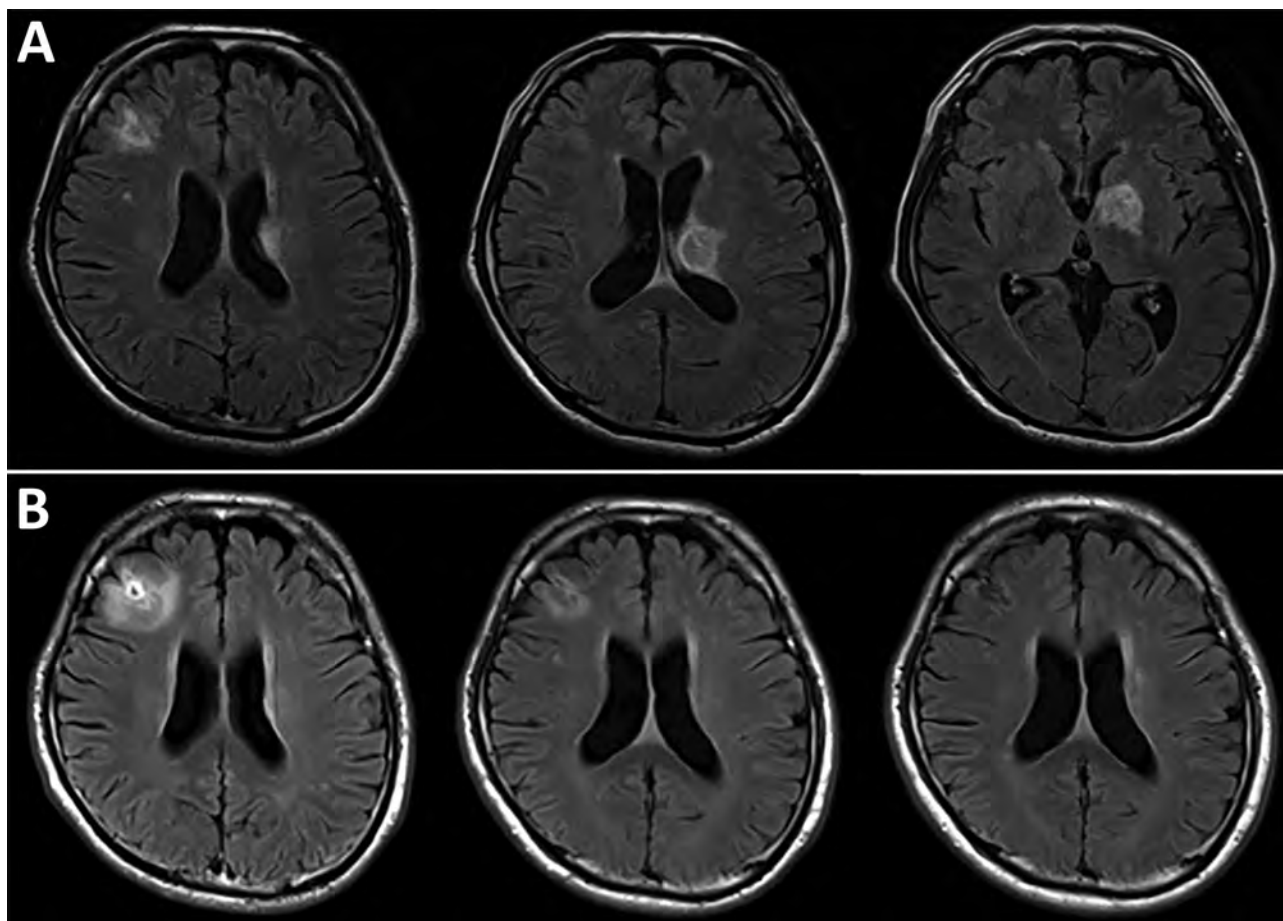


**Figure.** Serial brain magnetic resonance imaging results for a 57-year-old man with *Toxoplasma gondii* encephalitis, Tokyo, Japan. A) All 3 lesions were evident when the patient first sought care. B) Chronologic changes are shown of the lesion in the right frontal lobe in response to antitoxoplasmic therapy after 1 (left), 3 (center), and 12 (right) months.

clindamycin causes far fewer adverse events than sulfadiazine (2,4). Although the potency of clindamycin monotherapy has not been assessed, some case reports suggested its effectiveness (8). Therefore, a clindamycin-containing combination with potent agents other than pyrimethamine may be a reasonable treatment option for TE treatment.

Macrolides also have displayed substantial *in vitro* efficacy against *T. gondii* (9). A phase I/II dose-escalation study of oral azithromycin in combination with pyrimethamine revealed the relative efficacy and safety of the regimen (10). Azithromycin combined with a potent agent other than pyrimethamine, such as clindamycin, can be theoretically expected to be a safe and effective option. Further study should be conducted to establish safer treatment options for TE.

The continuous reduction in the size of the lesion in the patient we report was partly explained by his good immune recovery. Our results suggest that the combination of clindamycin and macrolides could be a safer and potent alternative therapy for patients who are intolerant of current standard regimens.

#### Acknowledgments

We thank Tokio Hoshina for detecting *Toxoplasma* nucleic acid by LAMP.

#### About the Author

Dr. Shiojiri is a fellow at the AIDS Clinical Centre, National Centre for Global Health and Medicine, Tokyo, Japan. His primary research interests include anal human papillomavirus infection and anal precancer among men who have sex with men in Japan.

#### References

1. US Department of Health and Human Services. Guidelines for the prevention and treatment of opportunistic infections in HIV-infected adults and adolescents [cited 2018 Aug 23]. <https://aidsinfo.nih.gov/guidelines>
2. Hernandez AV, Thota P, Pellegrino D, Pasupuleti V, Benites-Zapata VA, Deshpande A, et al. A systematic review and meta-analysis of the relative efficacy and safety of treatment regimens for HIV-associated cerebral toxoplasmosis: is trimethoprim-sulfamethoxazole a real option? *HIV Med.* 2017;18:115–24. <http://dx.doi.org/10.1111/hiv.12402>

3. Fallahi S, Seyyed Tabaei SJ, Pourmia Y, Zebardast N, Kazemi B. Comparison of loop-mediated isothermal amplification (LAMP) and nested-PCR assay targeting the RE and B1 gene for detection of *Toxoplasma gondii* in blood samples of children with leukaemia. *Diagn Microbiol Infect Dis*. 2014;79:347–54. <http://dx.doi.org/10.1016/j.diagmicrobio.2014.02.014>
4. Katlama C, De Wit S, O'Doherty E, Van Glabeke M, Clumeck N; The European Network for Treatment of AIDS (ENTA) Toxoplasmosis Study Group. Pyrimethamine-clindamycin vs. pyrimethamine-sulfadiazine as acute and long-term therapy for toxoplasmic encephalitis in patients with AIDS. *Clin Infect Dis*. 1996;22:268–75. <http://dx.doi.org/10.1093/clinids/22.2.268>
5. Katlama C, Mouthon B, Gourdon D, Lapierre D, Rousseau F; Atovaquone Expanded Access Group. Atovaquone as long-term suppressive therapy for toxoplasmic encephalitis in patients with AIDS and multiple drug intolerance. *AIDS*. 1996;10:1107–12.
6. Fichera ME, Bhopale MK, Roos DS. In vitro assays elucidate peculiar kinetics of clindamycin action against *Toxoplasma gondii*. *Antimicrob Agents Chemother*. 1995;39:1530–7. <http://dx.doi.org/10.1128/AAC.39.7.1530>
7. Gatti G, Malena M, Casazza R, Borin M, Bassetti M, Cruciani M. Penetration of clindamycin and its metabolite N-demethyl-clindamycin into cerebrospinal fluid following intravenous infusion of clindamycin phosphate in patients with AIDS. *Antimicrob Agents Chemother*. 1998;42:3014–7. <http://dx.doi.org/10.1128/AAC.42.11.3014>
8. Yapar N, Erdenizmenli M, Oğuz VA, Cakir N, Yüce A. Cerebral toxoplasmosis treated with clindamycin alone in an HIV-positive patient allergic to sulfonamides. *Int J Infect Dis*. 2005;9:64–6. <http://dx.doi.org/10.1016/j.ijid.2004.05.004>
9. Neville AJ, Zach SJ, Wang X, Larson JJ, Judge AK, Davis LA, et al. Clinically available medicines demonstrating anti-toxoplasma activity. *Antimicrob Agents Chemother*. 2015;59:7161–9. <http://dx.doi.org/10.1128/AAC.02009-15>
10. Jacobson JM, Hafner R, Remington J, Farthing C, Holden-Wiltse J, Bosler EM, et al.; ACTG 156 Study Team. Dose-escalation, phase I/II study of azithromycin and pyrimethamine for the treatment of toxoplasmic encephalitis in AIDS. *AIDS*. 2001;15:583–9. <http://dx.doi.org/10.1097/00002030-200103300-00007>

Address for correspondence: Daisuke Shiojiri, AIDS Clinical Centre, National Centre for Global Health and Medicine, 1-21-1, Toyama, Shinjuku-ku, Tokyo 192-8655, Japan; email: dshiojiri@hosp.ncgm.go.jp

prions *Plasmodium knowlesi* cholera tularemia  
*Eptesicus fuscus* syncytium *Klebsiella*  
 Kaposi *Leptospira* sapovirus yaws *Rickettsia*  
*Vibrio vulnificus* Quinine variola *Campylobacter* *Acinetobacter*  
 Chagas disease rotavirus Lyssavirus *Aspergillus*  
 botulism *Escherichia coli* *Babesia* hemozoin  
 syphilis knemidocoptic mange *Naegleria fowleri* *Ehrlichia* Leishmaniasis  
*Anopheles* *Bordetella* rabies  
 Verona integrin vaccination Artemisinin Dengue *Shigella*  
 Borna disease virus Ebola *Francisella tularensis* typhus *Rickettsia*  
 orf *Coxiella burnetii* kobuvirus *Candida* Q fever  
*Orientia tsutsugamushi* Bocavirus chimera *Brucella*  
 Norovirus tuberculosis quarantine Mange tetanus  
 Malaria measles Chikungunya pertactin *Borrelia* Leprosy influenza  
 Calcivirus quarantine Peste des petits ruminants  
 melioidosis Diphtheria Onyong-nyong virus *Pseudoterranova* azarasi  
 pertussis Merkel cells *Ignatzschineria* Glanders *Yersinia*  
 featured **EMERGING**  
 monthly in **INFECTIOUS DISEASES** <http://wwwnc.cdc.gov/eid/articles/etymologia>



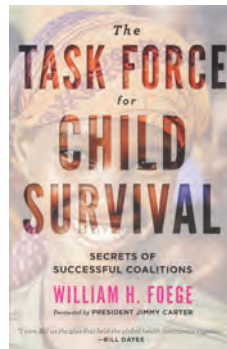
## The Task Force for Child Survival: Secrets of Successful Coalitions

William H. Foege; Johns Hopkins University Press, Baltimore, MD, USA, 2018; ISBN-10: 1421425602; ISBN-13: 978-1421425603; Pages: 160; Price: \$26.95

Well-written and inspirational, *The Task Force for Child Survival: Secrets of Successful Coalitions* is a firsthand perspective on the creation and history of one of the most successful coalitions in global health. An expert authority on vaccine programs and global health, author William H. Foege, former director of the US Centers for Disease Control and Prevention, was the lead architect of the Task Force.

Formed in 1984, the goal of the Task Force was to facilitate the work of the World Health Organization and UNICEF to improve global immunization coverage in children. At that time, 4.3 million deaths occurred per year, >12,000 children per day, from vaccine-preventable diseases measles, tetanus, and pertussis alone. To increase vaccine coverage, the Task Force had to overcome several complicated logistical issues, have an optimistic outlook despite the reality of what was feasible, and have the dedication of passionate individuals working as a team. Increasing vaccination coverage was a daunting task, yet they achieved success where other organizations had failed.

The Task Force also worked to increase access to Mectizan, a preventive medicine for onchocerciasis, also known as river blindness. Previous programs sought to control the black flies that transmit the disease-causing parasitic worm *Onchocerca volvulus*, without much success. The historical description of the Mectizan program, including how the drug was developed and donated free of charge by Merck



until the disease is eliminated, is captivating reading. The Task Force worked alongside Merck and became a crucial partner in the distribution and oversight of the drug, including surveillance for side effects. The program grew as the drug was shown to be safe and effective, reaching 6 million people within 4 years, and eventually 20 million people per year, with assistance from the World Bank.

A chronological account of the Task Force is the first aim of the book, which will be fascinating reading for those training or already working in global health, public health, infectious diseases, or immunization programs. The author's second purpose is to describe how successful coalitions develop and function. His insights are instructive reading for anyone currently a member of or tasked with creating a coalition or a collaborative endeavor. The short chapter "How Productive Coalitions Begin" and another, "Lessons Learned," contain crucial messages for building and sustaining functional coalitions, such as obtain commitment of partner agency leaders; have a shared, well-defined, and attainable goal (in this case 80% of the world's children would receive at least 1 vaccine by 1990); get input from those in the trenches on major barriers; prioritize good communications with all stakeholders; and emphasize the need for "ego suppression." Dr. Foege stresses that "guarding turf, seeking credit or becoming the spokesperson is hazardous to the health of the coalition." His description of great leadership and how successful coalitions and collaborations function underscores how vital both are to solving future problems in public health.

### Jane M. Gould

Author affiliation: Pennsylvania Department of Health, Harrisburg, Pennsylvania, USA

DOI: <http://dx.doi.org/10.3201/eid2504.181819>

Address for correspondence: Jane M. Gould, Pennsylvania Department of Health, Bureau of Epidemiology, 625 Forster St, Rm 912, Harrisburg, PA 17120-0012, USA; email: [c-jgould@pa.gov](mailto:c-jgould@pa.gov)



Untung Yuli Prastiawan (aka Wawan Geni) (1982–). *The Little Time*, 2017 (detail). Burning techniques applied to canvas, 35.4 in × 27.6 in/90 cm × 70 cm. Wawan Geni Collection. Digital image courtesy of Wawan Geni.

## Finesse and Fire, Creativity and Combustion

Byron Breedlove

The Republic of Indonesia is the world's fourth most populous country, the largest archipelago nation, one of the world's most biodiverse regions, and the country with the most active volcanoes. Vectorborne infections spread by mosquitoes pose a significant health burden for this equatorial nation. For Indonesia, World Health Organization data indicate that the incidence of malaria in 2015 was 26.10 new cases of malaria per 1,000 population at risk, 41st among all countries. Indonesia also has one of the highest burdens of dengue fever, and Japanese encephalitis and chikungunya are endemic there. Small wonder that a May 2014 article in the *Business Nikkei Asian Review* reports, "Some 4 billion mosquito coils are sold annually in the tropical archipelago."

Author affiliation: Centers for Disease Control and Prevention, Atlanta, Georgia, USA

DOI: <https://doi.org/10.3201/eid2504.AC2504>

Indonesian artist Untung Yuli Prastiawan, also known as Wawan Geni ("geni" in Javanese means fire), has purchased more than his fair share of those coils—but not for warding off mosquitoes. He uses them to create detailed works of art. Prastiawan is from Magelang in Central Java, Indonesia, and is a graduate of the Indonesian Institute of the Arts. He started his career as an oil painter. In 2003, he had the idea of creating images by burning them on drawing paper. Initially, he worked with incense, burnt sticks, and blackened firewood as his "brushes." Dissatisfied with those results, he continued experimenting and discovered that the glowing embers from mosquito coils and cigarettes accorded him the precision and control he was seeking from a combustible medium. His unusual painting technique has garnered Prastiawan many awards, including special recognition by the Indonesian World Records Museum in 2006.

Videos available on the Internet offer a glimpse of Prastiawan at work. He starts with a blank canvas or sheet of



thick drawing paper, a stack of mosquito coils, and numerous cigarettes piled pell-mell. After soaking the coils in water, Prastiawan snaps them apart, lights a section, and darkens the canvas by using the smoldering tip of the coil like a charcoal pencil and the cigarette like a miniature blowtorch on the tip of the coil. As he blows on an ember, he balances finesse and fire until detailed sepia-tinged shapes and images emerge. The artist cautiously and continually gauges how much heat he is applying and even heeds subtle shifts in wind direction throughout the process.

Completing each drawing, depending on its size and complexity, typically requires months of work, thousands of exhales, and, according to the artist, typically around 18 packages of mosquito coils. In a sense, Prastiawan's unusual approach to art embodies the notion of surrealist painter and sculptor Joan Miro that "the works must be conceived with fire in the soul but executed with clinical coolness."

According to Prastiawan, "The Little Time," this month's cover image, is "about my daily life when I was a child" (pers. comm., 2019 Feb. 14). In this drawing, he pays homage to his traditional culture by portraying a group of barefoot boys unfurling their kites and gazing toward the sky. More children can be seen near the fence that separates the field from a strip of forest. The temple visible on the hilltop before a low range of mountains is actually Borobudur, the 9th century Buddhist temple in Magelang that was built from volcanic stones and designated a UNESCO World Heritage Site. Prastiawan fills the canvas with delicately rendered textures of trees, grasses, and clouds, the interplay between light and shadow, and even a miniature scene on the pant leg of the boy on the right. "The Little Time" is an idyllic image, free from irony, save the fact that the artist said that it took him 5 months to finish.

It seems a safe assumption that Japanese entrepreneur Eiichiro Ueyama, who invented the spiral mosquito coil, never envisioned it could also be an instrument for creating art. For more than a decade, Ueyama persistently experimented with mixtures of pyrethrum powder and other ingredients and with various manufacturing techniques but failed to create a long-lasting combustible insect repellent. Early prototypes included sticks and bars, neither of which worked as he envisioned. His wife, Yuki, suggested the spiral shape, and Ueyama then spent 7 years perfecting the product, finally marketing the first coils in 1902.

Despite their widespread use, mosquito coils have not been demonstrated to prevent malaria infection, though

evidence indicates that they reduce nuisance bites from mosquitoes. To decrease the global health burden of disease caused by vectorborne infections, researchers and public health experts continue to develop and evaluate inventive approaches, including enhanced surveillance, smart mosquito traps, biotechnology tactics, and new and improved vaccines. Those endeavors will be aided by the blend of creativity, finesse, and tenacity exhibited by Prastiawan in his novel, painstaking approach to his art and by Ueyama in his unrelenting drive to create a viable mosquito repellent.

### Bibliography

1. Adelin F. This guy creates paintings using mosquito coils as paint [cited 2019 Jan 30]. <https://en.brilio.net/news/this-guy-creates-paintings-using-mosquito-coils-as-paint-coils-as-paint-151111b.html>
2. Debboun M, Frances SP, Strickman D. Insect repellents: principles, methods, and uses. Boca Raton (FL): CRC Press; 2006. p. 6.
3. Geni W. Artist profile [cited 2019 Jan 23]. <https://www.bbuzzart.com/profile/192345>
4. Hogarh JN, Agyekum TP, Bempah CK, Owusu-Ansah EDJ, Avicor SW, Awandare GA, et al. Environmental health risks and benefits of the use of mosquito coils as malaria prevention and control strategy. *Malar J*. 2018;17:265. <http://dx.doi.org/10.1186/s12936-018-2412-4>
5. IndexMundi. Incidence of malaria (per 1,000 population at risk) - country ranking [cited 2019 Feb 22]. <https://www.indexmundi.com/facts/indicators/SH.MLR.INCD.P3/rankings>
6. Lawrance CE, Croft AM. Do mosquito coils prevent malaria? A systematic review of trials. *J Travel Med*. 2004;11:92-6. <http://dx.doi.org/10.2310/7060.2004.17015>
7. Rosenberg R, Lindsey NP, Fischer M, Gregory CJ, Hinckley AF, Mead PS, et al. Vital signs: trends in reported vectorborne disease cases—United States and Territories, 2004–2016. *MMWR Morb Mortal Wkly Rep*. 2018;67:496–501. <http://dx.doi.org/10.15585/mmwr.mm6717e1>
8. Sanicas M. Innovations to stop mosquitoes from killing 830,000 humans every year [cited 2019 Feb 11]. <https://medium.com/@melvin.sanicas/innovations-to-stop-mosquitoes-from-killing-830-000-humans-every-year-f3ac12f57b36>
9. Watanabe S. Fumakilla smokes rivals in Indonesia insect-repellent market. [cited 2019 Jan 23]. <https://asia.nikkei.com/Business/Fumakilla-smokes-rivals-in-Indonesia-insect-repellent-market>
10. Wawan Geni on KOMPAS TV. "Pelangi Indonesia", At Limanjawi Art House, Borobudur, October 3, 2012, 08.00 WIB [cited 2019 Jan 29]. [https://www.youtube.com/watch?v=LMRphZo\\_sNk](https://www.youtube.com/watch?v=LMRphZo_sNk)
11. World Health Organization. Vector-borne diseases [cited 2019 Jan 23]. <https://www.who.int/en/news-room/fact-sheets/detail/vector-borne-diseases>

Address for correspondence: Byron Breedlove, EID Journal, Centers for Disease Control and Prevention, 1600 Clifton Rd NE, Mailstop H16-2, Atlanta, GA 30329-4027, USA; email: wbb1@cdc.gov



# EMERGING INFECTIOUS DISEASES®

## Upcoming Issue

- Outbreak of Nontuberculous Mycobacteria Joint Prosthesis Infections, Oregon, USA, 2010–2016
- Novel Sequence Type in *Bacillus cereus* Strains Associated with Nosocomial Infections and Bacteremia, Japan
- Formaldehyde and Glutaraldehyde Inactivation of Bacterial Tier I Select Agents in Tissues
- Infectious Dose of African Swine Fever Virus When Consumed Naturally in Liquid or Feed
- Serologic Prevalence of Ebola Virus in Equatorial Africa
- Management of Central Nervous System Infections, Vientiane, Laos, 2003–2011
- Recurrent Cholera Outbreaks, Democratic Republic of the Congo, 2008–2017
- Lassa Virus Targeting of Anterior Uvea and Endothelium of Cornea and Conjunctiva in Eye of Guinea Pig Model
- Neonatal Conjunctivitis Caused by *Neisseria meningitidis* of US Urethritis Clade, New York City, New York, USA, August 2017
- Estimating Risk to Responders Exposed to Avian Influenza A H5 and H7 Viruses in Poultry, United States, 2014–2017
- Genetic Characterization of Middle East Respiratory Syndrome Coronavirus, South Korea, 2018
- Anthrax Epizootic in Wildlife, Bwabwata National Park, Namibia, 2017
- Analysis of *Francisella tularensis* Group A.II Isolates from 5 Human Tularemia Cases, Arizona, USA, 2015–2017
- Value of PCR, Serology, and Blood Smears for Human Granulocytic Anaplasmosis Diagnosis, France
- Population-Based Estimate of Melioidosis, Kenya
- Severe Myasthenic Manifestation of Leptospirosis Associated with a New Sequence Type of *Leptospira interrogans*
- Lassa and Crimean-Congo Hemorrhagic Fever Viruses, Mali
- Nipah Virus Infections among Patient Contacts, India
- Nipah Virus Sequences from Humans and Bats during Nipah Outbreak, Kerala, India, 2018

Complete list of articles in the May issue at  
<http://www.cdc.gov/eid/upcoming.htm>

## Upcoming Infectious Disease Activities

April 13–16, 2019

European Congress of Clinical Microbiology  
and Infectious Diseases  
29th Annual Congress  
Amsterdam, Netherlands  
<http://www.eccmid.org/>

April 16–18, 2019

International Conference on  
One Health Antimicrobial Resistance  
Amsterdam, Netherlands  
<https://www.escmid.org/ICOHAR2019/>

May 5–9, 2019

ASM Clinical Virology Symposium  
Savannah, GA, USA  
<https://10times.com/clinical-virology-symposium>

June 20–24, 2019

ASM Microbe 2019  
San Francisco, CA, USA  
<https://www.asm.org/index.php/asm-microbe-2018>

June 23–28, 2019

Biology of Vector-borne Diseases  
Six-Day Training Course  
Moscow, ID, USA  
<https://www.uidaho.edu/cals/center-for-health-in-the-human-ecosystem/education/vector-borne-diseases>

July 14–17, 2019

STI and HIV 2019 World Congress  
Vancouver, BC, Canada  
<http://stihiv2019vancouver.com>

July 20–24, 2019

American Society for Virology  
Minneapolis, MN, USA  
<http://www.asv.org>

July 21–24, 2019

International Aids Society 2019  
Mexico City, Mexico  
<http://www.ias2019.org>

August 12–23, 2019

16th International Course on Dengue, Zika  
and other Emergent Arboviruses  
Havana, Cuba  
<http://instituciones.sld.cu/ipk/16th-international-course-on-dengue-zika-and-other-emergent-arboviruses/>

Email announcements to EIDEditor  
([eideditor@cdc.gov](mailto:eideditor@cdc.gov)). Include the event's  
date, location, sponsoring organization,  
and a website. Some events may appear  
only on EID's website, depending on  
their dates.

## Earning CME Credit

To obtain credit, you should first read the journal article. After reading the article, you should be able to answer the following, related, multiple-choice questions. To complete the questions (with a minimum 75% passing score) and earn continuing medical education (CME) credit, please go to <http://www.medscape.org/journal/eid>. Credit cannot be obtained for tests completed on paper, although you may use the worksheet below to keep a record of your answers.

You must be a registered user on <http://www.medscape.org>. If you are not registered on <http://www.medscape.org>, please click on the "Register" link on the right hand side of the website.

Only one answer is correct for each question. Once you successfully answer all post-test questions, you will be able to view and/or print your certificate. For questions regarding this activity, contact the accredited provider, [CME@medscape.net](mailto:CME@medscape.net). For technical assistance, contact [CME@medscape.net](mailto:CME@medscape.net). American Medical Association's Physician's Recognition Award (AMA PRA) credits are accepted in the US as evidence of participation in CME activities. For further information on this award, please go to <https://www.ama-assn.org>. The AMA has determined that physicians not licensed in the US who participate in this CME activity are eligible for AMA PRA Category 1 Credits™. Through agreements that the AMA has made with agencies in some countries, AMA PRA credit may be acceptable as evidence of participation in CME activities. If you are not licensed in the US, please complete the questions online, print the AMA PRA CME credit certificate, and present it to your national medical association for review.

### Article Title

## Clinical Manifestations and Molecular Diagnosis of Scrub Typhus and Murine Typhus, Vietnam, 2015–2017

### CME Questions

**1. You are advising a hospital in Hanoi, Vietnam, regarding anticipated needs for management of rickettsioses. According to the prospective, hospital-based study at 2 national referral hospitals in Hanoi by Trung and colleagues, which of the following statements about the epidemiological features of scrub typhus and murine typhus in northern Vietnam from 2015 to 2017 is correct?**

- A. Murine typhus was the predominant rickettsial disease diagnosed among hospitalized patients with acute undifferentiated fever in northern Vietnam
- B. Scrub typhus was confirmed in 5.5% of patients
- C. Rickettsioses peaked during the summer rainy season when vector populations are most abundant and active
- D. Average age of quantitative PCR (qPCR) (+) scrub typhus cases and eschar (+)-qPCR (–) cases in this study was 20.3 years

**2. According to the prospective, hospital-based study at 2 national referral hospitals in Hanoi by Trung and colleagues, which of the following statements about the clinical characteristics of scrub typhus and murine typhus in northern Vietnam is correct?**

- A. 20% of patients with scrub typhus had eschars
- B. Cough, vomiting, and diarrhea were the most common symptoms among patients with qPCR positivity

- C. Patients with murine typhus had a higher frequency of lymphadenopathy
- D. Complications of scrub typhus include jaundice, meningoencephalitis, myocarditis, acute respiratory distress syndrome, and renal failure; case-fatality rate was 4.9%

**3. According to the prospective, hospital-based study at 2 national referral hospitals in Hanoi by Trung and colleagues, which of the following statements about laboratory findings of scrub typhus and murine typhus in northern Vietnam is correct?**

- A. Prevalence of IgG against scrub typhus orientiae (STGO), typhus group rickettsiae (TGR), and spotted fever group rickettsiae (SFGR) among patients with suspected rickettsiosis was 5.0%, 1.7%, and 0.8%, respectively
- B. Prevalence of IgG against STGO, TGR, and SFGR in this study was highly similar to that previously reported among healthy persons in a rural and urban area of Hanoi
- C. Liver function test results were elevated in patients with scrub typhus but not in patients with murine typhus
- D. The diagnosis of scrub typhus can be serologically confirmed using only acute samples

**Emerging Infectious Diseases** is a peer-reviewed journal established expressly to promote the recognition of new and reemerging infectious diseases around the world and improve the understanding of factors involved in disease emergence, prevention, and elimination.

The journal is intended for professionals in infectious diseases and related sciences. We welcome contributions from infectious disease specialists in academia, industry, clinical practice, and public health, as well as from specialists in economics, social sciences, and other disciplines. Manuscripts in all categories should explain the contents in public health terms. For information on manuscript categories and suitability of proposed articles, see below and visit <http://wwwnc.cdc.gov/eid/pages/author-resource-center.htm>.

## Summary of Authors' Instructions

**Authors' Instructions.** For a complete list of EID's manuscript guidelines, see the author resource page: <http://wwwnc.cdc.gov/eid/page/author-resource-center>.

**Manuscript Submission.** To submit a manuscript, access Manuscript Central from the Emerging Infectious Diseases web page ([www.cdc.gov/eid](http://www.cdc.gov/eid)). Include a cover letter indicating the proposed category of the article (e.g., Research, Dispatch), verifying the word and reference counts, and confirming that the final manuscript has been seen and approved by all authors. Complete provided Authors Checklist.

**Manuscript Preparation.** For word processing, use MS Word. Set the document to show continuous line numbers. List the following information in this order: title page, article summary line, keywords, abstract, text, acknowledgments, biographical sketch, references, tables, and figure legends. Appendix materials and figures should be in separate files.

**Title Page.** Give complete information about each author (i.e., full name, graduate degree(s), affiliation, and the name of the institution in which the work was done). Clearly identify the corresponding author and provide that author's mailing address (include phone number, fax number, and email address). Include separate word counts for abstract and text.

**Keywords.** Use terms as listed in the National Library of Medicine Medical Subject Headings index ([www.ncbi.nlm.nih.gov/mesh](http://www.ncbi.nlm.nih.gov/mesh)).

**Text.** Double-space everything, including the title page, abstract, references, tables, and figure legends. Indent paragraphs; leave no extra space between paragraphs. After a period, leave only one space before beginning the next sentence. Use 12-point Times New Roman font and format with ragged right margins (left align). Italicize (rather than underline) scientific names when needed.

**Biographical Sketch.** Include a short biographical sketch of the first author—both authors if only two. Include affiliations and the author's primary research interests.

**References.** Follow Uniform Requirements ([www.icmje.org/index.html](http://www.icmje.org/index.html)). Do not use endnotes for references. Place reference numbers in parentheses, not superscripts. Number citations in order of appearance (including in text, figures, and tables). Cite personal communications, unpublished data, and manuscripts in preparation or submitted for publication in parentheses in text. Consult List of Journals Indexed in Index Medicus for accepted journal abbreviations; if a journal is not listed, spell out the journal title. List the first six authors followed by "et al." Do not cite references in the abstract.

**Tables.** Provide tables within the manuscript file, not as separate files. Use the MS Word table tool, no columns, tabs, spaces, or other programs. Footnote any use of bold-face. Tables should be no wider than 17 cm. Condense or divide larger tables. Extensive tables may be made available online only.

**Figures.** Submit editable figures as separate files (e.g., Microsoft Excel, PowerPoint). Photographs should be submitted as high-resolution (600 dpi) .tif or .jpg files. Do not embed figures in the manuscript file. Use Arial 10 pt. or 12 pt. font for lettering so that figures, symbols, lettering, and numbering can remain legible when reduced to print size. Place figure keys within the figure. Figure legends should be placed at the end of the manuscript file.

**Videos.** Submit as AVI, MOV, MPG, MPEG, or WMV. Videos should not exceed 5 minutes and should include an audio description and complete captioning. If audio is not available, provide a description of the action in the video as a separate Word file. Published or copyrighted material (e.g., music) is discouraged and must be accompanied by written release. If video is part of a manuscript, files must be uploaded with manuscript submission. When uploading, choose "Video" file. Include a brief video legend in the manuscript file.

## Types of Articles

**Perspectives.** Articles should not exceed 3,500 words and 50 references. Use of subheadings in the main body of the text is recommended. Photographs and illustrations are encouraged. Provide a short abstract (150 words), 1-sentence summary, and biographical sketch. Articles should provide insightful analysis and commentary about new and reemerging infectious diseases and related issues. Perspectives may address factors known to influence the emergence of diseases, including microbial adaptation and change, human demographics and behavior, technology and industry, economic development and land use, international travel and commerce, and the breakdown of public health measures.

**Synopses.** Articles should not exceed 3,500 words in the main body of the text or include more than 50 references. Use of subheadings in the main body of the text is recommended. Photographs and illustrations are encouraged. Provide a short abstract (not to exceed 150 words), a 1-line summary of the conclusions, and a brief

biographical sketch of first author or of both authors if only 2 authors. This section comprises case series papers and concise reviews of infectious diseases or closely related topics. Preference is given to reviews of new and emerging diseases; however, timely updates of other diseases or topics are also welcome. If detailed methods are included, a separate section on experimental procedures should immediately follow the body of the text.

**Research.** Articles should not exceed 3,500 words and 50 references. Use of subheadings in the main body of the text is recommended. Photographs and illustrations are encouraged. Provide a short abstract (150 words), 1-sentence summary, and biographical sketch. Report laboratory and epidemiologic results within a public health perspective. Explain the value of the research in public health terms and place the findings in a larger perspective (i.e., "Here is what we found, and here is what the findings mean").

**Policy and Historical Reviews.** Articles should not exceed 3,500 words and 50 references. Use of subheadings in the main body of the text is recommended. Photographs and illustrations are encouraged. Provide a short abstract (150 words), 1-sentence summary, and biographical sketch. Articles in this section include public health policy or historical reports that are based on research and analysis of emerging disease issues.

**Dispatches.** Articles should be no more than 1,200 words and need not be divided into sections. If subheadings are used, they should be general, e.g., "The Study" and "Conclusions." Provide a brief abstract (50 words); references (not to exceed 15); figures or illustrations (not to exceed 2); tables (not to exceed 2); and biographical sketch. Dispatches are updates on infectious disease trends and research that include descriptions of new methods for detecting, characterizing, or subtyping new or reemerging pathogens. Developments in antimicrobial drugs, vaccines, or infectious disease prevention or elimination programs are appropriate. Case reports are also welcome.

**Research Letters Reporting Cases, Outbreaks, or Original Research.** EID publishes letters that report cases, outbreaks, or original research as Research Letters. Authors should provide a short abstract (50-word maximum), references (not to exceed 10), and a short biographical sketch. These letters should not exceed 800 words in the main body of the text and may include either 1 figure or 1 table. Do not divide Research Letters into sections.

**Letters Commenting on Articles.** Letters commenting on articles should contain a maximum of 300 words and 5 references; they are more likely to be published if submitted within 4 weeks of the original article's publication.

**Commentaries.** Thoughtful discussions (500–1,000 words) of current topics. Commentaries may contain references (not to exceed 15) but no abstract, figures, or tables. Include biographical sketch.

**Another Dimension.** Thoughtful essays, short stories, or poems on philosophical issues related to science, medical practice, and human health. Topics may include science and the human condition, the unanticipated side of epidemic investigations, or how people perceive and cope with infection and illness. This section is intended to evoke compassion for human suffering and to expand the science reader's literary scope. Manuscripts are selected for publication as much for their content (the experiences they describe) as for their literary merit. Include biographical sketch.

**Books, Other Media.** Reviews (250–500 words) of new books or other media on emerging disease issues are welcome. Title, author(s), publisher, number of pages, and other pertinent details should be included.

**Conference Summaries.** Summaries of emerging infectious disease conference activities (500–1,000 words) are published online only. They should be submitted no later than 6 months after the conference and focus on content rather than process. Provide illustrations, references, and links to full reports of conference activities.

**Online Reports.** Reports on consensus group meetings, workshops, and other activities in which suggestions for diagnostic, treatment, or reporting methods related to infectious disease topics are formulated may be published online only. These should not exceed 3,500 words and should be authored by the group. We do not publish official guidelines or policy recommendations.

**Photo Quiz.** The photo quiz (1,200 words) highlights a person who made notable contributions to public health and medicine. Provide a photo of the subject, a brief clue to the person's identity, and five possible answers, followed by an essay describing the person's life and his or her significance to public health, science, and infectious disease.

**Etymologia.** Etymologia (100 words, 5 references). We welcome thoroughly researched derivations of emerging disease terms. Historical and other context could be included.

**Announcements.** We welcome brief announcements of timely events of interest to our readers. Announcements may be posted online only, depending on the event date. Email to [eideditor@cdc.gov](mailto:eideditor@cdc.gov).



# In This Issue

## Perspective

Resurgence of Vaccine-Preventable Diseases in Venezuela as a Regional Public Health Threat in the Americas.....	625
-----------------------------------------------------------------------------------------------------------------	-----

## Synopses

Clinical Manifestations and Molecular Diagnosis of Scrub Typhus and Murine Typhus, Vietnam, 2015–2017 .....	633
Mucosal Leishmaniasis in Travelers with <i>Leishmania braziliensis</i> Complex Returning to Israel ....	642
Tick-Borne Relapsing Fever in the White Mountains, Arizona, USA, 2013–2018 .....	649
Lobomycosis in Soldiers, Colombia .....	654

## Research

Cost-effectiveness of Latent Tuberculosis Infection Screening before Immigration to Low-Incidence Countries .....	661
Spatial Dynamics of Chikungunya Virus, Venezuela, 2014 .....	672
Sand Fly–Associated Phlebovirus with Evidence of Neutralizing Antibodies in Humans .....	681
Human-Origin Influenza A(H3N2) Reassortant Viruses in Swine, Southeast Mexico .....	691
<i>Staphylococcus aureus</i> Bacteremia in Children of Rural Areas of The Gambia, 2008–2015 .....	701
Pneumonia-Specific <i>Escherichia coli</i> with Distinct Phylogenetic and Virulence Profiles, France, 2012–2014 .....	710
Symptoms, Sites, and Significance of <i>Mycoplasma genitalium</i> in Men Who Have Sex with Men.....	719
Differences in Neuropathogenesis of Encephalitic California Serogroup Viruses.....	728
<i>Klebsiella pneumoniae</i> ST307 with <i>bla</i> <sub>OXA-181</sub> , South Africa, 2014–2016.....	739
Co-infections in Persons with Early Lyme Disease, New York, USA.....	748
Middle East Respiratory Syndrome Coronavirus Infection Dynamics and Antibody Responses among Clinically Diverse Patients, Saudi Arabia .....	753
<i>Francisella tularensis</i> Transmission by Solid Organ Transplantation, 2017 .....	767

## Dispatches

<i>Streptococcus agalactiae</i> Sequence Type 283 in Farmed Fish, Brazil .....	776
Genomic Survey of <i>Bordetella pertussis</i> Diversity, United States, 2000–2013 .....	780
Early Genomic Detection of Cosmopolitan Genotype of Dengue Virus Serotype 2, Angola, 2018 .....	784
Enterovirus A71 Phenotypes Causing Hand, Foot and Mouth Disease, Vietnam .....	788
Distribution, Host-Seeking Phenology, and Host and Habitat Associations of <i>Hemaphysalis longicornis</i> Ticks, Staten Island, New York, USA .....	792
Aerosol Transmission of <i>Aspergillus fumigatus</i> in Cystic Fibrosis Patients in the Netherlands .....	797
Pneumonic Plague in a Dog and Widespread Human Exposure in a Veterinary Hospital, United States.....	800
Seroprevalence of <i>Borrelia burgdorferi</i> , <i>B. miyamotoi</i> , and Powassan Virus in Residents Bitten by <i>Ixodes</i> Ticks, Maine, USA.....	804
Prolonged Shedding of Zika Virus RNA in Vaginal Secretions, Nicaragua .....	808
Self-Flagellation as Possible Route of Human T-Cell Lymphotropic Virus Type 1 Transmission.....	811
Seroprevalence of Zika and Dengue Virus Antibodies among Migrant Workers, Taiwan, 2017 .....	814
<i>Anopheles sudaicus</i> Mosquitoes as Vector for <i>Plasmodium knowlesi</i> , Andaman and Nicobar Islands, India .....	817